ЖУРНАЛ
ЭКСПЕРИМЕНТАЛЬНОЙ И ТЕОРЕТИЧЕСКОЙ
ФИЗИКИ
АКАДЕМИИ НАУК СССР

SOVIET PHYSICS

JETP

VOLUME 36 (9) NUMBER 1

A Translation

of the

Journal of Experimental and Theoretical Physics

of the

Academy of Sciences of the USSR

Volume 36

JULY, 1959

Published by the

AMERICAN INSTITUTE OF PHYSICS
INCORPORATED

SOVIET PHYSICS
JETP

A translation of the Journal of Experimental and Theoretical Physics of the USSR.

A publication of the

AMERICAN INSTITUTE OF PHYSICS

Governing Board

RALPH A. SAWYER, *Chairman*

Members:

WALTER S. BAIRD
JESSE W. BEAMS
RAYMOND T. BIRGE
R. H. BOLT
HARVEY BROOKS
J. W. BUCHTA
J. H. DILLON
VERNET E. EATON
HERBERT A. ERF
IRVINE C. GARDNER
S. A. GOUDSMIT
WINSTON E. KOCK
R. BRUCE LINDSAY
WALTER C. MICHELS
G. E. PAKE
R. RONALD PALMER
JOSEPH B. PLATT
RALPH A. SAWYER
H. D. SMYTH
JOHN STRONG
GEORGE E. UHLENBECK

Administrative Staff

ELMER HUTCHISSON
Director

HENRY A. BARTON
Associate Director

WALLACE WATERFALL
Secretary and Treasurer

THEODORE VORBURGER
Advertising Manager

RUTH F. BRYANS
Publication Manager

ALICE MASTRO
Circulation Manager

KATHRYN SETZE
Assistant Treasurer

EUGENE H. KONE
Director of Public Relations

EDWARD P. TOBER
Manager, Production and Distribution

W. C. KELLY
Director of Education Projects

EMILY WOLF
Office Manager

American Institute of Physics Advisory Board on Russian Translations

ROBERT T. BEYER, *Chairman*
FREEMAN J. DYSON, DWIGHT GRAY, DAVID HARKER,
MORTON HAMERMESH, VLADIMIR ROJANSKY, HAROLD F. WEAVER

Editor of SOVIET PHYSICS—JETP

J. GEORGE ADASHKO, 25 WEST 81ST ST., NEW YORK 24, NEW YORK

SOVIET PHYSICS—JETP is a monthly journal published by the American Institute of Physics and contains a complete translation of the JOURNAL OF EXPERIMENTAL AND THEORETICAL PHYSICS of the U.S.S.R. Academy of Sciences.

This translating and publishing project was undertaken by the institute in the conviction that dissemination of the results of researches everywhere in the world is invaluable to the advancement of science. The NATIONAL SCIENCE FOUNDATION of the United States has encouraged the project initially and is supporting it in large part by a grant.

The American Institute of Physics and its translators propose to translate faithfully all the material appearing in the original articles. The views expressed in the translations are therefore those of the original authors, and not those of the translators nor of the American Institute of Physics.

Volume 1 of SOVIET PHYSICS—JETP corresponds to Russian Volume 28 (1955). Two volumes are published annually, each of six issues. Each volume contains the translation of one volume of the JOURNAL OF EXPERIMENTAL AND THEORETICAL PHYSICS.

Beginning with Vol. 9(36), the transliteration of the names of Russian authors follows British Standard 2979, which is being adopted in 1959 by a large number of scientific journals in the United States. The Library of Congress transliteration is followed in the earlier volumes.

Subscription Prices

Per Year (12 issues)

General:

United States and Canada	$75.00
Elsewhere	79.00

Libraries and non-profit degree-granting Institutions:

United States and Canada	$35.00
Elsewhere	39.00
Back Numbers	$ 8.00

Subscriptions should be addressed to the American Institute of Physics, 335 East 45th Street, New York 17, New York.

SOVIET PHYSICS, JETP is published monthly by the American Institute of Physics, Inc. Application for Second Class mail privileges is pending at Ann Arbor, Michigan.

Copyright by American Institute of Physics 1959

SOVIET PHYSICS

JETP

A translation of the Journal of Experimental and Theoretical Physics of the USSR.

SOVIET PHYSICS JETP VOL. 36 (9), NO. 1, pp. 1-237 JULY, 1959

DEPTH OF PENETRATION AND CHARACTER OF DISTRIBUTION OF ATOMS INJECTED INTO Si^{30} ISOTOPE TARGETS

M. I. GUSEVA, E. V. INOPIN, and S. P. TSYTKO

Physico-technical Institute, Academy of Sciences, Ukrainian S.S.R.

Submitted to JETP editor October 5, 1957; resubmitted September 15, 1958

J. Exptl. Theoret. Phys. (U.S.S.R.) **36**, 3-9 (January, 1959)

We investigated the depth of penetration and distribution of silicon atoms injected in tantalum and copper backings. The targets, which were prepared in an electromagnetic separator by directly depositing the Si^{30} isotope on the backing, were bombarded with protons accelerated in an electrostatic generator. The shape of the resonance yield of gamma rays from a single gamma resonance in the $Si^{30}(p, \gamma)P^{31}$ reaction was observed in four targets and compared with the theoretical density distribution of the injected atoms. The penetration depth and nature of the distribution of the Si^{30} atoms injected in the tantalum backing are in satisfactory agreement with the theory.

INTRODUCTION

THE use of isotope targets in nuclear research is on the increase. The most effective among the various methods of preparing thin isotope targets is to force ions, accelerated in an electromagnetic separator to an energy of several tens of kev, to penetrate into a metal backing.

The essential characteristic of an isotope target prepared by the penetration method is the depth of penetration of the injected atoms and their distribution in the backing material. An investigation of the depth of penetration and of the character of distribution of the target atoms in the backing is of considerable interest both from the point of view of determining the optimum conditions under which isotope targets can be prepared in an electromagnetic separator, and from the point of view of the subsequent use of these targets in nuclear research. Furthermore, data obtained from these investigations can be of great importance in the formulation and verification of a theory of interaction between ions with energies of several kev and the backing substance, and also in the understanding of the phenomenon of cathode spattering. A theoretical examination of these problems is found in the papers by Bohr[1] and Nielson.[2]

Experimental data on the depth of penetration of injected atoms can be obtained from experiments on scattering of protons and alpha particles,[3] from resonant capture of protons,[2] and with the aid of tracer atoms.[4] One of the most convenient methods of investigating isotopic targets is the study of resonant capture of protons, for it yields directly the distribution density of the ions that penetrate into the backing.

The purpose of this study was an investigation of the depth of penetration of Si^{30} ions injected in copper and tantalum backings as a function of the backing material and ion energy. We also investigated the character of the distribution of the Si^{30} atoms injected into a surface layer of the backing. The depth of penetration and the character of the distribution were investigated on the basis of experimental data obtained in a study of the $Si^{30}(p, \gamma)P^{31}$ reaction. For the investigation of

TABLE I

Number of target	Backing material	Ion energy E_i, kev	Time of exposure in beam, min	Amount of silicon injected, μg
1	Ta	25	30	20
2	Cu	25	90	50
3	Cu	28	9	5
4	Cu	10	9	5

this reaction we used Si^{30} targets prepared as described in the following section. All the investigations were made at the same gamma resonance of the $Si^{30}(p, \gamma)P^{31}$ reaction at a proton energy of 940 kev, to permit ready comparison of the experimental data with each other and with experiment.

PREPARATION OF SILICON ISOTOPE TARGETS

The silicon targets were prepared in an electromagnetic separator by directly depositing the ions on metallic backings.[5] The ion source used for such a purpose is described in reference 6. The backings used were copper and tantalum disks 14 mm in diameter and 0.2 to 0.5 mm thick. The ion current into the target was 30 μa during the process. We prepared four Si^{30} targets. The conditions under which these targets have been prepared are listed in Table I.

The amount of Si^{30} injected into the backing, listed in the last column of Table I, is based on the measured target current. The total quantity of electricity flowing into the target during the time of the experiment was measured with a Coulomb meter. The actual concentration of the silicon atoms injected into the backing was determined by calorimetric analysis of several isotopic targets, prepared under analogous conditions. Experience has shown that at a given ion energy the fraction of trapped silicon atoms depends on the current density in the target. When the current density is increased to a fixed value that depends on the ion-metal combination, the number of penetrating atoms decreases. This decrease is due to an increase in the spattering coefficient of the backing material with increasing intensity of the bombarding ions. Thus, as the current density is increased from 20 to 200 $\mu a/cm^2$, the coefficient of spattering of copper by 25-kev silicon ions increases by one order of magnitude (from 0.3 to $\sim$ 3 atoms per ion[7]). At a target current density of ~ 20 $\mu a/cm^2$, maintained during the experiments, the actual concentration of the Si^{30} ions amounted to 85 or 90 percent of the value estimated from the target-current measurement.

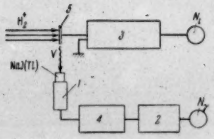

FIG. 1. Experimental setup and arrangement of apparatus: 1) FEU-19, 2) PS-64, 3) beam-current integrator, 4) amplifier, 5) target.

PROCEDURE

The investigation of the depth of penetration and the character of distribution of Si^{30} atoms in a surface layer of the target backing consisted of measuring the resonance gamma yield at a proton energy $E_p = 940$ kev in the $Si^{30}(p, \gamma)P^{31}$ reaction, and a determination of the width of the resonance peak and of its shape. Si^{30} isotope targets with the characteristics listed in Table I were used in these measurements. The gamma-ray resonance peak was measured with the precision electrostatic generator of the Physico-technical Institute of the Academy of Sciences of the Ukrainian S.S.R.[8] The accelerating voltage of the generator was stabilized with an accuracy of $\pm 0.05\%$, and the energy of the bombarding protons was measured with an electrostatic analyzer[8] having an energy resolution $\Delta E/E \approx 10^{-4}$.

The gamma-ray yield was measured with an NaI(Tl) crystal and an FEU-19 photomultiplier, amplifier, and PS-64 scaler. The current into the target was measured with a current integrator. The arrangement of the apparatus is shown in Fig. 1.

The number of gamma quanta, N_γ, registered by the detector, was referred to the number of counts N_i of the current integrator, corresponding to the charge of the protons incident on the target. The relative gamma yield from extraneous radiation sources and from the backing material was plotted as a function of the energy of the protons incident on the target. The total gamma background amounted to not more than 10% of the main effect measured with the gamma-ray detector. The statistical errors in the measurement of the relative gamma yield did not exceed 3%. With this, equally good reproducibility was obtained for the shape of the resonance curve both in repeated measurements with the same target, and in repeated measurements on different targets prepared in the electromagnetic separator under analogous conditions.

The width of the resonant peak at half maximum, Γ_{exp}, which characterizes the depth of penetration of the Si^{30} ions into the backing material, was determined from the resonance-peak curve in kev. If the stopping powers for protons of given energy in the target and backing material are known, and if

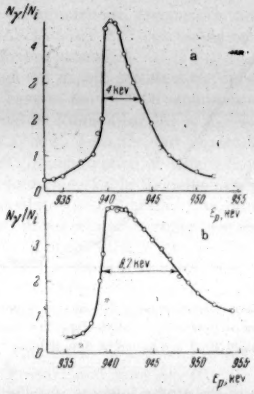

FIG. 2. Relative yield of gamma radiation from the $Si^{30}(p,\gamma)P^{31}$ reaction; resonance at E_p = 940 kev, a) target No. 1 – Si^{30} on tantalum backing; b) target No. 2 – Si^{30} on copper backing. Ion energy E_i = 25 kev.

the concentrations of the isotope atoms injected into the backing are also known, it is possible to determine from the width of the resonance peak (in kev) the depth of penetration of the ions of the target isotope in $\mu g/cm^2$.

Since the width of the resonance peak is determined by three independent quantities — the thickness Γ_t of the isotope target, the energy inhomogeneity Γ_i of the protons incident on the target, and the natural resonance width Γ_n, the experimentally determined with Γ_{exp} satisfies the relation

$$\Gamma_{exp}^2 = \Gamma_t^2 + \Gamma_i^2 + \Gamma_n^2. \quad (1)$$

The last two terms in (1) give the width of the gamma resonance for a thick target

$$\Gamma_{th} = \sqrt{\Gamma_i^2 + \Gamma_n^2}. \quad (2)$$

The width of the gamma resonance on a thick target was determined in a separate measurement, where a thick target of a natural mixture of silicon isotopes was used.

TABLE II

Target No.	Γ_{exp}, kev	Γ_t, kev	Γ_t, $\mu g/cm^2$	Γ_t^{theor}, $\mu g/cm^2$
1	4	3.46	30	31
2	8.7	8.45	35	13
3	6	5.65	42	15
4	3.7	3.11	21	5

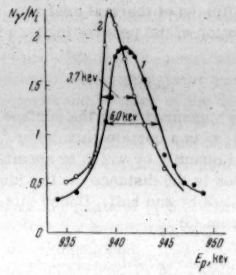

FIG. 3. Relative gamma yield in the Si^{30} (p, γ) reaction. 1) Target No. 3 – Si^{30} isotope on copper backing, ion energy E_i = 28 kev; 2) target No. 4 – Si^{30} on copper backing, ion energy E_i = 10 kev.

Inserting (2) in (1) we get

$$\Gamma_t = \sqrt{\Gamma_{exp}^2 - \Gamma_{th}^2}. \quad (3)$$

It is obvious that if

$$\Gamma_{th}^2/\Gamma_{exp}^2 \ll 1 \quad (4)$$

the curve of the gamma-ray yield will reproduce with sufficient accuracy the density distribution of the target atoms injected into the backing.

MEASUREMENT RESULTS AND DISCUSSION

Figures 2 and 3 show the results of the measurements of the relative gamma yield N_γ/N_i as a function of the energy E_p of the bombarding protons. The resonant peaks for four Si^{30} targets indicate the experimental widths Γ_{exp}, expressed in kev. The value of Γ_{th}, measured on a thick silicon target (natural isotope mixture) for resonance in the $Si^{30}(p,\gamma)P^{31}$ reaction at E_p = 940 kev, was found to be 2 kev. Condition (4) is thus quite well satisfied for all the investigated targets. The gamma-yield curves represent quite well the density distribution of the Si^{30} atoms injected into tantalum and copper backings.

Table II lists the widths of the targets, in kev, determined from the experimental values, Γ_{th} and Γ_{exp}.

A theoretical analysis of the interaction between ions of energy less than 50 kev and the material of the backing is given in the paper by Nielson[2] for two limiting cases: $A_1 \ll A_2$ and $A_1 \gg A_2$, where A_1 and A_2 are the mass numbers of the ions and atoms of the backing material. In the case of interest to us $A_1 \ll A_2$, when the ion transfers on the average in a single collision only a small fraction of its energy, the analysis is quite analogous

to that of diffusion of thermal neutrons. The density distribution of the penetrating ions is in this case

$$q(x) \sim e^{-x^2/4\tau}, \qquad (5)$$

where x is measured from the surface of the backing and τ is a certain parameter.[2]

A natural quantity by which to specify the depth of penetration is the distance x in which the density diminishes by one half. Under this condition we obtain from (5)

$$t = 2\sqrt{\tau \ln 2}. \qquad (6)$$

Nielson[2] has shown that

$$t = \Gamma_t = \frac{0.83}{(\xi(1-\overline{\cos\varphi}))^{1/2}} \frac{(z_1^{2/3}+z_2^{2/3})^{1/2}}{z_1 z_2} \frac{A_2^2 E_i}{A_1 + A_2} \ \mu g/cm^2, \qquad (7)$$

where z_1 and z_2 are the charges of the ion and of the backing atoms, while ξ and $\overline{\cos\varphi}$ are quantities familiar from neutron-diffusion theory.[9]

As applicable to our own measurements, a satisfactory agreement with (7) is expected for the Si^{30}-Ta combination, for here $A_2/A_1 \approx 6$. To compare the experimentally-determined width Γ_t = 3.46 kev (Table II) with the depth of penetration determined from (7), it is necessary to convert the former into $\mu g/cm^2$ units of the backing material. For this we must know the stopping power of the material through which the protons pass. It is necessary to recognize here that a considerable contribution to the stopping power S_p is made by the silicon ions injected into the tantalum base. This contribution depends in turn on the thickness of the layer in which the given amount of silicon has been injected. We thus obtain a system of equations for the thickness of the Si^{30} layer:

$$\Gamma_t[\text{kev}]/S_p[\text{kev}\cdot\text{cm}^2/\text{mg}] = \Gamma_t[\text{mg/cm}^2];$$
$$S_t = S_t^{Ta} + S_p^{Si}\delta[\text{mg/cm}^2]/\Gamma_t[\text{mg/cm}^2]. \qquad (8)$$

Here δ is the amount of the Si^{30} isotope (mg/cm^2) in a layer Γ_t(mg/cm^2), obtained by multiplying the silicon actually injected into the backing by a factor $^3/_4$, since, according to (5), a thickness $t = 2\sqrt{\tau \ln 2}$ contains approximately $^3/_4$ of all the atoms injected into the backing. Putting in (8) S_p^{Ta} = 60 kev-cm^2/mg and S_p^{Si} = 180 kev-cm^2/mg, we get Γ_t = 30 $\mu g/cm^2$, which is in good agreement with the width Γ_t^{theor} = 31 $\mu g/cm^2$, computed with the aid of Eq. (7).

Since the experimental and theoretical values of the depth of penetration of silicon atoms into tantalum are in good agreement, and the formula for the resonance peak represents accurately the distribution of the atoms injected into the backing, it becomes interesting to compare the theoretical distribution of the density of the injected atoms with the experimentally-observed shape of the resonance peak.

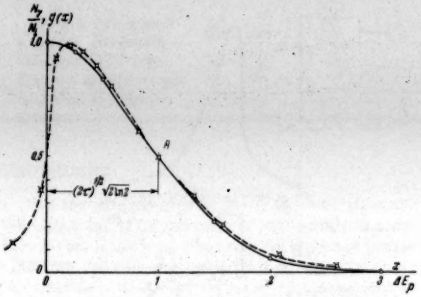

FIG. 4. Depth distribution of Si^{30} ions in a tantalum backing. Solid line – theoretical distribution. The experimental points for target No. 1 are joined by dotted lines.

Figure 4 shows a curve, calculated with the aid of Eq. (5), together with the experimental curve obtained with target No. 1. The curves are made to coincide at point A, where the density of the penetrated particles and the intensity of the gamma-ray yield decrease by one-half. Such an alignment of the curves determines their overall scale. The coordinates of the remaining points on the theoretical and experimental curves were recalculated to fit the scale so selected. We see that the experimental curve follows Eq. (5) rather closely. The portion of the experimental curve to the left of zero is apparently due to the "tail" of the Breit-Wigner curve, broadened by the energy inhomogeneity of the proton beam.

A simple calculation shows that in this case, a layer of thickness $\Gamma_t = 2\sqrt{\tau \ln 2}$, contains approximately two silicon atoms for each tantalum atom. Such a concentration ratio may correspond to the formation of an intermetallic compound $TaSi_2$. One might assume that so large an impurity of silicon atoms would also affect the character of diffusion of the silicon ions, causing a deviation from the law given by Eq. (5). However, one must take it into account that, firstly, the Si^{30}-Si^{30} and Si^{30}-Ta^{181} collision cross sections are related as the nuclear charges, i.e., the ratio of their cross sections is 14:73 = 0.19. Secondly, the 2:1 concentration ratio is attained only at the conclusion of the ion injection. Thirdly, one must consider that scattering at large angles (~ 180°) in the c.m. system cannot influence the diffusion of identical particles.

All these circumstances, apparently, make for only a slight effect of Si^{30}-Si^{30} scattering on the course of the diffusion process.

We must not expect satisfactory agreement with (7) in the case of the Si^{30}-Cu combination, which was derived by Nielson for $A_1 \ll A_2$, for in this case $A_2/A_1 \approx 2$. Actually, our experimental values of the depth of penetration of silicon ions into copper (see column 4, Table II) do not agree with the values calculated with Eq. (7). It is interesting that for all three copper-backing targets the depth of penetration of the silicon ions is 3 or 4 times greater than the theoretical value.

In Fig. 3 the maxima of the resonance peaks of targets 3 and 4 are displaced, owing to the different energies of the silicon ions (see Table I, data for E_i). This effect is expected both from the theory of N. Bohr and from Eq. (7).

It would be interesting to verify experimentally the correctness of Eq. (7) for several other ion and metal combination, and to investigate the other limiting case, when $A_1 \gg A_2$.

A very interesting fact is that isotope targets prepared by penetration in an electromagnetic separator were more stable in a proton beam than targets obtained by condensation of previously separated Si^{30} evaporated in vacuo.

CONCLUSIONS

1. The depth of penetration of Si^{30} ions into tantalum, at an ion energy of 25 kev, was found experimentally to be 30 $\mu g/cm^2$, a value in good agreement with theory.

2. The character of distribution of the silicon stoms penetrating in a tantalum backing is analogous to the distribution derivable from the theory of the diffusion of thermal neutrons.

3. A layer 30 $\mu g/cm^2$ thick contains on the average two silicon atoms for each tantalum atom; this indicates a considerable deformation of the tantalum lattice. It is probable that the penetration results in the formation of the intermetallic compound $TaSi_2$.

4. The experimental values of the depth of penetration of silicon ions into copper are 3 to 4 times greater than those computed by the Nielson formula, but smaller than those obtained from the theory of N. Bohr.

The authors are grateful to K. D. Sinel'nikov and A. K. Val'ter for continuous interest in the work and for valuable discussion, to Yu. P. Antuf'ev, V. Yu. Gonchar, A. N. L'vov, P. M. Tutakin, and E. G. Kopanets, who participated in the measurements with the electrostatic generator, and also to A. A. Tsygikalo and his associates, who ensured precise operation of the electrostatic generator during the time of these measurements.

[1] N. Bohr, Passage of Atomic Particles through Matter, Russ. Transl. M. IIL, 1950.

[2] K. O. Nielson, Electromagnetically Enriched Isotopes and Mass Spectrometry, London, 1956, p. 68.

[3] C. Milekowsky, Ark. Fys. 7, 89 (1951).

[4] S. Tuhlin, Ark. Fys. 9, 107 (1955).

[5] M. I. Guseva, Приборы и техника эксперимента (Instr. and Meas. Engg.) No. 5, 112 (1957).

[6] Gusev, Chkuaseli, and Guseva, Атомная энергия (Atomic Energy) 3, 215 (1957).

[7] M. I. Guseva, J. Tech. Phys. (U.S.S.R.), in press.

[8] A. K. Val'ter and A. A. Tsygikalo, Приборы и техника эксперимента (Instr. and Meas. Engg.) No. 4, 3 (1957).

[9] E. Fermi, Nuclear Physics, (Russ. Transl.) M. IIL, 1951.

Translated by J. G. Adashko
1

SHOWERS PRODUCED BY POSITRONS IN 100 to 400 Mev RANGE

Yu. D. PROKOSHKIN and T'ANG HSIAO-WEI

Joint Institute for Nuclear Research

Submitted to JETP editor April 23, 1958

J. Exptl. Theoret. Phys. (U.S.S.R.) **36**, 10-16 (January, 1959)

Cascade curves for 101, 224, and 407 Mev positrons in lead and copper were measured. The curves are in agreement with shower curves computed by the Monte Carlo method. Functions approximating the cascade curves were determined.

INTRODUCTION

THE passage of fast electrons through matter is accompanied by the production of electron-photon showers. Although this fact has been known for a long time,[1] no theory has so far been developed which could adequately describe the development of showers produced by electrons with energy E_e comparable with the critical energy ϵ (7 Mev in lead). The cascade theory[2] existing presently is correct for large energies, of a few orders of magnitude greater than the critical. Difficulties arise, however, even in the description of showers in heavy substances, since the cross section for pair production is then dependent on the energy, and because of the scattering of shower particles. The asymptotic formula for cross sections which is used in the cascade theory becomes incorrect with decreasing energy, which invalidates the results of the theory for $E_e < 1$ Bev, i.e., exactly in that energy range which has now become accessible to experimental investigation thanks to powerful particle accelerators. This gap has recently been filled by the work of Belen'kii and Ivanenko,[3] who calculated the cascade curves and the spectrum of shower particles using the moment method. However, the experimental data which would enable us to test the accuracy of these calculations (especially the most interesting ones concerning the spectrum) is still lacking. In connection with the above, the study of showers at $E_e < 1$ Bev is at present of considerable interest. Data concerning the cascade curves,* fluctuations, etc., in the above energy range have also an application which has increased in importance in recent years owing to the construction of spectrometers based on the detection of Cerenkov light pulses[4] associated with showers. In these spectrometers the magnitude of the light pulse is proportional to the area under the cascade curves $N(E_e, \epsilon, t) = n(t)$. The dependence of $n(t)$ on the electron energy E_e in the 50 to 500 Mev range was calculated by Wilson,[5] using the Monte-Carlo method. The purpose of the present work is to determine experimentally the cascade curves $n(t)$ in the above range, and to compare them with the calculations of Wilson.

*The cascade curves describe the number of electrons and positrons $N(E_0, E, T)$ with energy greater than E, contained in the shower at the depth t below the shower initiation point as a function of t. E_0 is the energy of the primary particle.

2. EXPERIMENTAL METHOD

The experiments were carried out with a beam of monoenergetic positrons. A collimated beam of high energy photons (produced by π^0-meson decay) from the phasotron chamber at the Joint Institute for Nuclear Research, was directed towards a lead target (1 mm thick) placed before the magnet (see Fig. 1). The positrons produced in the target were deflected in the magnetic field by an angle of 20° and then collimated by a counter telescope (a) and a lead diaphragm 5 cm in diameter. The energy of the positrons could be varied from 50 to 500 Mev by varying the intensity of the magnetic field. The energy spread amounted to 2 or 3%. Behind the last counter of the telescope (a), a 20×20 cm^2 copper or lead absorber was placed in the way of the positron beam and the number of fast electrons emerging from the absorber $n(t)$ was measured for different thicknesses t of the absorber.

Before the construction of the detector used for the measurement of $n(t)$ is discussed, it should be noted that in showers produced by electrons (here and in the following discussion we do not distinguish between electrons and positrons) of several hundred Mev energy there is a high probability that several electrons with a small angle of divergence will be produced simultaneously, especially at small thicknesses t. One can measure

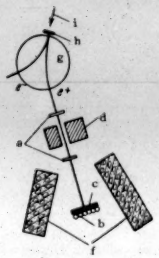

FIG. 1. Experimental set-up. a – telescope, b – tray of low-efficiency counters, c – absorber of thickness t, d – lead diaphragm, f – shield, e^+ – positron beam, g – magnet, h – lead target, i – photon and neutron beam.

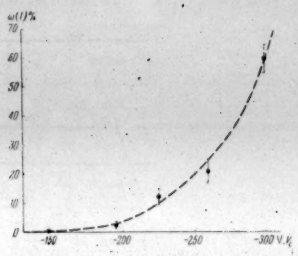

FIG. 2. Dependence of the probality w(1) on the value of the constant V_0 in the pulsed operation of the STS-8 counter. Delay of the high-voltage pulse equal to 0.6 μsec.

the number of these electrons, say, by means of a scintillation counter used together with a pulse-height analyzer. Such a method is in general complicated, and in our case, the difficulties are increased because of the large cross-section of the positron beam. For the measurement of the number of shower electrons, we used a tray of halogen counters (see Fig. 1) placed behind the absorber. The counters were fed by a triggered pulsed power supply.[6] The tray measured 15×15 cm and consisted of STS-8 counters of identical characteristics. Whenever a particle passed through the telescope (a), a high-voltage pulse (−1000 V) of 1.5 μsec duration with a rise time of 0.15 μsec, and delayed for 0.6 μsec with respect to the time of the passage of the particle, was applied to the cathodes of the counters, which were held at a constant voltage V_0. Since the high voltage pulse was delayed, the detection efficiency of the counters for single fast electrons w(1) was much smaller than unity for small values of V_0 (see Fig. 2).

The probability w(n) that a discharge will occur in the tray when n electrons pass simultaneously through it is given by the expression

$$w(n) = 1 - e^{-an}, \qquad (1)$$

where a is the mean number of ions produced by a single fast electron, which remain in the counter till the moment of the arrival of the high-voltage pulse. The dependence of the efficiency on n was measured, and the result is in good agreement with formula (1).

The necessary small value of w(1) which is determined by the condition

$$w(1)\,n \ll 1 \qquad (2)$$

can be obtained by adjusting V_0. When this condition is satisfied, the detector has almost linear counting characteristics

$$w(n) \approx an \approx w(1)\,n. \qquad (3)$$

Thus, for an energy of 400 Mev ($n \lesssim 3$), it is sufficient to choose w(1) = 0.04, in order that the maximum correction due to the nonlinearity of the characteristics amounts only to 6% of the counting rate of the tray.

When counters of such small efficiency are used, the problem of stability of the efficiency with respect to time becomes very serious, since small changes of the circuit parameters can change the value of w by factor of several times (from its normal value of $w \approx 1$). The stability of the array used was satisfactory.

The low efficiency of halogen counters used in the described method of operation is due not to the narrow zone of sensitivity, but to an almost identical decrease in the efficiency all over the counter volume.[6] The latter decrease is essential, since the diameter of the counters used (20 mm) is comparable with the dimensions of the positron beam. If the decrease of the efficiency were due to narrowing of the sensivity zone, the measurement would depend on the position of the tray with respect to the center of the beam. The radial dependence of the probability w(1) has been measured. The STS-8 counter was placed between two small counters which selected a beam of electrons 3 mm in width. The efficiency w(1), defined as the ratio of the counting rate of the investigated counter to the counting rate of the coincidences of the master counters, was measured for various distances between the anode of the counter and the electron beam. The measurements were carried out for several values of w(1), in the range of 3 to 25%. The results indicate that the sensitivity of the whole volume of the halogen counters is uniform, which is in agreement with Vishnyakov and Tyapkin.[6]

$E_e = 101 \pm 2$ Mev

t, mm Pb	0	5	8	10	15	20	25	30
$w(n)$, %	4.35	6.11	4.85	5.50	3.17	1.83	1.60	1.60
$\pm \Delta w(n)$, %	0.09	0.31	0.24	0.28	0.16	0.11	0.14	0.20

$E_e = 294 \pm 10$ Mev

t mm Pb	0	5	10	13	15	20	30	35
$w(n)$, %	5.80	13.5	14.8	15.1	12.8	9.4	6.9	4.4
$\pm \Delta w(n)$, %	0.17	0.6	0.6	0.6	0.5	0.4	0.3	0.2

$E_e = 407 \pm 10$ Mev

t mm Pb	0	5	10	15	20	25	30	35	40	50
$w(n)$, %	4.8	8.5	12.5	12.9	11.9	9.4	6.4	6.5	4.2	1.6
$\pm \Delta w(n)$, %	0.3	0.9	0.8	0.6	1.0	1.0	0.3	0.7	0.4	0.6

RESULTS OF MEASUREMENTS AND DISCUSSION

The measuring apparatus was placed in the immediate vicinity of the neutron beam (see Fig. 1). However, thanks to the fact that the resolving time of the whole array amounted to ~ 1 μsec, the background of chance coincidences was less than 1% for a counting rate of the tray equal to 200 pulses per minute (for the measurements of the number of chance coincidences, the triggering pulse was delayed for 2.5 μsec.).

The cascade curves $n(t)$ were measured for positrons with energy equal to 101 ± 2, 294 ± 10, and 407 ± 10 Mev. The positron energy was determined by the method of current-carrying wire.[7] We limited ourselves to an energy of 400 Mev, in view of the fact that for larger energies the background of chance coincidences increased sharply, and the intensity of the positron beam decreased. Simultaneously, the mixture of protons in the positron beam increased, which caused a fast drop of the counting rates with and without the target.

The value of $n(t)$ was determined by comparing the counting rate of the tray (b) and of the telescope (a) [the "tray-counting rate" to "telescope counting rate" ratio is equal to $w(n)$; for $t = 0$, the ratio is equal to $w(1)$]. The measured probabilities $w(n)$, related to the values of an by Eq. (1), are given in the table. The errors given are statistical.

Before comparing the cascade curves with the results of calculations of Wilson,[5] it was necessary to determine the energy threshold of the tray (b). For that purpose, an aluminum absorber was placed before the tray in order to cut off slow electrons. The threshold of the tray was found to be close to the critical energy $\epsilon = 7$ Mev, which made it possible to compare our results directly with the calculations of Wilson. It can be seen, by comparing the integrals J of the measured cascade curves $n(t)$ with the value of the ratio E_e/ϵ, that the apparatus does not detect soft electrons of the shower. The ratio $J/(E_e/\epsilon)$ is equal to 0.35. It follows that the detector detects roughly one-third of the total number of electrons in the shower.

The cascade curves calculated by Wilson and those obtained by us differ in the fact that the thickness of the lead absorber t is measured in different units: in g/cm^2 (present work) and in radiation units in lead, r.u. Pb (Wilson). A comparison of the data contained in the table and the cascade curves of Wilson makes it therefore possible to determine the value of one radiation unit in lead in units of g/cm^2, which is of interest since the values of the radiation unit in lead calculated by various authors[2,3,8] are considerably different from each other. The value of radiation unit in lead was found by the least-squares method to be

$$1 \text{ r.u. Pb} = 5.6 \pm 0.2 \text{ g/cm}^2,$$

which is in agreement with the value given in reference 8, if the latter is corrected according to the latest data on the energy dependence of the pair production cross-section in lead.[9]

The cascade curves obtained in the course of the present work (measured in radiation units) are compared with the curves of Wilson in Figs. 3 and 4. It can be seen from these figures that the two results are in agreement.

To test the present cascade theory, we measured the cascade curves $n(t)$ for lead and copper (see Figs. 3 and 4). It is well known that the theory predicts the following relation for the position of the maxima (t_{max}) of the cascade curves[8] in the

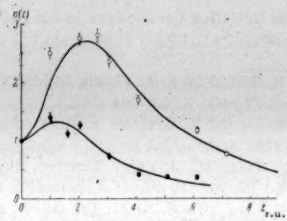

FIG. 3. Cascade curves n(t), measured for positrons: ● – with energy (101 ± 2) Mev, ○ – (294 ± 10) Mev in lead. 1 r.u. in lead = 5.6 g/cm². The curves shown in the figure were calculated by Wilson[5] for electrons with energy of 100 and 300 Mev.

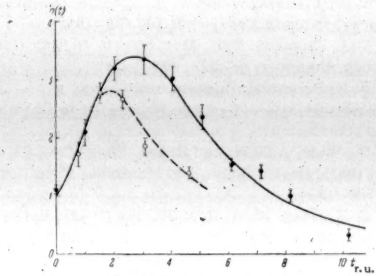

FIG. 4. Cascade curves n(t), measured for positrons of 407 ± 10 Mev in lead (●) and copper (○). 1 r.u. Pb = 5.6 g/cm², 1 r.u. Cu = 11.5 g/cm². The solid line was obtained for $E_0^* =$ 407 Mev by an interpolation of the results of Wilson.[5]

approximation B:

$$t_{\max\,Pb} / t_{\max\,Cu} = b_1 \ln (E_e / \varepsilon_{cr\,Pb}) / \ln (E_e / \varepsilon_{cr\,Cu}). \quad (4)$$

This ratio is equal to ≈ 1.7 for $E_e = 407$ Mev, which is in agreement with the experimentally found value of 1.5 ± 0.2.

The following relation holds for the maxima of cascade curves according to the cascade theory:

$$n_{\max\,Pb} / n_{\max\,Cu} = b_2 (\varepsilon_{cr\,Cu} / \varepsilon_{cr\,Pb}) \{\ln (E_e / \varepsilon_{cr\,Cu}) / \ln (E_e / \varepsilon_{cr\,Pb})\}^{1/2}. \quad (5)$$

For $E_e = 407$ Mev, the ratio (5) is equal to ≈ 1.5, which is close to the ratio 1.20 ± 0.25 obtained by us. It should be noted that, if the ratio (5) is calculated neglecting the dependence of the pair production cross section on energy (assuming $b_2 = 1$), then the value obtained is considerably different from that measured in our work: for $b_2 = 1$, the relation (5) is equal to 2.5.

The cascade curves n(t) obtained for lead can

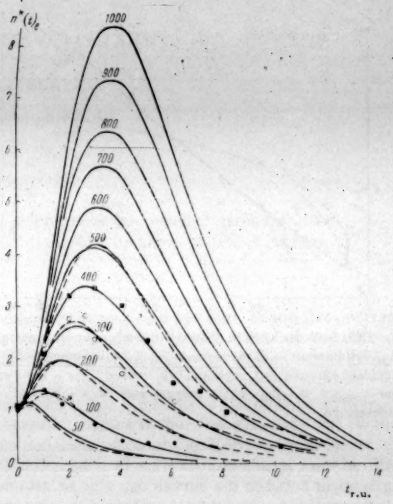

FIG. 5. Approximation of the cascade curves in lead (showers initiated by electrons). Solid curves – function $n^*(t)_e$, calculated according to formula (6). The numbers at the curves indicate the energy of the primary electron E_0 in Mev. Dashed curves were calculated by Wilson. ●, ○, ■ – data of the present work (errors not shown).

be approximated by the very simple functions

$$n^*(t)_e = (1 + 1.08\,\alpha t^{0.6\alpha})\, e^{-0.\alpha t}, \quad (6)$$

$$n^*(t)_\gamma = 1.08\,\alpha t^{0.\alpha}\, e^{-0.\alpha t} \quad (7)$$

(see Fig. 5), where $\alpha = 1 \ln (E_0/25)$, E_0 is the energy of the primary particle in Mev; and t is measured in radiation units. The index e or γ indicates the nature of the particle initiating the shower. Equations (6) and (7) enable us to find the dependence of the position of shower maximum on the energy of the primary particle in an analytic form:

$$t_{\max}(E_0)_\gamma = \alpha. \quad (8)$$

$$n^*_{\max}(E_0)_\gamma = 3(\alpha/e)^{0.6\alpha+1} \approx 0.008\,E_0. \quad (9)$$

The functions $t_{\max}(E_0)_e$ and $n_{\max}(E_0)_e$ are similar to Eqs. (8) and (7) (see Fig. 6), but are more complicated.

One advantage of Eqs. (6) to (9) given above is that they contain only one parameter α which depends on the energy of the primary particle. Formulae (6) to (9) may be used for calculating total absorption spectrometers, and also in other problems, where it is not necessary to know exactly the

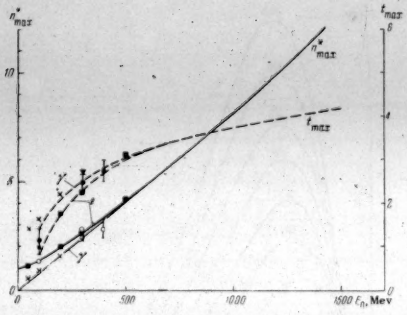

FIG. 6. Maxima of the showers in lead for various energies E_0. Solid curves – dependence of n^*_{max} on the energy of the incident electron (e) or photon (γ). Dashed lines – the same for t_{max}. ●, ○ – data of the present work; ■, × – data of reference 5.

tails of the cascade curves ($t > 10$ r.u.). The agreement between the curves can also be attained in the region $t > 10$ r.u., if we introduce a term $\exp(-0.24\,t)$ into the approximating functions, describing the tail of the cascade curves for large thicknesses.[5] The approximating functions then become complicated. It is at present difficult to establish the degree of applicability of the relations (6) to (9) for higher energies than those used in the present work. The results of experiments carried out so far with cosmic rays[10] cannot be used for such a purpose, since the energy of the particles initiating the showers is not sufficiently well known.

[1] D. B. Skobel'tsyn, Z. Physik **54**, 686 (1929); B. Rossi, Physik. Z. **33**, 304 (1932).

[2] B. Rossi and K. Greisen, Revs. Modern Phys. **13**, 240 (1941).

[3] S. Z. Belen'kiĭ, J. Exptl. Theoret. Phys. (U.S.S.R.) **19**, 940 (1949). I. P. Ivanenko, J. Exptl. Theoret. Phys. (U.S.S.R.) **32**, 491 (1957), Soviet Phys. JETP **5**, 413 (1957).

[4] C. E. Swartz, Nucleonics **14**, 4, 44 (1956); Cassels, Fidecaro, Wetherell, and Wormald, Proc. Phys. Soc. **A70**, 405 (1957).

[5] R. R. Wilson, Phys. Rev. **86**, 261 (1952).

[6] V. V. Vishnyakov and A. A. Tyapkin, Атомная энергия (Atomic Energy) **3**, 10, 298 (1957).

[7] J. J. Thomson, Phil. Mag. Ser. **6**, 13, 561 (1907); J. Loeb, Compt. rend. **222**, 488 (1957).

[8] S. Z. Belen'kiĭ, Лавинные процессы в космических лучах (Cascade Processes in Cosmic Rays) 1948.

[9] De-Wire, Ashkin, and Beach, Phys. Rev. **83**, 505 (1951); Davis, Bethe, and Maximon, Phys. Rev. **93**, 788 (1954).

[10] C. Y. Chao, Phys. Rev. **75**, 581 (1949); Butler, Rosser, and Barker, Proc. Phys. Soc. **A362**, 63, 145 (1950). Wang Kang-ch'ang, Ch'en Cheng-ch'ih and Li Ming, Chinese J. Phys. **11**, 421 (1955) (in Chinese).

Translated by H. Kasha
2

CLOUD CHAMBER INVESTIGATIONS IN THE CORES OF EXTENSIVE AIR SHOWERS

O. I. DOVZHENKO, S. I. NIKOL'SKII, and I. V. RAKOBOL'SKAYA

P. N. Lebedev Physics Institute, Academy of Sciences, U.S.S.R.

Submitted to JETP editor June 14, 1958

J. Exptl. Theoret. Phys. (U.S.S.R.) **36**, 17-23 (January, 1959)

The results of an experimental investigation of the structure of the cores of extensive air showers are presented. Photographs of the cores of extensive air showers traversing the chamber are shown.

INTRODUCTION

THE study of extensive air showers (EAS) has become of increasing interest in recent years. This is due to the fact that the investigation of the composition and energy distribution of the shower particles, and also of the Cerenkov light pulses associated with the EAS, makes it possible, in principle, to study the interaction of ultra-high-energy particles ($> 10^{13}$ ev). From this point of view, it is especially important to study the central region of the shower — its core. However, the core is the least known region, and at present it is even impossible to indicate its dimensions. The core structure might be understood through a detailed study of the energy fluxes and the energy spectra of particles contained in the central region of the EAS. In that respect, the study of the air-shower cores by means of a large number of ionization chambers yields rich quantitative material. More visual although less statistically founded data on the structure of shower cores can be obtained with cloud chambers. This method was used in the present experiment.

The measurements were carried out at sea level in Moscow in 1957.

1. MEASUREMENT PROCEDURE

For an effective observation of the cores of EAS, we used a rectangular cloud chamber with a special triggering system. This system selected only those showers in which the particle density, recorded by means of counters placed above the cloud chamber, was larger than the density of shower particles recorded by groups of counters placed further away. The position of the master group of counters can be seen in the general diagram of the array (see Fig. 1).

Groups 1 to 4 contain 12 counters each, and groups 5 and 6 contain 18 counters. The area of each counter was $\sigma = 100$ cm^2 in the first series of measurements, and $\sigma = 330$ cm^2 in the second series. The amplitude of the pulse in each group was proportional to the total number of discharged counters in it. If we denote the number of discharged counters in the i-th group by m_i, then the condition of recording EAS can be given by the formula

$$\sum_{i=5}^{6} m_i - \sum_{i=1}^{4} m_i \geqslant \xi, \quad m_5 \geqslant 2, \quad m_6 \geqslant 2.$$

The minimum value of ξ was 6 and 9 for the experiments with master counters 100 cm^2 and 330 cm^2 in area, respectively. Local showers produced in the cover above the array were practically excluded by the requirement of discharges in not less than 2 counters of each of the groups 5 and 6.

For the determination of the total number of particles in the recorded showers, we used a hodoscopic array consisting of 6 groups of counters with an area $\sigma = 100$ cm^2 each. Each group contained 24 counters (group 7 — 12 in Fig. 1). The resolving time of the master system amounted to about 10 μ sec.

The cloud chamber used[1] measured 60×60×30 cm. Six lead plates with a total thickness amounting to approximately 120 g/cm^2 were placed in the chambers. The plates were 1, 2, 2.5, 2, 2.5, and 1.5 cm Pb thick respectively. The cloud chamber was placed directly under the master counter groups 5 and 6 (dashed line in Fig. 1). A block diagram of the array is shown in Fig. 2.

For the experimental conditions described above, we calculated the differential spectrum of the showers with respect to the number of particles, the probability of recording the shower cores as a function of the distance from the center of the array, the number of EAS recorded by the given array per unit time, etc. In the calculations it was assumed that:

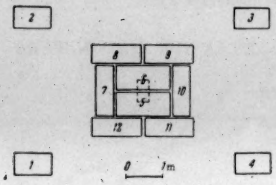

FIG. 1. General diagram of the array.

TABLE I

r(m)	n
0–1	0
1–12	1
12–50	1.5
50–200	2.0
200–500	2.5

(1) EAS possess circular symmetry, and their lateral distribution is independent of the number of particles in the shower and is given by the expression

$$p(r) = A_n N / r^n, \qquad (1)$$

where N is the number of particles in a shower, the exponent n depends on the distance as in Table I, and $A_n = 1.5 \times 10^{-3}$ for the distance range $1 < r < 12$ m from the axis. The value $n = 0$ for $r < 1$ m, although not corresponding to experimental results,[2] is caused by the fact that the linear dimensions of each of the master counter groups are larger than 1 m (cf. Fig. 1).

(2) The differential spectrum of showers with respect to the number of particles is of the shape $f(N)\,dN \sim N^{-(\gamma+1)}\,dN$, where N is the number of particles in the shower at the observation level, and the dependence of γ on N is that given in reference 3.

(3) The number of axes of EAS with $N > 10^5$ particles, arriving hourly per m^2 at sea level, is $7 \times 10^{-3}\ m^{-2}\ hour^{-1}$, which corresponds to the data of reference 3.

(4) The distribution of the recording probability of the EAS particles is described by the Poisson law.

The calculated differential size spectra of showers recorded by the given selecting system for $\xi \geq 9$, $\sigma = 330\ cm^2$ (curves 1 and 2) and $\xi \geq 6$, $\sigma = 100\ cm^2$ (curves 3 and 4) are shown in Fig. 3. Curves 1 and 3 correspond to showers, the axes of which pass not further than 2 m from the array center, and the curves 2 and 4 correspond to all showers recorded by the array independently of the position of the axes. It can be seen from Fig. 3 that the areas under the curves 1 and 3 are not much different from the corresponding areas under the curves 2 and 4, indicating a sharp concentration of the cores of recorded showers near the cloud chamber.

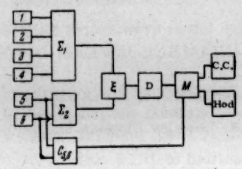

FIG. 2. Block diagram of the array. Σ_1, Σ_2 – circuit producing a pulse proportional to the number of discharged counters in the trays 1 to 4 and 5, 6, respectively; $C_{5,6}$ – double coincidence circuit of the trays 5 and 6; ξ – voltage comparator of circuit for the total pulses from trays 1 to 4 and 5, 6; D – discriminator; M – master pulse shaping; Hod – hodoscope circuit; C.C. – cloud chamber control; 1 to 6 – master counter trays.

A comparison between the experimental and theoretical numbers of recorded EAS and of the mean density of the charged particle flux recorded by the array for $\xi \geq 6$ and $\sigma = 100\ cm^2$ is given in Table II.

It can be seen from Table II that the results of the calculations are in good agreement with the experiment. This confirms the correctness of the assumptions underlying the calculations.

An advantage of the foregoing triggering system over the often-used triggering by counters connected in coincidence lies in a much greater efficiency of

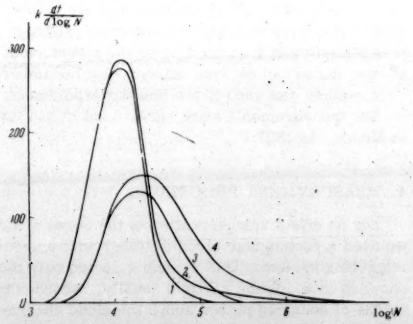

FIG. 3. Calculated differential size spectrum of the showers. The ordinate axis represents kdf/d log N, where k is a proportionality factor. The x axis represents the logarithm of the number of particles in the showers. The normalization is such that the areas under the corresponding curves correspond to the detection efficiency of the cores of the EAS. Curves 1 and 2 – $\xi \geq 9$, $\sigma = 330\ cm^2$, curves 3, 4 – $\xi \geq 6$, $\sigma = 100\ cm^2$.

TABLE II

	Experiment	Calculation
Number of particles recorded per hour	2.7 ± 0.2	1 – 2*
Mean value of the density of particles detected by the array	12 ± 1	10 – 13

*Best agreement with the experiment is obtained if we assume $A_n \sim 2 \times 10^{-3}$ in Eq. (1).

recording of the axes of EAS. In the given case this is important because of the large dead time of the cloud chamber which sharply diminished the time of measurements and makes it easier to select interesting cases in the reduction of data.

2. EXPERIMENTAL RESULTS

During the operation of the described array we recorded 1800 showers with $\xi \geq 6$, $\sigma = 100$ cm^2 and 100 showers with $\xi \geq 9$, $\sigma = 330$ cm^2.

A comparison between the experimentally observed and theoretically calculated numbers of the cores of the electron-photon component of EAS passing through the cloud chambers are given in Table III. It can be seen from this table that the experimentally observed and the expected number of cases where the core of the electron-photon component of EAS traversed the cloud chamber are in a good agreement, at least for showers with $N < 3.5 \times 10^4$. If we assume that the energy E_0 of the primary particle initiating the extensive shower

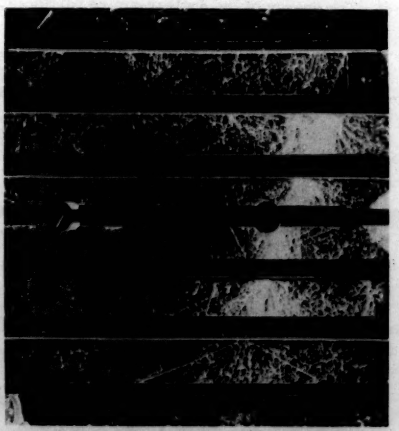

FIG. 5. Nuclear interactions in the lead of the chamber in the 5th and in the 6th plate. The energy of the nuclear-active particle initiating the interaction $\geq 10^{11}$ ev. The number of particles in the EAS is $N = 3.3 \times 10^4$.

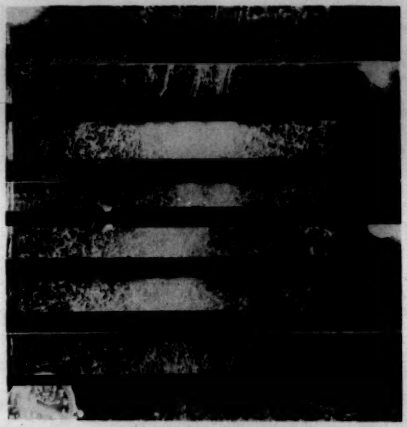

FIG. 4. A photograph of the electron-photon core of an EAS traversing the cloud chamber. The total number of particles in the shower is $N \approx 10^4$ ev.

is proportional to the number of particles in the showers, and that at sea-level $E_0 \approx 1.5 \times 10^{10} N$ ev, then such an energy of the primary particle corresponds to an energy at which, according to the data of reference 5, the structure of the cores of EAS might undergo a change. A photograph of an event in which the electron-photon core of an extensive air shower has traversed the cloud chamber is shown in Fig. 4. This corresponds to a case where a large number of high-energy ($> 10^9$ ev) electrons traverse the chamber simultaneously. It follows from the analysis of the events in which the cores of the electron-photon component traverse the cloud chamber that the high energy electrons are concentrated in a region whose linear dimensions are on the order of 20 or 30 cm, which can be seen in Fig. 4.

If we assume that one nuclear-active particle of $\gtrsim 10^{11}$ ev is present in the core region then, during the time of operation of the array, one should observe in the cloud chamber about five nuclear interactions for showers with a number of particles $N < 3.5 \times 10^4$ and one to two nuclear interactions for showers with $N > 3.5 \times 10^4$. During the total time of operation of the chamber, we observed four nuclear-active particles with energy $\gtrsim 10^{11}$ ev, associated with showers with $N \gtrsim 3.5 \times 10^4$ (cf. Table III).

A characteristic feature of these interactions is the absence of high-energy electrons in their immediate vicinity. This indicates that the nuclear-

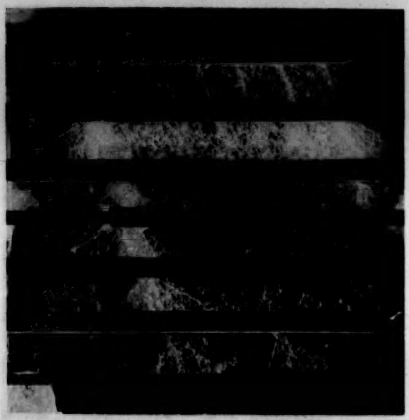

FIG. 6. Nuclear interaction produced by a charged particle in the first plate. The energy of the nuclear particle $\geq 3 \times 10^{11}$ ev. The number of particles in the extensive shower is $N = 2.5 \times 10^4$.

active particle can be present at a certain distance from the core of EAS determined from the electron-photon component.

We shall consider each of these interactions separately.

No. 1 (Fig. 5). Not less than seven particles were produced as a result of a nuclear interaction which took place in the cover of the cloud chamber. Three of these particles underwent nuclear interactions in traversing the lead plates (these interactions could be identified by means of heavy ionizing particles). The energy of the interacting particles can be estimated only for the nuclear-active particles that have undergone nuclear interactions in the top of the chamber and in the sixth plate. If we estimate the energy of nuclear-active particles from the number of secondary penetrating particles and from their angular distribution,[6] we obtain for the energy of the interaction in the chamber lid a value $E \geq 10^{10}$ ev. Since, however, the energy of the nuclear-active particle initiating a shower in the sixth plate is $E \sim 5 \times 10^{10}$ ev, we must ascribe an energy of $\sim 10^{11}$ ev to the primary particle. The total number of particles in the EAS is $N \sim 3.3 \times 10^4$.

No. 2 (Fig. 6). A nuclear interaction produced by a charged particle occurred in the first plate. As a result, about 15 particles were produced. The majority of these particles lie within a cone with an opening angle not larger than 5°. This corresponds to $\gamma_c \gtrsim 10$, i.e., to an energy of the incident nucleon $E \gtrsim 2 \times 10^{11}$ ev. At least four secondary nuclear-active particles undergo nuclear interactions in traversing the lead plate. It is difficult, however, to estimate their energy because of the large number of secondary electrons.

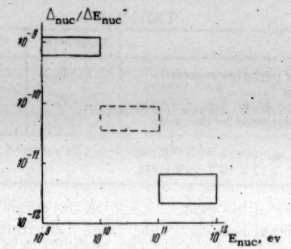

FIG. 7. Differential energy spectrum of the observed nuclear-active particles. The y axis represents the number of nuclear-active particles in the given energy range, and the x axis the energy of nuclear-active particles in electron-volts. The dashed figure indicates the expected number of nuclear-active particles in the energy range 10^{10} to 10^{11} ev.

This interaction is accompanied by a large number of high-energy electrons in spite of a relatively small number of particles in the extensive shower ($N \sim 2.5 \times 10^4$).

No. 3. A nuclear interaction produced by a charged particle in the third plate. The majority of secondary particles are concentrated in a very narrow cone with an opening angle not larger than 5°. The energy of the nuclear-active particle can

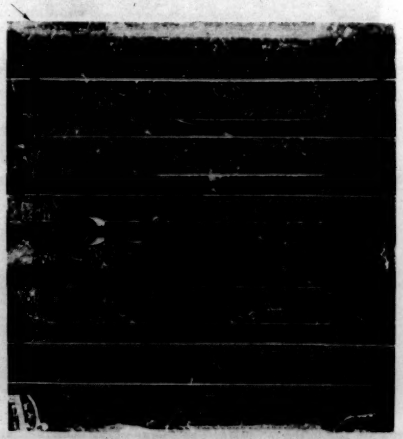

FIG. 8. Nuclear interaction produced by a nuclear-active particle with energy $< 10^{10}$ ev.

be estimated from the maximum of shower development. This occurs at the depth of ~ 10 t-units. If we assume that, in the given interaction, all the energy has been carried away by one π^0 meson, then the energy of the nuclear-active particle is $E \approx 1.5 \times 10^{11}$ ev. This is the lower limit of the energy. If we assume that, in lead, on the average $\sim 20\%$ of the energy of the incident nucleon is carried away by π mesons at interaction energies of 10^{11} to 10^{12} ev, then the energy of the nuclear-active particle initiating the given shower is $\sim (8 \text{ to } 10) \times 10^{11}$ ev.

It should be noted that the total number of particles in this EAS is very small ($N \lesssim 10^4$).

No. 4. An intensive electron-nuclear shower, the energy of which can be estimated only very roughly ($\gtrsim 10^{11}$ ev) because of the large number of high-energy electrons accompanying the nuclear-active particle, can be observed in one of the lower lead plates of the cloud chamber.

3. DISCUSSION OF RESULTS

As has been said above, the theoretically expected number of events in which the cores of EAS with $N < 3.5 \times 10^4$ traversed the cloud chamber, coincides with that observed experimentally. This indicates not only the correctness of the assumption underlying the calculations, but makes it possible to estimate the number of nuclear-active particles of high energy in the core of the shower. The expected and observed numbers of nuclear-interactions produced by these particles in the lead plates of the cloud chamber is given in Table III. These numbers are practically identical for showers with a number of particles $N < 3.5 \times 10^4$. Since it was assumed in the calculation of the expected number of nuclear interactions that only one particle in a given energy range is present in each shower, the agreement between the calculation and the experiment confirms this assumption for showers with $N < 3.5 \times 10^4$. A question arises as to whether the selection of the four cases among the remaining nuclear interaction events was objective. Twelve nuclear interactions were observed during the operation of the cloud chamber.* In eight cases (apart from those described above the energy was estimated by the method given in reference 6. The estimate showed that all the nuclear-active particles have a relatively low energy ($< 10^{10}$ ev).

*One can determine the mean value of the fraction of nuclear-active particles in a shower by using the mean value of the charged particle flux density in the detected showers. This fraction was found to be equal to $(1 \pm 0.3)\%$, which is in agreement with the data of reference 7.

TABLE III

	$N < 3.5 \cdot 10^4$		$N > 3.5 \cdot 10^4$	
	Calculation	Experiment	Calculation	Experiment
Number of cores of the electron-photon component	~ 10	9	~ 3	2
Number of nuclear-active particles with energy 10^{11} ev	~ 5	4	1–2	0

The differential energy spectrum of nuclear-active particles observed in the cloud chamber is given in Fig. 7. It is characteristic that in the energy range of nuclear-active particles, 10^{10} to 10^{11} ev, no nuclear interactions were observed. The probability of such an event is less than 0.05. This feature of the energy spectrum can be explained by errors in the estimate of the energy of nuclear-active particles. A photograph of a nuclear interaction produced by a nuclear-active particle with energy $< 10^{10}$ ev is shown in Fig. 8. A comparison of the particle under consideration and of other nuclear-active particles in the core of EAS. The question arises here as to the role of such a particle in the development of a shower in the depth of the atmosphere. A comparison of the energy of the particles observed by us ($\bar{E} = 2 \times 10^{11}$ ev) with the mean energy carried by the electron-photon component in the same showers ($\sim 2.5 \times 10^{12}$ ev), shows that the energy of one particle is not sufficient in order to change substantially the absorption of the shower and, consequently, a larger part of the secondary electron-photon component is produced in interactions of particles of lower energies. The energy of the particle is, however, fully sufficient for re-initiating the high-energy electron-photon component in the shower core. In fact, it follows from the analysis of the detected cores of EAS that the energy of the nuclear-active particle singled out is of the same order of magnitude as the energy of the electron-photon component in the core of the EAS. It should be noted that the position of the singled-out particle can be somewhat different from the position of the electron-photon component of high-energy and from the axis of the EAS, because of the transverse momenta (μc) gained by secondary particles in the nuclear interactions. Such a core region diffused up to a distance of ~ 1 m, was observed in our experiments, as well as in earlier investigations.[2]

We shall compare the mean energy of the detected singled-out particles with the energy of the primary particle initiating the EAS. The energy of the primary particle can be found from the total number of shower particles at the observation

level.[4] For showers with a number of particles 2×10^4, this amounts to $E_0 = 3 \times 10^{14}$ ev. The mean energy of the four nuclear-active particles detected in the cloud chamber amounts to $\sim 2 \times 10^{11}$ ev. If we assumed that the mean free path for nuclear interactions in air is 70 g/cm^2, and that we can neglect the fluctuations in the development of EAS, then the energy fraction conserved by these singled-out particles in each nuclear interaction development amounts, on the average, to ~ 0.6. We have already indicated in the introduction that more accurate quantitative results can be obtained using ionization chambers. It can be concluded from the photographs of cores traversing a cloud chamber that, in the central regions of EAS, high energy nuclear-active particles propagate in close vicinity of each other. In consequence, it is possible and worthwhile to use ionization chambers of sufficiently large dimensions for the study of the energy characteristics of the core of EAS.

In conculusion, the authors consider it their pleasant duty to express their gratitude to Prof. N. A. Dobrotin and G. T. Zatsepin for their interest in the work; to N. G. Birger and D. S. Chernyavskii for the discussion of the results, as well as to O. A. Kozhevnikov, A. M. Mozhaev, B. V. Subotin, and E. N. Tarasov for their help in carrying out the measurements.

[1] E. A. Ivanovskaya and A. G. Novikov, J. Tech. Phys. (U.S.S.R.) **26**, 209 (1956), Soviet Phys. JTP **1**, 206 (1956).

[2] O. I. Dovzhenko and S. I. Nikol'skii, Dokl. Akad. Nauk SSSR **102**, 241 (1955).

[3] R. J. Norman, Proc. Phys. Soc. **A69**, 443A, 804 (1956).

[4] K. Greisen, Progress in Cosmic Ray Physics III, Amsterdam (1956).

[5] Nikol'skiĭ, Vavilov, and Batov, Dokl. Akad. Nauk SSSR **111**, 71 (1956), Soviet Phys. "Doklady" **1**, 625 (1956).

[6] I. A. Ivanovskaya and D. S. Chernavsky, Nucl. Phys. **4**, 29 (1956).

[7] Abrosimov, Zatsepin, Solov'eva, Khristiansen, and Chikin, Izv. Akad. Nauk SSSR, Ser. Fiz. **19**, 677 (1956) [Columbia Tech. Transl. **19**, 616 (1956)].

Translated by H. Kasha
3

BETA-GAMMA ANGULAR CORRELATION IN Ba^{139} DECAY AND THE RELATIVE SIGN OF THE BETA-INTERACTION COUPLING CONSTANTS

N. A. VLASOV and V. P. RUDAKOV

Submitted to JETP editor July 11, 1958

J. Exptl. Theoret. Phys. (U.S.S.R.) **36**, 24-27 (January, 1959)

The differential β-γ angular correlation was measured for the cascade $E_\beta = 2.23$ Mev and $E_\gamma = 0.163$ Mev in the decay of Ba^{139}. The anisotropy coefficient was found to be $a = +0.058 \pm 0.023$ for β particles with total energy $4mc^2$. This result is compared with calculations based on the independent-particle model. The theoretical result is in agreement with experiment only if the ratio g_V/g_A is negative.

THE existing data on the ratio of the Fermi and Gamow-Teller β-interaction coupling constants come from an analysis of ft values in allowed transitions.[1] Such an analysis, however, gives only the absolute value of the ratio. The relative sign of the coupling constants can be determined from the shape of the β spectrum in forbidden transitions only. Thus a calculation of ratios of matrix elements for the β transitions becomes a necessary involvement. Morita, Fujita, and Yamada[2] analyzed, in calculations based on the independent particle model, the shape of the forbidden β spectra of Fe^{59}, Rb^{87}, Te^{99}, and Cs^{137}. They have shown that it agrees only with a negative g_S/g_T ratio. This conclusion was confirmed in a later work by Fujita[3] in which the same spectra were analyzed with the strong-coupling Bohr-Mottelson model. Lee-Whiting[4] deduced the opposite result ($g_S/g_T > 0$) from a study of the shape of the β spectrum of RaE. However, Takebe, Nakamura, and Taketani[5] have shown that it is impossible to determine the sign of g_S/g_T from an analysis of the spectrum shape of RaE.

All these attempts at a determination of the relative sign of the coupling constants were based on the assumption that only the scalar and tensor covariants contribute to the β interaction. It has recently become apparent that the main covariants are the vector and axial vector.[6] Clearly the problem of the relative sign requires further study.

The relative sign may be determined from data on β-γ angular correlation. Dolginov[7] has shown that the anisotropy coefficient a in the expression for β-γ angular correlation $W(\theta) = 1 + a\cos^2\theta$ may be expressed as an explicit function of the coupling-constant ratios (g_S/g_T or g_V/g_A) and certain ratios of β-transition matrix elements. For example, for $\Delta J = 1$ first-forbidden β transitions the expression for the coefficient a contains only three ratios x, y, and z of matrix elements:[7]

$$x = \int \psi^*_{l_1 s_1} r\,(\sigma Y^0_{1\Lambda})\,\psi_{l_2 s_2}\,d\mathbf{r} \Big/ \int \psi^*_{l_1 s_1} r Y_{1\Lambda} \psi_{l_2 s_2}\,d\mathbf{r};$$

$$y = -i \int \psi^*_{l_1 s_1}\,(\alpha Y^{-1}_{1\Lambda})\,\psi_{l_2 s_2}\,d\mathbf{r} \Big/ \int \psi^*_{l_1 s_1} r Y_{1\Lambda} \psi_{l_2 s_2}\,d\mathbf{r};$$

$$z = C^{l_1 l_2}_{1\Lambda l_2 s_2} \int \psi^*_{l_1 s_1} r\,(\sigma Y^{-1}_{1\Lambda})\,\psi_{l_2 s_2}\,d\mathbf{r} \Big/ C^{l_1 s_1}_{2\Lambda l_2 s_2} \int \psi^*_{l_1 s_1} r Y_{1\Lambda} \psi_{l_2 s_2}\,d\mathbf{r}.$$

To calculate x and z it is sufficient to assume that the nuclear levels involved in the β transition are described by the independent-particle model. Furthermore, only the angular momentum l of the odd nucleon in the nucleus is needed in the calculation of x and z. The computation of the third ratio y requires more detailed assumptions about the structure of the nucleus. However, as will be shown below, the uncertainties in y do not preclude the possibility of determining the relative sign of the ratio of coupling constants. Dolginov[7] listed the β decays of In^{117}, Ba^{139}, Ce^{141}, and possibly Hg^{203} and Tl^{208} as being of interest in this connection. We measured the differential β-γ angular correlation in the decay of Ba^{139}. An analysis of the results based on formulas given by Dolginov shows that the ratio g_V/g_A is negative.

The β-γ angular correlation was studied for the cascade:[8]

$$(^7/_2^-) \xrightarrow{\beta} (^5/_2^+) \xrightarrow{\gamma} (^7/_2^+).$$

The end point energy of the β-spectrum is 2.23 Mev, the energy of the γ-rays is 0.163 Mev.

According to the shell model[9] Ba^{139} has one $f_{7/2}$ neutron outside a closed shell of 82 neutrons which β-decays into a $d_{5/2}$ proton of La^{139}. The transition from the $d_{5/2}$ level to the $g_{7/2}$ ground state of La^{139} proceeds via magnetic dipole radia-

tion with a small admixture (4%) of electric quadrupole.[10] The structure of the Ba^{139} nucleus, namely (82 + 1) neutrons and an even (56) number of protons, raises the hope that a description of the ground state of this nucleus in terms of the independent particle model is justified. Existing data on Coulomb excitation of the 163-kev level of La^{139},[11] on the lifetime of this state,[12] on the multipole order of the γ transition,[10] and on the ft value of the β transition indicate that the 163-kev level of La^{139} also has a single-particle character.

Ba^{139} was obtained in the cyclotron from the $Ba^{138}(d,p)$ reaction and was chemically rid of the other active elements produced simultaneously. Practically no unwanted radiation was present in the purified samples. The measuring apparatus used was the standard type for this kind of experiment; a schematic diagram is given in Fig. 1. The

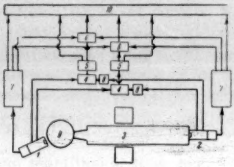

FIG. 1. Schematic diagram of experimental setup. 1,2) photomultipliers, 3) magnetic lens spectrometer, 4) fast-coincidence circuits, 5) amplifiers, 6) slow-coincidence circuits, 7) pulse-height analyzers, 8) variable-delay lines, 9) sample under study, 10) scaler circuit and electromechanical counters.

electrons were analyzed with a lens spectrometer of 5% resolution and detected by a photomultiplier with a plastic scintillator. A similar detector was used for the γ rays. The two counters were arranged in a fast-slow coincidence circuit. The resolving time of the coincidence scheme was 2.5×10^{-9} sec for 100% efficiency in the chosen range of incident pulse height. The counts of the β and γ counters and accidental coincidences were registered simultaneously with true coincidences. The measurements were performed for two positions of the γ-counter: at 180° and at 90° with respect to the direction of emission of the β particle.

The correlation measurements for Ba^{139} were performed for electrons with total energy $4mc^2$. Since the half-life of Ba^{139} is only 85 minutes, the measurements were performed in 30 series, each of 2 or 3 hours duration. The results of all series are consistent within statistical error. The anisotropy coefficient, averaged over all 30 series, is

$$a = \{N(\pi) - N(\pi/2)\} / N(\pi/2) = 0.058 \pm 0.023.$$

The indicated error is statistical. Results of control experiments with Sc^{46} and Sb^{124} indicate the absence of any systematic errors. In the case of Sc^{46} the angular distribution of the 0.89 and 1.12-Mev γ rays is isotropic with respect to the β electron ($E_\beta = 0.36$ Mev). As result of our measurement we found $a = 0.005 \pm 0.020$. In the case of Sb^{124} the differential angular correlation for the cascade $E_{\beta\,end} = 2.317$ Mev, $E_\gamma = 0.603$ Mev was measured for two values of β-particle energy, $3mc^2$ and $4mc^2$. The values of a were -0.12 ± 0.03 and -0.34 ± 0.03, in agreement with previous measurements.[13]

The calculation of the anisotropy coefficient a was performed for a mixture of vector and axial vector as well as scalar and tensor covariants. It was assumed that

$$g_S = -g_S';\ g_T = -g_T';\ g_V = g_V';\quad g_A = g_A',$$

where the primed constants refer to parity nonconservation. The calculation was performed for a mixture of magnetic dipole (96%) and electric quadrupole (4%) radiations.

The result of the calculation gives a as a function of the coupling-constant ratios g_S/g_T or g_V/g_A and the ratio y of matrix elements. For the other two ratios of matrix elements numerical values x = 0.7 and z = 0.9 were obtained.

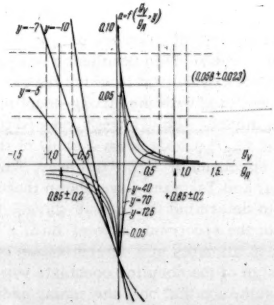

FIG. 2. Dependence of the anisotropy coefficient on the ratio of the vector and axial vector interaction coupling constants.

In Fig. 2 the dependence of the coefficient a is given as a function of g_V/g_A for various values of the parameter y. The horizontal lines give the experimentally determined limits for a and the vertical lines give the known limits on $|g_V/g_A|$.[1] Falling within the allowed region, for $g_V/g_A < 0$, is the curve for $y = -5$. For positive g_V/g_A there exists no value of y in agreement with

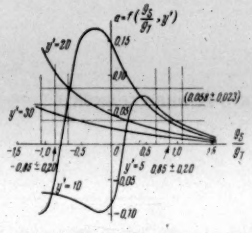

FIG. 3. Dependence of the anisotropy coefficient on the ratio of the scalar and tensor interaction coupling constants.

a = 0.058. This means that the ratio g_V/g_A is negative. It should be noted that varying x and z between 0.1 and 5 does not lead to values of a in agreement with experiment for positive g_V/g_A.

In Fig. 3 the analogous curves are given for a mixture of scalar and tensor covariants. In this case there exist curves in agreement with a positive or negative ratio g_S/g_T and no conclusions are possible.

The authors are grateful to A. Z. Dolginov for his kindness in communicating the results of his calculations and discussing the results, to S. P. Kalinin for constant interest in this work and collaboration in its completion, and also to L. A. Sliv and I. S. Shapiro for discussion of results.

[1] J. B. Gerhart, Phys. Rev. **95**, 288 (1954).

[2] Morita, Fujita, and Yamada, Progr. Theoret. Phys. (Japan) **10**, 630 (1953).

[3] J. Fujita, Progr. Theoret. Phys. (Japan) **13**, 260 (1955).

[4] G. E. Lee-Whiting, Phys. Rev. **97**, 463 (1955).

[5] Takebe, Nakamura, and Taketani, Progr. Theoret. Phys. (Japan) **14**, 317 (1955).

[6] R. P. Feynman and M. Gell-Mann, Phys. Rev. **109**, 193 (1958).

[7] A. Z. Dolginov and I. N. Toptygin, Izv. Akad. Nauk SSSR, Ser. Fiz. **20**, 1377 (1956) [Columbia Tech. Transl. **20**, 1260 (1956)]. A. Z. Dolginov, Nucl. Phys. **5**, 512 (1958). A. Z. Dolginov and N. P. Popov, Nucl. Phys. **7**, 591 (1958).

[8] A. Mitchell and E. Hebb, Phys. Rev. **95**, 727 (1954).

[9] P. F. A. Klinkenberg, Revs. Modern Phys. **24**, 63 (1952).

[10] Ambler, Hudson, and Temmer, Phys. Rev. **101**, 196 (1956).

[11] N. P. Heydenburg and G. M. Temmer, Phys. Rev. **100**, 150 (1955).

[12] T. R. Gerholm and H. DeWaard, Physica **21**, 601 (1955).

[13] D. T. Stevenson and M. Deutsch, Phys. Rev. **83**, 1202 (1951).

Translated by A. M. Bincer
4

Gd^{146} AND Eu^{146} CONVERSION-ELECTRON SPECTRA

N. M. ANTON'EVA, A. A. BASHILOV, B. S. DZHELEPOV, and B. K. PREOBRAZHENSKII

Leningrad State University

Submitted to JETP editor July 12, 1958

J. Exptl. Theoret. Phys. (U.S.S.R.) **36**, 28-31 (January, 1959)

The conversion electron spectra of the neutron-deficient isotopes Gd^{146} and Eu^{146} were investigated. The conversion electrons observed correspond to three nuclear transitions with energies of 114.8, 115.5, and 155 kev in the case of Gd^{146} and to two transitions with energies of 630 and 742 kev in the case of Eu^{146}. Decay schemes are proposed.

WHILE investigating[1] the conversion electron spectra of neutron-deficient isotopes of Gd formed in the fission of Ta nuclei by fast protons (660 Mev), we observed an activity with a half-life of 45 days.[2] First the usual chemical methods and then chromatography were employed to isolate the gadolinium fraction. The active material was then collected on a thin aluminum foil.

The Leningrad State University's "Ketron" magnetic spectrometer, with a resolving power of 0.5%, was used to investigate the conversion-electron spectrum of the gladolinium fraction. However, in the low-energy region the lines had a greater relative width because of the scattering and stopping of electrons in the material of the radioactive preparation. A film over the counter window admitted electrons with energies over 7 kev.

Figure 1 shows the portion of the conversion electron spectrum that contains lines due to γ rays from the 45-day gadolinium, with E_γ = 114.8, 115.5, and 155 kev. Figure 2 shows a decay curve constructed from the decaying heights of the K-114.8 and L-155 peaks.

The identification of the 45-day activity was attempted by Murin et al.[3] In their report they advanced several arguments in favor of the theory that this activity is due to Gd^{146}. However, their identification cannot be considered as proved.

Our study of the 114.8- and 115.5-kev γ transitions, in which we used a magnetic spectrometer (Ketron), were impaired by the nearness of the transition energies and because the L-114.8 and L-115.5 conversion lines were not separated from the K-155 conversion line. Therefore, V. M. Lobashev and one of the authors of this paper (Bashilov) used a magnetic spectrograph of high resolv-

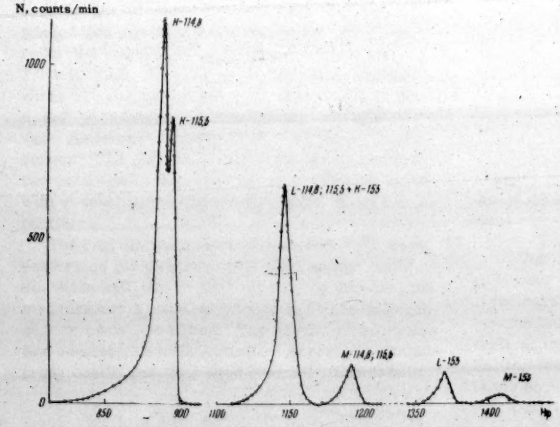

FIG. 1. The conversion electron spectra of Gd^{146}.

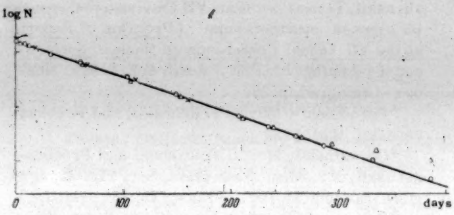

FIG. 2. Decay curve for Gd^{146}. o – 114.8; Δ – 114.8 + 115.5 + K-155; × – L-155.

ing power, available in our laboratory, for further study of the conversion electron spectrum of Gd^{146}. It has been in this way determined that the K-114.8 and K-115.5 lines possess approximately the same intensity and that for both transitions the K : L ratio is great (~ 7). Moreover, only L_1 lines were observed; no L_2 or L_3 lines appeared on the photographic plate. It is suggested that the most natural explanation of these facts is that the 114.8 and 115.5 kev γ transitions are of the M1 type and that their total intensities are approximately equal.

Murin and his co-workers[4] proved that these transitions occur in cascade.

Two factors complicated the investigation of the 155 kev transition. In the first place, as was mentioned, the K-155 conversion line was not separated in the spectrometric measurements from the L-114.8 and L-115.5 lines. Secondly, additional conversion electrons were present in our spectrum from a transition with the same energy (155 kev) but due to Gd^{151}.

A β spectrograph with a photographic plate was used to give a rough evaluation of the K : L ratio of the 155-kev γ transition immediately after the preparation of the compound, when the K-155 line of Gd^{146} was considerably more intense than the K-155 line of Gd^{151}. The ratio proved to be ~ 7.

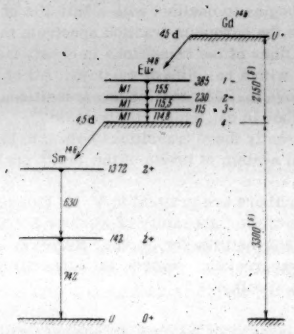

FIG. 3. $Gd^{146} \rightarrow Eu^{146} \rightarrow Sm^{146}$ decay scheme.

This indicates that the 155-kev γ transition of Gd^{146} is most likely of the M1 type.

Coincidence measurements[5] indicate that the 155-kev γ transition occurs in a cascade with at least one of the ~ 115-kev transitions. Since the 114.8- and 115.5-kev γ transitions have equal intensities, and since there are no intense lines with $E_\gamma \sim 40$ kev, it directly follows that all three transitions occur in a cascade. Moreover, the intensity of the 155-kev γ transition, based on a theoretical value for the internal conversion coefficient β_1, is also very close to the intensity of the 114.8- and 115.5-kev γ transitions. A suggested decay scheme is depicted in Fig. 3.

The daughter nucleus of Gd^{146} - Eu^{146} is radioactive and decays to the even-even Sm^{146} nucleus with $T_{1/2} = 45$ days. The decay process in Sm^{146} gives rise to at least two nuclear transitions with energies of 630 and 742 kev.

In the conversion electron spectrum of the gadolinium fraction the peaks for these conversions (Fig. 4) grow higher at first, during which time the half-life is ~ 5 days. After a while their in-

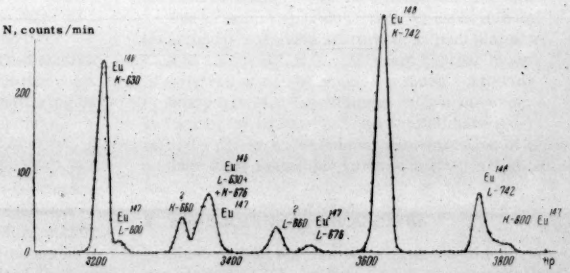

FIG. 4. The Eu^{146} conversion-electron spectrum.

tensity begins to decline, with a half-life of ~ 50 days. In the europium fraction spectrum the conversion lines of the transitions in question steadily decline, with a half-life of 4.5 days. All of these facts prove that 630 and 742 kev transitions must be ascribed to daughter activity of Gd^{146}.

Apparently these transitions belong to the vibrational system of levels of the Sm^{146} nucleus (Fig. 3).

The authors are grateful to V. M. Dzhelepov, Director of the Laboratory of Nuclear Problems in the Joint Institute for Nuclear Research, and to the synchrocyclotron crew for irradiating our tantalum specimens.

[1] Anton'eva, Bashilov, Dzhelepov, and Preobrazhenskii, Izv. Akad. Nauk SSSR, Ser. Fiz. **22**, 135, 895, 906 (1958) [Columbia Tech. Transl. **22**, 134 and in press].

[2] Anton'eva, Bashilov, Dzhelepov and Preobrazhenskii, Тезисы докладов VII Ежегодного Совещания по ядерной спектроскопии (Program of Reports at the VII Annual Conference on Nuclear Spectroscopy) Leningrad (1957), Acad. Sci. Press, Moscow-Leningrad, p. 28.

[3] Gorodinskii, Murin, Pokrovskii, and Preobrazhenskii, ibid. p. 22.

[4] Gorodinskii, Murin, Pokrovskii and Preobrazhenskii, Izv. Akad. Nauk SSSR, Ser. Fiz. **21**, 1624 (1957) [Columbia Tech. Transl. **21**, 1611 (1957)].

[5] Dzhelepov, Preobrazhenskii, and Sergienko, Материалы VIII Ежегодного Совещания по ядерной спектроскопии (Material from the VIII Annual Conference on Nuclear Spectroscopy) Leningrad, (January, 1958).

[6] Anton'eva, Bashilov, Dzhelepov, and Preobrazhenskii, Izv. Akad. Naul SSSR, Ser. Fiz. **23**, No. 2 (1959) [Columbia Tech. Transl., in press].

Translated by A. Skumanich
5

THE SCATTERING OF MUONS IN LEAD

A. I. ALIKHANYAN and F. R. ARUTYUNYAN

Physics Institute, Academy of Sciences, Armenian S.S.R.

Submitted to JETP editor July 14, 1958

J. Exptl. Theoret. Phys. (U.S.S.R.) **36**, 32-40 (January, 1959)

Muons with momenta between 1.0 and 1.8×10^8 ev were scattered in 7-mm thick lead plates. The experimental angular distribution is compared with the theoretical multiple scattering curve for a finite nucleus. It is shown that after all necessary corrections are made the experimental results are in good agreement with the calculations.

1. INTRODUCTION

In recent years a number of investigators have discovered that the scattering of muons with momenta above 100 Mev/c does not agree with the calculated angular distribution based purely on a Coulomb interaction between muons and nuclei. Whittemore and Shutt[1] studied the scattering of muons with momenta 0.3 to 3.1 Bev/c in a 5-cm lead plate mounted inside a cloud chamber and observed considerable scattering at larger angles than are predicted by Olbert's theory[2] for finite nuclei. The experiments of George, Redding, and Trent[3] at 60 m water equivalent (m.w.e.) underground also revealed an apparent excess of muon scattering in 2-cm lead plates, especially at angles greater than 15°. A cross section of the order of 4×10^{-27} cm^2/nucleon was obtained at 100 to 300 Mev, where the scattering results exceeded the theory.

McDiarmid,[4] working with a cloud chamber at a depth of 26 m.w.e., found that the scattering in lead of muons with momenta 200 to 600 Mev/c agrees with scattering theory, whereas at 500 to 1700 Mev/c the experimental results for angles greater than 4° considerably exceed the predictions of the theory for a finite nucleus. Leontic and Wolfendale[5] have also found a larger number of muons scattered in lead above 285 Mev/c.

The discrepancy between the observed angular distribution of scattered muons and the theoretical distribution calculated for Coulomb scattering by a finite nucleus has been called the "anomalous" scattering of muons.

All of the experimental work mentioned above was performed with fairly thick plates in which a considerable fraction of the mesons underwent multiple scattering. Kannangara and Shrikantia[6] investigated pure single scattering of muons at 100-600 Mev/c in an emulsion irradiated 60 m.w.e. underground, obtaining the anomalous scattering cross section $\sigma_{an} = (1.5 \pm 1.0) \times 10^{-27}$ cm^2/nucleon. Alikhanov and Eliseev[7] obtained the same order of magnitude for the anomalous muon scattering cross section in graphite at 200 to 800 Mev/c.

Alikhanyan and Kirillov-Ugryumov[8] investigated slow muon scattering in thin copper plates within a narrow momentum range from 80 to 140 Mev/c and detected excess scattering at projected angles greater than 15°. The small number of observed events did not permit any final conclusion regarding the existence of anomalous scattering in this energy region.

Establishment of the existence of anomalous muon scattering would be of fundamental significance for the theory of elementary particles but would disagree strongly with the known properties of muons. Specifically, it is known that the spectra of x-ray emission in μ-mesonic atomic transitions very accurately establishes the absence of appreciable non-Coulomb interaction between slow muons and nucleons.

It has been found impossible to account for the observed anomalous muon scattering by means of incoherent scattering accompanied by nuclear excitation, or by excess scattering resulting from anomalous muon and nucleon magnetic moments.

The present paper describes an experimental investigation of muon scattering in lead plates at $(1.0 \text{ to } 1.8) \times 10^8$ ev/c. An exact nuclear model is required to establish excess muon scattering by heavy nuclei. Experiments on fast electron scattering by Hofstadter[9] and Schiff[10] have permitted a direct experimental determination of a nuclear form factor for various nuclei, including lead.

2. EXPERIMENTAL PROCEDURE

Muon scattering was investigated at the cosmic-ray station on Mt. Aragats (3200 m above sea level)

using a magnetic mass spectrometer in conjunction with two multiplate cloud chambers. A detailed description of the apparatus has been given in references 12 and 13. Particle trajectories were selected which satisfied the conditions given in references 8 and 13. The present paper gives data on muon scattering in 7-mm lead plates.

Particle Identification

Momentum and range measurements by means of the mass spectrometer were used to determine the particle masses. Momenta were determined from the radius of curvature of trajectories in the magnetic field and ranges were determined from the amount of matter traversed by particles inside the chamber before stopping. Range measurements took into account the entrance angles of particles into the scattering plate and the systematic path lengthening due to multiple Coulomb scattering.[14] For 812 particles with masses measured at 150 to 360 m_e the experimental mass distribution is well approximated by two normal distribution curves with half-width corresponding to a root mean square error of 10%.

Assuming that all particles with measured mass below 240 m_e are muons and that all particles with mass greater than 250 m_e are pions, the average mass for the muon group is 209 m_e and for the pion group 278 m_e. An analysis of this mass spectrum with corrections for the transmission of the apparatus shows that the muon group should contain no more than 2% pions and that the pion group should not contain more than 12% muons.

Reference 8 gives the mass spectra when the chamber contained 5-mm and 2-mm copper plates, in which case the separation of pions and muons is considerably less clearcut.

Measurement of Angles

Large numbers of angle measurements, obtained by means of a special goniometer, were averaged, the accuracy being limited principally by cloud-chamber distortions (diffuseness of tracks, turbulent eddies, etc.). The root mean square error of angle measurements due to these factors is 0.6°. The error is constant over the entire angular range so that the relative error decreases as the angle increases.

The multiple Coulomb scattering of charged particles is usually determined theoretically for projections of the scattering angles on a plane passing through the original trajectory, which generally differs from projections on the plane of the photographic plate. The two angles are equal only when a trajectory before the scattering event is parallel to the photographing plane. The original trajectory makes an angle γ with the photographing plane because of scattering in the previous plate, so that the angle measured in the photograph is greater than the projection of the scattering angle on a plane passing through the original trajectory. Also, when a particle passes through the cloud chamber at a relatively great distance from the optical axis of the camera objective (compared with the distance from the objective to the scattering point inside the chamber) a nonorthogonal projection of the scattering angle is photographed. The true projection of the scattering angle is thus increased or decreased, depending on the orientation of the trajectory inside the chamber; this was pointed out to us by M. I. Daĭon.

The trajectories of mesons which, because of their large curvature in the magnetic field, enter the side regions of the chamber and are scattered in the plates at relatively large angles are subject to the indicated angular discrepancy. For mesons scattered at angles greater than 20° a stereocomparator was used for each angle separately to determine the trajectory in space, i.e., the coordinates of the intersections of the trajectory and the plate, after which the true projection of the scattering angle was determined from simple geometric relations.

From the distribution of the angle differences $\Delta\theta_\varphi = \theta'_\varphi - \theta_\varphi$, where θ'_φ is the true projection of the scattering angle and θ_φ is the angle measured directly in the photograph, we determined that the systematic excess in these directly measured angles was 0.45°. All angles smaller than 20° were corrected by this amount.

Measurement of Momentum at the Point of Scattering

The particle momentum at the point of scattering must be known for comparison of the observed and the expected scattering angle. When the particle mass is known the momentum can be determined in two ways: (1) From the residual range after scattering, which is taken to be the amount of matter traversed by the particle from the middle of the scattering plate to the middle of the plate in which the particle is stopped. (2) From the momentum measured in the magnetic field and the amount of matter traversed by the particle up to the scattering point.

When the plate in which a particle is stopped is denoted by $i = 0$ and the other plates above it are numbered serially $i = 1, 2, 3$ etc., the two methods

yield, for a plate of the same number i values of the average momentum which agree to within 2 to 3%.

The distribution function of multiple Coulomb scattering is derived on the assumption that the momentum loss in the scattering plate is negligibly small, but a calculation shows that when this momentum loss is taken into account the scattering curve is broadened. The broadening depends on the plate number i and for $i > 1$ does not exceed 5% (depending on the stopping point of the particle in plate $i = 0$); for $i = 1$ it varies from 5% to ∞. We therefore do not investigate scattering in plates with the number $i = 1$.

The residual range after scattering is thus known with maximum inaccuracy $\Delta R = t/2$, where t is the thickness of plate $i = 0$. This value of ΔR corresponds to a certain momentum difference Δp, which must be taken into account in plotting the scattering curves. Corrections were obtained for the multiple Coulomb scattering curves plotted for the mean momentum p_m by taking this uncertainty of the momentum measurement into account. At large scattering angles these corrections reach 30 or 40%.

Material and Thickness of the Scattering Plates

The lead plates in which scattering was investigated contained impurities which we took into account in calculating the rms scattering angle and distribution function. For example, 7% of antimony reduces by 1.5% the rms scattering angle calculated for pure lead. Particle tracks in a cloud chamber form different angles with the normal to a scattering plate first, because they enter the chamber at different angles and secondly, because of scattering in the plates, so that there was a certain distribution of scattering plate thickness which had to be taken into account.

For a given single scattering angle θ and particle momentum p, different scattering plate thicknesses $t_1, t_2, t_3, \ldots, t_k$ occurring with frequencies $n_{t_1}, n_{t_2}, \ldots, n_{t_k}$, respectively, correspond to different probabilities of observing the angle $\theta\varphi$: $f_{t_1}(\theta\varphi)$, $f_{t_2}(\theta\varphi), \ldots, f_{t_k}(\theta\varphi)$. We select a certain effective scattering plate thickness t_{eff} such that the relation

$$f_{t_{eff}}(\theta_\varphi) = \sum_{i=1}^{k} n_{t_i} f_{t_i}(\theta_\varphi) \Big/ \sum_{i=1}^{k} n_{t_i} \qquad (1)$$

is valid for the entire investigated angular range. For 7-mm lead plates this t_{eff} equalled the rms thickness calculated from the experimental thickness distribution and was 9% greater than the geometrical thickness of the plate.

Experimental Geometry

Our apparatus defined a certain region of space in which particle scattering was investigated. The projection of the total scattering angle θ on the plane in which scattering is investigated will be denoted by $\theta\varphi$, and the projection on a plane perpendicular to the plate of investigation will be denoted by $\theta\psi$. Because of the geometrical limitations in the investigated plane the probability of registration varies for different scattering angles. This was also pointed out by McDiarmid[4] and more recently by Cousins et al.[15] The same result is produced by geometrical limitations in the plane perpendicular to the plane of investigation, but this depends also on the distribution function of scattering angles. The registration of particles scattered at projected angle $\theta\varphi$ will depend on the corresponding angle $\theta\psi$; hence the observed distribution of $\theta\varphi$ will depend on the allowed distribution of $\theta\psi$.

The experimental geometry thus leads to a correction function $C(\theta\varphi)$ consisting of two parts, $C_1(\theta\varphi)$ and $C_2(\theta\varphi)$. $C_1(\theta\varphi)$ results from the experimental geometry in the investigated scattering plane and gives the probability that the scattering angle $\theta\varphi$ will be observed if there are no geometrical limitations in the perpendicular plane.

When a particle impinges on scattering plate i at angle γ to its normal and at the distance ϵl from one end of the chamber (l is the length of the illuminated region of the chamber in the photographing plane, which is generally simply the length of the chamber) and is then scattered at angle $\theta\varphi$, then we can always find in plate $i + 1$ a length b such that if the particle passes through this length it must be stopped in plate $i - 1$ within the illuminated region of the chamber.

Then, if above the scattering plate there is a certain angular distribution $\zeta(\gamma)\,d\gamma$ of incident particles, simple geometry leads to an expression for the total relative probability of observing the angle $\theta\varphi$, as follows:

$$P(\theta_\varphi) = \int_{\varepsilon=0}^{1} \left\{ 1 - \varepsilon - \frac{\varepsilon - (1/n)\tan\theta_\varphi}{1 + n\varepsilon\tan\theta_\varphi} \right\} \frac{n\varepsilon\,|\tan^{-1}(n\varepsilon) - \theta_\varphi|}{|1 + (n\varepsilon)^2|}\, d\varepsilon, \qquad (2)$$

where $n = l/a$, a is the plate separation and the correction function $C_1(\theta\varphi)$ is given by

$$C_1(\theta_\varphi) = P(\theta_\varphi) / P(0). \qquad (3)$$

It was very difficult to determine the exact angular distribution of incident particles in our apparatus; in calculating $C_1(\theta\varphi)$ we used the experimentally observed angular distributions of incident particles. $C_1(\theta\varphi)$ was then calculated

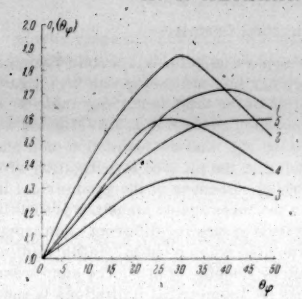

FIG. 1. Correction function $C_1(\theta_\varphi)$. 1) Muons in momemtum range (1.0 to 1.4) × 10^8 ev/c in 7-mm lead plates; 2) muons in momentum range (1.4 to 1.8) × 10^8 ev/c; 3) pions in momentum range (1.2 to 1.6) × 10^8 ev/c in 7-mm lead plates; 4) pions in momentum range (1.6 to 2.0) × 10^8 ev/c; 5) $C_1(C_\varphi)$ assuming $\zeta(\gamma)d\gamma = \cos^2\gamma d\gamma$.

by numerical integration of (2). The angular distributions differ according to the plate number i and also for muons and pions; $C_1(\theta_\varphi)$ is therefore not identical for muons and pions in different momentum ranges. Figure 1 shows values of $C_1(\theta_\varphi)$ for muon and pion scattering in 7-mm lead plates. $C_1(\theta_\varphi)$ is also shown when we assume $\zeta(\gamma)d\gamma = \cos^2\gamma d\gamma$.

$C_2(\theta_\varphi)$ is the correction function for the experimental geometry in a plane perpendicular to the plane of investigation. The multiple Coulomb scattering curve for a finite nucleus can be approximated very accurately by a normal distribution; it is easily shown that there is identical probability of registering different angles so that $C_2(\theta_\varphi)$ is independent of θ_φ.

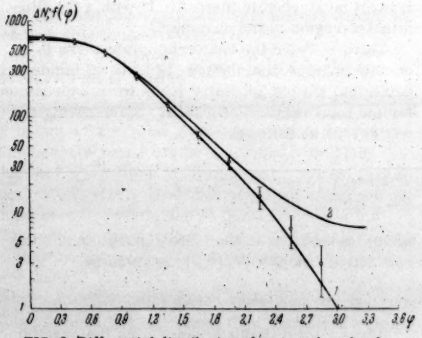

FIG. 2. Differential distribution of projected angles for muons scattered in 7-mm lead plates. Curves 1 and 2 represent multiple Coulomb scattering for an extended and a point nucleus, respectively.

Thus the multiple Coulomb scattering curves with which experimental results are to be compared need be corrected only by the function $C_1(\theta_\varphi)$.

3. EXPERIMENTAL RESULTS AND DISCUSSION

We investigated a total of 2337 muon scatterings and 818 pion scatterings in 7-mm lead plates. The total range in lead of muons with $p = (1.0 \text{ to } 1.8) \times 10^8$ ev/c is 19 m; for pions with $p = (1.2 \text{ to } 2.0) \times 10^8$ ev/c it is 6.7 m.

The experimental results for muon and pion scattering in 7-mm lead plates were compared with multiple Coulomb scattering for a point[16] and an extended[11] nucleus. Multiple Coulomb scattering curves for a finite nucleus were obtained by Ter-Mikaelian; in the calculation experimental results on the nuclear scattering of fast electrons were used.

In comparing the experimental and theoretical curves we used all corrections that were analyzed in Sec. 2. These corrections depend principally on the number of the plate in which scattering is investigated, i.e., on the momentum at the point of scattering; therefore the entire momentum range was divided into two groups, each of width 0.2×10^8 ev/c. After suitable corrections the muon and pion scattering curves were plotted for each group separately.

Figures 2 and 3 show the total scattering curves for muons and pions in lead for all groups combined. The horizontal axis represents the dimensionless quantity φ defined by

$$\varphi = \theta_\varphi / \chi_c B^{1/2},$$

where θ_φ is the projected scattering angle in degrees and $\chi_c B^{1/2}$ is the characteristic angle of multiple Coulomb scattering.[11] The advantage de-

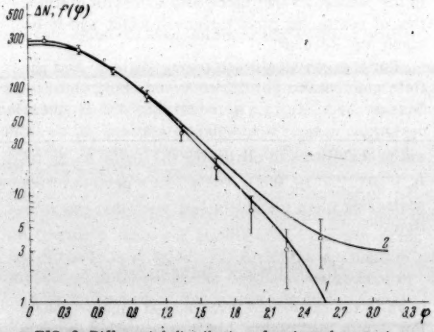

FIG. 3. Differential distribution of projected scattering angles for pions in 7-mm lead plates; 1) extended nucleus, 2) point nucleus.

rived from the use of φ is that scattering data in different momentum ranges and for different plate thicknesses can be combined.

Figures 2 and 3 show the statistical errors combined with errors in determining the correction function $C_1(\theta_\varphi)$; values of the latter were based on the experimental angular distribution of incident particles $\zeta(\gamma)d\gamma$. The error in measuring the scattering angle is much less than $\Delta\varphi = 0.3$ and is not shown in the figures.

It is evident from Fig. 2 that the experimental points are well fitted by the multiple Coulomb scattering curve for a finite nucleus.

A χ^2-type test showed that the experimental angular distribution is in very good agreement with theory for a finite nucleus ($P_{\chi^2} = 95\%$) and differs sharply from the curve for a point nucleus ($P_{\chi^2} = 0.33\%$).

Experimental data on pion scattering in lead also agree with the corresponding curves for multiple Coulomb scattering. It would seem at first that such agreement could not occur because of diffraction scattering of pions, but an investigation of multiple proton scattering in reference 18 showed that when the proton energy and scattering substance obey the relation $\lambda\!\!\!^{-}/R > \chi_c B^{1/2}$, which also holds true for the pions, diffraction scattering resulting from the absorption of particles by nuclei can occur only at very large angles which are outside of the investigated region.

As a control of our results we plotted the scattering curves of the muons with measured mass $< 220\ m_e$ and of pions with mass $> 270\ m_e$. These curves do not differ at all from those given above and are not reproduced here.

$\varphi >$	Number of scattered muons	
	Experimental	Theoretical
1.5	120	119.4
1.8	59	54.0
2.1	25	22.0
2.4	10	8.2
2.7	3	3.0

The magnitude of the possible anomaly can be determined from the table, which contains data (with all corrections) for the total number of scattered muons with φ larger than a given value. The small excess of the observed number of scattered muons over the values given by Ter-Mikaelyan lies within the limit of statistical fluctuations. The total amount of material traversed by the muons is 2.16×10^4 g/cm^2 of lead. It follows that the cross section for anomalous scattering, if it exists, does not exceed 10^{-28} cm^2/nucleon in the investigated momentum range.

It should be noted that if we neglect all of the corrections and refinements given in Sec. 2 (especially with reference to the geometry) we obtain strong disagreement between the experimental data and the theoretical multiple Coulomb scattering curves. In this case the experimental points also lie above the theoretical curve for a point nucleus and the cross section for "anomalous" muon scattering is $\sigma_{an} = (2 \text{ to } 5) \times 10^{-27}$ cm^2/nucleon, which has been obtained by many investigators.

In experiments on muon scattering it is very important to determine the momentum accurately at the point of scattering. We therefore cannot trust data on muon scattering at a few hundred million electron volts in which approximate momentum values were used.

Just as serious is the insufficient consideration (or, in the majority of experiments, the complete disregard) of the experimental geometry. The dimensions of the apparatus are often arbitrary and in some instances strongly distort the multiple Coulomb scattering curves. Incomplete consideration of these two factors has apparently led to "anomalous" muon scattering, at least for slow muons. In any event our data indicate that if anomalous muon scattering exists in the investigated momentum range it is smaller by a factor of tens than the observed value given by a number of investigators. This question can be answered by experiments in which single acts of scattering are observed.

Our data provide a useful indication of muon spin, which is usually assumed to be $\frac{1}{2}$, although there is still no direct experimental verification. Ter-Mikaelian's[11] calculations show that for spin $\frac{3}{2}$ the angular distribution curve lies considerably above our experimental curve.

In conclusion we wish to thank M. L. Ter-Mikaelian for very useful discussions and assistance. We are also indebted to B. A. Dolgoshein and B. I. Luchkov, who assisted with the preparations and measurements, and to M. I. Dalon and V. G. Kirillov-Ugryumov for discussions.

[1] W. L. Whittemore and R. P. Shutt, Phys. Rev. **88**, 1312 (1952).

[2] S. Olbert, Phys. Rev. **87**, 319 (1952).

[3] George, Redding and Trent, Proc. Phys. Soc. (London) **A66**, 533 (1953).

[4] J. B. McDiarmid, Phil. Mag. **45**, 933 (1954).

[5] B. Leontic and A. W. Wolfendale, Phil. Mag. **44**, 1101 (1953).

[6] M. L. T. Kannangara and G. S. Shrikantia, Phil. Mag. **44**, 1091 (1953).

[7] A. I. Alikhanov and G. P. Eliseev, Izv. Akad. Nauk SSSR, Ser. Fiz. **19**, 732 (1955) [Columbia Tech. Transl. **19**, 662 (1955)].

[8] A. I. Alikhanyan and V. G. Kirillov-Urgyumov, Izv. Akad. Nauk SSSR, Ser. Fiz. **19**, 737 (1955), [Columbia Tech. Transl. **19**, 667 (1955)].

[9] P. Hofstadter, Revs. Modern Phys. **28**, 214 (1956).

[10] L. I. Schiff, Phys. Rev. **98**, 756 (1955).

[11] M. L. Ter-Mikaelyan, J. Exptl. Theoret. Phys. (U.S.S.R.) **36**, 253 (1959); this issue, p. 171.

[12] Daĭon, Fedorov, Merzon, and Shostakovich, **Приборы и техника эксперимента** (Instruments and Measurement Engg.) **1**, 3 (1957).

[13] Alikhanyan, Shostakovich, Dadayan, Fedorov, and Deryagin, J. Exptl. Theoret. Phys. (U.S.S.R.) **31**, 955 (1956), Soviet Phys. JETP **4**, 817 (1957).

[14] I. Ya. Pomeranchuk, J. Exptl. Theoret. Phys. (U.S.S.R.) **18**, 759 (1948).

[15] Cousins, Nash, and Pointon, Nuovo cimento **6**, 1113 (1957).

[16] G. Z. Molière, Naturforsch. **3A**, 78 (1948).

[17] H. A. Bethe, Phys. Rev. **89**, 1256 (1953).

[18] F. R. Arutyunyan, J. Exptl. Theoret. Phys. (U.S.S.R.) **34**, 800 (1958), Soviet Phys. JETP **7**, 552 (1958).

Translated by I. Emin
6

IONIZATION OF AIR BY H^+ *AND* H_2^+ *IONS*

R. N. IL'IN, V. V. AFROSIMOV and N. V. FEDORENKO

Leningrad Physico-Technical Institute, Academy of Sciences, U.S.S.R.

Submitted to JETP editor July 29, 1958

J. Exptl. Theoret. Phys. (U.S.S.R.) **36**, 41-48 (January, 1959)

An investigation has been made of the secondary ions that are produced in single collisions between air molecules and H^+ and H_2^+ ions with energies between 5 and 180 kev. The following secondary ions were found: N_2^+, O_2^+, N^+, O^+, N^{2+}, O^{2+}, and Ar^+.

The cross sections for secondary ion formation have been measured. The cross sections for electron capture by H^+ and H_2^+ and the total cross section for ionization of the air molecules have also been investigated.

INTRODUCTION

THE ionization of air by protons has been studied chiefly in connection with investigations of the dependence of proton range on energy.[1] The magnitude and position of the maximum of the ionization cross section have been determined by various indirect methods, all of which are characterized by poor accuracy.[2] To the best of our knowledge, no direct measurements of the ionization cross section for air by protons or the dependence of cross section on energy have been carried out.

The present work was undertaken to investigate ionization in single collisions of H^+ and H_2^+ ions with air molecules. Collisions between fast positive ions and gas atoms are characterized by the detachment of electrons from the shells of both colliding particles and by electron exchange. These and other processes lead to the formation of singly-charged and multiply-charged secondary ions.[3] Because of electron capture by the fast primary ions the total charge of the secondary ions is usually greater than the total charge of the secondary electrons. Furthermore, since it is not a fixed quantity, the total charge of the secondary ions does not give a direct indication of the number of secondary ions. For this reason the "number of ion pairs," which is generally used to characterize ionization, is not a reliable parameter. The total ionization cross section is more properly denoted by the cross section for the formation of the free electrons, which are detached from the shells of the colliding particles. Hence, in the present work the total ionization cross section was determined directly by recording the electrons produced when an ion beam was passed through a chamber containing air. The total electron capture cross sections for H^+ and H_2^+ were also determined; this quantity was also reported in reference 4. In addition, mass-spectrometer measurements were carried out to determine the identity of the secondary ions. The cross sections for the formation of these ions were also measured.

MEASUREMENT PROCEDURE

The method of measurement has been described in detail in earlier papers[3,5] and will be discussed only briefly here.

A beam of primary H^+ or H_2^+ ions, which first passes through a monochrometer, enters a system of collimating slits and the collision chamber, which contains air at 1.5×10^{-4} mm Hg. It has been found that this pressure is low enough to satisfy the requirements for single collisions. A pressure less than 5×10^{-6} mm Hg is maintained in the rest of the system by means of differential pumping.

The collision chamber contains a measuring condenser; this condenser is used to collect the secondary ions and electrons which are formed when the primary ion beam passes through the chamber. The measuring condenser is used to determine the total cross section for the formation of positive ions [reduced to unit charge (σ_+)] and the total ionization cross section (σ_-) by the formulas

$$\sigma_+ = i_+ / i_1 n l; \quad (1)$$

$$\sigma_- = i_- / i_1 n l. \quad (2)$$

In Eqs. (1) and (2), i_1 is the current of primary ions, i_+ and i_- are the saturation currents for positive and negative particles respectively when the collision chamber is filled with air (taking

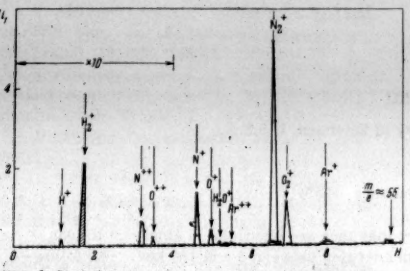

FIG. 1. Secondary-ion spectrogram. o) spectrum at an air pressure of 1.5×10^{-4} mm Hg in the collision chamber, •) spectrum with a residual pressure of 5×10^{-6} mm Hg. The lines due to the residual gases are shown cross-hatched.

account of the background due to the residual gas), n is the number of air molecules per cm^3, and l is the length of the electrodes. The total cross section for electron capture by primary ions (σ_{10}) is defined as

$$\sigma_{10} = \sigma_+ - \sigma_{-} \quad (3)$$

A magnetic mass analyzer is used with the collision chamber; this analyzer is used to analyze the e/m ratios of the secondary ions. Using the mass analyzer the cross section for the formation of secondary ions A^{n+} (σ_{An^+}) is determined from the expression

$$\sigma_{An^+} = \frac{1}{n} \sigma_+ \alpha_{An^+}, \quad (4)$$

where σ_{An^+} is the relative intensity of the line for the A^{n+} ion in the secondary-ion spectrum.

The primary-ion current and the saturation currents at the plates of the condenser are 5×10^{-6} to 5×10^{-8} amp and 4×10^{-7} to 8×10^{-10} amp respectively and are measured with a mirror galvanometer. The current at the collector of the mass analyzer is 8×10^{-10} to 4×10^{-14} amp and is measured with a vacuum-tube voltmeter with a sensitivity of 1×10^{-14} amp/division.

The air pressure in the collision chamber is measured with a radiometer gauge and is monitored with a manometer.

The errors in the cross section measurements are estimated at ±12% of the measured quantities and consist of the errors in the pressure measurements (±6%) and the errors in the current measurements (±6%).

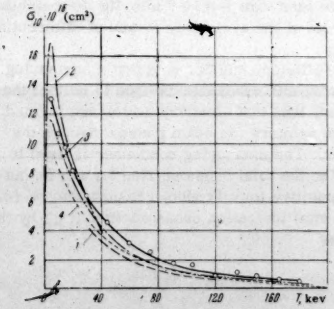

FIG. 2. Energy dependence of the total cross section for electron capture by protons. The solid curve represents the air data of the present work. The dotted curves are as follows: 1) data of reference 4 for air, 2) data of reference 7 for nitrogen, 3) and 4) data of reference 6 for N_2 and O_2 respectively.

RESULTS OF THE MEASUREMENTS AND DISCUSSION

1. Mass Spectrometric Analysis of the Secondary Ions

A spectrogram of the secondary ions formed in the passage of 75-kev protons through air is shown in Fig. 1. The spectrogram was taken at a pressure of 1.5×10^{-4} mm Hg; the residual pressure in the chamber was 5×10^{-6} mm Hg after evacuation. The intensity of the lines is plotted along the vertical axis while the strength of the magnetic field is plotted along the horizontal axis (both quantities are plotted in arbitrary units).

The strongest lines in the spectrum were assigned to the following ions: N_2^+, O_2^+, N^+, O^+, N^{2+}, O^{2+}, and Ar^+. Lines due to H^+, H_2^+, and H_2O^+ were observed; these were attributed to the residual gases. The H^+ and H_2^+ lines are due to the presence of a small amount of water (from the ion source) in the collision chamber while the line characterized by $m/e \approx 55$ is apparently due to vapors of organic compounds. The total contamination of the air was less than 2%.

2. Total Cross Section For Electron Capture by Primary Ions σ_{10}

The energy dependence of σ_{10}, the total electron capture cross section protons in air is shown in Fig. 2. This cross section falls off as the proton energy is increased (for the entire region which was investigated). The cross section for electron capture by protons has also been measured by Kanner.[4] The $\sigma_{10}(T)$ curve obtained in the present work lies above the curve obtained in reference 4; however the difference lies within the experimental errors. The figure also shows the electron capture cross sections measured by Stier and Barnett[6] in oxygen and nitrogen and by Gilbody and Hasted[7]

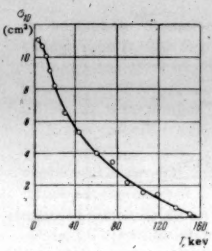

FIG. 3. Energy dependence of the total cross section for electron capture by H_2^+ ions in air (the quantity $\sigma_{10} \times 10^{16}$ is plotted along the ordinate axis).

in nitrogen. The capture cross sections in these gases are approximately the same as those in air.

Figure 3 shows the energy dependence of the total electron capture cross section (σ_{10}) for H_2^+ ions in air. This cross section is similar to the proton capture cross section in that both fall off with increasing energy over the entire range which was investigated.

3. Total Ionization Cross Section σ_-

In Fig. 4 is shown the total ionization cross section for air (σ_-) as a function of the energy of the primary ions, H^+ and H_2^+. The $\sigma_-(T)$ curve has a broad maximum for proton ionization at about 60 kev, at which $\sigma_- \approx 6.3 \times 10^{-16}$ cm². According to the data of reference 2 the maximum of the cross section for ionization of air by protons, as determined by indirect methods lies, in the 50 to 120 kev region; the maximum cross section is 8.6 to 12.5×10^{-16} cm², i.e., somewhat higher than the value obtained in the present work. The position of the ionization maximum found in the present work is in agreement with the position of the maximum of the stopping power of air for protons. According to the data of various authors, reported in the review paper by Allison and Warshaw,[8] this maximum lies in the 60 to 80 kev region.

Figure 5 shows the velocity dependence of the cross section for ionization of air by H^+ and H_2^+ ions and the cross section for ionization of nitrogen and oxygen by electrons as reported in reference 9. It is apparent from Fig. 5 that the ionization maximum for protons and H_2^+ ions lies in the

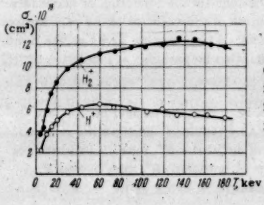

FIG. 4. The total cross section for ionization of air as a function of primary-ion energy (H^+ and H_2^+).

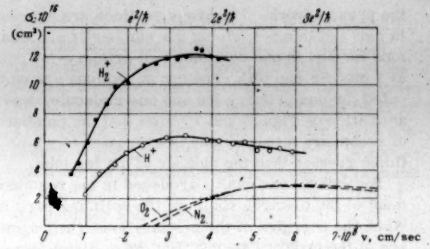

FIG. 5. Velocity dependence of the total ionization cross section. Solid curves are the data of the present work (the designations of the primary ions are given on the corresponding curves); the dotted curves are the data of reference 9 for ionization of nitrogen and oxygen by electrons.

velocity range $v \approx (1.5 \text{ to } 2)e^2/\hbar$ ($e^2/\hbar = 2.2 \times 10^8$ cm sec is the electron velocity in the Bohr hydrogen atom). The ionization maxima in oxygen and nitrogen for electrons corresponds to the higher velocity value $v \approx 3e^2/\hbar$. The maximum cross section for ionization of air by electron collision is approximately one half the value for proton ionization and four times smaller than that for ionization by H_2^+ ions. It is also apparent that ionization of air by protons and H_2^+ ions takes place in the velocity region $v \approx 3e^2/\hbar$, where ionization by electron impact does not occur.

4. Cross Section For the Formation of Secondary Ions

(a) Formation of Secondary ions in air. In Fig. 6 are shown the dependences of the cross sections for the formation of nitrogen and oxygen ions when air is ionized by protons. In Fig. 7 the same relations are shown for H_2^+ ions. Data on the ionization of argon atoms by H^+ and H_2^+ ions have been reported in reference 10 and have not been investigated in

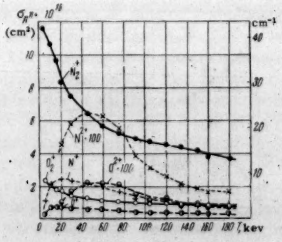

FIG. 6. Energy dependence of the cross sections for the formation of secondary ions in air for ionization by protons. The designations of the secondary ions are given on the corresponding curves.

the present work. The cross sections are expressed in cm^2 and in cm^{-1}, giving the number of secondary ions formed in one centimeter of primary-ion path at 1 mm Hg and 0°C. The cross sections are computed for one primary ion and one molecule. Examination of Figs. 6 and 7 shows that the number of secondary nitrogen ions is approximately four times greater than the number of oxygen ions.

Secondary ions can be produced in the readjustment of the electron shells of the colliding particles. When the energies of the primary ions (hydrogen) are of the order of several kev the collision time is less than 10^{-15} sec. Hence, in the ionization of air (which consists essentially of molecular gases) this readjustment process should be governed by the Franck-Condon principle. Under these conditions the collision of the primary ion with a molecule leads to the formation of a secondary molecular ion with charge equal to the number of electrons detached from the shell of the molecule. The molecular ions which are formed can be stable or unstable. In the latter case they dissociate into atomic particles.

In the interaction of protons with nitrogen molecules the most probable processes which lead to the formation of secondary ions are the following:

$$H^+ + N_2 \rightarrow H^0 + N_2^+, \quad \text{(I)}$$

$$H^+ + N_2 \rightarrow H^+ + N_2^+ + e, \quad \text{(II)}$$

$$H^{+*} + N_2 \rightarrow H^0 + N_2^{++} + e, \quad \text{(III)}$$

$$H^+ + N_2 \rightarrow H^+ + N_2^{++} + 2e. \quad \text{(IV)}$$

Here (I) is the reaction in which an electron is captured by a proton, (II) and (IV) are ionization reactions in which one and two electrons are detached respectively, and (III) is a capture reaction accompanied by ionization. It is obvious that there are also reactions in which three or more electrons are detached from the molecular shells and capture

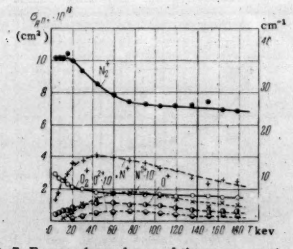

FIG. 7. Energy dependence of the cross sections for the formation of secondary ions in air for ionization by H_2^+ ions. The designations of the secondary ions are given on the corresponding curves.

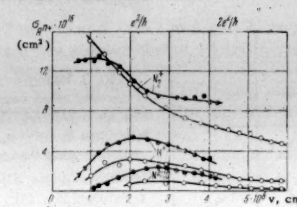

FIG. 8. The cross sections for the formation of secondary ions in nitrogen as a function of the velocity of the primary ion. The designations of the secondary ions are given on the corresponding curves. ○) ionization by protons; ●) ionization by H_2^+ ions.

reactions in which two electrons are captured by the proton. However, these reactions are much less probable than those given in (I) to (IV).

The N_2^+ ions which appear as a result of (I) and (II) and the N_2^{2+} ions which appear as a result of (III) and (IV) are predominantly stable.* The unstable secondary ions can dissociate by various modes, forming the atomic particles N, N^+ and N^{2+}. The O_2^+, O^+, and O^{2+} ions are formed as a result of similar processes.

(b) Cross sections for the formation of singly charged molecular ions in nitrogen and oxygen ($\sigma_{N_2^+}$ and $\sigma_{O_2^+}$). Figures 8 and 9 show the velocity dependences of the cross sections for the formation of various secondary ions for the passage of protons and H_2^+ ions through pure gases (nitrogen and oxygen). In computing these cross sections from the data given in Figs. 6 and 7 it has been assumed that the air is 78% nitrogen and 21% oxygen. Inspection of the curves in Figs. 8 and 9

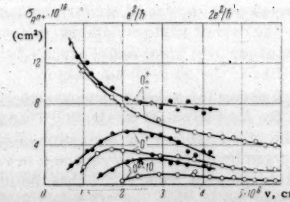

FIG. 9. The cross sections for the formation of secondary ions in oxygen as a function of the velocity of the primary ion. The designations of the secondary ions are given on the corresponding curves. ○) ionization by protons; ●) ionization by H_2^+ ions.

*It is apparent from Fig. 7 that the number of N^+ and N^{2+} atomic ions which arise as a result of dissociation is less than 50% of the number of molecular N_2^+ ions. It follows thus that the maximum number of unstable N_2^+ ions is less than one third of the total number.

shows that the formation cross sections for singly charged molecular ions fall off with increasing primary-ion velocity; the only exception is the cross section for the ionization of nitrogen by H_2^+, which has a maximum at $v \approx 1.2 \times 10^8$ cm/sec.

In the velocity region $v < e^2/\hbar$ the formation of secondary molecular ions is due chiefly to the capture of electrons by the primary ions. This follows from the fact that in this region the total capture cross section is greater than the cross sections $\sigma_{N_2^+}$ and $\sigma_{O_2^+}$ while the total ionization cross section is smaller than these cross sections. The shape of the $\sigma_{N_2^+}(v)$ and $\sigma_{O_2^+}(v)$ curves in this region is probably determined by the $\sigma_{10}(v)$ curve. On the other hand, in the velocity region $v > e^2/\hbar$ the molecular ions arise predominantly as a result of ionization. This result follows from the fact that the total electron capture cross section (σ_{10}) for $v > e^2/\hbar$ is considerably smaller than the cross sections $\sigma_{N_2^+}$ and $\sigma_{O_2^+}$.

(c) Cross sections for the formation of singly charged atomic ions in nitrogen and oxygen σ_{O^+} and σ_{N^+}. It is apparent from Figs 8 and 9 that the cross sections for the formation of singly charged atomic ions reach a maximum of about 50% of the cross sections for the formation of singly-charged molecular ions. The cross sections for the formation of the singly charged atomic ions (N^+ and O^+) reach a maximum in the region $v \approx (0.5 \text{ to } 1) \times e^2/\hbar$. It is interesting to note that the velocities corresponding to the appearance potentials of these ions in electron collision (according to the data of reference 11) are larger, being $2.6 \text{ to } 2.9 \times 10^8$ cm/sec.

It is important to note that the maxima for the formation of secondary atomic ions occur at lower velocities than the maxima for total ionization by H^+ and H_2^+ ions. This experimental fact may be explained qualitatively as follows. The $\sigma_{N^+}(v)$ curve (and the $\sigma_{O^+}(v)$ curve) must be a superposition of the curves for capture with dissociation and ionization with dissociation. According to the data reported by Lindholm,[12] processes involving capture with subsequent dissociation can have cross sections which are comparable with the cross sections for ordinary charge exchange (at primary ion energies of the order of 1 kev). Hence it is reasonable to assume that the basic contribution in σ_{N^+} and σ_{O^+} in the velocity region $v \gtrsim e^2/\hbar$ is due to processes involving capture with subsequent dissociation rather than ionization with dissociation, for which a relatively high energy is required.

The oxygen atom has a positive electron affinity; hence in the interaction of H^+ and H_2^+ ions with oxygen molecules the latter may dissociate with the formation of the negative atomic ions, O^-. In the present work we have estimated the cross section for the formation of negative oxygen ions for primary-ion energies between 11 and 29 kev. The results are shown in the table; the cross sections are given in units of 10^{-19} cm^2. It is apparent from the table that this cross section is much smaller than σ_{O^+} and falls off as the energy of the primary ions is increased.

Energy, kev	Primary ion	
	H^+	H_2^+
11	2.6	–
19	2	6
29	1.2	4

(d) Cross section for the formation of double charged atomic ions $\sigma_{O^{++}}$ and $\sigma_{N^{++}}$. The cross sections for the formation of doubly charged atomic ions have maxima which lie in the velocity region $v \approx (1 \text{ to } 1.5)\, e^2/\hbar$. The maximum values for ionization by protons are $\sigma_{O^{++}} \approx 1 \times 10^{-17}$ cm^2 and $\sigma_{N^{++}} \approx 8.3 \times 10^{-18}$ cm^2; for ionization by H_2^+ ions these cross sections are larger: $\sigma_{O^{++}} \approx 2.9 \times 10^{-17}$ cm^2 and $\sigma_{N^{++}} \approx 2.4 \times 10^{-17}$ cm^2. An estimate of the analogous cross sections for electron impact, made with the data of references 9 and 11, yields the values $\sigma_{O^{++}} < 3 \times 10^{-20}$ cm^2 and $\sigma_{N^{++}} \approx 8 \times 10^{-20}$ cm^2.

It is apparent from Figs. 8 and 9 that $\sigma_{O^{++}}$ and $\sigma_{N^{++}}$ and σ_{O^+} and σ_{N^+} for ionization by H_2^+ ions are 1.5 to 3 times greater than for ionization by protons. This would seem to indicate that the cross sections for processes which involve a sizeable consumption of energy increase with increasing atomic number of the primary ion. A similar conclusion was reached in earlier work, in which we investigated the ionization of argon by hydrogen ions.[10]

The experimental data of the present work lead to the following conclusions.

(1) Ionization of air by protons occurs at velocities smaller than $e^2/\hbar$, i.e., below the threshold for ionization by electron impact. The total cross section for ionization by H^+ and H_2^+ ions, at velocities corresponding to the threshold for electron ionization, are 6×10^{-16} cm^2 and 11×10^{-16} cm^2 respectively.

(2) In ionization of air by protons and H_2^+ ions, about one-third of the secondary ions produced at the total-ionization maxima are atomic ions.

These experimental findings and the data on the ionization of inert gases by positive ions[3,10] indicate that the ionization mechanism in atomic collisions

is different from that which operates in electron impact.

In conclusion the authors wish to thank Professors V. M. Dukel'skii and O. B. Firsov for valuable discussions of the results of the present work.

[1] Bethe and Ashkin, Experimental Nuclear Physics. Vol 1, edited by E. Segre, N. Y., Wiley, 1953. (Russ. Transl. I.I.L. 1955.)

[2] N. Feather, Nature, **147**, 510 (1942).

[3] N. V. Fedorenko and V. V. Afrosimov, J. Tech. Phys. (U.S.S.R.) 26, 1941 (1956), Soviet Phys. JTP **1**, 1872 (1956).

[4] H. Kanner, Phys. Rev. **84**, 1211 (1951).

[5] Fedorenko, Afrosimov, and Kaminker, J. Tech. Phys. (U.S.S.R.) **26**, 1929 (1956), Soviet Phys. JTP **1**, 1861 (1956).

[6] P. M. Stier and C. F. Barnett, Phys. Rev. **103**, 896 (1956).

[7] H. B. Gilbody and J. B. Hasted, Proc. Roy. Soc. **A238**, 334 (1957).

[8] S. K. Allison and S. D. Warshaw, Revs. Modern Phys. **25**, 779 (1953).

[9] J. T. Tate and P. T. Smith, Phys. Rev. **39**, 270 (1932).

[10] Afrosimov, Il'in and Fedorenko, J. Tech. Phys. (U.S.S.R.) **28**, 2266 (1958), Soviet Phys. JTP **3** (in press).

[11] H. D. Hagstrum and J. T. Tate, Phys. Rev. **59**, 354 (1941).

[12] E. Lindholm, Proc. Phys. Soc. **A66**, 1068 (1953).

Translated by H. Lashinsky
7

HODOSCOPE INVESTIGATION OF THE PENETRATING COMPONENT OF EXTENSIVE AIR SHOWERS

R. E. KAZAROV

Institute of Physics, Academy of Sciences, Georgian S.S.R.

Submitted to JETP editor July 31, 1958

J. Exptl. Theoret. Phys. (U.S.S.R.) 36, 49-51 (January, 1959)

A relation of the type $N_\mu \sim E_0^\kappa$ has been investigated for the flux of μ mesons possessing energies ≥ 0.41 Bev and moving 0 to 24 meters from the axis of extensive air showers. It is shown that for energies $1.54 \times 10^{14} \leq E_0 \leq 3.14 \times 10^{15}$ ev the exponent is $\kappa = 0.42 \pm 0.14$.

A dependence $N_\mu \sim E_0^\kappa$ has been established for the number of penetrating particles on the primary shower energy in several papers[1-3] devoted to the investigation of the penetrating component of extensive atomospheric showers under thin absorbers. We deemed it interesting to study an analogous dependence at our level of observation using available data on the flux density of μ mesons under lead in showers of various energies. The corresponding measurements were carried out in Tbilisi (~400 m above sea level) in the winter and spring of 1957.

The apparatus intended to fix the shower, to determine its magnitude, and to locate its axis was analogous to that used in reference 4. The only difference was that one of the lateral hodoscopes that were located symmetrically relative to the separating system was replaced by a penetrating-particle detector consisting of three rows of GS-60 hodoscopic counters, separated by layers of lead. Each row had 8 counters, and the total area of each row was 0.26 m^2. The minimum thickness of lead that a penetrating particle had to pass to produce a discharge in all three rows was 28 cm; a μ-meson energy greater than 0.41 Bev was thus necessary.

In the analysis of the hodoscopic data obtained with the penetrating-particle detector, an event was considered to be produced by a μ meson if:

(a) one counter was discharged in each of the rows in such a manner that the track of the particle could be reproduced,

(b) two or three neighboring counters in one of the rows operated together with single counters in the remaining rows. Thus μ mesons that produce a delta shower were also considered.

In the reduction of the material, we took into account the role played by different kinds of random coincidences of discharges in the detector counter. The contribution of random coincidences to the total number of μ mesons does not exceed 3% for all groups of investigated showers (the resolving time of the hodoscope was $\tau = 30\ \mu$sec, and the background of each counter was n = 1000 pulses/minute).

Based on the accuracy with which the magnitude of the shower was determined,[4] all extensive atmospheric showers were grouped in our experiments by the number of particles into the three groups shown in Table I.

TABLE I

Group No.	Interval	Average value	Primary energy
1	$7 \cdot 10^3 - 2.8 \cdot 10^4$	$1.4 \cdot 10^4$	$1.54 \cdot 10^{14}$
2	$2.8 \cdot 10^4 - 1.12 \cdot 10^5$	$7.2 \cdot 10^4$	$7.92 \cdot 10^{14}$
3	$1.12 \cdot 10^5 - 4.48 \cdot 10^5$	$2.85 \cdot 10^5$	$3.14 \cdot 10^{15}$

For each group of showers, the average density of the μ-meson flux was determined from the formula

$$p_\mu = \frac{1}{\sigma} \ln \frac{N}{N - N_\mu}, \qquad (1)$$

where σ is the area of one row of detectors, N the number of registered showers in a given group, and N_μ the number of showers of a given group in which a μ meson was registered. Of the total number of showers, N, we excluded those in which the μ-mesons could not be identified unambiguously. The data are summarized in Table II, which contains also the average distance r of the axis of the extensive atmospheric shower from the detector of the penetrating particles.

The values of the effective distance of the axis from the detector, given in Table II, were calculated in the following manner. If d is the distance between the detector and the center of the separating system, then the average distance R from the axis from the center of the separating system, the dis-

TABLE II

Energy of primary particle, ev	Total number of showers	Number of mesons	Density of meson flux, m^{-2}	Effective distance, m
$1.54 \cdot 10^{14}$	562	59	0.44 ± 0.06	10
$7.9 \cdot 10^{14}$	311	62	0.86 ± 0.13	10
$3.14 \cdot 10^{15}$	222	71	1.48 ± 0.25	10

tance r from the axis from the detector of the penetrating particle, and the azimuth angle φ are all related by

$$r^2 = R^2 + d^2 - 2Rd\cos\varphi. \quad (2)$$

We calculate N and N_μ from the following relations:

$$N = \iint_{R\varphi} P(R)\, RdRd\varphi; \quad (3)$$

$$N_\mu = \iint_{R\varphi} P(R)\,(1 - \exp\{-\rho_\mu(r)\,\sigma\})\, RdRd\varphi, \quad (4)$$

where P(R) is the distribution of the number of registered showers by distance from the axis of the center of the separating system, as obtained from the hodoscopic data, and $\rho_\mu(r)$ is the spatial distribution function of the μ mesons. For $\rho_\mu(r)$ we used an expression from the paper of Yu. Vavilov et al.[3] of the form $\rho_\mu = a/r^{0.6}$, at distances from 0 to 24 m.

Since our data did not include a single shower with an axis more than 24 m away from the center of the separating system, the use of a spatial distribution function in the form $\rho_\mu = a/r^{0.6}$ is well justified.

From the ratio of N_μ and N we calculated the probability of detector operation, $P(r) = N_\mu/N = 1 - \exp(-\rho_\mu\sigma)$ and estimated the corresponding value of r_{eff}. As can be seen from Table II, all distances were the same in our case ($r \approx 10$ m). This permits us to set up a relation of the type $N_\mu \sim E_0^\kappa$ for μ mesons incident within 24 m from the axis. Actually, it is easy to verify that

$$N_\mu = 2\pi \int_0^{24} \frac{a}{r^{0.6}}\, r\, dr = \text{const} \cdot a, \quad (5)$$

i.e., $N_\mu \sim a$. On the other hand, if the distance from the shower axis to the detector is the same for all showers and equals r_0, then $\rho_\mu(r_0) = a/r_0^{0.6}$, i.e., $\rho_\mu(r_0) \sim a$. Consequently, the dependence $\rho_\mu(r_0) \sim E_0^\kappa$ will have the same exponent as $N_\mu \sim E_0^\kappa$.

Analysis of our experiments has shown that in the energy range $1.54 \times 10^{14} \leq E_0 \leq 3.14 \times 10^{15}$ ev the exponent, as found by the least-squares method with allowance for the weights of the various measurements, is $\kappa = 0.42 \pm 0.14$. The results obtained are in agreement, within the limits of statistical error, with those of Vavilov[5] for μ mesons of energies ≥ 0.44 Bev and a corresponding primary-particle energy interval. This result does not contradict the value $\kappa = 0.62 \pm 0.12$, cited in reference 3 for μ mesons with energies ≥ 1 Bev.

In conclusion, I take this opportunity to express my deep gratitude to Academician of the Georgian S.S.R. E. L. Andronikashvili and to M. F. Bibilshvili and T. V. Varsimashvili for interest in the work and for a discussion of the results, and also to R. V. Kuridze, I. V. Khaldeeva, and M. M. Freĭdlin for help in the performance of the work.

[1] Cocconi, Cocconi, Tongiorgi, and Greisen, Phys. Rev. **75**, 1063 (1949).

[2] H. L. Kasnitz and K. Sitte, Phys. Rev. **94**, 977 (1954).

[3] Vavilov, Evstigneev, and Nikol'skiĭ, J. Exptl. Theoret. Phys. (U.S.S.R.) **32**, 1319 (1957), Soviet Phys. JETP **5**, 1078 (1959).

[4] R. E. Kazarov and E. L. Andronikashvili, J. Exptl. Theoret. Phys. (U.S.S.R.) **33**, 1528 (1957), Soviet Phys. JETP **6**, 1182 (1958).

[5] Yu. N. Vavilov, Dissertation, Phys. Inst. Acad. Sci. (U.S.S.R.), 1958.

Translated by J. G. Adashko
8

(d, p) STRIPPING REACTIONS IN THE SILICON ISOTOPES

V. G. SUKHAREVSKII

Nuclear Physics Institute, Moscow State University

Submitted to JETP editor August 5, 1958

J. Exptl. Theoret. Phys. (U.S.S.R.) **36**, 52-59 (January, 1959)

Thick emulsions were used to measure the angular distribution of protons from the ground and first excited states in the reactions $Si^{29,30}(d, p)Si^{30,31}$ at a deuteron energy of 4.3 Mev. The orbital angular momenta l of the captured neutrons were determined, as well as the absolute differential reaction cross sections and the reduced neutron widths of levels in the final nuclei. The experimental proton angular distributions were compared with the theoretical curves of Butler and Bhatia. The spin and parity of the ground and first excited states in Si^{31} confirm the calculations of Goldhammer.

THE angular distributions of protons or of neutrons in stripping reactions of the type (d, p) or (d, n) have become a generally accepted tool of nuclear spectroscopy for investigating the quantum numbers of states in the product nucleus.[1-3] As is well known, the orbital angular momentum l of the neutron captured by the nucleus in the (d, p) reaction is determined by the position of the peak in the angular distribution of the emitted protons, and can be used to find the parity π and a set of possible spins I_f of the final nucleus. The absolute value of the cross section for the stripping reaction is proportional to the probability that a particle with orbital angular momentum l will be captured on the surface of the nucleus, provided that the core remains unexcited. This probability is proportional to the reduced widths γ_l^2 and Θ_l^2 for the captured particle[4] or to the nuclear matrix element Λ_l.[2] If the states of the final nucleus can be described by the shell model, then the values of these parameters should be relatively large; they should at least be of the same order of magnitude for the excited states as they are for the ground states.

(d, p) reactions on enriched Silicon isotopes Si^{29} and Si^{30} were studied at deuteron energies of 4.3 Mev.[5] The energy spectra were calibrated using magnetic field measurements of the proton spectra[6] from the reactions $Si^{28,29,30}(d, p)Si^{29,30,31}$.

DESCRIPTION OF THE EXPERIMENT

A 4.3-Mev deuteron beam from the 72 cm cyclotron of the Institute of Nuclear Physics, Moscow State University was electromagnetically focused and, passing through a system of collimating slits, fell at 45° on the target, placed at the center of a cylindrical camera. The energy spread in the beam had been determined earlier in previous experiments[7] and was less than 40 kev; the beam did not diverge by more than 20′. Since the deuteron energy varied from one bombardment to another, the value of E_d used was obtained from the proton group of longest range and from a reaction with known Q. The protons emitted from the target were detected by type YA-2 NIKFI emulsions 100 and 200 μ thick and placed about 10 cm from the target at angles of 6.5 to 150° with the incident deuteron beam. Aluminum absorbers were placed between the target and the emulsions to suppress elastically-scattered deuterons and low-energy protons. The beam current was measured with a Faraday cylinder and integrator.

The targets for reactions on the enriched isotopes were made by depositing finely divided SiO_2 powder on a piece of gold tinsel 0.15 mg/cm^2 thick stretched over a frame. The silicon dioxide was enriched with Si^{29} or Si^{30} (see table I). The thickness of the target was found by weighing and turned out to be 0.30 mg/cm^2 for Si^{29} and 0.34 mg/cm^2 for Si^{30}. The Si^{28} target was made by evaporating a silicon sample with the natural isotopic abundances in vacuum. Only chemically pure materials were used in making the targets. Bombardments carried out as controls showed that there was a negligible amount of impurities in the targets and underlying tinsel foil.

The tracks were counted using an MBI-2 microscope with magnification 1.5×90×5. In the histograms below, the scale along the abscissa is in units of the scale in the ocular of the microscope. In the angular distributions shown below, the errors are statistical; the dotted lines show the isotropic

TABLE I

Isotope	Natural Abundance, %	Composition of the Si^{29} sample, %	Composition of the Si^{30} sample, %
Si^{28}	92.28	34.6	35.3
Si^{29}	4.67	63.9	12.5
Si^{30}	3.05	1.5	52.2

part of the angular distribution, which is presumably due to formation of the compound nucleus.

RESULTS

$Si^{29}(d, p)Si^{30}$. Figure 1 shows the proton spectra at angles $\theta_{lab.} = 6.5°$ and 40°. According to Dzhelepov and Peker,[8] Si^{30} has an excited state at 1.250 mev. It does not appear in our experiment. The dotted line in Fig. 1 shows the position of the proton group which should correspond to such a state. If this state is formed its intensity of formation is 0.3% of the corresponding quantity for the ground state of Si^{30} at $\theta_{lab.} = 6.5°$ and less than 0.6% for $\theta_{lab.} = 40°$. The energy resolution of the nuclear emulsions is insufficient to distinguish between the proton groups $Si^{30}(1)$ corresponding to reactions on the first excited state of Si^{30}, and the proton group $Si^{28}(0)$ corresponding to reactions

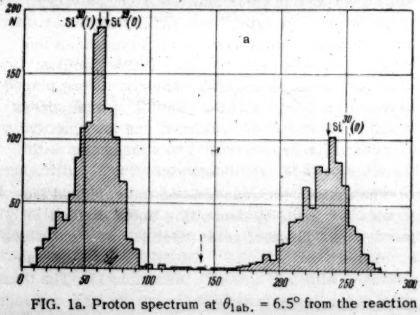

FIG. 1a. Proton spectrum at $\theta_{lab.} = 6.5°$ from the reaction $Si^{29}(d, p)Si^{30}$.

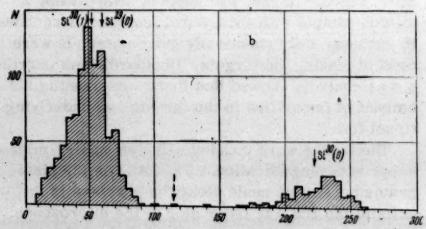

FIG. 1b. Proton spectrum at $\theta_{lab.} = 40°$ from the reaction $Si^{29}(d, p)Si^{30}$.

leading to the ground state of Si^{29}. The Q's for these reactions differ only by $\Delta Q = 0.098$ mev. The sum of the angular distributions has been plotted for these groups. Figure 2 shows the measured angular distributions together with the theoretical curve of Bhatia.[2] When the neutron was captured with orbital angular momentum $l = 0$, the radius of the target nucleus was taken to be $R = R_0 + 2 \times 10^{-13}$ cm, while $R = R_0 + 1 \times 10^{-13}$ cm was used for $l = 2$. R_0 was calculated as $R_0 = (1.7 + 1.22A^{1/3}) \times 10^{-13}$ cm. In Fig. 2a the angular distribution of the group $Si^{30}(0)$ agrees satisfactorily with theoretical curve for $l = 0$. The angular

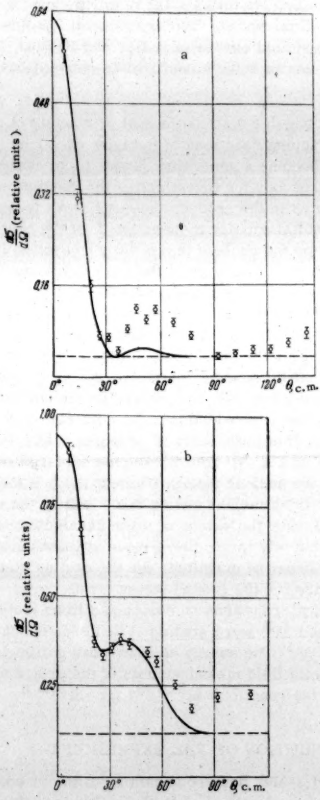

FIG. 2. Angular distribution of protons from the reaction $Si^{29}(d, p)Si^{30}$: a – ground state of Si^{30}, $l = 0$; b – first excited state of Si^{30} $l = 2$ and the ground state of Si^{29}, $l = 0$. $d\sigma/d\Omega$ is in units of 7.30 mbn/sterad.

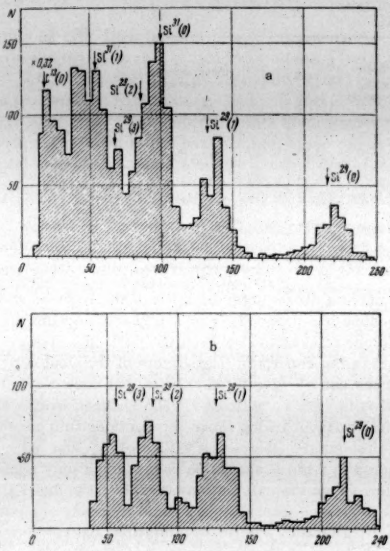

FIG. 3. Proton spectra: a – from the reactions Si^{30} (d, p) Si^{31} and Si^{28} (d, p) Si^{29} at an angle $\theta_{lab.} = 40°$; b – from the reaction Si^{28} (d, p) Si^{29} at an angle $\theta_{lab.} = 40°$.

distribution shown in Fig. 2b for the two groups $Si^{30}(1)$ and $Si^{29}(0)$ agrees with the sum of the curves for $l = 2 + 0$. Since the neutron is captured by the ground state of Si^{29} into an $l = 0$ state,[9,10] the angular distribution of the proton group $Si^{30}(1)$ corresponds to neutron capture with $l = 2$.

Si^{30} (d, p) Si^{31}. The proton spectra from the reactions Si^{30} (d, p) Si^{31} and Si^{28} (d, p) Si^{29} are shown in Fig. 3. The energy resolution is not enough to separate the proton groups $Si^{31}(0)$ from $Si^{29}(2)$ or $Si^{31}(1)$ from $Si^{29}(3)$ (the Q's for these reactions differ only by 0.144 and 0.212 mev). Figure 4 shows the sum of the angular distributions for these two groups. The bottom part of the figure shows the angular distributions of the proton groups $Si^{29}(2)$ and $Si^{29}(3)$, drawn to a scale which shows the contributions these groups make to the total angular distribution. A correction was made for the variation in deuteron energy ($\Delta E_d = 0.4$ mev), using the data of Tobocman and Kalos.[11] The correction never exceeded 0.5%. The angular distribution of the $Si^{29}(3)$ group is isotropic, while the $Si^{29}(2)$ protons correspond to capture of a neutron with $l = 2$ (the theoretical curve is drawn using Bhatia's formula with $R = R_0 + 1 \times 10^{-13}$ cm). These results agree with those of Holt and Marsham,[9] taken at a deuteron energy of 8 Mev. The final angular distributions for the proton groups $Si^{31}(0)$ and $Si^{31}(1)$ (obtained from the difference between the angular distributions of Fig. 4) are shown in Fig. 5, together with theoretical curves calculated from the formulas of Bhatia (solid curves, $R = R_0 + 1 \times 10^{-13}$ cm for $l = 2$ and $R = R_0 + 2 \times 10^{-13}$ cm for $l = 0$) and Butler (dotted curves, $R = R_0 + 1 \times 10^{-13}$ cm). The radius R was increased by 1×10^{-13} cm for $l = 2$ in order to obtain better agreement with experiment. The change displaces the peak in the theoretical curve by 3 or 4° toward the smaller angles.

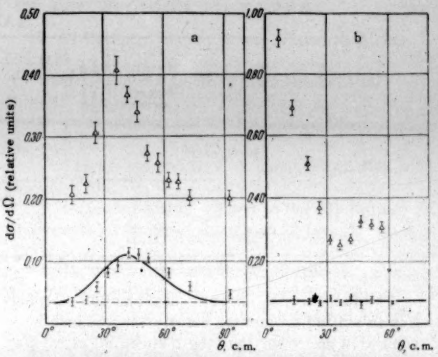

FIG. 4. Angular distributions of protons from the reactions Si^{30} (d, p) Si^{31} and Si^{28} (d, p) Si^{29}: a) Λ – ground state of Si^{31}, $l = 2$, and the second excited state of Si^{29}, $l = 2$; o – for the proton group Si^{29} (2); b) Λ – first excited state of Si^{31}, $l = 0$, and the third excited state of Si^{29} (isotropic). $d\sigma/d\Omega$ is in units of 9.30 mbn/sterad.

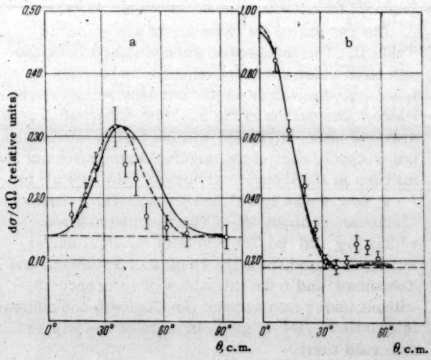

FIG. 5. Angular distribution of protons from the reaction Si^{30} (d, p) Si^{31}. a – ground state of Si^{31}, $l = 2$; b – first excited state of Si^{31}, $l = 0$. $d\sigma/d\Omega$ is in units of 9.30 mbn/sterad.

TABLE II

Reaction	Level position E Mev from reference 6	Level position E Mev from our data*	l	I_f, π_f	$d\sigma/d\Omega$, mbn/steradian	γ_l^2 Mev cm $\times 10^{-26}$	Θ_l^2	Shell model configuration
$Si^{29}(d, p)Si^{30}$	0	0	0	$0^+,(1^+)$	4.57 (0°)	0.88	0.029	$(2s_{1/2})^2$
	2.239± ±0.020	2.25± ±0.09	2	$2^+,(1^+,3^+)$	1.55 (38°)	0.57	0.019	$(2s_{1/2})^1(1d_{3/2})^1$
$Si^{30}(d, p)Si^{31}$	0	0	2	$^3/_2{}^+,(^5/_2{}^+)$	1.66 (38°)	0.31	0.011	$(2s_{1/2})^2(1d_{3/2})^1$
	0.757± ±0.007	0.76± ±0.08	0	$^1/_2{}^+$	7.25 (0°)	0.17	0.006	$(2s_{1/2})^1(1d_{3/2})^2$

*The indicated uncertainty is the root-mean-square error.

The fact that the experimental angular distribution is shifted toward the smaller angles and is somewhat narrower than the theoretical curve for $R = R_0$ indicates that there is a nuclear interaction not accounted for in the theories of Butler and Bhatia. In our case the deuteron energy was 4.3 Mev, almost equal to the height of the Coulomb barrier for the nuclei investigated, so that Coulomb effects cannot be neglected; their effect is to shift the peak in a direction opposite to that given by the nuclear forces, that is, toward larger angles. The Coulomb barrier of the nucleus Si^{29} is 3.70 Mev, while for the nucleus Si^{30} it is 3.66 Mev. However, when E_d is about the same as the Coulomb barrier, the shape of the angular distribution is not deformed enough to give a wrong value for l, at least for nuclei up to $Z = 19$ and for $l = 2$,[12] even though the Coulomb forces, together with other nuclear interactions, can have a big effect on the magnitude of the stripping cross section.

DISCUSSION

The results of the experiment are shown in Table II. The level spins were obtained from the selection rules corresponding to the formula $I_f = I_i + l + \frac{1}{2}$, the values in parentheses being less reliable. The values of the absolute differential cross sections were calculated without taking into account the isotropic part of the angular distributions at the maxima of the theoretical curves (for $\theta = 0°$ for $l = 0$ and $\theta = 36$ to 38° for $l = 2$). The accuracy of $d\sigma/d\Omega$ is about 40%. The reduced neutron widths γ_l^2 and Θ_l^2 for levels of the final nuclei were calculated from the results of Friedman and Tobocman[3] and from the tables of reference 13, without taking into account the Coulomb and nuclear interactions. Θ_l^2 is given in units of the Wigner sum rule limit.

In principle, a measurement of the absolute value of σ_{str} gives the value of γ_l^2 and the kind of nuclear excitation. However, it is not possible to make a direct determination of the reduced width because one cannot take properly into account the nuclear interaction between the particles taking part in the reaction. The effects of the Coulomb forces can be calculated exactly, but such a calculation is very complicated. The reduced widths obtained without taking these interactions into account are too small. Hence the values of γ_l^2 and Θ_l^2 quoted in table II should be regarded as only relative. From the calculations of Tobocman and Kalos, the neglected interactions should increase γ_l^2 and Θ_l^2 by a factor $N > 10$. Calculations carried out by Neudachin and Teplov[14] for the reaction $Ca^{40}(d, p)Ca^{41}$ for $E_d \approx 4$ Mev give a value of N about 40 or 50. Since the nuclear interactions have but little effect on the cross section, one can carry out an approximate calculation of the Coulomb corrections. Such estimates were obtained by Sawicki[15] and Butler[16] but the corrections obtained were small compared with the numerical computations of Tobocman and Kalos. According to Butler, a correction factor $\{R_\infty\}^2$ can be calculated in the limit of small l and for $E_d \gg Ze^2/R$, i.e., for relatively large angular momenta of the deuteron, λ_d, and proton L_p. (The correction factor $\{R_\infty\}^2$ is applied to decrease the value of $\sigma_{stripping}$ as calculated taking Coulomb corrections into account). The approximation improves with increasing λ_d and L_p, because of the short range of nuclear forces. For $E_d \approx Ze^2/R$, the factor $\{R_\infty\}^2$ is too small, but still can be used to obtain a lower limit for $\sigma_{stripping}$. The factor $\{R_\infty\}^2$ is almost exactly equal to $\exp[-\pi(\eta_p + \eta_d)]$ where η is the Coulomb parameter, $\eta = Ze^2m/\hbar^2k$ (k is the wave number). The second factor in $\{R_\infty\}^2$ is usually little different from one ($E_d \gtrsim Ze^2/R$, Q > binding energy of the deuteron).

For the reaction $Si^{29}(d, p)Si^{30}$ at $E_d = 4.30$ Mev, the correction decreases σ_{str} by a factor 10^3, which is clearly wrong but does provide a lower limit to the reaction cross section. From the values of the reduced width Θ_l^2 for the ground

state of Si^{30} (see table II), σ_{str} cannot be decreased by more than a factor 30, since $\{\Theta_l^2\}_{Coul.} = \Theta_l^2/\{R_\infty\}^2$ cannot be more than unity ($\{\Theta_l^2\}_{Coul.}$ is the reduced width taking Coulomb corrections into account). The reason for this discrepancy with experiment is not hard to find, since the orbital angular momentum of the incident deuteron is

$$\lambda_d = \hbar^{-1} R [2M_d (E_d - Ze^2/R)]^{1/2} \approx 1.$$

For the ground state of Si^{30}, the orbital angular momentum of the captured neutron is $l = 0$, i.e., the values $\lambda_d = L_p = 1$ are too small. In the case of the reaction $_9F^{19}(d, p)_9F^{20}$, proceeding from the ground state with $E_d = 14.3$ Mev, the Butler correction is small compared to the result given by the calculations of Tobocman and Kalos. Here $l = 2$, $\lambda_d = 4$, $E_d \gg Ze^2/R = 2.4$ Mev, but $\{R_\infty\}^2$ is less than the result given by Tobocman and Kalos by a factor 7.5. We may conclude that the approximations made by Butler are too crude, at least for deuteron energies up to 14 Mev.

The nucleus Si^{30}_{16} is even-even and has isotopic spin $T = 1$. The spin and parity of the ground state are 0^+. For even-even nuclei, the first excited state usually has spin and parity 2^+, which for this nucleus means that one of the two neutrons outside a closed shell has undergone the transition $(2s_{1/2}) \rightarrow (1d_{3/2})$. The close agreement between the values of the reduced widths for the ground and first excited states suggests that these can be pictured as two neutrons interacting outside a closed shell.

The nucleus Si^{31}_{17} is even-odd, with $T = 3/2$. Possible values for the spin and parity of the ground state are $3/2^+$, $5/2^+$; according to Dzhelepov and Peker the ground state is $3/2^+$. The spin of the first excited state is determined uniquely by this experiment; it is $1/2^+$. The values $3/2^+$, $1/2^+$ for the spins and parities of the ground and first excited states agree with the calculations carried out by Goldhammer;[17] for three neutrons outside a spherical core, his calculations involved a coupling between nucleons in orbits of the same parity introduced by surface oscillations of the core.

In conclusion, I should like to thank S. S. Vasil'ev for his guidance. I should like also to express my gratitude to the cyclotron crew of the Nuclear Physics Institute of the Moscow State University and especially G. V. Koshelyaev, A. A. Danilov, S. M. Kulakova and A. D. Shcheglova for helping to scan the plates.

[1] S. T. Butler, Proc. Roy. Soc. (London) **A208**, 559 (1951).

[2] Bhatia, Kun Huang, Huby, and Newns, Phil. Mag. **43**, 485 (1952).

[3] F. L. Friedman and W. Tobocman, Phys. Rev. **92**, 93 (1953).

[4] T. Teichmann and E. P. Wigner, Phys. Rev. **87**, 123 (1952).

[5] V. G. Sukharevskiĭ, Report to the All-Union Conference on Nuclear Reactions at Low Energies (1957).

[6] D. M. Van Patter and W. W. Buechner, Phys. Rev. **87**, 51 (1952).

[7] G. F. Timushev, Report of the Nuclear Physics Institute, Moscow State Univ. (1955).

[8] B. S. Dzhelepov and L. K. Peker, Схемы распада радиоактивных изотопов (Decay Schemes for Radioactive Isotopes) M.-L., Acad. Sci. Press (1957).

[9] J. R. Holt and T. N. Marsham, Proc. Phys. Soc. (London) **A66**, 467 (1953).

[10] I. B. Teplov and B. A. Yur'ev, J. Exptl. Theoret. Phys. (U.S.S.R.) **33**, 1313 (1957); Soviet Phys. JETP **6**, 1011 (1958).

[11] W. Tobocman and M. H. Kalos, Phys. Rev. **97**, 132 (1955).

[12] I. B. Teplov and B. A. Yur'ev, J. Exptl. Theoret. Phys. (U.S.S.R.) **34**, 334 (1958); Soviet Phys. JETP **7**, 233 (1958).

[13] H. A. Enge and A. Graue, Universitet i Bergen, Arbok 1955, Naturvitenskapelig rekke No. 13.

[14] V. G. Neudachin and I. B. Teplov, Тезисы докладов на Всесоюзной конференции по ядерным реакциям при малых и средних энергиях (Abstracts of talks given at the All-Union Conference on Nuclear Reactions at Low Energies) Acad. Sci. Press 1957 (page 37).

[15] J. Sawicki, Bulletin of the Polish Academy of Sciences, III, **3**, 313 (1955).

[16] S. T. Butler and O. H. Hittmair, Nuclear Stripping Reactions, Horwitz Publications Inc. Sydney 1957.

[17] P. Goldhammer, Phys. Rev. **101**, 1375 (1956).

Translated by R. Krotkov
9

THE ENERGY OF FORMATION AND MIGRATION OF VACANCIES IN GOLD AND PLATINUM

B. G. LAZAREV and O. N. OVCHARENKO

Physico-Technical Institute, Academy of Sciences, U.S.S.R.

Submitted to JETP editor August 8, 1958

J. Exptl. Theoret. Phys. (U.S.S.R.) **36**, 60-67 (January, 1959)

Values of $19 \pm 0.5 \times 10^3$ cal/mole and $27 \pm 0.5 \times 10^3$ cal/mole respectively were obtained for the energies of formation of a vacancy in gold and platinum. The activation energy for migration was found to be $20 \pm 1 \times 10^3$ and $25 \pm 1 \times 10^3$ cal/mole. These results were derived from data on the change of electrical resistance of the metals produced by quenching-in vacancies.

THERE is nowadays an increasing amount of work being devoted to the study of the diffusion mechanism in solids. By different experiments one obtains information on the basic characteristics of the diffusion phenomenon, the energy of formation of a vacancy, Q_1, and the activation energy for migration, Q_2. According to our present ideas, the sum of these two quantities gives the activation energy for self-diffusion: $Q = Q_1 + Q_2$. Q can be determined directly from measurement of the coefficient of self-diffusion, using the relation:

$$D = D_0 \exp\{-Q/RT\}.$$

One of the most direct means of measuring Q_1 and Q_2, and thus also Q, is based on the fact that the electrical resistance of a metal is increased by the presence of quenched-in vacancies, the increases being proportional to the vacancy concentration. This method is being more and more used, and in a previous communication[1] we gave some preliminary results obtained in this way on the self-diffusion of gold and platinum. In the present paper we describe the further development of this work.

EXPERIMENTAL PROCEDURE

Measurements were made on gold and platinum in the form of 0.05 and 0.1 mm diameter wires. These metals are convenient both because of their face-centered cubic lattices (one of the simplest structures) and because, as noble metals, they are easy to handle and can be heated in air.

We had available sufficiently pure metals — not less than 99.99% pure by chemical analysis — with resistance ratios (the ratio of the resistance at 4.2°K to that at room temperature) of 3.5×10^{-3} for gold and 2×10^{-3} for platinum in well-annealed samples.

The specimens were 50 to 70 mm long and current and potential leads of the same material were welded on in a hydrogen flame. After they had been mounted on their supports (quartz or glass) the specimens were thoroughly annealed by passing a current through them. This annealing current passed through leads long enough to ensure uniform heating of the working part of the specimen. The annealing temperature was determined from the resistance, the variation of which with temperature had been determined by heating in a furnace together with a standard platinum-platinum rhodium thermocouple. Before quenching, the specimens were kept at the appropriate temperature long enough for the equilibrium number of vacancies to be produced. The quenching was achieved either by simple cooling in air after switching off the current or, to increase the rate, by immersion in distilled water at room temperature, followed by switching off the current. Separate experiments on annealed specimens showed that the process of rapid immersion itself had negligible effect on the residual resistance (within the experimental uncertainties). Not more than one minute elapsed between quenching and immersion in liquid helium. The resistance of a specimen was measured in the annealed state, then with the quenched-in vacancies and, finally, after annealing again. The increase in resistance, ΔR, is then a measure of the concentration of vacancies at the high temperature. These operations were repeated many times for each temperature.

The temperature range was ~600 to ~1000°C for experiments on gold, and ~800 to ~1500°C for platinum.

Most of the determinations of the increase in resistance were made from measurements at liquid helium temperature, where the increase is appre-

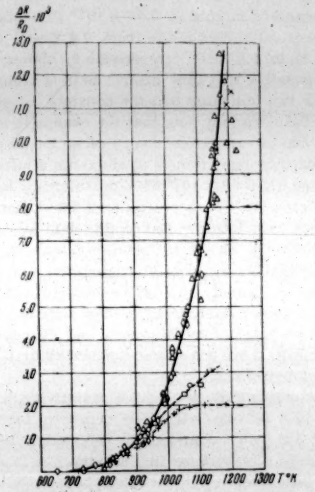

FIG. 1. The dependence of the resistance increase on the temperature, for quenching in vacancies in gold. △, +, ×) 0.1-mm diameter specimens; ◊, ○, □) 0.05-mm diameter specimens. The full curve is for quenching in water, the dashed curve for quenching in air. All the data are obtained from resistance measurements at 4.2°K, except for the points marked ×, which refer to liquid nitrogen temperature.

ciable in comparison with the resistance of an annealed specimen. Some measurements were also made of the change at liquid-hydrogen and liquid-nitrogen temperatures.

DETERMINATION OF THE ENERGY OF FORMATION OF VACANCIES

Figure 1 shows the results of measurements of the increase in resistance on quenching in vacancies, as a function of the temperature from which the quenching was carried out. The increase is plotted relative to the resistance at 20°C (R_0) to eliminate the influence of the dimensions of the great number of specimens measured.

For the results to be reliable one must ensure that all the vacancies are preserved during quenching. The quenching rate in air is sufficient for 0.1 mm diameter specimens at temperatures up to ~ 900°K and for 0.05 mm specimens up to ~ 950°K. This can be deduced from the agreement between the dotted and solid curves up to these temperatures. The solid curve follows an exponential variation over the whole temperature range, as can be seen from Fig. 2, where $\ln(\Delta R/R_0)$ is plotted against 1/T. The results fall on a straight line very well, so that one can be very certain that the mechanism of the resistance increase is the same throughout this temperature interval.

The rate of cooling in air was determined from an oscillograph record of the fall in temperature with time. It was found, for example, that a 0.1-mm specimen cooled from 900°K to 500°K in 0.14 sec. Cooling in water reduced this time by several factors of ten and preserved the vacancy concentration on quenching from all temperatures up to the melting point.

The slope (Q_1/R) of the straight line in Fig. 2 gives us the value of the energy of formation of vacancies in gold as $Q_1 = 19.0 \times 10^3$ cal/mole (0.82 ev). From the relatively small scatter of points the uncertainty in Q_1 is not more than 3%, i.e., 0.5×10^3 cal/mole. Within the limits of experimental errors this value of Q_1 agrees with the value given in the previous paper.[1]

The large number of points shown on the graph, obtained with a variety of specimens, were taken because during the course of this work values of Q_1 were published which were considerably different from our value.

Without knowing the exact conditions in other experiments it is difficult to find reasons for the discrepancies between the results. However, it can be said, for example, that the accuracy in determining Q_1 is evidently overestimated in the work of Koehler et al.[2] In one case they give a value 1.28 ± 0.03 ev and in the other 1.02 ± 0.06 ev; the 25% discrepancy is completely outside the estimated experimental error.

To approximate the experimental conditions used by these authors, we measured the increase

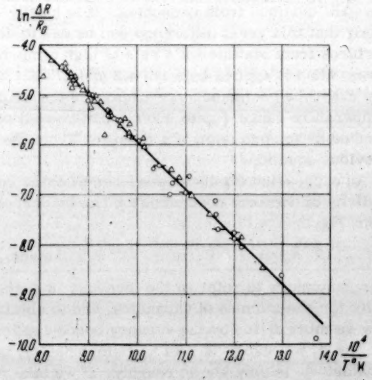

FIG. 2. The dependence of $\ln(\Delta R/R_0)$ on 1/T, for gold.

in resistance, ΔR, not only at helium temperatures, but also at liquid-nitrogen temperature and, as shown above, the results agreed. The uncertainty in ΔR is considerable at nitrogen temperature, as the resistance of the specimen is tens of times larger than ΔR, while at helium temperature ΔR is measured as an increase in the residual resistance, which is itself smaller than the increase produced.

The uncertainty in the work of Bradshaw and Pearson[3] is 10%, because of the few experimental points, and the value of Q_1 is 0.95 ± 0.1 ev. With this uncertainty, their result is close to ours.

It is appropriate here to consider methods[4,5] of determining Q_1 which depend on the temperature variation of the resistance of gold at high temperatures. These methods make use of the well established relation for the temperature variation of the resistance of gold,[6] $R = R_0 + AT + BT^2$, which holds for not too high temperatures. This relation fits the behavior up to 500 or 600°C, but the experimental curve lies above the curve given by this expression at higher temperatures. The authors ascribe this discrepancy to the effect of vacancies and determine ΔR from the difference between the two curves. From the temperature variation of ΔR, values of $Q_1 = 0.67$ ev[4] and $Q_1 = 0.69$ ev[5] were deduced.

We have also measured the R-T relation from rom temperature up to 950°C, and the results agree closely with those of Meechan and Eggleston.[4] This method of determining Q_1 is open to some doubt, as there is little justification for the extrapolation of the R-T curve up to the melting point.[7] The value of ΔR derived in this way and ascribed to vacancies is one order of magnitude larger than the ΔR obtained from quenching. It is hardly likely that this great difference can be due to departures from Matthiesen's rule at high temperatures, when it applies between 4.2 and 273°K. In any case, the resistance variation over the whole temperature range (up to 900°C) can be well described by the inclusion of a term in T^3 in the previous equation.

An expression for the dependence of extra resistivity on vacancy concentration can be derived from Fig. 2:

$$\Delta\rho = (\Delta R / R_0)\rho = 7.7 \cdot 10^{-2} \exp(-Q_1 / RT) \text{ ohm-cm}.$$

It is customary to refer to the increase in resistivity for one atom-% of vacancies, and to obtain this we must divide by the vacancy concentration, i.e., by $C = A \exp(-Q_1/RT)$. Unfortunately, the constant A is only known roughly. If we take $A = 1$ then increase in resistivity for one atom-% of vacancies in gold is 0.77×10^{-6} ohm-cm/atom-%. Theoretical values range from 0.4×10^{-6} (reference 8) to 1.5×10^{-6} (reference 9) ohm-cm/atom-%. It is possible that this difference by a factor of nearly two indicates that the constant A should be ~ 0.5. We may note that the change in resistance due to vacancies is very close to the change produced by one atom-% of elements similar to gold (e.g., 0.68×10^{-6} ohm-cm/atom-% for silver and 0.48×10^{-6} ohm-cm/atom-% for copper). From a rough calculation based on this data we can conclude that A should lie between 0.5 and 2.

We carried out similar experiments on platinum and obtained $Q_1 = 27.0 \pm 0.5 \times 10^3$ cal/mole. This is in satisfactory agreement with the value of 1.4 ev obtained by Bradshaw and Pearson,[10] especially if one takes into account their large experimental scatter.

Assuming that $A = 1$, the resistivity increase, $\Delta\rho = 12 \times 10^5 \exp(-Q_1/RT)$ ohm-cm, leads to the value 1.2×10^{-6} ohm-cm for the resistivity due to 1 atom-% of vacancies in platinum.

It is interesting to note that these results confirm LeClaire's calculation[11] of the ratio of the heat of formation of vacancies to the heat of vaporization. According to LeClaire, this ratio should be 0.22 for a face-centered metal, and from our results the values are 0.22 for gold and 0.23 for platinum.

DETERMINATION OF THE ACTIVATION ENERGY FOR VACANCY MIGRATION

In our preliminary communication we also derived the activation energy for migration of vacancies. This was 12×10^3 cal/mole for gold and 25×10^3 cal/mole for platinum. The value of Q_2 is obtained from curves of the reduction of the resistance increase, ΔR, during isothermal annealing.

The dependence of $\ln(\Delta R/\Delta R_0)$ on time for a 0.1-mm diameter gold wire is shown in Fig. 3 (ΔR_0 is the initial increase in resistance on quenching). The curves shown refer to one tem-

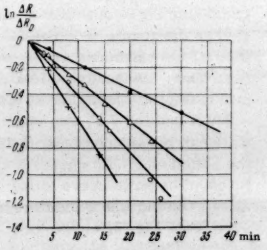

FIG. 3. Curves of the reduction of the resistance increment with annealing time.

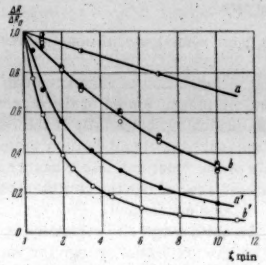

FIG. 4. The influence of wire diameter and concentration of quenched-in vacancies, for gold. Curves a and a') 0.1-mm diameter wire, Curves b and b') 0.05-mm diameter wire.

perature (in this case 100°C) and the different points correspond to different concentrations of quenched-in vacancies (i.e., to different initial values of $\Delta R_0/R_0$).

Similar curves were obtained for different annealing temperatures (75, 90, 100, 107 and 127°C) and for initial concentrations varying over a factor of more than 10 ($\Delta R_0/R_0$ from 1×10^{-3} to 12×10^{-3}).

The strong dependence of the kinetics of vacancy annihilation on concentration is noticeable — the curves of resistance removed become steeper with increasing resistance. It appears that the annihilation process is predominantly a diffusion process only for the smallest vacancy concentrations. For the largest concentrations vacancy coagulation plays a very important part. This is borne out by the curves of Fig. 4, which show the results of annealing specimens of two diameters at 120°C. For pure diffusion to the outside, the times for the concentrations to reach the same relative values, for different diameters, should be in the ratio of the squares of the diameters, i.e., 4 in our case. In fact, for small concentrations ($\Delta R_0/R_0 \sim 2 \times 10^{-3}$) the times for two different specimens (curves a and b) differ by a factor 3, so that even for these

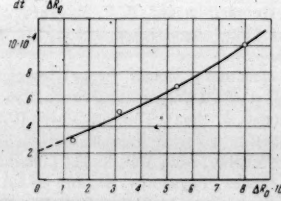

FIG. 5. The variation of slope of the annealing curves with initial vacancy concentration, for gold.

concentrations the process is not pure diffusion. For larger concentrations (up to $\Delta R_0/R_0 \sim 9 \times 10^{-3}$, curves a' and b') the time ratio becomes less than 2.

We can understand the fact that we do not have pure diffusion even for the smallest values of $\Delta R_0/R_0$ in a quenched specimen, if we bear in mind that for any measurement of concentration, the vacancy annihilation is taking place at a considerably lower temperature than that from which the quenching was carried out. This means that the vacancy solution is greatly supersaturated and there is inevitably a type of vacancy coagulation in it. Nevertheless, it seems possible to derive sufficiently reliable values for the activation energy of vacancy migration from such measurements. It is assumed that it is sufficient to extrapolate the kinetics curves to the limit of small concentrations. Such an extrapolation is shown carried out in Fig. 5, where the initial slopes of the annealing curves are plotted against the initial vacancy concentrations, ΔR_0.

Curves for each of the annealing temperatures given above were obtained in this way. Extrapolation of these curves gives the value of $d/dT \times \{\ln(\Delta R/\Delta R_0)\}$ for such small concentrations that we can consider the diffusion process to be dominant in vacancy annihilation.

As is well known, the solution of the diffusion problem for a cylinder of radius r, for sufficiently large times, gives a time dependence of concentration in the material in the form

$$\frac{N}{N_0} = \frac{\Delta R}{\Delta R_0} = \frac{4}{5.78} \exp\left\{-\frac{5.78}{r^2} D_v t\right\},$$

from which we obtain

$$\frac{d}{dt} \ln \frac{\Delta R}{\Delta R_0} = -\frac{5.78}{r^2} D_v,$$

where $D_V = D_0 \exp(-Q_2/RT)$ is the coefficient of diffusion of vacancies and Q_2 is the activation energy for their migration.

We should be able to calculate the diffusion coefficient for the whole temperature range of the experiments from these expressions.

The table gives values for the coefficient of diffusion (D_1) of vacancies in gold wire, taking $r = 5 \times 10^{-3}$ cm, the radius of the wire. For compari-

T °K	$c = \exp(-Q_1/RT)$	D_1 (cm²/sec)	$D_2 = D_0 c$ (cm²/sec)
348	$1.78 \cdot 10^{-12}$	$1.12 \cdot 10^{-10}$	$3.91 \cdot 10^{-15}$
363	$5.75 \cdot 10^{-12}$	$6.89 \cdot 10^{-10}$	$1.29 \cdot 10^{-14}$
373	$1.12 \cdot 10^{-11}$	$9.35 \cdot 10^{-10}$	$2.83 \cdot 10^{-14}$
380	$1.70 \cdot 10^{-11}$	$2.15 \cdot 10^{-9}$	$4.92 \cdot 10^{-14}$
400	$5.88 \cdot 10^{-11}$	$5.60 \cdot 10^{-9}$	$1.91 \cdot 10^{-13}$

son we give the diffusion coefficient derived from data on the self-diffusion of gold atoms obtained with radioactive isotopes.[12]

It can be seen that the value of D_1 is greater than the directly determined D_2 by a factor $\sim 4 \times 10^4$ over the whole temperature range. To explain the much greater value of D_1 one must assume that the diffusion length is not equal to the radius of the wire, but is considerably less and must be 2.5×10^{-5} cm.

We can then believe that vacancy annihilation is accomplished at small concentrations by a diffusion process, and use the results to determine the activation energy for vacancy migration. The dependence of $\ln D_1$ on $1/T$ is given in Fig. 6.

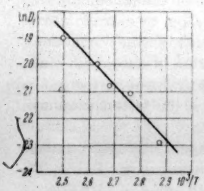

FIG. 6. Variation of ln D_1 with $1/T$, for gold.

The slope (Q_2/R) leads to the value $Q_2 = 20 \pm 1 \times 10^3$ cal/mole. This value is considerably different from our preliminary result $(12 \times 10^3$ cal/mole) when we were unaware of the great dependence of the annealing curves on the quenched-in concentration. This was also neglected in other work,[2,3] and probably accounts for the lower values of Q_2.

The sum $Q_1 + Q_2$ is the activation energy for self diffusion. Our value is $39.0 \pm 1.5 \times 10^3$ cal/mole, which is close to the most recent determinations by direct self-diffusion measurements: 39,360 ± 280 cal/mole,[12] 41,700 ± 300 cal/mole,[13] and 42,900 cal/mole.[14]

Annealing curves were also obtained for a wide concentration range in platinum. There is here a smaller concentration dependence than in gold, and only for large concentrations does the initial slope increase, while for small concentrations the curves coincide. These measurements were made on two specimens at temperatures from 500 to 300°C. There is only a few per cent uncertainty in Q_2, $25 \pm 1 \times 10^3$ cal/mole. The small dependence of the annealing curves on concentration explains the good agreement with our previous work $(25 \times 10^3$ cal/mole) and with the results of Bradshaw and Pearson $(25.3 \times 10^3$ cal/mole).

The activation energy for self diffusion in platinum $Q = 52 \pm 1 \times 10^3$ cal/mole. This value is known more accurately for platinum than for gold.

CONCLUSIONS

We can draw some general conclusions from our results.

The heat of formation of vacancies can be determined from the measurement of the increase in resistance on quenching, especially if the resistance change is measured at liquid-helium temperature. The results of the most reliable measurements on gold and silver are, within the limits of experimental error, in good agreement.

There are quite large discrepancies in the values found for the activation energy for vacancy migration in gold. When the concentration dependence of the annihilation process is taken into account, the results described above make it possible to derive a completely reliable value for this too.

The method of quenching-in vacancies can then yield a value for the activation energy for self diffusion with an accuracy as great as that achieved by use of radioactive isotopes.

There is, however, an inconsistency which must be pointed out. As has been noted, in the limit of small concentrations, vacancy annihilation is achieved by a diffusion process over a distance considerably less than the specimen diameter (it is hundreds of times less). We would then expect the cross-sectional dimensions not to matter. However, as can be seen from Fig. 4, there is a noticeable dependence of the annihilation kinetics during annealing on wire diameter, not only at small vacancy concentrations, but right up to the largest concentrations.

[1] B. G. Lazarev and O. N. Ovcharenko, Dokl. Akad. Nauk SSSR **100**, 875 (1955). Укр. физ. журн. (Ukr. Phys. J.) **1**, 106 (1956).

[2] J. W. Kauffman and J. S. Koehler, Phys. Rev. **97**, 555 (1955). J. E. Bauerle, C. E. Klabunde and J. S. Koehler, Phys. Rev. **102**, 1182 (1956).

[3] F. J. Bradshaw and S. Pearson, Phil. Mag. **2**, 379 (1957).

[4] C. J. Meechan and R. R. Eggleston, Acta Met. **2**, 680 (1954).

[5] C. D. Gertsriken and V. P. Slyusar, Укр. физ. журн. (Ukr. Phys. J.) **2**, 376 (1957), ibid. **3**, 140 (1958).

[6] N. F. Mott and H. Jones, Properties of Metals and Alloys, (Oxford University Press) 1936, p. 268. A. A. Smirnov, J. Exptl. Theoret. Phys. (U.S.S.R.) **4**, 229 (1934).

[7] J. F. Nicholas, Acta Met. **3**, 411 (1955).

[8] D. L. Dexter, Phys. Rev. **87**, 768 (1952).

[9] P. Jongenburger, Appl. Sci. Res. **B3**, 237 (1953).

[10] F. J. Bradshaw and S. Pearson, Phil. Mag. **1**, 812 (1956).
[11] A. D. LeClaire, Acta Met. **1**, 438 (1953).
[12] B. Okkerse, Phys. Rev. **103**, 1246 (1956).
[13] S. M. Makin, A. H. Rowe and A. D. LeClaire, Proc. Phys. Soc. **B70**, 545 (1957).
[14] H. W. Mead and C. E. Birchenall, J. of Metals **9**, 874 (1957).

Translated by R. Berman
10

ENERGY SPECTRA OF ALPHA PARTICLES FROM THE LONG-LIVED ISOTOPES Th^{232} *AND* U^{238}

G. E. KOCHAROV, A. P. KOMAR, and G. A. KOROLEV

Leningrad Physico-Technical Institute, Academy of Sciences, U.S.S.R.

Submitted to JETP editor August 8, 1958

J. Exptl. Theoret. Phys. (U.S.S.R.) **36**, 68-75 (January, 1959)

The alpha spectra of Th^{232} and U^{238} have been investigated by means of an ionization chamber with a grid. The energies and intensities of the transitions to the 2^+ and 4^+ states of the daughter nuclei were determined.

INTRODUCTION

INVESTIGATION of the fine structure in alpha-decay spectra opens a way for the study of weakly-excited states of heavy nuclei, and makes it possible to determine some of the parameters associated with their nuclear structure. The study of fine structure in alpha-decay spectra is carried out chiefly by means of magnetic spectrometers. However, the low aperture ratio (product of the source area by the solid angle used) of the latter does not permit their use in the study of fine structure in the alpha-decay spectra of long-lived isotopes such as Th^{232} and U^{238}, for example.

To solve this problem it is convenient to use ionization chambers whose aperture ratio is several orders of magnitude greater than that of a magnetic spectrometer. In spite of their high aperture ratio, however, ionization chambers are inferior to magnetic spectrometers in energy resolving power. Until recently, the half-width of alpha spectral lines from ionization chambers was of the order of 50 kev because of their poor energy resolution. But in many cases the separation between alpha lines is found to be less than 50 kev, and it is therefore impossible to resolve such lines completely. Hence any improvement in the resolving power of ionization chambers would be of great importance. During 1955 and 1956 a gridded ionization chamber was developed in our laboratories with a half-width of 30 kev for alpha lines.[1-4] The resolving power thus attained proved to be sufficient for a study of the fine structure of the alpha spectra of Th^{232} and U^{238}.

In studying the alpha transitions to excited levels of the daughter nuclei, particular attention had to be paid to the stability of the apparatus, since the measurements were carried out uninterruptedly for periods of several days or more. For instance, in studying the alpha transition to the 4^+ level of Ra^{228} the measurements were taken for 90 hours. During this time the drift of the apparatus used was less than 0.1% per day.

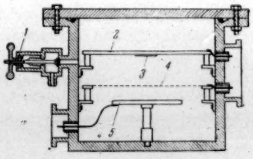

FIG. 1. Diagram of gridded ionization chamber. 1 – valve; 2 – high-voltage electrode; 3 – alpha-particle source; 4 – grid; 5 – collector electrode.

1. DESCRIPTION OF THE APPARATUS

1. The Ionization Chamber and Its Operation

A diagram of the chamber is shown in Fig. 1. The source of alpha particles is located inside the high-voltage electrode, and consists of a brass disk 220 mm in diameter and 4 mm thick. The grid is made of nichrome wires 0.1 mm in diameter welded to a ring of stainless steel. The distance between adjacent wires is 1.5 mm. The grid is 50 mm away from the high-voltage electrode and 25 mm away from the collector electrode. The potentials of the ion chamber electrodes were chosen so as to exclude the possibility of ion recombination or of electron capture by the grid. The chamber was filled with a mixture of 97% argon and 3% methane, to a pressure of 1.8 atmos. The pulses from the collector were amplified in a low-noise preamplifier before being fed into the main amplifier, which had a gain of 10^3 (see Fig. 2). 6Zh1P tubes were used in the preamplifier. Under optimum conditions the transconductance of the first tube was about 3000 μmho, with a grid current of 2×10^{-11} amp. A model-100 amplifier[5] was used for the main amplification. The time constants of the integrating and differentiating circuits were both equal to 15

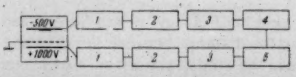

FIG. 2. Block diagram of the ionization alpha-spectrometer. 1 – preamplifiers; 2 – amplifiers; 3 – limiters; 4 – discriminator; 5 – 28 channel analyzer.

microseconds. To reduce the width of the analyzer channels, the output pulses from the amplifier were fed through a limiting amplifier.[6] From the output of this limiter the pulses went to a 28-channel amplitude analyzer. By varying the gain of the limiting amplifier, it was possible to change the effective width of the analyzer channels. The minimum channel width used in the present investigation was 0.1% of the alpha-particle energy. The pulses originating at the high-voltage electrode were used to provide electrical collimation.[3,4]

2. Energy Resolution of a Gridded Ionization Chamber

The energy resolving power of a gridded ionization chamber depends on the thickness of the source, the purity of the gas, the background electrical noise, and the geometry and operating conditions of the chamber. We shall now consider the most serious causes of straggling in the pulse amplitudes.

Fluctuations in the number of ion pairs, and also electrical noise, lead to a Gaussian distribution of pulse amplitudes; but the source thickness, lack of perfect screening by the grid, etc., lead to distributions which are not Gaussian. In spite of this, it is customary to use some value of effective mean-square deviation as a rough guide to the relative effects of each of the above-mentioned factors on the half-width of an alpha line. It will be understood that such estimates are not necessarily mathematically rigorous.

a. Ionization fluctuations. The mean square fluctuation in the number of ion pairs is equal to[7] $\Delta N^2 = FE/W$, where E is the alpha-particle energy, W is the mean energy required to form a single ion pair, and F is a parameter depending on the nature of the gas. According to Fano,[7] F is $\frac{1}{3}$ for argon. The corresponding value of the mean-square deviation for alpha particles from U^{238} is $s_i = 6.3$ kev.

b. Electrical noise. The signal-to-noise ratio at the amplifier output depends on the characteristics of the first amplifier tube as well as on the correct choice of the pass band. To obtain the maximum signal-to-noise ratio for a given amplifier bandwidth, the tubes must have high transconductance and low grid current. By a suitable selection of the first amplifier tube and its operating potentials, it was possible to reduce the mean-square value of electrical noise to a value equivalent to a spread of 6.8 kev.[1]

c. Effect of source thickness on resolution. In studies of long-lived isotopes the use of thick particle sources is unavoidable. Particles emitted from the deeper layers of the source, and particles coming off at large angles to the normal at the surface of the source, lose part of their energy within the source itself. The result is an increased half-width of the alpha line and the appearance of a "tail" on the low-energy side. The presence of this large "tail" in a pulse height distribution makes it difficult to study the fine-structure components. It is therefore necessary to apply some collimation. Mechanical collimators are ordinarily used for this purpose.[6,8] However, they suffer from a number of disadvantages: (1) some of the electrons produced by the alpha particles are lost because of the weakening of the electrical field in the collimator aperture, and (2) the geometry of the apparatus is seriously reduced. Another essential drawback is the difficulty of fabricating highly uniform collimators.

In our work we used the method of electrical collimation. To provide electrical collimation we made use of the pulses produced at the high-voltage electrode. It is well known that the differential distribution of the pulses is rectangular.[9] At the same time, the maximum amplitude V_{max} corresponds to a particle emitted parallel to the electrode, while the minimum amplitude V_{min} corresponds to one emitted perpendicularly. It is obvious that to achieve collimation it is necessary to record the number of collector pulses which coincide with the high-voltage electrode pulses whose amplitudes lie in the interval from V_{min} to $V_{min} + \Delta V$. By changing the magnitude of ΔV, the degree of collimation can be altered. In realizing electrical collimation we used an ordinary single-channel differential amplitude discriminator. The degree of collimation depends on the alpha-particle energy, thus distorting the natural intensity ratio. At the same time, it proved to be easy to allow for the intensity ratio.*

Taking into account the degree of collimation and the effect of source thickness on the shape of the alpha spectrum,[10] we arrive at an rms value $s_s \approx 4$ kev for U^{238} alpha particles.

d. Electron Trapping by Electronegative Impurities. The presence of electronegative gas impuri-

*G. E. Kocharov, Diploma thesis, Phys. Tech. Inst. Acad. Sci. U.S.S.R. (1956).

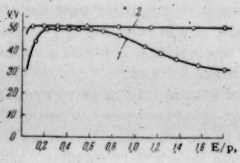

FIG. 3. Height of the collector electrode pulse as a function of the ratio E/p. 1 – A + 0.05% O_2; 2 – A + 0.05% O_2 + 3% CH_4.

ties in the ionization chamber leads to a loss of electrons moving toward the collector electrode and reduces the energy resolving power. The most active electronegative gas is oxygen. Gases are usually rid of oxygen by molten sodium or calcium. In a purified gas, for example argon, the electron drift velocity is small,[11] with the result that the resolution in time and energy is impaired (see item e). In this connection, it is of great practical value to use mixtures of gases. Facchini and Malvicini[12] have shown that the addition of a small amount of nitrogen to the argon prevents this trapping of electrons. The mixture of A and CH_4 which we have used behaves in the same way as a mixture of A and N_2. Figure 3 shows the experimental relationship which we observed between the pulse height and E/p for A + 0.05% O_2 and A + 0.05% O_2 + 3% CH_4. It is evident from these curves that the mixture of argon and methane is insensitive to oxygen impurities. In addition, the electron drift velocity is considerably increased in such a mixture,[11] and the total number of ion pairs formed by an alpha particle is also increased. The addition of 3% of CH_4 considerably improves the amplitude characteristics of the mixture.

e. Lack of Grid Screening. The grid is put into the chamber to suppress any disturbance of the collector electrode which might be induced by the positive ions. The inefficiency of the grid shielding can be determined from the size of the charge induced on the collector electrode by the ions formed in the space between the grid and the high-voltage electrode. As a measure of grid inefficiency we introduce the parameter $\sigma = dE_2/dE_1$, calculated from the formula[13]

$$\sigma = \frac{c}{2\pi b} \ln \frac{c}{2\pi r}, \qquad (1)$$

where c is the distance between grid wires, r is the wire radius, E_1 and E_2 are the electric field strengths in the regions between the grid and the high-voltage electrode and between the grid and the collector respectively, and b is the distance between the grid and the collector.

The grid inefficiency σ can be reduced by increasing the distance between the grid and the collector and the size of the wires, or by decreasing the separation between the grid wires. In so doing, it is essential to keep in mind that the electrons can settle on the grid wires.[13]

Incomplete grid screening makes the collector pulse amplitude depend on the angle at which the alpha particle is emitted, thus reducing the energy resolution. Bunemann et al[13] derived an analytical expression for the rms deviation

$$s = \sigma x E / 2f [d + l(1 - \sigma)], \qquad (2)$$

where x is the distance of the center of gravity of the ions along the alpha-particle track, E is the alpha-particle energy, d is the distance between the high-voltage electrode and the grid, l is a parameter depending on the grid geometry, and f is the degree of collimation.

The experimentally measured value of $\sigma = 0.014$ agrees with the calculated value.[13] Substituting all the necessary values into Eq. (2) we get $s \approx 3$ kev.

f. Effect of Different Collector-pulse Rise Times on Energy Resolution. The pulse rise time at the collector electrode depends on the angle of emission of the alpha particle, and is equal to

$$t = b / w_2 + R \cos \vartheta / w_1, \qquad (3)$$

where R is the range of the alpha particles in the chamber gas; w_1 and w_2 are the drift velocities in the regions between the high-voltage electrode and grid, and the collector and grid, respectively; and ϑ is the angle between the alpha track and the normal to the plane of the source.

During the process of amplification the pulses go through differentiation and integration networks, in which the output pulse amplitudes will depend upon the rise time. The dependence of the rise time on the angle impairs the energy resolving power. The use of mixed gases, A + 3% CH_4, to give a high drift velocity, together with the use of collimation, makes possible a considerable reduction in the straggling of pulse heights due to this effect. Using measured values of electron drift velocities in mixtures of argon and 3% methane,[11] and taking into account the degree of collimation, it is possible to estimate the effect of various pulse rise times on the resolution. The corresponding variance does not exceed 1 kev.

In addition to the above factors, the resolution also depends on the stability of the apparatus, etc. Hence the total rms variance, calculated from the formula $s = (\Sigma s_i^2)^{1/2}$, is equal to 11 kev, corresponding to a half-width of 26 kev in the curves.

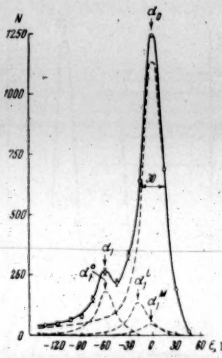

FIG. 4. Alpha particle spectrum of Th^{232}, taken over 25 hours. Half-width of alpha lines 30 kev. The resolution into components is shown dotted. α_0 is the fundamental group of alpha particles; α_1 is the group corresponding to transition to the 2^+ level of the daughter Ra^{228} nucleus. Half of the alpha of group α_1 are accompanied by conversion electrons from the L and M shells which cause excess ionization (groups α_1^L and α_1^M); α_1^0 corresponds to the cases where these electrons do not enter the working space of the chamber.

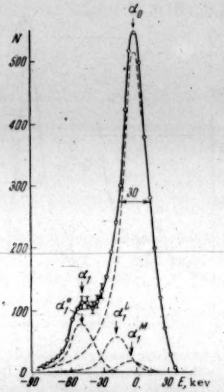

FIG. 5. Alpha particle spectrum of U^{238}, taken over 1.5 hours. Half-width of the lines is 30 kev. Resolution into components is shown dotted. Channel width 4.5 kev.

This is not significantly different from the experimental value of 30 kev.

2. RESULTS OF THE MEASUREMENTS

When a short-range alpha particle is emitted, the atom is left in an excited state. The transition to the ground state is accompanied by the emission of conversion electrons or gamma rays. Following the conversion electrons, the atom emits x-rays and Auger electrons. All these radiations which accompany the alpha-decay produce additional ionization in the chamber gas, thus increasing the ionization due to the short-range particle itself. The major portion of the additional ionization is due to the conversion electrons; the other radiations produce minor amounts of ionization which can be neglected. The working space of the chamber receives half of the conversion electrons. As a result, half of the pulses V_α from the alpha-particle fine structure lines coincide with pulses* from conversion electrons, V_e. This gives a total pulse equivalent to $V_\alpha + V_e$, corresponding to a group of alpha particles with an energy $E = E_\alpha + E_e$. The other half of the pulses register like pulses of alpha particles with the correct energy E_α. In the resulting pulse height distribution, a single group of alpha particles shows up at several different values of energy. This complicates the experimental determination of energies and intensities of alpha transitions. In working out the experimental results, therefore, account must be taken of the spectral distortion due to the conversion electrons.

*The ranges of the conversion electrons are all within the chamber working space.

1. Alpha Transitions to the First Excited Levels of the Daughter Nuclei Ra^{228} and Th^{234}

The alpha spectrum of Th^{232} is shown in Fig. 4. The measurement time was 25 hours. The stability and resolution were sufficiently good to permit the resolution of a well-developed peak α_1, corresponding to transitions to the first excited state of the daughter nucleus Ra^{228}. The distortion due to conversion electrons was taken into account in resolving the curve into its component lines. The intensity of the line α_1 is $23 \pm 3\%$. The energy of the first level is 60 ± 5 kev. This value is in good agreement with measurements made on conversion electrons.[14]

We also succeeded in resolving the α_1 group of particles in the U^{238} spectrum (Fig. 5). The energy of the corresponding level is 48 ± 5 kev, and the intensity of the transition is $23 \pm 4\%$.

It should be mentioned that after our measurements had been completed,[2] we learned that the α_1 group of U^{238} had also been obtained by Valladas,[15] using the coincidences of alpha particles with x-rays. He found the intensity of the transition to be about 20%.

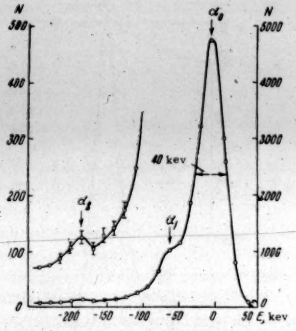

FIG. 6. Alpha particle energy spectrum of Th^{232}, taken over 90 hours. α_1 is the corresponding transition to the 2^+ level of the daughter nucleus. α_2 is apparently a group of alphas corresponding to a transition to the 4^+ level.

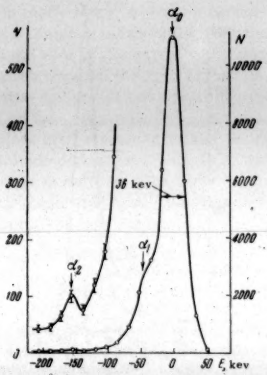

FIG. 7. Alpha energy spectrum of U^{238}, taken over 30 hours. The group α_2 obviously corresponds to a transition to the 4^+ level of the daughter nucleus Th^{234}.

2. Transitions to the Second Levels of the Daughter Nuclei Ra^{228} and Th^{234}

Up to the present time no data have been available on the second excited level of Ra^{228}, apparently because of the difficulties of studying the alpha spectra of nuclei with long half-lives.

The high aperture ratio and good energy resolution of our ionization chamber made it possible to observe an alpha-transition to the second excited level of the daughter nucleus in the spectrum of Th^{232} (Fig. 6). The time required for the measurement was 90 hours. From an analysis of the experimental curves thus obtained, the intensity of the alpha-transition was determined to be $0.2 \pm 0.08\%$. The excitation energy of the second level of the Ra^{228} nucleus is 185 ± 5 kev.

Figure 7 shows the alpha spectrum of U^{238}. This spectrum was taken over a period of 30 hours. The alpha-transition to the second excited level is clearly evident. The intensity of the transition is $0.23 \pm 0.07\%$, and the excitation energy of the level is 160 ± 5 kev.

The ratios of the energies of the first and second levels for these isotopes are in good agreement with the theoretical values obtained on the basis of the collective model of the nucleus.[16] Hence there are good grounds for taking the first and second levels to be rotational, with characteristics 2^+ and 4^+ respectively.

3. COMPARISON OF EXPERIMENTAL VALUES WITH THEORY

In this work we used the formulas of Nosov, who kindly showed us his paper before publication.[17] Nosov's formulas are simple and convenient for the purposes of comparison with experiment. From the comparison of the theoretical values of transition probabilities to the 2^+ level with the experimental values, we determined the deformation parameters of the nuclei Ra^{228}, Th^{230}, and Th^{234} (see column 3 of the table). These values of deformation parameter make it possible to derive theoretical values for the transition probabilities to the 4^+ levels (column 4). Column 5 contains the experimental values of the transition probabilities to the 4^+ level. This table includes also our previous data[18] on Th^{230}.

From the table it can be seen that, within the limits of the errors of measurement, the experimental values of transition probability to the 4^+ level are satisfactorily related to the calculated values. Best agreement is obtained for $r_0 > 1.4$. This agrees with measurements of alpha-particle interactions with nuclei.[19]

CONCLUSION

The high energy resolution of gridded ionization chambers, together with their satisfactory stability, have made possible a study of the previously unobserved alpha transitions to the first and second excited levels of daughter nuclei in the alpha spectra of Th^{232} and U^{238}. It has been shown that these levels are rotational.

Decay schemes for Th^{232} and U^{238}, constructed from the results of this study, are shown in Fig. 8. The half lives for the fundamental transition have been taken from the literature.[20,21]

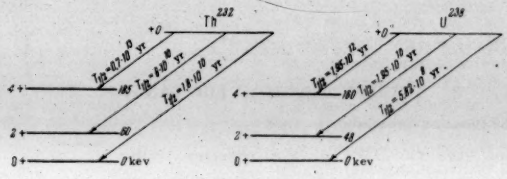

FIG. 8. Decay schemes for Th^{232} and U^{238}.

Daughter nucleus	Nuclear radius R_0 in units of 10^{-13} $A^{1/3}$	Deformation Parameter	Transition probability to the 4^+ level (relative to the fundamental transition)	
			Theory	Experiment
Ra^{228}	1.0	0.27	0.14	
	1.4	0.21	0.17	0.26±0.1
	1.6	0.19	0.19	
Th^{230}	1.0	0.23	0.34	
	1.4	0.19	0.39	0.48±0.2
	1.6	0.18	0.41	
Th^{234}	1.0	0.24	0.15	
	1.4	0.17	0.21	0.3 ±0.09
	1.6	0.15	0.23	

The authors express their sincere thanks to Yu. A. Surkov for providing the necessary thorium sources; to V. G. Nosov for discussions of the results of his work, and for making available the manuscript of his paper; to E. A. Damaskinskiĭ for his assistance in the work; and also to S. N. Nikolaev and V. A. Kireev for advice on matters of electronic equipment maintenance.

[1] Bochagov, Kocharov, and Kirshin, Приборы и техника эксперимента (Instruments and Meas. Engg.) **6**, 72 (1957).

[2] Bochagov, Komar, and Kocharov, J. Exptl. Theoret Phys. (U.S.S.R.) **32**, 1257 (1957), Soviet Phys. JETP **5**, 1026 (1957).

[3] B. A. Bochagov, Dissertation, Leningrad Phys. Tech. Inst. Acad. Sci. U.S.S.R. (1956).

[4] Bochagov, Vorob'ev and Komar, Izv. Akad. Nauk SSSR, Ser. Fiz. **20**, 1455 (1956) [Columbia Tech. Transl. **20**, 1331 (1956)].

[5] V. Elmore and M. Sands, Electronics in Nuclear Physics, (Russ. Transl.) I.I.L. (1953).

[6] D. W. Engelkemeir and L. B. Magnusson, Rev. Sci. Instr. **26**, 295 (1955).

[7] U. Fano, Phys. Rev. **72**, 26 (1947).

[8] Baranov, Zelenkov and Rodionov, Izv. Akad. Nauk SSSR Ser. Fiz. **21**, 909 (1957) [Columbia Tech. Transl. **21**, 911 (1957)].

[9] B. Rossi and G. Staub, Ionization Chambers and Counters, McGraw-Hill, 1949, (Russ. transl. I.I.L., 1951).

[10] Haeberli, Huber, and Baldinger, Helv. Phys. Acta **26**, 145 (1953).

[11] W. N. English and G. C. Hanna, Canad. J. Phys. **31**, 768 (1953).

[12] U. Facchini and A. Malvicini, Nucleonics **13**, (4), 36 (April 1955).

[13] Bunemann, Cranshaw, and Harvey, Canad. J. Res. **27A**, 191 (1949).

[14] S. W. Peat and M. A. S. Ross, Proc. Phys. Soc. **68A**, 923 (1955).

[15] G. Valladas, Thesis (Institut du Radium, Paris) (1955).

[16] A. Bohr, Rotational States of Atomic Nuclei, Copenhagen (1954).

[17] V. G. Nosov, Report presented at the Paris Conference on Nuclear Structure (1958).

[18] Komar, Korolev, and Kocharov, Report at the Eighth International Symposium on Nuclear Spectroscopy, Leningrad, Jan. 1958.

[19] I. Perlman and J. Rasmussen, Handb. Physik, **42**, 109 (1957).

[20] F. Picciotto and S. Wilgain, Nuovo cimento **4**, 6 (1956).

[21] B. S. Dzhelepov and L. K. Peker, Схемы распада радиоактивных изотопов (Decay Schemes of Radioactive Isotopes), Acad. Sci. Press, 1957.

Translated by D. C. West
11

A SEARCH FOR DOUBLE BETA DECAY IN Ca^{48}*

E. I. DOBROKHOTOV, V. R. LAZARENKO, and S. Yu. LUK'YANOV

Submitted to JETP editor September 6, 1958

J. Exptl. Theoret. Phys. (U.S.S.R.) 36, 76-87 (January, 1959)

The subject of this paper is an attempt to detect experimentally double β decay in Ca^{48}. The apparatus, procedure, and control tests used in the experimental work are described. The writers have reached the conclusion that if double β decay occurs in Ca^{48} its half-life is not smaller than 0.7×10^{19} years.

1. INTRODUCTION

THE search for double β decay is an amazing example of a fantastic succession of periods of hope and of disillusionment. Two times in the course of a single decade this phenomenon has been "discovered," and both times the discovery has been found to be erroneous. The history of the question is still not complete; the phenomenon has not been observed experimentally, and the succession of journal articles in recent years only gradually sets larger and larger lower limits on the lifetime of a nucleus capable of double β decay. In the present research we have again not succeeded in observing the event, but the limit on the half-life of the process has been raised to about 0.7×10^{19} years, and further steps in this direction (if indeed they are worth while) will depend on achieving considerable increases in the amount of material subjected to study.

The search for the phenomenon has been stimulated by the well known discussions[1,2] of the relation of the value of the period for double β decay with arguments in favor of or against the existence of neutrino and antineutrino as two different particles. Increase of the experimental limit of the decay period to the values now established has been regarded as strong evidence in favor of the existence of physically distinguishable neutrinos and antineutrinos.

Our views on this matter have been much changed, however, by the discovery that the law of conservation of parity is violated in the weak interactions. The result has been to give to the problem as a whole an incomparably more complex and involved character. Let us go into this in more detail.

A number of experiments performed in 1957 in the field of β decay have given evidence in favor of the concept of the neutrino as a longitudinally-polarized particle. Furthermore, in the two-component scheme for the neutrino, the neutrino and the antineutrino have different orientations of the spin relative to the momentum; the antineutrino, i.e., the particle emitted along with an electron in β decay, has its spin and momentum parallel, while the neutrino, emitted along with a positron, has them antiparallel. This picture corresponds to the idea of 100 percent polarization of the neutrino and the law of conservation of leptonic charge. So far as one can judge, it is not in contradiction with the available experimental facts, but also it does not follow from them as an automatic consequence — the measurements are still not sufficiently accurate. In this picture there is no place for such double processes as the "neutrinoless" double β decay; if before the decay the atomic system contained no light particles with one sign of the leptonic charge, and after the decay such particles have appeared (for example, two electrons), then along with these particles there must appear light particles with the opposite sign of this charge (two antineutrinos).

If, however, the law of the conservation of leptonic charge is violated,[3] then the process of neutrinoless decay is possible owing to the occurrence of mixed types of interaction. More precisely: part of the decays in the virtual first phase of the process can go through the scalar-tensor interaction with emission of a neutrino of one type, and part through the axial vector interaction with emission of a neutrino of the opposite type. During the second phase of the proeess these neutrinos can be absorbed, and the process as a whole will not be accompanied by neutrino emission. It turns out[4] that the process of such a decay with the mixed interaction appears only when forbidden transitions are involved; this brings about a reduction of the decay probability by four orders of magnitude as compared with previous estimates.[5]

*Preliminary results of this work were presented at the All-Union Conference on Nuclear Spectroscopy in January, 1957.

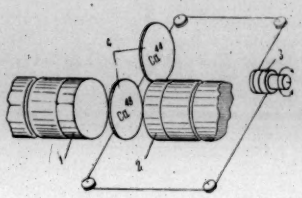

FIG. 1. Sketch of arrangement of measuring head. 1, 2) Scintillation counters; 3) shaft of motor for shifting of motor specimens; 4) specimens.

It must be noted that in case the two-component theory is incorrect (the longitudinal polarization of the neutrino is not 100 percent) the forbiddenness noted above can be weakened. The accuracy of the present experimental data in measurements of the longitudinal polarization of the electrons is to within 10 or 20 percent. If we assume (as is, however, not very probable) that the degree of polarization of β particles is 10 percent smaller than the maximum possible, we find that the probability of neutrinoless β decay is decreased by only two orders of magnitude instead of four.[4]

As for the leptonic charge, on this question there are practically no experimental data. Of the work done so far, that of Davis[6] might provide some information, but it is as yet unclear how it is to be interpreted. In principle, experiments on double β decay can also give information on the conservation of leptonic charge. It must be remembered, however, that the theory of the process involves one quantity that cannot be checked experimentally, namely the nuclear matrix element, for which one can only estimate an upper limit.[5]

Thus the situation in both experiment and theory indicates that continuation of experiments on double β decay can be of some interest.

2. THE PREPARATION OF THE SPECIMENS

The test and control specimens were prepared from calcium obtained by electromagnetic separation of the isotopes. To lower the proportion of extraneous atoms in the specimens, we used calcium fluoride as the chemical compound for their preparation. The test specimen, enriched in the isotope Ca^{48} to abundance 76.2 percent, contained 423 mg of Ca^{48}. The control specimen was enriched in the isotope Ca^{44} (94.7 %) and was equivalent to the test specimen in the number of molecules of calcium fluoride.

The two specimens were prepared by pressing powdered calcium fluoride and were in the shape of thin disks of diameter 37 mm. The binder was a 1 percent solution of agar in water. The disks were fixed in annular aluminum holders, with their sides covered with aluminum foil of thickness 30 μ. All the materials used in the preparation of the specimens were subjected to careful chemical analysis, and were checked for the absence of radioactivity. The results of the analyses showed that the foreign impurities in the specimens did not exceed 0.02%.

3. DESCRIPTION OF THE APPARATUS

The apparatus consisted of the measuring head, completely immersed in a shielding liquid scintillation counter, electronic registering equipment, and a unit for automatic control and monitoring. The apparatus had to operate for many hundreds of hours without interruption, and was designed for the registration of extremely rare events. Therefore the greatest care was taken to assure the stability and reliability of its functioning. These considerations determined the choice of the photomultipliers and the circuits and components of the electronic equipment, and also the arrangement of the automatic control system.

The arrangement of the measuring head is shown schematically in Fig. 1. The two scintillation counters, of diameter 50 mm, are placed facing each other in a sealed casing. Between the counters there is a steel frame, in which the specimens are fixed. The frame can be shifted by means of a reversible motor connected to the control unit, so as to place between the scintillation counters either the specimen enriched with Ca^{48} or that enriched with Ca^{44}. Springs included in the mechanism for shifting the frame assure that it always takes one of the extreme positions, and that the positions of the counters relative to the scintillation counters are established reproducibly.

The distance between the median plane of the specimen and the surface of the scintillator is 1.35 mm. The solid angle over which each of the scintillation counters "saw" the specimen was $0.464 \times 4\pi$. The method for calculating the solid angles between the disks is described in detail in reference 7.

Each liquid scintillation counter is a 70-liter tank with polished aluminum walls, into which 21 type FEU-19M photomultipliers are directed at all angles. The tank is filled with a solution of terphenyl in toluol; the concentration of terphenyl is 3 g/l. All of the photomultipliers of the tank, which will hereafter be called "shielding" photomultipliers, were operated at the same amplification coefficient.

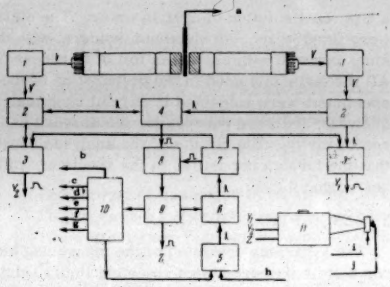

FIG. 2. Block diagram of the electronic part of the apparatus. 1) Cathode followers; 2) and 5) amplifiers; 3, 7, and 9) shaping units; 4) selection unit; 6) and 8) anticoincidence circuits; 10) control unit; 11) cathode-ray oscilloscope. a) To motor; b) Film advance; c) To motor; d) Time marker; e) $(check)_1$; f) $(check)_2$; g) Tank; h) From tank; i) Film advance; j) Time marker.

A block diagram of the electronic part of the apparatus is shown in Fig. 2. The total pulse from all the shielding photomultipliers was sent through the amplifier 5 into an electronic system, where after passing through the anticoincidence circuit 6 it was transformed by the shaping unit 7 to a rectangular pulse. The pulses coming from the photomultipliers of the measuring head were sent through the cathode followers 1 to the linear amplifiers 2 with strong negative inverse coupling. In the shaping units 3 they were transformed into pulses with flat tops and slanting trailing edges, and then went to the deflecting plates Y_1 and Y_2 of the two-beam cathode-ray oscilloscope 11. The formation of these "working" pulses occurred only in cases in which they were not accompanied by pulses from the screening photomultipliers.

Registration of the working pulses also occurred when quite definite conditions were fulfilled, namely when: (a) they were in coincidence to within 0.2μ sec, (b) their combined amplitude was above a prescribed value, and (c) there were no pulses from the screening photomultipliers during the time interval from 1 μ sec before the appearance of the "working" pulse to its termination. The first two conditions were imposed by the selection unit 4, and the last by the delayed anticoincidence circuit 8. If all these conditions were satisfied the shaping unit 9 was actuated; this developed a positive rectangular pulse to modulate the brightness of the oscilloscope beams. Since no alternating voltage was applied to the x axis of the oscilloscope, the pulses on the screen took the form of vertical lines directed toward each other and marked at both ends by points. A photographic attachment

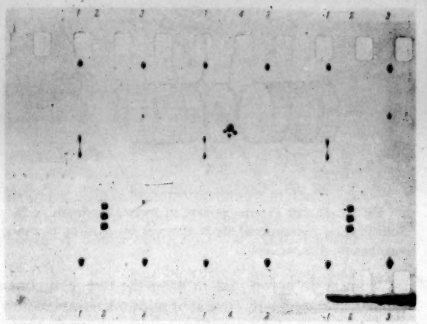

FIG. 3. Specimen of the film. 1) Control pulses; 2) mark indicating the beginning of measurements on the specimen of Ca^{45}; 3) coincident pulses registered in the course of an hour; 4) mark indicating the beginning of measurements on the specimen of Ca^{44}.

recorded this image on 35 mm film.

The anticoincidence circuit 6 shut off the pulses from the screening photomultipliers during the exposure. After each exposure the control unit 10 casued the film to be advanced by 1.5 mm.

In addition to advancing the film the control and monitoring unit performed the following functions:

(a) At the end of each hour it actuated the motor that accomplished the interchange of the specimens in the space between the photomultipliers of the measuring head.

(b) During the shifting of the frame carrying the specimens it sent out two series of standard pulses from a highly stable generator to check the stability and functioning of the electronic circuits;

(c) It actuated a device which marked the film with a conventional sign showing which specimen was in place for observation.

Figure 3 shows a reproduction of a piece of the film and gives the interpretation of all the elements of the registration. The amplitudes of the pulses registered on the film were measured by means of a projector. The measured spectrum of amplitudes was subjected to appropriate recalculation to obtain the energy spectrum.

4. THE SCINTILLATION COUNTERS. THE CALIBRATION

The liquid scintillation counter prevented registration by the measuring head of ionizing particles incident on the apparatus from the space outside, and considerably decreased the probability of the registration of neutral particles and photons. The lower the energy threshold of the shielding counter,

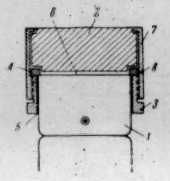

FIG. 4. Attachment of the plastic scintillator to the FEU-12 photoelectric cathode. 1) Photoelectric cathode; 2) scintillator; 3) brass ring; 4) rubber ring; 5) cement; 6) diffusion oil; 7) threaded brass fitting; 8) hole for injection needle.

the more effectively it should fulfill its protective function. It must be taken into account, however, that lowering of the threshold is accompanied by a rapid rise of the number of counts coming from the shielding photomultipliers, owing both to the registration of weak scintillations and also to the registration of its own noise pulses in the low-energy region. An increase of the number of shielding pulses would be accompanied by a lowering of the effective time for registration and an increase of the dead time of the system. The problem of choosing the permissible counting rate can be dealt with experimentally and will be considered later on.

The choice of the electric supplies to the dynodes made it possible to improve considerably the parameters of the FEU-19M photomultipliers owing to a sharp increase of the signal-to-noise ratio. More exactly, while keeping the voltage across the divider and the value of the discrimination threshold unchanged, we were able to raise the gain of the photomultipliers by a factor of several times, with a negligible increase of the number of noise pulses.

As for the choice of the liquid for filling the tank, it is desirable to have a scintillator with the greatest light yield and with sufficient transparency for its own radiation. From this point of view the most effective substance was a solution of terphenyl in toluol, to which was added a small amount of α-naphthyl phenyl oxazole (α NPO) or diphenyl-oxazolylbenzol (POPOP). We remark that to get good results one must use toluol purified by double distillation. Toluol is a very good solvent for many organic substances, and a liquid scintillator is extremely sensitive to impurities of any kind. Therefore all of the many gaskets were made either of lead or of fluorine plastic.

Tests of the liquid scintillation counter showed that with an energy threshold for β-ray quanta of 90 to 100 kev the number of noise pulses did not exceed 1000 to 1500 per minute. These figures were regarded as satisfactory.

For the measuring head one must have extremely stable photomultipliers with good amplitude resolution and capable of operating for many hundreds of hours without changes in their parameters. These requirements are satisfied by the type FEU-12 multipliers developed by Vil'dgrube.[8,9]

For the scintillators in the measuring head we used a solid solution of tetraphenyl butadiene in polystyrene, of concentration 16 g/l. Figure 4 shows schematically the construction of the attachments used to assure good optical contact between the photoelectric cathodes of the multipliers and the plastic scintillators.

The photoelectric cathodes of the multipliers in the measuring head were connected to the body of the apparatus, and the high voltage of positive polarity was applied through the collectors. The suitability of such connections was ascertained by tests on prolonged operation of the photomultipliers.

The energy calibration of the scintillation counters for the measuring head was carried out with the conversion line of Ba^{137} (0.625 Mev) and with the position of the maximum caused by cosmic-ray mesons of minimum ionization. The calibration of the point corresponding to the internal-conversion electrons of Ba^{137} was obtained in the following way. A small drop of a solution of a salt of radioactive Cs^{137} was placed on a thin organic film (0.3μ). After the water had evaporated from the drop, the film was mounted between two rings of organic glass in such a way that the dry residue from the drop, containing the Cs^{137}, was in the center. The source was placed on an aluminum disk 3 mm thick, which in turn was fastened against the working surface of the scintillation counter. The spectrum was taken twice with a single-channel differential amplitude analyzer — once with a hole in the aluminum disk toward the source, and the other time with a solid disk. In the latter case the γ-ray spectrum was taken. The difference of the two spectra gave the spectrum of the electrons, with its maximum at 0.625 Mev. The energy resolution of the two scintillation counters for 0.625 Mev electrons is 28 percent (the width of the peak at half its height). On the basis of this one draws the conclusion that for 4 Mev electrons one can expect that the half-value width for the resolution is 11 percent.

The second calibration point in the region of higher energies was obtained by an independent method. The apparatus was placed so that the working counters were one above the other, and below the lower one was placed a third (auxiliary) scintillation counter, connected for coincidences with the top one (Fig. 5). The oscilloscope with the photographic attachment registered only the pulses from the working counters, and this only in the case of coincidence of the counts from the top counter and the auxiliary counter. After the film was developed attention was given only to the

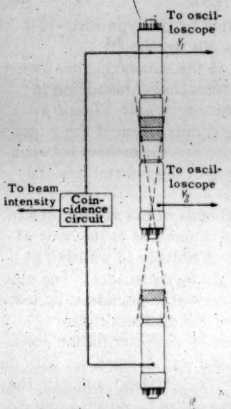

FIG. 5. Diagram of location of scintillation counters for calibration with cosmic-ray μ mesons.

cases in which pulses were registered from both working counters. This triple-coincidence method selected the vertical component of the cosmic radiation, incident normally on the working surfaces of the scintillators. After the spectrum had been constructed and the energy lost by minimum-ionization μ mesons in the polystyrene[10,11] had been computed, and the correction had been applied for the difference of the light yields for μ mesons and electrons,[12] a second calibration point was obtained in the neighborhood of 3.5 Mev. The Landau curve constructed on the basis of these measurements is shown in Fig. 6.

The linearity of the scintillation counters was checked by means of a β-ray spectrometer calibrated with the conversion line of Ba^{137}. This gave a number of points up to energy 2 Mev; to within 2.5 percent these fell on the straight line

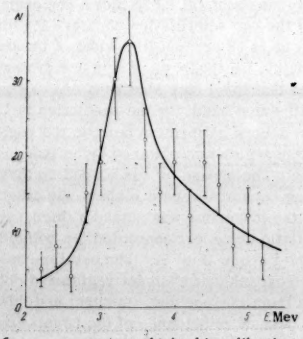

FIG. 6. μ-meson spectrum obtained in calibration of the scintillation counters.

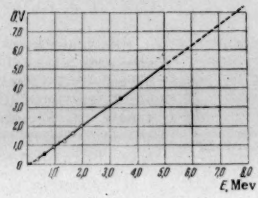

FIG. 7. Calibration curve of the scintillation counters of the measuring head (the abscissas are electron energies; the ordinates are amplitudes of pulses from the scintillation counter). •)– reference points; ○ – from β-ray spectrometer.

connecting the two reference points obtained with Ba^{137} and the Landau curve. The calibration curve for the scintillation counters of the measuring head is shown in Fig. 7.

5. THE CONTROL EXPERIMENTS

1. The electron-counting efficiency of the measuring-head scintillation counters for counting electrons was compared with the efficiency of end-window Geiger counters with window thickness 4 mg/cm^2. It was found that in all cases the counting rate when the scintillation counter was used was 8 percent higher than with the Geiger counter. Consequently the counters used in our apparatus had an efficiency for counting electrons not less than that of a Geiger counter, whose efficiency is known to be close to 100 percent.

2. The choice of the discrimination threshold in the liquid scintillation counter circuit was made experimentally. For this purpose a curve was obtained showing the dependence of the counting rate of the number of coincident pulses in the measuring head (for constant threshold of the total energy) on the counting rate of the liquid scintillator. The results of these measurements are shown in Fig. 8. The shape of the curve shows that when the number of inhibiting pulses is larger than 2×10^5 per minute

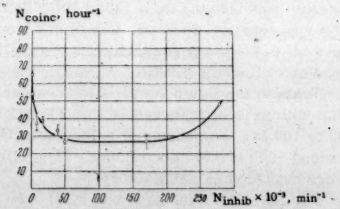

FIG. 8. Dependence of the counting rate of coincident pulses from the measuring head on the counting rate of the liquid scintillator.

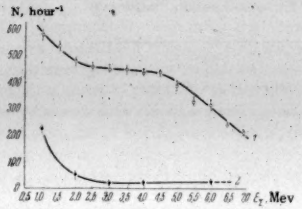

FIG. 9. Integrated spectrum of coincident pulses: 1) on the surface; 2) underground at a depth of 65 m water equivalent.

the shielding by anticoincidences becomes less effective owing to the increase of the dead time of the anticoincidence circuit, whereas for a number of inhibiting pulses less than 4×10^4 per minute the shielding effectiveness is still insufficient. The presence of a plateau indicates that there is adequate shielding effectiveness against most kinds of external radiation. In view of all this, the discrimination threshold of the liquid scintillation counter circuit, operated under these circumstances, was chosen at about 10^5 counts per minute. We estimate that the corresponding energy threshold is about 0.1 Mev for γ radiation.

3. A check on the identity of the calibration of the two counters in the measuring head was carried out under the following conditions. All the units of the apparatus were fully actuated, and photographic registration of the energy spectrum was obtained for 12 hours. To shorten the time of the measurement the tests were carried out not under the conditions of the experiment, under the ground, but on the surface. The energy spectra were compared with each other; besides this, comparisons were made between the sums of the amplitude values of the pulses for each of the channels. The total energy of all the pulses registered by one of the counters of the measuring head was 8959 Mev, that for the other counter, 8983 Mev. The good agreement of both the spectra and the amplitude totals indicates that there is identity of the calibrations of the two counters.

4. The integrated energy spectrum of the sum of the coincident pulses was taken both on the surface and underground. These tests were to determine the effect of the operating conditions on the background, i.e., on the counting rate of coincident pulses. The measurements were carried out with the measuring head not shielded by the liquid scintillator. The results are shown in Fig. 9.

The comparison of the counting rates for total energy 3 Mev shows that burying the apparatus under the ground leads to a decrease of the background by a factor of 23. Thus it is quite expedient

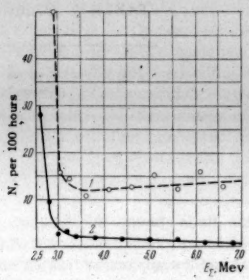

FIG. 10. Energy spectra of background of two sets of apparatus for measuring double β decay: 1) 1956; 2) 1957; ΔE = 0.2 Mev.

to make the measurements underground.

5. The effects of shielding by anticoincidences and of screening with lead were strikingly demonstrated in the following experiment. The completely assembled apparatus was set for registration of coincidences with the threshold at a total energy of 1 Mev. Numbers of coincidences in 1 hour were compared with the anticoincidence circuit turned on and with this circuit turned off; in the former case 17 coincidences were recorded, in the latter case 56. After this the apparatus was surrounded on all sides with a layer of lead 10 cm thick, and the measurement was repeated with the anticoincidence circuit turned on. Seven coincidences were registered during two hours. Thus the use of the lead shield leads to a further lowering of the background of coincidence counts by a factor of 5.

The control experiments that have been described confirmed the correctness of the calibration of the apparatus, provided a reasonable choice of the discrimination threshold, and demonstrated the effectiveness of the protections against background counts that were used in the experiment. This last point is illustrated by Fig. 10, which shows the energy spectra of the background for the apparatuses for measuring double β decay used by the writers in 1956[13]* and in the present work. It must be remarked, however, that the apparatus was relatively poorly shielded against neutron radiation.

6. THE MEASUREMENTS AND THE PROCESSING OF THE RESULTS

The conditions under which the measurements were made are, properly speaking, clear from the

*In Fig. 2 of reference 13, through an oversight of the editors, the energy scale is displaced to the right by 0.5 Mev.

TABLE I. Comparison of spectra from first and second series of measurements

E, Mev	Ca^{48}		Ca^{44}	
	Series 1	Series 2	Series 1	Series 2
3—4	1.16±0.52	1.00±0.58	0.93±0.47	2.00±0.82
4—5	1.16±0.52	0.67±0.47	0.93±0.47	0.00
5—6	0.92±0.47	1.00±0.58	0.23±0.23	0.33±0.33
6—7	0.23±0.23	0.33±0.33	0.47±0.33	0.33±0.33

information given above. The measurements were carried out under ground at a depth of 65 m water equivalent, and the apparatus was shielded against the effects of the external background by the anti-coincidence circuit and by a lead screen. Two series of measurements were carried out, the first in December 1956 – January 1957, and the second in July – August 1957. The time of measurement with each of the specimens was 430 hours in the first series and 300 hours in the second.

The stability of the parameters of the apparatus during the time of the measurements was checked automatically. The constancy of the operating conditions of the counters in the measuring head was checked regularly by the values of the voltage and current in the circuit of the VS-9 high-voltage rectifier that supplied the counters, and also by the constancy of the counts of both coincident and single pulses coming from the measuring head.

The measurements provided films on which were registered the amplitude distributions of the coincident pulses that came in the course of the experiment from the photomultipliers of the measuring head. After the amplitudes had been measured the spectra obtained were subjected to statistical analysis. For this purpose the whole time of the measurements was divided into equal intervals, and for each of the photomultipliers the numbers of pulses of amplitude exceeding a prescribed value that arrived within each interval were counted. The two series of numbers so obtained were analyzed both from the point of view of agreement with the Poisson distribution, and as to whether they agreed with each other. The results of the analysis showed that no crude errors came in in the process of handling the photographic films, verified the identical functioning of the two scintillation counters, and showed the stability of the operation of the apparatus as a whole.

As has already been mentioned, two series of measurements were made. For each of the series the spectra of the total energies of the coincident pulses were constructed, and a comparison of these spectra was made. The results of the comparison are shown in Table I. This table gives the counting rates per 100 hours of observation for the energy intervals indicated.

As can be seen from these data, the agreement of the spectra is quite satisfactory. After the processing of the results had shown that the laws of statistics are obeyed and that the spectra of the two series are in agreement with each other, these spectra were combined into the total spectra shown in Fig. 11

7. DISCUSSION OF THE RESULTS; CONCLUSIONS

To interpret the obtained results we have first to find out in what energy interval we must compare the spectra for Ca^{48} and Ca^{44}. The energy interval in which the effect of double β decay is to be sought depends on the expected energy of the decay, the assumptions about the process, and the energies lost by the electrons in the material of the specimens used. Let us examine this problem, starting from the assumption of the "neutrinoless" decay process, in which the entire energy released in the decay is divided between the two electrons.

For the case of Ca^{48} the energy of the decay is known with adequate accuracy from mass-spectrographic data,[14] and has the value 4.3 ± 0.1 Mev. The average total energy loss of the electrons that emerge from the material of the specimen in such

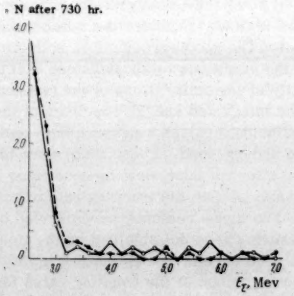

FIG. 11. Spectra of total energies of coincident pulses obtained in 730 hours of measurement with each of the specimens: solid line – Ca^{48}; dashed line – Ca^{44}; $\Delta E_2 = 0.2$ Mev.

a way that they go into different counters was determined by computation. For the specimens used in the present experiment it is 0.4 Mev, and corresponds to the energy loss of a relativistic electron in a path length equal to twice the thickness of the specimen. The computation was made on the assumption of absence of angular correlation between the decay electrons. According to this the search for the effect should be made in the region of 3.9 Mev.

The width of the energy interval in which one should compare the spectra of Ca^{48} and Ca^{44} depends both on the errors of the apparatus and also on a possible "smearing out" of the spectrum of the total energy of the electrons from double β decay. The probable errors introduced by the apparatus are the following:

1. The spread in amplitude introduced by each scintillation counter (± 5.6 percent).

2. The error in the energy calibration of the scintillation counters (± 3 percent).

3. The lack of stability of the gain coefficient of the apparatus (± 1.5 percent).

4. Errors in measurements on the film (± 1.5 percent).

Thus, taking account of the fact that two counters were functioning simultaneously, we get for the root-mean-square error of the apparatus ± 9 percent, which corresponds to a spread of ± 0.35 Mev in the energy. To be on the safe side we increase this figure to 0.5 Mev.

The effect of "smearing out" of the spectrum, owing to the spread of the amount of energy lost by the electrons in the material of the specimen, should lead to a shift of the maximum of the spectrum toward lower energies. This has been partly taken into account in the introduction of the correction for the loss of energy in the material of the specimen, and the part not so included can scarcely exceed 0.4 Mev.

Thus the spectra of the total energy of the electrons is to be analyzed in the region from 3.0 to 4.4 Mev. As can be seen from Fig. 11, in this energy range during the 730 hours there were registered 11 cases of coincidences when the specimen enriched in Ca^{48} was between the scintillation counters, and 12 cases for the specimen of Ca^{44}. The difference "Ca^{48} - Ca^{44}" consequently is $(-1 \pm 4.8)/730$ counts per hour, or (-0.14 ± 0.66) counts per 100 hours.

The half-life was determined from the formula

$$\tau = \ln 2 \frac{N_0}{A} \frac{k m \eta}{\Delta n},$$

where m is the amount of the substance to be studied contained in the specimen (in grams); A is the mass number; Δn is the difference of the numbers of counts per unit time from the working and control specimens; k is a factor corresponding to the geometrical effectiveness for coincidence counting, on the assumption of isotropic distribution of the decay electrons; η is a coefficient characterizing the "transparency" of the specimen for the decay electrons; and N_0 is Avogadro's number. The coefficient η was calculated on the assumption of no angular correlation between the decay electrons and for the energy distribution function of these electrons given in reference 5; it was found to be 0.52. The value of the coefficient k, as determined on the basis of the value of the solid angle over which each of the counters "saw" the specimen, was 0.43. After inserting the numerical values of the quantities one gets the following numerical formula for the half-value period:

$$\tau = \frac{0.9}{\Delta n} \cdot 10^{18} \text{ years},$$

where Δn is per hundred hours.

Following the established tradition, we shall give here the value of the half-life calculated on the assumption of no angular correlation between the decay electrons. Inclusion of the theoretically expected angular correlation[15] would lead to a decrease of both the figures given in the present paper and of those in other papers on searches for double β decay by about a factor of three.

The extremely small intensity of the count in the energy range in question, and the consequent high probability of considerable statistical fluctuations, lead to the danger of obtaining false conclusions if one regards as significant differences values of Δn greater than just a single standard error σ. Only results exceeding at least twice the standard error can be given any weight. An analysis of the spectra obtained here shows that there is not a single energy interval of reasonable width in the range from 2.4 to 7.0 Mev in which Δn would exceed 2σ. Therefore we can determine only a lower limit to the half-life for double β decay of Ca^{48}. Using the numerical formula and inserting instead of Δn the quantity 2σ, we find that the half-life for double decay of Ca^{48} is not less than $0.7 \cdot 10^{19}$ years.

Thus the result of our measurements is a negative one. Clearly a further reduction of the background could not bring any change in the situation, because a colossal length of time is needed for reliable measurements with a small quantity of the material. Thus there remains only one way to make further progress — increasing the actual

TABLE II

Year	Reference	Result	Method
1955	McCarthy[16]	1.1×10^{17} years (+)	Scintillation counters
1956	The writers[13]	$> 1 \times 10^{18}$ years	" "
1956	Awschalom[17]	$\geq 2 \times 10^{18}$ years	" "
1957	Present paper	$\geq 0.7 \times 10^{19}$ years	" "

mass of the isotopes studied. If besides this one is able to increase the dimensions of the counters, then the need will arise for a further decrease of the background. This last may be possible only after a detailed study of the factors determining the shape of the energy spectrum of the background. This problem is not considered in the present paper.

Let us sum up. In Table II are collected the results of the experiments made to search for double β decay in Ca^{48}. In this table the sign "plus" indicates a positive result of the search.

The lower limit now obtained on the half-value period of the double decay is larger by almost an order of magnitude than the value corresponding to incomplete polarization of the neutrino. Therefore it can be asserted that the experimental result of our study agrees with the two-component theory of the neutrino, in which the degree of polarization is 100 percent. The possibility of a two-component scheme with occurrence of double β decay through forbidden transitions (with nonconservation of the leptonic charge) remains open.

The necessary reservations limiting the certainty of the conclusions we have drawn, owing to lack of accurate knowledge of the nuclear matrix element and the degree of angular correlation of the electrons, have already been pointed out in the text.

The writers take occasion to express their sincere appreciation to I. S. Shapiro for an interesting and fruitful discussion of the problem of double β decay. We are also deeply grateful to I. V. Galkin for building the electronic part of our apparatus and to K. S. Mikhailov for the syntheses and the preparation of the scintillators.

[1] W. H. Furry, Phys. Rev. **56**, 1184 (1939).

[2] L. A. Sliv, J. Exptl. Theoret. Phys. (U.S.S.R.) **20**, 1035 (1950).

[3] M. G. Mayer and V. L. Telegdi, Phys. Rev. **107**, 1445 (1957).

[4] I. S. Shapiro, Report at the All-Union Conference on Nuclear Reactions at Low and Moderate Energies, 1957; Izv. AN SSSR, Ser. Fiz. (1958, in press).

[5] Zel'dovich, Luk'yanov, and Smorodinskii, Usp. Fiz. Nauk **54**, 361 (1954).

[6] R. Davis, Report at the International Conference on the Use of Radioactive Isotopes for Scientific Purposes, Paris 1957.

[7] K. A. Petrzhak and M. A. Bak, J. Tech. Phys. (U.S.S.R.) **25**, 636 (1955).

[8] Nemilov, Ovchinnikov, Pisarevskii, and Teterin, J. Atomic Energy (U.S.S.R.) No. 4, 51 (1956).

[9] Vil'dgrube, Zharkov, and Teterin, Izv. AN SSSR, Ser. Fiz. **21**, 1034 (1957) [Columbia Tech. Transl. 21, 1035 (1957)].

[10] N. A. Dobrotin, Космические лучи (Cosmic Rays), GTTI, Moscow 1954.

[11] B. Rossi, High-Energy Particles, (Russ. Transl.) GTTI, Moscow, 1955, p. 38 (New York, (1952).

[12] G. T. Wright, Phys. Rev. **91**, 1282 (1953).

[13] Dobrokhotov, Lazarenko, and Luk'yanov, Dokl. Akad. Nauk SSSR **110**, 966 (1956), Soviet Phys. "Doklady" **1**, 600 (1956).

[14] Collins, Nier, and Johnson, Phys. Rev. **86**, 408 (1952).

[15] H. Primakoff, Phys. Rev. **85**, 888 (1952).

[16] J. A. McCarthy, Phys. Rev. **97**, 1234 (1955).

[17] M. Awschalom, Phys. Rev. **101**, 1040 (1956).

Translated by W. H. Furry

SOVIET PHYSICS JETP VOLUME 36 (9), NUMBER 1 JULY, 1959

SYMMETRY GROUP OF THE ISOTROPIC OSCILLATOR

Yu. N. DEMKOV

Leningrad State University

Submitted to JETP editor January 23, 1958

J. Exptl. Theoret. Phys. (U.S.S.R.) **36**, 88-92 (January, 1959)

It is shown that the determination of the isotropic oscillator group by means of infinitesimal operators and generating elements, given earlier by the author, and the determination by means of canonical transformations, given by Baker, are equivalent. The explicit form of the unitary operators of the group is considered and their relation to the Green's function for the oscillator is demonstrated.

We consider an n-dimensional isotropic oscillator and we choose the system of units in such a way that the frequency, Planck's constant, and the mass are all equal to unity. Then the energy operator for the system has the form

$$H = \frac{1}{2}\sum_{k=1}^{n}(p_k^2 + x_k^2), \tag{1}$$

while the energy levels of the sytem

$$E_m = m + n/2 \quad (m = 0, 1, 2, \ldots) \tag{2}$$

are degenerate, with this degeneracy not being accounted for solely by the spherical symmetry of the system.

The symmetry group of the isotropic oscillator which explains the additional degeneracy of the energy levels and which is closely connected with the symmetry between the coordinates and momenta of the system was originally investigated by the author.[1,2] The group of unitary operators commuting with the Hamiltonian was determined by means of generating operators (rotations and one-dimensional Fourier transformations), all possible products of which from the group. Moreover, the infinitesimal operators of the group were obtained and the commutation relations between them were studied.

In Baker's paper[3] the symmetry group of the oscillator was investigated from a somewhat different point of view; the elements of the group were defined by means of a canonical transformation which leaves the Hamiltonian invariant. It was also shown that the symmetry group of the n-dimensional isotropic oscillator is isomorphic with the n-dimensional unitary group.

The relation between the two points of view in the case of the two dimensional oscillator was partially discussed by Alliluev.[4] It turned out that in this case in order to explain the additional degeneracy it is sufficient to consider the unimodular unitary group (which is isomorphic to the group of three dimensional rotations), whose infinitesimal operators are linear combinations of the corresponding operators of references 1 and 2.

We shall show here that the two methods of determining the symmetry group are equivalent in the general case.

We shall first of all establish that the commutation relations between the infinitesimal operators

$$\begin{aligned} H_x &= p_x^2 + x^2; \quad M_x = yp_z - zp_y, \quad N_x = p_y p_z + yz, \\ H_y &= p_y^2 + y^2, \quad M_y = zp_x - xp_z, \quad N_y = p_z p_x + zx, \\ H_z &= p_z^2 + z^2, \quad M_z = xp_y - yp_x, \quad N_z = p_x p_y + xy, \end{aligned} \tag{3}$$

which were obtained in references 1 and 2, coincide with the commutation relations between the infinitesimal matrices of the three dimensional linear unitary group. Indeed, the matrix of an infinitesimal linear unitary transformation may be written in the form

$$U = I + i\varepsilon L, \tag{4}$$

where I is the unit matrix, L is an arbitrary Hermitean matrix, and ϵ is the smallness parameter. It may be seen from this that as linearly independent infinitesimal matrices we can choose the n^2 matrices M^{ij}, N^{ij} with the following elements

$$M_{rs}^{ij} = i(\delta_{ir}\delta_{js} - \delta_{is}\delta_{jr}), \quad N_{rs}^{ij} = \delta_{ir}\delta_{js} + \delta_{is}\delta_{jr}. \tag{5}$$

The commutation relations between these matrices are of the form

$$\begin{aligned} [M^{ij}, M^{kl}] &= iM^{il}\delta_{jk} - iM^{ik}\delta_{jl} - iM^{jl}\delta_{ik} + iM^{jk}\delta_{il}, \\ [M^{ij}, N^{kl}] &= iN^{il}\delta_{jk} + iN^{ik}\delta_{jl} - iN^{jl}\delta_{ik} - iN^{jk}\delta_{il}, \\ [N^{ij}, N^{kl}] &= -iM^{il}\delta_{jk} - iM^{ik}\delta_{jl} - iM^{jl}\delta_{ik} - iM^{jk}\delta_{il}. \end{aligned} \tag{6}$$

If we now set n = 3

$$N^{11} = H_x, \quad N^{12} = N_z, \quad M^{12} = -M_z,$$
$$N^{22} = H_y, \quad N^{23} = N_x, \quad M^{23} = -M_y,$$
$$N^{33} = H_z, \quad N^{31} = N_y, \quad M^{31} = -M_z, \tag{7}$$

we obtain the commutation relations between the operators (3) which were given in reference 2.* Thus, the symmetry group determined in references 1 and 2 is isomorphic to the unitary group, and consequently is also isomorphic to the symmetry group discussed by Baker.† The generalization to the case n > 3 is trivial.

We now show that the two groups are equivalent, i.e., that the unitary operators which carry out Baker's canonical transformations coincide with the operators discussed in references 1 and 2.

Baker[3] introduces the non-Hermitian operators

$$a_k = (x_k + ip_k)/\sqrt{2}, \quad a_k^+ = (x_k - ip_k)/\sqrt{2}, \tag{8}$$

while the unitary matrix U corresponds to the canonical transformation

$$a_k' = \sum_{l=1}^{n} U_{kl} a_l, \quad a_k'^+ = \sum_{l=1}^{n} U_{kl}^* a_l^+. \tag{9}$$

It may be easily seen that such a transformation leaves invariant the operator H and the commutation relations between the operators a_k and a_k^+. To construct the unitary operator which corresponds to this canonical transformation we return to the variables x_k, p_k. On utilizing (8) and (9), we obtain

$$x_k' = \sum_{l=1}^{n} (A_{kl}x_l - B_{kl}p_l), \quad p_k' = \sum_{l=1}^{n} (B_{kl}x_l + A_{kl}p_l), \tag{10}$$

$$x_k = \sum_{l=1}^{n} (A_{lk}x_l' + B_{lk}p_l'), \quad p_k = \sum_{l=1}^{n} (-B_{lk}x_l' + A_{lk}p_l'), \tag{11}$$

where

$$U_{kl} = A_{kl} + iB_{kl} \tag{12}$$

and A_{kl}, B_{kl} are real. The unitary operator which corresponds to this transformation may be easily obtained in integral form; its kernel $f_U(x_1, x_2, \ldots, x_n;\ x_1', x_2', \ldots, x_n')$ will be an eigenfunction of the operators x_k in the x'-representation corresponding to the eigenvalues x_k, while f_U^* will be an eigenfunction of the operators x_k' in the x-representation corresponding to the eigenvalues x_k'. This condition determines the kernel f_U up to a factor independent of x_k, x_k'.

We consider a special case of the transformation (10), (11), when only one pair of coordinates and momenta is transformed. In this case we may without loss of generality consider the one-dimensional oscillator. Then U = exp iφ, A = cos φ, B = sin φ and the kernel of the corresponding integral operator satisfies the following equations

$$-i\sin\varphi\cdot\partial f/\partial x + \cos\varphi\cdot xf = x'f,$$
$$i\sin\varphi\cdot\partial f^*/\partial x' + \cos\varphi\cdot x'f = xf. \tag{13}$$

From this we obtain

$$f_\varphi(x, x') = C(\varphi)\exp[ixx'/\sin\varphi - (i/2)(x^2 + x'^2)\cot\varphi]. \tag{14}$$

The coefficient C(φ) may be determined by requiring that the operator acting on the ground state wavefunction $\exp(-x^2/2)$ should leave it unchanged. Finally we have

$$f_\varphi(x, x') = (2\pi\sin\varphi)^{-1/2}\exp[ixx'/\sin\varphi - (i/2)(x^2 + x'^2)\cot\varphi - i\varphi/2 + i\pi/4]. \tag{15}$$

The corresponding infinitesimal operator may be obtained by evaluating for small values of φ the expression

$$\int_{-\infty}^{+\infty} f_\varphi(x, x')\psi(x')\,dx' \tag{16}$$

(where ψ is an arbitrary function) up to terms proportional to φ. By using the method of steepest descents we obtain

$$\int_{-\infty}^{+\infty} f_\varphi(x, x')\psi(x')\,dx'$$
$$= \psi(x) + i\varphi\left(-\frac{1}{2}\frac{d^2}{dx^2} + \frac{1}{2}x^2 - \frac{1}{2}\right)\psi(x) + O(\varphi^2). \tag{17}$$

Thus, the infinitesimal operator which corresponds to this infinitesimal transformation does indeed coincide up to a constant factor with the operator H_x from formulas (3). The presence of the additional term $-1/2$ is not unavoidable; its introduction does not alter the commutation relations between the operators and leads only to the ground state wavefunction remaining unchanged when the group operator acts upon it.

By utilizing formula (17) we can easily obtain the expansion of the function f_φ in terms of the oscillator eigenfunctions

$$f_\varphi(x, x') = \sum_{m=0}^{\infty} \psi_m(x)\psi_m(x')e^{im\varphi}. \tag{18}$$

This leads directly to the relation between the function f and the Green's function for the one dimensional oscillator

*The commutation relations (19) of reference 2 contain an error: the sign of the right hand side should be reversed in formulas (8) and (11).

†To be more precise, it follows from this that there exists a one-to-one group correspondence between elements belonging to certain regions surrounding the unit elements of the two groups.

$$G(x, x', t) = \sum_{m=0}^{\infty} \psi_m(x)\,\psi_m(x')\,e^{-iEmt} = e^{-it/2} f_{-t}(x, x')$$

$$= (2\pi \sin t)^{-1/2} \exp[-ixx'/\sin t + (i/2)(x^2 + x'^2)\cot t - i\pi/4]. \quad (19)$$

When $t = \pi/2 = T/4$, where $T = 2\pi$ is the period of oscillation in terms of our units, we obtain up to a constant factor the operator for the one-dimensional Fourier transformation

$$G(x, x', T/4) = (2\pi)^{-1/2} \exp(-ixx' - i\pi/4). \quad (20)$$

Thus, if at time $t = 0$ the oscillator wavefunction in the x-representation is given by $\psi_0(x)$, while in the p-representation it is given by $\varphi_0(p)$, then at subsequent times it will vary in the following manner:

$t =$	0	$T/4$	$T/2$	$3T/4$	T
ψ:	$\psi_0(x)$	$e^{-i\pi/4}\varphi_0(x)$	$e^{-i\pi/2}\psi_0(-x)$	$e^{-i3\pi/4}\varphi_0(-x)$	$e^{-i\pi}\psi_0(x)$
φ:	$\varphi_0(p)$	$e^{-i\pi/4}\psi_0(-p)$	$e^{-i\pi/2}\varphi_0(-p)$	$e^{-i3\pi/4}\psi_0(p)$	$e^{-i\pi}\varphi_0(p)$.

Consequently the variation of the oscillator wavefunction with time may be obtained by operating on the initial wavefunction with the unitary operator of the symmetry group after setting $\varphi = -t$ in it. This unfolding in time represents a continuous transition from the coordinate wavefunction to the momentum wavefunction and conversely.

We now consider a second type of transformation in which two pairs of coordinates and momenta take part. Let the unitary matrix be of the form

$$U = \begin{pmatrix} \cos\varphi, & i\sin\varphi \\ i\sin\varphi, & \cos\varphi \end{pmatrix}. \quad (21)$$

These matrices form a group, and for small values of φ have the form

$$U = \begin{pmatrix} 1, & 0 \\ 0, & 1 \end{pmatrix} + i\varphi \begin{pmatrix} 0, & 1 \\ 1, & 0 \end{pmatrix} + O(\varphi^2), \quad (22)$$

i.e., the infinitesimal operator of this subgroup corresponds to the nondiagonal operator N^{ij} of the oscillator symmetry group. Transformation of coordinates in this case has the form

$$x_1' = \cos\varphi \cdot x_1 - \sin\varphi \cdot p_2, \quad x_1 = \cos\varphi \cdot x_1' + \sin\varphi \cdot p_2',$$
$$x_2' = \cos\varphi \cdot x_2 - \sin\varphi \cdot p_1, \quad x_2 = \cos\varphi \cdot x_2' + \sin\varphi \cdot p_1'. \quad (23)$$

By constructing a system of equations analogous to system (13) and by determining the normalization coefficient in the same manner we obtain

$$f_\varphi(x_1, x_2; x_1', x_2') \quad (24)$$
$$= (2\pi \sin\varphi)^{-1} \exp[i(x_1x_2' + x_1'x_2)/\sin\varphi - i(x_1x_2 + x_1'x_2')\cot\varphi].$$

Finally, by evaluating by the method of steepest descents the result of the action of the operator on an arbitrary function for small values of φ, we obtain

$$\int_{-\infty}^{+\infty}\int_{-\infty}^{+\infty} f_\varphi(x_1, x_2; x_1', x_2')\,\psi(x_1', x_2')\,dx_1'dx_2' \quad (25)$$
$$= \psi(x_1, x_2) + i\varphi(-\partial^2/\partial x_1\partial x_2 + x_1x_2)\,\psi(x_1, x_2) + O(\varphi^2).$$

The resultant infinitesimal operator coincides with the operators N in formulas (3).

The third type of transformation corresponding to the matrix

$$U = \begin{pmatrix} \cos\varphi, & -\sin\varphi \\ \sin\varphi, & \cos\varphi \end{pmatrix}, \quad (26)$$

as may be easily seen, does not mix coordinates and momenta, and represents a pure rotation in the x_1, x_2 plane. In this case the infinitesimal operator will be given by the corresponding component of angular momentum.

Thus, the infinitesimal operators of the groups determined in references 1, 2, and 3 are the same. Moreover, the generating elements of the group defined in references 1 and 2 are contained in the group defined in reference 3. From this it follows that the two groups coincide.

Finally, we shall obtain up to a normalizing factor the explicit form of the kernel of the integral operator for an arbitrary matrix U. In this case the function $f(X, X')$ satisfies the system of equations

$$(\tilde{A}X' - i\tilde{B}\nabla')f = Xf, \quad (AX - iB\nabla)f = X'f, \quad (27)$$

where obvious matrix notation has been used, while $\tilde{A}$, $\tilde{B}$ denote transposed matrices. By multiplying the two equations respectively by $\tilde{B}^{-1}$ and B^{-1} we obtain

$$\nabla' f/f = i\tilde{B}^{-1}X - i\tilde{B}^{-1}\tilde{A}X', \quad \nabla f/f = iB^{-1}X' - iB^{-1}AX. \quad (28)$$

From the fact that the matrix U is unitary it follows directly that the matrices $\tilde{B}^{-1}\tilde{A}$, $B^{-1}A$ are symmetric and, consequently, that the equations (28) are soluble. On solving them we obtain the general form for the kernel of the integral operator

$$f = C\exp[i\tilde{X}B^{-1}X' - (i/2)(\tilde{X}'AB^{-1}X' + \tilde{X}B^{-1}AX)]. \quad (29)$$

The coefficient C may again be determined from the requirement that the operator should leave the ground state function unchanged.

In conclusion we note that the isotropic oscillator is an example of a system in which the energy operator is completely expressed in terms of the infinitesimal operators of the symmetry group. In

such cases in principle it is possible to obtain from just the symmetry properties of the system all its other properties (energy levels, degree of degeneracy, the Green's function etc.).

[1] Yu. N. Demkov, J. Exptl. Theoret. Phys. (U.S.S.R.) **26** [sic!] 757 (1954).

[2] Yu. N. Demkov, Bull. Leningrad State Univ. No. 11, 127 (1953).

[3] G. A. Baker, Phys. Rev. **103**, 1119 (1956).

[4] S. P. Alliluev, J. Exptl. Theoret. Phys. (U.S.S.R.) **33**, 200 (1957), Soviet Phys. JETP **6**, 156 (1958).

Translated by G. Volkoff
13

ANGULAR MOMENTUM AND PARITY CONSERVATION LAWS IN THE STATISTICAL THEORY OF MULTIPLE PRODUCTION

V. B. MAGALINSKII

Moscow State University

Submitted to JETP editor April 26, 1958

J. Exptl. Theoret. Phys. (U.S.S.R.) **36**, 93-97 (January, 1959)

The general statistical method of the microcanonical distribution is employed to calculate the statistical weights of a many-particle system obeying an arbitrary statistics. The conservation laws for angular momentum and parity are taken into account. A general computational formula is obtained under the assumption that all particles obey Boltzmann statistics.

We consider a system of N identical particles obeying arbitrary statistics. The particles have an intrinsic parity λ. The total angular momentum L and the total parity I are given. Furthermore, it is assumed that the orbital angular momentum of each particle is bounded from above by some maximal value $\bar{l}$, since the particles are produced in a limited region and possess, by the conservation laws, a finite momentum. Hence $0 \leq l \leq \bar{l}$.

For the determination of the statistical weight (the number of states) of the system under consideration, for given L and I, it is sufficient to calculate the number of states $F_{N,\bar{l}}(M, I)$ with a given projection M of the total angular momentum (and with a given I). The number of states with given L and I, $G_{N,\bar{l}}(L, I)$, is then determined with the help of well-known Slater condition (see, e.g., reference 1):

$$G_{N,\bar{l}}(L, I) = F_{N,\bar{l}}(L, I) - F_{N,\bar{l}}(L+1, I). \quad (1)$$

For the calculation of $F_{N,\bar{l}}(M, I)$ one can effectively use the microcanonical distribution, since M is an additive integral of the system.

Each microstate of our system is completely determined by the set of occupation numbers n_s, where s denotes the set of magnetic (m) and azimuthal (l) quantum numbers defining the state of the particle.

The number of states with given M and I is equal to

$$F_{N,\bar{l}}(M, I) = \sum_{(n)} \delta\Big(M - \sum_s m n_s\Big)\, \delta\Big(N - \sum_s n_s\Big) \frac{1}{2} \prod_s \times \Big\{1 + I \prod_s [\lambda(-1)^{l n_s}]\Big\} \Omega(n) \equiv \frac{1}{2} F_{N,\bar{l}}(M) + \frac{I}{2} F'_{N,\bar{l}}(M), \quad (2)$$

where $\Omega(n)$ is the degeneracy of a given microstate:

$$\Omega(n) = \begin{cases} = 1 \text{ for bosons; } n_s = 0, 1, 2\ldots \\ = 1 \text{ for fermions; } n_s = 0, 1. \\ = N! \Big(\prod_s n_s!\Big)^{-1} \text{ in the case of Boltzmann} \\ \text{statistics; } n_s = 0, 1, 2\ldots \end{cases}$$

The factor $\frac{1}{2}\{1 + I \prod_s [\lambda(-1)^l]^{n_s}\}$ guarantees parity conservation in each microstate; $\delta(m-n) \equiv \delta_{m,n}$, the Kronecker symbol.

The summation goes over all microstates of the system, and also over all quantum numbers within each microstate:

$$\sum_s f(s) = \sum_{l=0}^{\bar{l}} \sum_{m=-l}^{l} f(l, m). \quad (3)$$

In the following calculations we make use of the integral representation of the δ symbol:

$$\delta(a-b) = (2\pi i)^{-1} \oint z^{b-a-1} dz, \quad (4)$$

Each term in the expression under the integral for $F_{N,\bar{l}}(M)$ and $F'_{N,\bar{l}}(M)$ is rewritten according to (4).

We obtain in the usual fashion (see, e.g., reference 2)

$$F'_{N,\bar{l}}(M) = (2\pi i)^{-2} \oint\oint x^{-M-1} y^{-N-1} dx\, dy \times \sum_{(n)} x^{\sum m n_s} y^{\sum n_s} \prod_s [\lambda(-1)^l]^{n_s} \Omega(n) = (2\pi i)^{-2} \oint\oint x^{-M-1} y^{-N-1} dx\, dy \prod_s \sum_{n_s} [\lambda y x^m (-1)^l]^{n_s} \Omega(n) = (2\pi i)^{-2} \oint\oint x^{-M-1} y^{-N-1} dx\, dy \exp \Phi(x, y), \quad (5)$$

where

$$\Phi(x, y) = \alpha \sum_s \ln |1 - \alpha y x^m (-1)^l|; \quad (6)$$

$\alpha = +1$ for bosons, and $\alpha = -1$ for fermions. Expanding the logarithm into a series and summing

each term over s, we obtain

$$\Phi(x, y) = \sum_{k=1}^{\infty} \frac{\alpha^{k+1} \gamma_k}{k} \Phi_1(x^k) y^k, \tag{7}$$

where

$$\Phi_1(z) = \sum_{l=0}^{\bar{l}} (-1)^l \sum_{m=-l}^{l} z^m$$

$$= z^{-\bar{l}} (-1)^{\bar{l}} (1 - z^{2(\bar{l}+1)}) / (1 - z^2). \tag{8}$$

We integrate (5) over y, and obtain, by the law of residues,

$$F'_{N,\bar{l}}(M) = (2\pi i)^{-1} \oint x^{-M-1} dx \frac{1}{N!} \left[\frac{d^N}{dy^N} \exp \Phi(x, y) \right]_{y=0}, \tag{9}$$

or, since $F'_{N,\bar{l}}(M) = F'_{N,\bar{l}}(-M)$,

$$F'_{N,\bar{l}}(M) = (2\pi i)^{-1} \oint x^{M-1} dx \frac{1}{N!} \left[\frac{d^N}{dy^N} \exp \Phi(x, y) \right]_{y=0}. \tag{9'}$$

Using the expression for the N-th derivative of a complex function (see, e.g., reference 3), we may also write this result in the explicit form

$$F'_{N,\bar{l}}(M) = \lambda^N (-1)^{N\bar{l}} \sum' \frac{\alpha^{N+l}}{1^{i_2 j} \dots l^{k} i! j! \dots k!} \times (2\pi i)^{-1} \oint x^{M-N\bar{l}-1} \varphi^{j}(x) \varphi^{j}(x^2) \dots \varphi^{k}(x^l) dx, \tag{10}$$

where the summation goes over all positive integral roots of the equation $i + 2j + \dots + lk = N$, and

$$\varphi(z) = (1 - z^{2(\bar{l}+1)}) / (1 - z^2). \tag{11}$$

In exactly the same way we obtain

$$F_{N,\bar{l}}(M) = \sum' \frac{\alpha^{N+l}}{1^{i_2 j} \dots l^{k} i! j! \dots k!} (2\pi i)^{-1} \times \oint x^{M-N\bar{l}-1} \psi^{2i}(x) \psi^{2j}(x^2) \dots \psi^{2k}(x^l) dx, \tag{12}$$

where

$$\psi(x) = (1 - x^{\bar{l}+1}) / (1 - x)$$

Finally,

$$F_{N,\bar{l}}(M, I) = \frac{1}{2} F_{N,\bar{l}}(M) + \frac{I}{2} F'_{N,\bar{l}}(M). \tag{13}$$

Formulas (10) to (13) give the solution of our problem in the general form, for an arbitrary statistics.

This result can be easily generalized to the case of a mixture of particles obeying different statistics, as was done in reference 2.

The formulas are considerably simplified in the case of Boltzmann statistics. The solution can then be given in explicit form. It is easily seen[2] that it is sufficient to sum the expressions (10) and (12) only over the terms with $i = N$, $j = \dots = k = 0$ and to multiply the result by N!. We then have

$$F_{N,\bar{l}}(M) = (2\pi i)^{-1} \oint x^{M-N\bar{l}-1} \psi^{2N}(x) dx$$

$$= (2\pi i)^{-1} \oint \frac{dx}{x^{N\bar{l}-M+1}} \frac{(1 - x^{\bar{l}+1})^{2N}}{(1 - x)^{2N}}, \tag{12'}$$

$$F'_{N,\bar{l}}(M) = \frac{\lambda^N (-1)^{N\bar{l}}}{2\pi i} \oint x^{M-N\bar{l}-1} \varphi^N(x) dx$$

$$= \frac{\lambda^N (-1)^{N\bar{l}}}{2\pi i} \oint \frac{dx}{x^{N\bar{l}-M+1}} \frac{(1 - x^{2(\bar{l}+1)})^N}{(1 - x^2)^N}. \tag{10'}$$

The integrals (10') and (12') are equal to the residue of the argument function at the point x = 0.

We apply the expansion

$$\left(\frac{1 - z^m}{1 - z} \right)^n = \sum_{i,j} (-1)^i \binom{n}{i} \binom{n + j - 1}{n - 1} z^{mi+j}, \tag{14}$$

where $\binom{n}{i} = C_n^i = n!/i!\,(n-i)!$, to the functions under the integral sign in (10') and (12'). By keeping the terms containing $x^{N\bar{l}-M}$, we find

$$F_{N,\bar{l}}(M) = \sum_{k=0}^{\left[\frac{N\bar{l}-M}{\bar{l}+1}\right]} (-1)^k \binom{2N}{k} \binom{N\bar{l} - M + 2N - 1 - (\bar{l}+1)k}{2N - 1}, \tag{15}$$

$$F'_{N,\bar{l}}(M) = \lambda^N (-1)^{N\bar{l}} \times \sum_{k=0}^{\left[\frac{N\bar{l}-M}{2(\bar{l}+1)}\right]} (-1)^k \binom{N}{k} \binom{(N\bar{l} - M)/2 + N - 1 - (\bar{l}+1)k}{N - 1}, \tag{16}$$

where [x] is the integral part of the number x.

We note that $F'_{N,\bar{l}}(M) = 0$ if $N\bar{l} - M$ is odd. The number of states with given M and I is given by formula (13). Here

$$F_{N,\bar{l}}(M) = \sum_{I=\pm 1} F_{N,\bar{l}}(M, I).$$

Using formula (1), we now find the number of states with given L and I:

$$G_{N,\bar{l}}(L, I) = F_{N,\bar{l}}(L, I) - F_{N,\bar{l}}(L+1, I)$$

$$= \frac{1}{2} [F_{N,\bar{l}}(L) - F_{N,\bar{l}}(L+1)]$$

$$+ \frac{I}{2} \begin{cases} F'_{N,\bar{l}}(L), & \text{if } N\bar{l} - L \text{ is even} \\ -F'_{N,\bar{l}}(L+1), & \text{if } N\bar{l} - L \text{ is odd,} \end{cases} \tag{18}$$

or, with obvious notations,

$$G_{N,\bar{l}}(L, I) = \frac{1}{2} G_{N,\bar{l}}(L) + \frac{1}{2} I (-1)^L G'_{N,\bar{l}} \left[L + \frac{1}{2} (1 - (-1)^{N\bar{l}-L}) \right]. \tag{19}$$

By termwise substitution of expansions (15) and (16) for M = L and M = L + 1, we find, with

$$\binom{n}{m} - \binom{n-1}{m} = \binom{n-1}{m-1},$$

that

$$G_{N,\bar{l}}(L) = \sum_{k=0}^{\left[\frac{N\bar{l}-L}{\bar{l}+1}\right]} (-1)^k \binom{2N}{k} \binom{N\bar{l}-L+2N-2-(\bar{l}+1)k}{2N-2}, \tag{20}$$

$$G'_{N,\bar{l}}(p) = \lambda^N \sum_{k=0}^{\left[\frac{N\bar{l}-p}{2(\bar{l}+1)}\right]} \binom{N}{k} \binom{\frac{1}{2}(N\bar{l}-p)+N-1-(\bar{l}+1)k}{N-1}. \tag{21}$$

It follows from (19) that

$$G_{N,\bar{l}}(L) = \sum_{l=\pm 1} G_{N,\bar{l}}(L, l) \tag{22}$$

is the number of states with a given L (and arbitrary l).

Corrections taking into account the type of statistics can, in any specific case, be calculated with the help of the general formulas (10) and (12).

This method allows the solution of a whole series of similar problems, as, for example, the determination of the statistical weight of a system of particles with arbitrary spin.

If the system consists of N particles with spin s obeying an arbitrary statistics, the statistical weight $g_{N,s} = \sum_S g_{N,s}(S)$ is given by

$$g_{N,s}(S) = f_{N,s}(S) - f_{N,s}(S+1), \tag{1'}$$

$$g_{N,s} = \begin{cases} f_{N,s}(0) & \text{for integer Ns,} \\ f_{N,s}(1/2) & \text{for half odd-integer Ns,} \end{cases} \tag{23}$$

where $g_{N,s}(S)$ is the number of states with total spin S, and

$$f_{N,s}(M) = \sum_{(n)} \delta\left(M - \sum_{m=-s}^{s} m n_m\right) \delta\left(N - \sum_{m=-s}^{s} n_m\right) \Omega(n), \tag{24}$$

is the number of states with a given projection M of the total spin.

Omitting intermediate calculations analogous to those done above, we give the final result.

In our notations, we obtain for an arbitrary statistics,

$$f_{N,s}(M) = \sum \frac{\alpha^{N+l}}{1^{k_1} j! \dots l^{k_l} l! \dots k!} (2\pi i)^{-1} \times \oint x^{M-Ns-1} \Phi^l(x) \Phi^l(x^2) \dots \Phi^k(x^l)\, dx, \tag{25}$$

$$\Phi(z) = (1 - z^{2s+1}) / (1 - z).$$

For the special case of Boltzmann statistics we obtain the closed expressions

$$g_{N,s}(S) = \sum_{k=0}^{\left[\frac{sN-S}{2s+1}\right]} (-1)^k \binom{N}{k} \binom{Ns-S+N-2-(2s+1)k}{N-2}, \tag{26}$$

$$g_{N,s} = \begin{cases} \sum_{k=0}^{\left[\frac{sN}{2s+1}\right]} (-1)^k \binom{N}{k} \binom{sN+N-1-(2s+1)k}{N-1}, \\ \qquad \text{if sN is integral,} \\ \sum_{k=0}^{\left[\frac{sN-1/2}{2s+1}\right]} (-1)^k \binom{N}{k} \binom{sN-1/2+N-1-(2s+1)k}{N-1}, \\ \qquad \text{if sN is half odd-integral.} \end{cases} \tag{27}$$

For the special case $s = 1/2$ formulas (26) and (27) give a well-known result (see, e.g., reference 1). For $s = 1$ we get the result[4] obtained by the combinatorial method.

A problem similar to the one just considered was solved by Barashenkov and Barbashev[5] with the use of recurrence relations. We further remark that the results of references 1, 4, and 5 were obtained for the case of Boltzmann statistics.

In conclusion I take this opportunity to express my gratitude to Prof. Ya. P. Terletskii for suggesting this problem and for his interest in this work.

[1] L. D. Landau and E. M. Lifshitz, Квантовая механика (Quantum Mechanics) Gostekhizdat, 1948, p. 250.

[2] V. B. Magalinskii and Ya. P. Terletskii, J. Exptl. Theoret. Phys. (U.S.S.R.) **32**, 584 (1957), Soviet Phys. JETP **5**, 483 (1957).

[3] I. M. Ryzhik and I. S. Gradshteĭn, Таблицы интегралов (Tables of Integrals), Gostekhizdat, 1951, p. 33.

[4] Y. Yeivin, Phys. Rev. **97**, 1084 (1955).

[5] V. S. Barashenkov and B. M. Barbashov, Nuovo cimento **7**, 19 (1958).

Translated by R. Lipperheide
14

DUAL SCATTERING OF RELATIVISTIC PIONS BY NUCLEONS

V. A. ASTAF' EV

Institute of Nuclear Physics, Moscow State University

Submitted to JETP editor May 9, 1958

J. Exptl. Theoret. Phys. (U.S.S.R.) 36, 98-107 (January, 1959)

The formalism of the dual scattering theory based on invariance of the interaction Hamiltonian under rotations in isotopic and x space is extended to relativistic energies. The expression for the differential cross section is obtained in a form which is convenient for analysis of the experimental data. To illustrate the application of the formal theory, the problem is considered in the approximation of radiation damping theory.

INTRODUCTION

THE production of pions in low-energy meson-nucleon collisions ("dual scattering" of pions) has been considered in a dissertation by d'Espagnat[1] and in a number of other papers.[2-4] The theory developed in these papers is subject to a number of formal limitations: (1) In deriving the equations for the scattering matrix T it is assumed that dual scattering is much less significant than single-meson scattering.* (2) Nucleon recoil is neglected, thus leading to the use of an approximate density function $\rho(1, 2)$ of the final states which is independent of angular variables, with the result that the angular distribution of scattered mesons is distorted at high energies. (3) The differential cross section is derived[1] on the assumption that only s and p waves are important in the scattering.

It is the purpose of the present paper to examine the formalism of the dual scattering theory at relativistic energies. Racah's procedure enables us to derive a formula for the differential cross section which is valid at any energy and can be used conveniently to analyze the experimental angular and momentum distributions of scattered pions (Sec. 3A). The scattering theory establishes an equation that relates the matrix T to the reaction matrix K. In Sections 1 and 2 this equation is studied for moderate relativistic energies, when effects associated with ternary scattering and the production of "new" particles are still small but the nucleon must be regarded as a relativistic particle.

The formalism that is developed is used for a solution of the problem in the approximation of the radiation damping theory (Sec. 3B). Although the damping theory cannot account for experimental scattering results[5] at low energies of the incident meson in the laboratory system $T_{kin} \ll M$ (nucleon rest mass), the results of this section may be of interest in explaining the role of damping at energies comparable with or greater than M.

*We here exclude the nonrigorous procedure based on the assumption that the dual scattering matrix can be represented by the product of a function depending on the energy of the incident meson and a function of the energy of the scattered mesons.[1]

1. K AND T MATRICES IN DUAL SCATTERING

Lippman and Schwinger[6] and Goldberger[7] have shown that an exact statement of the scattering problem leads to a set of two equations in the matrix T and reaction matrix K. The first is determined on a constant-energy surface while the second is determined both on and outside of a constant-energy surface:

$$K_{\beta a} = H_{\beta a} + \mathrm{P}\sum_{\gamma} H_{\beta\gamma} K_{\gamma a} / (E_a - E_\gamma), \tag{1}$$

$$T_{ba} = K_{ba} - i\pi \sum_{c} K_{bc} \delta (E_a - E_c) T_{ca}. \tag{2}$$

Here $H_{\beta a} = (\Phi\beta, \hat{H}\Phi_a)$ is the matrix element of the interaction Hamiltonian for the transition between states a and β (following reference 7, we use the indices b, c for states with $E_b = E_a$ and β, γ for $E_\beta \neq E_a$) and P in (1) indicates that the principal value of the integral is taken.

The probability of a transition from state a to state b is related to the matrix T_{ba} very simply as follows:[6]

$$w_{ba} = 2\pi |T_{ba}|^2 \rho(E_b), \tag{3}$$

where $\rho(E_b)$ is the density of states.*

Let us now consider dual scattering of a pion by a nucleon. In the center-of-mass system a meson with energy W_i and momentum $\mathbf{k}_i = \kappa_i \mathbf{n}_i$ ($\mathbf{n}_i$ is

*We use a system of units in which $m_\pi = c = \hbar = 1$.

the unit vector of direction), the isotopic state of which will be denoted by α ($\alpha = +, -, 0$), collides with a nucleon (energy E_i, momentum $\mathbf{p}_i$, spin s_i and isotopic spin t_i). In the final state we have a nucleon (E_f, $\mathbf{p}_f$, s_f, t_f) and two mesons (W_1, $\mathbf{k}_1$, β) and (W_2, $\mathbf{k}_2$, γ).

It is known that the solution of (1) is difficult and requires a number of field approximations. We confine ourselves to (2) and use (1) only to establish the general form of the reaction matrix K. The interaction operator of the nucleon and meson fields will be the Hamiltonian of symmetric pseudoscalar theory,

$$\hat{H}(x) = g\bar{\Psi}\gamma_5\tau\Psi\varphi + if\bar{\Psi}\gamma_5\gamma_\nu\tau\Psi\frac{\partial\varphi}{\partial x_\nu}, \qquad (4)$$

where Ψ is the nucleon field operator, φ is the meson field operator, τ is the nucleon isotopic spin vector, $\gamma_5 = \beta\gamma^1\gamma^2\gamma^3$ and $\gamma_5 = (\beta\alpha^k, \beta)$. $\hat{H}(x)$ is invariant under rotations and reflections in x space and under rotations in isotopic spin space.

Let Ω_i denote the set of variables that characterize the initial (nucleon-meson) state and let Ω_f denote the variables of the final (nucleon-2 meson) state. When isotopic spin is excluded the corresponding sets of variables will be denoted by ω_i and ω_f.

From the definition of the center-of-mass system,

$$\mathbf{p}_i + \mathbf{k}_i = \mathbf{p}_f + \mathbf{k}_1 + \mathbf{k}_2 = 0, \qquad (5)$$

the nucleon momenta $\mathbf{p}_i$ and $\mathbf{p}_f$ can be expressed in terms of the meson momenta $\mathbf{k}_i$ and $\mathbf{k}_i$, $\mathbf{k}_2$. We then have

$$\omega_i = \{\varkappa_i, \mathbf{n}_i; s_i\}, \qquad \omega_f = \{\varkappa_1, \mathbf{n}_1; \varkappa_2, \mathbf{n}_2; s_f\}, \qquad (6)$$

where $\varkappa_i$, $\varkappa_1$, $\varkappa_2$ are related by energy conservation as follows:

$$E = (M^2 + \varkappa_i^2)^{1/2} + (1 + \varkappa_i^2)^{1/2} \qquad (7)$$

$$= (M^2 + \varkappa_1^2 + \varkappa_2^2 + 2\varkappa_1\varkappa_2(\mathbf{n}_1\cdot\mathbf{n}_2))^{1/2} + (1 + \varkappa_1^2)^{1/2} + (1 + \varkappa_2^2)^{1/2}.$$

The matrix K in isotopic and momentum space is determined through its representation by an iteration series [see Eq. (1)]. It is easily shown from a study of the general term of this series that for interaction (4) the matrix element of K on a constant-energy surface is

$$\langle\Omega_f|K|\Omega_i\rangle = \langle t_f|\tau_\gamma^+\tau_\beta^+\tau_\alpha K_1 + \tau_\beta^+\tau_\gamma^+\tau_\alpha K_2 + \tau_\gamma^+\tau_\alpha\tau_\beta^+ K_3$$

$$+ \tau_\beta^+\tau_\alpha\tau_\gamma^+ K_4 + \tau_\alpha\tau_\gamma^+\tau_\beta^+ K_5 + \tau_\alpha\tau_\beta^+\tau_\gamma^+ K_6|t_i\rangle, \qquad (8)$$

where τ_α are related to the Cartesian components of τ by

$$\tau_\pm = \mp(\tau_x \pm i\tau_y)/\sqrt{2}, \quad \tau_0 = \tau_z. \qquad (9)$$

and each of the K_j ($j = 1, 2, \ldots 6$) can be represented by a linear combination of the pseudoscalars $(\sigma\cdot\mathbf{n}_1)$, $(\sigma\cdot\mathbf{n}_2)$, $(\sigma\cdot\mathbf{n}_i)$ and $i(\mathbf{n}_1\times\mathbf{n}_2\cdot\mathbf{n}_i)\eta$ (where η is the unit matrix) with coefficients that are invariant functions of $\mathbf{n}_1$, $\mathbf{n}_2$, $\mathbf{n}_i$ and $\varkappa_1$, $\varkappa_2$, $\varkappa_3$. Expressing $\varkappa_2$ of (7) as a function of $\varkappa_1$, E and $\cos\theta_{12} = \mathbf{n}_1\cdot\mathbf{n}_2$ and expanding these coefficients in series of the Legendre polynomials $P_{\lambda_1}(\mathbf{n}_1\cdot\mathbf{n}_2)$, $P_{\lambda_2}(\mathbf{n}_2\cdot\mathbf{n}_i)$ and $P_\lambda(\mathbf{n}_1\cdot\mathbf{n}_2)$, we obtain for K_j:

$$\begin{aligned}\langle\omega_f|K_j|\omega_i\rangle = {} & \{A_0 + B_0P_1(\mathbf{n}_1\cdot\mathbf{n}_i) + C_0P_1(\mathbf{n}_2\cdot\mathbf{n}_i) \\ & + D_0P_1(\mathbf{n}_1\cdot\mathbf{n}_2) + \ldots\}(\sigma\cdot\mathbf{n}_i)_{s_fs_i} \\ & + \{A_1 + B_1P_1(\mathbf{n}_1\cdot\mathbf{n}_i) + C_1P_1(\mathbf{n}_2\cdot\mathbf{n}_i) \\ & + D_1P_1(\mathbf{n}_1\cdot\mathbf{n}_2) + \ldots\}(\sigma\cdot\mathbf{n}_1)_{s_fs_i} \\ & + \{\text{symm. terms } 1 \rightleftarrows 2\} + \{A + \ldots\}\, i([\mathbf{n}_1\times\mathbf{n}_2]\cdot\mathbf{n}_i)(\eta)_{s_fs_i},\end{aligned} \qquad (10)$$

where A_0, B_0, ... depend only on $\varkappa_j$, $\varkappa_1$.

The complete matrix $\langle\Omega_f|K|\Omega_i\rangle$ must of course be symmetric with respect to the interchange of all variables of the emitted mesons, $1 \rightleftarrows 2$ (pions are bosons).

For not too high energies ($T_{kin} < 1.5$ Bev) we can in (2) neglect ternary scattering and the production of "new" particles. For dual scattering T is then determined from a system of equations written schematically as follows:

$$\begin{aligned}\langle 1_f, 2_f|T|1_i\rangle = {} & \langle 1_f, 2_f|K|1_i\rangle \\ & - i\pi\sum_{1'}\rho(1')\langle 1_f, 2_f|K|1'\rangle\langle 1'|T|1_i\rangle \\ & - i\pi\sum_{2'}\rho(2')\langle 2_f|K|2'\rangle\langle 1_f, 2'|T|1_i\rangle \\ & - i\pi\sum_{1'}\rho(1')\langle 1_f|K|1'\rangle\langle 1', 2_f|T|1_i\rangle \\ & - i\pi\sum_{1',2'}\rho(1', 2')\langle 1_f, 2_f|K|1', 2'\rangle\langle 1', 2'|T|1_i\rangle;\end{aligned} \qquad (11)$$

$$\langle 1_f|T|1_i\rangle = \langle 1_f|K|1_i\rangle - i\pi\sum_{1'}\rho(1')\langle 1_f|K|1'\rangle\langle 1'|T|1_i\rangle$$

$$- i\pi\sum_{1',2'}\rho(1', 2')\langle 1_f|K|1', 2'\rangle\langle 1', 2'|T|1_i\rangle.$$

Here $\langle 1_f, 2_f|T|1_f\rangle$ is the matrix of dual scattering and $\langle 1_f|T|1_i\rangle$ is the matrix of single-meson scattering. Then density functions $\rho(1)$ and $\rho(1, 2)$ are obtained from δ functions by integrating over the energy. The term

$$X_1 = \sum_{2'}\rho(2')\langle 2_f|K|2'\rangle\langle 1_f, 2'|T|1_i\rangle,$$

for example, describes rescattering of one of the two scattered mesons (meson "2") in another di-

rection (with observation of the conservation laws). The matrices $\langle 1_f | K | 1_i \rangle$ and $\langle 1_f, 2_f | K | 1', 2' \rangle$ are given similarly by (8) and (10).

2. K AND T MATRICES IN THE TOTAL MOMENTS REPRESENTATION

The state of our system is described by the following quantum numbers: The total isotopic spin I, its projection M_I, the total angular momentum J, its projection μ_J, and parity ξ. In addition, the initial state is characterized by the orbital angular momentum l and the final state by the total L and partial l_1, l_2 orbital moments as well as by the isotopic spin Λ of the two-meson system (the isotopic spin of a meson is 1). Since the interaction Hamiltonian is invariant under rotations and reflections K has the following diagonal form in the representation based on eigenstates of total isotopic spin and total angular momentum:

$$(l' M_l' \Lambda';\ J' \mu_J' L (l_1 l_2) \xi' | K | l M_l;\ J \mu_J l_\xi) = K^{I\Lambda}_{JlL(l_1 l_2)} \delta_{ll'} \delta_{JJ'} \delta_{M_l M_l'} \delta_{\mu_J \mu_J'} \delta_{\xi\xi'}, \quad (12)$$

where $l_1 + l_2 - l$ is odd (because of the pseudoscalar pion wave function). We have the following orthogonal transformation to the total isotopic spin representation:*

$$\langle \Omega_f | K | \Omega_i \rangle = \sum_{I=1/2}^{I=3/2} \sum_{\Lambda=l-1/2}^{l+1/2} C^{lM_l}_{\Lambda M_l;\ M\alpha_f} C^{\Lambda M}_{11;\ \beta\gamma} (\omega_f | K | \omega_i)^{I\Lambda} C^{lM_l}_{1\ \alpha_i;\ \beta\gamma_i}. \quad (13)$$

For the matrix $\langle \Omega_f | K | \Omega_i \rangle$ in the form (8) we have

$$(\omega_f | K | \omega_i)^{3/2;\ 2} = -\sqrt{10}\,(\omega_f | K_3 + K_4 | \omega_i),$$

$$(\omega_f | K | \omega_i)^{3/2;\ 1} = \sqrt{2}\,(\omega_f | 2(K_6 - K_5) + K_3 - K_4 | \omega_i),$$

$$(\omega_f | K | \omega_i)^{1/2;\ 1} = \sqrt{2}\,(\omega_f | 3(K_2 - K_1) + K_3 - K_4 + K_5 - K_6 | \omega_i), \quad (14)$$

$$(\omega_f | K | \omega_i)^{1/2;\ 0} = (\omega_f | 3(K_1 + K_2 + K_5 + K_6) - K_3 - K_4 | \omega_i).$$

We now expand the matrix $(\omega_f | K | \omega_i)^{I\Lambda}$ for arbitrary I and Λ in eigenfunctions of the total angular momentum:

$$(\omega_f | K | \omega_i)^{I\Lambda} = \sum_{J}\ \sum_{l,\ L=J-1/2 | l_1+l_2 | =L}\ \sum_{l'} K^{l\Lambda}_{JlL(l_1 l_2)}(\varkappa_1, \varkappa_i) \times \sum_{\mu_J} G^{J,\ \mu_J}_{L(l_1 l_2)}(s_f, \mathbf{n}_1, \mathbf{n}_2)\, g^{J,\ \mu_J +}_{l'}(s_i; \mathbf{n}_i). \quad (15)$$

Here

$$g^{J,\ \mu_J}_{l}(s_i, \mathbf{n}_i) = \sum_m C^{J\mu_J}_{l\ 1/2;\ ms_i} Y_{lm}(\mathbf{n}_i), \quad (16)$$

$$G^{J,\ \mu_J}_{L(l_1 l_2)}(s_f; \mathbf{n}_1, \mathbf{n}_2) = \sum_M C^{J\mu_J}_{L\ 1/2;\ Ms_f} Y^M_{L(l_1 l_2)}(\mathbf{n}_1, \mathbf{n}_2) = \sum_{m_1, m_2, M} C^{J\mu_J}_{L\ 1/2;\ Ms_f} C^{LM}_{l_1 l_2;\ m_1 m_2} Y_{l_1 m_1}(\mathbf{n}_1) Y_{l_2 m_2}(\mathbf{n}_2) \quad (17)$$

are orthogonal and normalized functions of the nucleon-meson system and of the nucleon-2 meson system, respectively; $Y_{lm}(\mathbf{n})$ is the usual spherical function.

When the matrix $(\omega_f | K | \omega_i)^{I\Lambda}$ is given by (10) its matrix elements in the J, μ_J representation, $K^{I\Lambda}_{JlL(l_1 l_2)}(\kappa_1, \kappa_i)$, will be linear combinations of A_0, B_0, ... etc. The expansions (13) and (15) also apply to the T matrix.

In order to obtain a set of equations relating T and K that are reduced with respect to total isotopic spin and total angular momentum we represent all matrices in (11) as expansions in functions of the total moments. When expanding the matrices $\langle 2_f | K | 2' \rangle$ that are in the X terms it must be taken into account that because of energy and momentum conservation these matrices will also depend on the momentum of meson 1_f, so that is more convenient to expand them in momentum space "on the left" in functions of the nucleon-2 meson system.

For elastic scattering $\kappa = \kappa_i$, whence the density function of nucleon-meson states becomes

$$\rho(1) = \rho_1(\varkappa_i) = \varkappa_i W_i (E - W_i) / (2\pi)^3 E. \quad (18)$$

From (7) the density function of nucleon-2 meson states is

$$\rho(1, 2) = \rho_2(\varkappa_1, \cos\vartheta_{12}) = \frac{1}{(2\pi)^5} \frac{\varkappa_1^2 \varkappa_2 W_2}{E - W_1 + (W_2/\varkappa_2)\varkappa_1 \cos\vartheta_{12}}, \quad (19)$$

where the angle θ_{12} is related to the emission angles ϑ_1, φ_1 and ϑ_2, φ_2 of the scattered pions by

$$\cos\vartheta_{12} = \cos\vartheta_1 \cos\vartheta_2 + \sin\vartheta_1 \sin\vartheta_2 \cos(\varphi_1 - \varphi_2). \quad (20)$$

At relativistic energies the dependence of $\rho(1, 2)$ on $\cos\theta_{12}$ becomes significant and complicates the reduction because, when integrating over angles, in terms containing $\rho(1, 2)$ we cannot directly make use of the orthogonality of the functions $Y^M_{L(l_1 l_2)}(\mathbf{n}_1 \cdot \mathbf{n}_2)$.

The separation of isotopic, angular and spin variables results in the following system of linear algebraic integral equations:

*Here and hereinafter $C^{c\gamma}_{ab;\ \alpha\beta}$ are Clebsch-Gordan coefficients, W(abcd; ef) are Racah coefficients, Z(abcd; ef) are the coefficients used in reference 8 and $U\begin{pmatrix} a & b & e \\ c & d & e' \\ f & f' & g \end{pmatrix}$ are generalized Racah coefficients.[9]

$$T^{I\Lambda}_{jl\,L\,(l_1 l_2)}(\varkappa_1, \varkappa_i)$$

$$= K^{I\Lambda}_{jl\,L\,(l_1 l_2)}(\varkappa_1, \varkappa_i) - i\pi\rho_1(\varkappa_i) K^{I\Lambda}_{jl\,L\,(l_1 l_2)}(\varkappa_1, \varkappa_i) T^{I}_{jl}(\varkappa_i)$$

$$- i\pi \sum_{I'', \Lambda', \ldots} a^{I\Lambda(I'')\Lambda'} \widetilde{\rho}_1(\varkappa_1) K^{I''}_{j''l''L'(l_1' l_2')}(\varkappa_1) T^{I\Lambda'}_{jl\,L'(l_1' l_2')}(\varkappa_1, \varkappa_i)$$

$$- i\pi\,\{\text{symm. terms } 1 \rightleftarrows 2\} \qquad (21)$$

$$- i\pi \sum_{\Lambda', L', \ldots} \int_0^{\varkappa_{1\max}'} d\varkappa_1' \widetilde{\rho}_2(\varkappa_1') K^{I\Lambda\Lambda'}_{jL'(l_1' l_2')L(l_1 l_2)}(\varkappa_1, \varkappa_1') T^{I\Lambda'}_{jlL'(l_1' l_2')}(\varkappa_1', \varkappa_i),$$

$$T^{I}_{jl}(\varkappa_i) = K^{I}_{jl}(\varkappa_i) - i\pi\rho_1(\varkappa_i) K^{I}_{jl}(\varkappa_i) T^{I}_{jl}(\varkappa_i)$$

$$- i\pi \sum_{\Lambda', L', \ldots} \int_0^{\varkappa_{1\max}'} d\varkappa_1' \widetilde{\rho}_2(\varkappa_1') K^{I\Lambda'}_{jL'(l_1' l_2')\,l}(\varkappa_i, \varkappa_1') T^{I\Lambda'}_{jlL'(l_1' l_2')}(\varkappa_1', \varkappa_i).$$

The summation in (21) is taken over all primed indices. We have here the coefficient

$$a^{(I\Lambda\ I'')\Lambda'} = (2I''+1)\sqrt{(2\Lambda+1)(2\Lambda'+1)}$$

$$\times W(11^1/_2 I; \Lambda I'')\, W(11^1/_2 I; \Lambda' I''). \qquad (22)$$

$\widetilde{\rho}_1(\kappa_1)$ and $\widetilde{\rho}_2(\kappa_1')$ are abbreviations for

$$\widetilde{\rho}_1(\varkappa_1) = \sum_\lambda A_\lambda \int d\cos\vartheta_{12} \rho_1(\varkappa_1, \cos\vartheta_{12'})\, P_\lambda(\cos\vartheta_{12'}), \qquad (23)$$

$$\widetilde{\rho}_2(\varkappa_1') = \sum_\lambda B_\lambda \int d\cos\vartheta_{1'2'} \rho_2(\varkappa_1', \cos\vartheta_{1'2'})\, P_\lambda(\cos\vartheta_{1'2'}), \qquad (24)$$

where

$$A_\lambda = \sum_{l''} \frac{1}{2\sqrt{4\pi}} (-1)^{L''+L'+L+l_1'+l_2'+l_2+l''+\lambda} i^{l_1''-l_1'-l_1-\lambda}$$

$$\times (2J''+1)(2\lambda+1)^{1/2} C^{l_2' 0}_{\lambda l'';\,00}\, W(LJL''J''; {}^1/_2 r)$$

$$\times W(L'Jl''J''; {}^1/_2 r)\, Z(l_1 L l_1'' L''; l_2 r)\, Z(l_1' L' l'' l''; l_2' r), \qquad (25)$$

$$B_\lambda = \frac{1}{2}(-1)^{L''+l_2'+l_2'} i^{l_1''-l_1'-\lambda} C^{\lambda 0}_{l_2' l_2';\,00}\, Z(l_1' l_2' l_1'' l_2'' L'' \lambda). \qquad (26)$$

3. DUAL SCATTERING CROSS SECTIONS

A. General Relations

Using (3), (13) and (19), we can represent the differential cross section for dual scattering by

$$d\sigma(l_f; \beta, \gamma | l_i, \alpha) = \sum_{I'\Lambda'} \sum_{I,\Lambda} \Delta^{I'\Lambda';\,I\Lambda}_{\alpha l_1';\,\beta\gamma l_f} d\sigma^{I'\Lambda';\,I\Lambda}, \qquad (27)$$

where the coefficient $\Delta^{I'\Lambda';\,I\Lambda}_{\alpha l_1';\,\beta\gamma l_f}$ contains the charge character of the process (see reference 10, for example) and

$$d\sigma^{I'\Lambda';\,I\Lambda} = \frac{2\pi}{v}\frac{1}{2} \sum_{s_{l_f} s_{l_i}} (\omega_f | T | \omega_i)^{I'\Lambda'+} (\omega_f | T | \omega_i)^{I\Lambda}$$

$$\times \rho_2(\varkappa_1, \cos\vartheta_{12})\, d\varkappa_1 d\Omega_1 d\Omega_2. \qquad (28)$$

Here $d\Omega_1 = \sin\vartheta_1 d\vartheta_1 d\varphi_1$ and $d\Omega_2 = \sin\vartheta_2 d\vartheta_2 d\varphi_2$ are the solid angles of pion scattering and v is the velocity of the incident meson. In (28) we assume that $(\omega_f | T | \omega_i)$ is represented by the expansion (15) with the functions g and G given by (16) and (17).

In the coordinate system where the polar axis has the direction of incident meson momentum,

$$g_l^{\mu\mu_f}(s_i, \mathbf{n}_i) = \sqrt{(2l+1)/4\pi}\, C^{s_{l_f}}_{\mu_f, 0, \mu_i}.$$

Following Racah,[8,9,11] we can obtain an equation for the differential cross section that is directly comparable with experiment. Integration of $d\sigma^{I'\Lambda';\,I\Lambda}$ in (28) over the azimuthal angles φ_1 and φ_2, followed by rather complicated transformations gives*

$$d\sigma^{I'\Lambda';\,I\Lambda}(\varkappa_1; \vartheta_1, \vartheta_2) = \frac{1}{32v} \sum_{J'l'L'(l_1' l_2')} \sum_{JlL(l_1 l_2)} T^{I'\Lambda'*}_{j'l'L'(l_1' l_2')}(\varkappa_1, \varkappa_i)\, T^{I\Lambda}_{jlL(l_1 l_2)}(\varkappa_1, \varkappa_i)$$

$$\times \sum_{L_1, L_2} \sum_\lambda D_{L, L_1; \lambda}\, \rho_\lambda(\varkappa_1)\, P_{L_1}(\cos\vartheta_1)\, P_{L_2}(\cos\vartheta_2)\, d\varkappa_1 d\cos\vartheta_1 d\cos\vartheta_2, \qquad (29)$$

where

$$\rho_\lambda(\varkappa_1) = \int_{-1}^{+1} \rho_2(\varkappa_1, \cos\vartheta_{12})\, P_\lambda(\cos\vartheta_{12})\, d\cos\vartheta_{12}, \qquad (30)$$

$$\times D_{L, L_2; \lambda} = (-1)^{l_1'+l_2'+L_1+L_2-L-\lambda} i^{l+L_1-l'-L_2} (2\lambda+1) \sqrt{(2J'+1)(2L'+1)(2l_1'+1)(2l_2'+1)(2J+1)(2L+1)(2l_1+1)(2l_2+1)}$$

$$\times \sum_{\Lambda_1, \Lambda_2} \sum_R (-1)^R C^{\Lambda_1 0}_{l_1' l_1';\,00}\, C^{\Lambda_2 0}_{l_2' l_2';\,00}\, C^{L 0}_{\Lambda_1 \Lambda_2;\,00}\, C^{L_2 0}_{\Lambda_2 R;\,00}\, W(LJL'J'; {}^1/_2 R)\, Z(lJl'J'; {}^1/_2 R)\, Z(L_1 \Lambda_1 L_2 \Lambda_2; \lambda R)\, U\begin{pmatrix} l_1' l_2' L' \\ l_1 l_2 L \\ \Lambda_1 \Lambda_2 l' \end{pmatrix}. \qquad (31)$$

*The integral functions $\rho_\lambda = \int_0^{\varkappa_{\max}} \rho_\lambda(\varkappa) d\varkappa$ diminish as λ increases. For example, when $T_{kin} \approx 1.5$ Bev we have $\rho_0 : \rho_1 : \rho_2 = 1 : (-0.27) : 0.085$. Therefore it is sufficient to use only small values of λ in practical calculations by means of (29). In the non-relativistic limit (for a static nucleon) all $\rho_{\lambda \neq 0} = 0$.

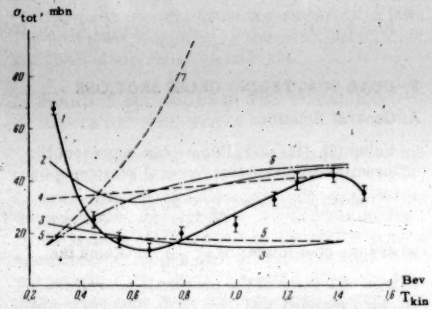

FIG. 1. Energy dependence of the total (elastic + inelastic) cross section for π^+ meson scattering by protons. Curve 1) experimental; curves 2 – 7) theoretical (including only dual scattering among the inelastic processes); 2 – 5) for ps(ps) coupling; 2, 3) by damping theory ($2-g^2=6$; $3-g^2=3$); 4, 5) by perturbation theory ($4-g^2=3$; $5-g^2=2.2$); 6, 7) for ps(pv) coupling; 6) by damping theory ($f^2=1/12$); 7) by perturbation theory ($f^2=1/12$)

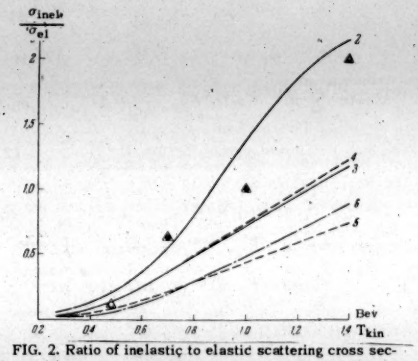

FIG. 2. Ratio of inelastic to elastic scattering cross section for π^+ meson scattering by protons. The notation is the same as in Fig. 1. Experimental data were taken from reference 14 for π^+, p scattering (T_{kin} = 0.5 Bev) and π^-, p scattering (T_{kin} 0.7 Bev, 1 Bev); also π^-, n (T_{kin} = 1.4 Bev) (since for this energy there are no corresponding data for π^+, p scattering).

The momentum distribution is obtained by integrating over $d\cos\vartheta_1$ and $d\cos\vartheta_2$, with the result

$$d\sigma^{I'\Lambda';\,I\Lambda}(\kappa_1)=\frac{1}{8\sigma}\sum_{JlL(l_1l_2)}\sum_{l_1'l_2'}T^{I'\Lambda'*}_{JlL(l_1'l_2')}(\kappa_1';\ \kappa_i)$$

$$\times\ T^{I\Lambda}_{JlL(l_1l_2)}(\kappa_1,\kappa_i)\sum_{\lambda}D_{00;\lambda}\rho_\lambda(\kappa_1)\,d\kappa_1, \qquad (32)$$

where

$$D_{00;\lambda}=(-1)^{l_2'-l_2-L_i^{l_1'-l_1-\lambda}}(2J+1)C^{\lambda 0}_{l_2'l_2;00}\,Z(l_1'l_2'l_1l_2;L\lambda). \qquad (33)$$

B. Damping Theory

The dual scattering cross section and the related single-meson scattering cross section were calculated according to the theory of radiation damping, where the first Born approximation is taken for the reaction matrix K. The covariant formalism of Fukuda[12] and Pirenne[13] was used; pseudoscalar ps(ps) and pseudovector ps(pv) coupling were considered [see (4)].

When we do not limit ourselves to nonrelativistic energies, $K^{I}_{J\ldots}(\kappa_1,\ldots)$ are complicated functions and the solution of (21) is difficult. We replace each $K^{I}_{J\ldots}(\kappa_1,\ldots)$ by its value for $\kappa_1=\kappa_2$, in which case (21) becomes an ordinary system of linear algebraic equations with its solution given by the ratio of two determinants consisting of equation coefficients. It can be shown by studying the character of the functions $K^{I}_{J\ldots}(\kappa_1,\ldots)$ and of the density function $\rho_2(\kappa_1,\cos\vartheta_{12})$ that the total dual scattering cross section is not essentially changed.

In the present work values of $K^{I\Lambda}_{JlL(l_1l_2)}(\kappa_1,\kappa_2)$ (for $\kappa_1=\kappa_2$) were calculated for four incident meson energies (in the laboratory system): T_{kin} = 0.275, 0.52, 0.84 and 1.4 Bev, and divided into two groups such that, for a given energy, each member of the second group was not greater in absolute magnitude than $1/3$ of any member of the first group.

In order to obtain the matrix elements $T^{I\Lambda}_{JlL(l_1l_2)}\times(\kappa_1,\kappa_2)$ corresponding to the first group we solved a set of approximate equations obtained from (21) by dropping the last term of the first and second equations (two mesons — 1′, 2′ — in the intermediate state). The single-meson scattering matrix elements $T^{I}_{Jl}(\kappa_1)$ were derived from the same equations.

We assumed $T^{I\Lambda}_{JlL(l_1l_2)}=K^{I\Lambda}_{JlL(l_1l_2)}$ for the second group, which in the present case represents the first approximation of damping theory with respect to the coupling constant. For purposes of comparison we also considered perturbation theory ($T^{I\Lambda}_{JlL(l_1l_2)}=K^{I\Lambda}_{JlL(l_1l_2)}$ for all scattering amplitudes). Figures 1 and 2 show the results for π^+, p scattering. A comparison of the curves calculated by perturbation theory and by damping theory for ps(ps) coupling shows that damping somewhat "improves" the energy dependence of the total cross section, although the pronounced resonant character of the experimental curves cannot be obtained with any of the coupling constants. Inclusion of damping enables us to increase the fraction of inelastic processes (dual scattering) for the same total cross section. (The experimental points

in Fig. 2 lie within a region bounded by curves calculated by the damping theory but go outside this region in the case of perturbation theory.)

With ps (pv) coupling damping sharply reduces the growth of the total cross section, but the same coupling constant cannot be used to obtain a total cross section and a cross section ratio which are both close to the experimental values.

A calculation of the total cross section for π^-, p scattering with ps (ps) coupling shows that the damping theory cannot account for the second peak in the energy-dependence curve of the total cross section. For any one coupling constant the theoretical curves for π^-, p scattering lie below the curves for π^+, p.

The author wishes to thank M. A. Markov for suggesting this topic and for his interest, G. F. Zharkov and A. M. Baldin for several valuable suggestions, and I. A. Egorova and L. A. Isaeva for assistance with the calculations.

APPENDIX

ANGULAR POLYNOMIALS FOR DUAL SCATTERING

For some features of the theory (the semiphenomenological theory and the derivation of dispersion relations) it is useful to know the expansion of matrix T in operators that project the initial (one-meson) eigenstate with given total isotopic spin and angular momentum into the final (two-meson) state.

We represent (15) for the T matrix as follows:

$$(\omega_f \mid T \mid \omega_i)^{I\Lambda} = \frac{1}{(4\pi)^{3/2}} \sum_{J} \sum_{l,L=J-1/2}^{J+1/2} \sum_{|l_1-l_2|}^{l_1+l_2} T^{I\Lambda}_{JlL(l_1l_2)} Q^{lf}_{JlL(l_1l_2)}; \quad (A.1)$$

$$Q^{lf}_{JlL(l_1l_2)} = (4\pi)^{3/2} \sum_{u_f} G^{J,u_f}_{L(l_1l_2)}(s_f; \mathbf{n}_1, \mathbf{n}_2)\, g^{J,u_f^+}_{l}(s_i, \mathbf{n}_i) \quad (A.2)$$

form a set of orthogonal operators for dual scattering (the so-called "angular polynomials").* If we confine ourselves to l, l_1, $l_2 \leq 2$ we have the following operators:†

$$Q^{(\pm)}_{[s]0,1(10)} = -\frac{1}{\sqrt{2}} (\sigma \cdot \mathbf{n}^{(\pm)}_{12}),$$

$$Q^{(\pm)}_{[s]0,1(21)} = \frac{3}{2} [(\mathbf{n}_2 \cdot \mathbf{n}_1) \mp 1/3] (\sigma \cdot \mathbf{n}^{(\pm)}_{12}),$$

$$Q^{(+)}_{[s]1,2(11)} = -3\sqrt{\frac{3}{10}} \Big[(\mathbf{n}_2 \cdot \mathbf{n}_i)(\sigma \cdot \mathbf{n}_1) + (\mathbf{n}_1 \cdot \mathbf{n}_i)(\sigma \cdot \mathbf{n}_2) - \frac{2}{3} (\mathbf{n}_2 \cdot \mathbf{n}_1)(\sigma \cdot \mathbf{n}_i) \Big],$$

$$Q^{(\pm)}_{[s]1,2(20)} = -\frac{3}{\sqrt{2}} \Big[(\mathbf{n}_1 \cdot \mathbf{n}_i)(\sigma \cdot \mathbf{n}_1) \pm (\mathbf{n}_2 \cdot \mathbf{n}_i)(\sigma \cdot \mathbf{n}_2) - \frac{1 \pm 1}{3} (\sigma \cdot \mathbf{n}_i) \Big],$$

$$Q^{(+)}_{[s]1,0(l_1l_1)} = (-1)^{l_1} \sqrt{2l_1+1}\, P_{l_1}(\cos\theta_{12})(\sigma \cdot \mathbf{n}_i),$$

$$Q^{(\pm)}_{[s]2,1(10)} = -\frac{3}{\sqrt{2}} \Big[(\mathbf{n}^{(\pm)}_{12} \cdot \mathbf{n}_i)(\sigma \cdot \mathbf{n}_i) - \frac{1}{3} (\sigma \cdot \mathbf{n}^{(\pm)}_{12}) \Big],$$

$$Q^{(-)}_{[s]1,1(11)} = \sqrt{\frac{3}{2}} \{ (\mathbf{n}_2 \cdot \mathbf{n}_i)(\sigma \cdot \mathbf{n}_1) - (\mathbf{n}_1 \cdot \mathbf{n}_i)(\sigma \cdot \mathbf{n}_2) - i ([\mathbf{n}_2 \times \mathbf{n}_1] \cdot \mathbf{n}_i)\, \gamma_i \},$$

$$Q^{(-)}_{[s]1,1(11)} = -\sqrt{\frac{3}{2}} \{ (\mathbf{n}_2 \cdot \mathbf{n}_i)(\sigma \cdot \mathbf{n}_1) - (\mathbf{n}_1 \cdot \mathbf{n}_i)(\sigma \cdot \mathbf{n}_2) + 2i ([\mathbf{n}_2 \times \mathbf{n}_1] \cdot \mathbf{n}_i)\, \gamma_i \}, \quad (A.3)$$

where

$$\mathbf{n}^{(\pm)}_{12} = \mathbf{n}_1 \pm \mathbf{n}_2.$$

*Ritus[15] has considered such operators for reactions of the type a + b → c + d (without the production of additional particles).

†The sign +(−) denotes a symmetric (antisymmetric) state of the system with respect to the exchange $\mathbf{n}_1 \rightleftarrows \mathbf{n}_2$.

[1] B. d'Espagnat, Kgl. Danske Videnskab Selskab, Mat.-fys. Medd. **28**, 11 (1954).
[2] J. Franklin, Phys. Rev. **105**, 1101 (1957).
[3] L. S. Rodberg, Phys. Rev. **106**, 1090 (1957).
[4] R. Omnes, Nuovo cimento **6**, 780 (1957).
[5] G. F. Zharkov, J. Exptl. Theoret. Phys. (U.S.S.R.) **27**, 296 (1954).
[6] B. A. Lippman and J. Schwinger, Phys. Rev. **79**, 469 (1950).
[7] M. L. Goldberger, Phys. Rev. **84**, 929 (1951).
[8] Biedenharn, Blatt, and Rose, Revs. Modern Phys. **24**, 249 (1952).
[9] Arima, Horie, and Tanabe, Progr. Theoret. Phys. **11**, 143 (1954).
[10] N. V. Dushin, Dokl. Akad. Nauk SSSR **106**, 977 (1956), Soviet Phys. "Doklady" **1**, 128 (1956).
[11] H. A. Jahn and J. Hope, Phys. Rev. **93**, 318 (1954).
[12] N. Fukuda and T. Miyazima, Progr. Theoret. Phys. **5**, 849 (1950).
[13] J. Pirenne, Phys. Rev. **86**, 395 (1952).
[14] R. P. Shutt, Proc. 6th Annual Rochester Conf. on High Energy Nuclear Physics, Ch. IV, Sec. 5, 1956.
[15] V. I. Ritus, J. Exptl. Theoret. Phys. (U.S.S.R.) **27**, 660 (1954); **32**, 1536 (1957), Soviet Phys. JETP **5**, 1249 (1957); **33**, 1264 (1957), Soviet Phys. JETP **6**, 972 (1958).

Translated by I. Emin
15

ELECTRICAL, OPTICAL, AND ELASTIC PROPERTIES OF CRYSTALS OF THE DIAMOND TYPE. III. DISPERSION AND ABSORPTION OF LIGHT

V. S. MASHKEVICH

Kiev Polytechnic Institute

Submitted to JETP editor May 16, 1958

J. Exptl. Theoret. Phys. (U.S.S.R.) **36**, 108-115 (January, 1959)

The dispersion, double refraction, and single-phonon absorption of light due to lattice vibrations are investigated in the infrared region. The parameters of the theory are determined and the numerical calculation of the effects mentioned above is performed.

IT is customarily assumed that the lattice vibrations of a homopolar crystal do not affect its optical properties in the harmonic approximation, since its atoms are electrically neutral. In reference 1 (which henceforth will be referred to as II) it is shown, however, that this is true only in the zero approximation with respect to d/λ (d is the lattice constant and λ the wavelength). A finite λ already leads to a coupling between the dipole moments of the atoms, which arise upon the passage of a light wave, and the displacements of the atoms and thus causes the lattice vibrations to affect the optical properties of the crystal. In particular, vibrations of a homopolar lattice cause dispersion and single-phonon absorption of light, effects hitherto not investigated (Lax and Burstein[2] have investigated qualitatively two-phonon absorption). In this paper we present a quantitative theory of the above phenomenon.

1. DISPERSION AND BIREFRINGENCE AWAY FROM THE SINGULARITY

The dependence of the index of refraction of the light wave on the frequency and on the direction of propagation away from the singularity (point of intersection of the light and optical branches of the zeroth approximation in d/λ; the coordinates of the singular point are $\Omega_{\lim}$, the limiting frequency of the optical vibrations, and n_0, the index of refraction of the extreme long waves; for more details see II) is determined by (26.II), from which we get

$$n_j = n_0 + \mu^2\Omega^2\{g_1 + [Q/(\Omega_{\lim}^2 - \Omega^2) - g_2]\, r_j(\mathbf{s})\},$$

$$r_j(\mathbf{s}) = s_x^4 + s_y^4 + s_z^4 + (-1)^j[(s_x^4 + s_y^4 + s_z^4 - 1)^2 - 12s_x^2s_y^2s_z^2]^{1/2},$$

$$g_1 = q[e_1^{(1)} + e_2^{(1)} + (e_1^{(3)} + e_2^{(3)})/2], \qquad (1)$$

$$g_2 = q(e_1^{(3)} + e_2^{(3)} - 2S^2/A)/2.$$

Here n_j is the index of refraction of the polarization wave, $j = 1, 2$; Ω is the dimensionless frequency; $\mu \sim 10^{-5}$ is a small parameter in which an expansion equivalent to the expansion in d/λ is made; $\mathbf{s}$ is the unit wave vector; numerical values of S and $e_i^{(k)}$ and expressions for q and Q are given in II; A is one of the parameters of the theory. It will be shown below that the light oscillations corresponding to various polarizations are mutually orthogonal. (This is difficult to see directly from Eqs. (25, 23a.II) which determine the directions of the oscillations, since the above system of equations is not self-adjoint).

Formulas (1) are valid if $|\Omega - \Omega_{\lim}| \gg \mu$. If, however, Ω is still not too far from $\Omega_{\lim}$, we obtain from (1) approximately

$$n_j = n_0 + \mu^2 Q\Omega^2 r_j(\mathbf{s})/(\Omega_{\lim}^2 - \Omega^2),$$

i.e., the usual dispersion formula away from the natural frequency. The value of n_j depends on the number of the polarization, so that birefringence takes place. The directions of the optical axes are determined from

$$(s_x^4 + s_y^4 + s_z^4 - 1)^2 - 12s_x^2s_y^2s_z^2 = 0$$

and are directions of the [100] and [111] type, i.e., the edges and diagonals of a cubic lattice. Thus, a crystal of the diamond type has seven axes; optical isotropy takes place only in the zeroth approximation in d/λ, to which the customary analysis is confined. For both polarizations, n_j depends on $\mathbf{s}$ so that both rays are extraordinary.

2. QUASI-NORMAL COORDINATES

It was shown in II that in the μ-vicinity of the singular point the normal oscillations connected with the propagation of the light wave are of mixed character: even in the zeroth approximation, neither

the dipole moments of the cells nor the displacements of the atoms are zero. These oscillations therefore do not contain purely light oscillations, which have no displacements in the zeroth approximation, and their corresponding normal coordinates are not suitable for a direct description of the light waves. The latter are described by the so-called quasi-normal coordinates,[3] which, for the case considered here, are introduced in the following manner. The general solution of the equations of motion (1.II) is

$$\mathbf{u}_s^l = \sum_{\alpha \mathbf{K}} q^\alpha(\mathbf{K}, t)\, \mathbf{u}_s^\alpha(\mathbf{K}) \exp(i\mathbf{K}\cdot\mathbf{r}_s^l),$$

$$\mathbf{P}_s^l = \sum_{\alpha \mathbf{K}} q^\alpha(\mathbf{K}, t)\, \mathbf{P}_s^\alpha(\mathbf{K}) \exp(i\mathbf{K}\cdot\mathbf{r}_s^l),$$

where $\mathbf{u}_S^l$ and $\mathbf{P}_S^l$ are respectively the displacement and the dipole moment due to deformation of the electron shell of the s-th atom of the l-th elementary cell; α is the number of the branch of the spectrum of normal oscillations, $\mathbf{K}$ is the wave vector, $\mathbf{u}_S(\mathbf{K})$ and $\mathbf{P}_S(\mathbf{K})$ are the amplitudes, $q^\alpha(\mathbf{K}, t)$ are the normal coordinates and $\mathbf{r}_S^l$ are the coordinates of the lattice sites. The following orthogonality condition holds[4]

$$I_{\alpha\beta} = \sum_s m_s \mathbf{u}_s^\alpha(\mathbf{K})\cdot\mathbf{u}_s^\beta(-\mathbf{K}) + (4\pi/\Delta) K^2 c^2 [(\mathbf{P}^\alpha(\mathbf{K}), \mathbf{P}^\beta(-\mathbf{K})) - (\mathbf{P}^\alpha(\mathbf{K}), \mathbf{S})(\mathbf{P}^\beta(-\mathbf{K}), \mathbf{s})] \times \{[n_\alpha^2(\mathbf{K}) - 1][n_\beta^2(-\mathbf{K}) - 1]\, \omega_\alpha^2(\mathbf{K})\, \omega_\beta^2(-\mathbf{K})\}^{-1} = 0, \quad \alpha \neq \beta, \tag{2}$$

$$\mathbf{P}^\alpha(\mathbf{K}) = \sum_s \mathbf{P}_s^\alpha(\mathbf{K}),$$

which is a generalization of the orthogonality relation

$$\sum_s m_s \mathbf{u}_s^\alpha(\mathbf{K})\cdot\mathbf{u}_s^\beta(-\mathbf{K}) = 0, \quad \alpha \neq \beta,$$

which applies if the theory does not take into account the retardation of the electromagnetic interaction;[5] m_S is the mass of the atom, ω the frequency, Δ the volume of the elementary cell, and c the velocity of light in vacuo. Considering that, according to (23, 23a.II), $\mathbf{u}_S = 0$ and $(\mathbf{P}^\alpha \cdot \mathbf{s}) = 0$ in the zeroth approximation for light oscillations, we obtain from (2) the above-mentioned orthogonality of $\mathbf{P}$ for light waves of different polarizations.

If we impose the normalization condition

$$I_{\alpha\alpha} = N^{-1}, \tag{3}$$

on the amplitudes, where N is the number of cells in the principal region, the energy of the crystal becomes[4]

$$E = \sum_{\alpha \mathbf{K}}{}' [\dot{q}^\alpha(\mathbf{K})\dot{q}^{*\alpha}(\mathbf{K}) + \omega_\alpha^2(\mathbf{K})\, q^\alpha(\mathbf{K})\, q^{*\alpha}(\mathbf{K})];$$

The prime indicates that the summation is in the half-space $\mathbf{K}$. We introduce new generalized coordinates $Q^\alpha(\mathbf{K}, t)$:

$$q^\alpha(\mathbf{K}, t) = \sum_\beta{}' c_{\alpha\beta}(\mathbf{K})\, Q^\beta(\mathbf{K}, t).$$

To these correspond new amplitudes

$$\tilde{\mathbf{u}}_s^\alpha(\mathbf{K}) = \sum_\beta{}' c_{\beta\alpha}(\mathbf{K})\, \mathbf{u}_s^\beta(\mathbf{K}), \quad \tilde{\mathbf{P}}_s^\alpha(\mathbf{K}) = \sum_\beta{}' c_{\beta\alpha}(\mathbf{K})\, \mathbf{P}_s^\beta(\mathbf{K}). \tag{4}$$

If we subject the coefficients $c_{\alpha\beta}$ to the normalization and orthogonality conditions

$$\sum_\beta{}' c_{\beta\gamma}^*(\mathbf{K})\, c_{\beta\gamma}(\mathbf{K}) = \delta_{\gamma\alpha}, \tag{5}$$

which indicate the equivalence of normalization of the old and new amplitudes and the orthogonality of the transformation of the kinetic energy, the energy in Q coordinates becomes

$$E = E^0 + E', E^0 = \sum_{\alpha \mathbf{K}}{}' [\dot{Q}^\alpha(\mathbf{K})\, \dot{Q}^{*\alpha}(\mathbf{K}) + \tilde{\omega}_\alpha^2(\mathbf{K})\, Q^\alpha(\mathbf{K})\, Q^{*\alpha}(\mathbf{K})],$$

$$E' = \sum_{\mathbf{K}} \sum_{\beta\alpha<\gamma}{}' c_{\beta\gamma}^*(\mathbf{K})\, c_{\beta\alpha}(\mathbf{K})\, \omega_\beta^2(\mathbf{K})\, Q^{*\gamma}(\mathbf{K})\, Q^\alpha(\mathbf{K}) + \text{compl. conj.}, \tag{6}$$

where

$$\tilde{\omega}_\alpha^2(\mathbf{K}) = \sum_\beta{}' |c_{\beta\alpha}(\mathbf{K})|^2\, \omega_\beta^2(\mathbf{K}). \tag{7}$$

The coefficients $c_{\alpha\beta}$ must be so chosen that the two Q coordinates described purely light-like oscillations. According to (23.II), there are no displacements of atoms in such oscillations, so that

$$\tilde{\mathbf{u}}_s^{0\alpha} = \sum_\beta c_{\beta\alpha}^0\, \mathbf{u}_s^{0\beta} = 0, \tag{8}$$

where $\alpha = 1, 2$ corresponds to the light oscillations. When formulating expressions (4) for light oscillations in the vicinity of the singular point in the zeroth approximation, one must use only the mixed oscillations, since in all others the dipole moment of the cell is zero. The orthogonality of the mixed oscillations of different polarizations can be derived from (2) and (29a, 30, 30a.II). Therefore different polarizations can be considered independently. We denote the coefficient c in terms of $c_{\alpha\beta}^j$, where $\alpha = 1, 2$, pertains to the two old (mixed) branches of the polarization j and $\beta = 1, 2$ pertains to the two new ones. Let q^{1j} describe the light oscillations. Then, changing to dimensionless amplitudes (see II) and inserting (3.II) into (8), we get

$$c_{11}^{0j}(\mathbf{w}^{01j} + \mathbf{s})/\rho^{1j} + c_{21}^{0j}(\mathbf{w}^{02j} + \mathbf{s})/\rho^{2j} = 0, \quad \rho \equiv \Omega_1^2, \tag{9}$$

where $\mathbf{w} = \mathbf{P}/ed$ (e is the absolute value of the electron charge), Ω_1^2 is the correction of first order to the square of frequency ($\Omega^2 = \Omega_{\lim}^2 + \mu\Omega_1^2 + \ldots$). It follows from (29a, 30, 30a.II) that $\mathbf{w}^{02j}$ is parallel to $\mathbf{w}^{01j}$. Putting

$$\mathbf{w}^{02j} = D^j \mathbf{w}^{01j}, \tag{10}$$

we find from (3), in the zero approximation

$$|D^j|^2 = [\chi p_j(\mathbf{s}) / (\rho^{1j})^2 + 1]/[\chi p_j(\mathbf{s}) / (\rho^{2j})^2 + 1],$$
$$p_j(\mathbf{s}) = \tfrac{1}{2} |\mathbf{w}^{01j} + \mathbf{s}\mathbf{\times}\mathbf{s}\mathbf{\times}|^2 / |\mathbf{w}^{01j}|^2, \tag{11}$$
$$\chi = n\omega Q_1^2 \Delta\omega_{\lim}^4 (n_0^2 - 1)^2 / 2\pi K_0^3 e^2.$$

Here $\omega_{\lim}$ and K_0 are the frequency and modulus of the wave vector of the singular point, and m is the mass of the atom. The expression for Q_1 is given in II. We obtain from (9), (10) and (5)

$$c_{11}^{0j} = -\rho^{1j} D^j / b^j, \quad c_{21}^{0j} = \rho^{2j} / b^j,$$
$$b^j = [(\rho^{2j})^2 + |D^j|^2 (\rho^{1j})^2]^{1/2}. \tag{12}$$

Using (12), we get from (5)

$$c_{12}^{0j} = \rho^{2j} / b^j, \quad c_{22}^{0j} = \rho^{1j} D^{*j} / b^j. \tag{13}$$

According to II, we have in the μ-vicinity of the singular point

$$\omega^2 = \omega_{\lim}^2 + \mu\Gamma^2\rho, \quad \Gamma^2 = e^2/md^3. \tag{14}$$

From (6), (14), and (5) it is seen that in the first approximation E' contains only $c_{\alpha\beta}^{0j}$. Taking this into account and inserting (12), (13), and (14) into (6) we get

$$E' = \mu\Gamma^2 \sum_{j\mathbf{K}} (D^j \rho^{1j} \rho^{2j} (\rho^{2j} - \rho^{1j}) / (b^j)^2)\, Q^{*2j} Q^{1j} + \text{compl. conj.}$$

3. DISPERSION AND BIREFRINGENCE IN THE VICINITY OF THE SINGULAR POINT

Inserting (12) and (14) into (7) we find in the first approximation the squares of the frequencies of the light branches:

$$\tilde{\omega}_{1j}^2 = \omega_{\lim}^2 + \mu\Gamma^2 [(\rho^{2j})^3 + (\rho^{1j})^3 |D^j|^2] / (b^j)^2. \tag{15}$$

For the mixed branches we obtain from (30, 30aII)

$$\rho^{nl} = \{\varkappa_0\varkappa_1 + (-1)^n [\varkappa_0^2\varkappa_1^2 + 2n_0^2 r_j(\mathbf{s}) r]^{1/2}\} n_0^{-2}, \quad n = 1, 2,$$
$$\varkappa = Kd/2\mu, \quad \varkappa_0 = K_0 d/2\mu,$$
$$\varkappa_1 = (\varkappa - \varkappa_0)/\mu, \quad r = -Q_1 R_1 > 0, \tag{16}$$

an expression for R_1 is given in II; (Eqs. (15), (16), and (27.II) give for the index of refraction

$$n_j = n_0 + \mu [\chi p_j(\mathbf{s}) - 2r_j(\mathbf{s}) r n_0^{-2}] \varkappa_1 / 2\Omega_{\lim} [\varkappa p_j(\mathbf{s}) + 2r_j(\mathbf{s}) r n_0^{-2} + 2\varkappa_0^3 \varkappa_1^2 n_0^{-4}]. \tag{17}$$

This expression describes the dispersion and the birefringence in the μ-vicinity of the singular point. The maximum departure of n_j from n_0 is

$$(\Delta n_j)_{\max} = \mu [n_0^2 \chi p_j(\mathbf{s}) - 2r r_j(\mathbf{s})] / 4\sqrt{2}\Omega_{\lim}^3 [n_0^2 \chi p_j(\mathbf{s}) + 2r r_j(\mathbf{s})]^{1/2}.$$

It follows from (30, 30a.II) that

$$w_x^{0j} \sim s_x [r_j(\mathbf{s}) + 1 - 2s_y^2] [r_j(\mathbf{s}) + 1 - 2s_z^2];$$

on this basis, Eq. (17) leads to the foregoing seven optical axes. For the principal directions $\mathbf{s}$ (the directions of the diagonals of the faces of the lattice cube, II) $r_1(\mathbf{s})$ and $p_1(\mathbf{s})$ vanish and consequently $n_1 = n_0$. Here $\mathbf{w}^{01}$ and $\mathbf{s}$ are in the plane of the same face.

4. ABSORPTION OF LIGHT

The energy of the crystal (6) corresponds to the Lagrangian

$$L = \sum_{\alpha\mathbf{K}}{}' [\dot{Q}^\alpha(\mathbf{K}) \dot{Q}^{*\alpha}(\mathbf{K}) - \omega_\alpha^2(\mathbf{K}) Q^\alpha(\mathbf{K}) Q^{*\alpha}(\mathbf{K})] - E';$$

from which we find the generalized momenta

$$P^\alpha(\mathbf{K}) = \partial L / \partial \dot{Q}^\alpha(\mathbf{K}) = \dot{Q}^{*\alpha}(\mathbf{K}),$$
$$P^{*\alpha}(\mathbf{K}) = \partial L / \partial \dot{Q}^{*\alpha}(\mathbf{K}) = \dot{Q}^\alpha(\mathbf{K})$$

and the Hamiltonian

$$H = \sum_{\alpha\mathbf{K}}{}' [P^\alpha(\mathbf{K}) P^{*\alpha}(\mathbf{K}) + \tilde{\omega}_\alpha^2(\mathbf{K}) Q^\alpha(\mathbf{K}) Q^{*\alpha}(\mathbf{K})] + E'.$$

In the vicinity of the singular point we have for the oscillations connected with the propagation of light

$$H = \sum_{\mathbf{K}}{}' \sum_{j=1,2} \sum_{n=1,2} [P^{nj}(\mathbf{K}) P^{*nj}(\mathbf{K}) + \tilde{\omega}_{nj}^2(\mathbf{K}) Q^{nj}(\mathbf{K}) Q^{*nj}(\mathbf{K})]$$
$$+ \Big\{ \mu\Gamma^2 \sum_{\mathbf{K}}{}' \sum_{j=1,2} [D^j \rho^{1j} \rho^{2j} (\rho^{2j} - \rho^{1j}) / (b^j)^2] Q^{*2j}(\mathbf{K}) Q^{1j}(\mathbf{K})$$
$$+ \text{compl. conj.} \Big\}. \tag{18}$$

In view of the small interaction energy ($\mu \sim 10^{-5}$), the absorption of light can be considered by the usual method of the theory of quantum transitions. Light oscillations of the polarization j are described by the coordinates $Q^{1j}(\mathbf{K})$. We shall call the corresponding quasi-particles, which appear as a result of quantization of (18), photophonons. The particles corresponding to $Q^{2j}(\mathbf{K})$ are ordinary phonons. The state of the unperturbed system (the perturbation is E') is characterized by the number of photons $n^j(\mathbf{K})$ and the number of photophonons $n_1^j(\mathbf{K})$. The probability of transition per unit time from the state $n^j(\mathbf{K})$, $n_1^j(\mathbf{K})$ into the state $n^j(\mathbf{K}) + \delta_{\mathbf{KK}'}$, $n_1^j(\mathbf{K}) - \delta_{\mathbf{KK}'}$ is

$$P_j(\mathbf{K}') = (2\pi/\hbar) |(n^j(\mathbf{K}) + \delta_{\mathbf{KK}'},$$
$$n_j^j(\mathbf{K}) - \delta_{\mathbf{KK}'} | E' | n^j(\mathbf{K}), \; n_j^j(\mathbf{K}))|^2 \delta(E - E_0),$$

where E and E_0 are the energies of the final and

Numerical values of certain quantities

	Diamond	Si	Ge
d (cm)	$3.6\cdot10^{-8}$	$5.4\cdot10^{-8}$	$5.6\cdot10^{-8}$
m (g)	$2.0\cdot10^{-23}$	$4.7\cdot10^{-23}$	$12\cdot10^{-23}$
n_0^2	5.8	12	16
c_{11} (dyne/cm^2)	$9.5\cdot10^{12}$	$1.7\cdot10^{12}$	$1.3\cdot10^{12}$
c_{12} "	$3.9\cdot10^{12}$	$0.64\cdot10^{12}$	$0.48\cdot10^{12}$
c_{44} "	$4.3\cdot10^{12}$	$0.80\cdot10^{12}$	$0.67\cdot10^{12}$
$\omega_{\mathbf{1im}}$ (sec^{-1})	$2.5\cdot10^{14}$	$1.2\cdot10^{14}$	$0.65\cdot10^{14}$
$\mu = (4\pi e^2 d/e^2)^{-1/2}$	$0.95\cdot10^{-5}$	$0.50\cdot10^{-5}$	$0.30\cdot10^{-5}$
A	53	43	40
D	$2.0\cdot10^2$	$1.7\cdot10^2$	$1.5\cdot10^2$
L	$2.8\cdot10^2$	$2.4\cdot10^2$	$2.2\cdot20^2$
F	59	23	20
C^{++}	53	29	27
C^{+-}	32	2.9	0.0
Q	$2.3\cdot10^2$	$7.9\cdot10^2$	$18\cdot10^2$
g_1	0.87	6.5	14
g_2	-0.14	-5.3	-14
χ	$1.2\cdot10^2$	$0.99\cdot10^2$	$1.4\cdot10^2$
a	60	0.62	0.063
r	$0.44\cdot10^2$	$5.5\cdot10^2$	$11\cdot10^2$
$a\,(2n_0^2+2r)\,n_0\,c \approx S_j$	0.77	0.16	0.037
$(n_2-n_1)_{\max}$	$\sim10^{-4}$	$\sim10^{-4}$	$\sim10^{-4}$

initial states, respectively, so that

$$E - E_0 = \hbar\omega^j(\mathbf{K}') - \hbar\omega^j_f(\mathbf{K}') \equiv \hbar\widetilde{\omega}_{2j}(\mathbf{K}') - \hbar\widetilde{\omega}_{1j}(\mathbf{K}').$$

The energy of light of polarization j, absorbed during the time dt, is

$$dE_j = dt\sum_{\mathbf{K}}\hbar\omega^j_f(\mathbf{K})\,P_j(\mathbf{K}) = dtV(2\pi)^{-3}\int\hbar\omega^j_f(\mathbf{K})\,P_j(\mathbf{K})\,K^2dKd\Omega,$$

where V is the volume of the principal region and $d\Omega$ is the solid-angle element in K space. Taking into account the readily-shown fact that the phonon and photophonon branches intersect at the point $\kappa_1 = 0$, changing from integration over K to integration over $E - E_0$, and carrying out this integration, we get

$$dE_j = dtV(2\pi)^{-2}n_0aK_0^2\hbar\omega_{\mathbf{1im}}\int u_j(\mathbf{s})\,[n^j_f(n^j+1)]_{\kappa_1=0}d\Omega,$$

$$u_j(\mathbf{s}) = \chi p_j(\mathbf{s})\,n_0^2 + 2rr_j(\mathbf{s}),\quad a = \mu^{3/2}\sqrt{4}dn_0\varkappa_0\omega_{\mathbf{1im}}. \quad (19)$$

The spectral density of the energy of light in the reciprocal wavelength scale (in vacuo), referred to unit solid angle, is

$$I^0_j = n_0(2\pi)^{-2}\hbar\omega^j_fn^j_fK^2. \quad (20)$$

Comparing (19) and (20) we obtain for the energy absorbed per unit volume

$$dE^0_j = dta\int u_j(\mathbf{s})\,[(n^j+1)\,I^0_j]_{\kappa_1=0}\,d\Omega.$$

For light propagating in the direction $\mathbf{s}$, this yields

$$dE^0_j = dtau_j(\mathbf{s})\,\{[n^j(\mathbf{s})+1]\,\varepsilon_j\}_{\kappa_1=0},$$

where ϵ_j is the spectral density of the energy. From this we obtain approximately[6] for the area of the absorption line

$$S_j(\mathbf{s}) = au_j(\mathbf{s})\,(\bar{n}+1)/v_j(\mathbf{s}), \quad (21)$$

where v_j is the group velocity

$$\bar{n} = [\exp(\hbar\omega_{\mathbf{1im}}/kT) - 1]^{-1}.$$

To find the width of the line it is necessary to take into account the anharmonicity of the displacements of the atoms, since the interaction due to this anharmonicity greatly exceeds E′. This is indeed why one can assume $n^j = \bar{n}$ (the absorption of light does not disturb noticeably the thermal equilibrium) and disregard the transitions involving annihilation of phonons and creation of photophonons.

According to (21), the area of the absorption line depends on the polarization and on the direction of propagation of the light wave. The dependence on $\mathbf{s}$ is particularly pronounced for j = 1. From (19), (11), and (1) it follows that $S_1(\mathbf{s})$ vanishes for the singular directions of $\mathbf{s}$. As indicated above, in this case $\mathbf{w}^0$ lies in the plane of the same face as $\mathbf{s}$ itself. Such light waves do not experience single-phonon absorption.

5. PARAMETERS OF THE THEORY. NUMERICAL RESULTS

The theory contains five parameters (see II)—A, D, L, F, and C. A is determined uniquely from (23.II):

$$A = 32\pi(n_0^2+2)/3\,(n_0^2-1).$$

The values of D and L (also unique) are obtained from (13, 16.II):

$$D = 2\,(d^3/e^2)\,(c_{11}+c_{12}),\quad L = 4\,(d^3/e^2)\,c_{11}.$$

Eq. (19.II) yields two values for F

$$F = \pm[A\,(2L - \Omega^2_{\mathbf{1im}})]^{1/2}/2. \quad (22)$$

When the value of F is fixed, Eqs. (13, 16.II) yield two values for C:

$$C = (2DF \pm \{4D^2F^2 - 2AL[D^2 - 2\Omega_{lim}^2(d^4/e^2)(c_{11} - c_{44})]\}^{1/2})/2L, \quad (23)$$

which lead, according to (22), to the four values $C^{--} = C^{++}$, $C^{-+} = -C^{+-}$ [the first sign of C is from (22), the second from (23)]. The quantities that characterize the optical properties contain F and C only in the combination $(C - 4FS/A)^2$ (cf. II), and therefore the four different sets of parameters lead to two different variants.

The table lists the experimental[7,8,2] (first seven lines of the table) and calculated values of the parameters and quantities that characterize the optical properties, for $F = |F|$ and $C = C^{+-}$. In calculating the area of the absorption band, the group velocity is approximately replaced by the phase velocity, $\bar{n}$ is taken to be zero, and it is assumed that $r_j(s) = p_j(s) = 1$. This latter simplification is used also in the estimate of $(n_2 - n_1)_{max}$, the maximum difference in the index of refraction.

The value obtained for $(n_2 - n_1)_{max}$ is $\sim 10^{-4}$, so that an attempt can be made to observe experimentally the birefringence in the region of the frequency ω_{lim}. An experimental investigation of absorption in the infrared region was made by Collins and Fan,[8] but their results give only the total absorption. An investigation of the dependence of the absorption on the direction of propagation and polarization of light would make it possible to separate the single-phonon absorption and to compare the theory with experiment.

CONCLUSIONS

1. The theory predicts the presence of dispersion and birefringence due to oscillations of the crystal atoms. Both effects are maximal near the limiting frequency of the experimental oscillations, where the difference in the indices of refraction for the two polarizations reaches 10^{-4}.

2. A diamond-like crystal has seven axes, while the directions of the optical axes are along the edges and diagonals of the cubic lattice.

3. The theory leads to a single-phonon absorption of light with a frequency equal to the limiting frequency of the optical oscillations, and predicts a substantial dependence of the absorption on the direction of propagation and polarization of the light.

4. It is desirable to verify experimentally the predictions of the theory; this verification would permit a comparison between experiment and the part of the theory that concerns the optical properties.

The author thanks K. B. Tolpygo for an evaluation of the results of this work.

[1] V. S. Mashkevich, J. Exptl. Theoret. Phys. (U.S.S.R.) **32**, 866 (1957), Soviet Phys. JETP **5**, 707 (1957).

[2] M. Lax and E. Burstein, Phys. Rev. **97**, 39 (1955).

[3] V. S. Mashkevich, Paper delivered to XI Conference on Spectroscopy (in press).

[4] V. S. Mashkevich, Dokl. Akad. Nauk SSSR **121**, 247 (1958), Soviet Phys. "Doklady" **3**, 768 (1958).

[5] M. Born and M. Goeppert Mayer, Theory of Solids (Russ. Transl.) ONTI, 1938.

[6] V. S. Mashkevich, Dissertation, Kiev, 1956.

[7] Bundy, Hall, Strong, and Wentorf, Nature, **176**, 51 (1955); W. C. Dunlap and R. L. Watters, Phys. Rev. **92**, 1396 (1953); S. Bhagavantan and J. Bhimasenacher, Proc. Roy. Soc. (London) **A187**, 381 (1946); H. J. McSkimin, J. Appl. Phys. **24**, 988 (1953); P. H. Keesom and N. Pearlman, Phys. Rev. **91**, 1347 (1953); K. Kohlrausch, Raman Spectra (Russ. Transl.) IIL, 1952.

[8] R. J. Collins and H. J. Fan, Phys. Rev. **93**, 674 (1954).

Translated by J. G. Adashko
16

FREQUENCY SPECTRUM OF ELECTRON SPIN DOUBLE RESONANCE AT COLOR CENTERS IN ALKALI HALIDE CRYSTALS

V. Ya. ZEVIN

Brest State Pedagogical Institute

Submitted to JETP editor May 17, 1958

J. Exptl. Theoret. Phys. (U.S.S.R.) **36**, 116-128 (January, 1959)

The dependence of frequencies in electron spin double resonance on crystal orientation in an external static magnetic field is found for U_2, F_2^+ and M centers in alkali halide crystals. Angular dependence is determined by the structure of the centers; the double-frequency resonance method can thus be used for a direct experimental study of the structure of color centers in alkali halide crystals.

1. STUDY OF SHORT-RANGE ORDER BY THE DOUBLE-FREQUENCY RESONANCE METHOD

THE electron spin double-resonance method[1,2] furnishes the frequencies of spin-nuclear transitions resulting from interactions between a localized electron and one of the nuclei surrounding the center where the electron is localized. These frequencies depend on the wave function of the localized electron and the direction of the external static magnetic field **H**. The dependence on the angle of **H** can be determined without knowing the analytic form of the electron wave function. This dependence is determined by the structure of the center and the symmetry of its neighborhood. The double-frequency resonance method can therefore be used to study the structure of different localization centers from their frequency spectra and angular dependences. When the wave function ψ falls off rapidly outside of the center the principal contribution to the frequency spectrum comes from nuclei of the first and second coordination spheres (i.e., only small frequencies result from interactions with the spins of distant nuclei). Therefore the frequency spectrum and its dependence on crystal orientation in an external magnetic field are sensitive to the short-range order of the localization centers.

Feher[2] investigated the frequency spectrum and angular dependence of double resonance at F centers in KCl. His experiments agree with the accepted view as to the nature of F centers and give the values of $|\psi|^2$ at the lattice sites which are closest to F centers.[3] Feher points out that the experiments obtain many other frequencies some of which are probably associated with defects other than F centers. It is therefore useful to obtain the dependence of double-resonance frequencies in spin-nuclear transitions on crystal orientation in an external field H when the crystal contains color centers other than F centers. This is all the more important because there is no direct experimental evidence showing the structures of a number of different electron localization centers.

2. SPIN HAMILTONIAN FOR INTERACTION BETWEEN A LOCALIZED ELECTRON AND THE MAGNETIC MOMENT OF A LATTICE NUCLEUS. SIMPLIFICATION OF THE HAMILTONIAN

We denote by **S** and $\mathbf{I}_k$ the spins of the electron and nucleus at the k-th lattice site, by μ, μ_k their magnetic moments and by ρ_k the distance from the k-th site. The spin Hamiltonian $\mathcal{H}_{sk}$ for the interaction between a localized electron and the k-th nucleus can be written as follows:[4]

$$\mathcal{H}_{sk} = 4\pi \frac{\mu\mu_k}{SI_k} |\psi(\rho_k = 0)|^2 (\mathbf{I}_k \cdot \mathbf{S}) + \sum_{p,q} A_{pqk} I_{pk} S_q, \quad (1)$$

$$A_{pqk} = \frac{\mu\mu_k}{SI_k} \int \frac{x_{qk}}{\rho_k^3} \frac{\partial |\psi|^2}{\partial x_{pk}} dV. \quad (2)$$

The axes of the Cartesian coordinate system centered at the k-th site are numbered by the subscripts p and q.

The spin Hamiltonian in (1) agrees essentially with the usual form for $\mathcal{H}_{sk}$ as the sum of a Fermi expression and a dipole-dipole interaction,[5] which is mathematically less accurate than (1) because the dipole-dipole term contains the difference between two divergent integrals. However, it is convenient in (1) to separate the Fermi term, which is proportional to $|\psi|^2$ at the k-th site.

When spherical coordinates are used for A_{pqk} in (2) it is easily shown that

$$A_{pqk} = -\frac{4\pi\mu\mu_k}{3SI_k}|\psi(\rho_k = 0)|^2\delta_{pq} + \frac{\mu\mu_k}{SI_k}\int|\psi|^2\frac{3x_{pk}x_{qk} - \rho_k^2\delta_{pq}}{\rho_k^5}dV, \quad (3)$$

where δ_{pq} is the Kronecker symbol. Inserting A_{pqk} from (3) into (1), we obtain

$$\mathcal{H}_{sk} = a(\mathbf{I}_k \cdot \mathbf{S}) + \sum_{p,q} D_{pqk} I_{pk} S_q. \quad (4)$$

The first expression on the right is the Fermi term while the second is the mean value of the dipole-dipole interaction. It follows from (1) and (3) that

$$a = \frac{8\pi}{3}\frac{\mu\mu_k}{SI_k}|\psi(\rho_k = 0)|^2, \quad (5a)$$

$$D_{pqk} = \frac{\mu\mu_k}{SI_k}\int|\psi|^2\frac{3x_{pk}x_{qk} - \rho_k^2\delta_{pq}}{\rho_k^5}dV. \quad (5b)$$

It is obvious that $D_{pq} = D_{qp}$. From considerations of symmetry the spin Hamiltonian (4) can be simplified further. Let $G_i^{(k)}$ be a symmetry operator satisfy the following requirements: (1) It does not affect the spatial position of the electron localization center. (2) It does not move the k-th nucleus of the lattice. (3) It interchanges identical crystal ions. Then

$$G_i^{(k)}|\psi|^2 = |\psi|^2. \quad (6)$$

From (6) we easily obtain the relation between different coefficients in (5b) resulting from symmetry:

$$D_{pqk} = G_i^{(k)} D_{pqk} = \sum_{s,r} b_{isr} D_{srk}. \quad (7)$$

The coefficients b_{isr} (which are generally also dependent on p, q, and k) are determined very simply in any specific case.

We note that the set of operations $G_i^{(k)}$ comprises a subgroup of the crystal point symmetry group. The fact that the present problem is subject to less than complete crystal symmetry accounts for the frequency anisotropy of spin-nuclear transitions (the dependence of double-resonance frequencies on crystal orientation in an external magnetic field H).

It is also evident that when the coordinate axes x_{1k}, x_{2k}, x_{3k} transform into each other under the operations of crystal point symmetry leaving lattice defects in their places, the coefficients D_{pqk} will not depend on the subscript k for a group of ions that are arranged identically with respect to the localization center and have the same symmetry elements of $G_i^{(k)}$. Each ion of this group can be transferred to any other site of the group by a crystal symmetry operation without effecting the spatial arrangement of the lattice defect. Hereinafter local coordinate systems will always satisfy the foregoing conditions.

3. U_2 CENTERS

There is indirect experimental evidence that the U_2 absorption band in KCl results from the presence of hydrogen atoms at interstices of the lattice.[6] It was shown in reference 6 that the U_2 optical absorption band is accompanied by the paramagnetic resonance of hydrogen atoms. The paramagnetic resonance line width ($\approx$ 68 gauss) results from the interaction between the electron spin and the magnetic moments of the surrounding nuclei.

We shall now obtain the electron spin double resonance frequencies resulting from the interaction between the U_2-center electron and eight surrounding nuclei, assuming that the hydrogen atom is at the center of a cube (Fig. 1). For each of the eight points the symmetry elements of $G_i^{(k)}$ form a group C_{3v} (a three-fold rotation axis and three planes of symmetry containing the rotation axis). The local coordinate system for ion 1 is chosen such that the axes x_{1k}, x_{2k} and x_{3k} are parallel to X, Y and Z. The coordinate axes for ion 2 are parallel to the directions [0 $\bar{1}$ 0], [1 0 0] and [0 0 1]. The local coordinate systems for other ions in Fig. 1 are then obtained by symmetry operations which leave the U_2 center fixed but transport ion 1 (or 2) together with its local coordinate system to equivalent points. In these coordinate systems all integrals in (5b) are identical for positive and negative ions, respectively.

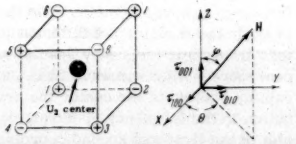

FIG. 1

Performing the symmetry operations of $G_i^{(k)}$ in group C_{3v} on the coefficients D_{pq}, we obtain

$$D_{11} = D_{22} = D_{33} = 0, \quad D_{12} = D_{23} = D_{31}. \quad (8)$$

The vanishing of the coefficients D_{pp} follows from the fact that $D_{11} + D_{22} + D_{33} = 0$. We denote the unit axes of the local systems by τ_{1k}, τ_{2k}, τ_{3k} and the coefficients D_{pq}, $p \neq q$, by $D^{\pm}$, where the upper sign refers to positive ions and the lower sign to negative ions. The spin Hamiltonian (4) with (8) taken into account can then be written as follows:

$$\mathcal{H}_{sk}^{\pm} = a^{\pm}(\mathbf{I}_k \cdot \mathbf{S}) + D^{\pm}\sum_{p \neq q}(\mathbf{I}_k \cdot \tau_{pk})(\mathbf{S} \cdot \tau_{qk}). \quad (9)$$

We assume at first that $a^{\pm} \gg D^{\pm}$, so that the

selection rules for double-resonance spin-nuclear transitions are $\Delta M_S = 0$; $\Delta M_I = \pm 1$, where M_S and M_I are the spin projections on the field $\mathbf{H}$, which is oriented with respect to the crystallographic axes as shown in Fig. 1. To calculate the mean value of $\mathcal{H}_{sk}$ we must know the projections of τ_{pq} $(p = 1, 2, 3)$ on the field direction. It is evident that

$$\tau_{pkH} = \tau_{pkX} \sin\varphi \cos\vartheta + \tau_{pkY} \sin\varphi \sin\vartheta + \tau_{pkZ} \cos\varphi. \quad (10)$$

In (10) τ_{pkX} is the projection of τ_{pk} on the X axis etc. In order to obtain the correct frequency, the Zeeman energy $g_n\beta_n(\mathbf{I}_k \cdot \mathbf{H})$ must be added to $\mathcal{H}_{sk}$, where g_n and β_n are the nuclear g-factor and nuclear magneton, respectively. Since the isotropic term in (10) makes the isotropic contribution $a^{\pm}/2$ to the frequency and the contribution of $D^{\pm}(\mathbf{I}_k \cdot \tau_{pk})(\mathbf{S} \cdot \tau_{qk})$ is $\frac{1}{2}D^{\pm}\tau_{pkH}\tau_{qkH}$, we obtain the following eight frequencies in the double-resonance spectrum of a U_2 center:

$$\begin{aligned}
h\nu_{1,8}^{\mp} &= g_{n_i}\beta_n H + {}^1/_2 a^{\pm} + {}^1/_2 (\sin^2\varphi \sin 2\vartheta + \sin 2\varphi (\cos\vartheta + \sin\vartheta)) D^{\pm}, \\
h\nu_{3,6}^{\mp} &= g_{n_i}\beta_n H + {}^1/_2 a^{\pm} + {}^1/_2 (\sin^2\varphi \sin 2\vartheta - \sin 2\varphi (\cos\vartheta + \sin\vartheta)) D^{\pm}, \\
h\nu_{5,2}^{\mp} &= g_{n_i}\beta_n H + {}^1/_2 a^{\pm} - {}^1/_2 (\sin^2\varphi \sin 2\vartheta - \sin 2\varphi (\cos\vartheta - \sin\vartheta)) D^{\pm}, \\
h\nu_{7,4}^{\mp} &= g_{n_i}\beta_n H + {}^1/_2 a^{\pm} - {}^1/_2 (\sin^2\varphi \sin 2\vartheta + \sin 2\varphi (\cos\vartheta - \sin\vartheta)) D^{\pm}
\end{aligned} \quad (11)$$

The subscripts of $h\nu$ in (11) refer to the numbered nuclei in Fig. 1.

When $\mathbf{H}$ lies in the XY plane we have $\varphi = \pi/2$ and

$$\begin{aligned}
h\nu_{1,8}^{\mp} &= h\nu_{3,6}^{\mp} = g_{n_i}\beta_n H + {}^1/_2 a^{\pm} + {}^1/_2 D^{\pm} \sin 2\vartheta, \\
h\nu_{5,2}^{\mp} &= h\nu_{7,4}^{\mp} = g_{n_i}\beta_n H + {}^1/_2 a^{\pm} - {}^1/_2 D^{\pm} \sin 2\vartheta.
\end{aligned} \quad (12)$$

In this case only four frequencies are obtained.

We shall now drop the assumption that $a^{\pm} \gg D^{\pm}$. As previously, the electron spin is oriented in the direction of $\mathbf{H}$, so that $M_S = \frac{1}{2}$ and the selection rule is $\Delta M_S = 0$.

Let $\mathcal{H}_{sk}$ be the spin Hamiltonian averaged over the electron spin wave functions. From (9), with $g_n\beta_n(\mathbf{I}_k \cdot \mathbf{H})$ taken into account, we then obtain

$$\overline{\mathcal{H}}_{sk} = g_{n_i}\beta_n (\mathbf{I}_k \cdot \mathbf{H}) + {}^1/_2 a^{\pm} I_{kH} + {}^1/_2 D^{\pm} \sum_{\substack{p,q \\ p+q}} \sum_{X,Y,Z} I_{kX} \tau_{pkX} \tau_{qkH}. \quad (13)$$

It is convenient to rewrite (13) by introducing the projection I_{kn} of the spin of the k-th nucleus on the "quantization axis."[7] If M_n is the quantum number of this projection of the spin operator the selection rule is $\Delta M_n = \pm 1$. It follows from (13) that

$$\begin{aligned}
\overline{\mathcal{H}}_{sk} = [&(m_{1k} + g_{n_i}\beta_n \alpha_1 H)^2 + (m_{2k} + g_{n_i}\beta_n \alpha_2 H)^2 \\
&+ (m_{3k} + g_{n_i}\beta_n \alpha_3 H)^2]^{1/2} I_{kn}.
\end{aligned} \quad (14)$$

Here α_1, α_2, α_3 are the projections of $\mathbf{H}/H$ on the X, Y, and Z axes,

$$m_{1k} = {}^1/_2 \alpha_1 a^{\pm} + \frac{D^{\pm}}{2} \sum_{p+q} \tau_{pkX} \tau_{qkH}, \quad (15)$$

and m_{2k} and m_{3k} are given by (15) with τ_{pkX} replaced by τ_{pkY} and τ_{pkZ}, respectively, and α_1 by α_2 and α_3. The frequencies are easily obtained from (14):

$$\begin{aligned}
h\nu_k = [&(m_{1k} + g_{n_i}\beta_n \alpha_1 H)^2 + (m_{2k} + g_{n_i}\beta_n \alpha_2 H)^2 \\
&+ (m_{3k} + g_{n_i}\beta_n \alpha_3 H)^2]^{1/2}.
\end{aligned} \quad (16)$$

It can be shown that when $a^{\pm} \gg D^{\pm}$ (16) becomes Eq. (11) as an expression for the frequencies.

The coefficients D_{pq} (the dipole-dipole interaction tensor) can most conveniently be written in the principal coordinate system where D_{pq} is diagonal. In the present case the symmetry group C_{3v} determines these coordinates, the x_{3k} axis being the three-fold rotation axis while the other two axes have any mutually perpendicular directions in a plane perpendicular to the C_3 axis. D_{pq} now has only the diagonal components $-D^{\pm}$, $-D^{\pm}$, and $2D^{\pm}$.

4. F_2^+ CENTERS

An F_2^+ center is a system consisting of two negative vacancies and an electron in an ionic crystal.[8] The electron ψ cloud can either be distributed symmetrically with respect to the two vacancies or be concentrated to a large degree around only one vacancy, giving what we shall call the symmetrical and asymmetrical F_2^+-center models, respectively. The second model possesses greater probability but both models are used in the literature.[9,10,11]

The angular dependences of a number of double-resonance frequencies will differ in the symmetrical and asymmetrical models. We shall determine the double-resonance frequency spectrum by considering only the interaction of the electron with the nearest neighbors of the F_2^+ center (Fig. 2). Table I is a list of the symmetry elements of $G_i^{(k)}$ for each of seven groups of "nearest neighbor" ions which are located identically with respect to the F_2^+ center. The spin Hamiltonian for ions of

FIG. 2. Immediate neighborhood of an F_2^+ center. Ions located one row above those shown in the figure are denoted by primes (3′a, a′, etc.); those located one row below by double primes (3″a, a″ etc.). The nearest neighbors include ions which are not farther distant than $\sqrt{2R}$ from a (upper circle) or b (lower circle).

groups I and VI will differ in the symmetrical and asymmetrical cases since the symmetry groups of the $G_i^{(k)}$ elements differ; frequencies resulting from interactions with ions of group I will be highest because these ions are closest to the vacant lattice sites a and b simultaneously. Moreover, in the asymmetrical case, the plane σ'' is not a plane of symmetry because the vacancies a and b are not equivalent in this instance. Therefore the coefficients in the spin Hamiltonian for ions of a single group are not equal when these ions have specularly symmetrical positions with respect to σ''. In the symmetrical case the coefficients of the spin Hamiltonian for all ions of a given group are identical. Compared with the asymmetrical case there are now only one half as many frequencies for groups of ions which are not in the σ'' plane. For the sake of simplicity we shall not supply the coefficients a and D_{pq} with additional indices but shall keep in mind the preceding discussion and the fact that the coefficients differ for ions of different groups.

Local coordinate systems are naturally selected so that the x_{1k} axis is parallel to the a-b direction, the x_{2k} axis is perpendicular to this direction and the x_{3k} axis is perpendicular to the plane of the F_2^+ center (the principal axes of D_{pq} can be given without knowing actual magnitudes only for ions of group I in the symmetrical model and for ions of group V; the axes are those already mentioned).

Table II gives the directions of τ_{pk} for some ions. Directions for other local coordinate systems are obtained by the procedure described in Sec. 2.

In the symmetrical model the symmetry group of

TABLE II

Local orthogonal unit axes for ions 1,3a,a′, 5a, 7a, 1′,3′a	F_2^+ center in (001) plane		F_2^+ center in (010) plane		F_2^+ center in (100) plane	
	$a-b$ [110]	Along [$\bar{1}$10]	$a-b$ [101]	Along [$\bar{1}$01]	$a-b$ [011]	Along [01$\bar{1}$]
τ_1	110	$\bar{1}$10	101	$\bar{1}$01	011	01$\bar{1}$
τ_2	$\bar{1}$10	$\bar{1}\bar{1}$0	10$\bar{1}$	$\bar{1}$0$\bar{1}$	01$\bar{1}$	0$\bar{1}\bar{1}$
τ_3	001	001	010	010	100	100

TABLE I. Symmetry elements of $G_i^{(k)}$

Ion group	Symmetrical model	Asymmetrical model
I: Ions 1, 2	σ, σ'', C_2	σ
II: Ions 3a, b; 4a, b	σ	σ
III: Ions a′, b′, a″, b″	σ'	σ'
IV: Ions 5a, b; 6a, b	σ	σ
V: Ions 7a, b	σ, σ', C_2'	σ, σ', C_2'
VI: Ions 1′, 2′, 1″, 2″	σ''	–
VII: Ions 3′a, b; 3″a, b 4′a, b; 4″a, b	–	–

σ – plane of F_1^+ center; σ' – plane perpendicular to σ and containing a and b; σ'' – plane perpendicular to σ and containing ions 1 and 2 (Fig. 2); C_2 – a,-b axis; C_2' – axis through ions 1 and 2.

$G_i^{(k)}$ for group I ions is C_{2v}. Therefore $D_{pqk} = 0$ when $p \neq q$:

$$\mathcal{H}_{sk}^{I} = a(\mathbf{I}_k\cdot\mathbf{S}) + D_{11}(\mathbf{I}_k\cdot\boldsymbol{\tau}_{1k})(\mathbf{S}\cdot\boldsymbol{\tau}_{1k}) + D_{22}(\mathbf{I}_k\cdot\boldsymbol{\tau}_{2k})(\mathbf{S}\cdot\boldsymbol{\tau}_{2k}) + D_{33}(\mathbf{I}_k\cdot\boldsymbol{\tau}_{3k})(\mathbf{S}\cdot\boldsymbol{\tau}_{3k}) = (a - D_{\parallel} - D_{\perp})(\mathbf{I}_k\cdot\mathbf{S}) + (2D_{\parallel} + D_{\perp})(\mathbf{I}_k\cdot\boldsymbol{\tau}_{1k})(\mathbf{S}\cdot\boldsymbol{\tau}_{1k}) + (2D_{\perp} + D_{\parallel})(\mathbf{I}_k\cdot\boldsymbol{\tau}_{2k})(\mathbf{S}\cdot\boldsymbol{\tau}_{2k}). \quad (17)$$

In deriving (17) we used the fact that the trace of D_{pq} is 0 and employed the notation

$$D_{11} = D_{\parallel};\ D_{22} = D_{\perp}.$$

In the asymmetrical model the symmetry group for the same ions is C_s, so that only the coefficients D_{13} and D_{23} vanish (the x_{3k} axis being perpendicular to the C_s plane). Consequently, in this case,

$$\mathcal{H}_{sk}^{I} = (a - D_{\parallel} - D_{\perp})(\mathbf{I}_k\cdot\mathbf{S}) + (2D_{\parallel} + D_{\perp})(\mathbf{I}_k\cdot\boldsymbol{\tau}_{1k})(\mathbf{S}\cdot\boldsymbol{\tau}_{1k}) + (2D_{\perp} + D_{\parallel})(\mathbf{I}_k\cdot\boldsymbol{\tau}_{2k})(\mathbf{S}\cdot\boldsymbol{\tau}_{2k}) + D_{12}[(\mathbf{I}_k\cdot\boldsymbol{\tau}_{1k})(\mathbf{S}\cdot\boldsymbol{\tau}_{2k}) + (\mathbf{I}_k\cdot\boldsymbol{\tau}_{2k})(\mathbf{S}\cdot\boldsymbol{\tau}_{1k})]. \quad (18)$$

The spin Hamiltonian of ion groups II and IV in both F_2^+-center models is also given by (18) (see Table I). For ions of Group III we have the following spin Hamiltonian:

$$\mathcal{H}_{sk}^{III} = (a - D_{\parallel} - D_{\perp})(\mathbf{I}_k\cdot\mathbf{S}) + (2D_{\parallel} + D_{\perp})(\mathbf{I}_k\cdot\boldsymbol{\tau}_{1k})(\mathbf{S}\cdot\boldsymbol{\tau}_{1k}) + (2D_{\perp} + D_{\parallel})(\mathbf{I}_k\cdot\boldsymbol{\tau}_{2k})(\mathbf{S}\cdot\boldsymbol{\tau}_{2k}) + D_{13}[(\mathbf{I}_k\cdot\boldsymbol{\tau}_{1k})(\mathbf{S}\cdot\boldsymbol{\tau}_{3k}) + (\mathbf{I}_k\cdot\boldsymbol{\tau}_{3k})(\mathbf{S}\cdot\boldsymbol{\tau}_{1k})]. \quad (19)$$

This equation does not contain D_{23} and D_{21} because the x_{2k} axis is perpendicular to the symmetry plane σ'.

For ions of group V the symmetry elements of $G_i^{(k)}$ form the group C_{2v}, and the corresponding spin Hamiltonian is given by (17). In the symmetrical F_2^+ center group VI ions possess a symmetry

plane σ''; consequently D_{12} and D_{13} vanish, so that

$$\mathcal{H}_{ik}^{VII} = (a - D_{\parallel} - D_{\perp})(\mathbf{I}_k \cdot \mathbf{S}) + (2D_{\parallel} + D_{\perp})(\mathbf{I}_k \cdot \boldsymbol{\tau}_{1k})(\mathbf{S} \cdot \boldsymbol{\tau}_{1k}) + (2D_{\perp} + D_{\parallel})(\mathbf{I}_k \cdot \boldsymbol{\tau}_{2k})(\mathbf{S} \cdot \boldsymbol{\tau}_{2k}) + D_{23}[(\mathbf{I}_k \cdot \boldsymbol{\tau}_{2k})(\mathbf{S} \cdot \boldsymbol{\tau}_{3k}) + (\mathbf{I}_k \cdot \boldsymbol{\tau}_{3k})(\mathbf{S} \cdot \boldsymbol{\tau}_{2k})]. \quad (20)$$

In the asymmetrical case, however, symmetry elements of $G_i^{(k)}$ are absent, so that

$$\mathcal{H}_{ik}^{VII} = (a - D_{\parallel} - D_{\perp})(\mathbf{I}_k \cdot \mathbf{S}) + (2D_{\parallel} + D_{\perp})(\mathbf{I}_k \cdot \boldsymbol{\tau}_{1k})(\mathbf{S} \cdot \boldsymbol{\tau}_{1k}) + (2D_{\perp} + D_{\parallel})(\mathbf{I}_k \cdot \boldsymbol{\tau}_{2k})(\mathbf{S} \cdot \boldsymbol{\tau}_{2k}) + \sum_{p \neq q} D_{pq}(\mathbf{I}_k \cdot \boldsymbol{\tau}_{pk})(\mathbf{S} \cdot \boldsymbol{\tau}_{qk}). \quad (21)$$

Group VII ions have the same spin Hamiltonian.

We shall now determine the frequencies for double-resonance spin-nuclear transitions. Let the static magnetic field **H** lie in the (001) plane forming an angle θ with the [100] direction. The isotropic part of the spin Hamiltonian is usually considerably larger than the anisotropic part,[2,3,7] so that for simplicity we shall assume $a \gg D_{pq}$. Therefore, if as previously M_S and M_I are the quantum numbers of the spin projections in the **H** direction, the selection rules for spin-nuclear transitions will be $\Delta M_S = 0$ and $\Delta M_I = \pm 1$. The frequencies are easily computed without assumptions regarding the orientation of **H** and the magnitudes of a and D_{pq}, as was shown for U_2 centers.

To determine the frequencies we must know the projections of the local axes on **H**. If the F_2^+ center lies in the (001) plane and is oriented along [110] the projections of the unit axes in Table II are given by

$$\tau_{1H} = (\sin\theta + \cos\theta)/\sqrt{2}; \quad \tau_{2H} = (\sin\theta - \cos\theta)/\sqrt{2}; \quad \tau_{3H} = 0. \quad (22)$$

If the F_2^+ center lies along $[\bar{1}10]$ it follows from Table II that

$$\tau'_{1H} = \tau_{2H}; \quad \tau'_{2H} = -\tau_{1H}; \quad \tau'_{3H} = \tau_{3H}. \quad (23)$$

The primed axes in (23) refer to the case in which the F_2^+ center is directed along $[\bar{1}10]$. For local coordinate axes not given in the table projections on **H** can differ from (22) in sign. If the F_2^+ center lies in the (100) plane the projections are

$$\tau_{1kH} = \pm\sin\theta/\sqrt{2}; \quad \tau_{2kH} = \pm\sin\theta/\sqrt{2}; \quad \tau_{3kH} = \pm\cos\theta. \quad (24)$$

The combination of signs in (24) depends on the number k of the ion. Finally, for an F_2^+ center in the (010) plane the result differs from (24) by the interchange of $\sin\theta$ and $\cos\theta$. The frequencies are determined in the same way as in the preceding section.

When F_2^+ centers lie in the (001) plane spin-nuclear transitions for ions of the first group in the symmetrical case are represented by

$$h\nu = g_n\beta_n H + \frac{1}{2}\left(a + \frac{D_{\parallel} + D_{\perp}}{2}\right) + \frac{D_{\parallel} - D_{\perp}}{4}\sin 2\theta;$$
$$h\nu' = g_n\beta_n H + \frac{1}{2}\left(a + \frac{D_{\parallel} + D_{\perp}}{2}\right) - \frac{D_{\parallel} - D_{\perp}}{4}\sin 2\theta. \quad (25)$$

For ions of the second group in the symmetrical case we have

$$h\nu^{\pm} = g_n\beta_n H + \frac{1}{2}\left(a + \frac{D_{\parallel} + D_{\perp}}{2}\right) \pm \frac{D_{\parallel} - D_{\perp}}{4}\sin 2\theta \mp \frac{1}{2}D_{12}\cos 2\theta;$$
$$h\nu'^{\pm} = g_n\beta_n H + \frac{1}{2}\left(a + \frac{D_{\parallel} + D_{\perp}}{2}\right) - \frac{D_{\parallel} - D_{\perp}}{4}\sin 2\theta \pm \frac{1}{2}D_{12}\cos 2\theta. \quad (26)$$

In (25) and (26) $h\nu$ and $h\nu'$ refer to two mutually perpendicular orientations of F_2^+ centers in the (001) plane.

For ions of groups III, V and VI spin-nuclear transition frequencies are given by (25), and for groups IV and VII by (26).

In the symmetrical case for F_2^+ centers in the (001) plane there are the single frequencies $h\nu$ and $h\nu'$ for groups I, III, V and VI, and pairs of frequencies for groups II, IV and VII.

For F_2^+ centers in the (100) plane in the symmetrical case spin-nuclear transition frequencies resulting from an interaction between the spin of a localized electron and the magnetic moment of the k-th nucleus are given by the following equations:

For groups I and V:

$$h\nu = g_n\beta_n H + \frac{1}{2}(a - D_{\parallel} - D_{\perp}) + \frac{3}{4}(D_{\parallel} + D_{\perp})\sin^2\theta. \quad (27)$$

For groups II and IV:

$$h\nu^{\pm} = g_n\beta_n H + \frac{1}{2}(a - D_{\parallel} - D_{\perp}) + \frac{3}{4}\left(D_{\parallel} + D_{\perp} \pm \frac{2}{3}D_{12}\right)\sin^2\theta. \quad (28)$$

For group III:

$$h\nu^{\pm} = g_n\beta_n H + \frac{1}{2}(a - D_{\parallel} - D_{\perp}) + \frac{3}{4}(D_{\parallel} + D_{\perp})\sin^2\theta \pm \frac{D_{12}}{2\sqrt{2}}\sin 2\theta. \quad (29)$$

For group VI:

$$h\nu^{\pm} = g_n\beta_n H + \frac{1}{2}(a - D_{\parallel} - D_{\perp}) + \frac{3}{4}(D_{\parallel} + D_{\perp})\sin^2\theta \pm \frac{D_{23}}{2\sqrt{2}}\sin 2\theta. \quad (30)$$

For group VII:

$$h\nu_2^{\pm} = g_n\beta_n H + \frac{1}{2}(a - D_{\parallel} - D_{\perp}) + \frac{3}{4}\left(D_{\parallel} + D_{\perp} + \frac{2}{3}D_{12}\right)\sin^2\theta \pm \frac{D_{13}+D_{23}}{2\sqrt{2}}\sin 2\theta;$$
$$h\nu_1^{\pm} = g_n\beta_n H + \frac{1}{2}(a - D_{\parallel} - D_{\perp}) + \frac{3}{4}\left(D_{\parallel} + D_{\perp} - \frac{2}{3}D_{12}\right)\sin^2\theta \pm \frac{D_{13}-D_{23}}{2\sqrt{2}}\sin 2\theta. \quad (31)$$

If the F_2^+ center lies in the (010) plane the results are the same as in the (100) plane with $\sin\theta$ in (27) to (31) replaced by $\cos\theta$.

Let us now consider the results for the asymmetrical F_2^+-center model. For ions of groups I and VI and F_2^+ centers in the (001) plane we have

$$h\nu^{\pm} = g_n\beta_n H + \frac{1}{2}\left(a + \frac{D_{\parallel}+D_{\perp}}{2}\right) + \frac{D_{\parallel}-D_{\perp}}{4}\sin 2\theta \pm \frac{1}{2}D_{12}\cos 2\theta;$$
$$h\nu'^{\pm} = g_n\beta_n H + \frac{1}{2}\left(a + \frac{D_{\parallel}+D_{\perp}}{2}\right) - \frac{D_{\parallel}-D_{\perp}}{4}\sin 2\theta \pm \frac{1}{2}D_{12}\cos 2\theta. \quad (32)$$

For group I and F_2^+ centers in the (100) plane we have

$$h\nu^{\pm} = g_n\beta_n H + \frac{1}{2}(a - D_{\parallel} - D_{\perp}) + \frac{3}{4}\left(D_{\parallel} + D_{\perp} \pm \frac{2}{3}D_{12}\right)\sin^2\theta, \quad (33)$$

and for group VI the frequencies are given by (31).

For the remaining ion groups the angular dependences of the frequencies are the same as for the corresponding groups in the symmetrical case.

In the asymmetrical model the frequencies for F_2^+ centers in the (010) plane are given by the symmetrical model in the (100) plane with $\sin\theta$ replaced by $\cos\theta$.

Each ion group in the asymmetrical case has twice as many different frequencies as the same groups in the symmetrical case.

It is evident from the foregoing that F_2^+ centers lying in mutually perpendicular directions in the (001) plane are represented by different angular dependences of the frequencies, whereas for F_2^+ centers in the other two planes the frequency spectrum is independent of the F_2^+-center orientation in the plane. If the F_2^+ center lies in the (001) plane the weight of each frequency for ion groups I, II, IV and V is one-half that of the corresponding frequency when the F_2^+ center lies in the (010) or (100) plane and is equal to N/6 and N/3 for the asymmetrical and symmetrical model, respectively (N is the number of F_2^+ centers in the crystal). For other frequencies the weight is independent of the plane in which the F_2^+ center is located and is twice as large as the values just given.

We may now inquire about the difference between the angular dependence of the double-resonance frequency for an F center and that for an F_2^+ center which is regarded as an F center that is polarized by a neighboring negative vacancy (the asymmetrical model). It is simplest to compare the two frequencies in the local coordinate system that was used for the nuclei surrounding the F center.[3] Denoting the coefficient of the dipole-dipole interaction in this system by $D_{p'q'}$, when for the positive ions nearest to the vacancy the primed axes are along the principal crystallographic axes and the x_3' axis passes through the vacancy, for k = 1, for example, we obtain

$$h\nu_{0,0,1}^{k=1} = g_n\beta_n H + \frac{1}{2}(a + D_{2'2'}) + \frac{1}{2}(D_{3'3'} - D_{2'2'})\sin^2\theta + \frac{1}{2}D_{3'2'}\sin 2\theta. \quad (34)$$

For F centers $D_{3'2'} = 0$, and we obtain the already known double-resonance frequency for this case[2,3] (in reference 3 $a + D_{2'2'} = A$, $D_{3'3'} - D_{2'2'} = BR^2$).

The angular dependences of other frequencies for F centers in the asymmetrical model can be determined in the local coordinate systems of the centers. However, without computing a and D_{pq} it is impossible to determine theoretically whether experiment can distinguish F-center and asymmetrical F_2^+-center frequencies (in (25) the difference in the angular dependence results from the term $\frac{1}{2}D_{3'2'}\sin 2\theta$). For an asymmetrical F_2^+ center the second vacancy has little effect on the ψ-cloud distribution of the F center, so that it is difficult to separate the frequencies. It is still an open question which of the frequencies in (25) to (33) can be resolved experimentally and how well this can be done.

5. M CENTERS

An M center is pictured as being formed by an electron localized near three vacancies resulting from two missing anions and one missing cation (Fig. 3).[8,12,13] As for F_2^+ centers, we have both a symmetrical and an asymmetrical model for M centers. In the symmetrical model the ψ cloud of the localized electron is distributed symmetrically with respect to the anion vacancies a and b, so that vacancies a and b are equivalent. In the more probable asymmetrical case the ψ cloud is concentrated to a greater extent around one of the anion vacancies.

Table III gives the symmetry elements of $G_i^{(k)}$ for nearest-neighbor ions. A knowledge of $G_i^{(k)}$ enables us to write the spin Hamiltonian $\mathcal{H}_{sk}$ at once. For ions of the first group in both M-center models

$$\mathcal{H}^{I}_{sk} = (a - D_1 - D_2)(\mathbf{I}_k \cdot \mathbf{S}) + (2D_1 + D_2)(\mathbf{I}_k \cdot \tau_{1k})(\mathbf{S} \cdot \tau_{1k}) + (2D_2 + D_1)(\mathbf{I}_k \cdot \tau_{2k})(\mathbf{S} \cdot \tau_{2k}) + D_{12}[(\mathbf{I}_k \cdot \tau_{1k})(\mathbf{S} \cdot \tau_{2k}) + (\mathbf{I}_k \cdot \tau_{2k})(\mathbf{S} \cdot \tau_{1k})]. \quad (35)$$

For group II in the symmetrical model $D_{11} = D_{22}$, so that

$$\mathcal{H}^{II}_{sk} = (a - 2D_1)(\mathbf{I}_k \cdot \mathbf{S}) + 3D_1[(\mathbf{I}_k \cdot \tau_{1k})(\mathbf{S} \cdot \tau_{1k}) + (\mathbf{I}_k \cdot \tau_{2k})(\mathbf{S} \cdot \tau_{2k})] + D_{12}[(\mathbf{I}_k \cdot \tau_{1k})(\mathbf{S} \cdot \tau_{2k}) + (\mathbf{I}_k \cdot \tau_{2k})(\mathbf{S} \cdot \tau_{1k})]. \quad (36)$$

In this case the principal axes of the tensor D_{pq} are along C_2 and two mutually perpendicular directions in a plane perpendicular to C_2. The principal values of the tensor are $D_1 - D_{12}$, $D_1 + D_{12}$ and $-2D_1$. In the asymmetrical model the spin Hamiltonian for these ions is given by (36).

For group III in the symmetrical case we have $D_{13} = D_{23}$, and $D_{11} = D_{22}$; otherwise we have (21). The asymmetrical model has the same spin Hamiltonian with different coefficients. Finally, group IV does not possess symmetry elements that simplify the Hamiltonian, so that $\mathcal{H}^{IV}_{sk}$ is given by (21).

The coefficients a and D_{pq} are identical for ions that are mirror reflections of each other in the σ plane. Moreover, in the symmetrical model there are identical coefficients for ions (k_a and k_b) that are located symmetrically with respect to the σ' plane, while all other ion groups have different coefficients. However, we shall not add additional subscripts to a and D_{pq}.

In calculating frequencies it must be remembered that there are four orientations of an M center in a given plane, which is thus divided into four quadrants by the sides of the M center.

Let the field H lie in the (001) plane and make an angle θ with the [100] direction. As previously, we shall assume that $a \gg D_{pq}$. The projections of unit local axes (Fig. 3) on H for M centers with different orientations in different planes will be $\pm\cos\theta$ or $\pm\sin\theta$.

Spin-nuclear transition frequencies in the symmetrical model for an M center in the (001) plane are as follows:

For ions of groups I and IV:

$$h\nu_a^{\pm} = g_n\beta_n H + \frac{1}{2}(a + D_2) + \frac{1}{2}(D_1 - D_2)\cos^2\theta \pm \frac{1}{2}D_{12}\sin 2\theta;$$
$$h\nu_b^{\pm} = g_n\beta_n H + \frac{1}{2}(a + D_2) + \frac{1}{2}(D_1 - D_2)\sin^2\theta \pm \frac{1}{2}D_{12}\sin 2\theta. \quad (37)$$

For groups II and III:

$$h\nu^{\pm} = g_n\beta_n H + \frac{1}{2}(a + D_1) \pm \frac{1}{2}D_{12}\sin 2\theta. \quad (38)$$

For M centers in the (100) plane in the symmetrical model the frequencies are:

For group I:

$$h\nu_a = g_n\beta_n H + \frac{1}{2}(a + D_1) - \frac{2D_1 + D_2}{2}\cos^2\theta;$$
$$h\nu_b = g_n\beta_n H + \frac{1}{2}(a + D_2) - \frac{2D_2 + D_1}{2}\cos^2\theta; \quad (39)$$

For group II:

$$h\nu = g_n\beta_n H + \frac{1}{2}(a + D_1) - \frac{3}{2}D_1\cos^2\theta; \quad (40)$$

For group III:

$$h\nu^{\pm} = g_n\beta_n H + \frac{1}{2}(a + D_1) - \frac{3}{2}D_1\cos^2\theta \pm \frac{1}{2}D_{13}\sin 2\theta; \quad (41)$$

For group IV:

$$h\nu_a^{\pm} = g_n\beta_n H + \frac{1}{2}(a + D_1) - \frac{2D_1 + D_2}{2}\cos^2\theta \pm \frac{1}{2}D_{13}\sin 2\theta; \quad (42)$$
$$h\nu_b^{\pm} = g_n\beta_n H + \frac{1}{2}(a + D_2) - \frac{2D_2 + D_1}{2}\cos^2\theta \pm \frac{1}{2}D_{23}\sin 2\theta.$$

In the asymmetrical model the number of different frequencies for each group is double that in the symmetrical model.

For groups I and IV of an M center in the (001) plane the angular dependences are the same as in the symmetrical model [Eq. (38)]. For groups II and III

TABLE III. Symmetry elements of $G_1^{(k)}$

Ion group	Symmetrical model	Asymmetrical model
I: Ions 1 – 6a, b	σ	σ
II: Ions 1, 3, 7	σ, σ', C_2	σ
III: Ions σ', σ'', 1', 1'', 3', 3'', 7'', 7''	σ'	–
IV: Ions on both sides of group I ions.	–	–

σ – plane of M center; σ' – diagonal plane; C_2 – intersection of these planes

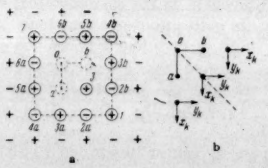

a b

FIG. 3. a) Nearest neighbors of an M center, which include ions in two parallel planes above and below those shown in the figure. The notation is the same as in Fig. 2.

b) Local coordinate systems. The z_k axis is perpendicular to the plane of the M center and is always directed away from it. (As for primed ions, the z_k axis in the figure is always along one of the three directions [0 0 1], [0 1 0] or [1 0 0].

FIG. 4. The Ψ cloud is largely concentrated at a on the left and at b′ on the right.

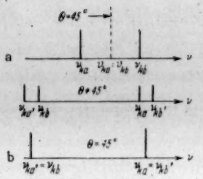

FIG. 5. a) The pair of nuclei k_a and k_b in the symmetrical model result in two frequencies which coincide at $\theta = 45°$.

b) In the asymmetrical model the same ions give four frequencies, two of which are smaller than for the symmetrical case. The weight of each frequency is one half that in the symsymmetrical model.

the frequencies are the same as $h\nu_a^{\pm}$ of (38) in the symmetrical model.

For M centers in the (100) plane in the asymmetrical model the frequencies for group I are

$$\begin{aligned} h\nu_a &= g_n\beta_n H + {}^1/_2(a + D_1) - {}^1/_2(2D_1 + D_2)\cos^2\theta; \\ h\nu'_a &= g_n\beta_n H + {}^1/_2(a + D_2) - {}^1/_2(2D_2 + D_1)\cos^2\theta; \\ h\nu_b &= g_n\beta_n H + {}^1/_2(a' + D'_2) - {}^1/_2(2D'_2 + D'_1)\cos^2\theta; \\ h\nu'_b &= g_n\beta_n H + {}^1/_2(a' + D'_1) - {}^1/_2(2D'_1 + D'_2)\cos^2\theta. \end{aligned} \tag{43}$$

For group IV we have

$$\begin{aligned} h\nu_a^{\pm} &= g_n\beta_n H + {}^1/_2(a + D_1) - {}^1/_2(2D_1 + D_2)\cos^2\theta \pm {}^1/_2 D_{12}\sin 2\theta; \\ h\nu_a'^{\pm} &= g_n\beta_n H + {}^1/_2(a + D_2) - {}^1/_2(2D_2 + D_1)\cos^2\theta \pm {}^1/_2 D_{23}\sin 2\theta; \\ h\nu_b'^{\pm} &= g_n\beta_n H + {}^1/_2(a' + D'_2) - {}^1/_2(2D'_2 + D'_1)\cos^2\theta \pm {}^1/_2 D'_{23}\sin 2\theta; \\ h\nu_b^{\pm} &= g_n\beta_n H + {}^1/_2(a' + D'_1) - {}^1/_2(2D'_1 + D'_2)\cos^2\theta \pm {}^1/_2 D'_{12}\sin 2\theta. \end{aligned} \tag{44}$$

For group II the frequencies are given by $h\nu_a$ and $h\nu'_a$ of (43) and for group III by $h\nu_a^{\pm}$ and $h\nu_a'^{\pm}$ of (44).

For an M center in the (010) plane in both the symmetrical and asymmetrical models frequencies are given by the preceding expressions for the (100) plane with $\cos\theta$ replaced by $\sin\theta$. We must expect large differences in the frequencies for ions of a single group even in the symmetrical model because of considerably different positions of ions in the group with respect to the M center.

We can make the following comments regarding the foregoing angular dependences. When an M center is in the (001) plane the angular dependences for ions k_a and k_b (Fig. 3) differ; also, M centers with sides along [001], [010] and [00$\bar{1}$], [0$\bar{1}$0] give frequencies different from the corresponding frequencies due to the two other M-center orientations in this plane (the sign of D_{12} is different). In the asymmetrical model each frequency is split into two. Thus ions 2a, 2a′, 2b, and 2b′ (Fig. 4) give four frequencies and ions 1o and 1o′ give two. (In our local coordinates D_{pq} for 2a and 2b′ coincide, and for ions 1o and 1o′ $D_{11} = D'_{22}$; $D_{22} = D'_{11}$). This is illustrated in Fig. 5.

When an M center lies in the (100) or (010) plane all four orientations in the symmetrical model give identical sets of frequencies, while in the asymmetrical model two pairs of orientations give different frequencies. However, the M centers shown in Fig. 4 give identical frequencies in this case.

We are deeply grateful to M. F. Deĭgen for directing this work.

[1] G. Feher, Phys. Rev. **103**, 500, 834 (1956).
[2] G. Feher, Phys. Rev. **105**, 1122 (1957).
[3] M. F. Deĭgen and V. Ya. Zevin, J. Exptl. Theoret. Phys. (U.S.S.R.) **34**, 1142 (1958), Soviet Phys. JETP **7**, 790 (1958).
[4] V. Ya. Zevin, Оптика и спектроскопия (Optics and Spectroscopy) **3**, 660 (1957).
[5] H. A. Bethe, Handbuch der Physik 24/2, 385, 1933; A. Abragam and M. H. L. Pryce, Proc. Roy. Soc. (London) **A205**, 135 (1951).
[6] Delbecq, Smaller and Yuster, Phys. Rev. **104**, 599 (1956).
[7] M. F. Deĭgen, J. Exptl. Theoret. Phys. (U.S.S.R.) **33**, 773 (1957), Soviet Phys. JETP **6**, 594 (1958).
[8] F. Seitz, Revs. Modern Phys. **18**, 384 (1946); **26**, 7 (1954).
[9] Nagamiya, Kojima and Kondoh, J. Phys. Soc. (Japan) **9**, 307 (1954).
[10] M. F. Deĭgen and V. Ya. Vinetskiĭ, J. Exptl. Theoret. Phys. (U.S.S.R.) **32**, 289 (1957), Soviet Phys. JETP **5**, 226 (1957).
[11] Yu. E. Perlin, J. Exptl. Theoret. Phys. (U.S.S.R.) **20**, 274 (1950).
[12] M. Ueta, J. Phys. Soc. (Japan) **7**, 107 (1952); J. Lambe and W. D. Compton, Phys. Rev. **106**, 684 (1957); N. W. Lord, Phys. Rev. **106**, 1100 (1957).
[13] Inui, Uemura, and Toyozawa, Progr. Theoret. Phys. (Japan) **8**, 355 (1952); B. S. Gourary and P. J. Luke, Phys. Rev. **107**, 960 (1957).

Translated by I. Emin
17

THE TWO-NUCLEON LS POTENTIAL IN NONRELATIVISTIC MESON THEORY

Yu. V. NOVOZHILOV and I. A. TERENT'EV

Leningrad State University

Submitted to JETP editor May 26, 1958; resubmitted September 27, 1958

J. Exptl. Theoret. Phys. (U.S.S.R.) **36**, 129-139 (January, 1959)

The potential between nucleons is calculated up to and including terms linear in the velocity (with recoil taken partially into account) without using perturbation theory. A potential is found which decreases as e^{-2R} and depends both on the coupling constant and on the cross section for π-N scattering.

ANALYSIS of experimental data shows[1] that it is impossible to explain nucleon-nucleon scattering even at an energy of 90 Mev without a potential which depends on the velocities. Also, the **LS** potential between nucleons has been considered earlier only in perturbation theory.[2] Therefore, it is of interest to clarify the procedure of obtaining a potential that depends on the velocities from meson theory without using perturbation theory.

In this article, the **LS** potential is calculated within the framework of a meson theory which is nonrelativistic with respect to the nucleons. In general, a number of objections have been raised against such a theory at one time or other: (a) The region of high virtual energies may be essential in the interaction of low-energy nucleons. (b) The interaction Hamiltonian is not completely defined within such a theory (this is connected with the problem of a proper calculation of the role of nucleon-antinucleon pairs). However, in the case of the two-nucleon problem, one can consider the nonrelativistic approach to be well founded. The favorable situation here arises because of the resonance character of π-N scattering. Because of this, the center of gravity of the matrix elements for π-N scattering lies in the nonrelativistic region, and just this matrix element enters into the velocity-dependent two-nucleon potential. As regards the interaction Hamiltonian, the method of calculating the potential developed below is not connected essentially with the type of interaction. We consider in this article only the potential that comes from pseudovector coupling.

Instead of the perturbation-theory expansion, an expansion in rate of fall-off with respect to the distance R between two nucleons will be carried out in this article. The n'th-order potential falls off as $\exp(-nR)$. (We use a system of units $\hbar = c = \mu = 1$, where μ is the mass of the meson.) We calculate below potentials of type $\exp(-R)$ and $\exp(-2R)$. (It would seem that potentials of higher order are not meaningful within the nonrelativistic approximation.) It turns out that only the potential $\exp(-2R)$ depends on the velocity. This potential contains, in addition to a term obtained in perturbation theory, a term which depends on the cross section σ_{tot} for π-N scattering.

With the present state of knowledge, this cross section σ_{tot} must be taken from experiment; in this way, the potential obtained might be called semi-phenomenological. In the static case, such a semi-phenomenological potential has been considered earlier by Klein and McCormick,[3] Miyazawa,[4] and one of the authors.[5]

The calculation in this article is based on the methods of a theory of the scattering of "dressed" particles, which was given in reference 6 by one of the authors (we denote reference 6 by I). We consider the meson cloud of both nucleons to be the same as it would be in the absence of interaction between the nucleons. The interaction arises both from meson exchange and from distortion of the meson clouds.

Renormalization causes considerable difficulty, in general, in calculations other than perturbation theory ones. In this work, this difficulty does not arise, because we consider only the approximation linear in velocity, in which the problem of renormalization is the same as in the static case.

In the classification of terms with respect to velocity, some arbitrariness arises, in the general case, in the definition of the potential[2,7] since, on the one hand, terms of the type of the kinetic energy $p^2/2M$ are equivalent to static potentials of higher order and, on the other hand, as Levy showed,[7] some terms in the velocity do not contribute to the scattering. The former is not important in our case, since we consider only potentials of the first

two orders, $\exp(-R)$ and $\exp(-2R)$, where this arbitrariness is connected with the well-investigated static potential of fourth order in perturbation theory.[2;7,8] Concerning the latter, those terms in the velocity which do not influence the scattering, have a characteristic form and are easily identified.

INITIAL FORMULAE FOR THE POTENTIAL

1. We denote by W_{ba} the matrix element of the potential, in momentum representation, between states a and b of the system of two free nucleons. (Two-nucleon states will be labelled by letters a, b, c ....) The initial formula for W_{ba} has the following form [see I(28)]:

$$W_{ba}^{\mathrm{I}} + W_{ba}^{\mathrm{II}} = W_{ba} = (\Phi_b (H - E_a)\,\Phi_a) - \sum_{\substack{n,c \\ \mathbf{p}_a = \mathbf{p}_n}} \frac{(\psi_{nc}^{(-)}, (H - E_b)\,\Phi_b)^*\,(\psi_{nc}^{(-)}, (H - E_a)\,\Phi_a)}{E_n + E_c - E_a - i\varepsilon}. \quad (1)$$

Here $\psi_{nc}^{(-)}$ is the eigenvector of the complete Hamiltonian H for a state with n mesons and energy E_n and two nucleons c with energy E_c; $\mathbf{q}_n$ is the total momentum of the n mesons. Summation over n in Eq. (1) begins with $n = 1$ (there are no states in the sum which do not contain real mesons). In comparison with I(28), a factor $(2\pi)^3 \delta(\mathbf{P}_a - \mathbf{P}_b)$ has been taken out, where $\mathbf{P}$ is the total momentum, and specialization has been made to the center-of-mass system (c.m.s.).

In the c.m.s., the Hamiltonian H for two nucleons, interacting with the meson field, is

$$H = -\frac{1}{M}\nabla_R^2 + \frac{u^2}{4M} + H_\pi + U_1(\mathbf{r}_1) + U_2(\mathbf{r}_2); \quad (2)$$

$$U_i(\mathbf{r}_i) = \sum_q \{V_{iq} e^{i\mathbf{q}\cdot\mathbf{r}_i} a_q + \mathrm{H.c.}\};\ V_{iq} = if\,(\boldsymbol{\sigma}_i \cdot \mathbf{q})\,\tau_{iq}/(2\omega_q)^{1/2};$$

$$\mathbf{r}_1 = -\mathbf{r}_2 = \mathbf{R}/2;\ \omega_q = (1 + q^2)^{1/2};\ \mathbf{u} = \sum \mathbf{q} a_q^+ a_q.$$

The operators σ_i and τ_i relate to the i-th nucleon; q denotes all quantum numbers of the meson. The term $u^2/4M$ appears in H from elimination of the center-of-mass coordinates.

The functionals Φ_a and Φ_b describe the asymptotic states of a system of two "dressed" nucleons; both Φ_a and Φ_b are solutions of the Schrödinger equation $(H - E_c)\,\Phi_c = 0$, with the full Hamiltonian H, for $R \to \infty$. The choice of Φ_a and Φ_b depends on the type of approximation in which the potential is calculated.

The connection between the desired potential W and the quantity W_{ba} is established in the following way. We represent W_{ba} as

$$W_{ba} = \int e^{i(\mathbf{p}_a - \mathbf{p}_b)\cdot\mathbf{R}}\, W_{\gamma'\gamma}(\mathbf{R}, \mathbf{v}_a, \mathbf{v}_b)\, d^3R. \quad (3)$$

Here $\mathbf{v}_a = \mathbf{p}_a/M$, $\mathbf{v}_b = \mathbf{p}_b/M$ are the nucleon velocities of the initial and final state in the c.m.s.; γ' and γ denote the totality of spin-charge variables of the nucleons, corresponding to states a and b. We calculate the quantity $W_{\gamma'\gamma}(\mathbf{R}, \mathbf{v}_a, \mathbf{v}_b)$ in the approximation linear in v and with neglect of terms from meson recoil of the type u^2/M. Here, as we shall show below, we can set $\mathbf{v}_a = \mathbf{v}_b = \mathbf{v}$ in the integrand in Eq. (3); i.e., in the calculation of $W_{\gamma'\gamma}$, the nucleon velocity can be considered as a parameter. The desired potential $W(\mathbf{R}, \mathbf{v})$, which depends on the velocity, is then determined by the formula

$$(\chi_{\gamma'}, W(\mathbf{R}, \mathbf{v})\,\chi_\gamma) = W_{\gamma'\gamma}(\mathbf{R}, \mathbf{v}, \mathbf{v}), \quad (3a)$$

where $\chi_{\gamma'}$ and χ_γ are the spin-charge functions for the two-nucleon system in the phenomenological treatment. In other words, the potential calculated in our approximation (linear approximation with respect to velocity, and neglect of the term u^2/M) is, in essence, a potential between nucleons surrounded by meson clouds and moving with constant velocities $\mathbf{v}$ and $-\mathbf{v}$. We calculate this potential, discarding terms which fall off as $\exp(-3R)$ and faster.

A consistent procedure of calculation of $W(\mathbf{R}, \mathbf{v})$ should start from a relativistic equation for the scattering amplitude. But no relativistic theory of the π-N interaction exists, and, therefore, we choose another way for the construction of W, based on the success of the static-meson theory in the low-energy range. Since the renormalized constants are quadratic in velocity, the renormalization will be carried out automatically in the linear approximation, if the meson cloud of the nucleon, described by the functional F, has the same character as in the static case. This situation makes it possible to base the approximation, linear with respect to velocity, on the solution of the static problem for the nucleon. The functional $F_{\alpha\mathbf{v}}(i)$ for the i-th nucleon, moving with velocity v, can be obtained from the functional for the fixed nucleon $F_{\alpha 0}(i)$ by transition to a moving system of reference (α represents all of the quantum numbers of the nucleon aside from the velocity $\mathbf{v}$).

In changing to the moving system, we make a Galilean transformation of the state vector of the dressed nucleon. The functional $F_{\alpha\mathbf{v}}(i)$ has the form

$$F_{\alpha\mathbf{v}}(i) = \exp\{i\,(\mathbf{p} - \mathbf{u})\cdot\mathbf{r}_i\}\,|\,i\alpha\mathbf{v}\rangle, \quad (4)$$

where $i\alpha\mathbf{v}$ does not depend on $\mathbf{r}_i$, and the one-nucleon Hamiltonian

$$H_{1\mathbf{v}}(0) = \{-(\mathbf{v}\cdot\mathbf{u}) + H_\pi + U_i(0)\} \quad (5)$$

differs from the static Hamiltonian $H_{i0}(0) = H_\pi + U_i(0)$ by the substitution of ω_k in H_π by $\omega_k - (\mathbf{v}\cdot\mathbf{k})$. Thus, we have

$$H_{iv}(0)\,|\,i\alpha v\rangle = 0. \tag{6}$$

We note that in so far as the Hamiltonian for the fixed nucleon $H_{i0}(0)$ does not contain recoil terms of the type u^2/M, these terms are not in the Hamiltonian (5). Thus, the term u^2/M in the Hamiltonian (2) will also be omitted.

With the aid of the formulae (4), (5), and (6) for the one-nucleon function $F_{\alpha v}$, we can write the explicit form of the vector Φ which enters into Eq. (1) [see I(8)]:

$$\begin{aligned}\Phi_a &= Z_{aa}^{-1/2}\sum_{\alpha\beta} C_{\alpha\beta}^{a} F_{\alpha v_a}(1,\ a^+)\,F_{\beta,-v_a}(2,\ a^+)\,\Lambda_0\\ &= Z_{aa}^{-1/2}\,e^{i\rho_a\cdot\mathbf{R}}\,|\,av\rangle,\end{aligned} \tag{7}$$

where the velocities of nucleons 1 and 2 have been set equal to $\mathbf{v}_a$ and $-\mathbf{v}_a$, respectively. Here

$$Z_{ba}(\mathbf{R}) = (bv_b\,|\,av_a) \tag{8}$$

normalizes the amplitude Φ_a to unity (In all matrix elements of the type $(bv|\,L\,|av)$, the integration over R is not carried out.).

2. We shall show that, in the approximation linear with respect to $\mathbf{v}$ and with neglect of recoil terms of the type u^2/M, we can set $\mathbf{v}_a = \mathbf{v}_b$ in $W_{\gamma'\gamma}(\mathbf{R}, \mathbf{v}_a, \mathbf{v}_b)$ [see Eq. (3)]. To do this, we investigate the dependence of $W_{\gamma'\gamma}(\mathbf{R}, \mathbf{v}_a, \mathbf{v}_b)$ on $\mathbf{v}_a$ and $\mathbf{v}_b$. We represent $W_{\gamma'\gamma}(\mathbf{R}, \mathbf{v}_a, \mathbf{v}_b)$ in the form

$$\begin{aligned}W_{\gamma'\gamma} &= \int d^3k e^{i\mathbf{k}\cdot\mathbf{R}} w'_{\gamma'\gamma}(\mathbf{k},\ \mathbf{v}_a,\ \mathbf{v}_b)\\ &+ \int d^3q d^3k e^{i(\mathbf{k}+\mathbf{q})\cdot\mathbf{R}} w''_{\gamma'\gamma}(\mathbf{k},\mathbf{q},\mathbf{v}_a,\mathbf{v}_b),\end{aligned} \tag{9}$$

where w′ and w″ correspond to the potentials which fall off as $\exp(-R)$ and $\exp(-2R)$ respectively.

Since the entire dependence of w′ and w″ on $\mathbf{v}_a$ and $\mathbf{v}_b$ occurs through the one-nucleon matrix elements of the type

$$\begin{aligned}&\langle\alpha' v_b|\,V_k\,|\alpha v_a\rangle; \qquad &&\langle\alpha' v_b|\,a_k|\,\alpha v_a\rangle;\\ &\langle\alpha' v_b|\,a_k a_q|\,\alpha v_a\rangle; \qquad &&\langle\alpha' v_b|\,V_k a_q|\,\alpha v_a\rangle,\end{aligned} \tag{10}$$

we should first elucidate the way in which the quantities (10) depend upon $\mathbf{v}_a$ and $\mathbf{v}_b$. Here we employ the formulae

$$\begin{aligned}a_k F_{\alpha v} &= -[H_v + \omega_k(v)]^{-1} V_k^+ \exp(-i\mathbf{k}\cdot\mathbf{r})\,F_{\alpha v},\\ a_k a_q F_{\alpha v} &= \exp[-i(\mathbf{k}+\mathbf{q})\cdot\mathbf{r}]\,[H_v + \omega_q(v) + \omega_k(v)]^{-1}\\ &\times\{V_k^+[H_v + \omega_q(v)]^{-1} V_q^+ + V_q^+[H_v + \omega_k(v)]^{-1} V_k^+\}\,F_{\alpha v},\\ \omega_q(\pm v) &= \omega_q^{\pm} = \omega_q \mp (\mathbf{q}\cdot\mathbf{v}),\end{aligned} \tag{11}$$

which go over into the well-known relations of the static theory for $v = 0$. Using Eqs. (11), the matrix elements (10) can be expressed through matrix elements of the form

$$\langle\alpha' v_b|\,V_q\,\frac{1}{H_v(0)+\omega_q(v)}\cdots\frac{1}{H_v(0)+\omega_{q'}(v)}\cdots V_{q'}\,|\alpha v_a\rangle, \tag{12}$$

containing the product of operators V and $[H_V(0) + \omega(v)]^{-1}$ in various orders. Here the v without a suffix in Eq. (12) is equal to one of the vectors $\mathbf{v}_a$, $\mathbf{v}_b$. Using the unitary inversion operator I of the pseudoscalar meson field[9]

$$I = \exp\left\{-\frac{i\pi}{4}\sum_q (a_q^+ - a_{-q}^+)(a_q + a_{-q})\right\}, \tag{13}$$

$$Ia_qI^+ = -a_{-q}; \qquad Ia_q^+I^+ = -a_{-q}^+, \tag{14}$$

we find

$$\begin{aligned}IH_0(0)\,I^+ &= H_0(0); \qquad Iu I^+ = -u;\\ IH_v(0)\,I^+ &= H_{-v}(0).\end{aligned} \tag{15}$$

In addition

$$I\,|\alpha, v\rangle = |\alpha, -v\rangle, \tag{16}$$

since the state $\alpha, \pm v$ relates, for fixed velocity v, to the lowest eigenvalue of $H_{\pm v}(0)$, which is nondegenerate (not considering the degeneracy with respect to α). With Eqs. (14), (15), and (16) we can obtain the following relations for (12)

$$\begin{aligned}&\langle\alpha' v_b|\,I^+ I V_q \frac{1}{H_v(0)+\omega_q(v)}\cdots\frac{1}{H_v(0)+\omega_{q'}(v)}\cdots V_{q'} I^+ I\,|\alpha v_a\rangle\\ &\quad= \langle\alpha', -v_b|\,V_q\\ &\quad\frac{1}{H_{-v}(0)+\omega_q(v)}\cdots\frac{1}{H_{-v}(0)+\omega_{q'}(v)}\cdots V_{q'}\,|\alpha, -v_a\rangle.\end{aligned} \tag{17}$$

If follows from Eq. (17) that the matrix element (12) does not change if v is changed to $-v$ throughout, except in $\omega(v)$. Consequently, the entire matrix element (12) depends on $\mathbf{v}_a$ and $\mathbf{v}_b$ only through v_a^2, v_b^2 and $(\mathbf{v}_a\mathbf{v}_b)$, aside from the dependence through $\omega(v)$. Therefore, in the approximation linear in velocity, we can set $\mathbf{v}_a = \mathbf{v}_b = 0$ everywhere in Eq. (12) except in $\omega(v)$. From this it follows that the dependence of the quantities (12) and, through them, also w′ and w″, is completely through $\omega(v)$, i.e., through scalar products $(\mathbf{v}_a\cdot\mathbf{k})$, $(\mathbf{v}_b\cdot\mathbf{q})$ etc.

As can be seen from Eqs. (3) and (7), the multiplication of $W(\mathbf{R}, \mathbf{v}_a, \mathbf{v}_b)$ by $(\mathbf{v}_a - \mathbf{v}_b)$ is equivalent to multiplication of the Fourier transforms w′ and w″ by $-\mathbf{k}/M$ and $-(\mathbf{k}+\mathbf{q})/M$, respectively. Therefore, terms $(\mathbf{v}_a - \mathbf{v}_b, \mathbf{q})$ and $(\mathbf{v}_a - \mathbf{v}_b, \mathbf{k})$ in w′ and w″ are equivalent to terms $-k^2/M$ and $-(\mathbf{k}+\mathbf{q}, \mathbf{k})/M$, which are characteristic of the meson recoil of type u^2/M. Consequently, if we neglect the quadratic recoil terms u^2/M, we can set $\mathbf{v}_a = \mathbf{v}_b$ in the potential $W(\mathbf{R}, \mathbf{v}_a, \mathbf{v}_b)$.

3. Starting from Eq. (1), we introduce formulae for the potential $W(\mathbf{R}, \mathbf{v})$. The first term in Eq.

(1) pertains to a number of matrix elements, methods of calculation of which were considered in I. In this case, additional terms arise because of the factor Z, which was not taken into account in the derivation of I(20). With this in mind, we find as we go from Eq. I(20) to separate coordinates for the meson clouds, that with the choice of the functional Φ_a and Φ_b in the form Eq. (7) (and in our approximation), the term $(\Phi_b, (H - E_a)\Phi_a)$ leads to the potential W^I with matrix elements

$$W^I_{\gamma\gamma} = \langle bv | (1+\hat{N}) | U_1^{(+)}(a_2) + U_2^{(+)}(a_1) | av \rangle (Z_{aa}Z_{bb})^{-1/2} + i(\mathbf{v}\cdot\nabla Z_{aa}) Z_{ab} (Z_{bb}Z_{aa}^2)^{-1/2}; \quad Z_{ab} = \langle av | (1+\hat{N}) | bv \rangle. \tag{18}$$

Here and throughout $|av\rangle$ denotes the two-nucleon state vector with separate coordinates:

$$|av\rangle = \sum_{\alpha\beta} C^a_{\alpha\beta} e^{-i\mathbf{p}_a\cdot\mathbf{R}} F_{\alpha v}(1, a_1^+) F_{\beta,-v}(2, a_2^+)\Lambda_0 = \sum_{\alpha\beta} C^a_{\alpha\beta} e^{-i\mathbf{p}_a\cdot\mathbf{R}} e^{-i(\mathbf{u}_1-\mathbf{v}_\beta)\cdot\mathbf{R}/2} |1, \alpha v\rangle |2, \beta, -v\rangle, \tag{19}$$

where the functional of the i-th nucleon $|i\alpha v\rangle$, defined by Eqs. (4) and (6), depends only on the operators a_1^+; $\mathbf{u}_i = \sum_q \mathbf{q} a_{iq}^+ a_{iq}$.

To obtain the potential of order $\exp(-2R)$, it is necessary to insert into the term $(\mathbf{v}\cdot\nabla Z_{ab})$ in Eq. (18) the first two terms of the expansion I(22) for the operator $\hat{N}$:

$$\hat{N} = \sum_q (a_{1q}^+ a_{2q} + a_{2q}^+ a_{1q}) + \frac{1}{2}\sum_{kq} (a_{2q}^+ a_{2k}^+ a_{1q}a_{1k} + a_{1q}^+ a_{1k}^+ a_{2q}a_{2k} + 2a_{2q}^+ a_{1k}^+ a_{1q}a_{2k}). \tag{20}$$

In the calculation of the first term in Eq. (18), the first term in Eq. (20) is sufficient.

We transform the second term of Eq. (1). We introduce the notation

$$\Gamma_a = (H - E_a)\Phi_a. \tag{21}$$

As shown above, Γ falls off as $\exp(-R)$. Therefore, the second term in Eq. (1) in which Γ occurs twice, can be written in the following form:

$$-W^{II}_{ba} = (\Gamma_b | (H-E_a)^{-1} | \Gamma_a) - \sum_{\substack{c \\ \mathbf{p}_c = 0}} (\Gamma_b | \Phi_c)(E_c - E_a - i\varepsilon)^{-1}(\Phi_c | \Gamma_a). \tag{22}$$

Here we have substituted the vector Φ_c for $\psi_{0c}^{(-)}$, since the terms discarded here lead to a potential $\exp(-3R)$.

We adopt the convention that the double line in the functional

$$\| G(a_1, a_2, a_1^+, a_2^+)\Lambda_0$$

means that we should first calculate the expression $G\Lambda_0$ to the right of the double line, that is, we should first free it from all annihilation operators a_1, a_2, moving them to the right to the vacuum Λ_0, taking account of commutation relations, and then set $a_1^+ = a_2^+ = a^+$.

For transformation of the first term in Eq. (22), it is convenient to use Eq. (11) to represent Γ_a in the form $\Gamma_a = \| \Gamma_a(a_1^+, a_2^+)\Lambda_0\|$, where

$$\Gamma_a(a_1^+, a_2^+)\Lambda_0 = \sum_{\mathbf{k},\alpha\beta} C^a_{\alpha\beta} g(\mathbf{k}+\mathbf{p}_a, \mathbf{R}) \hat{M}(\mathbf{k}, \mathbf{v}, 0) |\alpha v\rangle |\beta, -v\rangle;$$
$$\hat{M}(\mathbf{k}, \mathbf{v}, \mathbf{R}) = e^{i\mathbf{k}\cdot\mathbf{R}}\{-(\mathbf{v}\cdot\mathbf{k}) Z_{aa}(\mathbf{k}) + \left[\frac{1}{H_{1v}+\omega_k^*(-v)} + \frac{1}{H_{2,-v}+\omega_k(-v)}\right] V_{1k}V_{2k}\}; \tag{23}$$
$$g = \exp\left\{i\left[\frac{\mathbf{u}_2-\mathbf{u}_1}{2} + \mathbf{p}_a + \mathbf{k}\right]\cdot\mathbf{R}\right\}; \quad Z_{aa}(\mathbf{R}) = \sum_{\mathbf{k}} e^{i\mathbf{k}\cdot\mathbf{R}} Z_{aa}(\mathbf{k}).$$

The quantity $(H-E_a)^{-1}\Gamma_a$ in Eq. (22) can be transformed in the following way:

$$[H_\pi + U_1 + U_2 - E_a]^{-1} \| \Gamma_a) = \| [H_{10} + H_{20} - E_a]^{-1}\Gamma_a(a_1^+, a_2^+)\Lambda_0) - [H_\pi + U_1 + U_2 - E_a]^{-1} \| (U_1^{(+)}(a_2) + U_2^{(+)}(a_1)) \times [H_{10} + H_{20} - E_a]^{-1} \Gamma_a(a_1^+, a_2^+)\Lambda_0); \tag{24}$$
$$H_{iv} = H_\pi(a_i^+, a_i) + U_i(a_i^+, a_i) - (\mathbf{v}\cdot\mathbf{u}_i).$$

The second term on the right-hand side falls off as $\exp(-2R)$ and can be discarded. With the aid of Eq. (24), the following expression for the potential corresponding to the first term in Eq. (22) is obtained

$$\sum_k \langle bv | [U_1^{(-)}(a_2^+) + U_2^{(-)}(a_1^+) - i(\mathbf{v}, \nabla Z_{bb})] [H_{1,v+v_k} + H_{2,-v-v_k} + 2E(p+k) - 2E(p) - i\varepsilon]^{-1} \hat{M}(\mathbf{k}, \mathbf{v}, \mathbf{R}) | av\rangle, \quad \mathbf{v}_k = \mathbf{k}/M. \tag{25}$$

Integrating over the second term in Eq. (22), we find the following expression for the potential corresponding to this term

$$\sum_{k,c} \frac{\langle bv | [U_1^{(-)}(a_2^+) + U_2^{(-)}(a_1^+) - i(\mathbf{v}, \nabla Z_{bb})] | c, v + \frac{k}{M}\rangle\langle v + \frac{k}{M}, c | \hat{M}(\mathbf{k}, \mathbf{v}, \mathbf{R}) | av\rangle}{2E(k+p) - 2E(p) - i\varepsilon}, \tag{26}$$

where the label c in Eq. (26) denotes summation only over spin-charge indices of the two-nucleon state. Unifying Eqs. (25) and (26), we find the potential W^{II} to be

$$-W^{II}_{\gamma'\gamma}(\mathbf{R},\ \mathbf{v})$$

$$=\sum_k \langle b,\ v\,|\,[U_1^{(-)}(a_2^+)+U_2^{(-)}(a_1^+)-i(\mathbf{v},\ \nabla Z_{bb})] \quad (27)$$

$$\times[H_{1,v+v_k}+H_{2,-v-v_k}-2(\mathbf{k}\cdot\mathbf{v})]^{-1}$$

$$\times(1-P_0)\,\hat{M}(\mathbf{k},\ \mathbf{v},\ \mathbf{R})\,|\,av\rangle,$$

where P_0 is the projection operator on the ground state of the Hamiltonian $H_{1,\,v+v_k}+H_{2,\,-v-v_k}$ (not containing real mesons). In Eq. (27) we have set $E(p+k)-E(p)\approx(\mathbf{k}\cdot\mathbf{v})$. Neglecting, as earlier, terms of the type u^2/M, one can take $k=0$ in the operators H_1, H_2 and P_0 in Eq. (27). Terms with $(\mathbf{v}\cdot\nabla Z_{aa})$ and $(\mathbf{v}\cdot\nabla Z_{bb})$ do not then contribute to Eq. (27).

The total potential is the sum of W^I and W^{II} [Eqs. (18) and (27)]. Direct calculation from Eqs. (18) and (27) leads, in general, to a complicated dependence on velocity. In the approximation linear in the velocity, which we consider, the only parts which are meaningful are W_{st} (static potential) and the part W_{LS}, which is linear in velocity, of the sum $W(\mathbf{R},\ \mathbf{v})=W^I+W^{II}$:

$$W_{st}=W(\mathbf{R},\ 0);\ W_{LS}=(\mathbf{v},\ [\nabla_v W(\mathbf{R},\ \mathbf{v})]_{v=0}). \quad (28)$$

THE POTENTIAL

In Eqs. (18) and (27) for the potential, the meson variables relating to the clouds of nucleons 1 and 2 are completely separated, so that the calculation of (18) and (27) reduces to the calculation of one-nucleon matrix elements. Here, as follows from the form of H_{iv} and the discussion in connection with Eq. (17), in the approximation linear in the velocity, the one-nucleon matrix elements differ from the static matrix elements only in the substitution of ω_k by $\omega_k\pm(\mathbf{k}\cdot\mathbf{v})$ in the energy denominators, so that the results of the static theory can be used for their calculation. We calculated these matrix elements, which have the form (12) for $v_a=v_b$, using an expansion in terms of the system of functions of the one-nucleon Hamiltonian. Because of this, the two-nucleon potential turned out to be connected with the π-N scattering, as in the static case.[3-5] In summing over the intermediate states, the following formula[3] was employed:

$$\langle\alpha'\,|\,V_{ik}\,G(H_i)\,V_{ia}^+\,|\,\alpha\rangle=\sum_\nu\langle\alpha'\,|\,V_{ik}\,|\,\nu\rangle\langle\nu\,|\,V_{ia}^+\,|\,\alpha\rangle\,G(E_\nu)$$

$$-\sum_{l,\,j}(2J+1)^{-1}P_{kq}^{(l)}(2I)F_{kq}^{(l)}(2J)\frac{4\,kq}{(\omega_k\omega_q)^{1/2}}$$

$$\times\int d\omega_n\frac{G(\omega_n)}{k_n}\sigma_{2I,\,2J}(\omega_n), \quad (29)$$

where $\sigma_{2I,2J}$ is the total cross section for π-N scattering in the state with isotopic spin I and angular momentum J; P(2I) and F(2J) are projection operators on the state of isotopic spin I and angular momentum J (matrix elements $P_{kq}\equiv(k\,|\,P\,|\,q)$ and $F_{kq}\equiv(k\,|\,F\,|\,q)$ are in the notation of reference 3); $G(H_i)$ is some function of the one-nucleon Hamiltonian H_i. In Eq. (29) for W^{II}, the function G depends both on H_1 and H_2. In this case, the result of applying Eq. (29) to the calculation of matrix elements between states of the first nucleon [first part of Eq. (29)] will be functions of the Hamiltonian of the second nucleon. This function $\tilde{G}(H_2)$ should be considered the starting point for the application of Eq. (29) to summation over the states of the second nucleon.

We shall not dwell on the details of the calculation, in view of the analogy with the calculation of the potential in the static case.[5] Since the influence of the factor Z is of interest, we first give the result for $Z_{ab}\neq\delta_{ab}$, and then indicate the change introduced by $Z_{ab}\neq\delta_{ab}$. Calculation in this case gives the following expression for the operator $W(\mathbf{R},\ \mathbf{v})$ from which — according to Eq. (28) — both the static part W_{st} of the potential and the part depending on the velocity, W_{LS}, can be obtained

$$W(\mathbf{R},\ \mathbf{v})=W_0^{(1)}(\mathbf{R},\ \mathbf{v})+W_0^{(2)}(\mathbf{R},\ \mathbf{v})$$

$$+W_{e0}(\mathbf{R},\ \mathbf{v})+W_{ee}(\mathbf{R},\ \mathbf{v}). \quad (30)$$

The first term in Eq. (30), which falls off as $\exp(-R)$, comes from the term $\langle bv\,|\,[U_1^{(+)}(a_2)+U_2^{(+)}(a_1)]\,|\,av\rangle$ in Eq. (18):

$$W_0^{(1)}=-2(2\pi)^{-3}\int d^3k e^{i\mathbf{k}\cdot\mathbf{R}}V_{1k}^+V_{2k}/\omega_k^-. \quad (31)$$

The remaining part $W(\mathbf{R},\mathbf{v})$ falls off as $\exp(-2R)$. It can be conveniently expressed through the functions h_1, h_2 and h_3:

$$h_1(\omega_t,\ \omega_s) \quad (32)$$

$$=\frac{1}{\omega_k^-+\omega_q^-}\left[\frac{1}{\omega_t+\omega_q^+}\frac{1}{\omega_s+\omega_k^-}+\frac{1}{\omega_t+\omega_k^-}\frac{1}{\omega_s+\omega_q^+}\right].$$

$$h_2(\omega_t,\ \omega_s) = \frac{1}{\omega_k^- + \omega_q^-}\left(\frac{1}{\omega_t + \omega_q^+}\,\frac{1}{\omega_s + \omega_q'}\right.$$

$$+ \frac{1}{\omega_t + \omega_q^+}\,\frac{1}{\omega_t + \omega_k^-} + \frac{1}{\omega_s + \omega_q^-}\,\frac{1}{\omega_s + \omega_q'} + \frac{1}{\omega_t + \omega_k^-}\,\frac{1}{\omega_s + \omega_k^+}\,\frac{1}{\omega_s + \omega_q'}$$

$$\left. + \frac{1}{\omega_k^- + \omega_q^-}\,\frac{1}{\omega_t + \omega_k^-}\,\frac{1}{\omega_s + \omega_k^+}\right), \qquad (33)$$

$$h_3(\omega_t,\ \omega_s) = \frac{1}{\omega_s + \omega_t + 2(\mathbf{k}\cdot\mathbf{v})}\left[\frac{1}{\omega_s + \omega_q^+}\,\frac{1}{\omega_s + \omega_k^-}\right.$$

$$+ \frac{1}{\omega_t + \omega_q^+}\,\frac{1}{\omega_s + \omega_k^-} + \frac{1}{\omega_s + \omega_q^+}\,\frac{1}{\omega_t + \omega_k^-}$$

$$\left. + \frac{1}{\omega_t + \omega_q^+}\,\frac{1}{\omega_t + \omega_k^-}\right]. \qquad (34)$$

Here the terms in the operators $W_0^{(2)}$, $W_{\sigma 0}$, $W_{\sigma\sigma}$ which contain h_1 and h_2 come from the term $\langle \mathrm{bv}\,|\,N[U_1^{(+)}(a_2) + U_2^{(+)}(a_1)]\,|\,\mathrm{av}\rangle$ in Eq. (18), and the terms with h_3 come from the operator W^{II}. The operator $W_0^{(2)}$, which does not depend on the π-N scattering cross section, is of the form

$$W_0^{(2)} = -(2\pi)^{-6}\int d^3q\,d^3k\,e^{i(\mathbf{k}+\mathbf{q})\cdot\mathbf{R}}(V_{1q}V_{1k}V_{2q}V_{2k}h_1(0,\ 0) + V_{1q}V_{1k}V_{2q}h_2(0,\ 0)). \qquad (35)$$

This operator leads to a potential of fourth order in perturbation theory. The operators $W_{\sigma 0}$ and $W_{\sigma\sigma}$ depend on the cross section $\sigma_{2I,2J}$ for π-N scattering. $W_{\sigma 0}$ is linear in $\sigma_{2I,2J}$:

$$W_{\sigma 0} = -4(2\pi)^{-6}\sum_{IJ}(2J+1)^{-1}\int d^3k\,d^3q\,e^{i(\mathbf{k}+\mathbf{q})\cdot\mathbf{R}}\int_0^\infty dt\,\frac{qk\sigma_{2I,2J}(t)}{\omega_t(\omega_q\omega_k)^{1/2}}$$

$$\times\{P_{qk}^{(1)}(2I)\,F_{qk}^{(1)}(2J)\,V_{2q}^{+}V_{2k}[h_1(\omega_t,\ 0) + h_3(\omega_t,\ 0)]$$

$$+ V_{1q}^{+}V_{1k}P_{qk}^{(2)}(2I)\,F_{qk}^{(2)}(2J)\,[h_1(0,\ \omega_t) + h_3(0,\ \omega_t)]$$

$$+ P_{qk}^{(1)}(2I)\,F_{qk}^{(1)}(2J)\,V_{2k}^{+}V_{2q}h_2(\omega_t,\ 0)$$

$$+ V_{1q}^{+}V_{1k}P_{kq}^{(2)}(2I)\,F_{kq}^{(2)}(2J)\,h_2(0,\ \omega_t)\}. \qquad (36)$$

The operator $W_{\sigma\sigma}$ depends quadratically on the cross section $\sigma_{2I,2J}$:

$$W_{\sigma\sigma} = -16(2\pi)^{-6}\sum_{I,I',J,J'}(2J+1)^{-1}(2J'+1)^{-1}$$

$$\times\int d^3q\,d^3k\int_0^\infty dt\,ds\,\sigma_{2I,2J}(t)\,\sigma_{2I',2J'}(s)\,\frac{q^2k^2}{\omega_q\omega_k\omega_s}\,e^{i(\mathbf{k}+\mathbf{q})\cdot\mathbf{R}}$$

$$\times\{P_{qk}^{(1)}(2I)\,F_{qk}^{(1)}(2J)\,P_{qk}^{(2)}(2I')\,F_{qk}^{(2)}(2J')[h_1(\omega_t,\ \omega_s) + h_3(\omega_t,\ \omega_s)]$$

$$+ P_{qk}^{(1)}(2I)\,F_{qk}^{(1)}(2J)\,P_{kq}^{(2)}(2I')\,F_{kq}^{(2)}(2J')\,h_2(\omega_t,\ \omega_s)\}. \qquad (37)$$

In Eqs. (31) to (37), the dependence on the velocities enters only through the quantities $\omega^{\pm}$ in the denominators of the functions h_1, h_2 and h_3. The potential W_{st} calculated from Eqs. (30) to (37) coincides with the potential obtained by Klein and McCormick,[3]

We consider the dependence of the integrands on the velocity and on the vectors $\mathbf{k}$, $\mathbf{q}$ and $\boldsymbol{\sigma}$, keeping the terms of the operator $W(\mathbf{R}, \mathbf{v})$ [Eq. (30)] which are linear in velocity. These vectors occur here only in the combinations

$$(\mathbf{k}+\mathbf{q},\ \mathbf{v})(\mathbf{k}\cdot\mathbf{q})^2,\ (\mathbf{k}+\mathbf{q},\ \mathbf{v})(\boldsymbol{\sigma}_1\cdot[\mathbf{k}\times\mathbf{q}])(\boldsymbol{\sigma}_2\cdot[\mathbf{k}\times\mathbf{q}]), \qquad (38)$$

$$(\mathbf{k}\cdot\mathbf{v})(\mathbf{k}\cdot\mathbf{q})(\mathbf{S}[\mathbf{k}\times\mathbf{q}]),\ (\mathbf{q}\cdot\mathbf{v})(\mathbf{k}\cdot\mathbf{q})(\mathbf{S}[\mathbf{k}\times\mathbf{q}]), \qquad (39)$$

(aside from $\exp[i(\mathbf{k}+\mathbf{q})\cdot\mathbf{R}]$), where $\mathbf{S} = \boldsymbol{\sigma}_1 + \boldsymbol{\sigma}_2$. The combinations (38) and (39) come from the symmetric and antisymmetric terms (relative to $\mathbf{k}$ and $\mathbf{q}$) entering into the part of the function h_i which is linear in velocity. Only the terms with the combinations (39) lead to our **LS** type potential, after integration over angles. This potential falls off as $\exp(-2R)$. Terms of the type $(\mathbf{k}+\mathbf{q})\cdot\mathbf{v}$ in the potential $\exp(-2R)$ and of the type $(\mathbf{k}\cdot\mathbf{v})$ in the potential $\exp(-R)$ correspond in the more exact treatment to an expansion of the differences of kinetic energies, $E(\mathbf{p}) - E(\mathbf{p}+\mathbf{k}+\mathbf{q})$ or $E(\mathbf{p}) - E(\mathbf{p}+\mathbf{k})$ in the denominators. But, as Levy showed,[7] terms involving the difference in kinetic energies of the initial and final states do not contribute to the scattering, so that terms of this character can be discarded.

We now consider the influence of the factor $Z_{ab} \neq \delta_{ab}$ on the potential. After taking this factor into account, the result calculated for the potential differs from the potential (30) in the following ways.*

1. The potential W_{st} coincides in this case with the potential calculated by Miyazawa and one of the authors[5†] and differs from the potential of reference 3 by a factor Z^{-1}.

2. No part linear in the velocity will occur in the operator $W_0^{(1)}$.

3. In the terms linear in the velocity in the functions h_i [Eqs. (32) to (34)], parts symmetric in the

*It is convenient to choose the states a and b such that $Z_{ab}^{(\omega)} = Z_{aa}^{(\omega)}\delta_{ab}$, where $Z^{(\omega)}$ comes from the first term in Eq. (20).

†In reference 5 the term $W_{\sigma\sigma}(\mathbf{R}, 0)$ was not calculated and the elastic, rather than total, cross section was considered. We note the following misprints and inaccuracies in reference 5: in Eq. (39), the square bracket in the last term should come before the round one, that is, the expression should be:

$$(\tau_1\tau_2 - 1)\,[2(\mathbf{k}\cdot\mathbf{k}')^2 - (\boldsymbol{\sigma}_1\cdot[\mathbf{k}\times\mathbf{k}'])\,(\boldsymbol{\sigma}_2\cdot[\mathbf{k}\times\mathbf{k}'])](2k_0q_0 + 2k_0^2 + k_0k_0').$$

Further, in Eq. (44) a factor $\exp(iq\cdot R)$ was left out before the group of terms beginning with $\frac{7}{6}(\boldsymbol{\sigma}_1\cdot\mathbf{k}')(\boldsymbol{\sigma}_2\cdot\mathbf{k})(\mathbf{k}\cdot\mathbf{k}')$. These terms lead to a potential of the type $\exp(-3R)$.

variables q and k will not be present, except for the symmetric part of the term resulting from taking into account the $2(\mathbf{k}\cdot\mathbf{v})$ in the first factor of Eq. (34). The antisymmetrical part here will be unchanged.

Thus, when one takes into account $Z_{ab} \neq \delta_{ab}$, all terms with $(\mathbf{k}+\mathbf{q})\cdot\mathbf{v}$ and $(\mathbf{k}\cdot\mathbf{v})$ disappear from the potential $W(R, v)$, with the exception noted above, whereas the terms with **LS** are unchanged. In other words, normalization of the asymptotic functions does not change the potential W_{LS}. In both cases the potential W_{LS} depends on the velocity only through **(LS)**, as it should.

If we retain only the largest cross section σ_{33} out of all the cross sections $\sigma_{2I,2J}$, then we obtain the following expression for the potential W_{LS}:

$$W_{LS} = \frac{(LS)}{MR^3}(w_{00} + w_{\sigma 0} + w_{\sigma\sigma}),$$

$$w_{00} = \frac{f^4}{2(2\pi)^3}[3 - 2(\tau^1\tau^2)]\int_0^\infty \frac{dk dq\,(kq)^{1/2}}{\omega_k\omega_q} J_{\nu_{1/2}}(kR) J_{\nu_{1/2}}(qR)\, A_1(k, q, i, i),$$

$$w_{\sigma 0} = \frac{f^2}{3(2\pi)^4}\int_0^\infty dk\,dq\,dt\,\frac{(kq)^{1/2}\sigma_{33}(t)}{\omega_k\omega_q\omega_t}\{3A_3(k, q, t)(3 - (\tau^1\tau^2)) + [A_1(k, q, t, i) + A_2(k, q, t, i)](3 + (\tau^1\tau^2))\} J_{\nu_{1/2}}(kR)\, J_{\nu_{1/2}}(qR)_{\nu_{1/2}},$$

$$w_{\sigma\sigma} = -\frac{2}{9(2\pi)^3}[6 - (\tau^1\tau^2)]\int_0^\infty dk\,dq\int_0^\infty dt\,ds\,\frac{(kq)^{1/2}}{\omega_k\omega_q\omega_t\omega_s}\sigma_{33}(t)\,\sigma_{33}(s)\{A_1(k, q, t, s) + A_2(k, q, t, s)\} J_{\nu_{1/2}}(kR)\, J_{\nu_{1/2}}(qR). \qquad (40)$$

Here we have introduced the following notation

$$A_1(k, q, t, s) = \frac{(\omega_s+\omega_q)^2(\omega_t+\omega_k) + (\omega_t+\omega_q)^2(\omega_s+\omega_k)}{(\omega_s+\omega_q)^2(\omega_t+\omega_q)^2(\omega_k+\omega_q)(\omega_t+\omega_k)(\omega_s+\omega_k)},$$

$$A_2(k, q, t, s) = (\omega_t+\omega_s+2\omega_k)\frac{[(\omega_t+\omega_q)^2 + (\omega_s+\omega_q)^2](\omega_t+\omega_s) + (\omega_t+\omega_s+2\omega_q)(\omega_t+\omega_q)(\omega_s+\omega_q)}{(\omega_s+\omega_t)^2(\omega_s+\omega_q)^2(\omega_t+\omega_q)^2(\omega_s+\omega_k)(\omega_t+\omega_k)},$$

$$A_3(k, q, t) = \frac{\omega_t[(\omega_t+\omega_k)\omega_k + (\omega_k+\omega_q)(\omega_t+\omega_k+\omega_q)]}{\omega_q^2\omega_k(\omega_k+\omega_q)(\omega_t+\omega_q)^2(\omega_t+\omega_k)}.$$

The term w_{00} in Eq. (40), which is proportional to f^4, would be a potential of 4th order in perturbation theory.[2] It is well known that the sign of this term is opposite to that necessary to explain the experimental data.[1] The terms $w_{\sigma 0}$ and $w_{\sigma\sigma}$ depend on the total cross section for π-N scattering. From the form of the expression for W_{LS} and the asymptotic expansion (see below) one might think that the sum $w_{\sigma 0} + w_{\sigma\sigma}$ is of the same order of magnitude as w_{00}. In view of the complexity of Eqs. (40), the sign of the sum for $R \sim 1$ can be determined only through numerical integration. In calculating the potential W_{LS}, one should keep in mind the fact that it is necessary to introduce a cut off factor (nuclear form-factor) into the calculation of the potential W_{LS}; otherwise, the calculation within the framework of static meson theory is meaningless. Then it is clear that one can consider the potential W_{LS} to be satisfactory only for such distances R that the influence of the cut off is small. In the case of the static potential this region is $R \geq 0.4$, where the potentials of order e^{-R} and e^{-2R} are of main importance. One might hope that the LS potential, which falls off as e^{-2R} will also depend weakly on the cut off in this region.

ASYMPTOTIC EXPANSION FOR W_{LS}

In Eq. (40) for the **LS**-potential, asymptotic integration over q and k can be carried out by deforming the contour of integration to a contour C, starting from $+i\infty$, going around the point i, and returning to $+i\infty$ (both in the integration over q and over k). In addition, poles should be taken into account.

As a result, an asymptotic series in inverse integral and half-integral powers of R, with a common multiplier e^{-2R}/R^3, is obtained. Here the series for w_{00} contains only inverse integral powers of R and begins with a constant term. Series in inverse integral and half-integral powers of R are obtained for $w_{\sigma 0}$ and $w_{\sigma\sigma}$, with the series for $w_{\sigma 0}$ beginning with $R^{-1/2}$, and the series for $w_{\sigma\sigma}$ with $R^{-3/2}$. The coefficients of these terms can be expressed in terms of integrals of the form

$$L_n = \int_0^\infty \frac{\sigma_{33}(p)\,dp}{\omega_p^{n+1}}, \quad n = 1, 2, 3\ldots, \qquad (41)$$

which can easily be calculated from the experimental values of the cross section σ_{33}.

In this way we calculated the expansion up to terms of R^{-6} in the expressions for w_{00}, $w_{\sigma 0}$ and $w_{\sigma\sigma}$. In view of the complexity of these expansions, we give here only the asymptotic series up to terms in $R^{-3/2}$. They are

$$w_{00} = \frac{f^2}{2(2\pi)^3} e^{-2R} \left\{3 - 2(\tau^1\tau^2)\left(1 + \frac{15}{4} R^{-1}\right)\right\},$$

$$w_{\sigma 0} = \frac{f^2}{3(2\pi)^3} e^{-2R} \left\{2\sqrt{\pi}(6 - (\tau^1\tau^2)) L_1 R^{-1/2} - 2\pi(3 - 2(\tau^1\tau^2)) L_2 R^{-1} + R^{-3/2}\sqrt{\pi}\left[\left(\frac{79}{8} - L_1 + 3L_3\right)\right]\left[6 - (\tau^1\tau^2)\right]\right\},$$

$$w_{\sigma\sigma} = -\frac{2\sqrt{\pi}}{9(2\pi)^3} e^{-2R} [6 - (\tau^1\tau^2)] R^{-3/2} L_1 L_2. \qquad (42)$$

The coefficients L_n which enter into these formulae were calculated from the data of reference 10. The cross section for elastic scattering was used for the cross section σ_{33}. The numerical values of these coefficients were

$$L_1 = 3.2,\ L_2 = 1.8,\ L_3 = 1.0.$$

From Eqs. (42) it can be seen that the main term at large distances is w_{00}. It is well known that sometimes the asymptotic expressions are good approximations up to $R \sim 1$. If we assume that this is so in our case, then in the region $R \sim 1$, the terms w_{00} and $w_{\sigma 0}$ will be of the same order of magnitude, and $w_{\sigma\sigma}$, an order of magnitude smaller.

We note that the expressions obtained for the potential W_{LS}, together with the static potential W_{st} found earlier, permit one, for the first time, to judge the extent of validity of the nonrelativistic meson theory for the N-N scattering in the low-energy region.

We thank Acad. V. A. Fock for valuable advice concerning the problem of the asymptotic expansion of the potential.

[1] P. S. Signell and R. E. Marshak, Phys. Rev. **106**, 832 (1957); I. L. Gammel and R. Thaler, Phys. Rev. **107**, 291 (1957).

[2] A. Klein, Phys. Rev. **90**, 1101 (1953).

[3] A. Klein and B. H. McCormick, Phys. Rev. **104**, 1747 (1956).

[4] H. Miyazawa, Phys. Rev. **104**, 1741 (1956).

[5] Yu. V. Novozhilov, J. Exptl. Theoret. Phys. (U.S.S.R.) **32**, 1262, **33**, 901 (1957). Soviet Phys. JETP **5**, 1030 (1957); **6**, 692 (1958).

[6] Yu. V. Novozhilov, J. Exptl. Theoret. Phys. (U.S.S.R.) **35**, 742 (1958), Soviet Phys. JETP **8**, 515 (1959).

[7] M. Lévy, Phys. Rev. **88**, 72 (1952).

[8] Taketani, Machida, and Onuma, Progr. Theor. Phys. **7**, 45 (1952); K. M. Brueckner and K. N. Watson, Phys. Rev. **92**, 1073 (1953); I. Sato, Progr. Theor. Phys. **10**, 323 (1953); Fukuda, Sawada, and Taketani, Progr. Theor. Phys. **12**, 156 (1954).

[9] Drell, Friedman, and Zachariasen, Phys. Rev. **104**, 236 (1956).

[10] H. L. Anderson, Proceedings of the Sixth Annual Rochester Conference, Interscience, 1956.

Translated by G. E. Brown
18

REMARKS REGARDING HEISENBERG'S PAPER ON THE LEE MODEL

L. A. MAKSIMOV

Submitted to JETP editor June 7, 1958

J. Exptl. Theoret. Phys. (U.S.S.R.) **36**, 140-144 (January, 1959)

The case of two real discrete states of the V particle in the Lee model is considered. It is shown that Heisenberg's method can be extended to this case.

1. Heisenberg[1] showed, with the Lee model as an example, that in the special case when an unphysical discrete state with negative norm is combined with a discrete state with positive norm one can exclude transitions to unphysical states in a consistent way, at the same time guaranteeing the unitarity of the S matrix for scattering between physical states. We shall show that the requirement of combining the discrete states is unnecessary, at least in the Lee model. We make use of the results and notations of Heisenberg.

The Lee model introduces three real particles that interact according to the scheme $V \rightleftarrows N + \theta$. All states are divided into the sectors $(N + z\theta, V + (z-1)\theta)$ which do not go over into each other. Each sector can therefore be considered separately.

The sector $(N+\theta, V)$ contains the eigenstates of the continuous spectrum (describing the scattering of θ particles by N particles) and two discrete states. The state with the highest energy has a positive norm and may be interpreted as a physical state of the V particle. The other state has a negative norm. It is called a "ghost state" of the V particle.

Any state of the sector $(N+z\theta, V+(z-1)\theta)$ can be considered as a superposition of states formed by a state of the sector $(N+\theta, V)$ and $(z-1)$ free θ particles. These states are not eigenstates of the system. This means, in particular, that transitions are possible from states with positive norm, which can be interpreted physically, to states with negative norm, which have no physical meaning. This led Pauli and Källén[2] to the conclusion that the Lee model is inadequate. We shall show, however, that it is indeed possible to derive meaningful physical results from a theory involving states with negative norm, if the initial states are subjected to certain conditions.

2. We first discuss the scattering of a θ particle from a V particle (sector $(N+2\theta, V+\theta)$). This is meaningful, since one obtains, in contrast to the case considered by Heisenberg, a discrete V particle state with positive norm for the two discrete states. We seek a solution of the Schrödinger equation

$$H\Phi\rangle = E\Phi\rangle \tag{1}$$

in the form

$$\Phi\rangle = (\psi_V^* \int \varphi(\mathbf{k})\, a^*(\mathbf{k})\, d\mathbf{k} + \psi_N^* \int \varphi(\mathbf{k}_1, \mathbf{k}_2)\, a^*(\mathbf{k}_1)\, a^*(\mathbf{k}_2) d\mathbf{k}_1 d\mathbf{k}_2)|0\rangle \tag{2}$$

or shorter,

$$\Phi = \begin{cases} \varphi(\mathbf{k}), \\ \varphi(\mathbf{k}_1, \mathbf{k}_2). \end{cases} \tag{3}$$

Repeating the calculations of Heisenberg (reference 1, sec. 3.1), we find that the function $\varphi(\mathbf{k})$, describing the scattering of the θ particle in the momentum representation, satisfies the equation [formula (68) of reference 1]

$$h^+(E-\omega)\varphi(\omega) = \int_{m_\theta}^{\infty} K(\omega\omega')\varphi(\omega')\, d\omega', \tag{4}$$

where

$$K(\omega\omega') = -\frac{1}{2}\frac{k'}{\omega+\omega'-E-i\gamma}\sqrt{\omega'/\omega},$$

the other notations are, as always, taken from reference 1. Formula (4) differs from formula (68) of Heisenberg's paper[1] only by the fact that the function $h^+(E-\omega)$ has two separate roots and that the inhomogeneous term $\varphi_{0i}(\mathbf{k})$ is absent, since in our case the state $N+2\theta$ is not present in the initial state. The general solution of (4) is of the form

$$\varphi(\omega) = a\delta(\omega-\omega_p) + b\delta(\omega-\omega_g) + \chi(\omega)/h^+(E-\omega), \tag{5}$$

where $\omega_{p,g} = E - E_{p,g}$; E_p and E_g are the energies of the physical state and the unphysical "ghost state" of the V particle, i.e., the zeroes of the function $h^+(\omega)$; $\chi(\omega)$ is a function which is regular at the points $\omega_{p,g}$. We rewrite the last term in (5):

$$\frac{\chi(\omega)}{h^+(E-\omega)} = \left[\frac{(\omega-\omega_p)(\omega-\omega_g)\chi(\omega)}{(E_p-E_g)h^+(E-\omega)}\right]\frac{1}{\omega-\omega_g-i\gamma} - \left[\frac{(\omega-\omega_p)(\omega-\omega_g)\chi(\omega)}{(E_p-E_g)h^+(E-\omega)}\right]\frac{1}{\omega-\omega_p-i\gamma}. \quad (6)$$

The function inside the square brackets is regular at the points $\omega_{p,g}$.

The first two terms in (5) thus describe stationary S waves, while the last term describes outgoing waves of the system $V+\theta$ in the physical and "ghost" states. A physical interpretation of the solution (5) is possible only if there are no transitions of the system from the physical to the unphysical states. This requirement can be met by setting $\chi(\omega_g) = 0$. This corresponds to the absence of divergent scattered waves of the unphysical state at infinity. It is not necessary to assume that the amplitude of the stationary wave of the unphysical state is zero, since the stationary wave corresponds to an unchanged state of an unphysical system at $t = \pm\infty$, which may readily be left out of the physical interpretation (see also reference 3). We therefore choose this amplitude such that

$$\chi(\omega_g) = 0 = K(\omega_g, \omega_p)\,a + K(\omega_g, \omega_g)\,b + \int_{m_\theta}^{\infty} K(\omega_g, \omega')\,(\chi(\omega')/h^+(E-\omega'))\,d\omega'. \quad (7)$$

$\chi(\omega)$ is then uniquely determined by the equation

$$\chi(\omega) = G(\omega, \omega_p)\,a + \int_{m_\theta}^{\infty} G(\omega, \omega')\frac{\chi(\omega')\,d\omega'}{h^+(E-\omega')}, \quad (8)$$

where

$$G(\omega, \omega') = K(\omega, \omega') - \frac{K(\omega, \omega_g)K(\omega_g, \omega')}{K(\omega_g, \omega_g)} = -\frac{k'}{2}\sqrt{\frac{\omega'}{\omega}}\frac{(\omega-\omega_g)(\omega'-\omega_g)}{(\omega-E_g)(\omega'-E_g)(\omega+\omega'-E_g)}. \quad (9)$$

For $E > 2m_\theta$ inelastic processes ($V+\theta \to N+2\theta$) are possible. They are described by an outgoing wave [formula (66) of reference 1]:

$$\varphi(\mathbf{k}_1, \mathbf{k}_2) = \frac{g_0}{2\sqrt{4\pi}(\omega_1+\omega_2-E-i\gamma)}\left[\frac{\varphi(\omega_2)}{\sqrt{2\omega_1}} + \frac{\varphi(\omega_1)}{\sqrt{2\omega_2}}\right]. \quad (10)$$

Then the wave of the unphysical state will not be scattered, if its amplitude is related to the amplitude a of the physical wave by the equation [cf. formula (7)]

$$b = -a\left\{\frac{K(\omega_g, \omega_p)}{K(\omega_g, \omega_g)} + \int_{m_\theta}^{\infty}\frac{K(\omega_g, \omega')}{K(\omega_g, \omega_g)}\frac{[\chi(\omega')/a]\,d\omega'}{h^+(E-\omega')}\right\}; \quad (11)$$

the function $\chi(\omega')/a$ is independent of a [cf. formula (8)].

3. In exactly the same way it is easily shown that the scattered wave of "ghost states" can be made to vanish for the system $(V+(z-1)\theta, N+z\theta)$, if a definite unphysical state amplitude is added to the initial state of the system. This obviously guarantees the conservation of the probability for finding the system in the physical region, i.e., the unitarity of the physical S matrix.

Repeating Heisenberg's calculations, we arrive at an interesting result: the scattered wave of "ghost states" vanishes for a definite value, not of the amplitude b of the incoming wave of the "ghost states" itself, but of the following integral of b:

$$B = \int b(\mathbf{k}_1 \ldots \mathbf{k}_{z-1})\,\delta\left(E - E_g - \sum_{i=1}^{z-1}\omega_i\right)d\mathbf{k}_{z-1}. \quad (12)$$

The adding of an arbitrary "ghost" wave giving a prescribed value to the integral (12), to the incoming physical wave does not alter any physical results.

4. We now discuss in more detail the question of the choice of basis states of the system. To be definite, we shall talk about the sector $(N+2\theta, V+\theta)$. We seek eigenstates of the Hamiltonian in the form of expansions in terms of states with a definite number of bare particles [cf. formula (2)]. The state $\psi_V^* a^*|0\rangle$ has a negative norm. Nevertheless, we look for a physical interpretation for the amplitude $\varphi(\mathbf{k})$ of this state, and show that it can be found. In order to resolve this seeming contradiction, we look at the solutions of the previous sector $(N+\theta, V)$. The discrete states of this sector are described by the function [formula (7R) of reference 1]

$$\Phi_{p,g}\rangle = c\left[-\psi_V^* + \frac{g_0}{\sqrt{4\pi}}\psi_N^*\int\frac{1}{\sqrt{2\omega}(\omega-E_{p,g})}a^*(\mathbf{k})\,d\mathbf{k}\right]|0\rangle. \quad (13)$$

Its norm is [formula (34) of reference 1]

$$\langle\Phi|\Phi\rangle_{p,g} = \left[-1+|g_0|^2\int\frac{k^2dk}{2\omega(\omega-E_{p,g})^2}\right]|c|^2. \quad (14)$$

The second term is greater than unity for the physical state of the V particle, and the system is mainly in the state $N+\theta$. We have the opposite situation for the "ghost state."

In the sector $(N+2\theta, V+\theta)$ it would have more physical meaning, if we expanded in terms of eigenstates of the system $(N+\theta, V)$ plus a θ particle in a free state, as was done by Heisenberg in the discussion of the higher sectors (reference 1, Sec. 5.1). However, it is more convenient for the calculations to use an expansion in terms of bare particle states. $\varphi(\mathbf{k})$ can then be regarded as a

superposition of the amplitudes of the two states of the V particle, which is what is effectively done in reference 1 as well as in this paper [if $E > 2m_\theta$, $\varphi(\mathbf{k})$ also contains the amplitude of the virtual state of the V particle coming from the continuous spectrum of the $(N+\theta, V)$ system].

The use of $\varphi(\mathbf{k})$ is justified by the fact that it possible, as a consequence of the formal conservation laws concerning the asymptotic behavior of the function $\varphi(\mathbf{k})$ at great distances (the δ-function in the Hamiltonian (2R) in reference 1), to tell which one of the states of the system $(N+\theta, V)$ belongs to the scattered θ particle. In view of what has been said earlier, we shall regard the basis states of the following section as states of the type $(N+\theta, V) + z\theta$.

5. In conclusion we investigate the conditions which have to be imposed on the unphysical states in the more general case.

Let the initial state of the system be described by the function $\begin{pmatrix}\Phi\\ G\end{pmatrix}$, where Φ is a state with positive norm, and G is a state with negative norm. Writing this function in the form of a column vector underscores the orthogonality of Φ and G with respect to each other. Φ and G may themselves be many-component functions.

The scattering matrix mixes states with positive and negative norm belonging to the same energy eigenvalue (other integrals of the motion may also be identical). Owing to the pseudo-unitarity of the scattering matrix $(S^+S = 1)$,[1] the norm of the system remains unchanged:

$$|\Phi|^2 - |G|^2. \tag{15}$$

If the initial state contains only states with either positive or negative norm, the final state will be a mixture of both:

$$S\begin{pmatrix}1\\0\end{pmatrix} = \begin{pmatrix}A\\b\end{pmatrix}, \quad |A|^2 - |b|^2 = +1, \tag{16}$$

$$S\begin{pmatrix}0\\1\end{pmatrix} = \begin{pmatrix}a\\B\end{pmatrix}, \quad |a|^2 - |B|^2 = -1. \tag{17}$$

If the initial state is a mixture, then

$$S\left[\begin{pmatrix}1\\0\end{pmatrix} + \xi\begin{pmatrix}0\\1\end{pmatrix}\right] = \begin{pmatrix}A+\xi a\\ b+\xi B\end{pmatrix}, \tag{18}$$

$$|A+\xi a|^2 - |b+\xi B|^2 = 1 - |\xi|^2.$$

Choosing ξ such that

$$|\xi|^2 = |b+\xi B|^2, \tag{19}$$

we obtain

$$|A+\xi a|^2 = 1 \tag{20}$$

The S matrix then takes the form

$$\begin{pmatrix}S_1 & 0\\ 0 & S_2\end{pmatrix}, \tag{21}$$

with both $S_1^+S_1 = 1$ and $S_2^+S_2 = 1$, where the hermitian conjugation is to be understood in the usual sense.

With the unitarity of the S matrix describing transitions between states with positive norm guaranteed, one may now construct physical quantities by postulating that they are completely defined by states with positive norm. The probability $\langle\Phi|\Phi\rangle$, the energy $\langle\Phi|H|\Phi\rangle$, and the other integrals of the motion will be conserved, as should be required of these physical quantities.

With regard to the foregoing section we emphasize again that the states Φ must have a physical meaning, whereas the states with negative norm G have the character of boundary conditions and arise solely from unitarity considerations for the scattering matrix for physical transitions.

We add a few remarks on the uniqueness of the determination of the states G. The only condition on the amplitude of the admixture G is the requirement that the scattering matrix for transitions between unphysical states be unitary [cf. formula (19)]. Then we can apply physical language to the "ghost states." In particular, if there is only one unphysical state, condition (19) can be said to be the requirement of elastic scattering of the unphysical admixture.

It is clear that the requirement of elastic scattering of the "ghost state" makes the problem nonunique, since it depends on the choice of the scattering phase of this state. In this respect the case of an indefinite metric is different from the case considered by Heisenberg. There the exclusion of the unphysical states is unique. The simplest procedure to obtain unique physical results is given by the more incisive requirement (which we used in the present paper) that the unphysical admixture does not scatter at all.[3] In this case condition (19)

$$|G_{t=+\infty}|^2 = |G_{t=-\infty}|^2 \tag{19a}$$

is replaced by the condition

$$G_{t=+\infty} = G_{t=-\infty}. \tag{19b}$$

I am grateful to Prof. Ya. A. Smorodinskii for a discussion of the results and for helpful advice during the writing of this paper.

[1] W. Heisenberg, Nucl, Phys. **4**, 532 (1957).

[2] G. Källén and W. Pauli, Dan. Mat. Fys. Medd. **30**, No. 7 (1955). Russ. Transl. in Usp. Fiz. Nauk **60**, No. 3 (1956).

[3] Bogolyubov, Medvedev, and Polivanov, Научн. докл. Высш. школы серия физ.-мат. (Scient. Reports of the Higher Schools Phys.-Math. Series) **1**, (1958).

Translated by R. Lipperheide
19

ELECTROACOUSTIC PHENOMENA IN A DEGENERATE ELECTRON-ION PLASMA

P. S. ZYRYANOV and G. G. TALUTS

Institute of Metal Physics, Academy of Sciences, U.S.S.R.

Submitted to JETP editor June 7, 1958

J. Exptl. Theoret. Phys. (U.S.S.R.) **36**, 145-148 (January, 1959)

Electrical phenomena occurring in an electron-ion plasma in which acoustic waves are propagated are considered. The space attenuation coefficient (absorption coefficient) of the waves is computed.

THE spectrum of characteristic oscillations of an electron-ion plasma consists of two modes: plasma or electronic oscillations with the limiting Langmuir frequency, and acoustic or ion oscillations. Thermal motion excites in the plasma only acoustic oscillations, which largely determine the temperature dependence of the physical properties of the plasma (for example, electric conductivity, thermal conductivity, absorption of sound, etc.).

Certain properties of real metals can be explained on the basis of the so-called plasma model,[1,2] in which the metal is regarded as an isotropic electron-ion plasma. This model is useful for describing those phenomena in which the characteristic length is considerably greater than the average distance between the particles of the metal. In particular, such phenomena include effects, considered below, which are associated with the propagation of supersonic waves in the metal.

In the first section of this paper, the problem is formulated and the fundamental equations are discussed, on the second section the potential of the electric field of supersonic waves is calculated, and in the third section the absorption coefficient of a longitudinal supersonic wave in the plasma is calculated.

1. When a longitudinal supersonic wave is propagated in an electron-ion plasma the amplitudes of the ion and electron densities will differ in magnitude due to the large difference in the volume compressibility of electron and ion fluids. This circumstance will result in the appearance of a space charge that produces a longitudinal electric field which varies at the supersonic frequency. The interaction of the spreading supersonic wave with thermal acoustic vibrations will lead to absorption and dissipation of energy of the supersonic wave. These effects can be taken into account by introducing a finite value for the electrical conductivity σ of the plasma, i.e., by taking into account the collisions between the electrons and the thermal vibrations of the plasma. For finite values of σ, the energy of the longitudinal electric field excited by the supersonic wave will be dissipated as Joule heat. We shall show that this mechanism of dissipation of supersonic vibrations in the metal gives the correct order of magnitude for the absorption coefficient.

We consider a dynamical system consisting of a large number of electrons and ions in which an ultrasonic wave is propagated. If the interactions between the particles are taken into account in the self-consistent field approximation, the initial equations may be written in the following form:

$$i\hbar\dot{\psi}_{\gamma j} = -(\hbar^2/2m_\gamma)\,\Delta\psi_{\gamma j} + e_\gamma\Phi\psi_{\gamma j},$$
$$\Delta\Phi = -4\pi\sum_{j\gamma} e_\gamma |\psi_{\gamma j}|^2. \qquad (1)$$

Here $\psi_{\gamma j}$ is the self-consistent wave function for the j-th particle. The subscript γ takes on two values, 1 for electrons, and 2 for ions. The equations in (1) are a system of Hartree's equations generalized to the case of nonstationary states. Our problem consists of evaluating the potential of the longitudinal electric field of ultrasonic waves in terms of constants characterizing the plasma and the amplitude of the supersonic wave.

Equations (1) have an exact solution for the system in a state of constant density $|\psi_{\gamma j}|^2 = \text{const}$. In states with a density that does not differ much from a constant, (1) can be linearized. To do this it is convenient to write (1) in the so-called hydrodynamic form,[3] by setting

$$\psi_{\gamma j} = \rho_{\gamma j}^{1/2}\exp\{is_{\gamma j}/\hbar\}.$$

If we seek solutions of the linearized equations in the form of a superposition of plane progressive waves $\exp\{i\mathbf{k}\cdot\mathbf{r} - i\omega(k)t\}$, then we obtain the following system of equations for the Fourier amplitudes of the quantities $\rho_{\gamma j}$ and $s_{\gamma j}$:

$$\{-i\omega + i\mathbf{k}\cdot\mathbf{v}_{\gamma j}\}\, s_{\gamma j} + e_\gamma \Phi_k + (\hbar^2/4m_\gamma)\, k^2 \rho_{\gamma j} = 0,$$

$$\{-i\omega + i\mathbf{k}\cdot\mathbf{v}_{\gamma j}\}\, \rho_{\gamma j} - (k^2/m_\gamma)\, s_{\gamma j} = 0, \qquad (2)$$

$$\Phi_k = 4\pi k^{-2} \sum_{\gamma j} e_\gamma \rho_{\gamma j},$$

where $\mathbf{v}_{\gamma j}$ is the velocity of the j particle in the state with homogeneous density, equal to $\nabla s_{\gamma j}^{(0)}/m_\gamma$. The system of equations (2) leads to the dispersion equation[3]

$$1 = (k^2 G\ (k)/L^3) \sum_{j\gamma} (e_\gamma^2/m_\gamma)\, [(\omega - \mathbf{k}\cdot\mathbf{v}_{\gamma j})^2 - \hbar^2 k^4/4m_\gamma^2]^{-1}, \qquad (3)$$

where

$$G(k) = \int \frac{1}{|r|} e^{i\mathbf{k}\cdot\mathbf{r}}\, d\mathbf{r} = \frac{4\pi}{k^2},$$

and L^3 is the volume of the system. If the velocity distribution of the electrons obeys Fermi statistics and the random motion of the ions can be neglected in the state with a spatially homogeneous density, then, taking into account the inequality $(\omega/k)^2 \ll v_F^2$ (v_F is the limiting velocity on the Fermi surface), which is justified by the result obtained, we obtain from (3)

$$\omega^2(k) = \omega_{i02}^2 u_0^2 k^2/(\omega_{i2}^2 + u_0^2 k^2), \qquad (4)$$

where

$$\omega_{i02}^2 = 4\pi n_{i02} e_2^2/m_2, \quad u_0^2 = {}^1/_3 |m_1 e_2 / m_2 e_1|\, v_F^2;$$

n_{02} is the average ion density. As $k \to 0$ expression (4) coincides with the corresponding formula of Silin's paper.[1]

2. From (2) we can easily obtain the Fourier component of the longitudinal electric field Φ_k, which can be conveniently expressed in terms of only the ion characteristics and $\omega(k)$. On using the approximations adopted in deriving Eq. (4) we obtain

$$\Phi_k = \frac{m_2}{e_2} \frac{\omega^2(k)}{k} A_k, \qquad (5)$$

where A_k is the amplitude of displacement of the ions equal to $\sum_j \rho_{2,j}/(n_{02}k)$, while $\omega(k)$ is the frequency of the supersonic wave.

Let us consider the case of a standing supersonic wave. The position in space of the loops and nodes of the amplitude of the displacement of the ions A_k will not depend upon the time in this case. On the basis of (5) we can assert that between a node and a loop there exists a difference of potential Φ_k which varies in time with the frequency of the supersonic wave. Preliminary experiments support this conclusion.[4] In these experiments we measured the magnitude of the variable electromotive force that arises in a polycrystalline copper sample when stationary supersonic waves are excited in it. When the standing waves had a wavelength of 5 cm and the amplitude of oscillations was $\sim 10^{-5}$ cm the magnitude of the electromotive force was of the order of 10 microvolts, which agrees with the estimate in Eq. (5). The distribution of the variable electromotive force along the sample corresponded to the nodes and loops of the standing wave.

3. The potential (5) can also be obtained by considering oscillations in a system containing not two, but only one kind of particles of mass m_2 with the interaction potential between these particles being given by

$$V(r) = (e_2/r) \exp\{-\omega_{02}/u_0)\, r\}.$$

From this it follows that the effect of electrons on the interaction between ions reduces to screening the ionic charge. Since the average velocity of the random motion of the electrons is large compared with the same quantity for the ions, the Debye electron cloud practically does not differ in shape from a sphere. At the same time the velocities of the ordered (hydrodynamic) motions of the electrons and the ions are the same, since the Debye polarization cloud consisting of electrons moves practically together with the ion which is at the center of this cloud. The ratio of the kinetic energies of ordered motion of electrons and ions will be equal to the ratio of their mass densities $T_1/T_2 = m_1 z/m_2$ (where $z = |e_2/e_1|$ is the number of electrons per ion). This conclusion follows directly from Eq. (2).

We now proceed to evaluate the coefficient of sound absorption α in an electron-ion plasma. We consider the absorption due to the viscosity of the electron gas which arises as a result of collisions between the electrons and the thermal vibrations of the lattice. The existence of viscosity leads to the dissipation of kinetic energy of the ordered (hydrodynamic) motion. Consequently, the quantity q (the energy converted into heat per unit time per unit volume) is a function of the kinetic energy T_1 of the ordered motion of the electrons. By expanding this function into a series in powers of T_1, and by restricting ourselves to the first term of the expansion, we obtain

$$q = \beta\, (m_1 z/m_2) \left\{\tfrac{1}{2} n_{02} m_2 v_2^2\right\}. \qquad (6)$$

(β is the expansion constant). Since the average density of kinetic energy in a supersonic wave is equal to the average density of potential energy, which in turn is equal to the energy density of the longitudinal electric field with the potential given by (5), formula (6) may be written in the form

$$q = (\beta/8\pi)\, (m_1 z/m_2)\, |\nabla \Phi_k|^2. \qquad (7)$$

The quantity $\{(m_1 z/m_2)|\nabla\Phi_k|^2\}^{1/2}$ can be interpreted as a certain effective electric field which gives rise to the ordered motion of the electrons. If formula (7) is interpreted in such a way, the constant $\beta/8\pi$ can be identified with the electrical conductivity of the electron-ion plasma.

By equating q to the divergence of the energy flux density in the sound wave, which is equal to $2\alpha u_0 m_2 n_0 \omega^2(k)|A_k|^2$, we obtain the following expression for the absorption coefficient:

$$\alpha = (\sigma m_1 z/2m_2)|\nabla\Phi_k|^2/u_0 m_2 n_{02}\omega^2(k)|A_k|^2. \quad (8)$$

By utilizing (5), Eq. (8) can be rewritten as

$$\alpha = (m_1 \sigma z/2e^2 n_{02} u_0)\,\omega^2. \quad (9)$$

This expression for the absorption coefficient coincides with the corresponding expression of references 5, 6, and 7, in which the formula for α was obtained by other methods. The numerical value of the quantity α and its dependence on the electrical conductivity are apparently confirmed by experimental data.[5]

We note that in the electron-ion plasma of a metal other mechanisms of absorption of supersonic waves also exist in addition to the mechanism of absorption considered above. The absorption of supersonic waves may be due, for example, to thermal conductivity. In this case the correction to Eq. (9), according to reference 8, will be of order $(1-c_v/c_p)$. Since the ratio of specific heats c_v/c_p for metals at not very high temperatures is close to unity the corrections to formula (9) due to thermal conductivity will be small.

[1] V. P. Silin, J. Exptl. Theoret. Phys. (U.S.S.R.) **23**, 649 (1952).

[2] P. S. Zyryanov, J. Exptl. Theoret. Phys. (U.S.S.R.) **29**, 193 (1955), Soviet Phys. JETP **2**, 247 (1956).

[3] P. S. Zyryanov and V. M. Eleonskii, J. Exptl. Theoret. Phys. (U.S.S.R.) **30**, 592 (1956), Soviet Phys. JETP **3**, 620 (1956).

[4] Zyryanov, Borisov, and Taluts, Физика металлов и металловедение (Physics of Metals and Metal Research) (in press).

[5] W. P. Mason, Phys. Rev. **97**, 557 (1955).

[6] R. W. Morse, Phys. Rev. **97**, 1716 (1955).

[7] Akhiezer, Kaganov, and Lyubarskiĭ, J. Exptl. Theoret. Phys. (U.S.S.R.) **32**, 837 (1957), Soviet Phys. JETP **5**, 685 (1957).

[8] L. D. Landau and E. M. Lifshitz, Механика сплошных сред (Mechanics of Continuous Media) Moscow, Gostekhizdat, 1953.

Translated by G. Volkoff
20

ON THE ENERGY SPECTRUM OF A MOTT EXCITON IN IONIC CRYSTALS

S. A. MOSKALENKO and K. B. TOLPYGO

Institute of Physics, Academy of Sciences, Ukrainian S.S.R.

Submitted to JETP editor June 9, 1958

J. Exptl. Theoret. Phys. (U.S.S.R.) 36, 149-163 (January, 1959)

A qualitative study of the levels of a Mott exciton in ionic crystals is made from the point of view of a many-electron theory. A many-electron discussion of the exciton reduces to the problem of the motion of two quasi-particles which in the case of triplet states (ortho-exciton) interact through Coulomb forces and in the case of singlet states (para-exciton) through Coulomb and exchange forces. These forces are approximately evaluated using a model in which the electron states at the cation site and the vacant states at the anion site are supposed to be spherically symmetric. The ortho- and para-exciton series of a non-polarizable exciton of large radius are evaluated using a generalized effective mass method. An estimate is given of the influence of the difference from a point charge Coulomb potential on the magnitude of the l-splitting. Using group theory a general level scheme is given for an exciton for the case $\mathbf{K} = 0$ for the O_h group, and the results are compared with the yellow exciton series in a Cu_2O crystal. The properties of an exciton in a magnetic field are discussed.

1. A MANY-ELECTRON DISCUSSION OF THE PROBLEM

A Mott exciton in strongly polar crystals is the result of a transition of an electron from an external, filled p shell of the anion into a vacant state of the s shell of the cation. The extra electron and hole obtained in this way form a system similar to a hydrogen atom. Its states have been considered in many papers.[1-9] In the paper by one of the authors [reference 9, Eq. (8)] the wave function of the exciton in a crystal with undisplaced ions was written as a linear combination of wave functions $C(\mathbf{G}, s, \mathbf{H}, M, S_1, S_2)$ of all electrons in the crystal for which an electron from the external p shell of the anion site $\mathbf{H}$ with magnetic quantum number M had gone into the s shell of the cation site $\mathbf{G}$ with spin S_1, while the anion site remained with a spin S_2. These were of the form

$$C(\mathbf{G}, s, \mathbf{H}, M, S_1, S_2) = \sum{}' (-1)^\nu P^\nu \prod_{\mathbf{h}m\sigma} \Theta_{\mathbf{h}m\sigma}(\mathbf{q}_{\mathbf{h}m\sigma} S_{\mathbf{h}m\sigma}) \Theta_{\mathbf{G}s S_1}(\mathbf{q}_{\mathbf{G}s} S_1), \quad (\mathbf{h}, m, \sigma) \neq (\mathbf{H}, M, -S_2), \quad (1)$$

where $\Theta \ldots$ are one-electron orthonormal functions, P the electron permutation operator, ν the parity of the permutation, $\mathbf{q}$ and S_z the coordinate and spin of the electron; $\mathbf{h}$ numbers the anion sites of the lattice, m and σ number the states in the anion p shell.

It is convenient to choose as the basis functions linear combinations of the C functions which are eigenfunctions of the operator of the square of the total spin of the system. For a singlet state $S = 0$ and the corresponding function, designated by an index Σ, is equal to

$$\Psi(\mathbf{G}, s, \mathbf{H}, M | \Sigma) = [C(\mathbf{G}, s, \mathbf{H}, M, {}^1/_2, -{}^1/_2) - C(\mathbf{G}, s, \mathbf{H}, M, -{}^1/_2, {}^1/_2)]/\sqrt{2}. \quad (2)$$

For $S = 1$ there are three functions. It is convenient to choose these in such a way that they go over into one another under the action of the O_h group.[10] We distinguish them by indices ξ, η, and ζ:

$$\begin{aligned}
\Psi(\mathbf{G}, s, \mathbf{H}, M | \xi) &= [-C(\mathbf{G}, s, \mathbf{H}, M, {}^1/_2, {}^1/_2) + C(\mathbf{G}, s, \mathbf{H}, M, -{}^1/_2, -{}^1/_2)]/\sqrt{2}, \\
\Psi(\mathbf{G}, s, \mathbf{H}, M, | \eta) &= [C(\mathbf{G}, s, \mathbf{H}, M, {}^1/_2, {}^1/_2) + C(\mathbf{G}, s, \mathbf{H}, M, -{}^1/_2, -{}^1/_2)](i/\sqrt{2}), \quad (3) \\
\Psi(\mathbf{G}, s, \mathbf{H}, M | \zeta) &= [C(\mathbf{G}, s, \mathbf{H}, M, {}^1/_2, -{}^1/_2) + C(\mathbf{G}, s, \mathbf{H}, M, -{}^1/_2, {}^1/_2)]/\sqrt{2}.
\end{aligned}$$

The wave function of the crystal in the general case will be

$$\Psi = \sum_{\mathbf{G}\mathbf{H}MI} \Phi(\mathbf{G}, \mathbf{H}, M | I) \Psi(\mathbf{G}, s, \mathbf{H}, M | I), \quad (4)$$

where I takes on four values Σ, ξ, η, and ζ, while M takes on three values. The sum over $\mathbf{G}$ and $\mathbf{H}$ extends over the whole of the crystal.

For an exciton moving with wave vector $\mathbf{K}$, the function Φ must tend to zero as $|\mathbf{G} - \mathbf{H}|$ increases,

and if G and H are translated over a lattice vector distance it must be multiplied by an exponential factor, so that

$$\Phi(\mathbf{G}, \mathbf{H}, M \mid l) = \exp[i\mathbf{K}, \alpha\mathbf{G} + \beta\mathbf{H}]\, \varphi_\nu(\mathbf{G} - \mathbf{H}, M \mid l), \quad (5)$$

where ν denotes all the quantum numbers characterizing the relative motion in the exciton. The average of the crystal Hamiltonian taken over the function $\Psi(4)$ is equal to

$$\begin{aligned}
{}^{s}E_\nu(\mathbf{K}) = {} & \frac{1}{N}\sum_{\mathbf{GG'HM}l} L_{\text{eff}}(\mathbf{G}-\mathbf{G}', s)\exp[i\mathbf{K}, \alpha(\mathbf{G}-\mathbf{G}')] \\
& \times \varphi^*_\nu(\mathbf{G}'-\mathbf{H}, \quad M \mid l)\, \varphi_\nu(\mathbf{G}-\mathbf{H}, M \mid l) \\
& - \frac{1}{N}\sum_{\mathbf{HH'GMM'}l} L_{\text{eff}}(\mathbf{H}-\mathbf{H}', M, M')\exp[i\mathbf{K}, \beta(\mathbf{H}-\mathbf{H}')] \\
& \times \varphi^*_\nu(\mathbf{G}-\mathbf{H}', M' \mid l)\, \varphi_\nu(\mathbf{G}-\mathbf{H}, M \mid l) \\
& + \frac{1}{N}\sum_{\mathbf{GG'HH'MM'}l} \exp[i\mathbf{K}, \alpha(\mathbf{G}-\mathbf{G}') \\
& + \beta(\mathbf{H}-\mathbf{H}')][-F(\mathbf{G}, s, \mathbf{H}', M'; \mathbf{G}', s, \mathbf{H}, M) \\
& + 2\delta(S)F(\mathbf{G}, s, \mathbf{H}', M'; \mathbf{H}, M, \mathbf{G}', s)] \\
& \times \varphi^*_\nu(\mathbf{G}'-\mathbf{H}', M' \mid l)\, \varphi_\nu(\mathbf{G}-\mathbf{H}, M \mid l)
\end{aligned} \quad (6)$$

if we neglect the spin-orbit interaction. This expression separates into two parts corresponding to $S = 0$ when $I = \Sigma$, and $S = 1$ when I takes on the three values ξ, η, ζ. In our approximation the states with $I = \xi, \eta, \zeta$ can be also separated, but in the following we shall choose linear combinations of them corresponding to a well determined symmetry. According to reference 9, the coefficients L_{eff} are equal to

$$\begin{aligned}
L_{\text{eff}}(\mathbf{G}-\mathbf{G}', s) = {} & L(\mathbf{G}, s,; \mathbf{G}', s) \\
& + 2\sum_{\mathbf{h}m} F(\mathbf{G}, s, \mathbf{h}, m; \mathbf{G}', s, \mathbf{h}, m) \\
& - \sum_{\mathbf{h}m} F(\mathbf{G}, s, \mathbf{h}, m; \mathbf{h}, m, \mathbf{G}', s),
\end{aligned} \quad (7)$$

$$\begin{aligned}
L_{\text{eff}}(\mathbf{H}-\mathbf{H}', M, M') = {} & L(\mathbf{H}, M; \mathbf{H}', M') \\
& + 2\sum_{\mathbf{h}m} F(\mathbf{h}, m, \mathbf{H}', M'; \mathbf{h}, m, \mathbf{H}, M) \\
& - \sum_{\mathbf{h}m} F(\mathbf{h}, m, \mathbf{H}', M'; \mathbf{H}, M, \mathbf{h}, m).
\end{aligned}$$

Here

$$\begin{aligned}
L(\mathbf{f}, \lambda; \mathbf{f}', \lambda') = {} & \int \Theta^*_{\mathbf{f}\lambda}(\mathbf{q})\left[-\frac{\hbar^2}{2m}\nabla^2_{\mathbf{q}} + V(\mathbf{q})\right]\Theta_{\mathbf{f}'\lambda'}(\mathbf{q})\, d\mathbf{q}, \\
& F(\mathbf{f}_1, \lambda_1, \mathbf{f}_2, \lambda_2; \mathbf{f}'_1, \lambda'_1, \mathbf{f}'_2, \lambda'_2) \\
= {} & e^2 \int \frac{\Theta^*_{\mathbf{f}_1\lambda_1}(\mathbf{q}_1)\,\Theta^*_{\mathbf{f}_2\lambda_2}(\mathbf{q}_2)\,\Theta_{\mathbf{f}'_1\lambda'_1}(\mathbf{q}_1)\,\Theta_{\mathbf{f}'_2\lambda'_2}(\mathbf{q}_2)\, d\mathbf{q}_1 d\mathbf{q}_2}{|\mathbf{q}_1 - \mathbf{q}_2|},
\end{aligned} \quad (8)$$

where $V(\mathbf{q})$ is the potential produced by the cores of all the ions in the lattice, $\mathbf{f}$ takes on the values G and H; λ takes on the values M and s. For $\mathbf{G} = \mathbf{G}'$ $L_{\text{eff}}(\mathbf{G}-\mathbf{G}', s)$ can be interpreted as the average kinetic and potential energy (including exchange) of the interaction of an excited electron with the cores of the ions and with all of the 6N valence electrons (the background). For $\mathbf{H} = \mathbf{H}'$ and $M = M'$ $L_{\text{eff}}(\mathbf{H}-\mathbf{H}', M, M')$ plays a similar role for a hole which has, as can be seen from the signs, the opposite mass, charge, and spin. The third sum in (6) can, if $\mathbf{G} = \mathbf{G}'$, $\mathbf{H} = \mathbf{H}'$, $M = M'$, be interpreted as the Coulomb and exchange interaction of the extra electron and the hole. In the triplet states there is no exchange interaction between the hole and the electron. Since the form of the "interaction potential" is different, states with $S = 0$ and $S = 1$ will have different energies. We shall call them para- and ortho-excitons. Since the electron spin can change during a photo-transition due to the spin-orbit interaction, but with a rather small probability, we must expect that the ortho-exciton series will have a very low intensity. Since there are two quasi-particles present, the exciton states will be to some extent similar to the states of the He atom, but since the interaction potential is different for the two series from a point charge Coulomb potential, the l-degeneracy will be lifted.

Overhauser[10] has investigated the lowest states of a Mott exciton for $\mathbf{K} = 0$ in crystals of the NaCl and CsCl type, assuming that the electron goes over from the halide only to the first spherical configuration of Na^+ or Cs^+ ions. He also showed the existence of singlet and triplet states using group theoretical methods and gave the systematics of the lowest exciton terms. However, the restriction to the first spherical configuration is clearly insufficient for a consideration of the excited states. Moreover, Overhauser did not determine the exciton levels. In a recent paper[11] Takeuti considered the exciton in elemental semiconductors with one valence band and one conduction band, using Bloch functions. Restricting himself to a qualitative investigation he also arrived at the result that there are singlet and triplet states present, and concluded that the difference between their levels in the so-called "hydrogen case" are negligible. Ortho- and para-excitons are thus described in his paper by the same equation. Our consideration is more general, and includes, in particular, his scheme and enables us to determine the exciton levels in a well defined approximation. Using the more general description of the wave functions (2) to (5) we shall consider arbitrary exciton states and the case

$\mathbf{K} \neq 0$. For $\mathbf{K} = 0$ we made a group-theoretical analysis of all exciton states for crystals of the group O_h; the result of this analysis is given in the following, but an account of the method is given in a separate paper. In that way a method is found to understand the details of the exciton spectrum which is experimentally observed. Finally, we reduce the determination of the exciton energy (6) to the problem of the motion of two quasi-particles, and in the case of excitons with a sufficiently large radius we shall give a numerical estimate of the Coulomb and exchange integrals and of the energy levels of the para- and ortho-exciton series, taking l-splitting into account.

2. THE REDUCTION OF THE MANY-ELECTRON PROBLEM TO THE EQUATION OF MOTION OF TWO QUASI-PARTICLES

The functional (6) can be rewritten in the form used by Dresselhaus[8] who earlier assumed the presence of two quasi-particles, where one of them is described by the states of a degenerate band. To do this we use the identity

$$\frac{1}{N}\sum_{\mathbf{HH'G}} L_{\mathbf{eff}}(\mathbf{H}-\mathbf{H'}, M, M') \exp[i\mathbf{K}, \beta(\mathbf{H}-\mathbf{H'})] \times \varphi_\nu^*(\mathbf{G}-\mathbf{H'}, M' \mid I)\, \varphi_\nu(\mathbf{G}-\mathbf{H}, M \mid I)$$

$$= \sum_{\mathbf{f}_1} L_{\mathbf{eff}}(\mathbf{f}_1, M, M') \varphi_\nu^*(\mathbf{f}, M' \mid I)\, \varphi_\nu(\mathbf{f}-\mathbf{f}_1, M \mid I) \times \exp[i\mathbf{K}, \beta\mathbf{f}_1] = \sum_{\mathbf{f}} \varphi_\nu^*(\mathbf{f}, M' \mid I) \sum_{\mathbf{f}_1} L_{\mathbf{eff}}(\mathbf{f}_1, M, M') \times \exp[i\mathbf{f}_1, \beta\mathbf{K} + i\nabla_{\mathbf{f}}]\, \varphi_\nu(\mathbf{f}, M \mid I)$$

$$= \sum_{\mathbf{f}} \varphi_\nu^*(\mathbf{f}, M' \mid I)\, E(\beta\mathbf{K} + i\nabla_{\mathbf{f}}, M, M')\, \varphi_\nu(\mathbf{f}, M \mid I), \tag{9}$$

where we have put

$$E(\mathbf{x}, M, M') = \sum_{\mathbf{f}} L_{\mathbf{eff}}(\mathbf{f}, M, M') \exp(i\mathbf{x}\mathbf{f}).$$

The first term in Eq. (6) can be similarly transformed. In the last term we retain only the two-center integrals with $\mathbf{G} = \mathbf{G'}$ and $\mathbf{H} = \mathbf{H'}$. We have then

$$^{S}E_\nu(\mathbf{K}) = \sum_{\mathbf{f}MI} \varphi_\nu^*(\mathbf{f}, M \mid I)\, E(\alpha\mathbf{K} + i\nabla_{\mathbf{f}}, s)\, \varphi_\nu(\mathbf{f}, M, \mid I) - \sum_{\mathbf{f}MM'I} \varphi_\nu^*(\mathbf{f}, M' \mid I)\, E(\beta\mathbf{K} + i\nabla_{\mathbf{f}}, M, M')\, \varphi_\nu(\mathbf{f}, M \mid I) + \sum_{\mathbf{f}MM'I} [-\mathbf{K}(\mathbf{f}, M, M', s) + 2\delta(S)\, A(\mathbf{f}, M, M', s)] \times \varphi_\nu^*(\mathbf{f}, M' \mid I)\, \varphi_\nu(\mathbf{f}, M \mid I), \tag{10}$$

where

$$E(\mathbf{x}, s) = \sum_{\mathbf{f}} L_{\mathbf{eff}}(\mathbf{f}, s) \exp(i\mathbf{x}\mathbf{f});\ K(\mathbf{f}, M, M', s) = F(\mathbf{G}, s, \mathbf{H}, M'; \mathbf{G}, s, \mathbf{H}, M);$$

$$A(\mathbf{f}, M, M' s) = F(\mathbf{G}, s, \mathbf{H}, M'; \mathbf{H}, M, \mathbf{G}, s).$$

Minimizing the functional (7) with respect to φ_ν^* leads to a matrix equation for φ_ν which is the same as Eq. (19) of Dresselhaus' paper.[8] The physical meaning of the coefficients $E(\kappa, s)$ and $E(\kappa, M, M')$ is easily ascertained, if we neglect the interaction between the electron and the hole and assume $\varphi_\nu = N^{-1/2}\varphi(M)\exp(i\mathbf{K}\mathbf{f})$, where

$$\sum_M |\varphi(M)|^2 = 1. \tag{11}$$

In that case Eq. (10) separates into two parts:

$$E(\alpha\mathbf{K} - \mathbf{k}_1, s) - \sum_{MM'} \varphi_\nu^*(M')\, E(\beta\mathbf{K} - \mathbf{k}_1, M, M')\, \varphi_\nu(M). \tag{12}$$

The first term is the energy of the electron in the band with wave vector $\alpha\mathbf{K} - \mathbf{k}_1$, and the second term gives after diagonalization the energy of the three hole bands corresponding to a wave vector $\beta\mathbf{K} - \mathbf{k}_1$.

The next problem is to find the form of the function $\varphi_\nu(\mathbf{f}_1 M \mid I)$. In the general case φ_ν and the exciton levels depend on the exciton wave vector $\mathbf{K}$ which enters as a parameter into the functional (10). The next step in the investigation is performed only for the states with $\mathbf{K} = 0$, into which transitions from the ground state of the crystal are allowed. We can write φ_ν in the form of an expansion in spherical harmonics $Y_{lm}(\theta, \varphi)$ which enables us to classify not only states of small radius, but also states of large radius:

$$\varphi_\nu(\mathbf{f}, M \mid I) = \sum_{lm} Y_{lm}(\theta_{\mathbf{f}}, \phi_{\mathbf{f}})\, R_{\nu lm}(|\mathbf{f}|, M \mid I). \tag{13}$$

Here $\theta_{\mathbf{f}}$, $\varphi_{\mathbf{f}}$ are the polar angles which determine the discrete lattice vector $\mathbf{f}$. Using group theory one can show, how, indeed, a combination of spherical harmonics leads to the expansion (13)

3. GROUP THEORETICAL CLASSIFICATION OF EXCITON STATES WITH $\mathbf{K} = 0$

In contradistinction to Overhauser's considerations which assumed to begin with that the electron moved around a fixed hole and along the nearest spherical configuration, and then let the system as a whole be translated, we shall start from the very beginning with arbitrary motion of the electron and the hole.

Substituting the expression for an arbitrary func-

tion which possesses translational symmetry (5) and (4) we get for K = 0:

$$\Psi_\nu = \sum_{lM\mathbf{f}} \varphi_\nu(\mathbf{f}, M|l)\,\Psi(\mathbf{f}, M|l), \qquad (14)$$

where

$$\Psi(\mathbf{f}, M|l) = \sum_{\mathbf{H}} \Psi(\mathbf{H}+\mathbf{f}, s, \mathbf{H}, M|l). \qquad (15)$$

We choose to begin with the functions $\Psi(\mathbf{f}, M|I)$ as the basis functions for the classification of the states. Since in our approximation the Hamiltonian does not contain the spin variable I, we can at first classify the states only according to the coordinate part of the function $\Psi(\mathbf{f}, M)$. In the case of states of small radius, when we can restrict ourselves to the first spherical configuration, $\mathbf{f}$ will take on, for a lattice of the NaCl type, all six values $(\pm d, 0, 0)$, $(0, \pm d, 0)$, $(0, 0, \pm d)$ which we shall denote by $\pm f_x$, $\pm f_y$, $\pm f_z$. Each value of $\mathbf{f}$ can be combined with one of the three values of M. The indices M_x, M_y, M_z will denote states of an electron in the p-shell of the type $xf(r)$, $yf(r)$, $zf(r)$. The space of the eighteen functions splits up into invariant subspaces corresponding to the irreducible representations:

$$\Gamma^{18} = \Gamma_1 + \Gamma_3 + \Gamma_4 + 2\Gamma_4' + \Gamma_5'. \qquad (16)$$

As will become clear in a moment, only transitions into states arising from Γ_4' and Γ_5' are allowed, after multiplication by the spin functions. These irreducible representations correspond to the functions

$$\begin{array}{l}
\Gamma_4' \\
[\Psi(f_x, M_x) + \Psi(-f_x, M_x)]/\sqrt{2} \\
[\Psi(f_y, M_y) + \Psi(-f_y, M_y)]/\sqrt{2} \\
[\Psi(f_z, M_z) + \Psi(-f_z, M_z)]/\sqrt{2} \\
\Gamma_4' \\
\tfrac{1}{2}[\Psi(f_y, M_x) + \Psi(-f_y, M_x) + \Psi(f_z, M_x) + \Psi(-f_z, M_x)] \\
\tfrac{1}{2}[\Psi(f_x, M_y) + \Psi(-f_x, M_y) + \Psi(f_z, M_y) + \Psi(-f_z, M_y)] \\
\tfrac{1}{2}[\Psi(f_x, M_z) + \Psi(-f_x, M_z) + \Psi(f_y, M_z) + \Psi(-f_y, M_z)] \\
\Gamma_5' \\
\tfrac{1}{2}[\Psi(f_y, M_x) + \Psi(-f_y, M_x) - \Psi(f_z, M_x) - \Psi(-f_z, M_x)] \\
\tfrac{1}{2}[\Psi(f_x, M_y) + \Psi(-f_x, M_y) - \Psi(f_z, M_y) - \Psi(-f_z, M_y)] \\
\tfrac{1}{2}[\Psi(f_x, M_z) + \Psi(-f_x, M_z) - \Psi(f_y, M_z) - \Psi(-f_y, M_z)]
\end{array} \qquad (17)$$

Instead of the functions Γ_4' which we have written down we can also take a linear combination of the corresponding lines of the two equivalent representations. In that case we get, in particular, the completely symmetric function $6^{-1/2}\sum_{\mathbf{f}} \Psi(\mathbf{f}, M_X)$, and also the function

$$3^{-1/2}\{\Psi(f_x, M_x) + \Psi(-f_x, M_x) - {}^1/_2[\Psi(f_y, M_x) + \Psi(-f_y, M_x) + \Psi(f_z, M_x) + \Psi(-f_z, M_x)]\}, \qquad (18)$$

which occurs in Overhauser's paper.[10]

For states of arbitrary radius we can choose, according to the expansion (13) and Eq. (14) as basis functions

$$\chi_\nu(lm|M) = \sum_{\mathbf{f}} \Psi(\mathbf{f}, M)\, Y_{lm}(\theta_f \varphi_f)\, R_{\nu lm}(|\mathbf{f}|M). \qquad (19)$$

One can easily see that now expansion (13) must contain either only even, or only odd l. The allowed transitions correspond to the first states. If we restrict ourselves to only harmonics with $l = 0$ and $l = 2$, the space of the eighteen functions splits into subspaces according to the irreducible representations $\Gamma_2' + \Gamma_3' + 3\Gamma_4' + 2\Gamma_5'$.

The wave functions of the bases of the irreducible representations Γ_4' and Γ_5' will be the following: for the first representation of Γ_4' we have three functions of the kind

$$\sum_{\mathbf{f}} R_{v0}(|\mathbf{f}|)\, Y_{00}(\theta_f \varphi_f)\, \Psi(\mathbf{f}, M_x), \qquad (20)$$

which differ in the index M; similarly for the second representation of Γ_4'

$$\sum_{\mathbf{f}} R_{v20}(|\mathbf{f}|)\, \tfrac{1}{2}[3\cos^2(\widehat{fx}) - 1]\, \Psi(\mathbf{f}, M_x); \qquad (21)$$

and for the third representation of Γ_4'

$$\sum_{\mathbf{f}} R_{v22}(|\mathbf{f}|)[\cos(\widehat{fx})\, \Psi(\mathbf{f}, M_x) + \cos(\widehat{fz})\, \Psi(\mathbf{f}, M_z)]\cos(\widehat{fy}). \qquad (22)$$

For the first representation of Γ_5' we have

$$\sum_{\mathbf{f}} \sin^2(\widehat{fz}) \cos(2\varphi_{fxz})\, R_{v22}(|\mathbf{f}|)\, \Psi(\mathbf{f}, M_z), \qquad (23)$$

where φ_{xz} is the angle between $\mathbf{f}$ and the xz-plane; for the second representation of Γ_5'

$$\sum_{\mathbf{f}} R_{v22}(|\mathbf{f}|)[\cos(\widehat{fx})\, \Psi(\mathbf{f}, M_x) - \cos(\widehat{fz})\, \Psi(\mathbf{f}, M_z)]\cos(\widehat{fy}). \qquad (24)$$

If we write down the wave functions of the spin variable I, the basis remains the same for the singlet states, and transitions into Γ_4' states are allowed. For a triplet state the number of basis functions increases by a factor three and the 54 functions fall into groups according to the following irreducible representations:

$$(\Gamma_2' + \Gamma_3' + 3\Gamma_4' + 2\Gamma_5') \times \Gamma_4 = 3\Gamma_1' + 2\Gamma_2' + 5\Gamma_3' + 6\Gamma_4' + 7\Gamma_5'. \qquad (25)$$

We shall give one function of each of the irreducible representations of Γ_4'.

The first representation of Γ_4':

$$\sum_l R_{v20}(|\mathbf{f}|)\, Y_{60}(\vartheta_f \varphi_f)\,[-\Psi(\mathbf{f},\, M_y|\zeta) + \Psi(\mathbf{f},\, M_z|\eta_l)]/\sqrt{2}, \tag{26}$$

the two other functions are obtained by a cyclic permutation of the variables x, y, z and ξ, η, ζ. The second representation of Γ_4':

$$\frac{1}{2}\sum_l R_{v20}(|\mathbf{f}|)\,[(3\cos^2(\widehat{fy}) - 1)\,\Psi(\mathbf{f},\, M_y|\zeta) + (3\cos^2(\widehat{fz}) - 1)\,\Psi(\mathbf{f},\, M_z|\eta_l)]. \tag{27}$$

The third representation of Γ_4':

$$\sum_l R_{v22}(|\mathbf{f}|)\,[\sin^2(\widehat{fz})\cos(2\hat{\varphi}_{xz})\,\Psi(\mathbf{f},\, M_z|\eta_l) + \sin^2(\widehat{fy})\cos(2\hat{\varphi}_{xy})\Psi(\mathbf{f},\, M_y|\zeta)]. \tag{28}$$

The fourth representation of Γ_4':

$$\sum_l R_{v22}(|\mathbf{f}|)\,\{\cos(\widehat{fx})\,[\cos(\widehat{fy})\,\Psi(\mathbf{f},\, M_y|\zeta) + \cos(\widehat{fz})\,\Psi(\mathbf{f},\, M_z|\zeta)] \tag{29}$$

$$-\cos(\widehat{fz})[\cos(\widehat{fx})\,\Psi(\mathbf{f},\, M_x|\xi) + \cos(\widehat{fy})\,\Psi(\mathbf{f},\, M_y|\xi)]\}$$

and so on.

The exciton eigenfunctions will be linear combinations of the corresponding lines of these irreducible representations, different for S = 0 and for S = 1. From the point of view of this more general consideration, the level schemes for a NaCl and for a CsCl crystal must be identical, since their lattice symmetry is the same. The different number of states obtained by Overhauser is connected only with the different number of basis functions, he took, since he restricted himself to only one coordination sphere. The differences between the exciton spectra of these crystals must lie only in the individual spacing and intensity of the different lines.

4. EXCITON LEVELS IN THE MACROSCOPIC APPROXIMATION AND A VERY SIMPLE VARIANT OF THE EFFECTIVE MASS METHOD

If the expansion in spherical harmonics contains a limited number of terms, it was shown by the foregoing considerations that the wave functions without spin are not separated as far as the quantum number M is concerned. As a result there will enter into the functional (10) not only diagonal terms in M, and the equation corresponding to this will for K = 0 have the form

$$E(i\nabla_f,\, s)\,\varphi_\nu(\mathbf{f},\, M) - \sum_{M'} E(i\nabla_f,\, M,\, M')\,\varphi_\nu(\mathbf{f},\, M') + \sum_{M'}[-K(\mathbf{f},\, M,\, M',\, s) + 2\delta(S)\,\hat{A}(\mathbf{f},\, M,\, M',\, s)] \times \varphi_\nu(\mathbf{f},\, M') = {}^S E_\nu \varphi_\nu(\mathbf{f},\, M). \tag{30}$$

In the present paper we shall, in order to simplify the calculation, neglect the off-diagonal elements in M in Eq. (30). Account will be taken of these terms in a separate calculation. Equation (27) then simplifies to:

$$E(i\nabla_f,\, s)\,\varphi_\nu(\mathbf{f}) - E(i\nabla_f,\, M,\, M')\,\varphi_\nu(\mathbf{f}) + [-K(\mathbf{f},\, M,\, M,\, s) + 2\delta(S)\,A(\mathbf{f},\, M,\, M,\, s)]\,\varphi_\nu(\mathbf{f}) = {}^S E_\nu \varphi_\nu(\mathbf{f}). \tag{31}$$

We restrict our considerations to an exciton of large radius. We can then consider $\mathbf{f}$ to be a continuous variable and go over to the effective mass method (E.M.M.) equation. We shall consider the simplest case when both the electron and the hole band have a unique minimum at K = 0, and, moreover, F(k, M, M) does not depend on the value of M. Both bands are then spherically symmetric. It is known that for a number of real crystals the bands have several energy minima and do not possess spherical symmetry, and in the case of degenerate bands one can not expand in powers of K. The corresponding exciton spectra will be much more complicated than the ones obtained in our approximation. We shall concentrate our attention here mainly on ascertaining the role of the exchange potential and an estimate of the magnitude of the l-splitting and of the level shift compared to the hydrogen series. As is clear from (6), the many-electron approach to the problem leads to the appearance of another interaction, apart from the Coulomb and exchange potentials namely of each quasi-particle with the background electrons. The influence of the background on the interaction of the electron and the hole was considered by Samoĭlovich and Korenblit.[4] This interaction leads, moreover, to the fact that at large distances the Coulomb interaction is divided by the square of the index of refraction n_0^2. This was in different approximations shown in the papers of Kohn[12] and Liberberg-Kucher.[13] At distances of the order d and $d\sqrt{2}$ (d is the distance between nearest neighbor ions) the error in dividing by n_0^2 is about 10 to 20%. In our considerations this last effect will not enter explicitly, but the final result for both functions will be divided by n_0^2. If $\mathbf{f} = |\mathbf{G} - \mathbf{H}| \geq d$ the error is again small and the contribution of this potential at smaller distances is small (especially for a para-exciton). Expanding $E(i\nabla_f, s)$ and $E(i\nabla_f, M, M)$ in powers of $i\nabla_f$ up to ∇_f^4 inclusive, we can write Eq. (31) in the form

$$-\frac{\hbar^2}{2\mu}\nabla^2\varphi_\nu - \frac{\hbar^2 d^2}{\mu c}\nabla^4\varphi_\nu - \frac{e^2}{n_0^2}[K(r) - 2\delta(S)\,A(r)]\,\varphi_\nu = {}^S E_\nu \varphi_\nu. \tag{32}$$

It is different from the equation used by other au-

thors[2-8] through the presence of the exchange potential $A(r)$, the fact that $K(r)$ differs from $1/r$ and the fact that the following E.M.M. approximations are taken into account. The quantity c depends on the structure of the cation and anion lattices (see Appendix 1). Here $r = |G - H|$ is a continuous parameter. The approximate estimate of the integrals $K(r)$ and $A(r)$ is performed with hydrogen-like functions of the 1s type. The equation which is then obtained is quite complicated (see Appendix 2) but can be approximated quite simply:

$$-{}^{S}V(r)/(e^2/n_0^2) = K(r) - 2\delta(S)A(r) = \frac{1}{r} + \sum_{k=1}^{2} V_k^S \exp(-\gamma_k^S r) + V_3^S \frac{\exp(-\gamma_3^S r)}{r} \qquad (33)$$

through a suitable choice of the parameters V_k^S, γ_k^S for each value of the spin $S = 0$ and $S = 1$.

Equation (32) was solved by the variational method using the trial functions

$$\varphi_{nlm}(r) = x_S^{3/2} R_{nl}\left(\frac{x_S r}{na}\right) Y_{lm}(\theta\phi), \qquad (34)$$

where $a = a_B n_0^2 m/\mu$ is the effective Bohr radius, $a_B = \hbar^2/me^2$, x_S the variational parameter. The average value of the energy, evaluated by using the functions (34) and taking (A2.8) and (A2.9) into account, is equal to

$${}^{S}E_{nl}(x_S) = \frac{e^2}{2an_0^2n^2}\left[x_S^2 - 2x_S - \frac{8}{c}\left(\frac{d}{a}\right)^2 \frac{x_S^4}{n}\left(\frac{1}{l+1/2} - \frac{3}{4n}\right) - {}^{S}L(x_S|nl)\right]. \qquad (35)$$

The first two terms within the brackets correspond purely to the hydrogen problem, the third term is due to the term in ∇^4 and the fourth one to the difference between $K(r) - 2\delta(S)A(r)$ and $1/r$. ${}^{S}L(x_S|nl)$ is given in Appendix 2.

After finding the minimization parameter x_S, the expression (35) for the energy turns out to depend on the orbital quantum number l. One sees easily that the l-splitting between s and p levels varies as $1/n^3$. A numerical estimate will be given for a Cu_2O crystal.

5. THE THEORY OF EXCITONS IN A CRYSTAL OF THE Cu_2O TYPE

Since at the point $\mathbf{K} = 0$ the difference between all groups vanishes, the classification of the states of large radius which was obtained for NaCl remains valid also for Cu_2O. We shall assume that, in accordance with reference 14, the hole can be on one of the O^{--} sites in one of three p states, and the electron on one of the Cu^{+} sites in an s state. Such a mechanism of the formation of an exciton is not possible in only one way. At the present time also other possibilities are considered, on which we shall report separately.

In Fig. 1 we have depicted the scheme of those levels of the para-exciton ($S = 0$) and the ortho-exciton ($S = 1$) for which transitions from the ground state are possible only through spin-orbit interactions. We have given only S and d states of relative motion, transitions into which are allowed. The distances between the levels are drawn

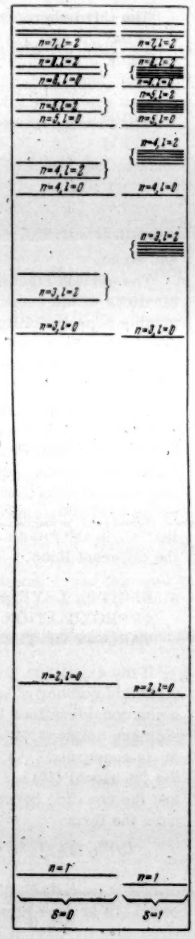

FIG. 1. Scheme of the exciton levels in the crystal, into which a transition from the ground state is allowed.

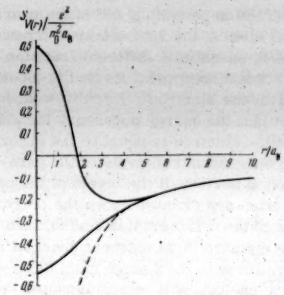

FIG. 2. Potential energy curves for the para- (S = 0) and ortho- (S = 1) exciton in the macroscopic approximation.

arbitrarily. The para-exciton levels must lie somewhat higher, thanks to the presence of the repulsive exchange potential. Pavinskii and Zhilich[15] have shown that due to the presence of two O^{--} ions in the elementary cell of Cu_2O two hole states are possible: even and odd states. Taking this fact into account in our scheme led just to the occurrence of the second exciton series.

Our considerations cannot give us the correct distances between the levels since from the various factors which produce the splitting we have only taken into account the difference in the potentials in their dependence on the total spin. For our numerical calculations we took for the parameters in the atomic functions (A2.1) for Cu $\alpha = 0.743/a_B$ according to Slater[16] and for O^{--} according to the results of Zhilich[14] (for the radial part) $\beta = 1.03/a_B$. As a result of this calculation we obtained an expression for $K - 2A$ (Appendix 2) and found the values of the coefficients in the simplified Eq. (33):

$$S=0:\quad V_1^0=-48.47/a_B;\quad V_2^0=46.46/a_B;\quad V_3^0=-1;$$
$$\gamma_1^0=1.44/a_B;\quad \gamma_2^0=1.503/a_B;\quad \gamma_3^0=1.5/a_B. \qquad (36)$$
$$S=1:\quad V_1^1=-1.554/a_B;\quad V_2^1=0;\quad V_3^1=-1;$$
$$\gamma_1^1=1.42/a_B;\quad \gamma_3^1=2.1/a_B.$$

For $\beta = 1.18/a_B$ we obtained values close to these. The corresponding curves are given in Fig. 2: $-K(r) + 2A(r)$ for S = 0, and $-K(r)$ for S = 1. The dotted line gives the point charge Coulomb potential. The rest of the evaluation of the exciton energy through Eqs. (35) and (A2.8) was performed for $n_0^2 = 2.5$; $\mu = 0.253\,m$, $a = 24.7\,a_B$.

In Fig. 3 we have given the para-exciton levels taking the exchange potential and the term in ∇^4 into account. We assumed also that the effective masses of the electron and the hole were the same. In that case c = 1/16 according to Appendix 1.

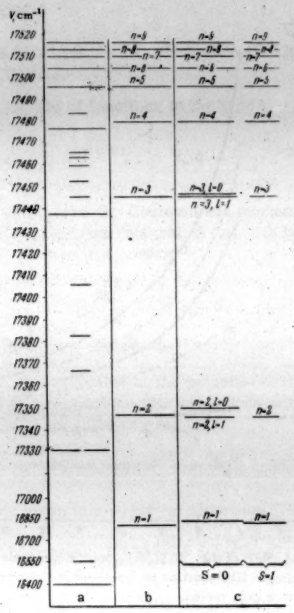

FIG. 3. Comparison of the yellow exciton series observed experimentally with the calculated ones: a – experimental data;[17,18] b – calculated from a hydrogen-like exciton model; c – according to the representation of the present paper.

Side by side we have given for comparison the results of the experiments of Gross and coworkers[17,18] and also the position of the lines for a purely hydrogen series $K(r) = 1/r$, $A(r) = 0$.

As can be seen from the figure the shift is appreciable for the s level of the para-exciton series and insignificant for all other levels of the para- and ortho-series. The lines with n = 1 (they are drawn to a different scale) turned out to be very weak experimentally; this cannot be explained in our scheme. The calculations show that the distances between s and p levels of the same n vary for the given values of the parameters as $30/n^3\ cm^{-1}$ for the para-series and as $1/n^3\ cm^{-1}$ for the ortho-series. The comparative smallness of the l-splitting produced by the difference of $K - 2A$ from $1/r$ and by taking the terms in ∇^4 into account is connected with the large radii of the exciton states in Cu_2O.

We also investigated the influence of the difference between $K - 2A$ and $1/r$ and of the correc-

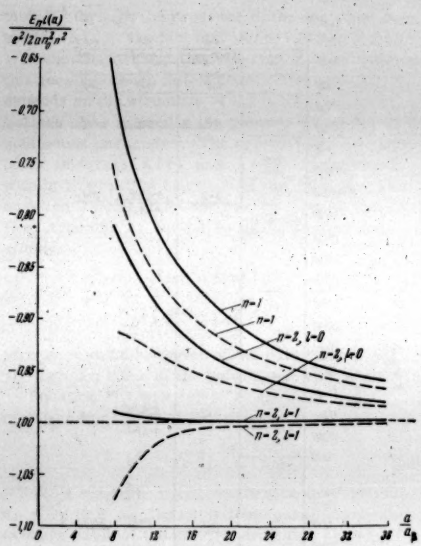

FIG. 4. Shift of the $^0E_{1s}$, $^0E_{2s}$, and $^0E_{2p}$ levels from the usual hydrogen-like position as functions of the magnitude of the effective Bohr radius.

tions to the E.M.M. $\sim\nabla^4$ on the magnitude of the l-splitting for different radii of the state in the simplest case when the effective masses of the electron and hole are assumed to be equal in the correction term $\sim\nabla^4$. The results are given in Fig. 4 for the 1s, 2s, and 2p levels. The solid curves are the ones obtained without taking the term ∇^4 into account, and the dotted lines those with taking this term into account. The horizontal line gives the level of the purely hydrogen problem. The magnitude of the splitting increases steeply with decreasing effective Bohr radius. Simultaneously the role of the corrections to the E.M.M. increases. The exact calculation of the l-splitting and the position of the lowest levels for small radii of the states must thus take into account the discrete structure of the crystal.

In conclusion we note some peculiarities of the behavior of excitons in a magnetic field. The ground state of the crystal in which all spins and orbital momenta are compensated is diamagnetic and its energy in a magnetic field increases as H^2. As a result of the absorption of light due to the presence of the spin-orbit interaction exciton states with $S = 0$ and $S = 1$ are formed. Since their energy levels differ appreciably because of the differences in the interaction potentials and in the character of the orbital motion, the spin-electron resonance in an exciton is essentially different from the spin-electron resonance in polarons and in localized centers with one electron. This difference consists in the fact that the energy necessary for a spin-flip of the exciton electron is equal to the difference between the corresponding levels of the para- and ortho-exciton series. If the levels of the para-exciton series are situated above the corresponding levels of the ortho-exciton series, then the spin-flip of the electron in an external constant magnetic field which leads to the change of an ortho-exciton into a para-exciton, will be accompanied by the absorption of two quanta of energy

$$\hbar\omega = |^0E_{nl} - {}^1E_{nl} \pm 2\hbar O_L|,$$

where O_L is the Larmor frequency. In crystals where the levels of the para-exciton series are situated below the corresponding levels of the ortho-exciton series during the same mechanism of transformation of a para-exciton into an ortho-exciton quanta

$$\hbar\omega = |^1E_{nl} - {}^0E_{nl} \pm 2\hbar O_L|$$

will be absorbed. The absorbed quanta in spin-electron resonance in excitons can correspond to an infrared frequency for some values of the quantity $|^0E_{nl} - {}^1E_{nl}|$. This is one of the different peculiarities of exciton spin-resonance absorption. Another property of it is, according to Deigen and Pekar[19] the narrowness of the spin-resonance absorption band.

The exciton model considered by us can be generalized both for the case of an exciton in elemental semiconductors and dielectrics and, in particular, for the case of a delta-function form of the function $\varphi_\nu(\mathbf{G}-\mathbf{H})$, that is, for a Frenkel exciton. One needs only let the position vector of the electron $\mathbf{G}$ take on the same values as the position vector of the hole $\mathbf{H}$. The atomic functions in the case $\mathbf{G} = \mathbf{H}$ will then be different from the case of differing $\mathbf{G}$ and $\mathbf{H}$.

APPENDIX 1

EXPANSION OF $E(-i\nabla)$ IN POWERS OF $i\nabla$

The behavior of $E_1(\mathbf{k})$ for lattices with identical ions with a face centered cubic cell of edge length $D = 2d$ and an extremum at $\mathbf{k} = 0$ is given in reference 20. Apart from a constant it has for small k the form

$$E_1(\mathbf{k}) = \frac{\hbar^2k^2}{2\mu_1} - \frac{\hbar^2d^2}{16\mu_1}k^4 + \frac{\hbar^2d^2}{48\mu_1}(k_x^4 + k_y^4 + k_z^4). \quad (1.1)$$

We shall approximate by replacing the cubically symmetric expression by a spherically symmetric one. We perform a similar operation for the expression $E_2(k)$ for a body-centered cubic lattice[20] and replacing k by $-i\nabla$ we get, apart from a constant

$$E_1(-i\nabla) - E_2(-i\nabla) = -\frac{\hbar^2}{2\mu}\nabla^2 - \frac{\hbar^2 d^2}{c\mu}\nabla^4, \quad (1.2)$$

where

$$c = \frac{40(\mu_1+\mu_2)}{2\mu_2+3\mu_1}, \quad \frac{1}{\mu} = \frac{1}{\mu_1} + \frac{1}{\mu_2},$$

and μ is the reduced effective exciton mass.

APPENDIX 2

EVALUATION OF THE COULOMB AND EXCHANGE INTEGRALS

With the aid of functions of the type

$$\Theta_G(q) = \frac{\alpha^{3/2}}{\sqrt{\pi}} e^{-\alpha|q-G|}; \qquad \Theta_H(q) = \frac{\beta^{3/2}}{\sqrt{\pi}} e^{-\beta|q-H|} \quad (2.1)$$

we can write down the Coulomb and exchange integrals. The exchange integral $A(r)$ can be estimated by Hellmann's method[21]

$$A(r) = \frac{\alpha^3\beta^3}{\pi^2}\int \frac{1}{q_{12}} \exp\{-\alpha|q_1-G| - \beta|q_1-H| - \alpha|q_2-G| - \beta|q_2-H|\} dq_1 dq_2 \approx \frac{\alpha^3\beta^3}{\pi^2}\eta_1(r)\int\left[\frac{1}{|q_1-G|} + \frac{1}{|q_1-H|}\right]$$

$$\times \exp\{-\alpha|q_1-G| - \beta|q_1-H| - \alpha|q_2-G| - \beta|q_2-H|\}\, dq_1\, dq_2, \quad (2.2)$$

with only one difference, namely that we use for $\eta(r)$ a different analytical expression which is more convenient for the integration:

$$\eta_1(r) = \frac{5}{8}\{1 - 0.5\exp[-0.11(\beta+0.4\alpha)r]\}, \quad (2.3)$$

where

$$r = |G-H| \text{ and } \beta > \alpha.$$

Using the expressions for the two-center integrals[21] we find

$$K(r) - 2A(r) = \frac{1}{r} + e^{-2\alpha r}\sum_{n=0}^{n=2}\frac{A_n}{r^n} + e^{-2\beta r}\sum_{n=0}^{n=2}\frac{B_n}{r^n} + e^{-(\alpha+\beta)r}\sum_{n=0}^{n=2}\frac{C_n}{r^n} + e^{-2\alpha' r}\sum_{n=0}^{n=2}\frac{A'_n}{r^n} + e^{-2\beta' r}\sum_{n=0}^{n=2}\frac{B'_n}{r^n} + e^{-(\alpha'+\beta')r}\sum_{n=0}^{n=2}\frac{C'_n}{r^n}, \quad (2.4)$$

where

$$A_0 = -\frac{\alpha\beta^4}{(\beta^2-\alpha^2)^2} - \frac{40\alpha^3\beta^4}{(\beta^2-\alpha^2)^3}; \qquad A'_0 = \frac{20\alpha^3\beta^4}{(\beta^2-\alpha^2)^3};$$

$$B_0 = -\frac{\alpha^4\beta}{(\beta^2-\alpha^2)^2} + \frac{40\alpha^4\beta^3}{(\beta^2-\alpha^2)^3}; \qquad B'_0 = -\frac{20\alpha^4\beta^3}{(\beta^2-\alpha^2)^3};$$

$$C_0 = \frac{40\alpha^3\beta^3(\beta-\alpha)}{(\beta^2-\alpha^2)^3}; \qquad C'_0 = -\frac{20\alpha^3\beta^3(\beta-\alpha)}{(\beta^2-\alpha^2)^3};$$

$$A_1 = -\frac{(\beta^6 - 3\alpha^2\beta^4)}{(\beta^2-\alpha^2)^3} + \frac{80\alpha^3\beta^3(3\alpha\beta-\beta^2)}{(\beta^2-\alpha^2)^4}; \quad (2.5)$$

$$B_1 = -\frac{(3\alpha^4\beta^2 - \alpha^6)}{(\beta^2-\alpha^2)^3} + \frac{80\alpha^3\beta^3(3\alpha\beta-\alpha^2)}{(\beta^2-\alpha^2)^4};$$

$$C_1 = -\frac{80\alpha^3\beta^3[4\alpha\beta-(\beta-\alpha)^2]}{(\beta^2-\alpha^2)^4};$$

$$A'_1 = -\frac{40\alpha^3\beta^3(3\alpha-\beta^2)}{(\beta^2-\alpha^2)^4}; \qquad B'_1 = -\frac{40\alpha^3\beta^3(3\alpha\beta-\alpha^2)}{(\beta^2-\alpha^2)^4};$$

$$C'_1 = \frac{40\alpha^3\beta^3[4\alpha\beta-(\beta-\alpha)^2]}{(\beta^2-\alpha^2)^4};$$

$$A_2 = B_2 = -\frac{C_2}{2} = \frac{320\alpha^4\beta^4(\beta-\alpha)}{(\beta^2-\alpha^2)^5};$$

$$A'_2 = B'_2 = -\frac{C'_2}{2} = \frac{160\alpha^4\beta^4(\beta-\alpha)}{(\beta^2-\alpha^2)^5};$$

$$2\alpha' = 2\alpha + \delta, \quad 2\beta' = 2\beta + \delta, \quad \delta = 0.11(\beta + 0{,}4\alpha).$$

In evaluating the value of the potential (33) averaged over the functions (34) one comes across integrals of the following form:

$$x^3\int_0^\infty R^2_{nl}(xr/na)\, r^\rho e^{-\gamma r} r^2\, dr = J^{\rho,\gamma}_{nl,nl}(x).$$

They are given in a paper by Alder and Winther:[22]

$$J^{\rho,\gamma}_{nl,nl}(x) = \frac{4(n+l)!\,(2l+p+2)!\,x^{2l+3}\gamma^{2l}}{|(2l+1)!|^2 n^{4+2l}(n-l-1)!\,\gamma^\rho(\gamma a)^{2l+3}}$$

$$\times F_2\left(2l+p+3,\ l+1+n,\ l+1-n,\right. \quad (2.6)$$

$$\left. 2l+2,\ 2l+2,\ -\frac{2x}{na\gamma},\ \frac{2x}{na\gamma}\right),$$

where F_2 is the generalized hypergeometric function with a circle of convergence $4x/\gamma na \le 1$. The average value of $^SV(r)$ is, according to (34) and (2.6), equal to

$$-\frac{e^2}{2an_0^2}[2x_S + {}^SL(x_S|nl)], \quad (2.7)$$

where

$${}^SL(x_S|nl) = 2an^2\left[\sum_{k=1}^{k=2} V^S_k J^{0,\gamma^S_k}_{nl,nl} + V^S_3 J^{-1,\gamma^S_3}_{nl,nl}\right]$$

$$= \frac{8(n+l)!\,2^{2l}x_S^{2l+3}}{n^{2l+2}(2l+1)!\,(n-l-1)!\,a^{4l+2}}\left\{(2l+2)\sum_{k=1}^{k=2}\frac{V^S_k}{(\gamma^S_k)^{2l+3}}\right.$$

$$\times F_2\left(2l+3,\ l+1+n,\ l+1-n,\right.$$

$$\left. 2l+2,\ 2l+2,\ -\frac{2x_S}{na\gamma^S_k},\ \frac{2x_S}{na\gamma^S_k}\right) \quad (2.8)$$

$$+\frac{V^S_3}{(\gamma^S_3)^{2l+2}}F_2(2l+2,\ l+1+n,\ l+1-n,$$

$$\left. 2l+2,\ 2l+2,\ -\frac{2x_S}{na\gamma^S_3},\ \frac{2x_S}{na\gamma^S_3}\right)\Big\}.$$

Since the functions (34) are the solutions of the hydrogen problem, the average values of the operators $(-\hbar^2/2\mu)\nabla^2$ and $(-\hbar^2 d^2/\mu c)\nabla^4$ are respectively equal to

$$\frac{e^2 x_S^2}{2an_0^2 n^2} \text{ and } -\frac{8}{c}\left(\frac{d}{a}\right)^2 \frac{e^2}{2an_0^2 n^3}\left[\frac{1}{l+1/2}-\frac{3}{4n}\right] x_S^4. \quad (2.9)$$

[1] G. H. Wannier, Phys. Rev. **52**, 191 (1937).

[2] I. M. Dykman and S. I. Pekar, Тр. ИФАН УССР (Transactions of the Institute of Physics, Academy of Sciences, Ukrainian S.S.R.) No. 3, 92 (1952).

[3] I. M. Dykman, Тр. ИФАН УССР (Transactions of the Institute of Physics, Academy of Sciences, Ukrainian S.S.R.) No. 5, 48 (1954).

[4] A. G. Samoilovich and L. L. Korenblit, Usp. Fiz. Nauk, **60**, No. 2 (1956).

[5] K. B. Tolpygo, Doctoral thesis, Kiev (1958).

[6] T. Muto and H. Okuno, J. Phys. Soc. Japan 11, 633 (1956).

[7] S. A. Moskalenko, Уч. зап. Кишиневского гос. ун-та (Sci. Notes, Kishinev State University) **17**, 103 (1955).

[8] G. Dresselhaus, J. Phys. Chem. Solids 1, 14 (1956).

[9] S. A. Moskalenko, Оптика и спектроскопия (Optics and Spectroscopy) **5**, 147 (1958).

[10] A. Overhauser, Phys. Rev. **101**, 1702 (1956).

[11] Y. Takeuti, Progr. Theoret. Phys. **18**, 421 (1957).

[12] W. Kohn, Phys. Rev. **105**, 509 (1957).

[13] T. I. Liberberg-Kucher, J. Exptl. Theoret. Phys. (U.S.S.R.) **30**, 724 (1956), Soviet Phys. JETP **3**, 580 (1956).

[14] A. G. Zhilich, Вестн. ЛГУ (Bulletin Leningrad State University) **4**, 31 (1957).

[15] P. P. Pavinskii and A. G. Zhilich, Вестн. ЛГУ (Bulletin, Leningrad State University) **4**, 50 (1957).

[16] Eyring, Walter, and Kimball, Quantum Chemistry (Russ. Transl.) GIIL, M. 1954, p. 218.

[17] E. F. Gross, Usp. Fiz. Nauk **63**, 575 (1957).

[18] Gross, Zakharchenya, and Reĭnov, Dokl. Akad. Nauk SSSR **99**, 231 (1954).

[19] M. F. Deĭgen and S. I. Pekar, J. Exptl. Theoret. Phys. (U.S.S.R.) **34**, 684 (1958), Soviet Phys. JETP **7**, 471 (1958).

[20] K. B. Tolpygo, J. Exptl. Theoret. Phys. (U.S.S.R.) **21**, 443 (1951).

[21] H. Hellmann, Einführung in die Quantenchemie (Russ. Transl.) ONTI 1937, p. 516.

[22] K. Alder and A. Winther, Kg. Danske Videnskab. Selskab, Mat.-fys. Medd. **29**, Nr 18 (1955).

Translated by D. Ter Haar
21

EFFECTS OF A RESONANT PION-PION INTERACTION IN FERMI'S STATISTICAL THEORY OF MULTIPLE PARTICLE PRODUCTION

V. I. RUS' KIN

Nuclear Physics Institute, Academy of Sciences of the Kazakh S.S.R.

Submitted to JETP editor June 14, 1958

J. Exptl. Theoret. Phys. (U.S.S.R.) **36**, 164-168 (January, 1959)

The statistical theory of Fermi is applied to π^--p scattering at 4.5 Bev, including effects of a possible resonant interaction between two pions. Production of strange particles is also included. The results are compared with experiment.

SEVERAL authors[1-4] have suggested that two pions have a resonant interaction. In a statistical theory, the effect of such a resonant interaction can be consistently included by treating the resonant state as a virtual particle.[5,6]

Nikishov[7] made a calculation along these lines, treating the resonant pion-nucleon interaction as an "isobar" effect, and thereby improved the agreement between the theory and experiment.* However, the ratio of strange-particle production to pion production remained considerably too high.[6] To be consistent, one should also include effects of a possible pion-pion resonance.

At present there are no direct experiments on pion-pion scattering, and it is hard to imagine such experiments being done in the near future. But indirect evidence can be used. For example, we see from the work of Dyson[1] and Takeda[2] that the second

TABLE I. Charge distribution of the products of $\pi^- - p$ collisions for processes involving K-particle and hyperon production

Type of process	Charge state	Statistical weight of the charge state	Type of process	Charge state	Statistical weight of the charge state
$\Lambda\Theta$	$\Lambda^0\Theta^0$	1.000	$\Sigma K1$	$\Sigma^0K^+\pi^-$	0.189
	Σ^-K^+	0.555		$\Sigma^-K^+\pi^0$	0.189
ΣK	$\Sigma^0\Theta^0$	0.445		$\Sigma^0\Theta^0\Pi^0$	0.211
	$\Lambda^0\Theta^0\pi^0$	0.445	$\Sigma K\Pi$	$\Sigma^+\Theta^0\Pi^-$	0.233
$\Lambda\Theta1$	$\Lambda^0K^+\pi^-$	0.555	Takeda	$\Sigma^-\Theta^0\Pi^+$	0.178
				$\Sigma^0K^+\Pi^-$	0.189
$\Lambda\Theta\Pi$	$\Lambda^0\Theta^0\Pi^0$	0.445		$\Sigma^-K^+\Pi^0$	0.189
Takeda	$\Lambda^0K^+\Pi^-$	0.555	$\Sigma K\Pi$	$\Sigma^-\Theta^0\Pi^0$	0.445
$\Lambda\Theta\Pi$	$\Lambda^0\Theta^0\Pi_0$	1.000	Dyson	$\Sigma^-K^+\Pi^0$	0.555
Dyson				$N\Theta^0\bar{\Theta}^0$	0.278
	$\Sigma^0\Theta^0\pi^0$	0.211	$NK\bar{K}$	$N\bar{K}^+K^-$	0.278
$\Sigma K1$	$\Sigma^+\Theta^0\pi^-$	0.233		$P\bar{K}^-\Theta^0$	0.444
	$\Sigma^-\Theta^0\pi^+$	0.178	ΞKK	$\Xi^-K^+\Theta^0$	1.000

TABLE II. Statistical weights of $\pi^- - p$ collision processes at 4.5 Bev.

Number of secondary mesons		0	1			2				3					4					Strange particles							
Type of process		$N1$	$N2$	$N'1$	$N\Pi$	$N3$	$N'2$	$N\Pi1$	$N'\Pi$	$N4$	$N'3$	$N'\Pi1$	$N\Pi2$	$N\Pi\Pi$	$N5$	$N'4$	$N'\Pi2$	$N'\Pi\Pi$	$N\Pi3$	$\Lambda\Theta$	$\Sigma\Theta$	$\Lambda\Theta1$	$\Lambda\Theta\Pi$	$\Sigma K1$	$\Sigma K\Pi$	ΞKK	$NK\bar{K}$
Statistical weight	Takeda version	0	3	1	0	5	5	6	1	2	6	13	14	2	0	2	17	3	9	0	0	2	1	4	3	0	1
	Dyson version	1	5	1	0	7	8	5	0	4	9	9	10	1	1	3	11	1	6	0	1	3	2	6	4	0	2

*There seems to be an error in the calculation of the frequency of stars with various numbers of prongs in reference 7. The relative probabilities for elastic non-diffractive scattering, 2-prong, 4-prong and 6-prong stars should be respectively 0.75, 45, 28.5, and 0.75 instead of 1, 49, 24.5, and 0.5.

TABLE III. Charge distribution of $\pi^- - p$ collision products, including effects of Π-particle production

Type reaction	Reaction products	Statistical weights of charge states	
		Dyson version	Takeda version
$N'\Pi$	$P + - -$	0.222	0.081
	$P - 00$	0.111	0.193
	$N + - 0$	0.445	0.726
	$N\,000$	0.222	—
$N\Pi1$	$P + - -$	0.371	0.189
	$P - 00$	0.185	0.189
	$N + - 0$	0.296	0.622
	$N\,000$	0.148	—
$N\Pi\Pi$	$P + - - 0$	—	0.378
	$N + + - -$	0.444	0.155
	$N + - 00$	0.445	0.467
	$N\,0000$	0.111	—
$N'\Pi1$	$P + - - 0$	0.183	0.355
	$P - 000$	0.092	0.071
	$N + + - -$	0.375	0.181
	$N + - 00$	0.296	0.393
	$N\,0000$	0.054	—
$N\Pi2$	$P + - - 0$	0.252	0.465
	$P - 000$	0.126	0.074
	$N + + - -$	0.311	0.130
	$N + - 00$	0.259	0.331
	$N\,0000$	0.052	—
$N'\Pi\Pi$	$P + + - - -$	0.148	0.032
	$P + - - 00$	0.148	0.395
	$P - 0000$	0.037	—
	$N + + - - 0$	0.296	0.425
	$N + - 000$	0.296	0.148
	$N\,00\,000$	0.075	—
$N'\Pi2$	$P + + - - -$	0.173	0.096
	$P + - - 00$	0.201	0.324
	$P - 0000$	0.054	0.025
	$N + + - - 0$	0.339	0.364
	$N + - 000$	0.212	0.191
	$N\,00000$	0.021	—
$N\Pi3$	$P + + - - -$	0.144	0.057
	$P + - - 00$	0.180	0.306
	$P - 0\,000$	0.054	0.015
	$N + + - - 0$	0.385	0.428
	$N + - 000$	0.222	0.194
	$N\,00\,000$	0.015	—

maximum in the $\pi^- - p$ scattering around 1 Bev might be explained by a resonant interaction between two pions. Using the Fermi statistical theory, we can handle such an interaction by supposing that a new "virtual particle" Π is being produced, having mass $\mu = 0.47$,* ordinary spin $S = 0$ and isotopic spin $T = 0$[1] or $T = 1$.[2]

By comparing the results of the theory with experiment, we can find out which of the two isotopic spin values is more correct, within the limits of the statistical model.† We calculate here the effect of the pion-pion interaction on π^--p scattering at 4.5 Bev.

We take the statistical weights from the formula

$$s(n) = [\Omega/(2\pi)^3]^{n-1}\, dQ(E)/dE,\quad \Omega = \Omega_0/\gamma_2',\quad \Omega_0 = {}^4/_3\pi R_0^3.$$

Here $R_0 = 1.4 \times 10^{-13}$ cm is the pion Compton wavelength, and γ_2' is the nucleon energy in the π-p center-of-mass system. In all cases the statistical weights are calculated with conservation of energy, momentum, spin, isotopic spin and its components, and identity of particles. In the case of strange particles, we also take into account the conservation of strangeness.

The calculations for two and three particles were made with the exact formulae of reference 6. For four and five particles, we made the approximation of treating the nucleons and nucleon-isobars non-relativistically, the pions and the Π-particles ultra-relativistically. We neglected processes in which more than four secondary pions are produced, such processes being certainly unimportant at these energies.

In calculating the production of K-particles and hyperons, we assumed the K-particles to have spin zero, the hyperons to have spin ½. At 4.5 Bev, allowing for the conservation of strangeness, only the following processes are energetically possible: $\Lambda\Theta$, $\Sigma\Theta$, $\Lambda\Theta 1$, $\Sigma\Theta 1$, $\Lambda\Theta\Pi$, $\Sigma\Theta\Pi$, $\Xi\Theta\Theta$, $N\Theta\tilde{\Theta}$. Table I enumerates the charge-states arising from these processes.

Table II shows the statistical weights of the various processes. To compare the theoretical results with experiment, the charge-distribution of all the reaction products was calculated (Tables I and III). The charge-distribution of the products of $\pi^- - p$ collisions, assuming only pions and isobars to be produced, is shown in Table II of reference 6. In our calculations we have assumed[6] that the isobar,

TABLE IV. Distribution by prong-number of charged products of $\pi^- - p$ collisions, normalized to 100%

Type of collision	Experiment	Statistical Theory			
		Including isobars only*	Including isobars and strange particles only	Takeda version**	Dyson version**
2-prong inelastic	60	61	72	48	51
4-prong inelastic	38	38	27	49	45
6-prong inelastic	2	1	1	3	3

*Corrected value, see first footnote of text.

**The Dyson and Takeda versions are calculated including isobars, strange particles and Π-particles, the latter possessing isotopic spin 0 according to Dyson, 1 according to Takeda.

*We use units such that $\hbar = c = M_{nucl} = 1$.

†This kind of treatment of a resonant interaction is also interesting, because it allows us indirectly to incorporate into the statistical theory the effects of a matrix element H'_{if} in the expression $W_{i\to f} = \frac{2\pi}{\hbar}|H'_{if}|^2\rho_E$. In the original Fermi theory such matrix elements were neglected.

which can have the T_z component of its isotopic spin equal to $\pm 3/2$ or $\pm 1/2$, decays from the state with $T_z = 3/2$ into $p\pi^+$; from the state $T_z = -3/2$ into $N\pi^-$; from the state $T_z = 1/2$ with probability $2/3$ into $p\pi^0$ and with probability $1/3$ into $N\pi^+$; from the state $T_z = -1/2$ with probability $1/3$ into $p\pi^-$ and with probability $2/3$ into $N\pi^0$. In the theory of Takeda ($T_\Pi = 1$), the Π-particle has three states with $T_z = \pm 1, 0$. It decays from the state $T_z = +1$ into $\pi^+\pi^0$; from the state $T_z = -1$ into $\pi^-\pi^0$; from the state $T_z = 0$ into $\pi^+\pi^-$. In the Dyson theory ($T_\Pi = 0$) the Π-particle has only one state $T_z = 0$, and decays with probability $2/3$ into $\pi^+\pi^-$, with probability $1/3$ into $\pi^0\pi^0$.

For the comparison with experiment we have used references 8 and 9. Reference 9 concerns π^--p scattering at 5 Bev, but the experimental results at this energy differ very little from the results at 4.5 Bev.

Table IV shows the distribution of the reaction products according to the number of prongs, calculated from Tables I to III. Comparison of these numbers with experiment shows that the number of two-prong stars is too small, especially in the Takeda theory. However, the Dyson theory gives better agreement than a calculation including only isobars and strange particles. It should also be remembered that the reaction $\Lambda\Theta 2$ will make some contribution to the statistical weights, and this will increase the number of two-prong stars.

The ratio between strange particles and observable pions is 0.08 to 0.09 in Takeda's theory, 0.14 in Dyson's theory, and 0.3 to 0.4 in the theory which includes only isobars. The experimental value of this ratio[9] is 0.04 to 0.05.

The average multiplicity is 2.7 in Takeda's theory, 2.4 in Dyson's theory and 2.3 ± 0.1 experimentally.[9]

From these results we draw the following conclusions:

1. The statistical theory, including only isobars, K-particles and hyperons, disagrees significantly with experiment, both in the distribution of numbers of prongs (Table IV) and in the ratio of strange particles to pions.

2. When a resonant pion-pion interaction, or Π-particle, is included in the statistical theory in addition to the isobar, the agreement with experiment is much improved so far as K-particle and hyperon production is concerned.

3. The Dyson theory agrees with experiment better than the Takeda theory, although there are some discrepancies in both cases. Such discrepancies are to be expected, since our calculations have ignored the conservation of angular momentum.

In conclusion, it is my pleasant duty to thank Professor Zh. S. Takibaev and his collaborators P. A. Usik and Ya. M. Granovskii for valuable advice and help, and A. Akhmedshin for his assistance with the calculations.

Note added in proof (October 15, 1958). After this paper was submitted for publication, we learned of the work of R. Gatto and M. A. Ruderman [Nuovo cimento **8**, 775 (1958)], in which a similar treatment of a resonant pion-pion interaction is used in a calculation of proton-antiproton annihilation.

[1] F. J. Dyson, Phys. Rev. **99**, 1037 (1955).

[2] G. Takeda, Phys. Rev. **100**, 440 (1955).

[3] A. N. Mitra and R. P. Saxena, Phys. Rev. **108**, 1083 (1957).

[4] J. S. Kovacs, Phys. Rev. **101**, 397 (1956).

[5] S. Z. Belen'kiĭ, Nucl. Phys. **2**, 259 (1956); G. Uhlenbeck and H. A. Bethe, Physica, **3**, 729 (1936) and **4**, 195 (1937).

[6] Belen'kiĭ, Maksimenko, Nikishov, and Rozental', Usp. Fiz. Nauk, **62**, 1 (1959).

[7] A. I. Nikishov, J. Exptl. Theoret. Phys. (U.S.S.R.) **30**, 990 (1956), Soviet Phys. JETP **3**, 783 (1956).

[8] Maenchen, Powell, Saphir, and Wright, Phys. Rev. **99**, 1619 (1955).

[9] Maenchen, Fowler, Powell, and Wright, Phys. Rev. **108**, 850 (1957).

Translated by F. J. Dyson
22

A SYSTEM OF MAGNETIC MOMENTS IN A WEAK VARIABLE MAGNETIC FIELD

G. V. SKROTSKII and A. A. KOKIN

Ural Polytechnical Institute

Submitted to JETP editor June 23, 1958

J. Exptl. Theoret. Phys. (U.S.S.R.) **36**, 169-175 (January, 1959)

A study is made of a system of magnetic moments subject to electric exchange and weak magnetic dipole-dipole interactions and situated in an external magnetic field $\mathbf{H}_0 + \mathbf{h}(t)$. Equations of motion for the magnetization vector are obtained up to terms of second order perturbation theory[5] and for weak variable fields $\mathbf{h}(t) \ll \mathbf{H}_0$. The limits of applicability of the equations obtained are discussed.

1. The microscopic theory of the behavior of nuclear magnetization in an external magnetic field has been developed in the paper by Wangsness and Bloch.[1] In that paper it was assumed that nuclear magnetic moments interact weakly with their molecular surroundings which are regarded as a heat reservoir.

In the cases when the nuclear spins are $I \leq 1$ the equation of motion in weak variable fields has the form:

$$d\mathbf{M}/dt + (\mathbf{i}M_x + \mathbf{j}M_y)/T_\perp + \mathbf{k}(M_z - M_0)/T_\parallel = \gamma[\mathbf{M}\times\mathbf{H}]. \quad (1)$$

For values of spin $I > 1$, Eqs. (1) are valid only in sufficiently weak constant fields H_0. In subsequent papers[2,3] Bloch took into account the direct and the indirect interactions of the nuclei and has investigated strong variable circularly polarized fields. The theory developed in references 1 – 3 in principle allows one to compute the relaxation times $T_\perp$ and $T_\parallel$ occurring in (1).

Bloch's equations have been widely used to describe the behavior not only of a system of nuclear magnetic moments but also of electronic magnetic moments in an external field. The phenomenon of ferromagnetic resonance in strong radio-frequency fields is also often discussed on the basis of the system of equations (1).[4]

Experimental data on the observation of relaxation and resonance phenomena in paramagnetic and ferromagnetic substances are analyzed on the basis of Bloch's equations; in such an analysis the relaxation times $T_\perp$ and $T_\parallel$ are obtained. However, the computation of these relaxation times is carried out on the basis of assumptions which are frequently different from those utilized in the derivation of equations (1). Therefore a comparison with experiment of the theoretically calculated values of $T_\perp$ and $T_\parallel$ based on the application of Bloch's equations is not consistent.

A more consistent method consists of finding the variation of magnetization with time (equation of motion) starting with a given form of the Hamiltonian, and of finding the coefficients appearing in these equations.

Kubo and Tomita[5] have developed a quite general and flexible method for determining the line shape of magnetic resonance absorption in radio-frequency fields. This method is more convenient than the method of Wangsness and Bloch for the description both of nuclear and of electronic magnetic resonance and relaxation. It was successfully applied to the study of line shape in nuclear and electronic resonance in a weak constant field ($\hbar\omega_0 \ll kT$).[6-8]

In this paper we obtain with the aid of the method of Kubo and Tomita the equation of motion for the magnetization vector of a system of magnetic moments coupled by electric exchange and weak magnetic dipole-dipole interactions. The coefficients occurring in these equations may be calculated in specific cases.

2. The expression for the components of the magnetization vector

$$\mathbf{M}(t) = \mathrm{Sp}\,\hat{\rho}(t)\,\hat{\mathbf{M}} \quad (2)$$

is determined by the density operator $\hat{\rho}(t)$ which obeys the equation of motion:

$$i\hbar\dot{\hat{\rho}}(t) = \hat{\mathcal{H}}(t)\,\hat{\rho}(t) - \hat{\rho}(t)\,\hat{\mathcal{H}}(t), \quad (3)$$

where

$$\hat{\mathcal{H}}(t) = \hat{\mathcal{H}} - \hat{\mathbf{M}}\cdot\mathbf{h}(t), \quad \hat{\mathbf{M}} = g\mu_0\sum_j \hat{\mathbf{I}}_j, \quad (4)$$

and $\mathbf{h}(t)$ is a variable radio-frequency field which is assumed to be weak, $\mathbf{h}(t) \ll \mathbf{H}_0$.

Following Kubo and Tomita[5] we write the time-independent part of the Hamiltonian $\hat{\mathcal{H}}$ in the form

$$\hat{\mathcal{H}} = \hat{\mathcal{H}}_1 + \hat{\mathcal{H}}_2 + \hat{\mathcal{H}}', \tag{5}$$

in such a way that

$$[\hat{\mathcal{H}}_2, \hat{\mathbf{M}}] = [\hat{\mathcal{H}}_1, \hat{\mathcal{H}}_2] = 0. \tag{6}$$

In order to do this we assume that $\hat{\mathcal{H}}_2$ contains, in addition to terms which do not depend on the spins $\hat{\mathbf{I}}_j$, other terms that describe electric exchange interactions, while the operator

$$\hat{\mathcal{H}}_1 = -\hbar\omega_0 \sum_j \hat{\mathbf{I}}_{jz}, \quad \hbar\omega_0 = g\mu_0 H_0 \tag{7}$$

determines the interaction of the magnetic moments with the external constant field $H_0 = H_z$.

The operator

$$\hat{\mathcal{H}}' = g^2\mu_0^2 \sum_{j>k} r_{jk}^{-3} (\hat{\mathbf{I}}_j \hat{\mathbf{I}}_k - 3(\hat{\mathbf{I}}_j \mathbf{r}_{jk})(\hat{\mathbf{I}}_k \mathbf{r}_{jk}) / r_{jk}^2) \tag{8}$$

is regarded as a perturbation.

To solve the equation of motion (3) we set

$$\hat{\rho}(t) = \exp(-i\hat{\mathcal{H}}t/\hbar)\,\hat{\rho}'(t)\exp(i\hat{\mathcal{H}}t/\hbar). \tag{9}$$

Then in the new representation we shall have for $\hat{\rho}'(t)$

$$i\hbar\dot{\hat{\rho}}' = [\hat{\rho}'(t), \hat{\mathbf{M}}(t)]\,\mathbf{h}(t), \tag{10}$$

where

$$\hat{\mathbf{M}}(t) = \exp(i\hat{\mathcal{H}}t/\hbar)\,\hat{\mathbf{M}}\exp(-i\hat{\mathcal{H}}t/\hbar). \tag{11}$$

On integrating (10) by the method of successive approximations we obtain, up to terms linear in $\mathbf{h}(t)$,

$$\hat{\rho}'(t) = \hat{\rho}'(-\infty) + \frac{1}{i\hbar}\int_{-\infty}^{t} [\hat{\rho}'(-\infty), \hat{\mathbf{M}}(t')]\,\mathbf{h}(t')\,dt'. \tag{12}$$

Further, in the same approximation we obtain from (9)

$$\hat{\rho}(t) = \hat{\rho}_0 + \frac{1}{i\hbar}\int_{-\infty}^{t} [\hat{\rho}_0, \hat{\mathbf{M}}(t'-t)]\,\mathbf{h}(t')\,dt', \tag{13}$$

where

$$\hat{\rho}_0 = \exp\{(F - \hat{\mathcal{H}})/kT\} \tag{14}$$

is the equilibrium density operator in the absence of the radio-frequency field $\mathbf{h}(t)$ which is switched on at $t = -\infty$.

We introduce the following notation:

$$\begin{aligned} \hat{M}_{-1} &= \mp(\hat{M}_x \pm i\hat{M}_y)/\sqrt{2}, \quad \hat{M}_0 = \hat{M}_z, \\ h_{-1} &= \mp(h_x \pm ih_y)/\sqrt{2}, \qquad h_0 = h_z, \end{aligned} \tag{15}$$

then

$$\hat{\mathbf{M}}\cdot\mathbf{h}(t) = \sum_\alpha (-1)^\alpha \hat{M}_\alpha h_{-\alpha} = \sum_\alpha \hat{M}_\alpha h_\alpha^*,$$

where $\alpha = 0, \pm 1$.

Now by using (13) expression (2) can be written in terms of its components

$$M_\alpha(t) = M_{0\alpha} + \sum_\beta \int_{-\infty}^{t} \frac{i}{\hbar}\,\mathrm{Sp}\,\hat{\rho}_0 [\hat{M}_\alpha(t-t'), M_\beta]\,h_\beta^*(t')\,dt', \tag{16}$$

where

$$M_{0\alpha} = \mathrm{Sp}\,\hat{\rho}_0 \hat{M}_\alpha \delta_{\alpha 0},$$

and where we have taken into account the fact that

$$\mathrm{Sp}\,[\hat{\rho}_0, \hat{M}_\beta(t'-t)]\,\hat{M}_\alpha = -\mathrm{Sp}\,\hat{\rho}_0 [\hat{M}_\alpha(t-t'), \hat{M}_\beta]. \tag{17}$$

We introduce the tensor relaxation function

$$\begin{aligned} G_{\alpha\beta}(\tau) = \mathrm{Sp}\,\hat{\rho}_0 \int_0^{1/kT} \frac{1}{2}\{&M_\alpha(\tau - i\hbar\sigma)\,M_\beta \\ &+ M_\beta(-\tau - i\hbar\sigma)\,M_\alpha\}\,d\sigma - \frac{1}{kT} M_{0\alpha} M_{0\beta}, \end{aligned} \tag{18}$$

which, as can be easily seen, satisfies the following relations

$$G_{\alpha\beta}(\tau) = G_{\beta\alpha}(-\tau), \tag{19}$$

$$-dG_{\alpha\beta}(\tau)/d\tau = (i/\hbar)\,\mathrm{Sp}\,\hat{\rho}_0 [\hat{M}_\alpha(\tau), \hat{M}_\beta]. \tag{20}$$

By noting that at $\tau = t - t'$ the right-hand side of the expression coincides with the integrand in (16), we obtain

$$M_\alpha(t) - M_{0\alpha} = -\sum_\beta \int_0^\infty \frac{d}{d\tau} G_{\alpha\beta}(\tau)\, h_\beta^*(t-\tau)\,d\tau. \tag{21}$$

Thus, to calculate the components of the magnetization $M_\alpha(t)$ it is enough to find the components of the tensor $G_{\alpha\beta}(\tau)$.

3. To calculate the components of the tensor $G_{\alpha\beta}(\tau)$ we shall write the expression for the operator $\hat{M}_\alpha(t)$ occurring in it in the form of the following expansion:

$$\begin{aligned} \hat{M}_\alpha(t) = \hat{M}_\alpha^0(t) &+ (1/i\hbar)\int_0^t [\hat{M}_\alpha^0(t_1), \hat{\mathcal{H}}'(t_1)]\,dt_1 \\ &+ (i\hbar)^{-2}\int_0^t dt_1 \int_0^{t_1} dt_2 [[\hat{M}_\alpha^0(t), \hat{\mathcal{H}}'(t_1)], \hat{\mathcal{H}}'(t_2)] + \ldots, \end{aligned} \tag{22}$$

where

$$\hat{M}_\alpha^0(t) = \exp(i\hat{\mathcal{H}}_0 t/\hbar)\,\hat{M}_\alpha \exp(-i\hat{\mathcal{H}}_0 t/\hbar), \tag{23}$$

$$\hat{\mathcal{H}}'(t) = \exp(i\hat{\mathcal{H}}_0 t/\hbar)\,\hat{\mathcal{H}}' \exp(-i\hat{\mathcal{H}}_0 t/\hbar). \tag{24}$$

Then

$$G_{\alpha\beta}(\tau) = G_{\alpha\beta}^{(0)}(\tau) + G_{\alpha\beta}^{(1)}(\tau) + G_{\alpha\beta}^{(2)}(\tau) + \ldots. \tag{25}$$

In the following we shall restrict ourselves to the approximation of second order in $\mathcal{H}'$.

We obtain for $G_{\alpha\beta}^{(0)}$:

$$\begin{aligned} G_{\alpha\beta}^{(0)} = \int_0^{1/kT} &\mathrm{Sp}\,\hat{\rho}_0 \frac{1}{2}\{\hat{M}_\alpha^0(\tau - i\hbar\sigma)\,\hat{M}_\beta \\ &+ \hat{M}_\beta^0(-\tau - i\hbar\sigma)\,\hat{M}_\alpha\}\,d\sigma - \frac{1}{kT} M_{0\alpha} M_{0\beta}. \end{aligned} \tag{26}$$

By utilizing (6), (7), (23), we obtain:

$$\hat{M}^0_\alpha(\tau - i\hbar\sigma) = \exp(-i\alpha\omega_0\tau - \alpha\hbar\omega_0\sigma)\,\hat{M}_\alpha. \quad (27)$$

Now by noting that $\mathrm{Sp}\,\hat{\rho}_0\hat{M}_\alpha\hat{M}_\beta = 0$ for $\alpha \neq -\beta$, we obtain

$$G^{(0)}_{\alpha\beta} = (-1)^\alpha \chi_\alpha \exp(-i\alpha\omega_0\tau)\,\delta_{\alpha,-\beta} - \frac{1}{kT} M^2_{0z}\,\delta_{\alpha 0}\,\delta_{\beta 0}, \quad (28)$$

where

$$\chi_\alpha = \mathrm{Sp}\,\hat{\rho}_0 |M_\alpha|^2 \sinh(\alpha\hbar\omega_0/kT)/\alpha\hbar\omega_0. \quad (29)$$

In the case of weak fields $\hbar\omega_0 \ll kT$ as a result of the isotropic nature of the operator (14) in spin space we have

$$\chi_{+1} = \chi_{-1} \equiv \chi_\perp = \chi_0 \equiv \chi_\parallel. \quad (30)$$

In strong fields, generally speaking, $\chi_\perp \neq \chi_\parallel$.

In the case of isotropic surroundings $G^{(1)}_{\alpha\beta} = 0$. This follows from the fact that $G^{(1)}_{\alpha\beta}$ contains only the first power of $\mathcal{H}'$.

For the computation of $G^{(2)}_{\alpha\beta}$ it is convenient to write the operator $\hat{\mathcal{H}}'$ in the form

$$\hat{\mathcal{H}}' = \sum_\lambda \sum_{j>k} \Phi^\lambda_{jk}\{jk\}_\lambda, \quad (31)$$

where

$$\{jk\}_{\pm 2} = 2\hat{I}_{j\pm 1}\hat{I}_{k\pm 1},$$
$$\{jk\}_{\pm 1} = \mp\sqrt{2}\,(\hat{I}_{j\pm 1}\hat{I}_{k0} + \hat{I}_{j0}\hat{I}_{k\pm 1}), \quad (32)$$
$$\{jk\}_0 = \hat{I}_{j0}\hat{I}_{k0} + {}^1/_2\,(\hat{I}_{j+1}\hat{I}_{k-1} + \hat{I}_{j-1}\hat{I}_{k+1});$$

$$\Phi^{\pm 2}_{jk} = -\sqrt{6\pi/5}\,g^2\mu_0^2 r_{jk}^{-3} Y_{2,\pm 2}(\vartheta_{jk}, \varphi_{jk}),$$
$$\Phi^{\pm 1}_{jk} = -\sqrt{6\pi/5}\,g^2\mu_0^2 r_{jk}^{-3} Y_{2,\pm 1}(\vartheta_{jk}, \varphi_{jk}), \quad (33)$$
$$\Phi^0_{jk} = -\sqrt{16\pi/5}\,g^2\mu_0^2 r_{jk}^{-3} Y_{2,0}(\vartheta_{jk}, \varphi_{jk}),$$

Y_{lm} is the normalized spherical harmonic, and

$$\hat{I}_{\pm 1} = \mp(\hat{I}_x \pm i\hat{I}_y)/\sqrt{2}, \quad \hat{I}_0 = \hat{I}_z. \quad (34)$$

By utilizing (6), (7) and (24) we obtain:

$$\hat{\mathcal{H}}'(t - i\hbar\sigma) = \sum_\lambda \exp(-i\lambda\omega_0 - \lambda\hbar\omega_0\sigma)\,\hat{\mathcal{H}}'_\lambda(t - i\hbar\sigma), \quad (35)$$

where

$$\hat{\mathcal{H}}'_\lambda(t - i\hbar\sigma) = \exp(i\hat{\mathcal{H}}_2 t/\hbar + \hat{\mathcal{H}}_2\sigma)\,\hat{\mathcal{H}}'_\lambda \exp(-i\hat{\mathcal{H}}_2 t/\hbar - \hat{\mathcal{H}}_2\sigma). \quad (36)$$

Now

$$G^{(2)}_{\alpha\beta}(\tau) = -\frac{1}{2\hbar^2}\int_0^{1/kT} d\sigma \exp(-i\alpha\omega_0\tau)\sum_{\lambda\lambda'}\int_0^\tau dt_1 \int_0^{t_1} dt_2$$
$$\times \exp(-i\lambda\omega_0 t_1 - i\lambda'\omega_0 t_2)\,\mathrm{Sp}\,\hat{\rho}_0 \{\exp(-(\alpha+\lambda+\lambda')\hbar\omega_0\sigma)$$
$$\times([[\hat{M}_\alpha, \hat{\mathcal{H}}'_\lambda(t_1 - i\hbar\sigma)], \hat{\mathcal{H}}'_{\lambda'}(t_2 - i\hbar\sigma)]\hat{M}^\beta)$$
$$+\exp((\alpha+\lambda+\lambda')\hbar\omega_0\sigma)$$
$$\times(\hat{M}_\beta [\hat{\mathcal{H}}'_{\lambda'}(t_2 + i\hbar\sigma), [\hat{\mathcal{H}}'_\lambda(t_1 + i\hbar\sigma), \hat{M}_\alpha]])\}. \quad (37)$$

The magnitude of the trace does not depend on the choice of the origin of time, since the trace is invariant with respect to a unitary transformation of an operator which follows the trace sign:

$$\exp(i\hat{\mathcal{H}}_0\Delta T/\hbar)\ldots\exp(-i\hat{\mathcal{H}}_0\Delta T/\hbar).$$

Therefore

$$\mathrm{Sp}\,\hat{\rho}_0([[\hat{M}_\alpha, \hat{\mathcal{H}}'_\lambda(t_1 - i\hbar\sigma)], \hat{\mathcal{H}}'_{\lambda'}(t_2 - i\hbar\sigma)]\hat{M}_\beta)$$
$$= \exp(-i(\alpha+\lambda+\lambda'+\beta)\omega_0\Delta T)$$
$$\times \mathrm{Sp}\,\hat{\rho}_0([[\hat{M}_\alpha, \hat{\mathcal{H}}'_\lambda(t_1 - i\hbar\sigma)], \hat{\mathcal{H}}'_{\lambda'}(t_2 - i\hbar\sigma)]\hat{M}_\beta),$$

from which we obtain

$$\alpha + \lambda + \lambda' + \beta = 0. \quad (38)$$

Since expression (31) for $\hat{\mathcal{H}}'$ contains spherical harmonics, only the terms with $\lambda = -\lambda'$ differ from zero in averaging at $t_1 = t_2$ in the case of isotropic surroundings. For $t_1 \neq t_2$ the terms with $\lambda = -\lambda'$ give the principal contribution to (37). Therefore, in accordance with (38) we may set $\alpha = -\beta$.

We then have:

$$G^{(2)}_{\alpha\beta}(\tau) = -\frac{1}{2\hbar^2}\int_0^{1/kT} d\sigma \exp(-i\alpha\omega_0\tau)\sum_\lambda\int_0^\tau d\vartheta\,(\tau - \vartheta)\exp(i\lambda\omega_0\vartheta)$$
$$\times \mathrm{Sp}\,\hat{\rho}_0\{\exp(-\alpha\hbar\omega_0\sigma)[[\hat{M}_\alpha, \hat{\mathcal{H}}'_\lambda(-\vartheta - i\hbar\sigma)], \hat{\mathcal{H}}'_{-\lambda}(-i\hbar\sigma)]\,\hat{M}_{-\alpha}$$
$$+\exp(\alpha\hbar\omega_0\sigma)\,\hat{M}_{-\alpha}[\hat{\mathcal{H}}'_{-\lambda}(\vartheta + i\hbar\sigma), [\hat{\mathcal{H}}'_\lambda(i\hbar\sigma), \hat{M}_\alpha]]\}\,\delta_{\alpha,-\beta}, \quad (39)$$

where $\vartheta = t_2 - t_1$.

We introduce the notation

$$\frac{1}{2\hbar^2}\int_0^{1/kT} d\sigma\,\mathrm{Sp}\,\hat{\rho}_0\{\exp(-\alpha\hbar\omega_0\sigma)$$
$$\times[[\hat{M}_\alpha, \hat{\mathcal{H}}'_\lambda(-\vartheta - i\hbar\sigma)], \hat{\mathcal{H}}'^*_\lambda(i\hbar\sigma)]\,\hat{M}^*_\alpha + \exp(\alpha\hbar\omega_0\sigma)\,\hat{M}^*_\alpha$$
$$\times[\hat{\mathcal{H}}'^*_\lambda(\vartheta - i\hbar\sigma), [\hat{\mathcal{H}}'_\lambda(i\hbar\sigma), \hat{M}_\alpha]]\} = \gamma_\alpha\,\Omega^2_{\alpha\lambda}\,f_{\alpha\lambda}(\vartheta) \quad (40)$$

under the condition $f_{\alpha\lambda}(0) = 1$. Then

$$G^{(2)}_{\alpha\beta}(\tau) = -(-1)^\alpha \chi_\alpha \exp(-i\alpha\omega_0\tau)\,\psi_\alpha(\tau)\,\delta_{\alpha,-\beta}, \quad (41)$$

$$\psi_\alpha(\tau) = \sum_\lambda \Omega^2_{\alpha\lambda}\int_0^\tau (\tau - \vartheta)\exp(i\lambda\omega_0\vartheta)\,f_{\alpha\lambda}(\vartheta)\,d\vartheta. \quad (42)$$

The tensor $G_{\alpha\beta}(\tau)$ can now be written in the form

$$G_{\alpha\beta}(\tau) = (-1)^\alpha \chi_\alpha \exp(-i\alpha\omega_0\tau)(1 - \psi_\alpha)\,\delta_{\alpha,-\beta}$$
$$-\frac{1}{kT} M^2_{0z}\,\delta_{\alpha 0}\,\delta_{\beta 0}. \quad (43)$$

As can be seen from (40) and (42), the function $\psi_\alpha(\tau)$ has the following properties:

$$\psi_\alpha(\tau) = \psi^*_\alpha(-\tau) = \psi^*_{-\alpha}(\tau). \quad (44)$$

4. If (43) is taken into account, Eq. (21) found above for the magnetization $\hat{M}_\alpha$ determines its

variation with time in weak variable fields. The function $\psi_\alpha(\tau)$ can be obtained if the specific form of the correlation function $f_{\alpha\lambda}(t)$ is known. The function $f_{\alpha\lambda}(t)$ falls off rapidly with time. In the case that

$$\Omega_{\alpha\lambda}\tau_c \ll 1, \tag{45}$$

where τ_c is the time interval that characterizes the function $f_{\alpha\lambda}(t)$, then we can use for $\psi_\alpha(\tau)$ the following asymptotic expression

$$\psi_\alpha(\tau) = \tau \sum_\lambda \Omega_{\alpha\lambda}^2 \int_0^\infty \exp(i\lambda\omega_0\vartheta) f_{\alpha\lambda}(\vartheta)\, d\vartheta, \quad \tau > 0. \tag{46}$$

The term neglected in the integral (42) is of order $(\Omega_{\alpha\lambda}\tau_c)^2$.

We can now write $\psi_\alpha(\tau)$ in the form

$$\psi_\alpha(\tau) = (1/T_\alpha)|\tau| + i\varkappa\Delta\omega_0\tau, \tag{47}$$

where

$$\frac{1}{T_\alpha} = \sum_\lambda \Omega_{\alpha\lambda}^2 \operatorname{Re} \int_0^\infty \exp(i\lambda\omega_0\vartheta) f_{\alpha\lambda}(\vartheta)\, d\vartheta, \tag{48}$$

$$\varkappa\Delta\omega_0 = \sum_\lambda \Omega_{\alpha\lambda}^2 \operatorname{Im} \int_0^\infty \exp(i\lambda\omega_0\vartheta) f_{\alpha\lambda}(\vartheta)\, d\vartheta. \tag{49}$$

Taking into account the fact that $\psi_\alpha(\tau)$ is small and the limiting condition $G(\infty) = 0$ we obtain in accordance with (21) and (43), up to terms of second-order perturbation theory:

$$M_\alpha = M_{0\alpha} + \chi_\alpha \int_0^\infty (i\varkappa\omega_0 + \dot{\psi}_\alpha(\tau)) \times \exp(-i\varkappa\omega_0\tau - \psi_\alpha(\tau)) h_\alpha(t-\tau)\, d\tau. \tag{50}$$

The last expression completely determines the dependence of M_α on the time for a given $h(t)$.

It is now easy to obtain the differential equation that is satisfied by the components of the magnetization vector. On differentiating M_α with respect to time we obtain after simple transformations

$$\begin{aligned} \dot{M}_\alpha + [i\varkappa(\omega_0 + \Delta\omega_0) + 1/T_\alpha](M_\alpha - M_{\alpha 0}) \\ = -[i\varkappa(\omega_0 + \Delta\omega_0) + 1/T_\alpha]\chi_\alpha h_\alpha(t). \end{aligned} \tag{51}$$

By going over to the Cartesian coordinate system we obtain:

$$\begin{aligned} \dot{M}_x + (1/T_\perp)M_x &= (1/T_\perp)\chi_\perp h_x(t) + \gamma M_y H_0 - \gamma M_0 h_y(t) \\ &\quad - \gamma(\chi_\perp H_0 - M_0) h_y(t), \\ \dot{M}_y + (1/T_\perp)M_y &= (1/T_\perp)\chi_\perp h_y(t) + \gamma M_0 h_x(t) \\ &\quad - \gamma M_x H_0 + \gamma(\chi_\perp H_0 - M_0) h_x(t), \\ \dot{M}_z + (1/T_\parallel)(M_z - M_0) &= (1/T_\parallel)\chi_\parallel h_z(t), \end{aligned} \tag{52}$$

where

$$\gamma H_0 = \omega_0 + \Delta\omega_0, \tag{53}$$

and $T_\perp = T_{\pm 1}$ and $T_\parallel = T_0$ are the transverse and longitudinal relaxation times.

Equations (52) differ from the linearized Bloch equations (1) by their last terms, and also by the terms containing $\chi_\perp$ and $\chi_\parallel$.

In weak fields, $\hbar\omega_0 \ll kT$, as we have pointed out earlier, we have $\chi_\perp = \chi_\parallel = \chi$ independent of the field H_0. In this case $M_0 = \chi H_0$.

The quantity γ appearing in the equation differs from the gyromagnetic ratio for the free magnetic moment $\gamma_0 = g\mu_0/\hbar$ by the correction term (53)

$$\gamma = \gamma_0 + \Delta\omega_0/H_0, \tag{54}$$

where $\Delta\omega_0$ is determined by (49).

In the case $\omega_0\tau_c \ll 1$ we obtain from (49)

$$\Delta\omega_0/H_0 = \sum_\lambda \Omega_{1\lambda}^2 \int_0^\infty \lambda\gamma_0\vartheta\, f_{1\lambda}(\vartheta)\, d\vartheta. \tag{55}$$

In the case under consideration this correction to γ is due certainly not to the spin-orbit interactions, which were not taken into account, but to dipole-dipole interactions. The magnitude of the correction depends in an essential manner on the nature of the thermal motion of the magnetic moments and on the exchange interaction. When $\omega_0\tau_c \gg 1$ the correction to the gyromagnetic ratio can be neglected.

The condition for the applicability of (52) is the inequality $\Omega_{\alpha\lambda}\tau_c \ll 1$.

In paramagnetic solutions τ_c is the correlation time which is determined by

$$\tau_c = (4\pi/3)a^3\eta/kT, \tag{56}$$

where a is the kinetic radius of the molecule. If we take into account that $\Omega_{\alpha\lambda} \sim \mu_0^2/d^3\hbar$, where d is the average distance between the magnetic moments, then

$$\Omega_{\alpha\lambda}\tau_c \sim (4\pi\mu_0^2\eta/3kkT)(a/d)^3. \tag{57}$$

For aqueous solutions of paramagnetic salts at room temperatures $\Omega_{\alpha\lambda}\tau_c \sim (a/d)^3 < 1$ and rapidly decreases upon dilution.

For ferromagnetic substances at temperatures below the Curie temperature we always have $\Omega_{\alpha\lambda}\tau_c \ll 1$.

[1] R. K. Wangsness and F. Bloch, Phys. Rev. **89**, 728 (1953).

[2] F. Bloch, Phys. Rev. **102**, 104 (1956).

[3] F. Bloch, Phys. Rev. **105**, 1206 (1957).

[4] N. Bloembergen and S. Wang, Phys. Rev. **93**, 72 (1954).

[5] P. Kubo and K. Tomita, J. Phys. Soc. Japan **9**, 888 (1957).

[6] M. Yokota and S. Koide, J. Phys. Soc. Japan **9**, 953 (1954).

[7] D. Kivelson, J. Chem. Phys. **27**, 1087 (1957).

[8] A. K. Chirkov and A. A. Kokin, J. Exptl. Theoret. Phys. (U.S.S.R.) **35**, 50 (1958), Soviet Phys. JETP **8**, 36 (1959).

Translated by G. Volkoff

PARAMAGNETIC RESONANCE OF F CENTERS IN STATIC MAGNETIC FIELDS OF ARBITRARY STRENGTH

M. F. DEĬGEN and L. B. ROĬTSIN

Institute of Physics, Academy of Sciences, Ukrainian S.S.R.

Submitted to JETP editor June 21, 1958

J. Exptl. Theoret. Phys. (U.S.S.R.) 36, 176-185 (January, 1959)

The hyperfine interaction of an F center electron with the magnetic moments of nuclei of the first coordinational sphere surrounding the vacancy is examined for the case when a static field of arbitrary strength is present. The hyperfine splitting has been evaluated for F centers in a KCl crystal. Transitions between hyperfine levels induced by a radio-frequency field are considered. In the absence of an external static field, these transitions are found to be allowed.

Special attention is paid to paramagnetic resonance of F centers in which only one of the first coordinational sphere has a magnetic moment. In this case the frequencies and intensities of paramagnetic resonance absorption depend on the orientation of the crystal in the static magnetic field. The absorption intensity depends also on the orientation of the crystal relative to the vector of the magnetic field of the wave incident on the crystal.

1. INTRODUCTION

EXPERIMENTAL and theoretical investigations of paramagnetic resonance of F centers in ionic crystals have been reported by several authors.[1-6] An essential feature of all these investigations has been the presence of strong magnetic fields, i.e., the inequality $\mu H \gg A$ (μ is the Bohr magneton, H is the intensity of the external staticmagnetic field, and A is the hyperfine splitting constant). In this case the correct quantum numbers are S_z and I_z.

Quantum transitions under the influence of a microwave field satisfy the condition $\Delta S_z = \pm 1$, $\Delta I_z = 0$. It becomes possible to obtain the shape and half width of the spin-electron resonance curve. The Gaussian form of the curve, which is obtained theoretically, is in good agreement with experiment.

It is of interest to consider paramagnetic resonance of local electron centers for arbitrary value of intensity of external static magnetic field. Judging from references 7 and 8, devoted to an experimental investigation of paramagnetic resonance in hydrogen and deuterium in weak magnetic fields, we can likewise expect qualitatively new features, not inherent in the spin-electron resonance in strong fields, in paramagnetic resonance of local electron centers in crystals.

Of particular interest is an investigation of the possibility of realizing paramagnetic resonance in the absence of an external static magnetic field. We develop below the theory of paramagnetic resonance of F centers for arbitrary value of the intensity of the external static field and, in particular, for zero field.

2. HYPERFINE SPLITTING OF ENERGY LEVELS OF THE F CENTER IN THE PRESENCE OF AN EXTERNAL STATIC MAGNETIC FIELD

The spin-Hamiltonian of the system under consideration can be written[9]

$$\hat{W} = \mu H\Big(g\hat{S}_z - \sum_{k=1}^{6} g_{kI}\hat{I}_{kz}\Big) + \sum_{k=1}^{6} a_k(\hat{\mathbf{S}}\cdot\hat{\mathbf{I}}_k) + \sum_{k=1}^{6}\sum_{p,q=1}^{3} A_{pqk}\hat{I}_{kq_k}\hat{S}_{p_k}, \qquad (1)$$

and

$$a_k = (4\pi/3)\mu_{kI}\mu/I_k S)\,|\psi(\rho_k = 0)|^2, \quad g_I = g_{\text{nuc}}\mu_N/\mu,$$
$$A_{pqk} = \frac{\mu^2 I_k}{SI_k}\int \frac{x_q}{\rho_k^3}\frac{\partial|\psi|^2}{\partial x_p}\,d\tau, \qquad (2)$$

where g is the Landé factor of the electron; g_{nuc} is the nuclear g factor; μ_N is the nucleon magneton; $\mathbf{S}$, $\mathbf{I}_k$, S_z and I_{kz} are the spin vectors of the electron and the k-th nucleus and their projections on the z axis; μ_k is the magnetic moment of the k-th nucleus, and ψ is the wave function of the F center. The integration in (2) is in a frame with origin in the k-th nucleus.

Separating the Fermi terms in the last component of (1), the spin-Hamiltonian of the system is more conveniently rewritten as

$$\hat{W} = \mu H\left(g\hat{S}_z - \sum_{k=1}^{6} g_{Ik}\hat{I}_{kz}\right) + \sum_{k=1}^{6} A_k(\mathbf{S}\cdot\mathbf{I}_k) + \sum_{k=1}^{6}\sum_{q=1}^{3}\sum_{p=1}^{3} A'_{pqk}\hat{I}_{kq}\hat{S}_{pL}, \quad (3)$$

$$A_k = \frac{8\pi\mu\mu_k}{3SI_k}|\psi(r_k=0)|^2, \quad (4)$$

$$A'_{pqk} = \frac{\mu\mu_k}{SI_k}\int|\psi|^2\frac{3x_{kp}x_{kq} - r_k^2\delta_{pq}}{r_k^5}d\tau. \quad (5)$$

Estimates show that $A'_{pqk} \ll A_k$ for F centers. Therefore the spin Hamiltonian (3) can be approximately written

$$\hat{W} = \mu H(g\hat{S}_z - g_I\hat{I}_z) + A(\hat{\mathbf{S}}\cdot\hat{\mathbf{I}}). \quad (6)$$

It is taken into account in (6) that for all nuclei of the first coordination sphere the value of A_k is the same ($A_k = A$); I and I_z are respectively the total spin of the nuclei of the first coordinational sphere and its projection on the z axis.

The energy levels of a system with a spin Hamiltonian (6) have been calculated by Breit and Rabi[10] and are written

$$E_1 = AI/2 + \mu H(g/2 - g_I I) \quad \text{for } F_z = S_z + I_z = I + 1/2, \quad (7)$$

$$E_2 = AI/2 - \mu H(g/2 - g_I I) \quad \text{for } F_z = -I - 1/2, \quad (7a)$$

$$E_{3,4} = -A/4 - \mu H g_I F_z \pm 1/2\{(g+g_I)^2\mu^2H^2 + 2AF_z(g+g_I)\mu H + A^2(I+1/2)^2\}^{1/2}. \quad (7b)$$

In Eq. (7b), F_z assumes values from $-I + \frac{1}{2}$ to $I - \frac{1}{2}$, and the indices 3 and 4 designate the aggregate of energy levels. It follows from (7) that the energy levels correspond to definite values of F_z. This quantum number, however, does not determine the levels uniquely [see (7b)]. It is therefore convenient to describe arbitrarily the energy levels by still another quantum number F, which characterizes the eigenvalue of the square of the total momentum. The latter characteristic has meaning only if $H = 0$ ($F = I + \frac{1}{2}$ and $F = I - \frac{1}{2}$). We shall assign the first value to the E_3 level and the second to the E_4 level. All energy levels of this system are obtained from (7) at different values of F_z and I.

By way of illustration, we calculated the numerical values of the energy levels for the alkali-halide crystals with lattices of the NaCl type (halides of K, Na, Rb, and Li). The spins of the nuclei of the metal ions in these lattices are $^3/_2$. Using the rules for addition of vector operators,[11] we obtain for the total spin of the six nuclei in the first coordinational sphere the following values:

$I =$	0	1	2	3	4	5	6	7	8	9
$N =$	34	90	120	120	96	64	35	15	5	1

N determines the statistical weight of the quantum state corresponding to a definite I.

Available data on double paramagnetic resonance[9,12,13] make it possible to determine the binding constants of the spin Hamiltonian (1). In particular, for the spin-Hamiltonian of the F center in KCl we obtain for the constant A [Eq. (6)] $A/\mu = 15.43$ gausses. We note, furthermore, that in high-accuracy numerical calculations it is possible to neglect the second component of the Zeeman term of (6), since it is on the order of 10^{-4} of the first term.

It is easy to see that the total number of levels in this case is $\sum_{I=0}^{9} 2(2I+1) = 200$. Numerical claculations of the energy levels in the presence of an external magnetic field have been carried out for H = 50 oersteds. Since we do not wish to clutter up the article with tables, we omit the numerical values of the energy levels and cite only the transition frequencies.

3. QUANTUM TRANSITIONS IN THE SPECTRUM OF HYPERFINE SPLITTING. SELECTION RULES. INTENSITIES OF PARAMAGNETIC-RESONANCE LINES

The wave function of the system is written

$$\Phi = C_1\chi'_I(I_z)\chi_{+1/2}(S_z) + C_2\chi'_{-I}(I_z)\chi_{-1/2}(S_z) + \sum_{F_z=-I+1/2}^{I-1/2}[C_3(F_z)\chi'_{F_z+1/2}(I_z)\chi_{-1/2}(S_z) + C_4(F_z)\chi'_{F_z-1/2}(I_z)\chi_{1/2}(S_z)]. \quad (8)$$

Here χ and χ' are the electronic and nuclear spin functions respectively, while C are the linear-combination coefficients.

The inclusion of the perturbation (6) removes the degeneracy completely and leads to the appearance of 200 levels. Each level has its own wave function, obtained from (8) by substituting into this expression the corresponding set of coefficients C. We note that for levels with $F_z = I + \frac{1}{2}$ and $F_z = -(I + \frac{1}{2})$ only one of the coefficients differs from zero. For levels having the same values of F_z only $C_3(F_z)$ and $C_4(F_z)$ differ from zero. They are determined by solving the system of equations

$$\begin{aligned}[W_{33}(F_z) - E]C_3(F_z) + W_{34}(F_z)C_4(F_z) &= 0,\\ W_{43}(F_z)C_3(F_z) + [W_{44}(F_z) - E]C_4(E_z) &= 0,\end{aligned} \quad (9)$$

where $W_{33}(F_z)$ and $W_{44}(F_z)$ are respectively the diagonal matrix elements of the states with $I = F_z + \frac{1}{2}$, $S_z = -\frac{1}{2}$ and $I = F_z - \frac{1}{2}$, $S_z = \frac{1}{2}$, while $|W_{34}(F_z)| = |W_{43}(F_z)|$ is the non-diagonal ele-

ment, constructed from the wave functions of the state indicated above:

$$W_{33}(F_z) = -\mu Hg/2 - (A/2)(F_z + {}^1/_2),$$
$$W_{44}(F_z) = \mu Hg/2 + (A/2)(F_z - {}^1/_2), \qquad (10)$$
$$W_{34}(F_z) = W_{43}(F_z) = (A/2)[(I + F_z + {}^1/_2)(I - F_z + {}^1/_2)]^{1/2}$$

with the normalization condition

$$|C_3(F_z)|^2 + |C_4(F_z)|^2 = 1. \qquad (11)$$

We finally obtain the following system of wave functions

$$\Phi_1 = \chi'_{1/2}\chi_{1/2}, \qquad (12a)$$
$$\Phi_2 = \chi''_{-1/2}\chi_{-1/2}, \qquad (12b)$$
$$\Phi_3(F_z) = C'_3(F_z)\chi'_{F_z+1/2}\chi_{-1/2} + C''_4(F_z)\chi'_{F_z-1/2}\chi_{1/2}, \qquad (12c)$$
$$\Phi_4(F_z) = C''_3(F_z)\chi'_{F_z+1/2}\chi_{-1/2} + C''_4(F_z)\chi'_{F_z-1/2}\chi_{1/2}. \qquad (12d)$$

In (12c) and (12d) F_z assumes values from $-I + \frac{1}{2}$ to $I - \frac{1}{2}$. C′ corresponds to the value of energy E, obtained from (7b) using the root with the positive sign; C″ corresponds to the negative root. The first three wave functions in (12) describe states characterized by $F = I + \frac{1}{2}$, while the last one describes states with $F = I - \frac{1}{2}$.

It follows directly from (9) and (11) that

$$C_3(F_z) = -W_{34}(F_z)/[W_{34}^2(F_z) + [W_{33}(F_z) - E]^2]^{1/2}, \qquad (13a)$$

$$C_4(F_z) = (W_{33}(F_z) - E)/[W_{34}^2(F_z) + [W_{33}(F_z) - E]^2]^{1/2}. \qquad (13b)$$

Using (13a), (13b), and also (7b), we can show that

$$C'_3(F_z) = -C''_4(F_z), \quad C''_3(F_z) = C'_4(F_z). \qquad (14)$$

Going to the limit of strong fields, we obtain the following values for the coefficients:

$$C'_3(F_z) \to 0; \quad C''_3(F_z) \to -1;$$
$$C'_4(F_z) \to -1; \quad C''_4(F_z) \to 0. \qquad (15)$$

A radio-frequency field produces transitions between the stationary states of the system which were considered in Sec. 2.

The solution of the corresponding Schrödinger temporal equation is sought in the following form

$$\varphi = D_1\Phi_1 + D_2\Phi_2 + \sum_{F_z=-I+1/2}^{I-1/2}[D_3(F_z)\Phi_3(F_z) + D_4(F_z)\Phi_4(F_z)], \qquad (16)$$

where D are time-dependent coefficients.

As usual, at the instant $t = 0$ all the coefficients D, with the exception of one, are assumed to be zero. At a time $t \neq 0$, according to perturbation theory,

$$D_i^{(1)} = (1/i\hbar)\int_0^t V_{ik}\exp\{i\omega_{ik}\tau\}\,d\tau + \delta_{ik}, \qquad (17)$$

where the index k indicates the level from which the transition takes place to a certain level i, and

$$\hat{V} = -(\boldsymbol{\mu}\cdot\mathbf{H}'(t)), \quad \omega_{ik} = (E_i - E_k)/\hbar. \qquad (18)$$

To calculate D_i it is first necessary to determine V_{ik}. It is easy to see that all the matrix elements V_{ik} can be obtained by applying the perturbation operator (18) to the functions Φ_1 and Φ_2, and also to the system of functions $\Phi_3(F_z)$ $\Phi_4(F_z)$.

The first two functions correspond to levels E_1 and E_2, while the third and fourth functions are ascribed to levels E_3 and E_4. We therefore encounter a total of eight different types of matrix elements V_{ik}. The calculations yield

$$V_{12} = 0 \text{ for } I \neq 0,$$
$$V_{12} = {}^1/_2\mu g(H'_x - iH'_y) \text{ for } I = 0, \qquad (19a)$$

$$V_{13} = {}^1/_2\mu g(H'_x - iH'_y)\,C'_3(F_z)\,\delta(F_z, I - {}^1/_2). \qquad (19b)$$

The symbol $\delta(F_z, I - \frac{1}{2})$ indicates that the matrix element (19b) differs from 0 only for transitions from level 3 (when $F_z = I - \frac{1}{2}$) to level 1. For the remaining values of F_z, the transitions from levels 3 to level 1 are forbidden. Inserting into (19b) the values $F_z = I - \frac{1}{2}$ and the values of the coefficient $C'_3(F_z)$ for $F_z = I - \frac{1}{2}$ [from (13a)] we determine V_{13}.

Analogously we have for the matrix element V_{14}, V_{23}, V_{24}, and V_{33}

$$V_{14} = {}^1/_2\mu g(H'_x - iH'_y)\,C''_3(F_z)\,\delta(F_z, I - {}^1/_2), \qquad (19c)$$

$$V_{23} = {}^1/_2\mu g(H'_x + iH'_y)\,C'_4(F_z)\,\delta(F_z, -I + {}^1/_2), \qquad (19d)$$

$$V_{24} = {}^1/_2\mu g(H'_x + iH'_y)\,C''_4(F_z)\,\delta(F_z, -I + {}^1/_2), \qquad (19e)$$

$$V_{33} = {}^1/_2\mu g(H'_x - iH'_y)\,C'_4(F_z^+)\,C'_3(F_z)\,\delta(F_z, F_z^+ - 1). \qquad (19f)$$

The matrix element V_{33} corresponds to a transition from the level F_z to the level $F_z^+ = F_z + 1$

$$V_{44} = {}^1/_2\mu g(H'_x + iH'_y)\,C''_3(F_z^+)\,C''_4(F_z)\,\delta(F_z, F_z^+ + 1). \qquad (19g)$$

When calculating V_{34} it must be borne in mind that the transitions possible here are both between identical F_z and between different ones. Accordingly, three matrix elements of type V_{34} appear:

$$V'_{34} = {}^1/_2\mu g H'_z[C'_4(F_z^+)\,C''_4(F_z) - C'_3(F_z^+)\,C''_3(F_z)]\,\delta(F_z^+, F_z), \qquad (19h)$$

$$V''_{34} = {}^1/_2\mu g(H'_x + iH'_y)\,C'_3(F_z^+)\,C''_4(F_z)\,\delta(F_z, F_z^+ + 1), \qquad (19i)$$

$$V'''_{34} = {}^1/_2\mu g(H'_x - iH'_y)\,C'_4(F_z^+)\,C''_3(F_z)\,\delta(F_z, F_z^+ - 1). \qquad (19j)$$

It follows from the above that selection rules $\Delta F_z = 0$ apply to transitions caused by the com-

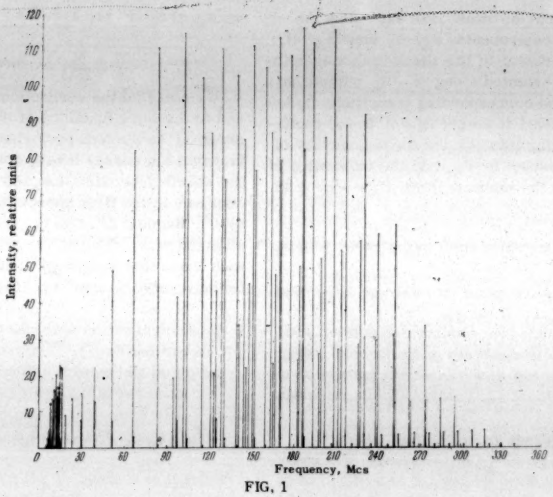

FIG. 1

ponent H'_Z of the alternating field, while selection rules $\Delta F_Z \pm 1$ hold for the transitions corresponding to the components H'_X and H'_Y.

Expressions (19) allow us to determine the probabilities of the corresponding transitions; multiplication of the latter by the statistical weights of the states yields the intensities of the absorption lines in relative units.

The results of calculations are shown in Figs. 1 and 2.

4. FIELD-FREE PARAMAGNETIC RESONANCE

In this case the Hamiltonian (6) becomes

$$\hat{W} = A\hat{\mathbf{S}} \cdot \hat{\mathbf{I}}. \qquad (20)$$

Its eigenvalues are

$$E = {}^1/_2 A [F(F+1) - I(I+1) - S(S+1)]. \qquad (21)$$

In view of the fact that F assumes only two values, two levels $E^{(1)} = AI/2$ and $E^{(2)} = -(A/2)(I+1)$ correspond to each value of I. The transition frequency is $E^{(1)} - E^{(2)} = A(I + \frac{1}{2})$.

It is interesting to investigate the possibility of quantum transitions between levels $E^{(1)}$ and $E^{(2)}$. Using the results of the preceding section, it is easy to show that when $H = 0$ only the matrix elements V_{14}, V_{24}, and V_{34} will play any role (V_{12}, V_{13}, V_{23}, V_{33} and V_{44} are not significant, since the corresponding levels have merged). It is convenient in this case to retain the previous coordinate system

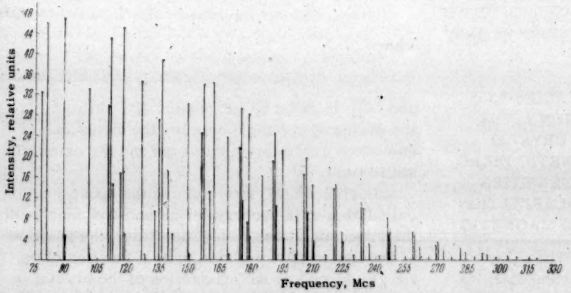

FIG. 2

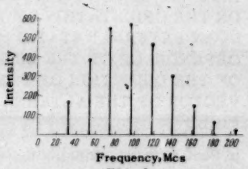

FIG. 3

($H = H_Z$) and speak of transitions caused by the alternating-field components H'_X, H'_Y and H'_Z. If, for example, the vector of the alternating magnetic-field intensity is oriented along z (H'_Z component) the intensity of the corresponding transitions is determined from (19h); if we put $H = 0$ in the coefficient C and, taking into account the degeneracy of the levels with respect to F_Z, add the intensities of the transitions in the interval from $F_Z = -I + \frac{1}{2}$ to $I - \frac{1}{2}$, we obtain

$$J' = 4 \sum_{F_Z=-I+1/2}^{I-1/2} [C'_3(F_z) C'_4(F_z)]^2. \qquad (22)$$

The relations (14) are taken into account here. Putting $H = 0$ in Eqs. (13) we get

$$C'_4(F_z) = -\left[\frac{1}{2}\left(1 + \frac{F_z}{I+1/2}\right)\right]^{1/2}, \qquad (23a)$$

$$C'_3(F_z) = -\left[\frac{1}{2}\left(1 - \frac{F_z}{I+1/2}\right)\right]^{1/2}. \qquad (23b)$$

Inserting (23) into (22) and summing, we get

$$J' = \frac{8I}{3}\,\frac{I+1}{2I+1}. \qquad (24)$$

The intensities of the individual lines in relative units are obtained by multiplying (24) by the statistical weights of the states with definite $I - N$.

Analogous calculations, but using (19i) and (19k), also lead to expression (24) for the two other components.

It is thus obvious that, for an arbitrary orientation of the external alternating magnetic field, the intensity of the lines of field-free paramagnetic resonance is again determined by the product $J'N$.

The results of the calculation of the frequencies and the transition intensities (in relative units) in field-free paramagnetic resonance are shown in Fig. 3.

It is easy to show that the intensities of the lines of field-free paramagnetic resonance are comparable with the intensities of the lines of spin-electron resonance in strong fields. It therefore becomes possible to realize field-free paramagnetic resonance experimentally.

5. DEPENDENCE OF THE FREQUENCIES AND INTENSITIES OF THE ABSORPTION LINES ON THE ORIENTATION OF THE CRYSTAL IN AN EXTERNAL STATIC MAGNETIC FIELD. DEPENDENCE OF THE LINE INTENSITIES ON THE DIRECTION OF THE POLARIZATION VECTOR OF THE ALTERNATING MAGNETIC FIELD

In Sec. 2, in considering the hyperfine splitting of the energy levels of the F centers, we omitted terms of the form

$$\hat{Q} = \sum_{k=1}^{6} \sum_{p,\,q=1}^{3} A'_{pqk} \hat{I}_{kq} \hat{S}_{pk}. \qquad (25)$$

We now find the corrections to the energy levels and to the wave functions of the system, by considering $\hat{Q}$ as a small perturbation. In view of the fact that the energy levels are not degenerate in the zeroth approximation, the correction to the energies in the first approximation are determined by the diagonal elements of the matrix Q_{min}, constructed with the functions Φ_1 and Φ_2, and also with the entire system of functions corresponding to the levels E_3 and E_4. The calculations yield

$$Q_{11} = {}^1/_2 \sum_{k=1}^{6} A'_{k33} (I_k)^I_I, \qquad (26a)$$

$$Q_{22} = Q_{11}, \qquad (26b)$$

$$Q_{33} = \left[-\frac{F_z}{2}(C'^2_4(F_z) - C'^2_3(F_z)) - \frac{1}{4} - \frac{1}{2} C'_4(F_z) C'_3(F_z) \sqrt{(I+1/2)^2 - F_z^2}\right] \sum_{k=1}^{6} (I_k)^I_I A'_{k33}, \qquad (26c)$$

$$Q_{44} = \left[-\frac{F_z}{2}(C'^2_4(F_z) - C'^2_3(F_z)) - \frac{1}{4} + \frac{1}{2} C'_4(F_z) C'_3(F_z) \sqrt{(I+1/2)^2 - F_z^2}\right] \sum_{k=1}^{6} (I_k)^I_I A'_{k33}. \qquad (26d)$$

The symbol $(I_k)^I_I$ for the matrix elements is borrowed from reference 11. In obtaining formulas (26) we used relations (14) and the equality $A'_{k11} + A'_{k22} + A'_{k33} = 0$. It must be borne in mind that the spin Hamiltonian (1), and consequently also the coefficients, are written in a coordinate system that is connected with the external static magnetic field. In specific calculations it is convenient to calculate expressions for the coefficients in a frame with its origin in the k-th nucleus, but with the z axis along one of the crystallographic axes.

The corrections (26) to the energy depend only on one of the coefficients A'_{k33}. It is easy to show that

$$A'_{k33} = A_{11} + a/3 + (A_{33} - A_{11}) n_3^2, \qquad (27)$$

where

$$a = (4\pi |\psi_k(\mu_k S)|^2, \quad A_{11} = A_{22}, \quad 2A_{11} + A_{33} = -a,$$

and A_{33} is given by expression (2), while n_3 is the cosine of the angle between the directions of one of the crystallographic axes and the external static field.

Insertion of (27) into (26) and the subsequent calculation of the energy terms and frequencies of the absorption lines cause, naturally, the position of the line in the spectrum to be a function of n_3, i.e., to depend on the orientation of the crystal in the external static magnetic field.

TABLE I

$\Delta F_z = 0$		$\Delta F_z = \pm 1$	
Frequency, Mcs	Intensity in relative units	Frequency, Mcs	Intensity in relative units
$54.51+5.146\ n_3^2$	0.198	$56.04+8.54\ n_3^2$	0.948
$50.49+0.438\ n_3^2$	0.394	$52.5\ +2.35\ n_3^2$	0.848
$45.22-4.578\ n_3^2$	0.589	$47.85-2.51\ n_3^2$	0.749
$38.51-8.058\ n_3^2$	0.779	$41.86-6.32\ n_3^2$	0.651
$29.45-11.46\ n_3^2$	0.952	$33.98-9.76\ n_3^2$	0.552
		$15.51+0.234\ n_3^2$	0.390

Specific calculations have been made for the F centers in an MgO crystal. In this case the task becomes simpler, for this crystal most probably has two types of F centers:[14] (1) F centers in which the first coordination sphere has no nuclei with magnetic moments different from zero; (2) F centers in which one of the nuclei of the first coordination sphere has a non-zero magnetic moment.

It is obvious that for the F centers of the first there will be no such angular dependence. Calculation of the angular dependence was made for the F centers of the second type. By way of an example, the field was assumed to equal 10 oersteds, and there were calculated frequencies and intensities of lines that are sufficiently remote from each other and were easiest to resolve experimentally in the spectrum. The results of the calculations for two directions of the polarization vector of the incident wave are given in Table I.

The wave functions can be calculated in the first approximation using the ordinary procedure of perturbation theory. Cumbersome calculations, but not difficult in principle, make it possible to determine the wave functions in the first approximation, and to calculate with the aid of the latter the probabilities of the transitions under the influence of the radio-frequency field. By way of an example, the calculations have been made for two arbitrarily chosen levels (with $F = I + \frac{1}{2}$, $F_Z = I + \frac{1}{2}$ and $F = I - \frac{1}{2}$, $F_Z = I - \frac{1}{2}$), the quantum transitions between which were then considered.

The square of the corresponding matrix element was found to be

$$V_{14}^2 = \mu^2 H_x'^2 \left\{ C_3'^2(F_z) + 2C_3'(F_z) \left[\frac{Q_{34} C_3'(F_z)}{E_4^0 - E_3^0} + \frac{(A'_{11} - A'_{22})\sqrt{21}}{4} \left(\frac{C_3'^2(F_z^+)}{E_3^0 - E_3^{0+}} + \frac{C_3'^2(F_z^+)}{E_1^0 - E_4^{0+}} \right) C_4'(F_z) \right] \right\} \times \delta(F_z, F_z^+ + 1)\, \delta(F_z, I - {}^1/_2). \quad (28)$$

Inserting into (28) the values A'_{11} and A'_{22} yields, after subsequent calculation,

$$(\mu H_x')^{-2} V_{14}^2 = 0.9225 + 0.00555 n_3^2 + 0.0705 n_1^2, \quad (29)$$

where n_1 is the cosine of the angle between the x axis (which determines the polarization of the alternating component in the magnetic field) in a coordinate system stationary with respect to the static field, and the z axis of the local system of coordinates.

TABLE II

Direction along which the ions are located	Frequency	Intensity according to (29)
$[0\bar{1}0]$	$56.04+8.54\sin^2\Omega$	$0.928 - \cos^2\Omega\ (0.0705\sin^2\gamma_x - 0.00555)$
$[0\bar{1}0]$	$56.04+8.54\cos^2\Omega$	$0.9225 + \sin^2\Omega\ (0.0705\sin^2\gamma_x + 0.00555)$
$[\bar{1}00]$		
$[00\bar{1}]$	56.04	$0.9225+0.0705\cos^2\gamma_x$
$[00\bar{1}]$		

It follows from (29) that the intensities of the lines will depend on the orientation of the crystal both relative to the external static field and relative to the component of the alternating high-frequency magnetic field that causes the transitions.

To obtain the angular dependences of the intensities and frequencies for any ion of the first coordination sphere, we introduce, as in reference 13, the following angles in the principal system of coordinates: (1) γ and Ω to specify the vector **H**, (2) θ and φ to specify the z axis of the local system of coordinates, and (3) γ_X and Ω_X to specify the x component of the alternating magnetic field.

For $\gamma = 90°$ (intensity vector of the external static field lies in the xy plane of the principal system of coordinates), we obtain, for the sixth of the frequencies (see Table I), the summary of the angular dependences of the frequency and intensity listed in Table II.

Estimates show that the angular dependences of the frequencies and intensities are sufficiently large to be experimentally observable.

[1] C. Hutchison and G. Noble, Phys. Rev. **87**, 1125 (1952).

[2] Kip, Kittel, Levy, and Portis, Phys. Rev. **91**, 1066 (1953).

[3] E. Schneider and T. England, Physica **17**, 221 (1951).

[4] A. H. Kahn and C. Kittel, Phys. Rev. **89**, 315 (1953).

[5] M. F. Deĭgen and L. A. Shul'man, Оптика и спектроскопия (Optics and Spectroscopy) **3**, 21 (1957).

[6] M. F. Deĭgen, J. Exptl. Theoret. Phys. (U.S.S.R.) **33**, 773 (1957), Soviet Phys. JETP **6**, 594 (1958).

[7] J. E. Nafe and E. B. Nelson, Phys. Rev. **73**, 718 (1948).

[8] A. G. Prodell and P. Kusch, Phys. Rev. **88**, 184 (1952).

[9] M. F. Deĭgen and V. Ya. Zevin, J. Exptl. Theoret. Phys. (U.S.S.R.) **34**, 1142 (1958), Soviet Phys. JETP **7**, 790 (1958).

[10] G. Breit and I. I. Rabi, Phys. Rev. **38**, 2082 (1931).

[11] L. D. Landau and E. M. Lifshitz, Квантовая механика (Quantum Mechanics) part I, Gostekhizdat, 1948 (Engl. Transl., Pergamon, 1958).

[12] G. Feher, Phys. Rev. **105**, 1122 (1957).

[13] M. F. Deĭgen and A. B. Roĭtsin, Укр. физ. журн. (Ukr. Phys. J.) **3**, 439 (1958).

[14] Wertz, Auzins, Weeks, and Silsbee, Phys. Rev. **107**, 1535 (1957).

Translated by J. G. Adashko
24

PARENTAGE COEFFICIENTS IN THE GENERALIZED NUCLEAR MODEL

V. G. NEUDACHIN and Yu. F. SMIRNOV

Institute of Nuclear Physics, Moscow State University

Submitted to JETP editor June 24, 1958

J. Exptl. Theoret. Phys. (U.S.S.R.) 36, 186-192 (January, 1959)

We consider the construction of a wave function of a system of n nucleons, with prescribed values of isobarin spin T, from the wave functions of individual states N_1, N_2, ... N_n that are not coupled vectorially. The number of independent states with a given T is determined by algebraic methods. The problem is primarily of interest in relation to the unified model of a light nucleus.

NUMEROUS experimental data[1] evidence that the generalized model of a nucleus with a strong coupling between the particle and the surface holds not only for heavy nuclei, but also for elements between O^{16} and Ca^{40} (1d and 2s shells), i.e., where the isobaric spin is a good quantum number for the lower states. In connection with this, it becomes necessary to evaluate for the Nilsson model[2] in this region the parentage coefficients[3] necessary to calculate the matrix moments of the operators $F = \Sigma f_i$ or $G = \Sigma g_{if}$.

In this paper we make a general analysis of this problem and derive a general formula for the parentage coefficients.

1. NUMBER OF INDEPENDENT STATES

The nucleon in the nucleus is characterized by the charge and by four quantum numbers, for example nljΩ, where Ω is the projection of the nucleon momentum on the symmetry axis of the nucleus. The particular form of this set of numbers is immaterial in our problem. We denote this set by N.

The wave function of n particles is

$$|N_1 N_2 \dots N_n \alpha T T_Z\rangle = \Psi_{T, T_Z}, \qquad (1.1)$$

where T is the isobaric spin, $T_Z = Z - \frac{1}{2}A$ is antisymmetric over all particles if the charge coordinate of the nucleon is introduced.

It is easy to see that by changing the order of the nucleon coupling we can obtain other independent states from (1.1). Such states are identified by the symbol α. The number of such independent states is determined by the theory of permutation groups[4] in the following manner. The antisymmetric function Ψ is constructed from the spin-orbit functions $\Phi^{[\lambda]}(r)$ and the charge functions $\Gamma^{[\tilde{\lambda}]}(r)$, where λ is the symbol of the Young tableau, r is the Yamanouchi symbol,[4] while $[\tilde{\lambda}]$ and $[\tilde{r}]$ are the symbols for the tableaus that are conjugate[5] to [λ] and r in the following manner

$$\Psi_{T, T_Z} = (f^{[\lambda]})^{-1/2} \sum_r \Phi^{[\lambda]}_r(r)\, \Gamma^{[\tilde{\lambda}]}_{T, T_Z}(\tilde{r}), \qquad (1.2)$$

where $f^{[\lambda]}$ is the dimensionality of the representation of the group S_n of permutation of n numbers, with [λ] determining the isobaric spin T.[5] It is necessary to determine how many independent states $\Phi^{[\lambda]}(r)$ exist with given [λ] and r.

We first consider the case when all N_i are different (at least one number out of four different for each compared pair).

We introduce

$$\Phi_0 = |N_1(1) N_2(2) \dots N_n(n)\rangle, \qquad (1.3)$$

i.e., Φ_0 is simply the product of individual functions. All the functions $P\Phi_0$ for all n! permutations of the number of states P are orthogonal to each other. From these we construct the functions

$$\omega^{[\lambda]}_{rs} \Phi_0, \qquad (1.4)$$

where $\omega^{[\lambda]}_{rs}$ are the normalized orthogonal Young operators,[4] [λ] is the symbol for the Young tableau, while r and s are the Yamanoochi symbols. The symbols [λ] and r represent the permutation properties with respect to permutation of particles, while the symbols [λ] and s pertain to permutation of the number of states.

All the states $\omega^{[\lambda]}_{rs_i} \Phi_0$ ($i = 1, 2, f^{[\lambda]}$) are orthogonal to each other. In addition, since

$$P\omega^{[\lambda]}_{rs} = \sum_t \theta^{[\lambda]}_{rt}(P)\, \omega^{[\lambda]}_{ts}, \qquad (1.5)$$

(where $\theta^{[\lambda]}_{rt}(T)$ is the matrix of the irreducible orthogonal representation[4] of the group S_n) any state with specified [λ] and r can be expressed in terms of these states. Thus, if all N_i are

ferent, the number of independent states with specified T is $f^{[\lambda]}$.

Now let there be one pair of identical N_i, for example, $N_1 = N_2$. Then

$$\Phi_1 = |N_1(1)N_1(2)N_3(3)\ldots N_n(n)\rangle \quad (1.6)$$

has the same properties with respect to permutation as

$$[\epsilon + P_{12}]\Phi'_0, \quad (1.7)$$

where ϵ is the unit of the group; P_{12} is the permutation of the number of states 1 and 2; $[\epsilon + P_{12}] = 2e^{[2]}$ is the symmetrizer with respect to the numbers 1 and 2, and the function Φ'_0 has the same properties with respect to permutation as Φ_0.

Thus, the problem reduces to the following: how many of the operators

$$\omega^{[\lambda]}_{rs_i} e^{[2]}, \quad i = 1, 2 \ldots f^{[\lambda]}, \quad (1.8)$$

are linearly independent?

The problem is solved by successive expansion of $\omega^{[\lambda]}_{rs}$ in idempotent operators of the Young tableaus with an ever-diminishing number of cells[4] until $\omega^{[\lambda]}_{rs}$ assumes the form of an operator product on the right end of which will be either $e^{[11]}$ — the anti-symmetrizer over numbers 1 and 2, or $e^{[2]}$:

$$e^{[11]}e^{[2]} = 0, \quad e^{[2]}e^{[2]} = e^{[2]}.$$

Thus

$$\omega^{[\lambda]}_{rs_i} e^{[2]} = \omega^{[\lambda]}_{rs_i},$$

if in a table of s_i the numbers 1 and 2 are in the first row (i.e., $[\lambda] = [\lambda_1, \lambda_2, \ldots, \lambda_m]$ should have $\lambda_1 = 2$), and

$$\omega^{[\lambda]}_{rs_i} e^{[2]} = 0$$

in the opposite case. The number of non-vanishing operators $\omega^{[\lambda]}_{rs_i} e^{[2]}$, as can be readily concluded from the above, is $f^{[\lambda^*]}$, where $[\lambda^*] = [\lambda_2, \ldots \lambda_m]$ is the Young tableau without the first line. All are independent of each other.

Finally, let us consider the case of k identical pairs N from a total number and $n \geq 2k$. It is necessary to determine how many independent operators will be among

$$\omega^{[\lambda]}_{rs_i} e^{[2]_1} e^{[2]_2} \ldots e^{[2]_k}, \quad i = 1, 2 \ldots f^{[\lambda]}, \quad (1.9)$$

where $e^{[2]}_j$ is the symmetrizer over the j-th pair of states. Making use of the results of the foregoing analysis and solving the problem by analogy, we find that the number of independent operators is $f^{[\lambda^k]}$ where $[\lambda^k]$ is obtained from $[\lambda]$ by removing the k upper rows, each of which consist of two cells. The number of independent operators equals the number of independent states.

The method of constructing the function $\Phi^{[\lambda]}_{rs} = \omega^{[\lambda]}_{rs}\Phi$ (where Φ is Φ_0 or Φ_1, etc.) i.e., the Yamanouchi symbol s, is determined, as can be readily seen, by all the intermediate particle couplings over T:

$$|(N_1N_2)T_{12}, N_3, T_{123}, \ldots, N_n, TT_Z\rangle = (f^{[\lambda]})^{-1/2}\sum_\tau \omega^{[\lambda]}_{rs}\Phi\Gamma^{[\tau]}_\tau(\tau(1), \tau(2)\ldots, \tau(n)\,TT_Z). \quad (1.10)$$

Actually, the transition from T_{12} to T_{123} etc. describes the successive filling of the Young tableau by numbers; this determines the Yamanouchi symbol.

2. PARENTAGE COEFFICIENTS AND THEIR CALCULATION

The parentage coefficients make it possible to express the complete asymmetric wave function of n nucleons in the form of a linear combination of antisymmetric wave functions of $n-1$ particles, vectorially coupled through the isobaric spin with the wave function of the n-th particle. In the spin-orbit portion of the wave function, there is no vector addition:

$$\begin{aligned}
&|N_1N_2\ldots N_n\alpha TT_Z\rangle \\
&= \sum_{\alpha' T's}\langle N_1N_2\ldots N_n\alpha T|N_1N_2\ldots N_{s-1}N_{s+1}\ldots N_n\alpha' T'\rangle \\
&\quad\times|N_1N_2\ldots N_{s-1}N_{s+1}\ldots N_n\alpha' T',\ N_s(n):TT_Z\rangle, \\
&|N_1N_2\ldots N_{s-1}N_{s+1}\ldots N_n\alpha' T',\ N_s(n):TT_Z\rangle \\
&= \sum_{T'_z\tau_z(n)}(T'T'_z, {}^1/_2\tau_z(n)|T'{}^1/_2TT_Z) \\
&\quad\times|N_1N_2\ldots N_{s-1}N_{s+1}\ldots N_n\alpha' T'T'_z\rangle|N_s{}^1/_2\tau_z(n)\rangle.
\end{aligned} \quad (2.1)$$

Here $\langle N_1N_2\ldots N_n\alpha T|N_1\ldots N_{s-1}N_{s+1}\ldots N_n\alpha' T'\rangle$ is the parentage coefficient. We shall use henceforth a shorter symbol:

$$\begin{aligned}
&\langle N_1N_2\ldots N_n\alpha T|N_1\ldots N_{s-1}N_{s+1}\ldots N_n\alpha' T'\rangle \\
&\equiv\langle n\alpha T|(n-1)_s\alpha' T'\rangle;
\end{aligned} \quad (2.2)$$

$\tau_Z(m)$ in formula (2.1) is the projection of the isobaric spin of the n-th nucleon. $(T'T'_Z, \frac{1}{2}\tau_Z(m)|T'\frac{1}{2}TT_Z)$ is the Clebsch-Gordan coefficient.

To calculate the genealogical coefficients we use the Redmond method.[6] If we take some state $|N_1\ldots N_{i-1}N_{i+1}\ldots N_n\alpha''T'', N_i(n):TT_Z\rangle$ from the right half of formula (2.1) as the initial state, and act on it with the antisymmetrizing operator $\hat{O} = 1 - \sum_{k=1}^{n-1} P_{kn}$, we obtain, with accuracy to within a normalizing factor Q, the antisymmetric state $|N_iN_2\ldots N_n\alpha TT_Z\rangle$. The operator P_{kn} is the operator of

TABLE I. Parentage coefficients for n = 3

$\langle N_1 N_2 N_3 \alpha T \,|\, (2)_s T', N_s \rangle$

T'	0			1		
s / αT	1	2	3	1	2	3
$^1/_2 a$	$1/2\sqrt{3}$	$-1/\sqrt{3}$	$1/2\sqrt{3}$	$-1/2$	0	$1/2$
$^1/_2 b$	$1/2$	0	$-1/2$	$1/2\sqrt{3}$	$1/\sqrt{3}$	$1/2\sqrt{3}$
$^3/_2$				$1/\sqrt{3}$	$-1/\sqrt{3}$	$1/\sqrt{3}$

$\langle N_1 N_1 N_2 {}^1/_2 \,|\, N_1 N_2 0, N_1 \rangle = -1/\sqrt{6}$, $\langle N_1 N_1 N_2 {}^1/_2 \,|\, N_1 N_2 1, N_1 \rangle = -1/\sqrt{2}$,
$\langle N_1 N_1 N_2 {}^1/_2 \,|\, N_1 N_1 0, N_2 \rangle = 1/\sqrt{3}$

permutation of the spin, isobaric, and ordinary coordinates of the k-th and n-th nucleons. Multiplying (2.2) by $|N_1 \dots N_{s-1} N_{s+1} \dots N_n \alpha' T', N_s(n) : TT_Z\rangle^*$ and integrating over the corresponding variables, we get

$$\begin{aligned} & Q\langle n\alpha T \,|\, (n-1)_s \alpha' T'\rangle \\ &= \langle (n-1)_s \alpha' T', N_s(n) : TT_Z \,|\, \hat{O} \,|\, (n-1)_t \alpha'' T'', N_t(n) : TT_Z\rangle \\ &= \delta(is)\,\delta(\alpha'\alpha'')\,\delta(T'T'') - \sum_{k=1}^{n-1} \langle (n-1)_s \alpha' T', \end{aligned} \tag{2.3}$$

$$N_s(n) : TT_Z \,|\, P_{kn} \,|\, (n-1)_t \alpha'' T'', \; N_t : TT_Z\rangle.$$

Consider the matrix element of the permutation $P_{n-1,n}$. This is best performed if we use the parentage coefficients to separate also the (n − 1)-st particle:

$$\begin{aligned} & P_{n-1,n} \,|\, (n-1)_t \alpha'' T'', N_t(n) : TT_Z\rangle \\ &= P_{n-1,n} \sum_{\alpha''' T'''_r} \langle (n-1)_t \alpha'' T'' \,|\, (n-2)_{tr} \alpha''' T'''\rangle \\ &\times |\, (n-2)_{tr} \alpha''' T''', \; N_r(n-1) : T''; \; N_t(n) : TT_Z\rangle \\ &= \sum \langle (n-1)_t \alpha'' T'' \,|\, (n-2)_{tr} \alpha''' T'''\rangle \\ &\times |\, (n-2)_{tr} \alpha''' T''', N_r(n) : T''; \; N_t(n-1) : TT_Z\rangle \\ &= \sum_{\alpha''' T''' r T'} \langle (n-1)_t \alpha'' T'' \,|\, (n-2)_{tr} \alpha''' T'''\rangle \\ &\times |\, (n-2)_{tr} \alpha''' T''', N_t(n-1) : T'; \; N_r(n) : TT_Z\rangle \\ &\times U\left(\tfrac{1}{2} T''' T \tfrac{1}{2}; T'' T'\right) (-1)^{T-T'-T''+T'''}. \end{aligned} \tag{2.4}$$

The last transition is carried out by introducing the Racah coefficients $U(\frac{1}{2}T'''T\frac{1}{2}; T''T')$, which are connected with the Racah coefficients W as follows

$$U(abcd; ef) = \sqrt{(2e+1)(2f+1)}\, W(abcd; ef).$$

It is now easy to obtain from (2.4) the permutation matrix element $P_{n-1,n}$, which enters into the right half of (2.3). If all N_S are different, we obtain for $s \neq i$, by using the orthogonality of the single-nucleon functions with different N_S,

$$\begin{aligned} & \langle (n-1)_s \alpha' T', \; N_s(n) : TT_Z \,|\, P_{n-1,n} \,|\, (n-1)_t \alpha'' T'', \; N_t(n) : TT_Z\rangle \\ &= \sum_{\alpha''' T'''} \langle (n-1)_s \alpha' T' \,|\, (n-2)_{ts} \alpha''' T'''\rangle \\ &\times \langle (n-1)_t \alpha'' T'' \,|\, (n-2)_{ts} \alpha''' T'''\rangle, \\ &\times (-1)^{T-T'-T''+T'''} U\left(^1/_2 T''' T^1/_2; T'' T'\right). \end{aligned} \tag{2.5}$$

When s = r, the matrix element is obviously equal to zero.

From the antisymmetry of the functions that determine the matrix elements of the operators P_{kn} in (2.3), it follows with respect to the permutation of the particles 1, 2, . . . , n − 1, that all the matrix elements in (2.3) are identical and have the value given by Eq. (2.5).

We thus obtain for the case when all N_S are different

$$\begin{aligned} Q\langle n\alpha T \,|\, (n-1)_s' \alpha' T'\rangle &= \delta(is)\,\delta(\alpha'\alpha'')\,\delta(T'T'') - (n-1) \\ &\times (1 - \delta(is)) \sum_{\alpha''' T'''} \langle (n-1)_s \alpha' T' \,|\, (n-2)_{is} \alpha''' T'''\rangle \\ &\times \langle (n-1)_t \alpha'' T'' \,|\, (n-2)_{is} \alpha''' T'''\rangle \\ &\times (-1)^{T-T'-T''+T'''} U\left(^1/_2 T''' T^1/_2; T'' T'\right). \end{aligned} \tag{2.6}$$

To determine the normalizing factor Q, we multiply (2.2) by its complex conjugate and integrate over the corresponding variables:

$$\begin{aligned} Q^2 = \langle (n-1)_t \alpha'' T'', \; N_t(n) : TT_Z \,|\, \hat{O} \,|\, (n-1)_t \alpha'' T'', N_t(n) : TT_Z\rangle \\ - \sum_{k=1}^{n-1} P_{kn} \{\langle (n-1)_t \alpha'' T'', N_t(n) : TT_Z\rangle \\ \times |\, \hat{O} \,|\, (n-1)_t \alpha'' T'', N_t(n) : TT_Z\rangle. \end{aligned} \tag{2.7}$$

From calculations analogous to the proceeding ones, we find that $Q^2 = n$ for the case when all N_S are different.

According to the Pauli principle, the same N_S can be found among $N_1, N_2, \dots, N_n$ not more than twice. Consequently, the most general case is that when the $N_1 N_2 \dots N_n$ contains k pairs of equal N, i.e., when the wave function of the n nucleons has the form

TABLE II. Parentage coefficients for n = 4

$\langle N_1N_2N_3N_4\alpha_i T \mid (3)_s\, \alpha' T',\ N_s\rangle$

$T'\alpha'$	$^1/_2a$				$^1/_2b$				$^3/_2$			
T_α \ s	1	2	3	4	1	2	3	4	1	2	3	4
0a	1/2	−1/4	−1/4	1/2	0	$\sqrt{3}/4$	$-\sqrt{3}/4$	0	·	·	·	·
0b	0	$-\sqrt{3}/4$	$-\sqrt{3}/4$	0	−1/2	−1/4	1/4	1/2	·	·	·	·
1a	$-1/\sqrt{6}$	$1/\sqrt{6}$	$-1/\sqrt{6}$	0	$-1/3\sqrt{2}$	$1/3\sqrt{2}$	$-1/3\sqrt{2}$	0	1/6	−1/6	1/6	1/2
1b	0	1/4	−1/4	1/2	$1/2\sqrt{3}$	$-\sqrt{3}/4$	$1/4\sqrt{3}$	0	$1/\sqrt{6}$	0	$-1/\sqrt{6}$	0
1c	$-1/2\sqrt{3}$	$-1/4\sqrt{3}$	$1/4\sqrt{3}$	0	1/3	−1/12	−5/12	1/2	$-1/3\sqrt{2}$	$-\sqrt{2}/3$	$-1/3\sqrt{2}$	0
2									−1/2	1/2	−1/2	1/2

$\langle N_1N_1N_2N_2\,0 \mid N_1N_2N_2\,{}^1/_2,\ N_1\rangle = 1/\sqrt{2}$; $\langle N_1N_1N_2N_2\,0 \mid N_1N_1N_2\,{}^1/_2,\ N_2\rangle = 1/\sqrt{2}$;

$\langle N_1N_1N_2N_3\,0 \mid N_1N_2N_3\,{}^1/_2\,a,\ N_1\rangle = (1/2\sqrt{2})$; $\langle N_1N_1N_2N_3\,0 \mid N_1N_2N_3\,{}^1/_2\,b,\ N_1\rangle = \sqrt{3}/2\sqrt{2}$;

$\langle N_1N_1N_2N_3\,0 \mid N_1N_1N_3\,{}^1/_2,\ N_2\rangle = {}^1/_2$; $\langle N_1N_1N_2N_3\,0 \mid N_1N_1N_3\,{}^1/_2,\ N_3\rangle = {}^1/_2$;

$\langle N_1N_1N_2N_3\,1 \mid N_1N_2N_3\,{}^1/_2\,a,\ N_1\rangle = (1/2\sqrt{2})$; $\langle N_1N_1N_2N_3\,1 \mid N_1N_2N_3\,{}^1/_2\,b,\ N_1\rangle = -1/2\sqrt{6}$;

$\langle N_1N_1N_2N_3\,1 \mid N_1N_1N_3\,{}^1/_2,\ N_2\rangle = -{}^1/_2$; $\langle N_1N_1N_2N_3\,1 \mid N_1N_1N_3\,{}^1/_2,\ N_3\rangle = 1/2$;

$\langle N_1N_1N_2N_3\,1 \mid N_1N_1N_3\,{}^3/_2,\ N_1\rangle = 1/\sqrt{3}$

$\mid N_1N_1N_2N_2 \ldots;\ N_kN_kN_{k+1}N_{k+2} \ldots, N_{n-k}\alpha TT_Z\rangle$.

The formula for the parentage coefficients is derived for such a state of a system of nucleons in the same way as (2.6). We finally obtain

$$\langle n\alpha T \mid (n-1)_i\alpha' T'\rangle = Q^{-1}\Big\{\delta_{is}\delta_{\alpha'\alpha''}\,\delta_{T'T''} - (n-1)$$
$$\times\Big(1-\delta_{is}+\sum_{l=1}^{k}\delta_{il}\delta_{sl}\Big)\sum_{\alpha''T''}\langle (n-1)_s\,\alpha' T' \mid (n-2)_{is}\,\alpha'' T''\rangle$$
$$\times\langle (n-1)_l\,\alpha'' T'' \mid (n-2)_{is}\,\alpha'' T''\rangle\,.$$
$$\times(-1)^{T-T'-T''+T''}U\,({}^1/_2 T''T'{}^1/_2;\ T''T')\Big\};$$
$$Q^2 = n\Big[1-(n-1)\sum_{\alpha''T''}\sum_{l=1}^{k}(-1)^{T-2T''+T''}U\,({}^1/_2 T''T'{}^1/_2;\ T''T'')\delta_{il}$$
$$\times\langle (n-1)_l\alpha'' T''\mid (n-2)_{ll'}\,\alpha'' T''\rangle^2\Big]. \qquad (2.8)$$

In the case of a purely proton or purely neutron configuration, i.e., in the case of maximum isobaric spin, the wave function is merely the Slater determinant and it is obvious that

$$\langle n, T = \frac{n}{2}\Big|(n-1)_s,\ T' = \frac{n-1}{2}\rangle = (-1)^{n+s}(n)^{-1/2}.$$

Not all the states $|n\alpha TT_Z\rangle$, obtained with the aid of all possible initial states, are linearly independent. It is necessary to select from among them the linearly-independent and the orthogonal states. This selection is made easier by the fact that if all N_S are different, the initial states $|(n-1)_i\alpha' T'\rangle$ and $|(n-1)_i\alpha'' T''\rangle$ lead to mutually orthogonal states of the n nucleons. It is also useful to know the total number of linearly independent states, which we have determined by algebraic analysis. A unique construction of the wave function is possible only from experimental data, but for the cases of practical importance, when all the nucleons in the configuration form pairs, or else there are one, two, or three nucleons that form no pairs, the matter is rather simple, since the number of linearly-independent states does not exceed two.

Tables I and II give the parentage coefficients for n = 3 and 4. For n = 3 our coefficients coincide with those of Yoshida,[3] whose results, however, are incomplete. The calculations were carried out with the aid of formulas (2.6), (2.7), and (2.8) and can be extended without difficulty to include the case of more particles.

[1] A. E. Litherland et al., Phys. Rev. **102**, 208 (1956). Can. J. Phys. **36**, 378 (1958); **35**, 1057 (1957). G. Racavy, Nucl. Phys. **4**, 289 (1957).

[2] S. G. Nilsson, Dan. Mat. Fys. Medd. **29**, No. 16, 1955.

[3] S. Yoshida, Progr. Theoret. Phys. **12**, 141 (1954).

[4] D. E. Rutherford, Substitutional Analysis, Edinburgh, 1948. A. H. Jahn, Phys. Rev. **96**, 989 (1954).

[5] A. R. Edmonds and B. H. Flowers, Proc. Roy. Soc. **A214**, 515 (1952).

[6] P. J. Redmond, Proc. Roy. Soc. **A222**, 94 (1954). A. Hassit, Proc. Roy. Soc. **A229**, 110 (1955).

Translated by J. G. Adashko
25

BETA-GAMMA CORRELATION IN FIRST-FORBIDDEN BETA TRANSITIONS

Yu. V. GAPONOV

Nuclear Physics Institute, Moscow State University

Submitted to JETP editor June 30, 1958

J. Exptl. Theoret. Phys. (U.S.S.R.) **36**, 193-203 (January, 1959)

A general formula is derived for the β-γ correlation of β-decay electrons and circularly polarized γ rays emitted by the excited daughter nucleus. First-forbidden β transitions are considered. The calculation is performed for an arbitrary mixture of β couplings, with the nuclear Coulomb field, in particular the so called "Coulomb terms," taken into account. Two special cases are considered, unique and Coulomb transitions.

ONE of the experimental consequences of parity nonconservation in weak interactions[1] is the appearance of spatial asymmetries in the angular distributions of β-decay electrons and circularly polarized γ rays emitted by the excited daughter nucleus. A theoretical calculation of the degree of asymmetry for first-forbidden β transitions was given by Alder, Stech, and Winther.[2] Assuming the β interaction to be a mixture of the s, t, and p covariants, they calculated the angular distribution of β electrons and of γ rays emitted immediately following the β decay. They included effects due to the nuclear Coulomb field but neglected the terms which, in heavy nuclei, give rise to so called "Coulomb" transitions.

The aim of the present work is to study the β-γ angular correlation of circularly polarized γ rays in first-forbidden β transitions, in particular in Coulomb transitions, for an arbitrary mixture of covariants and including Coulomb effects.

The probability that in a γ transition following β decay the γ ray is emitted at an angle θ with respect to the direction of the electron momentum is given by

$$W(\theta) = \sum_R \beta_R \gamma_R P_R(\cos\theta)(2R+1), \qquad (1)$$

where β_R is a coefficient which depends on the characteristics of the β-decay (interaction coupling constants, nuclear matrix elements, electron and neutrino energy and momentum, nuclear charge), and γ_R is a coefficient that depends on the characteristics of the γ transition (spin of the final nucleus, multipole order). The quantity R, which determines the order of the Legendre polynomial $P_R(\cos\theta)$, is related to the order of forbiddeness l by $0 \le R \le 2l+1$, and varies between 0 and 3 in the case of first forbidden β transitions.

The quantity γ_R can be calculated for an arbitrary γ transition — pure electric, or pure magnetic, or mixed. In the case of a pure transition γ_R does not depend on the transition type and is given by

$$\gamma_R = C^{L-\mu R_0}_{L-\mu}\sqrt{(2j_2+1)(2L+1)}\,W(j_2 j_3 RL; Lj_2), \qquad (2)$$

where j_2 is the spin of the excited nucleus formed after β-decay, j_3 is the spin of the final state to which the γ-transition proceeds, and L is the multipole order of the γ-radiation; $\mu = \pm 1$ corresponds to right- and left-circular polarization of the γ ray. $C^{L-\mu R_0}_{L-\mu}$ is a Clebsch-Gordan coefficient[3] and $W(j_2 j_3 RL; Lj_2)$ is a Racah coefficient tabulated in reference 4.

Occasionally the nuclear γ radiation is a mixture of electric radiation of multipole order $L+1$ and magnetic radiation of multipole order L. We denote the ratio of the amplitudes of electric and magnetic radiations in the mixture by a constant Δ, so that the ratio of the corresponding intensities is Δ^2. For such a radiation

$$\gamma_R = C^{L-\mu R_0}_{L-\mu}\sqrt{(2j_2+1)(2L+1)}\,W(j_2 j_3 RL; Lj_2) + 2\mu\Delta\sqrt{\frac{L+2}{2L+1}\frac{2L+1}{2L+3}}\,C^{L-\mu R_0}_{L+1-\mu}\sqrt{(2j_2+1)(2L+1)}\,W \times (j_2 j_3 RL; L+1 j_2) + \Delta^2 C^{L+1-\mu R_0}_{L+1-\mu}\frac{L+2}{2L+3}\sqrt{(2j_2+1)(2L+3)}\,W(j_2 j_3 RL+1; L+1 j_2). \qquad (3)$$

$W(\theta)$ is also given by formula (1) if angular correlation of a β electron with any γ ray from a cascade accompanying the β decay is considered. In that case γ_R will depend on the characteristics of that γ transition as well as on those of the γ transitions preceding it. Thus, if an excited nucleus of spin j_2 is formed following β decay, which emits successive γ rays of multipole order L_1, $L_2 \ldots L_n$ as it cascades through the levels of spin $j_3 \ldots j_{n+2}$, the angular correlation function $W(\theta)$

of the electron and n-th γ ray will contain for a pure radiation

$$\gamma_R = C^{L_n-\mu_n R_0}_{L_n-\mu_n} \sqrt{(2j_{n+1}+1)(2L_n+1)}\, W(j_{n+1} j_{n+2} RL_n; L_n j_{n+1}) \times \prod_{i=1}^{n-1} \sqrt{(2j_{i+1}+1)(2j_{i+2}+1)}\, W(j_{i+1} L_i R j_{i+2}; j_{i+2} j_{i+1}). \quad (4)$$

and for a mixed radiation

$$\gamma_R = [C^{L_n-\mu_n R_0}_{L_n-\mu_n} \sqrt{(2j_{n+1}+1)(2L_n+1)}\, W(j_{n+1} j_{n+2} RL_n; L_n j_{n+1}) + 2\mu_n \Delta_n \sqrt{\frac{L_n+2}{2L_n+1}\frac{2L_n+1}{2L_n+3}}\, C^{L_n-\mu_n R_0}_{L_n+1-\mu_n} \sqrt{(2j_{n+1}+1)(2L_n+3)} \times W(j_{n+1} j_{n+2} RL_n; L_n+1 j_{n+1}) + \Delta_n^2 C^{L_n+1-\mu_n R_0}_{L_n+1-\mu_n} \frac{L_n+2}{2L_n+3} \times \sqrt{(2j_{n+1}+1)(2L_n+3)}\, W(j_{n+1} j_{n+2} RL_n+1; L_n+1 j_{n+1})] \times \prod_{i=1}^{n-1} [\sqrt{(2j_{i+1}+1)(2j_{i+2}+1)}\, W(j_{i+1} L_i R j_{i+2}; j_{i+2} j_{i+1}) + \Delta_i^2 \sqrt{(2j_{i+1}+1)(2j_{i+2}+1)}\, W(j_{i+1} L_i+1 R j_{i+2}; j_{i+2} j_{i+1})], \quad (5)$$

where $\Delta_1, \Delta_2 \ldots \Delta_n$ describe the relative amount of electric and magnetic radiations in the γ transitions $L_1, L_2 \ldots, L_n$, and μ_n gives the circular polarization of the n-th γ ray.

The quantity β_R is calculated in this work for first forbidden β transitions without taking into account finite nuclear size corrections. It has the following form:

$$\beta_R = \sum_{JJ'} f(J, J', R) \sqrt{2j_2+1}\, W(Jj_1 Rj_2; j_2 J'). \quad (6)$$

Here j_1 and j_2 are the spins of the nucleus before and after the β transition, and J and J′ represent the total angular momentum of the electron-neutrino pair and may be equal to l, $l \pm 1$ where l is the order of forbiddenness. $W(Jj_1Rj_2; j_2J')$ is a Racah coefficient.[4] $f(J, J', R)$ is a complicated expression which depends only on the interaction coupling constants and nuclear matrix elements. The form of $f(J, J', R)$ for a general first forbidden transition is given in the Appendix. Some special cases, easy to interpret, are discussed below. The calculations were performed with the β-interaction Hamiltonian as given by Lee and Yang.[1]

The electron wavefunction can be written as follows:[5]

$$\psi_e = \left[A \cdot 1 + B\gamma_4 + Ci\mathbf{p}\cdot\mathbf{r} \cdot 1 + Di\mathbf{p}\cdot\mathbf{r}\gamma_4 + iN\frac{\mathbf{r}}{r}\boldsymbol{\gamma} + iM\frac{\mathbf{r}}{r}\gamma_4\boldsymbol{\gamma}\right] u_\xi, \quad A = {}^1/_2(\gamma_1+1) + i\frac{\alpha Z}{2p}E;$$

$$C = \zeta\frac{\gamma_2+2}{4} + i\frac{\alpha Z}{2p}E\zeta; \quad N = \frac{\gamma_1-1}{2p}; \quad B = -i\frac{\alpha Z}{2p};$$

$$D = -i\frac{\alpha Z}{4p}\zeta; \quad M = i\frac{\alpha Z}{2} + \frac{(\gamma_1-1)}{2p}E; \quad \gamma_1 = \sqrt{1-\alpha^2Z^2};$$

$$\gamma_2 = \sqrt{4-\alpha^2Z^2}; \quad \zeta = \frac{12\Gamma(2\gamma_1+1)}{\Gamma(2\gamma_2+1)}\frac{\Gamma(\gamma_2+i\alpha ZE/p)}{\Gamma(\gamma_1+i\alpha ZE/p)}; \quad (7)$$

where p is the electron momentum, E its total energy, Z is the charge of nucleus 1, γ_4, $\boldsymbol{\gamma}$ are four-by-four matrices, and u_ξ is the unit two-component spinor.

It is easy to see that this form of ψ_e will give rise to three types of terms in first forbidden β transitions: relativistic terms, whose matrix elements are of order v_N/c (v_N is the nucleon velocity in the nucleus), ordinary nonrelativistic terms of order pR_N (R_N is the average nuclear radius), and Coulomb terms of order αZ due to the nuclear Coulomb field. In heavy nuclei the Coulomb terms are dominant and all others may be neglected. Beta transitions of this type are called Coulomb transitions and they are in many respects similar to ordinary allowed transitions. However there is one important difference. Whereas in allowed β transitions terms testing time reversal invariance appear as small corrections, in the case of Coulomb transitions they can play a leading role. This circumstance makes a study of these terms particularly interesting.

Whereas the quantity γ_R can always be calculated from the formulas (2) to (5) if the spins of the excited states of the final nucleus and the multipole order of the γ rays are known, the computation of β_R is complicated by nuclear matrix elements which can be estimated only with great difficulties. This naturally leads to a consideration of various special cases of the general formula where the number of unknown nuclear matrix elements is at a minimum.

1. COULOMB TRANSITIONS

This type of transitions is found in heavy nuclei when the conditions $\alpha Z \gg pR_N$ and $\alpha Z \gg v_N/c$ are satisfied. In this case β_R depends on three kinds of nuclear matrix elements whose numerical value is unknown: $\langle r/r\rangle_1$, $\langle (r/r)\sigma\rangle_0$, $\langle (r/r)\sigma\rangle_1$. All three enter into $\Delta j = 0$ transitions, only $\langle r/r\rangle_1$ and $\langle (r/r)\sigma\rangle_1$ enter into $\Delta j = \pm 1$ transitions so that the asymmetry coefficient depends on two ratios of nuclear matrix elements in the former case and on one ratio in the latter. $\Delta j = \pm 2$ transitions are forbidden. The quantity β_R is given by

$$\beta_0 = [2\mathrm{Re}\, g_{sv} |\langle r/r\rangle_1|^2 - 2\sqrt{2}\,\mathrm{Re}(g_{vt} + g_{sa})\langle r/r\rangle_1 \langle (r/r)\sigma\rangle_1 + 2\mathrm{Re}\, g_{ta}(3|\langle (r/r)\sigma\rangle_0|^2 + 2|\langle (r/r)\sigma\rangle_1|^2)]\left(X_{21}\frac{1}{E} + X_{22}\right)$$
$$- [(g_{ss} + g_{vv})|\langle r/r\rangle_1|^2 - 2\sqrt{2}\,\mathrm{Re}(g_{st} + g_{va})\langle r/r\rangle_1 \langle (r/r)\sigma\rangle_1 + (g_{tt} + g_{aa})(3|\langle (r/r)\sigma\rangle_0|^2 + 2|\langle (r/r)\sigma\rangle_1|^2)]\left(X_{21} + \frac{1}{E}X_{22}\right). \quad (8)$$

$$\beta_1 = \frac{p}{E}\sum_{JJ'}\frac{(\gamma_1-1)^2+\alpha^2Z^2}{4}\Big[(g'_{ss}-g'_{pp})\langle r/r\rangle_J\langle r/r\rangle_{J'}\frac{\sqrt{6}}{3}\delta_{J1}\delta_{J'1}$$

$$-2\,\mathrm{Re}\,(g'_{st}-g'_{pa})\langle r/r\rangle_J\langle(r/r)\sigma\rangle_{J'}\Big(\delta_{J'0}\delta_{J1}+\frac{2\sqrt{3}}{3}\delta_{J'1}\delta_{J1}\Big)$$

$$+2\,\mathrm{Re}\,(g'_{tt}-g'_{aa})\langle(r/r)\sigma\rangle_J\langle(r/r)\sigma\rangle_{J'}\frac{2\sqrt{6}}{3}\delta_{J'1}\delta_{J1}\Big]$$

$$+\frac{\alpha Z}{2p}(1-\gamma_1)\Big[2\,\mathrm{Im}\,g'_{ps}\langle r/r\rangle_J\langle r/r\rangle_{J'}\frac{\sqrt{6}}{3}\delta_{J1}\delta_{J'1}$$

$$-2\,\mathrm{Im}\,(g'_{st}-g'_{sa})\langle r/r\rangle_J\langle(r/r)\sigma\rangle_{J'}\Big(\delta_{J'0}\delta_{J1}+\frac{2\sqrt{3}}{3}\delta_{J1}\delta_{J'1}\Big)$$

$$+2\,\mathrm{Im}\,g'_{at}\langle(r/r)\sigma\rangle_J\langle(r/r)\sigma\rangle_{J'}\frac{2\sqrt{6}}{3}\delta_{J1}\delta_{J'1}\Big]\Big\}$$

$$\times\sqrt{2j_2+1}\,W(Jj_1\,1j_2;\,j_2J').$$

Since R can only be either 0 or 1 it is convenient to write formula (1) as

$$W(\theta) = 1 + \lambda\frac{v}{c}\cos\theta, \qquad (9)$$

where v is the electron velocity and the angular asymmetry coefficient λ is given in terms of β_R and γ_R by

$$\lambda = \frac{E}{p}\frac{\beta_1\gamma_1}{\beta_0\gamma_0}. \qquad (10)$$

Coulomb transitions are of interest mainly in connection with the question of time reversal invariance. Should even one combination of the imaginary parts of the interaction coupling constants turn out to be different from zero, violation of time-reversal invariance would be proven. It is easy to see that the expressions multiplying the imaginary and the real parts of the coupling constants behave differently, namely the former contain an additional factor $\alpha Z/p$ which increases with decreasing electron energy and increasing nuclear charge. Consequently a study of the energy dependence of the asymmetry coefficient λ in heavy nuclei would give an estimate of the contribution of time reversal non-invariant terms in β decay.

Recently a number of hypotheses have been put forward regarding the covariants involved in β decay. One of them, proposed by Feynman and Gell-Mann[6] and consistent with the two-component neutrino theory developed by Landau[7] and Lee and Yang,[8] states that

$$C_s = C'_s = C_t = C'_t = 0; \quad C'_v = C_v; \quad C'_a = C_a, \qquad (11)$$

In that case formula (8) becomes

$$\beta_0 = -[2|C_v|^2|\langle r/r\rangle_1|^2 - 4\sqrt{2}\,\mathrm{Re}\,C_v^*C_a\langle r/r\rangle_1\langle(r/r)\sigma\rangle_1 + 2|C_a|^2(3|\langle(r/r)\sigma\rangle_0|^2+2|\langle(r/r)\sigma\rangle_1|^2)]\Big(X_{21}+\frac{1}{E}X_{22}\Big).$$

$$\beta_1 = -\frac{p}{E}\sum_{JJ'}\frac{(\gamma_1-1)^2+\alpha^2Z^2}{4}\Big[2|C_v|^2\langle r/r\rangle_J\langle r/r\rangle_{J'}\frac{\sqrt{6}}{3}\delta_{J1}\delta_{J'1} - 4\,\mathrm{Re}\,C_vC_a^*\langle r/r\rangle_J\langle(r/r)\sigma\rangle_{J'}\Big(\delta_{J'0}\delta_{J1}+\frac{2\sqrt{3}}{3}\delta_{J1}\delta_{J'1}\Big)$$

$$+2|C_a|^2\langle(r/r)\sigma\rangle_J\langle(r/r)\sigma\rangle_{J'}\frac{2\sqrt{6}}{3}\delta_{J'1}\delta_{J1}\Big]\sqrt{2j_2+1}\,W(Jj_1\,1j_2;\,j_2J'). \qquad (12)$$

Formula (12) permits the study of ratios of nuclear matrix elements and can be used to determine unknown spins of nuclear levels.

Examples of Coulomb β transitions are: Re^{186}, Ir^{194}, Au^{196}, An^{198}, Bi^{212}, Np^{238}.

2. UNIQUE TRANSITIONS $\Delta j = \pm 2$

In this case, as a consequence of selection rules for the nuclear matrix elements, most of the terms in expression (16) are to be omitted. β_R becomes independent of the nuclear matrix elements and is given by

$$\beta_0 = 2\,\mathrm{Re}\,g_{at}\Big[q^2\Big(X_1\frac{1}{E}+X_2\Big)+\frac{p^2}{3}\Big(X_{13}\frac{1}{E}+X_{14}\Big)\Big]$$

$$+(g_{tt}+g_{aa})\Big[q^2\Big(X_1+\frac{1}{E}X_2\Big)+\frac{p^2}{3}\Big(X_{13}+\frac{1}{E}X_{14}\Big)\Big];$$

$$\beta_1 = -\frac{\sqrt{30}}{6}\frac{p}{E}\Big[(g'_{tt}-g'_{aa})\Big(q^2X_3+\frac{p^2}{5}X_{15}\Big)$$

$$+2\,\mathrm{Im}\,g'_{at}\Big(q^2X_4+\frac{p^2}{5}X_{16}\Big)\Big]\sqrt{2j_2+1}\,W(2j_1\,1j_2;\,j_2 2);$$

$$\beta_2 = -\frac{\sqrt{70}}{90}p^2\Big[2\,\mathrm{Re}\,g_{at}\Big(X_{13}\frac{1}{E}+X_{14}\Big)$$

$$+(g_{tt}+g_{aa})\Big(X_{13}+\frac{1}{E}X_{14}\Big)\Big]\sqrt{2j_2+1}\,W(2j_1\,2j_2;\,j_2 2);$$

$$\beta_3 = \frac{\sqrt{70}}{35}\frac{p^3}{E}[(g'_{tt}-g'_{aa})X_{15}$$

$$+2\,\mathrm{Im}\,g'_{at}X_{16}]\sqrt{2j_2+1}\,W(2j_1\,3j_2;\,j_2 2). \qquad (13)$$

The X_i are given in the Appendix, formulas (17).

As in the case of Coulomb β transitions the terms violating time reversal invariance have an additional factor $\alpha Z/p$. If time-reversal invariance holds and the hypothesis (11) is valid the quantities β_R may be calculated exactly since they are then independent of the interaction coupling constants. Omitting factors common to all β_R and irrelevant for $W(\theta)$ we obtain from (13)

$$\beta_0 = q^2\Big(X_1+\frac{1}{E}X_2\Big)+\frac{p^2}{3}\Big(X_{13}+\frac{1}{E}X_{14}\Big);$$

$$\beta_1 = \frac{\sqrt{30}}{6}\frac{v}{c}\Big(q^2X_3+\frac{p^2}{5}X_{15}\Big)\sqrt{2j_2+1}\,W(2j_1\,1j_2;\,j_2 2);$$

$$\beta_2 = -\frac{\sqrt{70}}{90}p^2\Big(X_{13}+\frac{1}{E}X_{14}\Big)\sqrt{2j_2+1}\,W(2j_1\,2j_2;\,j_2 2);$$

$$\beta_3 = -\frac{v}{c}p^2\frac{\sqrt{70}}{35}X_{15}\sqrt{2j_2+1}\,W(2j_1\,3j_2;\,j_2 2). \qquad (14)$$

$\langle A\rangle_J\,\langle B\rangle_{J'}$	$K(A,B,R)$
$\langle\gamma_5\rangle_0\,\langle\gamma_5\rangle_0$	$\left[(g_{aa}+g'_{pp})\left(X_1+\frac{1}{E}X_2\right)-2\mathrm{Re}\,g_{ap}\left(X_1\frac{1}{E}+X_3\right)\right]3\delta_{R0}$
$\langle\gamma_5\rangle_0\,\langle\alpha\rangle_1$	$[2\mathrm{Re}\,(g'_{ap}-g'_{pt})X_3+2\mathrm{Im}\,(g'_{at}-g'_{pa})X_4]\frac{p}{E}3\delta_{R1}$
$\langle\alpha\rangle_1\,\langle\alpha\rangle_1$	$\left[(g_{vv}+g_{tt})\left(X_1+\frac{1}{E}X_2\right)-2\mathrm{Re}\,g_{vt}\left(X_1\frac{1}{E}+X_3\right)\right]3\sqrt{3}\delta_{R0}+[(g'_{vv}-g'_{tt})X_3-2\mathrm{Im}\,g'_{tv}X_4]\frac{p}{E}\sqrt{6}\delta_{R1}$
$\langle r\rangle_1\,\langle r\rangle_1$	$\left[2\mathrm{Re}\,g_{sv}\left(X_1\frac{1}{E}+X_2\right)+(g_{ss}+g_{vv})\left(X_1+\frac{1}{E}X_2\right)\right]\left(q^2\sqrt{3}\delta_{R0}+\frac{p^2}{3}\sqrt{3}\delta_{R0}-p^2\frac{\sqrt{30}}{15}\delta_{R2}\right)$
	$+[2\mathrm{Re}\,(g_{ss}-g_{vv})X_3+2\mathrm{Im}\,(g_{vs}-g_{sv})X_5]\frac{p^2q}{E}\left(-\frac{\sqrt{3}}{3}\delta_{R0}+\frac{\sqrt{30}}{15}\delta_{R2}\right)$
$\langle r\rangle_1\,\langle r\sigma\rangle_0$	$[2\mathrm{Re}\,(g'_{st}-g'_{vv})X_{15}+2\mathrm{Im}\,(g'_{vt}-g'_{sa})X_{16}]\frac{p^3}{E}\frac{1}{3}\delta_{R1}+[2\mathrm{Re}\,(g'_{st}-g'_{va})X_3+2\mathrm{Im}\,(g'_{vt}-g'_{sa})X_4]\frac{pq^2}{E}\frac{1}{3}\delta_{R1}$
	$+\left[4\mathrm{Re}\,(g'_{vt}+g'_{sa})\left(X_5\frac{1}{E}+X_6\right)+4\mathrm{Re}\,(g'_{st}+g'_{va})\left(X_5+\frac{1}{E}X_6\right)\right]\frac{pq}{3}\delta_{R1}$
$\langle r\rangle_1\,\langle r\sigma\rangle_1$	$[2\mathrm{Re}\,(g'_{va}-g'_{st})X_3+2\mathrm{Im}\,(g'_{sa}-g'_{vt})X_4]\frac{pq^2}{E}\frac{\sqrt{3}}{3}\delta_{R1}+[2\mathrm{Re}\,(g_{sv}-g_{ts})X_7+2\mathrm{Im}\,(g_{as}-g_{tv})X_8]\frac{p^2q}{E}\left(\frac{\sqrt{6}}{3}\delta_{R0}-\frac{2\sqrt{15}}{15}\delta_{R2}\right)$
	$+[2\mathrm{Re}\,(g_{st}-g_{va})X_7+2\mathrm{Im}\,(g_{vt}-g_{sa})X_8]\frac{p^2q}{E}\left(\frac{\sqrt{6}}{3}\delta_{R0}+\frac{2\sqrt{15}}{15}\delta_{R2}\right)$
	$+\left[2\mathrm{Re}(g'_{vt}+g'_{sa})\left(X_5\frac{1}{E}+X_6\right)+2\mathrm{Re}(g'_{st}+g'_{va})\left(X_5+\frac{1}{E}X_6\right)\right]pq\frac{\sqrt{3}}{3}\delta_R$
$\langle r\rangle_1\,\langle r\sigma\rangle_2$	$[2\mathrm{Re}\,(g'_{st}-g'_{va})X_3+2\mathrm{Im}\,(g'_{vt}-g'_{sa})X_4]\frac{p}{E}\left(q^2\frac{\sqrt{5}}{3}\delta_{R1}+p^2\frac{2\sqrt{5}}{15}\delta_{R1}-p^2\frac{\sqrt{70}}{35}\delta_{R3}\right)+[2\mathrm{Re}(g_{st}-g_{va})X_7+2\mathrm{Im}(g_{vt}-g_{sa})X_8]$
	$\times\frac{p^2q}{E}\frac{\sqrt{5}}{5}\delta_{R2}+\left[2\mathrm{Re}\,(g'_{vt}+g'_{sa})\left(X_5\frac{1}{E}+X_6\right)+2\mathrm{Re}\,(g'_{st}+g'_{va})\left(X_5+\frac{1}{E}X_6\right)\right]pq\frac{\sqrt{5}}{3}\delta_{R1}$
$\langle r\sigma\rangle_0\,\langle r\sigma\rangle_0$	$\left[2\mathrm{Re}\,g_{at}\left(X_1\frac{1}{E}+X_2\right)+(g_{tt}+g_{aa})\left(X_1+\frac{1}{E}X_2\right)\right]q^2\delta_{R0}+\left[2\mathrm{Re}\,g_{at}\left(X_{13}\frac{1}{E}+X_{14}\right)+(g'_{tt}+g_{aa})\left(X_{13}+\frac{1}{E}X_{14}\right)\right]\frac{p^2}{3}\delta_{R0}$
	$+[2\mathrm{Re}\,(g_{aa}-g_{tt})X_7+2\mathrm{Im}\,(g_{ta}-g_{at})X_8]\frac{p^2q}{E}\delta_{R0}$
$\langle r\sigma\rangle_1\,\langle r\sigma\rangle_0$	$\left[2\mathrm{Re}\,g'_{at}\left(X_5\frac{1}{E}+X_6\right)+2\mathrm{Re}\,(g'_{tt}+g'_{aa})\left(X_5+\frac{1}{E}X_6\right)\right]pq\frac{\sqrt{2}}{3}\delta_{R1}$
$\langle r\sigma\rangle_0\,\langle r\sigma\rangle_2$	$[2\mathrm{Re}\,(g_{tt}-g_{aa})X_7+2\mathrm{Im}\,(g_{at}-g_{ta})X_8]\frac{p^2q}{E}\frac{\sqrt{10}}{5}\delta_{R2}$
$\langle r\sigma\rangle_1\,\langle r\sigma\rangle_1$	$[2\mathrm{Re}\,(g_{tt}-g_{aa})X_7+2\mathrm{Im}\,(g_{at}-g_{ta})X_8]\frac{p^2q}{E}\left(\frac{2\sqrt{3}}{3}\delta_{R0}+\frac{\sqrt{30}}{15}\delta_{R2}\right)$
	$+\left[2\mathrm{Re}\,g_{at}\left(X_1\frac{1}{E}+X_2\right)+(g_{tt}+g_{aa})\left(X_1+\frac{1}{E}X_2\right)\right]q^2\sqrt{3}\delta_{R0}-[(g'_{tt}-g'_{aa})X_3+2\mathrm{Im}\,g'_{at}X_4]\frac{pq^2}{E}\frac{\sqrt{6}}{6}\delta_{R1}$
	$+\left[2\mathrm{Re}\,g_{at}\left(X_{13}\frac{1}{E}+X_{14}\right)+(g_{tt}+g_{aa})\left(X_{13}+\frac{1}{E}X_{14}\right)\right]\frac{p^2}{3}\left(\sqrt{3}\delta_{R0}+\frac{\sqrt{30}}{30}\delta_{R2}\right)-[(g'_{tt}-g'_{aa})X_{15}+2\mathrm{Im}\,g'_{at}X_{16}]\frac{p^3}{E}\frac{\sqrt{6}}{6}\delta_{R1}$
	$+\left[4\mathrm{Re}\,g'_{at}\left(X_5\frac{1}{E}+X_6\right)+2\mathrm{Re}\,(g'_{tt}+g'_{aa})\left(X_5+\frac{1}{E}X_6\right)\right]pq\frac{\sqrt{6}}{3}\delta_{R1}$
$\langle r\sigma\rangle_1\,\langle r\sigma\rangle_2$	$[2\mathrm{Re}\,(g_{tt}-g_{aa})X_7+2\mathrm{Im}\,(g_{at}-g_{ta})X_8]\frac{p^2q}{E}\frac{\sqrt{10}}{5}\delta_{R1}+\left[4\mathrm{Re}\,g'_{at}\left(X_5\frac{1}{E}+X_6\right)+2\mathrm{Re}\,(g'_{tt}+g'_{aa})\left(X_5+\frac{1}{E}X_6\right)\right]pq\frac{\sqrt{10}}{3}\delta_{R1}$
$\langle r\sigma\rangle_2\,\langle r\sigma\rangle_2$	$\left[2\mathrm{Re}\,g_{ta}\left(X_1\frac{1}{E}+X_2\right)+(g_{tt}+g_{aa})\left(X_1+\frac{1}{E}X_2\right)\right]q^2\sqrt{5}\delta_{R0}-[(g'_{tt}-g'_{aa})X_3+2\mathrm{Im}\,g'_{at}X_4]\frac{pq^2}{E}\frac{\sqrt{30}}{6}\delta_{R1}$
	$+\left[2\mathrm{Re}\,g_{ta}\left(X_{13}\frac{1}{E}+X_{14}\right)+(g_{tt}+g_{aa})\left(X_{13}+\frac{1}{E}X_{14}\right)\right]\frac{p^2}{3}\left(\sqrt{5}\delta_{R0}-\frac{\sqrt{70}}{30}\delta_{R2}\right)-[(g'_{tt}-g'_{aa})X_{15}+2\mathrm{Im}\,g'_{at}X_{16}]\frac{p^3}{E}\left(\frac{\sqrt{30}}{30}\delta_{R1}-\frac{\sqrt{70}}{35}\delta_{R3}\right)$
$\langle r\,|\,r\rangle_1\,\langle r\rangle_1$	$\left[2\mathrm{Re}\,(g_{sv}-g_{vs})\left(X_9+\frac{1}{E}X_{10}\right)+2(g_{vv}-g_{ss})X_{10}\right]p\sqrt{3}\delta_{R0}+[4\mathrm{Re}\,g'_{sv}X_{11}+2(g'_{ss}+g'_{vv})X_{12}]\frac{p^2}{E}\frac{\sqrt{6}}{3}\delta_{R1}$
	$+[4\mathrm{Re}\,g_{sv}X_{19}+2\mathrm{Re}\,(g_{ss}+g_{vv})X_{20}]\frac{p^2}{E}\left(-\frac{\sqrt{3}}{3}\delta_{R0}+\frac{\sqrt{30}}{15}\delta_{R2}\right)$
$\langle r\,|\,r\rangle_1\langle r\sigma\rangle_0$	$-[2\mathrm{Re}\,(g'_{ts}+g'_{as})X_{11}+2\mathrm{Re}\,(g'_{ts}+g'_{av})X_{12}]\frac{p^2}{E}\delta_{R1}+\left[2\mathrm{Re}\,(g'_{av}-g'_{ts})\left(X_{17}\frac{1}{E}+X_{18}\right)+2\mathrm{Re}(g'_{ts}-g'_{as})\left(X_{17}+\frac{1}{E}X_{18}\right)\right]\frac{p}{3}\delta_{R1}$

$\langle A\rangle_J\langle B\rangle_{J'}$	$K(A,B,R)$
$\langle r/r\rangle_1\langle r\sigma\rangle_1$	$\left[2\mathrm{Re}\,(g_{ao}-g'_{to})\left(X_9\frac{1}{E}+X_{10}\right)+2\mathrm{Re}(g_{to}-g_{as})\left(X_9+\frac{1}{E}X_{10}\right)\right]p\sqrt{6}\,\delta_{R0}$
	$+[2\mathrm{Re}\,(g'_{to}+g'_{as})X_{11}+2\mathrm{Re}\,(g'_{ts}+g'_{av})X_{12}]\frac{p^2}{E}\frac{2\sqrt{3}}{3}\delta_{R1}$
	$+[2\mathrm{Re}\,(g_{ct}+g_{sa})X_{19}+2\mathrm{Re}\,(g_{st}+g_{va})X_{20}]\frac{p^2}{E}\left(\frac{\sqrt{6}}{3}\delta_{R0}+\frac{\sqrt{15}}{15}\delta_{R2}\right)$
	$+\left[2\mathrm{Re}\,(g'_{av}-g'_{ts})\left(X_{17}\frac{1}{E}+X_{18}\right)+2\mathrm{Re}(g'_{to}-g'_{as})\left(X_{17}+\frac{1}{E}X_{18}\right)\right]p\frac{\sqrt{3}}{3}\delta_{R1}$
$\langle r/r\rangle_1\langle r\sigma\rangle_2$	$[2\mathrm{Re}\,(g_{ct}+g_{sa})X_{19}+2\mathrm{Re}\,(g_{st}+g_{va})X_{20}]\frac{p^2}{E}\frac{\sqrt{5}}{5}\delta_{R2}+\left[2\mathrm{Re}\,(g'_{av}-g'_{ts})\left(X_{17}\frac{1}{E}+X_{18}\right)+2\mathrm{Re}(g'_{to}-g'_{as})\left(X_{17}+\frac{1}{E}X_{18}\right)\right]p\frac{\sqrt{5}}{3}\delta_{R1}$
$\langle(r/r)\sigma\rangle_0\langle r\rangle_1$	$[2\mathrm{Re}\,(g'_{to}+g'_{sa})X_{11}+2\mathrm{Re}\,(g'_{st}+g'_{va})X_{12}]\frac{p^2}{E}\delta_{R1}+\left[2\mathrm{Re}\,(g'_{sb}-g'_{va})\left(X_{17}\frac{1}{E}+X_{18}\right)+2\mathrm{Re}\,(g'_{ct}-g'_{sa})\left(X_{17}+\frac{1}{E}X_{18}\right)\right]p\delta_{R1}$
$\langle(r/r)\sigma\rangle_0\langle r\sigma\rangle_0$	$\left[2\mathrm{Re}\,(g_{aa}-g_{tt})X_{10}+2\mathrm{Re}\,(g_{ta}-g_{at})\left(X_9+\frac{1}{E}X_{10}\right)\right]p3\delta_{R0}-[4\mathrm{Re}\,g_{ta}X_{10}+2\mathrm{Re}\,(g_{tt}+g_{aa})X_{20}]\frac{p^2}{E}\delta_{R0}$
$\langle(r/r)\sigma\rangle_0\langle r\sigma\rangle_1$	$[4\mathrm{Re}\,g'_{at}X_{11}+2\,(g'_{tt}+g'_{aa})X_{12}]\frac{p^2}{E}\sqrt{2}\,\delta_{R1}$
$\langle(r/r)\sigma\rangle_0\langle r\sigma\rangle_2$	$[4\mathrm{Re}\,g_{ta}X_{19}+2\mathrm{Re}\,(g_{tt}+g_{aa})X_{20}]\frac{p^2}{E}\frac{\sqrt{10}}{5}\delta_{R2}$
$\langle(r/r)\sigma\rangle_1\langle r\rangle_1$	$\left[2\mathrm{Re}\,(g_{st}-g_{va})\left(X_9\frac{1}{E}+X_{10}\right)+2\mathrm{Re}\,(g_{ct}-g_{sa})\left(X_9+\frac{1}{E}X_{10}\right)\right]p\sqrt{6}\delta_{R0}$
	$-[2\mathrm{Re}\,(g'_{ct}+g'_{sa})X_{11}+2\mathrm{Re}\,(g'_{st}+g'_{va})X_{12}]\frac{p^2}{E}\frac{2\sqrt{3}}{3}\delta_{R1}$
	$+[2\mathrm{Re}\,(g_{to}+g_{as})X_{19}+2\mathrm{Re}\,(g_{ts}+g_{av})X_{20}]\frac{p^2}{E}\left(\frac{\sqrt{6}}{3}\delta_{R0}-\frac{2\sqrt{15}}{15}\delta_{R2}\right)$
$\langle(r/r)\sigma\rangle_1\langle r\sigma\rangle_0$	$-[4\mathrm{Re}\,g'_{to}X_{11}+2\,(g'_{tt}+g'_{aa})X_{12}]\frac{p^2}{E}\sqrt{2}\,\delta_{R1}+\left[2\mathrm{Re}\,(g'_{tt}-g'_{aa})X_{18}-2\mathrm{Im}\,g'_{at}\left(X_{17}+\frac{1}{E}X_{18}\right)\right]p\frac{\sqrt{2}}{3}\delta_{R1}$
$\langle(r/r)\sigma\rangle_1\langle r\sigma\rangle_1$	$[2\mathrm{Re}\,(g_{tt}-g_{aa})X_{19}+2\mathrm{Re}\,(g_{at}-g_{ta})X_9]p2\sqrt{3}\,\delta_{R0}+[4\mathrm{Re}\,g'_{ta}X_{11}+2(g'_{tt}+g'_{aa})X_{12}]\frac{p^2}{E}\delta_{R1}\left(-\frac{2\sqrt{6}}{3}\right)$
	$+[4\mathrm{Re}\,g_{ta}X_{19}+2\mathrm{Re}\,(g_{tt}+g_{aa})X_{20}]\frac{p^2}{E}\left(-\frac{2\sqrt{3}}{3}\delta_{R0}-\frac{\sqrt{30}}{15}\delta_{R2}\right)+\left[2\mathrm{Re}\,(g'_{tt}-g'_{aa})X_{18}-2\mathrm{Im}\,g'_{at}\left(X_{17}+\frac{1}{E}X_{18}\right)\right]p\frac{\sqrt{6}}{3}\delta_{R1}$
$\langle(r/r)\sigma\rangle_1\langle r\sigma\rangle_2$	$-[4\mathrm{Re}\,g_{ta}X_{19}+2\mathrm{Re}\,(g_{tt}+g_{aa})X_{20}]\frac{p^2}{E}\frac{\sqrt{10}}{5}\delta_{R2}+\left[2\mathrm{Re}\,(g'_{tt}-g'_{aa})X_{18}-2\mathrm{Im}\,g'_{at}\left(X_{17}+\frac{1}{E}X_{18}\right)\right]p\frac{\sqrt{10}}{3}\delta_{R1}$
$\langle(r/r)\sigma\rangle_1\langle r/r\rangle_1$	$\left[2\mathrm{Re}\,g_{sv}\left(X_{21}\frac{1}{E}+X_{22}\right)-(g_{ss}+g_{vv})\left(X_{21}+\frac{1}{E}X_{22}\right)\right]\sqrt{3}\,\delta_{R0}+[(g'_{ss}-g'_{vv})X_{23}+2\mathrm{Im}\,g'_{sv}X_{24}]\frac{p}{E}\frac{\sqrt{6}}{3}\delta_{R1}$
$\langle r/r\rangle_1\langle(r/r)\sigma\rangle_0$	$[2\mathrm{Re}\,(g'_{va}-g'_{st})X_{23}+2\mathrm{Im}\,(g'_{sa}-g'_{vt})X_{24}]\frac{p}{E}\delta_{R1}$
$\langle r/r\rangle_1\langle(r/r)\sigma\rangle_1$	$-\left[2\mathrm{Re}\,(g_{vt}+g_{sa})\left(X_{21}\frac{1}{E}+X_{22}\right)-2\mathrm{Re}(g_{st}+g_{va})\left(X_{21}+\frac{1}{E}X_{22}\right)\right]\sqrt{6}\,\delta_{R0}$
	$+[2\mathrm{Re}\,(g'_{va}-g'_{st})X_{23}+2\mathrm{Im}\,(g'_{sa}-g'_{vt})X_{24}]\frac{p}{E}\frac{2\sqrt{3}}{3}\delta_{R1}$
$\langle(r/r)\sigma\rangle_0\langle(r/r)\sigma\rangle_0$	$\left[2\mathrm{Re}\,g_{ta}\left(X_{21}\frac{1}{E}+X_{22}\right)-(g_{tt}+g_{aa})\left(X_{21}+\frac{1}{E}X_{22}\right)\right]3\delta_{R0}$
$\langle(r/r)\sigma\rangle_1\langle(r/r)\sigma\rangle_1$	$\left[2\mathrm{Re}\,g_{ta}\left(X_{21}\frac{1}{E}+X_{22}\right)-(g_{tt}+g'_{aa})\left(X_{21}+\frac{1}{E}X_{22}\right)\right]2\sqrt{3}\,\delta_{R0}+[(g'_{tt}-g'_{aa})X_{23}+2\mathrm{Im}\,g'_{at}X_{24}]\frac{p}{E}\frac{2\sqrt{6}}{3}\delta_{R1}$

Comparison of these exact results with experiment makes it possible to check the validity of time reversal invariance for β decay. For unique β transitions the experiments could be performed with the Y^{91} nucleus, for which $j_1 = 1/2$ and $j_2 = 5/2$.[9] Formulas (14) then give

$$\begin{aligned}
&\beta_0 = q^2\left(X_1+\frac{1}{E}X_2\right)+\frac{p^2}{3}\left(X_{13}+\frac{1}{E}X_{14}\right);\\
&\beta_1 = \frac{\sqrt{42}}{18}\frac{v}{c}\left(q^2X_3+\frac{p^2}{5}X_{15}\right);\\
&\beta_2 = -\frac{\sqrt{21}}{9\cdot15}p^2\left(X_{13}+\frac{1}{E}X_{14}\right);\quad \beta_3 = -\frac{\sqrt{7}}{35}p^2\frac{v}{c}X_{15}.
\end{aligned}\tag{15}$$

To summarize: the study of β-γ angular correlation of circularly polarized γ-rays in first forbidden β-transitions is of interest in two cases: Coulomb transitions in heavy nuclei and unique transitions. Apparently only in these cases is a simple interpretation of the results possible.

The author expresses his gratitude to Prof. I. S. Shapiro, who suggested this research, for valuable advice and constant attention.

APPENDIX

For a general first forbidden β transition the quantity $f(J, J', R)$ [cf. formula (6)] has the form

$$f(J, J', R) = \sum_{A,B} \langle A \rangle_J \langle B \rangle_{J'} K(A, B, R), \qquad (16)$$

where $\langle A \rangle_J$ and $\langle B \rangle_{J'}$ denote arbitrary nuclear reduced matrix elements. Thus $f(J, J', R)$ is the sum of all possible products of pairs of such elements weighted by the factor $K(A, B, R)$ which depends on their specific form. The table lists all nonzero values of $K(A, B, R)$ for different pairs of matrix elements $\langle A \rangle_J$ and $\langle B \rangle_{J'}$. In the calculations $\langle A \rangle_J$ and $\langle B \rangle_{J'}$ were assumed to be real.

The table contains a number of abbreviations. The quantities g_{yz} and g'_{yz} stand for the following combinations of coupling constants:

$$g_{yz} = C_y C_z^* + C'_y C'^*_z; \quad g'_{yz} = C_y C'^*_z + C'_y C_z^*.$$

Here C_y, C'_y are the coupling constants for the covariant y (y corresponds to s, t, p, etc.), where the primed ones take into account parity nonconservation in β decay.

The quantities X_i have the following values:

$$X_1 = \frac{(\gamma_1+1)^2}{4} + \frac{\alpha^2 Z^2}{4}\frac{E^2+1}{p^2}; \quad X_2 = -\frac{\alpha^2 Z^2}{2}\frac{E}{p^2}; \quad X_3 = \frac{(\gamma_1+1)^2+\alpha^2 Z^2}{4}; \quad X_4 = \frac{\alpha Z}{2p}(\gamma_1+1);$$

$$X_5 = \zeta^* \frac{1}{8}\left[(\gamma_1+1)(\gamma_2+2) + \frac{\alpha^2 Z^2 (E^2+1)}{p^2} + i\frac{\alpha Z E}{p}(\gamma_2-\gamma_1+1)\right]; \quad X_6 = -\frac{1}{8}\zeta^*\left[\frac{\alpha^2 Z^2}{p^2}E + i\frac{\alpha Z}{p}(\gamma_2-\gamma_1+1)\right];$$

$$X_7 = \frac{1}{8p}\zeta^*[p(\gamma_1+1)(\gamma_2+2) + \alpha^2 Z^2 p + i\alpha Z E(\gamma_2-\gamma_1+1)]; \quad X_8 = \frac{\alpha Z}{8p}(\gamma_2+\gamma_1+3)\zeta^*; \quad X_9 = i\frac{\alpha^2 Z^2}{2p}; \quad X_{10} = \frac{\alpha Z}{2}\gamma_1;$$

$$X_{11} = \frac{\alpha Z E}{2p^2}(1-\gamma_1); \quad X_{12} = \frac{\alpha Z}{4p^2}(E^2+1)(\gamma_1-1) - \frac{\alpha Z}{4}(\gamma_1+1); \quad X_{13} = \frac{|\zeta|^2}{16}\left[(\gamma_2+2)^2 + \alpha^2 Z^2\frac{E^2+1}{p^2}\right]; \quad X_{14} = -|\zeta|^2\frac{\alpha^2 Z^2}{8}\frac{E}{p^2};$$

$$X_{15} = |\zeta|^2\frac{(\gamma_2+2)^2+\alpha^2 Z^2}{16}; \quad X_{16} = \frac{\alpha Z}{8p}|\zeta|^2(\gamma_2+2); \quad X_{17} = i\zeta\frac{(\gamma_2+2)(\gamma_1-1)-\alpha^2 Z^2}{8p};$$

$$X_{18} = X_{20} = \frac{\zeta}{8p}[\alpha Z p(\gamma_2-\gamma_1+3) + i(\gamma_2+2)(\gamma_1-E) + i\alpha^2 Z^2 E]; \quad X_{19} = \zeta\left[\frac{\alpha Z E}{p^2}(\gamma_1-1)^2 - i\frac{(\gamma_2+2)(\gamma_1-1)+\alpha^2 Z^2}{8p}\right];$$

$$X_{21} = \frac{(\gamma_1-1)^2}{4}\frac{E^2+1}{p^2} + \frac{\alpha^2 Z^2}{4}; \quad X_{22} = \frac{(\gamma_1-1)^2 E}{2p^2}; \quad X_{23} = \frac{(\gamma_1-1)^2+\alpha^2 Z^2}{4}; \quad X_{24} = \frac{\alpha Z}{2p}(1-\gamma_1). \qquad (17)$$

The general expression for $f(J, J', R)$ contains a number of reduced matrix elements satisfying definite selection rules in the total angular momentum $J(J')$ of the electron-neutrino pair and in parity. Our notation for the reduced matrix elements differs from the generally accepted one, but it simplifies the final results. We give these matrix elements below in the notation of Rose and Osborn[10] together with the appropriate selection rules. Nuclear matrix elements differing by the operator $\beta = \gamma_4$ were assumed to be the same.

$$\langle r \rangle_J = (j_2 \| Y_1(\mathbf{r}) \| j_1); \quad J = 1, \quad |j_2 - j_1| \leqslant J \leqslant j_2 + j_1, \text{ yes};$$

$$\langle r\sigma \rangle_J = (j_2 \| T_{j_1}(\mathbf{r}, \sigma) \| j_1); \quad 0 \leqslant J \leqslant 2, \quad |j_2 - j_1| \leqslant J \leqslant j_2 + j_1, \text{ yes}; \quad \langle \gamma_5 \rangle_J = \frac{1}{M}(j_2 \| Y_0(\mathbf{r})\, \sigma \cdot \mathbf{p} \| j_1); \quad J = 0, \quad j_2 = j_1, \text{ yes};$$

$$\langle \alpha \rangle_J = -\frac{1}{M}(j_2 \| T_{10}(\mathbf{r}, \mathbf{p}_n) \| j_1); \quad J = 1, \quad |j_2 - j_1| \leqslant J \leqslant j_2 + j_1, \text{ yes};$$

$$\langle r/r \rangle_J = \left(j_2 \left\| \frac{1}{r} Y_1(\mathbf{r}) \right\| j_1\right); \quad J = 1, \quad |j_2 - j_1| \leqslant J \leqslant j_2 + j_1, \text{ yes};$$

$$\langle (r/r)\sigma \rangle_J = \left(j_2 \left\| \frac{1}{r} T_{j_1}(\mathbf{r}, \sigma) \right\| j_1\right); \quad J = 0, 1, \quad |j_2 - j_1| \leqslant J \leqslant j_2 + j_1, \text{ yes}. \qquad (18)$$

Note added in proof (August 28, 1958). Recently M. Morita and S. Morita published an article (Phys. Rev. 109, 2048 (1958)) containing formulas for β-γ correlation of circularly polarized γ-rays for arbitrary mixtures of covariants but without interference terms between the s, t, p and v, a covariants. The case $\alpha Z \gg 1$ is considered, but the concept of Coulomb β-transitions is not introduced.

[1] T. D. Lee and C. N. Yang, Phys. Rev. **104**, 254 (1956).

[2] Alder, Stech, and Winther, Phys. Rev. **107**, 728 (1957).

[3] G. Racah, Phys. Rev. **62**, 438 (1942).

[4] Biedenharn, Blatt, and Rose, Revs. Modern Phys. **24**, 249 (1952).

[5] Berestezky, Joffe, Rudik, and Ter-Martirosyan, Nucl. Phys. **5**, 464 (1958).

[6] R. P. Feynman and M. Gell-Mann, Phys. Rev. **109**, 193 (1958).

[7] L. D. Landau, J. Exptl. Theoret. Phys. (U.S.S.R.) **32**, 407 (1957), Soviet Phys. JETP **5**, 337 (1957).

[8] T. D. Lee and C. N. Yang, Phys. Rev. **105**, 1671 (1957).

[9] B. S. Dzhelepov and L. K. Peker, Схемы распада радиоактивных изотопов (Decay Schemes of Radioactive Isotopes), Acad. Sci. Press, 1957.

[10] M. E. Rose and R. K. Osborn, Phys. Rev. **93**, 1326 (1954).

Translated by A. M. Bincer
26

GREEN'S FUNCTION FOR THE RESONANCE RADIATION DIFFUSION EQUATION

V. A. VEKLENKO

Moscow Power Institute

Submitted to JETP editor June 30, 1958

J. Exptl. Theoret. Phys. (U.S.S.R.) **36**, 204-211 (January, 1959)

An analytic expression for the Green's function of the resonance radiation diffusion equation has been derived for the case of a homogeneous infinite space. The properties of the Green's function have been investigated for dispersion and Doppler spectral lines. An analytic expression has been derived for the mean time required for photon to move as a result of diffusion over a distance greater than some prescribed value. In conclusion, the Green's function has been determined for the stationary equation and its asymptotic expression is given in explicit form for a dispersion spectral line.

1. INTRODUCTION

THE theory of resonance radiation leads to a Fredholm integral equation of the second order relative to the concentration of the excited atoms. Biberman[1,7] formulated this equation for stationary problems under the following assumptions: (1) all the atoms have one resonant level, (2) the diffusion of the atoms can be neglected compared with the diffusion of the photons; (3) one can neglect the reduction in the number of normal atoms due to excitation or ionization of some of the normal atoms; (4) the role of negative absorption is unimportant; (5) the mean-free-path time of the photon is small compared with the duration of the excited state of the atom; (6) the frequency of the photon emitted by the atom is independent of the frequency of the absorbed quantum within the limits of the given spectral line.

The integral equation of diffusion of resonance radiation is first encountered for non-stationary problems in the papers of Holstein.[2,3] However, since he investigated the rate of emission of the gases by determining the cessation of their excitation, Holstein was interested only in the first eigenvalue of the equation, which he calculated by the Ritz method.

We shall show here that by retaining Biberman's assumptions and by considering the diffusion of radiation in an infinite homogeneous medium it is possible to obtain an analytic expression for the Green's function $f(\mathbf{r}, t)$ for this problem.

In this case the function $f(\mathbf{r}, t)dV$ is the probability of the excited atom staying at the instant t in the vicinity of the point $\mathbf{r}$, if at the initial instant of time $(t = 0)$ the space contains only one excited atom, located at $\mathbf{r} = 0$. The unknown Green's functions should satisfy the following equation, considered in the papers of Biberman and Holstein,

$$\frac{\partial f(\mathbf{r}, t)}{\partial t} = \frac{1}{4\pi\tau}\int_{V}\int_{0}^{\infty}\varepsilon_{\nu}k_{\nu}f(\mathbf{r}_1, t)\frac{\exp(-k_{\nu}|\mathbf{r}-\mathbf{r}_1|)}{|\mathbf{r}-\mathbf{r}_1|^2}d\nu\,dV_1 - \left(\frac{1}{\tau}+\sigma\right)f(\mathbf{r}, t) \tag{1.1}$$

with the initial condition $f(\mathbf{r}, t) = \delta(\mathbf{r})$ when $t = 0$.

The following symbols are used in Eq. (1.1): τ is the average lifetime of the excited state of the atom, σ is the probability of an extinction collision per single excited atom, and ν is the frequency of the photon. The functions ϵ_ν and k_ν characterize the shapes of the emission and absorption lights respectively.

2. SOLUTION OF THE RADIATION DIFFUSION EQUATION

By virtue of the symmetry of the problem, we have for a homogeneous unbounded medium, $f(\mathbf{r}, t) = f(r, t)$, where r is the modulus of the vector $\mathbf{r}$.

We use the Ambartsamyan transformation.[4] We write Eq. (1.1) in a rectangular system of coordinates (x, y, z) and integrate it over the two variables y and z from $-\infty$ to $+\infty$.

Let us consider the transformation term by term. We have

$$\int\int_{-\infty}^{\infty} f(\sqrt{x^2+y^2+z^2}, t)\,dy\,dz = 2\pi \int_{|x|}^{\infty} f(r,t)\,r\,dr,$$

where $r^2 = x^2 + y^2 + z^2$.

We introduce the notation

$$A(x,t) = 2\pi \int_{|x|}^{\infty} f(r,t)\,r\,dr. \qquad (2.1)$$

Differentiating Eq. (2.1) with respect to x we find

$$f(x,t) = -(1/2\pi x)\,\partial A(x,t)/\partial x. \qquad (2.2)$$

Next we have

$$\int\int_{-\infty}^{\infty} \frac{\exp[-k_\nu|\mathbf{r}-\mathbf{r}'|]}{|\mathbf{r}-\mathbf{r}'|^2}\,dy\,dz = 2\pi\,\mathrm{Ei}(k_\nu|x-x'|).$$

Here Ei is the exponential integral.

We thus obtain for the function A(x, t) a one-dimensional integro-differential equation.

$$\frac{\partial A(x,t)}{\partial t} = \frac{1}{2\tau}\int_{-\infty}^{\infty}\int_{0}^{\infty} \varepsilon_\nu k_\nu\,\mathrm{Ei}(k_\nu|x-x'|)\,A(x',t)\,d\nu\,dx'$$

$$-\left(\frac{1}{\tau}+\sigma\right)A(x,t) \qquad (2.3)$$

with an initial condition $A(x,t) = \delta(x)$ when $t = 0$. We apply the Fourier transformation to Eq. (2.3), denoting the Fourier transforms with the same symbols as the originals, merely changing the arguments from x to p. We find

$$\frac{\partial A(p,t)}{\partial t} = \frac{\sqrt{2\pi}}{2\tau}A(p,t)\int_0^{\infty}\varepsilon_\nu k_\nu\,\mathrm{Ei}(k_\nu p)\,d\nu - \left(\frac{1}{\tau}+\sigma\right)A(p,t). \qquad (2.4)$$

The initial conditions becomes $A(p,t) = 1/\sqrt{2\pi}$ when $t = 0$.

By definition

$$\mathrm{Ei}(k_\nu p) = \frac{1}{\sqrt{2\pi}}\int_{-\infty}^{\infty}\mathrm{Ei}(k_\nu|x|)\,e^{ipx}\,dx$$

$$= \frac{1}{\sqrt{2\pi}}\int_{-\infty}^{\infty}\int_0^1 e^{ipx}\,\frac{\exp(-k_\nu|x|/y)}{y}\,dy\,dx.$$

After integrating first with respect to x and then with respect to y we get

$$\mathrm{Ei}(k_\nu p) = \frac{1}{p}\sqrt{\frac{2}{\pi}}\tan^{-1}\frac{p}{k_\nu}. \qquad (2.5)$$

Solving Eq. (2.4) and using Eq. (2.5) we get

$$A(p,t) = \frac{1}{\sqrt{2\pi}}\exp\left[t\left(\frac{1}{\tau p}\int_0^{\infty}\varepsilon_\nu k_\nu\tan^{-1}\frac{p}{k_\nu}\,d\nu - \frac{1}{\tau} - \sigma\right)\right].$$

Using the inverse Fourier and Ambartsamyan transformations, we obtain finally

$$f(r,t) = -\frac{e^{-t(1/\tau+\sigma)}}{(2\pi)^2 r}$$

$$\times\frac{\partial}{\partial r}\int_{-\infty}^{\infty} e^{-ipr}\left[\exp\left\{\frac{t}{\tau}J(p)\right\} - 1\right]dp + 2\pi\delta(r)\Big\}. \qquad (2.6)$$

where

$$J(p) = \frac{1}{p}\int_0^{\infty}\varepsilon_\nu k_\nu\tan^{-1}\frac{p}{k_\nu}\,d\nu. \qquad (2.7)$$

We shall henceforth replace the argument x, which denotes the distance between two points in space, by r.

Equation (2.6) gives a complete solution of the problem for an arbitrary form of the spectral line. The first term in (2.6) takes into account the diffusion portion of the solution. The second corresponds to the probability of the excited atom staying at the point $r = 0$ during the entire time t, without experiencing a single act of radiation or extinction.

We turn now to the limiting case. Let the spectral line be monochromatic. Then

$$J(p) = \frac{k}{p}\tan^{-1}\frac{p}{k}. \qquad (2.8)$$

The Green's function can be calculated further by approximate methods. Its asymptotic expression for larger values of r can be obtained by expanding J(p) in powers of small p and retaining the first two terms. We then obtain

$$f(r,t) \approx \frac{e^{-\sigma t}}{(2\pi)^2 r}\,\frac{\partial}{\partial r}\int_{-\infty}^{\infty}\exp\left\{-ipr - \frac{tp^2}{3\tau k^2}\right\}dp$$

$$= (4\pi Dt)^{-3/2}\exp\left(-\sigma t - \frac{r^2}{4Dt}\right), \qquad (2.9)$$

where

$$D = 1/3\tau k^2.$$

The diffusion of monochromatic radiation is thus analogous in the first approximation to the diffusion of particles. This analogy was noted by Compton.[6]

3. DIFFUSION OF PHOTONS FOR A DISPERSION SPECTRAL LINE

A dispersion spectral line is defined by the functions

$$k_\nu = \frac{k_0}{1+[2(\nu-\nu_0)/\Delta\nu_c]^2}; \qquad \varepsilon_\nu = \frac{2}{\pi\Delta\nu_c}\,\frac{1}{1+[2(\nu-\nu_0)/\Delta\nu_c]^2}. \qquad (3.1)$$

Here ν_0 is the frequency of the center of the spectral line, $\Delta\nu_c$ is the width of the line, and k_0 is the coefficient of absorption at the frequency ν_0.

If the spectral line is of this form, the integral (2.7) can be calculated explicitly.[5] For an asymptotic expression of the Green's function it is

enough to know the behavior of the function $J(p)$ for small arguments only. We determine this expression:

$$J(p)=\int_0^\infty\int_0^1 \frac{\varepsilon_\nu k_\nu^2}{k_\nu^2+p^2\mu^2}\,d\mu d\nu$$

$$=\frac{k_0^2}{\pi}\int_{-2\nu_c/\Delta\nu_c}^{\infty}\int_0^1 \frac{1}{(1+\omega^2)^3}\,\frac{d\mu d\omega}{\left(\frac{k_0}{1+\omega^2}\right)^2+p^2\mu^2},$$

where $\omega=2(\nu-\nu_0)/\Delta\nu_c$. Since $\Delta\nu_c \lesssim \nu_0$ for the spectral lines of the atoms, the lower limit of integration can be extended to $-\infty$. Using the normalization condition of the function ϵ_ν and making the following change in the integration variable

$$(k_0/p\mu)/(1+\omega^2)=x; \qquad (p\gg 0),$$

we obtain

$$J(p)=1+\frac{1}{\pi}\int_0^1 \sqrt{\frac{p\mu}{k_0}}\int_{k_0/p\mu}^{0}\frac{dx\,d\mu}{(1+x^2)\sqrt{(1-xp\mu/k_0)\,x}}. \tag{3.2}$$

At small values of p the lower limit of integration can be extended to infinity and the second term under the radical can be neglected. Then

$$J(p)\approx 1-1/3\sqrt{\frac{2p}{k_0}}; \qquad (p\gg 0). \tag{3.3}$$

Inserting (3.3) into (3.6) we get

$$f(r,t)\approx -\frac{e^{-\alpha t}}{(2\pi)^2 r}\,\frac{\partial}{\partial r}\int_{-\infty}^{\infty} e^{-ipr}\exp\left(-\frac{t}{3\tau}\sqrt{\frac{2|p|}{k_0}}\right)dp.$$

After making the substitution $rp=q^2$ for the integration variable and integrating by parts we obtain as the final result

$$f(r,t)=-\frac{1}{\pi^2 r}\,\frac{\partial}{\partial r}\left(\frac{e^{-\alpha t}}{r}\,\varphi(y)\right), \tag{3.4}$$

where

$$\varphi(y)=y\int_0^\infty e^{-2yq}\sin q^2 dq; \quad y=t/3\tau\sqrt{2k_0 r}. \tag{3.5}$$

For very large distances it follows from (3.4) and (3.5) that

$$f(r,t)\approx \frac{1}{(4\pi)^{3/2}}\,\frac{t}{\tau}\,\frac{e^{-\alpha t}}{\sqrt{k_0 r}}\,\frac{1}{r^3}. \tag{3.6}$$

Compared with (3.9), the distribution (3.6) diminishes slowly at infinity. This is explained by the slow character of decrease in the kernel of Eq. (1.1), as pointed out by Biberman.[1]

The function $\varphi(y)$ can be expressed in terms of the Fresnel integrals:[7]

$$\varphi(y)=\sqrt{\frac{\pi}{2}}\,y\left\{\sin y^2\left[\frac{1}{2}-S(y)\right]+\cos y^2\left[\frac{1}{2}-C(y)\right]\right\}, \tag{3.7}$$

where

$$S(y)=\frac{2}{\sqrt{2\pi}}\int_0^y \sin t^2 dt; \qquad C(y)=\frac{2}{\sqrt{2\pi}}\int_0^y \cos t^2 dt.$$

It is easy to verify that the distribution (3.4), like (3.9), satisfies the following normalization condition

$$e^{\alpha t}\int_0^\infty f(r,t)\,4\pi r^2 dr=1. \tag{3.8}$$

For the subsequent calculations we shall find it convenient to use certain integral relations. We have

$$\int_0^r A(r_1,t)\,dr_1=\frac{1}{2}-S(y)[1-S(y)]-C(y)[1-C(y)]. \tag{3.9}$$

Using the properties of the Fresnel integrals, we obtain the following asymptotic formulas

$$\int_0^r A(r_1,t)\,dr_1\approx\frac{1}{2\pi y^2} \qquad \text{for } y\to\infty,$$
$$\int_0^r A(r_1,t)\,dr_1\approx\frac{1}{2}-\frac{2y}{\sqrt{2\pi}} \qquad \text{for } y\to 0. \tag{3.10}$$

Furthermore

$$\int_0^t A(r,t')\,dt'=\frac{1}{\sqrt{2\pi}}\,\frac{t}{yr}\left(\frac{1}{2}-\sqrt{\frac{2}{\pi}}\int_0^\infty e^{-2yq}\cos q^2 dq\right),$$
$$\int_0^t\int_0^r A(r_1,t')\,dr_1 dt'=t\int_0^r A(r_1,t)\,dr_1+2r\int_0^t A(r,t')\,dt'. \tag{3.11}$$

4. DIFFUSION OF PHOTONS FOR A DOPPLER SPECTRAL LINE

The Doppler spectral line, resulting from the thermal motion of atoms with Maxwellian velocity distribution, is determined by the functions

$$k_\nu=k_0\exp\left\{-\left[\frac{2(\nu-\nu_0)}{\Delta\nu_D}\sqrt{\ln 2}\right]^2\right\};$$
$$\varepsilon_\nu=\frac{2}{\Delta\nu_D}\sqrt{\frac{\ln 2}{\pi}}\exp\left\{-\left[\frac{2(\nu-\nu_0)}{\Delta\nu_D}\sqrt{\ln 2}\right]^2\right\}, \tag{4.1}$$

where $\Delta\nu_D$ is the Doppler width.

The integral (2.7) cannot be calculated in explicit form for a Doppler spectral line. For small values of the argument p, it is possible to obtain by the method indicated above the asymptotic value

$$J(p)\approx 1-\sqrt{\pi}p/4k_0\sqrt{\ln k_0-\ln p}. \tag{4.2}$$

Equations (2.6) and (4.2) lead to the following asymptotic expression for the Green's function

$$f(r,t)=-\frac{e^{-\alpha t}}{2\pi^2 r}\,\frac{\partial}{\partial r}\,\mathrm{Re}\int_0^{k_0} e^{-ipr} \tag{4.3}$$
$$\times\exp\left(-\frac{t}{\tau}\,\frac{\sqrt{\pi}}{4}\,\frac{p}{k_0}\,\frac{1}{\sqrt{\ln k_0-\ln p}}\right)dp.$$

For large optical distances $k_0 r$, formula (4.3) can be further simplified to

$$f(r, t) \approx \frac{2}{(4\pi)^{3/2}} \frac{t}{\tau} \frac{e^{-ct}}{k_0 r^4 \sqrt{\ln k_0 r}}. \qquad (4.4)$$

It follows from (4.4), like from (3.6), that the photon distribution function $f(r, t)$ diminishes slowly with increasing distance.

5. NUMERICAL CHARACTERISTICS OF THE DIFFUSION OF PHOTONS

The principal numerical characteristics of photon diffusion, like those of any distribution, are the mathematical expectation value and the dispersion. The mathematical expectation value vanishes because the function $f(r, t)$ is even. The dispersion $\overline{r^2}$ provides an estimate of the mean distance covered by the photon during the time t.

Let the photons diffuse without a change of frequency and in the absence of extinction ($\sigma = 0$). Calculating r^2 with the aid of (2.9), we arrive at the Einstein equation $r^2 = 6Dt$.

If the spectral lines have Doppler or dispersion shapes, the slow decrease in the function $f(r, t)$ at infinity causes the integral that determines r^2 to diverge, and the foregoing arguments lose their meaning. We must forego the definition of the mean distance covered by the photon during the time t. We can speak, however of the mean time t required for the photon to shift more than a specified distance r.

Assume that there is no extinction. Then the expression

$$\int_0^r 4\pi r_1^2 f(r_1, t)\, dr_1$$

represents the probability of the photon staying within a sphere of radius r. Therefore

$$-\frac{\partial}{\partial t}\int_0^r 4\pi r_1^2 f(r_1, t)\, dr_1 dt \qquad (5.1)$$

is the probability of the photon leaving this sphere within a time dt. Consequently, the average time required for the photon to shift a distance greater than r is defined as the mathematical expectation value of the function (5.1)

$$\bar{t} = -\int_0^\infty t \frac{\partial}{\partial t}\int_0^r 4\pi r_1^2 f(r_1, t)\, dr_1 dt. \qquad (5.2)$$

Let us turn now to the dispersion spectral line. Integration of expression (5.2) by parts and relations (3.10) lead to

$$\bar{t} = \int_0^\infty \int_0^r 4\pi r_1^2 f(r_1, t)\, dr_1 dt. \qquad (5.3)$$

Integrating by part once more

$$\bar{t} = -2r\int_0^\infty A(r, t)\, dt + 2\int_0^\infty \int_0^r A(r_1, t)\, dr_1 dt.$$

These integrals have been given above. We therefore obtain as the final result

$$\bar{t} = 3\tau\sqrt{k_0 r/\pi} = 1.7\tau\sqrt{k_0 r}. \qquad (5.4)$$

Formula (5.4), obtained with the aid of an asymptotic expression for the function $f(r, t)$, does not hold for small $k_0 r$. In practice it gives correct results even if $k_0 r$ is on the order of several units.

Since we consider the photon to have an infinite velocity, the time t owes its existence to the finite duration τ of the excited state of the atom. Consequently $\bar{t} = n\tau$, where n is the average number of photon reradiation events over an optical distance greater than r. From this we get

$$n = 3\sqrt{k_0 r/\pi}.$$

Holstein[2,3] investigated the de-excitation of finite volumes of gas after cessation of the excitation of the atoms. He considered a planar layer of gas of thickness L and a cylindrical volume of radius R. For the mean de-excitation times of these volumes he obtained (using our symbols) the following expressions, respectively:

$$\bar{t} = 2.2\tau\sqrt{k_0 L/2};\quad \bar{t} = 1.6\tau\sqrt{k_0 R}. \qquad (5.5)$$

Comparison of (5.5) with (5.4) shows that Holstein's results are close to ours. The difference lies only in the numerical factor, which is determined by the configuration of the scattering space.

Let us turn now to the Doppler spectral line. From (5.2) and (4.3) we find

$$\bar{t} = \frac{2}{\pi}\int_0^\infty t \frac{\partial}{\partial t}\int_0^r r_1 \frac{\partial}{\partial r_1}\int_0^{k_0} \cos pr_1$$

$$\times \exp\left(-\frac{t}{\tau}\frac{\sqrt{\pi}}{4}\frac{p}{k_0}\frac{1}{\sqrt{\ln k_0 - \ln p}}\right) dp\, dr_1 dt.$$

Interchanging the order of integration and performing operations connected with t and r_1 we arrive at the expression

$$\bar{t} = \frac{8}{\pi^{3/2}}\tau k_0 r \int_0^{k_0 r}\left(\frac{\sin x}{x^2} - \frac{\cos x}{x}\right)\sqrt{\ln k_0 r - \ln x}\, dx,$$

where $x = pr$. If the optical distance $k_0 r$ is sufficiently small, then

$$\bar{t} = 8\pi^{-3/2}\tau k_0 r\sqrt{\ln k_0 r}\int_0^\infty \left(\frac{\sin x}{x^2} - \frac{\cos x}{x}\right) dx.$$

After integrating, we obtain the final result

$$\bar{t} = 8\pi^{-3/2}\tau k_0 r\sqrt{\ln k_0 r} = 1.4\tau k_0 r\sqrt{\ln k_0 r}. \qquad (5.6)$$

Compare these with Holstein's calculated results

$$\bar{t} = 1.9\tau k_0 \frac{L}{2}\sqrt{\ln k_0 \frac{L}{2}}; \quad \bar{t} = 1.1\tau k_0 R\sqrt{\ln k_0 R}. \quad (5.7)$$

His first formula is for a planar layer, the second for a volume with cylindrical configuration. Holstein's relations (5.7) are in good agreement with experiment.[8]

Comparison of (5.6) and (5.7) leads to the same results as obtained for a dispersion spectral line.

6. CONCERNING STATIONARY SOLUTIONS

Let a source of excited atoms act for an infinitely long time at a certain point in space ($\mathbf{r} = 0$). The distribution function $f(\mathbf{r})$ satisfies in this case the equation

$$\frac{1}{4\pi\tau}\int_V\int_0^\infty \varepsilon_\nu k_\nu f(\mathbf{r}_1)\frac{\exp(-k_\nu|\mathbf{r}-\mathbf{r}_1|)}{|\mathbf{r}-\mathbf{r}_1|^2}\,d\nu dV_1$$

$$-f(\mathbf{r})\left(\frac{1}{\tau}+\sigma\right)+\delta(\mathbf{r})=0. \quad (6.1)$$

Using, as previously, the Ambartsamyan and Fourier transformations, we find

$$f(r) = -\frac{1}{(2\pi)^2 r}\frac{\partial}{\partial r}\int_{-\infty}^{\infty}\frac{e^{-ipr}\,dp}{\sigma+\tau^{-1}[1-J(p)]}, \quad (6.2)$$

where the function $J(p)$ is defined by Eq. (2.7).

Assume that there is no extinction and that the spectral line has a dispersion shape. Using (3.3) we arrive at the asymptotic expression

$$f(r) \approx 3\tau\sqrt{\pi k_0 r}/2\,(2\pi)^2 r^3.$$

The same result can be obtained by using the solution of Eq. (1.1) and the formula

$$f(r) = \int_0^\infty f(r,t)\,dt.$$

In conclusion, I express deep gratitude to L. M. Biberman, who was in charge of this research.

[1] L. M. Biberman, J. Exptl. Theoret. Phys. (U.S.S.R.) **17**, 416 (1947).

[2] T. Holstein, Phys. Rev. **72**, 1212 (1947).

[3] T. Holstein, Phys. Rev. **83**, 1159 (1951).

[4] V. A. Ambartsumyan, Бюллетень Ереванской Астрономической обсерватории (Bulletin, Erevan Astr. Observ.) **6**, 3 (1945).

[5] B. A. Veklenko, J. Exptl. Theoret. Phys. (U.S.S.R.) **33**, 817 (1957), Soviet Phys. JETP **6**, 629 (1958).

[6] K. T. Compton, Phys. Rev. **20**, 283 (1922).

[7] I. M. Ryzhik and I. S. Gradshtein, Таблицы интегралов, сумм, рядов и произведений (Tables of Integrals, Sums, Series, and Products), Moscow, 1951.

[8] Alpert, McCoubrey, and Holstein, Phys. Rev. **76**, 1257 (1949).

Translated by J. G. Adashko
27

POLARIZATION EFFECTS IN Σ^-- HYPERON CAPTURE BY DEUTERONS

S. G. MATINYAN and O. D. CHEISHVILI

Physics Institute, Academy of Sciences, Georgian S.S.R.

Submitted to JETP editor July 2, 1958

J. Exptl. Theoret. Phys. (U.S.S.R.) **36**, 212-215 (January, 1959)

A phenomenological treatment is given of Σ^--hyperon capture by deuterons with formation of Λ^0-particles. A study of the polarization correlation of the strange particles yields information on the polarization of the Σ^--hyperon.

A phenomenological study of Σ^--hyperon capture by protons was recently given by Pais and Treiman.[1] The process is of interest for determination of the relative parity of Λ and Σ particles and for determination of the degree of polarization of the Σ particle using the decay process as analyzer. (As is well known, experiments on the "up-down" asymmetry coefficient in the associated production process give drastically different results for Λ and Σ particles which makes a determination of Σ polarization important.)

In this note we consider the capture of a polarized Σ^- hyperon by a deuteron

$$\Sigma^- + d \to 2n + \Lambda^0. \qquad (1)$$

We assume that the spin of Λ and Σ particles is $\frac{1}{2}$. A quantitative study of this process indicates that it is of definite interest as a source of additional information on the question of the degree of polarization of the Σ^- particle.

We investigated the capture process in the impulse approximation (cf., e.g., references 2 and 3). In this approximation the amplitude for the process has the form[4]

$$T_d = J_{12}T(1,2) + J_{13}T(1,3), \qquad (2)$$

where the index 1 refers to the strange particles, and 2 and 3 refer to the nucleons composing the deuteron;

$$J_{1l} = \int \Psi_f^+(\mathbf{r}_1, \mathbf{r}_2, \mathbf{r}_3)\, \Psi_i(\mathbf{r}_1, \mathbf{r}_2, \mathbf{r}_3)\, \delta(\mathbf{r}_1 - \mathbf{r}_l)\, d\mathbf{r}_1 d\mathbf{r}_2 d\mathbf{r}_3$$

$$(l = 2,3),$$

Ψ_i and Ψ_f are the initial and final wave functions of the three particle system; and T is the amplitude introduced by Pais and Treiman, for Σ^--hyperon capture by a proton.

Proceeding in a manner analogous to that of reference 4 we find the following formula for the polarization of the Λ particle produced in the capture of a polarized Σ^- hyperon by a deuteron:

$$R_d \mathbf{p}_\Lambda = \tfrac{1}{3}\{|F^-|^2 \mathrm{Sp}[\Pi_t(2,3)\, T(1,2)\, \rho_\Sigma\, \Pi_t(2,3)\, T^+(1,2)\, \sigma_1]$$

$$+ |F^+|^2 \mathrm{Sp}[\Pi_s(2,3)\, T(1,2)\, \rho_\Sigma\, \Pi_t(2,3)\, T^+(1,2)\, \sigma_1]\}. \qquad (3)$$

Here the trace is over the spin variables of all three particles, $\rho_\Sigma = [1 + \mathbf{p}_\Sigma \cdot \boldsymbol{\sigma}_1]/2$ is the spin density matrix of Σ^- particles of polarization $\mathbf{p}_\Sigma$,

$$\Pi_t(2,3) = \tfrac{1}{4}[3 + \boldsymbol{\sigma}_2 \cdot \boldsymbol{\sigma}_3], \qquad \Pi_s(2,3) = \tfrac{1}{4}[1 - \boldsymbol{\sigma}_2 \cdot \boldsymbol{\sigma}_3],$$

$$F^\pm = \int \Phi_g^{\pm *} \Phi_d e^{i\varkappa \cdot \rho} d\rho,$$

Φ_g is the wave function of two neutrons with relative momentum $\mathbf{g}$, Φ_d is the deuteron wave function, $2\varkappa$ is the momentum transferred to the nucleons;

$$R_d = \tfrac{1}{3}\{|F^-|^2 \mathrm{Sp}[\Pi_t(2,3)\, T(1,2)\, \rho_\Sigma \Pi_t(2,3)\, T^+(1,2)]$$

$$+ |F^+|^2 \mathrm{Sp}[\Pi_s(2,3)\, T(1,2)\, \rho_\Sigma \Pi_t(2,3)\, T^+(1,2)]\}. \qquad (4)$$

As in reference 1, it is easy to obtain the following relation between $\mathbf{p}_\Lambda$ and $\mathbf{p}_\Sigma$:

$$R_d \mathbf{p}_\Lambda = \alpha \mathbf{p}_\Sigma + \beta (\mathbf{p}_\Sigma \cdot \mathbf{N})\, \mathbf{N}, \qquad (5)$$

where $\mathbf{N}$ is a unit vector in the direction of motion of the Λ particle.

The values of R_d, α and β are determined by the type of transition from the initial to the final state and depend on the dynamics of the Σ^--proton interaction leading to capture. We shall consider the various transition types separately.

1. S → S Transition

In this case the amplitude for Σ^- capture by a proton has the form

$$T = a_1 \Pi_t(1,2) + a_2 \Pi_s(1,2), \qquad (6)$$

where a_1 and a_2 are the amplitudes for the transitions $^3S_1 \to {}^3S_1$ and $^1S_0 \to {}^1S_0$ of the strange particle-nucleon system respectively (we use

standard spectroscopic notation).

R_d, α, and β are given by the following expressions:

$$R_d = \frac{1}{16}\{(11\,|a_1|^2 + 3|a_2|^2 + 2\mathrm{Re}\,a_1a_2^*)|F^-|^2 + (|a_1|^2 + |a_2|^2 - 2\,\mathrm{Re}\,a_1a_2^*)|F^+|^2\}, \quad (7a)$$

$$\alpha = \frac{1}{48}\{(25\,|a_1|^2 + |a_2|^2 + 22\,\mathrm{Re}\,a_1a_2^*)|F^-|^2 - (|a_1|^2 + |a_2|^2 - 2\mathrm{Re}a_1a_2^*)|F^+|^2\}, \quad (7b)$$

$$\beta = 0. \quad (7c)$$

For $\kappa \approx 0$ (i.e., for small momentum transfer to the nucleons) one has $F^- \approx 0$ and $\mathbf{p}_\Lambda = -\mathbf{p}_\Sigma/3$, independent of any assumption about the coherence or incoherence of the states with a_1 and a_2.

Consequently, in this case it is possible to obtain definite information about the Σ^- polarization by studying the asymmetry in the Λ-decay for both the instance where the Σ^- was captured from the continuum and where it came from an S-orbit.

In the case of capture by protons the inequality $\mathbf{p}_\Lambda \leq {}^2/_3\mathbf{p}_\Sigma$ is obtained only for transitions from S-orbits.[1]

2. S → P Transitions

$$T = (^3/_2)^{1/2}b_1\mathbf{N}\cdot\mathbf{S} + \sqrt{3}b_2\mathbf{N}\cdot\mathbf{S}'\Pi_t + b_3\mathbf{N}\cdot\mathbf{S}'\Pi_s,$$

where

$$\mathbf{S} = (\boldsymbol{\sigma}_1 + \boldsymbol{\sigma}_2)/2, \qquad \mathbf{S}' = (\boldsymbol{\sigma}_1 - \boldsymbol{\sigma}_2)/2;$$

b_1, b_2 and b_3 are the amplitudes for the transitions ${}^3S_1 \to {}^3P_1$, ${}^3S_1 \to {}^1P_1$ and ${}^1S_0 \to {}^3P_0$ respectively.

$$R_d = \frac{1}{8}\Big\{\Big(5|b_1|^2 + \frac{9}{2}|b_2|^2 + \frac{3}{2}|b_3|^2 + \sqrt{2}\,\mathrm{Re}\,b_1b_2^* + \sqrt{\frac{2}{3}}\,\mathrm{Re}b_1b_3^* + \frac{1}{\sqrt{3}}\,\mathrm{Re}\,b_2b_3^*\Big)|F^-|^2 + \Big(|b_1|^2 + \frac{3}{2}|b_2|^2 + \frac{1}{2}|b_3|^2 - \sqrt{2}\,\mathrm{Re}b_1b_2^* - \sqrt{\frac{2}{3}}\,\mathrm{Re}\,b_1b_3^* - \sqrt{\frac{1}{3}}\,\mathrm{Re}\,b_2b_3^*\Big)|F^+|^2\Big\}, \quad (8a)$$

$$\alpha = \frac{1}{8}\Big\{-\Big(|b_1|^2 + \frac{1}{2}|b_2|^2 + \frac{1}{6}|b_3|^2 + 5\sqrt{2}\,\mathrm{Re}\,b_1b_2^* + 5\sqrt{\frac{2}{3}}\,\mathrm{Re}\,b_1b_3^* + \sqrt{\frac{1}{3}}\,\mathrm{Re}\,b_2b_3^*\Big)|F^-|^2 + \Big(|b_1|^2 + \frac{1}{2}|b_2|^2 + \frac{1}{6}|b_3|^2 - \sqrt{2}\,\mathrm{Re}\,b_1b_2^* - \sqrt{\frac{2}{3}}\,\mathrm{Re}\,b_1b_3^* + \sqrt{\frac{1}{3}}\,\mathrm{Re}\,b_2b_3^*\Big)|F^+|^2\Big\}, \quad (8b)$$

$$\beta = \frac{1}{4}\Big\{\Big(3|b_1|^2 + \frac{1}{2}|b_2|^2 + \frac{1}{6}|b_3|^2 + 3\sqrt{2}\,\mathrm{Re}b_1b_2^* + \sqrt{6}\mathrm{Re}\,b_1b_3^* + \frac{5}{\sqrt{3}}\,\mathrm{Re}\,b_2b_3^*\Big)|F^-|^2 + \Big(-\frac{1}{2}|b_2|^2 - \frac{1}{6}|b_3|^2 + \frac{1}{\sqrt{3}}\,\mathrm{Re}\,b_2b_3^*\Big)|F^+|^2\Big\}. \quad (8c)$$

Let us again consider the case $\kappa \approx 0$ (experimentally this corresponds to the observation of a Λ particle with energy larger than a given E_0).

If the Σ^- particle is captured from a discrete level the interference terms $b_1b_3^*$ and $b_2b_3^*$ vanish.[1] In addition, if the amplitude b_1 of the transition ${}^3S_1 \to {}^3P_1$ dominates the others the simple expression $\mathbf{p}_\Lambda \approx \mathbf{p}_\Sigma$ results. In the case when the amplitude b_2 or b_3 (or both)

$$\mathbf{p}_\Lambda = {}^1/_3\mathbf{p}_\Sigma - {}^2/_3(\mathbf{p}_\Sigma\cdot\mathbf{N})\,\mathbf{N}$$

is obtained.

3. P → S Transition

In this case the amplitude T has the same form as for S → P transitions with the unit vector $\mathbf{N}$ replaced by the unit vector $\mathbf{n}$ in the direction of the relative momentum of the $(\Sigma^- - p)$ system. In the final expressions for R_d, α and β an average over $\mathbf{n}$ was performed.

$$R_d = \frac{1}{8}\Big\{\Big(5|c_1|^2 + \frac{9}{2}|c_2|^2 + \frac{3}{2}|c_3|^2 + \sqrt{2}\,\mathrm{Re}c_1c_2^* + \sqrt{\frac{2}{3}}\,\mathrm{Re}\,c_1c_3^* + \sqrt{\frac{1}{3}}\,\mathrm{Re}\,c_2c_3^*\Big)|F^-|^2 + \Big(|c_1|^2 + \frac{3}{2}|c_2|^2 + \frac{1}{3}|c_3|^2 - \sqrt{2}\,\mathrm{Re}\,c_1c_2^* - \sqrt{\frac{2}{3}}\,\mathrm{Re}\,c_1c_3^* - \sqrt{\frac{1}{3}}\,\mathrm{Re}\,c_2c_3^*\Big)|F^+|^2\Big\}, \quad (9a)$$

$$\alpha = \frac{1}{8}\Big\{\Big(|c_1|^2 - \frac{1}{6}|c_2|^2 - \frac{1}{18}|c_3|^2 - 3\sqrt{2}\,\mathrm{Re}\,c_1c_2^* - \sqrt{6}\,\mathrm{Re}\,c_1c_3^* + \frac{7}{9}\sqrt{3}\mathrm{Re}c_2c_3^*\Big)|F^-|^2 + \Big(|c_1|^2 + \frac{1}{6}|c_2|^2 + \frac{1}{18}|c_3|^2 - \sqrt{2}\,\mathrm{Re}\,c_1c_2^* - \sqrt{\frac{2}{3}}\,\mathrm{Re}\,c_1c_3^* + \frac{5}{9}\sqrt{3}\,\mathrm{Re}\,c_2c_3^*\Big)|F^+|^2\Big\}, \quad (9b)$$

$$\beta = 0. \quad (9c)$$

Here c_1, c_2, c_3 are transition amplitudes for ${}^3P_1 \to {}^3S_1$, ${}^1P_1 \to {}^3S_1$ and ${}^3P_0 \to {}^1S_0$ respectively of the $(\Sigma^- - p)$ system.

Considering again the case $\kappa \approx 0$ and taking into account the fact that all three amplitudes c_1, c_2, and c_3 are incoherent (i.e., all interference

terms vanish), we obtain the inequality

$$^1/_9 p_\Sigma \leqslant p_\Lambda \leqslant p_\Sigma.$$

The limiting value $p_\Lambda \approx p_\Sigma$ occurs when the amplitude c_1 dominates the others; the other limiting value $p_\Lambda \approx {}^1/_9 p_\Sigma$ is obtained when one of the amplitudes c_2, c_3 is dominant.

As was to be expected, these results could be obtained by averaging the equalities found in section 2.

4. P → P Transitions*

$$T = (^3/_4)^{1/2} \{ \frac{1}{3} d_1 [4\mathbf{N}\cdot\mathbf{n}\Pi_t - 3i\mathbf{S}\cdot[\mathbf{N}\times\mathbf{n}] - (\mathbf{n}\cdot\mathbf{S})(\mathbf{N}\cdot\mathbf{S})]$$
$$+ d_2 [i\mathbf{S}\,[\mathbf{N}\times\mathbf{n}] + (\mathbf{n}\cdot\mathbf{S})(\mathbf{N}\cdot\mathbf{S})] + \sqrt{2} i\mathbf{S}'\cdot[\mathbf{N}\cdot\mathbf{n}](d_3\Pi_t + d_4\Pi_s)$$
$$+ 2d_5 (\mathbf{N}\cdot\mathbf{n})\Pi_s + \frac{2}{3} d_6 [(\mathbf{N}\cdot\mathbf{n})\Pi_t - (\mathbf{n}\cdot\mathbf{S})(\mathbf{N}\cdot\mathbf{S})] \}.$$

The amplitudes d_1, d_2, d_3, d_4, d_5 and d_6 refer to the transitions $^3P_2 \to {}^3P_2$, $^3P_1 \to {}^3P_1$, $^3P_1 \to {}^1P_1$, $^1P_1 \to {}^3P_1$, $^1P_1 \to {}^1P_1$ and $^3P_0 \to {}^3P_0$ respectively of the $(\Sigma^- p)$ system.

If the conditions for incoherence are satisfied we obtain (after averaging over $\mathbf{n}$):

$$R_d = \frac{1}{16} \Big\{ \Big(\frac{35}{6} |d_1|^2 + \frac{19}{6} |d_2|^2 + 3(|d_3|^2 + |d_4|^2 + |d_5|^2)$$
$$+ |d_6|^2 + \frac{\sqrt{2}}{3} \operatorname{Re} d_2 d_3^* \Big) |F^-|^2$$
$$+ \Big(\frac{5}{6} |d_1|^2 + \frac{5}{6} |d_2|^2 + |d_3|^2 + |d_4|^2 + |d_5|^2$$
$$+ \frac{1}{3} |d_6|^2 - \frac{\sqrt{2}}{3} \operatorname{Re} d_2 d_3^* \Big) |F^+|^2 \Big\}, \qquad (10a)$$

$$\alpha = \frac{1}{48} \Big\{ \Big(\frac{97}{9} |d_1|^2 + |d_2|^2 + |d_5|^2 + \frac{1}{9} |d_6|^2$$
$$- 4\sqrt{2} \operatorname{Re} d_2 d_3^* \Big) |F^-|^2 + \Big(\frac{11}{9} |d_1|^2 - |d_2|^2 - |d_5|^2 - \frac{1}{9} |d_6|^2$$
$$- 2\sqrt{2} \operatorname{Re} d_2 d_3^* \Big) |F^+|^2 \Big\}, \qquad (10b)$$

$$\beta = \frac{1}{24} \Big\{ \Big(-\frac{97}{36} |d_1|^2 + \frac{7}{4} |d_2|^2 - \frac{1}{2} |d_3|^2$$
$$- \frac{1}{2} |d_4|^2 - \frac{1}{9} |d_6|^2 + \frac{3}{\sqrt{2}} \operatorname{Re} d_2 d_3^* \Big) |F^-|^2$$
$$+ \Big(-\frac{11}{36} |d_1|^2 + \frac{5}{4} |d_2|^2 + \frac{1}{2} |d_3|^2$$
$$+ \frac{1}{2} |d_4|^2 + \frac{1}{9} |d_6|^2 + \frac{3}{\sqrt{2}} \operatorname{Re} d_2 d_3^* \Big) |F^+|^2 \Big\}. \qquad (10c)$$

In conclusion the authors thank Prof. G. R. Khutsishvili for useful discussions and advice.

Note added in proof (November 24, 1958). The amplitudes of Pais and Treiman[1] characterize the transition of the strange particle-nucleon system. On the other hand in the deuteron case it is necessary to consider transitions of the system strange particle – two nucleons. However it is clear that for $\kappa \approx 0$ the two definitions coincide.

*There are a number of misprints in reference 1. This is true in particular of formulas (7) and (9) and of the form of the P → P amplitude.

[1] A. Pais and S. B. Treiman, Phys. Rev. **109**, 1759 (1958).

[2] G. F. Chew, Phys. Rev. **80**, 196 (1950).

[3] I. Ya. Pomeranchuk, J. Exptl. Theoret. Phys. (U.S.S.R.) **21**, 1113 (1951).

[4] S. G. Matinyan and O. D. Cheishvili, Сообщ. АН ГрузССР (Reports, Acad. Sci., Georgian S.S.R.) (in press).

Translated by A. Bincer
28

ON THE THEORY OF RELAXATION PROCESSES IN FERRODIELECTRICS AT LOW TEMPERATURES

A. I. AKHIEZER, V. G. BAR'YAKHTAR, and S. V. PELETMINSKII

Physico-Technical Institute, Academy of Sciences, Ukrainian S.S.R.

Submitted to JETP editor July 5, 1958

J. Exptl. Theoret. Phys. (U.S.S.R.) **36**, 216-223 (January, 1959)

A theory of relaxation of the magnetic moment of ferrodielectrics is given. It is shown that exchange interaction between the spin waves causes first a Bose distribution to be established, with given non-equilibrium values of the square and projection of the magnetic moment on the axis of preferred magnetization. Because of magnetic interaction and interaction due to the anisotropy energy, equilibrium values of these quantities are gradually attained. The relaxation times are computed.

1. The kinetic and relaxation phenomena in ferrodielectrics are determined by various processes of interaction of spin waves with each other and with phonons. The strongest interaction between spin waves in the temperature region $\Theta_c \gg \Theta \gg \Theta_c (\mu M_0/\Theta_c)^{4/7}$ (Θ_c is the Curie temperature, μ the Bohr magneton, and M_0 the magnetic moment of such a region) is the exchange interaction that establishes a Bose distribution of the spin waves. This distribution, however, does not correspond to the equilibrium value of the magnetic moment. To the contrary, since the Hamiltonian of the exchange interaction commutes with the total magnetic moment of the body $\mathfrak{M}$ and with its projection of the axis of the lightest magnetization $\mathfrak{M}_z$, the latter quantities can be arbitrary.

The transition to equilibrium values of these quantities, together with the equalization of the spin and lattice temperatures, is due to the magnetic dipole interaction between the spin waves, to the interaction caused by the anisotropy energy, and to the interaction between the spin waves and the phonons. All these interactions are weak compared with the exchange interaction between the spin waves, and the relaxation of the magnetic moment and equalization of the temperatures are therefore slow compared with the establishment of the Bose distribution for spin waves with specified values of magnetic moment.

The first to be established is the equilibrium value of the absolute magnetic moment. This process is caused principally by magnetic dipole interaction. The equalization of the spin-wave and lattic temperatures and the establishment of the equilibrium value of the projection of the magnetic moment on the axis of the least magnetization are slower.

2. The Hamiltonian of interaction of the spin waves with each other or with phonons can be represented in the following form

$$\mathcal{H}_{\text{int}} = \mathcal{H}_e + \mathcal{H}_w + \mathcal{H}_a + \mathcal{H}_p,$$

where $\mathcal{H}_e$ and $\mathcal{H}_w$ are the Hamiltonians of the exchange and magnetic interactions, $\mathcal{H}_a$ is the anisotropy energy, and $\mathcal{H}_p$ is the Hamiltonian that describes the interaction between the spin waves and the phonons.

To find $\mathcal{H}_e$, we start with the expression for the exchange energy of a ferromagnet:[1]

$$\mathcal{H}_e = \frac{\alpha}{2}\int \frac{\partial M_l}{\partial x_i}\frac{\partial M_l}{\partial x_i}\,dV,$$

where M is the magnetic moment per unit volume and α is the exchange integral ($\alpha = \Theta_c a^2/2\mu M_0$, and a is the lattice constant). Let us put[2]

$$\begin{aligned} M^+ &= M_x + iM_y = (4\mu M_0)^{1/2} a^+ [1 - (\mu/M_0)\, a^+ a]^{1/2}, \\ M^- &= M_x - iM_y = (4\mu M_0)^{1/2} [1 - (\mu/M_0)\, a^+ a]^{1/2} a, \\ M_z &= M_0 - 2\mu a^+ a, \end{aligned} \tag{1}$$

where a^+ and a are the spin-wave creation and absorption operators, satisfying the commutation conditions

$$[a(\mathbf{r}),\ a^+(\mathbf{r}')] = \delta(\mathbf{r} - \mathbf{r}').$$

Expanding the operators a in a Fourier series

$$a(\mathbf{r}) = V^{-1/2}\sum_{\mathbf{k}} e^{i\mathbf{k}\cdot\mathbf{r}} a_{\mathbf{k}},\quad a^+(\mathbf{r}) = V^{-1/2}\sum_{\mathbf{k}} e^{-i\mathbf{k}\cdot\mathbf{r}} a_{\mathbf{k}}^+, \tag{1'}$$

we obtain the following expression for the exchange-interaction Hamiltonian

$$\begin{aligned} \mathcal{H}_e = \frac{\mu^2\alpha}{V}\sum_{\mathbf{k}_1\mathbf{k}_2\mathbf{k}_3\mathbf{k}_4} &\{(\mathbf{k}_2 - \mathbf{k}_1)^2 + (\mathbf{k}_3 - \mathbf{k}_1)^2 - \mathbf{k}_1^2 - \mathbf{k}_4^2\} \\ &\times a_{\mathbf{k}_1}^+ a_{\mathbf{k}_2} a_{\mathbf{k}_3}^+ a_{\mathbf{k}_4} \Delta(\mathbf{k}_1 + \mathbf{k}_3 - \mathbf{k}_2 - \mathbf{k}_4), \end{aligned} \tag{2}$$

where

$$\Delta(\mathbf{k}) = \begin{cases} 1, & \mathbf{k} = 0 \\ 0, & \mathbf{k} \neq 0 \end{cases}$$

and $a_{\mathbf{k}}^{+}$, $a_{\mathbf{k}}$ are the operators of creation and annihilation of a spin wave of momentum $\mathbf{k}$. These operators satisfy the commutation condition

$$[a_{\mathbf{k}},\ a_{\mathbf{k}'}^{+}] = \Delta(\mathbf{k} - \mathbf{k}').$$

The number of spin waves with momentum $\mathbf{k}$ is $n_{\mathbf{k}} = a_{\mathbf{k}}^{+} a_{\mathbf{k}}$.

The operator $\mathcal{H}_e$ is responsible for the scattering of the spin waves by the spin waves, i.e., for transitions of the type $n_1,\ n_2,\ n_3,\ n_4 \rightarrow n_1+1,\ n_2-1,\ n_3+1,\ n_4-1$.

The Hamiltonians $\mathcal{H}_w$ and $\mathcal{H}_e$ are defined by the formulas

$$\mathcal{H}_w = -\frac{8\pi\mu\sqrt{\mu M_0/V}}{} \times \sum_{\mathbf{k}_1\mathbf{k}_2\mathbf{k}_3} \frac{k_1^{+}k_1^{-}}{k_1^2} a_{\mathbf{k}_1} a_{\mathbf{k}_2} a_{\mathbf{k}_3}^{+} \Delta(\mathbf{k}_1 + \mathbf{k}_2 - \mathbf{k}_3) + \text{compl. conj.}, \tag{3}$$

$$\mathcal{H}_a = -\frac{2\mu^2\beta}{V} \sum_{\mathbf{k}_1\mathbf{k}_2\mathbf{k}_3\mathbf{k}_4} a_{\mathbf{k}_1}^{+} a_{\mathbf{k}_2} a_{\mathbf{k}_3}^{+} a_{\mathbf{k}_4} \Delta(\mathbf{k}_1 + \mathbf{k}_3 - \mathbf{k}_2 - \mathbf{k}_4), \tag{4}$$

where β is the anisotropy constant [the latter expression can be obtained from the anisotropy energy $\frac{1}{2}\beta\int(M_X^2 + M_Y^2)\,dV$]. It is easy to see that the operator $\mathcal{H}_w$ is responsible for the processes of the merging of two spin waves into one and for the splitting of one spin wave into two, i.e., for processes of the type $n_1,\ n_2,\ n_3 \rightarrow n_1+1,\ n_2-1,\ n_3-1$ and $n_1,\ n_2,\ n_3 \rightarrow n_1-1,\ n_2+1,\ n_3+1$. The Hamiltonian $\mathcal{H}_a$, like $\mathcal{H}_e$, is responsible for the scattering of the spin waves.

The energy of the interaction between the spin waves and the lattice can be represented in the following form[3,4]

$$\mathcal{H}_p = \delta_1 \int \frac{\partial M_i}{\partial x_i}\frac{\partial M_i}{\partial x_k} u_{ik} dV + \delta_2 \int \frac{\partial M_i}{\partial x_i}\frac{\partial M_i}{\partial x_i} u_{kk} dV,$$

where u_{ik} is the deformation tensor; δ_1 and δ_2 are constants connected with the exchange integral:

$$\delta_1 = \beta_1(\Theta_c/\mu M_0)\,a^2,\quad \delta_2 = {}^1/_2\beta_2(\Theta_c/\mu M_0)\,a^2$$

(β_1 and β_2 are quantities on the order of unity). We have written in $\mathcal{H}_p$ only the energy connected with the exchange interaction, and did not take into account the magnetostriction energy, which necessitates small corrections.

Introducing the creation and annihilation operators $b_{\mathbf{fs}}^{+}$ and $b_{\mathbf{fs}}$ of a phonon with momentum $\mathbf{f}$ and polarization $\mathbf{s}$, in accordance with the formula

$$u = \sqrt{\frac{\hbar}{\rho V}} \sum_{fs} \frac{\mathbf{e}_{fs}}{\sqrt{2\omega_{fs}}} \{b_{fs} e^{i\mathbf{f}\cdot\mathbf{r}} + b_{fs}^{+} e^{-i\mathbf{f}\cdot\mathbf{r}}\}$$

(ρ is the density of the matter, $\mathbf{e}_{\mathbf{fs}}$ is the vector of polarization of a phonon with momentum $\mathbf{f}$; the number of phonons with momentum $\mathbf{f}$ and polarization $\mathbf{s}$ is $N_{\mathbf{fs}} = b_{\mathbf{fs}}^{+} b_{\mathbf{fs}}$), and using (1) and (1′) we obtain the following expression for $\mathcal{H}_p$:

$$\mathcal{H}_p = i\Theta_c a^2 \sqrt{\frac{2\hbar}{\rho V}} \sum_{\mathbf{k}\mathbf{k}'fs} \{\beta_1[(\mathbf{e}_{fs}\cdot\mathbf{k})(\mathbf{f}\cdot\mathbf{k}') + (\mathbf{e}_{fs}\cdot\mathbf{k}')(\mathbf{f}\cdot\mathbf{k})] + \beta_2(\mathbf{k}\cdot\mathbf{k}')(\mathbf{e}_{fs}\cdot\mathbf{f})\}\, a_{\mathbf{k}}^{+} a_{\mathbf{k}} b_{fs} \frac{\Delta(\mathbf{k}' - \mathbf{k} - \mathbf{f})}{\sqrt{\omega_{fs}}} + \text{compl. conj.} \tag{5}$$

This Hamiltonian is responsible for the emission and absorption of a phonon by a spin wave, i.e., for transitions of the type

$$n_1,\ n_2,\ N_{fs} \rightarrow n_1 - 1,\ n_2 + 1,\ N_{fs} \pm 1.$$

3. The change per unit time in the number of spin waves with momentum $\mathbf{k}$, due to the above interactions, is determined by the following formulas.

$$\dot{n}_{\mathbf{k}} = \dot{n}_{\mathbf{k}}^{\text{col}} \equiv L\{n_{\mathbf{k}},\ N_{fs}\}, \tag{6}$$

$$L\{n_{\mathbf{k}},\ N_{fs}\} = L_e\{n_{\mathbf{k}}\} + L_w\{n_{\mathbf{k}}\} + L_a\{n_{\mathbf{k}}\} + L_p\{n_{\mathbf{k}},\ N_{fs}\},$$

where L_e, L_w, L_a, and L_p are collision operators connected with the Hamiltonians $\mathcal{H}_e$, $\mathcal{H}_w$, $\mathcal{H}_a$, and $\mathcal{H}_p$ as follows:

$$L_e\{n_{\mathbf{k}}\} = (24\pi\mu^2\Theta_c^2 a^4/\hbar M_0^2 V^2) \times \sum_{\mathbf{k}_1\mathbf{k}_2\mathbf{k}_3} (\mathbf{k}_2\cdot\mathbf{k}_4 + \mathbf{k}_1\cdot\mathbf{k}_3)(\mathbf{k}_2\cdot\mathbf{k}_4 + \mathbf{k}_1\cdot\mathbf{k}_3 + 8\beta_1\mu M_0/\Theta_c a^2) \times \{(n_{\mathbf{k}_1}+1)\,n_{\mathbf{k}_2} n_{\mathbf{k}_3}(n_{\mathbf{k}_4}+1) - n_{\mathbf{k}_1} n_{\mathbf{k}_2}(n_{\mathbf{k}_3}+1)(n_{\mathbf{k}_4}+1)\} \times \delta(\varepsilon_1 + \varepsilon_3 - \varepsilon_2 - \varepsilon_4)\,\Delta(\mathbf{k}_1 + \mathbf{k}_3 - \mathbf{k}_2 - \mathbf{k}_4); \tag{7}$$

$$L_w\{n_{\mathbf{k}}\} = (2\pi/\hbar) \sum_{\mathbf{k}_1\mathbf{k}_2\mathbf{k}_3} \{A_{\mathbf{k}_1\mathbf{k}_2\mathbf{k}_3}[n_{\mathbf{k}_2} n_{\mathbf{k}_3}(n_{\mathbf{k}_1}+1) - (n_{\mathbf{k}_2}+1)(n_{\mathbf{k}_3}+1)\,n_{\mathbf{k}_1}]\,\delta(\varepsilon_3 + \varepsilon_2 - \varepsilon_1)\,\Delta(\mathbf{k}_3 + \mathbf{k}_2 - \mathbf{k}_1) + A_{\mathbf{k}_1\mathbf{k}_3\mathbf{k}_2}[(n_{\mathbf{k}_1}+1)\,n_{\mathbf{k}_3}(n_{\mathbf{k}_2}+1) - n_{\mathbf{k}_1}(n_{\mathbf{k}_3}+1)\,n_{\mathbf{k}_2}] \times \delta(\varepsilon_3 - \varepsilon_2 + \varepsilon_1)\,\Delta(\mathbf{k}_3 - \mathbf{k}_2 - \mathbf{k}_1) + A_{\mathbf{k}_2\mathbf{k}_3\mathbf{k}_1}[n_{\mathbf{k}_1}(n_{\mathbf{k}_2}+1) \times (n_{\mathbf{k}_3}+1) - (n_{\mathbf{k}_1}+1)\,n_{\mathbf{k}_2} n_{\mathbf{k}_3}]\,\delta(\varepsilon_3 - \varepsilon_2 - \varepsilon_1)\Delta(\mathbf{k}_3 - \mathbf{k}_2 - \mathbf{k}_1)\}; \tag{8}$$

$$A_{\mathbf{k}_1\mathbf{k}_2\mathbf{k}_3} = (64\pi^2\mu^3 M_0/V)\,|\sin\vartheta_1\cos\vartheta_1\exp i\varphi_1 + \sin\vartheta_2\cos\vartheta_2\exp i\varphi_2|^2;$$

$$L_a\{n_{\mathbf{k}}\} = (24\pi\beta^2\mu^4/\hbar V^2) \sum_{\mathbf{k}_1\mathbf{k}_2\mathbf{k}_3} \{(1 + n_{\mathbf{k}_1} + n_{\mathbf{k}_2})\,n_{\mathbf{k}_3} n_{\mathbf{k}_4} - (1 + n_{\mathbf{k}_3} + n_{\mathbf{k}_4})\,n_{\mathbf{k}_1} n_{\mathbf{k}_2}\} \times \delta(\varepsilon_1 + \varepsilon_3 - \varepsilon_2 - \varepsilon_4)\,\Delta(\mathbf{k}_1 + \mathbf{k}_3 - \mathbf{k}_2 - \mathbf{k}_4); \tag{9}$$

$$L_p\{n_{\mathbf{k}},\ N_{fs}\} = (4\pi a^4\Theta_c^2/\rho V) \sum_{\mathbf{k}_1 fs} \omega_{fs}^{-1} \{\beta_1[(\mathbf{e}_{fs}\cdot\mathbf{k}_1)(\mathbf{f}\cdot\mathbf{k}_2) + (\mathbf{e}_{fs}\cdot\mathbf{k}_2)(\mathbf{f}\cdot\mathbf{k}_1)] + \beta_2(\mathbf{k}_1\cdot\mathbf{k}_2)(\mathbf{e}_{fs}\cdot\mathbf{f})\}^2 \{(N_{fs} n_{\mathbf{k}_1} - n_{\mathbf{k}_2} n_{\mathbf{k}_1} - n_{\mathbf{k}_1} - N_{fs} n_{\mathbf{k}_1})\,\delta(\varepsilon_1 - \varepsilon_2 - \hbar\omega_{fs})\,\Delta(\mathbf{k}_1 - \mathbf{k}_2 - \mathbf{f}) + (n_{\mathbf{k}_1} n_{\mathbf{k}_2} + n_{\mathbf{k}_1} N_{fs} + n_{\mathbf{k}_2} - n_{\mathbf{k}_1} N_{fs}) \times \delta(\varepsilon_2 - \varepsilon_1 - \hbar\omega_{fs})\,\Delta(\mathbf{k}_2 - \mathbf{k}_1 - \mathbf{f})\}. \tag{10}$$

By using the expression for the collision operators it is possible to obtain the mean probabilities

of various interactions of spin waves and phonons.

The mean probability of scattering of a spin wave by a spin wave, due to exchange interaction, is:[4]

$$w_e \approx (\Theta_c/\hbar)(\Theta/\Theta_c)^4. \quad (11)$$

The mean probability of splitting of a spin wave into two and of merging of two spin waves into one[3] is

$$w_w \approx 4\pi^{1/2}(\Theta_c/\hbar)(\mu M_0/\Theta_c)^2(\Theta/\Theta_c)^{1/2}\ln^2(\Theta/\mu M_0). \quad (12)$$

The probabilities of the remaining processes are less than w_e or w_w. In the temperature range $\Theta_c(\mu M_0/\Theta_c)^{4/7} < \Theta \ll \Theta_c$ the inequality $w_e \gg w_w$ holds, and therefore when $\Theta > \Theta_c(\mu M_0/\Theta_c)^{4/7}$ the largest term in $\dot{n}_k^{col}$ will be $L_e\{n_k\}$. The remainder of L, i.e., $L' = L_w + L_p + L_a$, can be considered in this temperature region as a small perturbation.

It is easy to see that the general solution of the equation

$$L_e\{n_k\} = 0$$

has the form

$$n_k = \begin{cases} [e^{(\varepsilon_k-\gamma)/\Theta_s}-1]^{-1}, & k \neq 0, \\ n_0, & k = 0, \end{cases} \quad (13)$$

where γ and n_0 are arbitrary constants. They can be connected with the initial values of the square of the magnetic moment $\mathfrak{M}^2$ and the projection of the magnetic moment $\mathfrak{M}_z$ on the axis of least magnetization. According to (1), these values are

$$\mathfrak{M}_z = \int_V M_z dV = M_0 V - 2\mu n_0 - 2\mu \sum_{k\neq 0} n_k$$
$$\mathfrak{M}^2 = \left\{\int_V \mathbf{M} dV\right\}^2 = (M_0 V)^2 - 4\mu V M_0 \sum_{k\neq 0} n_k. \quad (14)$$

We note that $\mathfrak{M}^2$ and $\mathfrak{M}_z$ commute with the Hamiltonian of exchange interaction $\mathcal{H}_e$ ($\mathfrak{M}_z$ commutes also with $\mathcal{H}_a$, but $\mathfrak{M}^2$ does not).

The time required to establish the Bose distribution (13) is of the following order of magnitude

$$\tau_e = 1/w_e \approx (\hbar/\Theta_c)(\Theta_c/\Theta)^4.$$

We now take into consideration the weak interactions $\mathcal{H}_a$, $\mathcal{H}_w$, and $\mathcal{H}_p$. Then the distribution (13), which satisfies the equation $L_e\{n_k\} = 0$, will no longer satisfy the equation $L\{n_k, N_{fs}\} = 0$. Since, however, the mean probability of the exchange interaction of the spin waves w_e is considerably greater than the probabilities of all the remaining processes, the distribution (13) with slowly varying parameters γ, n_0, and Θ_s, can satisfy approximately the equation

$$\dot{n}_k = L\{n_k, N_{fs}\}, \quad N_{fs} = [\exp\{\hbar\omega_{fs}/\Theta_p\} - 1]^{-1}$$

(here the phonon temperature Θ_p also changes slowly with time). By finding the form of the functions $\gamma(t)$, $n_0(t)$, $\Theta_s(t)$, and $\Theta_p(t)$ we can, in accordance with formulas (14), determine the variation of $\mathfrak{M}^2$ and $\mathfrak{M}_z$ with time, and also find the equalization time of the spin-wave and the phonon temperatures.

To determine the time derivatives of γ, n_0, Θ_s, and Θ_p we insert the distribution (13) into the expressions

$$\sum_{k\neq 0} \dot{n}_k = \sum_{k\neq 0} \dot{n}_k^{col}, \quad \dot{n}_0 = \dot{n}_0^{col}$$
$$\sum_{fs} \hbar\omega_{fs}\dot{N}_{fs} = -\sum_{k} \varepsilon_k \dot{n}_k = -\sum_{k} \varepsilon_k \dot{n}_k^{col}, \quad (15)$$
$$\sum_{k} \varepsilon_k n_k + \sum_{fs} \hbar\omega_{fs} N_{fs} = E_0.$$

The third equality determines the amount of heat transferred to the lattice from the spin system, while the last relation is the law of conservation of energy.

The change in γ and n_0 can be found from the first two equations. Since γ, being the "chemical potential" of the spin waves, is determined by the total number of the spin waves, which does not change if only the strong interaction $\mathcal{H}_e$ is taken into account, it is possible to determine $\dot{\gamma}$ by finding the change in $\sum_{k\neq 0} n_k$. Inserting the expression for the collision operators into (15) and linearizing over the quantities γ, $\Delta\Theta = \Theta_s - \Theta_p$, and $\eta = \epsilon_0 n_0/N$ (N is the total number of atoms in the body, and the quantity n_0/N is considered small but finite when $N \to \infty$), we obtain after simple transformations:

$$\Delta\dot{\Theta} + \Gamma_1\dot{\gamma} - \dot{\gamma}_i/c_p = B_{\gamma\gamma}\gamma + B_{\gamma\eta}\gamma_i,$$
$$\Delta\dot{\Theta} + \Gamma_2\dot{\gamma} + \dot{\gamma}_i/c_s = B_{\Theta\Theta}\Delta\Theta, \quad \dot{\gamma}_i = B_{\eta\eta}\gamma_i, \quad (16)$$

where c_s and c_p are the specific heats of the phonons, referred to one atom:

$$c_s = \frac{15\zeta(3/2)}{32\pi^{3/2}}\left(\frac{\Theta}{\Theta_c}\right)^{3/2}, \quad c_p = \frac{2\pi^2}{5}\left(\frac{\Theta}{\Theta_D}\right)^3 = \frac{2\pi^2\Theta^3}{5}\left(\frac{1}{\Theta_l^3} + \frac{2}{\Theta_t^3}\right)$$

($\Theta_l = \hbar s_l/a$, $\Theta_t = \hbar s_t/a$ are the Debye temperatures for the longitudinal and transverse sound); Γ_1 and Γ_2 are defined as

$$\Gamma_1 = -\frac{1}{c_p}\left\{\frac{\Theta}{N}\sum_{k\neq 0}\frac{\partial n_k}{\partial\Theta} + (c_s + c_p)\sum_{k\neq 0}\frac{\partial n_k}{\partial\varepsilon_k}\Big/\sum_{k\neq 0}\frac{\partial n_k}{\partial\Theta}\right\},$$
$$\Gamma_2 = \frac{\Theta}{c_s}\frac{1}{N}\sum_{k\neq 0}\frac{\partial n_k}{\partial\Theta}, \quad (16')$$

and the quantities $B_{\gamma\gamma}$, $B_{\gamma\eta}$, $B_{\Theta\Theta}$, and $B_{\eta\eta}$ are related to the collision operators by

$$\gamma B_{\gamma\gamma} = \frac{c_s + c_p}{c_s c_p}\frac{\Theta}{\Gamma_2}\frac{1}{N}\sum_{\mathbf{k}\neq 0} L_w\{n_{\mathbf{k}}\},$$

$$\gamma_1 B_{\gamma\eta} = -\frac{c_s + c_p}{c_s c_p}\frac{\Theta}{\Gamma_2}\frac{1}{N} L_a\{n_{\mathbf{k}}\}_{\mathbf{k}=0},$$

$$\Delta\Theta B_{\Theta\Theta} = \frac{c_s + c_p}{c_s c_p}\frac{1}{N}\sum_{\mathbf{k}\neq 0}\varepsilon_{\mathbf{k}} L_p\{n_{\mathbf{k}}, N_{1\mathbf{k}}\},$$

$$\eta_1 B_{\eta\eta} = \frac{\varepsilon_0}{N} L_a\{n_{\mathbf{k}}\}_{\mathbf{k}=0}$$

($L_a\{n_{\mathbf{k}}\}_{\mathbf{k}=0}$ is the value of the collision integral L_a when $\gamma = 0$ and a value n_0 is specified).

Using formulas (8) and (10) we obtain for the coefficients B

$$B_{\gamma\gamma} = -\frac{4}{5\pi}\frac{\mu^3 M_0}{\hbar a^3}\left(\frac{\Theta}{\Theta_c}\right)^2\frac{c_s + c_p}{c_s c_p}\frac{K(\xi)}{\Theta_c\Gamma_2};$$

$$B_{\gamma\eta} = \frac{3}{(2\pi)^3}\frac{\beta^2}{\beta_1^2}\frac{\mu^4}{\hbar a^6}\left(\frac{\Theta}{\Theta_c}\right)^2\frac{c_s + c_p}{c_s c_p}\frac{G(\xi)}{\Theta_c\Gamma_2};$$

$$B_{\eta\eta} = -\frac{3}{(2\pi)^3}\frac{\beta^2}{\beta_1^2}\frac{\mu^4\varepsilon_0\Theta}{\hbar a^6\Theta_c^3}G(\xi); \qquad (17)$$

$$B_{\Theta\Theta} = -\frac{1}{(2\pi)^3}\frac{\hbar}{\rho a^5}\left(\frac{\Theta}{\Theta_t}\right)^5\frac{c_s + c_p}{c_s c_p}J_t(\alpha_t)$$

$$-\frac{1}{(2\pi)^3}\frac{\hbar}{\rho a^5}\left(\frac{\Theta_t}{\Theta_c}\right)^3\left(\frac{\Theta}{\Theta_t}\right)^5 J_t(\alpha_t)\frac{c_s + c_p}{c_s c_p},$$

where

$$\xi = \varepsilon_0/\Theta,\quad \alpha_t = \Theta_t^2/\Theta\Theta_c,\quad \gamma_t = \Theta_t^2/\Theta\Theta_c;$$

$$K(\xi) = \xi^2\int_0^\infty dx\int_{1/4x}^\infty \frac{1/2 + 1/4xy}{(e^{\xi(1+x)} - 1)(e^{\xi(1+y)} - 1)(1 - e^{-\xi(x+y+2)})}dy;$$

$$G(\xi) = \int_\xi^\infty \frac{dx}{(e^x - 1)(1 - e^{-x})}\ln\frac{1 - e^{-x_0}}{1 - e^{-\xi}};$$

$$J_t(\alpha_t) = \frac{\beta_1^2}{\beta_1^2}\int_0^\infty \frac{y^4 dy}{e^y - 1}\int_{\underbrace{(y+\alpha_t)^2/4\alpha_t}}^\infty \frac{x - (y+\alpha_t)^2/4\alpha_t}{(1 - e^{-x})(e^{x-y} - 1)}dx;$$

$$J_t(\alpha_t) = \int_0^\infty \frac{y^4 dy}{e^y - 1}$$

$$\times\int_{(y+\alpha_t)^2/4\alpha_t}^\infty \frac{(1/2\beta_1)(\alpha_t^2 - y^2) + \beta_2[\alpha_t x - 1/2y(y+\alpha_t)]^2}{(1 - e^{-x})(e^{x-y} - 1)}dx.$$

Assuming in (16) that the quantities γ, η, and $\Delta\Theta$ vary as $\exp\{-\lambda t\}$, we obtain the following value for the relaxation constants:

$$\lambda_1 = \frac{\Gamma_1 B_{\Theta\Theta} + B_{\gamma\gamma} + ((\Gamma_1 B_{\Theta\Theta} - B_{\gamma\gamma})^2 + 4\Gamma_2 B_{\Theta\Theta} B_{\gamma\gamma})^{1/2}}{2(\Gamma_2 - \Gamma_1)};$$

$$\lambda_2 = \frac{\Gamma_1 B_{\Theta\Theta} + B_{\gamma\gamma} - ((\Gamma_1 B_{\Theta\Theta} - B_{\gamma\gamma})^2 + 4\Gamma_2 B_{\Theta\Theta} B_{\gamma\gamma})^{1/2}}{2(\Gamma_2 - \Gamma_1)}; \qquad (18)$$

$$\lambda_3 = -B_{\eta\eta}.$$

In the temperature range $\Theta_c \gg \Theta \gg \epsilon_0\,(\xi \ll 1)$, the expressions for λ_2 and λ_3 are greatly simplified and become

$$\lambda_2 \approx \frac{32\chi}{5}\frac{\mu M_0}{\hbar}\frac{\mu M_0}{\sqrt{\varepsilon_0\Theta_c}}\frac{\Theta}{\Theta_c},\quad \lambda_3 \approx \frac{\beta^2}{16\pi}\frac{\mu^4}{\hbar a^6\Theta_c}\left(\frac{\Theta}{\Theta_c}\right)^2, \qquad (19)$$

where

$$\chi = \frac{1}{12}\int_0^\infty dx\int_{1/4x}^\infty \frac{4 + 3/xy}{(1+x)(1+y)(2+x+y)}dy \sim 10^{-1}.$$

We present expressions for λ_1 in the limiting cases of "low" and "high" temperatures:[3,4]

$$\lambda_1 = \begin{cases} \dfrac{155\zeta(5)}{2\pi^5}\dfrac{\varepsilon_0^2}{\beta_1^2}\left(2 + \dfrac{\Theta_t^3}{\Theta_c^3}\right)\dfrac{\hbar}{\rho a^5}\dfrac{\Theta^5}{\Theta_c^3\Theta_t^3}\exp\left\{-\dfrac{\Theta_t^2}{4\Theta\Theta_c}\right\}, & \Theta \ll \dfrac{\Theta_t^2}{\Theta_c}, \\ \dfrac{2^6\pi^{4/3}}{765\zeta(2/3)}\dfrac{\hbar}{\rho a^5}[2\beta_1^2 + (2\beta_1 + \beta_2)^2]\left(\dfrac{\Theta}{\Theta_c}\right)^{5/2}, & \Theta \gg \dfrac{\Theta_t^2}{\Theta_c}. \end{cases} \qquad (20)$$

Using (14) to (16) we can show that the time variation of $\Delta\Theta$, $\mathfrak{M}_z$, and $\mathfrak{M}^2$ is determined by the following formulas

$$\Delta\Theta = \frac{n_1}{N}\frac{\lambda_3}{\lambda_1}\frac{\varepsilon_0}{c_s}e^{-\lambda_3 t} + \Delta\Theta_1 e^{-\lambda_1 t} + \Delta\Theta_2 e^{-\lambda_2 t};$$

$$\mathfrak{M}_z = \overline{\mathfrak{M}_z} - 2\mu n_0(1-\zeta)e^{-\lambda_3 t} - 2\mu N\frac{c_p c_s}{c_p + c_s}\frac{\Gamma_2 B_{\gamma\gamma}}{\lambda_1\Gamma_1 + B_{\gamma\gamma}}\frac{\Delta\Theta_1}{\Theta}e^{-\lambda_1 t}$$
$$- 2\mu N\frac{c_p c_s}{c_p + c_s}\frac{\Gamma_2 B_{\gamma\gamma}}{\lambda_2\Gamma_1 + B_{\gamma\gamma}}\frac{\Delta\Theta_2}{\Theta}e^{-\lambda_2 t},$$

$$\mathfrak{M}^2 = \overline{\mathfrak{M}^2} + 4\mu M_0 V\zeta n_0 e^{-\lambda_3 t} \qquad (21)$$
$$- 4\mu M_0 NV\frac{c_p c_s}{c_p + c_s}\frac{\Gamma_2 B_{\gamma\gamma}}{\Gamma_1\lambda_1 + B_{\gamma\gamma}}\frac{\Delta\Theta_1}{\Theta}e^{-\lambda_1 t}$$
$$- 4\mu M_0 NV\frac{c_p c_s}{c_p + c_s}\frac{\Gamma_2 B_{\gamma\gamma}}{\Gamma_1\lambda_2 + B_{\gamma\gamma}}\frac{\Delta\Theta_2}{\Theta}e^{-\lambda_2 t},$$

where $\overline{\mathfrak{M}_z}$ and $\overline{\mathfrak{M}^2}$ are the equilibrium values of $\mathfrak{M}_z$ and $\mathfrak{M}^2$ for the given temperature,

$$\zeta = -\frac{\lambda_3}{\lambda_1} + \frac{\varepsilon_0}{\Theta}\frac{\Gamma_2}{c_s + c_p}\left(c_s - \frac{\lambda_3}{\lambda_1}c_p\right) \ll 1$$

and the integration constants n_0, $\Delta\Theta_1$, and $\Delta\Theta_2$ are determined by the initial values of $\Delta\Theta$, $\mathfrak{M}_z$, and $\mathfrak{M}^2$.

We note that of the three quantities λ_1, λ_2, and λ_3 the smallest is λ_3. Therefore, if $t \gg 1/\lambda_1$ or $1/\lambda_2$, it is necessary to retain in (21) only one term, proportional to $\exp\{-\lambda_3 t\}$. The values of $\mathfrak{M}_z$, $\mathfrak{M}^2$, and $\Delta\Theta$ now become

$$\mathfrak{M}_z = \overline{\mathfrak{M}_z} - 2\mu n_0\zeta e^{-\lambda_3 t},\quad \mathfrak{M}^2 = \overline{\mathfrak{M}^2} + 4\mu M_0 V n_0\zeta e^{-\lambda_3 t},$$
$$\Delta\Theta = \frac{n_1}{N}\frac{\lambda_3}{\lambda_1}\frac{\varepsilon_0}{c_s}e^{-\lambda_3 t}. \qquad (22)$$

Since $\zeta \ll 1$, $(\mathfrak{M}_z - \overline{\mathfrak{M}_z})/\overline{\mathfrak{M}_z}$ is considerably greater than $(\mathfrak{M}^2 - \overline{\mathfrak{M}^2})/\overline{\mathfrak{M}^2}$. In other words, first to be established is the equilibrium of the square of the moment at $\mathfrak{M}^2$, this is followed by a slow rotation of the magnetic moment towards the axis of least magnetization, which in turn establishes the equilibrium value of $\mathfrak{M}_z$. Such a relaxation process can be described phenomenologically by the well-known Landau-Lifshitz equation.[1] The time

of relaxation of the magnetic moment towards the axis of least magnetization is

$$\tau = 1/\lambda_3 = (16\pi/\beta^2)(\hbar a^6\Theta_c/\mu^3)(\Theta_c/\Theta)^2.$$

Putting $\beta \sim 10$, $\Theta_c \sim 10^{-13}$ erg, $a \sim 2 \times 10^{-8}$ cm, and $\Theta/\Theta_c \sim 10^{-1}$, we get $\tau \sim 10^{-5}$ sec.

In conclusion, the authors thank Academician L. D. Landau and M. I. Kaganov for valuable discussions.

[1] L. D. Landau and E. M. Lifshitz, Sow. Phys. **8**, 153 (1935).

[2] T. Holstein and H. Primakoff, Phys. Rev. **58**, 1098 (1940).

[3] A. I. Akhiezer, J. of Phys. (U.S.S.R.) **10**, 217 (1946).

[4] M. I. Kaganov and V. M. Tsukernik, J. Exptl. Theoret. Phys. (U.S.S.R.) **35**, 474 (1958), Soviet Phys. JETP **8**, 327 (1959).

[5] L. D. Landau and E. M. Lifshitz, Статистическая физика (Statistical Physics) 2d ed., GITTL, 1951.

Translated by J. G. Adashko
29

PHENOMENOLOGICAL THEORY OF KINETIC PROCESSES IN FERROMAGNETIC DIELECTRICS. II. INTERACTION OF SPIN WAVES WITH PHONONS

M. I. KAGANOV and V. M. TSUKERNIK

Physico-Technical Institute, Academy of Sciences, Ukrainian S.S.R.

Submitted to JETP editor July 8, 1958

J. Exptl. Theoret. Phys. (U.S.S.R.) **36**, 224-232 (January, 1959)

The interaction between spin waves and phonons is considered. The time for establishment of equilibrium between phonons and spin waves is calculated.

In a previous work,*[1] a phenomenological method was used to obtain the magnetic part of the energy spectrum of a ferromagnetic dielectric, and the interaction of spin waves with one another was considered. Besides the spin waves there are in a ferromagnetic dielectric, as in any solid body, energy branches connected with vibrations of the crystal lattice (phonons). Three of these, the acoustic, play a basic part both in thermal properties and in kinetic processes. The present work deals with the study of the interaction of spin waves with phonons.

Interaction of elementary excitations (quasiparticles) with each other leads to the establishment of statistical equilibrium in the body. We calculate here the time for establishment of such equilibrium. For this purpose the process of establishment of equilibrium is regarded as a process of equalization of the temperatures of the phonons and of the spin waves. Such an approach is permissible if the time for establishment of equilibrium within each of the subsystems (phonons and spin waves) is considerably shorter than the time of relaxation between the subsystems; as will be shown below, this condition is satisfied over a wide temperature range.

Similar questions have been considered by Akhiezer[2] from a microscopic point of view. Besides the processes studied by him, processes are here considered in which two phonons take part.

1. THE INTERACTION HAMILTONIAN

In a phenomenological approach to the study of interaction between spin waves and phonons, it is appropriate to describe the spin waves by the vector density of magnetic moment, $\mathbf{M} = \mathbf{M}(\mathbf{r}, t)$, and the phonons by the strain tensor, $u_{ik} = \frac{1}{2}(\partial u_i/\partial x_k + \partial u_k/\partial x_i)$ [$\mathbf{u} = \mathbf{u}(\mathbf{r}, t)$ = displacement vector]. The interaction Hamiltonian will then be the sum of all those terms, in the expansion of the energy of the ferromagnetic in powers of M_i, $\partial M_i/\partial x_k$, and u_{ik}, that have the form*

$$\gamma_{iklm}\int M_i M_k u_{lm}\,dv, \qquad \lambda_{iklmrs}\int \frac{\partial M_i}{\partial x_k}\frac{\partial M_l}{\partial x_m}u_{rs}\,dv.$$

These terms include all the invariant combinations that contain the tensor u_{ik} linearly, and the vector M_i and its spatial derivatives quadratically. The terms quadratic in u_{ik} are responsible for the two-phonon processes and will be considered below. Terms linear in M_i cannot enter, since M_i is a pseudovector.

The first of the terms written corresponds to magnetostrictive energy, which in the isotropic case (we shall henceforth restrict ourselves to it) can be written in the following form:

$$\gamma_0\int M^2 \operatorname{div}\mathbf{u}\,dv + \gamma\int M_i M_k u_{ik}\,dv.$$

The first of the integrals vanishes, since $M^2 \equiv M_0^2$. The second contains an anisotropic combination of the components of the vector $\mathbf{M}$ and consequently is of relativistic origin. The value of the constant γ may be taken from magnetostriction measurements at low temperatures.

The term quadratic in the derivatives of $\mathbf{M}$ drops out when the magnetization is uniform and therefore does not enter into the ordinary magnetostrictive effects. The largest among the constants λ are those that are connected with (isotropic) exchange interaction.

On the basis of these remarks, we write the interaction Hamiltonian in the following form:

$$\mathcal{H}_{int} = \mathcal{H}_{ms} + \mathcal{H}_{ex}, \qquad (1)$$

*The notation of the present work coincides with the notation of reference 1.

*Summation over repeated indices is understood.

where

$$\mathcal{H}_{ms} = \gamma \int M_i M_k u_{ik}\, dv;$$

$$\mathcal{H}_{ex} = \lambda_1 \int \frac{\partial M_l}{\partial x_i}\frac{\partial M_l}{\partial x_k} u_{ik}\, dv + \lambda_2 \int \frac{\partial M_l}{\partial x_i}\frac{\partial M_i}{\partial x_l} u_{kk}\, dv. \quad (2)$$

The energy $\mathcal{H}_{ex}$ may be considered the result of expansion of the exchange interaction energy $\int \alpha_{ik} (\partial M_l/\partial x_i)(\partial M_l/\partial x_k)\, dv$ (cf. reference 1) in powers of u_{ik}. Therefore the constants $\lambda_{1,2}$ are conveniently written $(\beta_{1,2}/2)(\Theta_c/\mu M_0)a^2$, where $\beta_{1,2}$ are dimensionless constants of order unity.

In the ground state the density of magnetic moment is uniform and constant and equal to $\mathbf{M}_0$. We choose the z axis along the vector $\mathbf{M}_0$. Then near the ground state, to terms quadratic in the deviation of the magnetic moment from $\mathbf{M}_0$, we get

$$\begin{aligned}\mathcal{H}_{ms} &= 2\gamma M_0 \int (M_x u_{xz} + M_y u_{yz})\, dv \\ &+ \frac{1}{4}\gamma \int \{(M^+)^2 (u_{xx} - u_{yy} - 2iu_{xy}) \\ &+ (M^-)^2 (u_{xx} - u_{yy} + 2iu_{xy}) \\ &+ 2M^+M^- (u_{xx} + u_{yy}) + 2M_0 M_z' u_{zz}\}\, dv,\end{aligned} \quad (3)$$

$$\mathcal{H}_{ex} = \frac{\beta_1}{2}\frac{\Theta_c}{\mu M_0} a^2 \int \frac{\partial M^+}{\partial x_i}\frac{\partial M^-}{\partial x_k} u_{ik}\, dv + \frac{\beta_2}{2}\frac{\Theta_c}{\mu M_0} a^2 \int \frac{\partial M^+}{\partial x_i}\frac{\partial M^-}{\partial x_i} u_{kk} dv, \quad (4)$$

where

$$M^{\pm} = M_x \pm iM_y; \quad M_z' = M_z - M_0. \quad (5)$$

We remark that M_z' is quadratic in M_x and M_y.

The first integral in the expression (3) describes the connection between elastic and spin waves in a ferromagnetic[3,4] and is not connected with transitions between stationary states of the system of spin waves and phonons. Therefore it is hereafter omitted.

For the study of kinetic processes, the magnetic moment density $\mathbf{M}$ and the strain tensor u_{ik} are to be considered operators. In terms of the second-quantization operators a_λ and a_λ^*, the components of the moment are expressed as (cf. reference 1):*

$$M^+ = (2\mu M_0)^{1/2}\hat{a}^*; \quad M^- = (2\mu M_0)^{1/2}\hat{a}, \quad M_z' = -\mu \hat{a}^*\hat{a},$$

$$\hat{a} = V^{-1/2}\sum_\lambda \hat{a}_\lambda(t)\, e^{i\mathbf{k}_\lambda \mathbf{r}}; \quad \hat{a}_\lambda(t) = \hat{a}_\lambda e^{-i\varepsilon_\lambda t/\hbar}, \quad (6)$$

$\mathbf{k}_\lambda$ and ϵ_λ are the wave vector and energy of the spin wave.

In the temperature range of interest to us ($T \gg 2\pi\mu M_0$), we may, in the spectrum, neglect the magnetic interaction and limit ourselves to the Bloch dispersion law

$$\varepsilon_\lambda = \Theta_c (ak_\lambda)^2. \quad (7)$$

In the representation based on occupation numbers n_λ of the spin waves, the nonvanishing matrix elements of the operators a_λ and a_λ^* are respectively equal to

$$(n_\lambda | \hat{a}_\lambda | n_\lambda + 1) = \sqrt{n_\lambda + 1}; \quad (n_\lambda | \hat{a}_\lambda^* | n_\lambda - 1) = \sqrt{n_\lambda}. \quad (8)$$

The strain tensor component operators u_{ik} are expressed in terms of the creation and annihilation operators $\hat{b}_{\lambda s}$ and $\hat{b}_{\lambda s}^*$ for phonons in the following form:

$$u_{ik} = {}^1/_2 (\partial u_i/\partial x_k + \partial u_k/\partial x_i);$$
$$\mathbf{u} = V^{-1/2}\sum_{\lambda, s} \sqrt{\hbar/2\rho\omega_{\lambda s}}\, \mathbf{p}_{\lambda s} [\hat{b}_{\lambda s}(t)\, e^{i\mathbf{k}_\lambda \mathbf{r}} + \hat{b}_{\lambda s}^*(t)\, e^{-i\mathbf{k}_\lambda \mathbf{r}}]; \quad (9)$$

$$\hat{b}_{\lambda s}(t) = e^{-i\omega_{\lambda s} t}\hat{b}_{\lambda s};$$
$$(N_{\lambda s} | \hat{b}_{\lambda s} | N_{\lambda s} + 1) = \sqrt{N_{\lambda s} + 1},$$
$$(N_{\lambda s} | \hat{b}_{\lambda s}^* | N_{\lambda s} - 1) = \sqrt{N_{\lambda s}}. \quad (10)$$

Here ρ is the density of matter, $\mathbf{p}_{\lambda s}$ is a unit vector of polarization of a sound wave, the index s identifies the polarization, and $\mathbf{f}_\lambda$ and $\omega_{\lambda s}$ are the wave vector and frequency of a phonon.

For longitudinal polarization,

$$\omega_{\lambda s} = \omega_{\lambda l} = c_l f_\lambda; \quad (11)$$

for transverse polarization,

$$\omega_{\lambda s} = \omega_{\lambda t} = c_t f_\lambda, \quad (11')$$

c_l and c_t are the longitudinal and transverse sound velocities ($c_l > c_t$).

On substituting the expansions (6) and (9) in formulas (3) and (4) and integrating over the volume, we get

$$\mathcal{H}_{ms} = \frac{i\gamma\sqrt{\mu M_0}}{2}\sqrt{\frac{\hbar}{2\rho V}}\sum_{\lambda\lambda' s s'}\frac{1}{\sqrt{\omega_{\lambda' s'}}}\{p_{\lambda' s'}^- f_{\lambda'} a_\lambda^* a_{\lambda'}^* b_{\lambda' s'} + (p_{\lambda' s'}^+ f_{\lambda'} - p_{\lambda' s'}^z f_{\lambda'}^z) a_\lambda^* a_{\lambda'} b_{\lambda' s'}\} + \text{complex conjugate}. \quad (12)$$

*In formulas (6) we have omitted terms of the third order in the operators a_λ and a_λ^*, since they play no part in the processes considered below.

$$\mathcal{H}_{ex} = -\frac{ia^2\Theta_c}{V^{1/2}}\sqrt{\frac{\hbar}{2\rho}}\sum_{\lambda\mu\nu s}\frac{1}{V\sqrt{\omega_{\nu s}}}\left\{\frac{\beta_1}{2}(p^i_{\nu s}f^k_\nu + p^k_{\nu s}f^i_\nu)k^i_\lambda k^k_\mu\right.$$

$$\left. + \beta_2(k^i_\lambda k^i_\mu)(f^k_\nu p^k_{\nu s})\right\}a^*_\lambda a_\mu b_{\nu s} + \text{complex conjugate}. \quad (13)$$

Here $p^\pm = p^x \pm ip^y$, $f^\pm = f^x \pm if^y$. The operator $a^*_\lambda a_\mu b_{\nu s}$ describes the process of creation of a phonon by a spin wave. To this process corresponds the following law of conservation of momentum:

$$\mathbf{k}_\lambda = \mathbf{k}_\mu + \mathbf{f}_\nu. \quad (14)$$

The operator $a^*_\lambda a^*_\mu b_{\nu s}$ describes the annihilation of two spin waves with formation of a phonon. To it corresponds the conservation law

$$\mathbf{k}_\lambda + \mathbf{k}_\mu = \mathbf{f}_\nu. \quad (15)$$

Both conservation laws (14) and (15) are obtained naturally upon integration over the volume.

2. GENERATION AND ABSORPTION OF PHONONS BY SPIN WAVES

Since the dispersion law (7) for spin waves coincides with the dispersion law for ordinary free particles, the generation of phonons by spin waves is analogous to the Cerenkov radiation of sound waves by particles in motion at supersonic speed. From this it follows that the condition for radiation of a phonon has the form: for longitudinal phonons $v_S > c_l$, for transverse phonons $v_S > c_t$, where $v_S = 2\Theta_c a^2 k_\lambda/\hbar$ is the speed of the spin wave. By expressing k_λ in terms of ϵ_λ, we may write the radiation condition

$$\varepsilon_\lambda > \Theta^2_{ul}/4\Theta_c, \quad (16)$$

where Θ_0 is the Debye temperature; $\Theta_0 = \hbar c_l/a$ for longitudinal phonons, and $\Theta_0 = \hbar c_t/a$ for transverse phonons. From the condition (16) it is clear that the generation of a phonon by a spin wave is an activation process.

As follows from formulas (12) and (13), the Hamiltonian that describes this process has the form

$$\mathcal{H}_e = \frac{i}{2}\sqrt{\frac{\hbar}{2\rho V}}\sum_{\lambda\mu\nu s}\frac{1}{V\sqrt{\omega_{\nu s}}}\{\gamma\mu M_0(p^+_{\nu s}f^-_\nu + p^-_{\nu s}f^+_\nu - p^z_{\nu s}f^z_\nu)$$

$$+ \Theta_c a^2[\beta_1(p^i_{\nu s}f^k_\nu + p^k_{\nu s}f^i_\nu)k^i_\lambda k^k_\mu + 2\beta_2 k^i_\lambda k^i_\mu f^k_\nu p^k_{\nu s}]\}a^*_\lambda a_\mu b_{\nu s} + \text{c. c.}$$

On comparing the terms inside the curly brackets we find that for $T \gg \mu M_0$ the second term is considerably larger than the first, since $\Theta_c a^2 k^i_\lambda k^k_\mu \sim \epsilon \sim T$. Therefore

$$\mathcal{H}_e = \frac{i}{2}a^2\Theta_c\sqrt{\frac{\hbar}{2\rho V}}\sum_{\lambda\mu\nu s}\frac{1}{V\sqrt{\omega_{\nu s}}}[\beta_1(p^i_{\nu s}f^k_\nu + p^k_{\nu s}f^i_\nu)k^i_\lambda k^k_\mu$$

$$+ 2\beta_2 k^i_\lambda k^i_\mu f^k_\nu p^k_{\nu s}]a^*_\lambda a_\mu b_{\nu s} + \text{c. c.} \quad (17)$$

The nonvanishing matrix elements of the Hamiltonian $\mathcal{H}_e$ correspond to a transition n_λ, n_μ, $N_{\nu s} \to n_\lambda - 1$, $n_\mu + 1$, $N_{\nu s} + 1$ and to the reverse transition. According to (8) and (10) we have for the indicated transitions

$$(n_\lambda, n_\mu, N_{\nu s}|\mathcal{H}_e|n_\lambda - 1, n_\mu + 1, N_{\nu s} + 1)$$

$$= \frac{i}{2}\sqrt{\frac{\hbar}{2\rho V\omega_{\nu s}}}\Theta_c a^2\{\beta_1(p^i_{\nu s}f^k_\nu + p^k_{\nu s}f^i_\nu)k^i_\lambda k^k_\mu + 2\beta_2 k^i_\lambda k^i_\mu f^k_\nu p^k_{\nu s})\}$$

$$\times\sqrt{n_\lambda(n_\mu+1)(N_{\nu s}+1)}\exp\left\{\frac{i}{\hbar}(\varepsilon_\lambda - \varepsilon_\mu - \hbar\omega_{\nu s})t\right\}.$$

Hence the transition probability is

$$(n_\lambda, n_\mu, N_{\nu s}|W|n_\lambda - 1, n_\mu + 1, N_{\nu s} + 1)$$

$$= \frac{\pi\Theta_c^2 a^4}{4\rho V\omega_{\nu s}}\{\beta_1(p^i_{\nu s}f^k_\nu + p^k_{\nu s}f^i_\nu)k^i_\lambda k^k_\mu + 2\beta_2 k^i_\lambda k^i_\mu f^k_\nu p^k_{\nu s})^2 \quad (18)$$

$$\times n_\lambda(n_\mu+1)(N_{\nu s}+1)\delta(\varepsilon_\lambda - \varepsilon_\mu - \hbar\omega_{\nu s}).$$

The δ-function guarantees the energy conservation law

$$\varepsilon_\lambda = \varepsilon_\mu + \hbar\omega_{\nu s}. \quad (19)$$

We recall that the momentum conservation law for the process under study has the form (14).

We now consider the transfer of energy from spin waves to phonons. The energy received by the phonon system in unit time is

$$\dot{U}_e = \sum_{\nu s}\hbar\omega_{\nu s}\dot{N}_{\nu s}, \quad (20)$$

where $\dot{N}_{\nu S}$ is the change in the number of phonons in unit time resulting from radiation and absorption of sound waves by spin waves. According to (18),

$$\dot{N}_{\nu s} = \frac{\pi\Theta_c^2 a^4}{4\rho V\omega_{\nu s}}\sum_{\lambda\mu}A^2_s\{n_\lambda(n_\mu+1)(N_{\nu s}+1)$$

$$-(n_\lambda+1)n_\mu N_{\nu s}\}\delta(\varepsilon_\lambda - \varepsilon_\mu - \hbar\omega_{\nu s}), \quad (21)$$

$$A_s = \beta_1[(\mathbf{p}_{\nu s}\cdot\mathbf{k}_\lambda)(\mathbf{f}_\nu\cdot\mathbf{k}_\mu) + (\mathbf{p}_{\nu s}\cdot\mathbf{k}_\mu)(\mathbf{f}_\nu\cdot\mathbf{k}_\lambda)] + 2\beta_2(\mathbf{k}_\lambda\cdot\mathbf{k}_\mu)(\mathbf{f}_\nu\cdot\mathbf{p}_{\nu s}).$$

Here and hereafter, the sum extends over those values of the wave vectors that satisfy the momentum conservation law.

On inserting the value of $\dot{N}_{\nu S}$ into (20), we get

$$\dot{U}_e = \frac{\pi\Theta_c^2 a^4\hbar}{4\rho V}\sum_{\lambda\mu\nu s}A^2_s\{n_\lambda(n_\mu+1)(N_{\nu s}+1)$$

$$-(n_\lambda+1)n_\mu N_{\nu s}\}\delta(\varepsilon_\lambda - \varepsilon_\mu - \hbar\omega_{\nu s}). \quad (22)$$

Upon replacement of n_λ and $N_{\nu s}$ by the Bose equilibrium distribution, U_e naturally vanishes. On deviation of the system from the equilibrium state, the return to the equilibrium state will proceed thus: equilibrium will be established first within each subsystem (spin waves and phonons), and then — considerably more slowly — between the subsystems. The second stage can be described as a process of equalization of the temperatures of the spin waves and of the phonons. Clearly such a view is correct if the time for temperature equalization is much longer than the relaxation time of spin waves.[1] As will be clear below, this condition is satisfied over a wide temperature range.

Thus we shall consider that the spin waves and the phonons are described by Bose equilibrium distribution functions with different temperatures, respectively equal to $T_s = T$ and to $T_{ph} = T - \Delta T$. Hereafter we shall always consider that $\Delta T \ll T$.

On the basis of these remarks, we get from formula (22)

$$\dot{U}_e = \frac{\pi\Theta_c^2 a^4 k^2}{4\rho V T^2}\,\Delta T \sum_{\lambda;\nu s} A_s^2 \omega_{\nu s}\,\frac{e^{\varepsilon_\lambda/T}\,\delta(\varepsilon_\lambda - \varepsilon_{\lambda'} - \hbar\omega_{\nu s})}{(e^{\varepsilon_\lambda/T}-1)(e^{\varepsilon_{\lambda'}/T}-1)(e^{\hbar\omega_{\nu s}/T}-1)} \tag{23}$$

or

$$\dot{U}_e = \dot{U}_e^l + \dot{U}_e^t, \tag{24}$$

where $\dot{U}_e^{l,t}$ is the amount of energy transferred to a longitudinal (transverse) phonon in one second. $\dot{U}_e^{l,t}$ is determined by formula (23) with A_s^2 replaced by $A_{l,t}^2$. From expression (21), with account taken of the momentum conservation law (14), we have:

$$A_l^2 = 2\,\{\beta_1 f_\nu k_\lambda \cos\theta_{\lambda\nu}\,(k_\lambda \cos\theta_{\lambda\nu} - f_\nu) + \beta_2 f_\nu k_\lambda\,(k_\lambda - f_\nu \cos\theta_{\lambda\nu})\}, \tag{25}$$

$$A_t^2 = \beta_1 f_\nu k_\lambda \sin\theta_{\lambda\nu}\,(2k_\lambda \cos\theta_{\lambda\nu} - f_\nu) \tag{26}$$

($\theta_{\lambda\nu}$ is the angle between the vectors $\mathbf{k}_\lambda$ and $\mathbf{f}_\nu$).

On going over from summation to integration, we get after integration over angles

$$\dot{U}_e^l = \frac{V\hbar}{6\,(2\pi)^3\,\rho a^5}\left(\frac{T}{\Theta_l}\right)^5 \Delta T J_{el}(\alpha_l),$$
$$\dot{U}_e^t = \frac{V\hbar}{16\,(2\pi)^3\,\rho a^5}\,\frac{T^5}{\Theta_c^3\Theta_t^2}\,\Delta T J_{et}(\alpha_t), \tag{27}$$

where

$$J_{el}(\alpha) = \int_0^\infty \frac{y^4 dy}{e^y - 1}$$
$$\int_{(1/4\alpha)^2(y+\alpha)^2}^\infty \frac{e^x\,\{\beta_1(\alpha^2 - y^2) + 2\beta_2\,[2\alpha x - y(y+\alpha)]\}^2 dx}{(e^x - 1)(e^{x-y} - 1)}; \tag{28}$$

$$J_{et}(\alpha) = \beta_1^2 \int_0^\infty \frac{y^4 dy}{e^y - 1} \int_{(1/4\alpha)^2(y+\alpha)^2}^\infty \frac{e^x\,[x - (y+\alpha)^2/4\alpha]\,dx}{(e^x - 1)(e^{x-y} - 1)},$$

$$\alpha_l = \Theta_l^2/\Theta_c T, \quad \alpha_t = \Theta_t^2/\Theta_c T. \tag{29}$$

We consider the limiting cases of high and low temperatures.

High temperatures ($\alpha_l,\ \alpha_t \ll 1$). Here

$$J_{el}(\alpha) \approx \frac{2^7\pi^4\alpha^4}{15}\,\frac{\beta_1^2 + 2(\beta_1+\beta_2)^2}{3}; \quad J_{et}(\alpha) \approx 8\zeta(3)\,\alpha^2\beta_1^2. \tag{30}$$

On substituting in (22) the asymptotic value of the integrals, we find

$$\dot{U}_e^l \approx \frac{\pi V\hbar}{60\rho a^5}\,\frac{\beta_1^2 + 2(\beta_1+\beta_2)^2}{3}\left(\frac{T}{\Theta_c}\right)^4 \Delta T \quad (T \gg \Theta_l^2/\Theta_c), \tag{31}$$

$$\dot{U}_e^t \approx \frac{\zeta(3)\,\beta_1^2 V\hbar}{16\pi^3\rho a^5}\,\frac{\Theta_t^2}{\Theta_c^2}\left(\frac{T}{\Theta_c}\right)^3 \Delta T \quad (T \gg \Theta_t^2/\Theta_c). \tag{32}$$

On comparison of expressions (31) and (32), we find that for $T \gg \Theta_l/\Theta_c$, always $\dot{U}_e^l \gg \dot{U}_e^t$ ($\beta_1 \sim \beta_2$). Therefore

$$\dot{U}_e \approx \frac{\pi V\hbar}{60\rho a^5}\,\frac{\beta_1^2 + 2(\beta_1+\beta_2)^2}{3}\left(\frac{T}{\Theta_c}\right)^4 \Delta T, \quad (T \gg \Theta_l^2/\Theta_c). \tag{33}$$

Low temperatures ($\alpha_l,\ \alpha_t \gg 1$). In this case

$$J_{el}(\alpha) \approx 24\cdot 31\zeta(5)\,\alpha^4 e^{-\alpha/4}\,(\beta_1+\beta_2)^2,$$
$$J_{et}(\alpha) \approx 24\cdot 31\zeta(5)\,\beta_1^2 e^{-\alpha/4}.$$

Hence

$$\dot{U}_e^l \approx \frac{3V\hbar}{2\pi^2\rho a^5}\,(\beta_1+\beta_2)^2\left(\frac{T}{\Theta_c}\right)^4 \exp\left\{-\frac{\Theta_l^2}{4\Theta_c T}\right\}\Delta T,$$
$$(T \ll \Theta_l/\Theta_c), \tag{34}$$

$$\dot{U}_e^t \approx \frac{6\beta_1^2 V\hbar}{\pi^2\rho a^5}\,\frac{T^5}{\Theta_c^3\Theta_t^2}\exp\left\{-\frac{\Theta_t^2}{4\Theta_c T}\right\}\Delta T, \quad (T \ll \Theta_t^2/\Theta_c). \tag{35}$$

Since $\Theta_l > \Theta_t$ (cf. reference 5), the fundamental role in energy transfer at low temperatures is played by the process of generation of transverse phonons, i.e.,

$$\dot{U}_e \approx \frac{6\beta_1^2 V\hbar}{\pi^2\rho a^5}\,\frac{T^5}{\Theta_c^3\Theta_t^2}\exp\left\{-\frac{\Theta_t^2}{4\Theta_c T}\right\}\Delta T, \quad (T \ll \Theta_t^2/\Theta_c). \tag{36}$$

As was to be expected, the coefficient of heat emission for the activation process of radiation and absorption of phonons decreases exponentially with temperature.

3. ANNIHILATION OF TWO SPIN WAVES WITH FORMATION OF A PHONON, AND DISSOCIATION OF A PHONON INTO TWO SPIN WAVES

The processes indicated in the section title occur by virtue of the magnetostrictive part (12) of the Hamiltonian. Because of the relativistic origin of the magnetostrictive energy, the probability of these processes is small. However, as will be evident below, the corresponding coeffi-

cient of heat transfer does not contain an exponential dependence on temperature (at low temperatures). Therefore it becomes necessary to make a comparison of the coefficient of heat emission resulting from generation and absorption of phonons with the corresponding coefficient resulting from the processes to be investigated.

By use of the Hamiltonian (12) and of a formula analogous to formula (20), we find [with the aid of the expressions (8) and (10) for the matrix elements of the operators a_λ and b_λ] that the energy given up by the spin waves to the lattice in unit time by virtue of the processes under investigation is equal to

$$\dot{U}_a = \frac{\pi\hbar\gamma^2(\mu M_0)^2}{\rho V}\sum_{\lambda\mu\nu s}{}' B_s^2\{(N_{\nu s}+1)n_\lambda n_\mu - N_{\nu s}(n_\lambda+1)(n_\mu+1)\}\,\delta(\varepsilon_\lambda+\varepsilon_\mu-\hbar\omega_{\nu s}), \tag{37}$$

where

$$B_s = |p_{\nu s}^{+}f_\nu^{+}|. \tag{38}$$

As before, we get from (37) and (38)

$$\dot{U}_a = \dot{U}_a^l + \dot{U}_a^t,$$

where

$$\dot{U}_a^l = \frac{\gamma^2 V\hbar}{60\pi^3\rho a^5}\left(\frac{\mu M_0}{\Theta_c}\right)^2\left(\frac{T}{\Theta_l}\right)^6\Delta T J_a(\alpha_l),$$
$$\dot{U}_a^t = \frac{\gamma^2 V\hbar}{40\pi^3\rho a^5}\left(\frac{\mu M_0}{\Theta_c}\right)^2\left(\frac{T}{\Theta_t}\right)^4\Delta T J_a(\alpha_t), \tag{39}$$

here

$$J_a = \int_0^{2\alpha} y^4 e^y dy \int_{x_1}^{x_2}\frac{dx}{(e^x-1)(e^{y-x}-1)},$$
$$x_{1,2} = \frac{y}{2}\left(1 \mp \sqrt{\frac{2y}{\alpha}-\frac{y^2}{\alpha^2}}\right), \tag{40}$$

and the quantities α_l and α_t are determined by equations (29).

On finding the asymptotic expressions for the integral (40) for the cases of high and of low temperatures, we find:

$$\dot{U}_a \approx \frac{7}{90\pi^2}\frac{\gamma^2 V\hbar}{\rho a^5}\left(\frac{\mu M_0}{\Theta_c}\right)^2\frac{\Theta_c^2+{}^3/_2\Theta_t^2}{\Theta_c^2}\frac{T}{\Theta_c}\Delta T \qquad (T \gg \Theta_l^2/\Theta_c). \tag{41}$$

$$\dot{U}_a \approx 0{,}25\,\frac{\gamma^2 V\hbar}{\rho a^5}\left(\frac{\mu M_0}{\Theta_c}\right)^2\Theta_c^5\left(\frac{1}{\Theta_l^5}+\frac{3}{2\Theta_t^5}\right)\left(\frac{T}{\Theta_c}\right)^{5}\Delta T, \qquad (T \ll \Theta_l^2/\Theta_c). \tag{42}$$

By comparison of formulas (33) and (41), it can easily be shown that for $T \gg \Theta_l^2/\Theta_c$ the fundamental role is played by the processes of generation and absorption of phonons (i.e., $\dot{U}_a \ll \dot{U}_e$).

For $T \ll \Theta_l^2/\Theta_c$ two cases are possible, as is clear from comparison of formulas (36) and (42).

For

$$\Theta_l^2/8\Theta_c \ln(\Theta_l^2/\mu M_0\Theta_c) \ll T \ll \Theta_l^2/\Theta_c,$$

as for high temperatures, spin-wave annihilation processes play no part in the transfer of energy to phonons. For

$$T \ll \Theta_l^2/8\Theta_c \ln(\Theta_l^2/\mu M_0\Theta_c)$$

these processes should be the ones of greatest importance. However, since the whole treatment is valid only down to temperatures of order μM_0, the last statement may prove to be incorrect [in case $\mu M_0 \gtrsim \Theta_t^2/8\Theta_c \ln(\Theta_t^2/\mu M_0\Theta_c)$, which usually occurs].

Practically, therefore, for all temperatures above μM_0 the fundamental role, among single-phonon processes, is played by the processes of generation and absorption of phonons by spin waves.

4. THE ROLE OF TWO-PHONON PROCESSES

Two-phonon processes are described by the quadratic terms in the expansion of the energy of the ferromagnetic in powers of the strain tensor. Here, as in the single-phonon processes, there can be terms of exchange origin and of relativistic origin. It can be shown that the relativistic terms are small in comparison with the analogous terms in the single-phonon processes by virtue of the smallness of the parameter $M^2/\rho c^2$.

Therefore it is necessary to compare with the single-phonon processes only the exchange terms, which have the form

$$\mathcal{H}_2 = L_{lmrs}^{ik}\int\frac{\partial M_q}{\partial x_i}\frac{\partial M_q}{\partial x_k}u_{lm}u_{rs}dv, \tag{43}$$

where the coefficients L_{lmrs}^{ik} are in order of magnitude equal to $\Theta_c a^2/\mu M_0$.

On going over to a second-quantization representation, we get from (38)

$$\mathcal{H}_2 = -\frac{\Theta_c a^3 h}{4V\rho}\sum_{\substack{\varkappa\lambda\mu\nu\\ ss'}}{}' F_{\varkappa\lambda\mu\nu}^{ss'}\frac{k_\varkappa k_\lambda l_\mu l_\nu}{\sqrt{\omega_{\mu s}\omega_{\nu s'}}} \tag{44}$$
$$\times(a_\varkappa a_\lambda^* b_{\mu s}b_{\nu s'} - a_\varkappa a_\lambda^* b_{\mu s}^* b_{\nu s'}^* + \text{c.c.}).$$

The coefficients F are of order unity. They are complicated functions of the angles; their precise form is not important for the estimates carried out below.

As is clear from equation (44), there are two types of process: scattering of a phonon by a spin wave (or vice versa) and radiation (or abosrption) of two phonons by a spin wave. The radiation of two phonons, like the radiation of a single phonon,

is an activation process. It is less probable (by comparison with the radiation of a single phonon), as being a higher-order process. On the other hand the scattering of a phonon by a spin wave is a non-activation process. Therefore at low temperatures ($T \ll \Theta_0^2/\Theta_c$, where Θ_0 is the Debye temperature) the energy transferred to phonons by spin waves by virtue of this process varies with temperature in a moderate fashion, and so, it might seem, can play a larger part at low temperatures than does the activation process of phonon radiation. A calculation analogous to the preceding one gives, apart from a numerical factor,

$$\dot{U}_2 \sim \frac{\beta^2 V\hbar}{\rho a^{10}} \frac{T^3}{\Theta_c^3 \Theta_0^2} \left(\frac{T}{\Theta_1}\right)^{5/2} \left(\frac{T}{\Theta_2}\right)^4 \Delta T \quad (T \ll \Theta_1), \tag{45}$$

where

$$\Theta_1 = \Theta_0^2/\Theta_c; \quad \Theta_2^4 = mc^2\Theta_0^3 \quad (m = \rho a^3).$$

On comparison of equations (45) and (36), we find that two-phonon processes can be important at temperatures below $\Theta_1/[52 \ln 2 + 16 \ln(\Theta_2/\Theta_1)] \sim 0.1°K$, where our treatment, as we have pointed out, does not apply.

Thus, finally, according to formulas (33) and (36),

$$\dot{U} \approx \frac{6\beta_1^2 V\hbar}{\pi^3 \rho a^8} \frac{T^3}{\Theta_c^2 \Theta_t^2} \exp\left\{-\frac{\Theta_t^2}{4\Theta_c T}\right\} \Delta T, \qquad (T \ll \Theta_t^2/\Theta_c),$$

$$\dot{U} \approx \frac{\pi V\hbar}{60\, a^6} \left(\frac{T}{\Theta_c}\right)^4 \frac{\beta_1^2 + 2(\beta_1+\beta_2)^2}{3} \Delta T, \quad (T \gg \Theta_t^2/\Theta_c). \tag{46}$$

5. THE TIME FOR ESTABLISHMENT OF EQUILIBRIUM

By use of the results obtained, we shall calculate the time for establishment of thermal equilibrium (the relaxation time) between spin waves and phonons.

The heat balance equation clearly has the form

$$C_s \partial T_s/\partial t = \dot{U}; \quad C_{ph}\partial T_{ph}/\partial t = -\dot{U}, \tag{47}$$

where C_s and C_{ph} are the specific heats of spin waves and of phonons:

$$C_s \approx \frac{15\zeta(3/2)}{32\pi^{3/2}} \frac{V}{a^3} \left(\frac{T}{\Theta_c}\right)^{3/2}; \quad C_{ph} \approx \frac{2\pi^2}{5} \frac{V}{a^3} \left(\frac{T}{\Theta_0}\right)^3, \tag{48}$$

($3/\Theta_0^3 = 1/\Theta_l^3 + 2/\Theta_t^3$), and $\dot{U}$ is determined by formula (46).

At low temperatures ($T \ll \Theta_t^2/\Theta_c$), the phonon specific heat is much smaller than the spin ($C_{ph} \ll C_s$). Therefore the temperature of the spin-wave gas may be considered constant.

Then for the temperature difference ΔT we get the equation

$$C_{ph}\frac{\partial \Delta T}{\partial t} = -\varkappa \Delta T, \quad \varkappa = \frac{6\beta_1^2 V\hbar}{\pi^3 \rho a^8} \frac{T^3}{\Theta_c^2 \Theta_t^2} \exp\left\{-\frac{\Theta_t^2}{4\Theta_c T}\right\}.$$

Hence

$$\frac{1}{\tau_{sph}} = \frac{15\beta_1^2}{\pi^3} \frac{\Theta_0^3}{\Theta_c mc_t^2 \hbar} \left(\frac{T}{\Theta_c}\right)^2 \exp\left\{-\frac{\Theta_t^2}{4\Theta_c T}\right\} \quad (T \ll \Theta_t^2/\Theta_c). \tag{49}$$

At high temperatures ($T \gg \Theta_t^2/\Theta_c$), the temperature of the phonons must be considered constant. As before we find

$$\frac{1}{\tau_{sph}} = \frac{8\pi^{5/2}}{225\zeta(3/2)} \frac{\Theta_t^2}{mc_t^2\hbar} \left(\frac{T}{\Theta_c}\right)^{5/2} \frac{\beta_1^2 + 2(\beta_1+\beta_2)^2}{3} \quad (T \gg \Theta_t^2/\Theta_c). \tag{50}$$

As was indicated in the introduction, the expressions obtained here for the relaxation time must be compared with the relaxation time within the spin system. For the relaxation time τ_{ss} within the spin system, there were obtained in reference 1 the formulas

$$\frac{1}{\tau_{ss}} \approx \begin{cases} (\Theta_c/\hbar)(T/\Theta_c)^4 & \text{for } T \gg \mu M_0 (\Theta_c/\mu M_0)^{3/4}, \\ gM_0(\mu^2/a^3\Theta_c)(T/\Theta_c)^{1/2} & \text{for } T \ll \mu M_0 (\Theta_c/\mu M_0)^{3/4}. \end{cases} \tag{51}$$

We have omitted in the second formula a logarithmic factor unimportant for our estimate. The characteristic temperature for spin-spin relaxation $\mu M_0 (\Theta_c/\mu M_0)^{3/4}$, agrees in order of magnitude with the temperature Θ_0^2/Θ_c. Therefore the expression (49) must be compared with the second formula (51), and the expression (48) with the first. The comparison shows that both for $\mu M_0 \ll T \ll \Theta_0^2/\Theta_c$ and for $\Theta_0^2/\Theta_c \ll T \ll \Theta_0$, Θ_c, the relaxation time τ_{ss} is much smaller than the time τ_{sph}. This justifies the introduction of two temperatures in the treatment of spin-phonon relaxation.

[1] M. I. Kaganov and V. M. Tsukernik, J. Exptl. Theoret. Phys. (U.S.S.R.) **34**, 1610 (1958), Soviet Phys. JETP **7**, 1107 (1958).

[2] A. I. Akhiezer, J. Phys. (U.S.S.R.) **10**, 217 (1946).

[3] Akhiezer, Bar'yakhtar, and Peletminskiĭ, J. Exptl. Theoret. Phys. (U.S.S.R.) **35**, 228 (1958), Soviet Phys. JETP **8**, 157 (1959).

[4] Yu. P. Irkhin and E. A. Turov, Физика металлов и металловедение (Physics of Metals and Metal Research) **3**, 15 (1956).

[5] L. D. Landau and E. M. Lifshitz, Механика сплошных сред (Mechanics of Continuous Media) M.-L. Gostekhizdat, 1953.

Translated by W. F. Brown, Jr.
30

GAMMA OSCILLATIONS OF THE SURFACE OF AN ATOMIC NUCLEUS

A. S. DAVYDOV and D. A. ZAIKIN

P. N. Lebedev Physics Institute, Academy of Sciences, U.S.S.R.

Submitted to JETP editor July 10, 1958

J. Exptl. Theoret. Phys. (U.S.S.R.) **36**, 233-237 (January, 1959)

The energy and probability of excitation of γ oscillations of the surface of an atomic nucleus are computed on the basis of the shell model assuming an anisotropic harmonic oscillator potential. It is shown that in order of magnitude the energy of the first excited state of this type is close to that of single-nucleon excitations, and that the probability of excitation of these states is much smaller than the probability of excitation of rotational states of the nucleus.

INTRODUCTION

RECENTLY an opinion has been expressed in a number of papers that some of the excited energy levels of even-even nuclei should be interpreted as so-called γ oscillations (reference 1, V, D, 1). However, Davydov and Filippov[2] have shown that these excited states may be regarded as rotational energy levels of non-axially-symmetric nuclei. It turned out that the sequence of energy levels, the values of their spins and the probabilities of electromagnetic transitions between them depend on only one parameter γ_0, which describes the deviation of nuclear shape from axial symmetry. The value of this parameter may be determined by measuring, for example, the ratio of the energies of the first two excited states of spin 2. In order to obtain agreement between experimental data and theory it was sufficient to assume that $\gamma_0 = 8.1°$ for Pu^{238}, $\gamma_0 = 13.5°$ for Sm^{152}, $\gamma_0 = 26.5°$ for Te^{122}, etc. The hypothesis of a non-axially-symmetric equilibrium shape of the nucleus is supported by the work of Gurskiĭ,[3] Geĭlikman,[4] and Zaikin[5] who have shown that the minimum energy of nucleons moving in an oscillator[3,4] or in a rectangular[5] potential corresponds to a non-axially-symmetric nuclear shape, if the number of nucleons (of the same type) outside a closed shell exceeds 2.

In this paper we investigate the question of the stability of a nucleus with respect to a change in the equilibrium value of γ_0 which corresponds to the minimum potential energy. By means of a simple model of an anisotropic harmonic oscillator field for individual nucleons it is shown that the energy of the first excited state corresponding to γ oscillations in order of magnitude is close to the energy of single-nucleon excitation. Further it is shown that the reduced probability of electric quadrupole transitions to levels corresponding to γ oscillations is smaller by a factor of approximately several hundred compared to the probability of transition to the first rotational level of an axially-symmetric nucleus. It appears to us that these results confirm the great stability of nuclear shape with respect to γ oscillations.

1. POTENTIAL ENERGY OF SURFACE OSCILLATIONS OF AN ATOMIC NUCLEUS

We assume that nucleons of mass m move subject to a potential of the form

$$V = \frac{m\omega^2}{2}\sum_{k=1}^{3}(x_k/R_k)^2, \tag{1.1}$$

where

$$R_k = R\exp(\xi_k),\quad \xi_k = \sqrt{5/4\pi}\,\beta\cos\left(\gamma - \frac{2\pi}{3}k\right); \tag{1.2}$$

β and γ determine the shape of the nucleus; here $R_1R_2R_3 = R^3$, since $\Sigma\xi_k = 0$. By introducing the three frequencies

$$\omega_k = \omega R/R_k \approx \omega\left\{1 - \xi_k + \frac{1}{2}\xi_k^2 + \cdots\right\}, \tag{1.3}$$

we easily see that the energy of each nucleon will depend on three quantum numbers n_k, so that

$$E_s/\hbar\omega = n_s + {}^3/_2 - \sum_{k=1}^{3} n_{sk}\xi_k + \frac{1}{2}\sum_{k=1}^{3}(n_{sk} + {}^1/_2)\xi_k^2 + \cdots,\quad n_s = \sum_{k=1}^{3} n_{sk}. \tag{1.4}$$

If, in accordance with the Pauli exclusion principle, we fill the lowest energy levels (1.4) using Z protons and N neutrons, we obtain their total energy as a function of the parameters of the nuclear deformation (β and γ). By treating this energy as the potential energy for surface oscillations about

the equilibrium values β_0 and γ_0 corresponding to the minimum energy, we can determine the energy of excited states corresponding to β and γ oscillations.

It may be easily seen that for each filled shell

$$\sum_{sk} n_{sk}\xi_k = 0,$$

and that the total energy of the nucleons filling several shells (magic-number nucleus) may be written in the form

$$E_M = \hbar\omega(\varepsilon_0 + {}^1/_2 D\beta^2), \quad \varepsilon_0 = \sum_s (n_s + {}^3/_2), \tag{1.5}$$

where $D > 0$ and determines the stiffness of the nuclear surface with respect to β oscillations.

It follows from (1.5) that for nuclei with filled shells the minimum energy corresponds to spherical shape of the nucleus, i.e., to $\beta_0 = 0$.

We now suppose that outside the filled shells the shell with $n_s = N$ contains ν nucleons of one kind, then the total energy of all the nucleons has the form

$$E(\nu) = E_M + \left[\nu(N + {}^3/_2) - \sum_{sk} n_{sk}\xi_k + \frac{1}{2}\sum_{sk}(n_{sk} + {}^1/_2)\xi_k^2\right]\hbar\omega, \tag{1.6}$$

where $\sum_k n_{sk} = N$; the summation $\sum_k$ here and in subsequent equations is taken over all the nucleons of the shell N.

If we introduce the notation

$$\tan\gamma_0 = \sqrt{3}\sum_s (n_{s1} - n_{s2}) \Big/ \sum_s (3n_{s3} - N), \tag{1.7}$$

$$\beta_0 = \sqrt{4\pi/45}\sum_s (3n_{s3} - N) / D\cos\gamma_0, \tag{1.8}$$

then (1.6) is brought into the form

$$E(\nu) = E_0(\nu) + {}^1/_2 C(\beta - \beta_0)^2 + C\beta\beta_0[1 - \cos(\gamma - \gamma_0)], \tag{1.9}$$

where

$$C = 15D\hbar\omega/8\pi, \quad E_0(\nu) = \hbar\omega[\varepsilon_0 + \nu(N + {}^3/_2) - {}^1/_2 C\beta_0^2].$$

It follows from (1.9) that when $\beta = \beta_0$ the potential energy regarded as a function of γ has the form

$$V(\gamma) = E_0(\nu) + F[1 - \cos(\gamma - \gamma_0)], \tag{1.10}$$

where

$$F = (15D\hbar\omega/8\pi)\,\beta_0^2 = {}^1/_4\sqrt{5/\pi}\hbar\omega\beta_0\left\{\sum_s (3n_{s3} - N)\right\} \Big/ \cos\gamma_0. \tag{1.11}$$

In obtaining (1.11) we have utilized (1.8).

2. γ-OSCILLATIONS OF THE SURFACE OF AN ATOMIC NUCLEUS

According to A. Bohr,[6] the operator for the kinetic energy of the γ-oscillations may be written, when $\beta = \beta_0$, in the form

$$T_\gamma = -\frac{\hbar^2}{2B\beta_0^2}\frac{1}{\sin 3\gamma}\frac{\partial}{\partial\gamma}\sin 3\gamma\frac{\partial}{\partial\gamma}, \tag{2.1}$$

where B is the mass parameter. Taking into account the explicit form of the potential energy (1.10), we can write the Schrödinger equation, which determines the energy of the γ oscillations, in the form

$$[T_\gamma - F\cos(\gamma - \gamma_0) - (E_\gamma - E_0(\nu) + F)]\,\Phi(\gamma) = 0. \tag{2.2}$$

By making use of (1.7) it is easily seen that the transformations $\gamma_0 \to -\gamma_0$, $\gamma_0 \to \gamma_0 + 2\pi/3$ correspond to an interchange of the axes 1, 2, 3. Since the shape of the nucleus, which is defined in terms of γ by means of (1.2), is also invariant with respect to the transformations $\gamma \to -\gamma$, $\gamma \to \gamma + 2\pi/3$, it is necessary to seek the solutions of (2.2) in the form of periodic even functions of γ (of period $2\pi/3$). For these conditions to be fulfilled, it is sufficient to set

$$\Phi(\gamma) = \Phi(\cos 3\gamma). \tag{2.3}$$

By introducing the variable $\zeta = 3\gamma$, we bring (2.2) into the form

$$[T_\zeta - M\cos(\zeta/3 - \gamma_0) - W]\,\Phi(\cos\zeta) = 0, \tag{2.4}$$

where

$$T_\zeta = -\frac{1}{\sin\zeta}\frac{\partial}{\partial\zeta}\sin\zeta\frac{\partial}{\partial\zeta}, \tag{2.5}$$

$$M = \frac{2B\beta_0^2}{9\hbar^2}F = \frac{1}{18}\sqrt{\frac{5}{\pi}}\frac{\hbar\omega}{(\hbar^2/B\beta_0^2)}\sum_s (3n_{s3} - N)\beta_0/\cos\gamma_0, \tag{2.6}$$

$$W = (2B\beta_0^2/9\hbar^2)(E_\gamma - E_0(\nu) + F). \tag{2.7}$$

To calculate W it is convenient to expand the function Φ in (2.4),

$$\Phi(\cos\zeta) = \sum_{\lambda=0}^{\infty} a_\lambda\psi_\lambda(\zeta), \tag{2.8}$$

where $\psi_\lambda(\zeta)$ are the eigenfunctions of the operator T_ζ, i.e., they satisfy the equation

$$[T_\zeta - \lambda(\lambda + 1)]\,\psi_\lambda(\zeta) = 0. \tag{2.9}$$

The functions $\psi_\lambda(\zeta)$ normalized to unity may be directly expressed in terms of Legendre polynomials:

$$\psi_\lambda(\zeta) = \sqrt{(2\lambda + 1)/2}\,P_\lambda(\cos\zeta). \tag{2.10}$$

On substituting (2.8) into (2.9) we obtain the sys-

tem of equations

$$\sum_{\lambda=0}^{\infty} \{[\lambda(\lambda+1) - W]\delta_{\lambda\mu} - V_{\lambda\mu}\} a_\lambda = 0, \qquad (2.11)$$

where

$$V_{\lambda\mu} = M\int_0^\pi \psi_\lambda(\zeta)\cos\left(\frac{\zeta}{3} - \gamma_0\right)\psi_\mu(\zeta)\sin\zeta\, d\zeta.$$

It may be easily shown that

$$V_{\lambda\mu} = \begin{cases} \frac{2}{\sqrt{3}} M I_{\lambda\mu}\cos\left(\frac{\pi}{6} - \gamma_0\right), & \text{if } \lambda-\mu \text{ is even} \\ 2MI_{\lambda\mu}\sin\left(\frac{\pi}{6} - \gamma_0\right), & \text{if } \lambda-\mu \text{ is odd} \end{cases}$$

where

$$I_{\lambda\mu} = \frac{4}{2}\sqrt{(2\lambda+1)(2\mu+1)}\int_0^\pi P_\lambda(\cos\zeta)\cos\frac{\zeta}{3}P_\mu(\cos\zeta)\sin\zeta d\zeta.$$

We restrict ourselves to four terms in the expansion (2.8). Then (2.10) reduces to a system of four homogeneous equations in the coefficients a_λ. By setting the determinant of the system equal to zero we shall obtain the values for the energies of the γ oscillations. Numerical results were obtained for $\gamma_0 = 0$, $\pi/12$, and $\pi/6$, and M = 5, 10, and 20. The result of this is that within the range of variation of M that was investigated the difference between the ground state and the first excited γ-oscillation level may be approximately represented in the form

$$\begin{aligned} \Delta E_\gamma &= (9\hbar^2/2B\beta_0^2)(2 + 0.11M), \quad \text{for } \gamma_0 = 0, \\ \Delta E_\gamma &= (9\hbar^2/2B\beta_0^2)(2 + 0.052M), \quad \text{for } \gamma_0 = \pi/12, \\ \Delta E_\gamma &= (9\hbar^2/2B\beta_0^2)(2 + 0.024M), \quad \text{for } \gamma_0 = \pi/6. \end{aligned} \qquad (2.12)$$

From these expressions it may be seen that even if the contribution of $V = M\cos(\gamma - \gamma_0)$ to the difference ΔE_γ is not great, nevertheless the first excited γ level lies at a value one order of magnitude higher than the first rotational level. If β_0 is small then the rotational levels lie very high and the energy of the γ oscillations falls into the range of single particle excitations. In the case of large β_0 the value of γ_0 differs little from zero. On setting $\gamma_0 \approx 0$ and on substituting (2.6) into (2.12) we obtain

$$\Delta E_\gamma \approx 9\hbar^2/B\beta_0^2 + (0.9/36)\sqrt{5/\pi}\,\hbar\omega\sum_s(3n_{s3} - N). \qquad (2.13)$$

Large values of β_0 can be realized when a certain not very small number of nucleons exists outside a closed shell. We consider the filling of the shell with N = 5. For a number of nucleons exceeding four $\sum_s(3n_{s3} - N) > 40$. Consequently, for large β_0 the second term in (2.13) is of order $\hbar\omega$, i.e., of order of magnitude of single particle excitations.

The results obtained above are based on the assumption that the series (2.8) converges sufficiently rapidly, starting with the third term of the series. Calculations show that for not very large values of M this assumption is satisfied. Thus, for $\gamma_0 = 0$ and M = 5:

$$\begin{aligned} \Phi_0 &= 0.971\,\psi_0 + 0.239\,\psi_1 + 0.0022\,\psi_2 + \sim 10^{-4}\psi_3, \\ \Phi_1 &= -0.239\,\psi_0 + 0.961\,\psi_1 + 0.198\,\psi_2 + 0.0039\,\psi_3. \end{aligned}$$

For $\gamma_0 = 0$ and M = 10:

$$\begin{aligned} \Phi_0 &= 0.923\,\psi_0 + 0.383\,\psi_1 + 0.029\,\psi_2 + 0.0018\,\psi_3, \\ \Phi_1 &= -0.342\,\psi_0 + 0.894\,\psi_1 + 0.290\,\psi_2 + 0.0053\,\psi_3. \end{aligned}$$

3. PROBABILITY OF EXCITATION OF γ OSCILLATIONS

The probability given above for the transition of a nucleus from the ground state into the first excited γ-oscillation state under the action of an electromagnetic field is given by the expression

$$B_\gamma(E2) = (5e^2/16\pi)\,Q_0^2\,|\langle\Phi_1 \mid \cos\gamma \mid \Phi_0\rangle|^2, \qquad (3.1)$$

where Q_0 is the internal nuclear quadrupole moment; Φ_0 and Φ_1 are wave functions of the ground and of the first γ-oscillation level respectively.

Calculations show that over a sufficiently wide range of variation of M the ratio of (3.1) to the reduced probability of electric quadrupole transition to the first rotational level of an axially-symmetrical nucleus ($5e^2Q_0^2/16\pi$) is very small. Thus, for $\gamma_0 = 0$ and M = 0 this ratio is equal to 0.01, for M = 5 and 20 this ratio respectively amounts to 0.009 and 0.003.

Thus, the reduced probability of excitation of the first γ-oscillation state is by a factor of several hundred smaller than the corresponding probability of excitation of the first rotational state of the nucleus.

[1] Alder, Bohr, Huus, Mottelson and Winter, Revs. Modern Phys. **28**, 432 (1956).

[2] A. S. Davydov and G. F. Filippov, J. Exptl. Theoret. Phys. (U.S.S.R.) **35**, 440 (1958), Soviet Phys. JETP **8**, 303 (1959); Nucl. Phys. **8**, 237 (1958).

[3] M. Gursky, Phys. Rev. **98**, 1205 (1955). L. Wilets and M. Jean, Phys. Rev. **102**, 788 (1956).

[4] B. T. Geilikman, J. Exptl. Theoret. Phys. (U.S.S.R.) **35**, 989 (1958), Soviet Phys. JETP **8**, 690 (1959).

[5] D. A. Zaikin, J. Exptl. Theoret. Phys. (U.S.S.R.) **35**, 529 (1958), Soviet Phys. JETP **8**, 365 (1959).

[6] A. Bohr, Danske Mat.-fys. Medd. **26**, 14 (1952).

Translated by G. Volkoff
31

CERENKOV RADIATION OF AN ELECTRON MOVING IN A MEDIUM WITH SPATIAL DISPERSION

V. N. AGRANOVICH, V. E. PAFOMOV, and A. A. RUKHADZE

P. N. Lebedev Physics Institute, Academy of Sciences, U.S.S.R.

Submitted to JETP editor July 10, 1958

J. Exptl. Theoret. Phys. (U.S.S.R.) **36**, 238-243 (January, 1959)

An analysis is given of Cerenkov radiation in an isotropic gyrotropic medium, with spatial dispersion taken into account. The angular distribution of the Cerenkov radiation and the emergence of the radiation at the boundary of the medium are considered.

1. INTRODUCTION

DIELECTRICS are usually characterized by a dielectric constant which depends only on frequency ω. However, the electric induction can also depend on the spatial derivatives of the field intensity. For example, if one takes account of the first spatial derivatives it is possible to describe the effects due to natural optical activity. The terms containing derivatives in the expressions which relate the electric field intensity and the electric induction are, generally speaking, of higher order than the electromagnetic field equations. These lead to the new solutions and new waves which have been investigated by a number of authors.[1-3] As has already been noted,[2] one of the possible methods of observing effects related to spatial dispersion is to examine the Cerenkov radiation.

It has been shown in reference 4 that the total energy loss of an electron which moves in an arbitrary medium characterized by spatial dispersion is given by the following expression:

$$F = -\frac{ie^2}{2\pi^2 c^2 v} \times \int (\mathbf{q}\cdot\mathbf{v}) \frac{|v_i b_{ik}^{-1} q_k|^2 - (v_i b_{ik}^{-1} v_k)(q_i b_{ik}^{-1} q_k) + (v_i b_{ik}^{-1} v_k)}{1 - (q_i b_{ik}^{-1} q_k)} dq, \quad (1.1)$$

where the tensor b_{ik} is expressed in terms of the dielectric permittivity tensor as follows:

$$b_{ik} = q^2 \delta_{ik} - \frac{(\mathbf{q}\cdot\mathbf{v})^2}{c^2} \varepsilon_{ik}. \quad (1.2)$$

The permittivity tensor ϵ_{ik} depends only on frequency (ω) if spatial dispersion is neglected; however, if spatial dispersion is considered ϵ_{ik} also depends on the propagation vector $\mathbf{q}$, i.e.

$$D_i = \varepsilon_{ik}(\omega, \mathbf{q}) E_k. \quad (1.3)$$

We first consider an isotropic medium. In this case Eq. (1.3) assumes the form

$$\varepsilon_{ik}(\omega, q) = \varepsilon_1(\omega, q)\delta_{ik} + \varepsilon_2(\omega, q) q_i q_k / q^2, \quad (1.3a)$$

while the expression for the total energy loss becomes:*

$$F = -\frac{ie^2}{\pi} \int_{-\infty}^{+\infty} \omega\, d\omega \times \int_0^{k_0} k\, dk \frac{v^{-2} - c^{-2}\bar{\varepsilon}(\omega, k^2 + \omega^2/v^2) + \dfrac{\omega^2}{(v^2k^2 + \omega^2)} \varepsilon_2(\omega, k^2 + \omega^2/v^2)}{\bar{\varepsilon}(\omega, k^2 + \omega^2/v^2)\{k^2 + \omega^2[v^{-2} - c^{-2}\varepsilon_1(\omega, k^2 + \omega^2/v^2)]\}}, \quad (1.4)$$

where $\bar{\epsilon} = \epsilon_1 + \epsilon_2$.

It follows from Eq. (1.4) that Cerenkov radiation will be excited at frequency ω if the following condition is satisfied:

$$v > c/n_i(\omega), \quad (1.5)$$

where the quantity $n_i(\omega)$ satisfies the relation

$$n^2(\omega) = \varepsilon_1(\omega, n^2\omega^2/c^2). \quad (1.6)$$

If spatial dispersion of the medium is neglected Eq. (1.6) defines a single function $n(\omega)$. On the other hand, if spatial dispersion is taken into account this equation will in general, have several solutions $n_i = n_i(\omega)$. If ϑ is the angle between the direction of motion of the particle and the radiation direction, since

$$\cos\vartheta_i = c/vn_i(\omega), \quad (1.7)$$

we find that the Cerenkov radiation at frequency ω is distributed over cones with opening angles ϑ_i which are determined from Eq. (1.7). It is of interest to consider the intensity distribution of the Cerenkov radiation over these cones.

2. INTENSITY DISTRIBUTION OF THE CERENKOV RADIATION

Carrying out the integration indicated in Eq.(1.4) with appropriate circuits of the poles in the complex

*The upper limit of the integration over k and k_0 is determined by the range of validity of the macroscopic analysis.

plane for k (cf. reference 5), we find that the energy loss due to Cerenkov radiation in the frequency interval ω, $\omega+d\omega$ is given by the expression

$$dF = \frac{e^2}{c^2} \times \sum_i \left(1 - \frac{c^2}{v^2 n_i^2(\omega)}\right) \left|1 - \frac{d}{dn_i^2(\omega)}\, \varepsilon_1\left(\omega, \frac{\omega^2}{c^2} n_i^2(\omega)\right)\right|^{-1} \omega d\omega. \quad (2.1)$$

Eq. (2.1) represents the total intensity of the Cerenkov radiation as a function of frequency; this intensity is a sum of intensities which are distributed over the individual Cerenkov cones defined by Eq. (1.7).

We now examine the different possibilities which arise when spatial dispersion of the medium is considered.

At Cerenkov frequencies far from the resonance frequencies of the medium the solution of Eq. (1.6) can be found through the use of a "direct" dispersion expansion. Limiting ourselves to second spatial derivatives,[2] we have for the transverse waves

$$\mathbf{D} = (\varepsilon_0(\omega) - \alpha(\omega) n^2)\, \mathbf{E} \equiv \varepsilon_1(\omega, n^2\omega^2/c^2)\, \mathbf{E}. \quad (2.2)$$

Hence, in the frequency regions considered here Eq. (1.6) has the single solution

$$n^2(\omega) = \varepsilon_0(\omega)/(1 + \alpha(\omega)), \quad (2.3)$$

and the Cerenkov radiation is distributed over a single cone given by Eq. (1.7). In this frequency region $\alpha(\omega) \ll 1$; thus spatial dispersion of the medium has essentially no effect on the Cerenkov radiation of an electron in these cases. Equation (2.2), which gives the intensity of the Cerenkov radiation at frequency ω, assumes the form

$$dF = \frac{e^2}{c^2} \frac{1 - c^2(1 + \alpha(\omega))/v^2\varepsilon_0(\omega)}{|1 - \alpha(\omega)|} \omega d\omega = \frac{e^2}{c^2} \frac{1 - c^2/v^2 n^2}{2 - \varepsilon_0/n^2} \omega d\omega. \quad (2.4)$$

On the other hand, dispersion becomes important at Cerenkov frequencies close to the resonance frequencies of the medium. In this case, it is necessary to use the "inverse" dispersion expansion in solving Eq. (1.6). If, as in the above paragraph, we limit ourselves to second spatial derivatives,[2] we have

$$\mathbf{E} = \mathbf{D}/\hat{\varepsilon}(\omega, n^2\omega^2/c^2) = [1/\varepsilon_0 + \beta n^2]\, \mathbf{D}. \quad (2.5)$$

Thus, at these frequencies the dispersion equation (1.6) has two roots:

$$n_{1,2}^2(\omega) = -1/2\,\varepsilon_0\beta \pm \sqrt{(2\varepsilon_0\beta)^{-2} + 1/\beta}. \quad (2.6)$$

Ginzburg has shown[2] that when $\beta > 0$, one of the roots of Eq. (2.6) is always smaller than unity and the Cerenkov condition (1.5) may not be satisfied. In this case the Cerenkov radiation is distributed over a single cone. However, when $\beta < 0$, the Cerenkov condition can be satisfied for both roots of (2.6) and the Cerenkov radiation will be distributed over two cones. The total intensity of the Cerenkov radiation is then given by the sum of two terms — the intensities of radiation over these cones:

$$dF = \frac{e^2}{c^2} \sum_{1,2} \frac{1 - c^2/v^2 n_i^2}{|1 + \beta n_i^4|} \omega\, d\omega. \quad (2.7)$$

In accordance with Eq. (2.7), the ratio of these intensities is given by the following expression:

$$\frac{I_2}{I_1} = \left(1 - \frac{c^2}{v^2 n_2^2}\right) |1 + \beta n_1^4| \Big/ \left(1 - \frac{c^2}{v^2 n_1^2}\right) |1 + \beta n_2^4|. \quad (2.8)$$

It follows from Eqs. (2.6) and (2.7) that when $\epsilon_0^2|\beta| \ll 1$, $n_2^2 \gg n_1^2$ and

$$I_2/I_1 \approx \varepsilon_0^2|\beta|/(1 - c^2/v^2 n_1^2) \ll 1. \quad (2.9)$$

It follows from the foregoing that if the condition $\epsilon_0^2|\beta| \ll 1$ is satisfied the Cerenkov radiation is concentrated almost entirely in the first (ordinary) cone. As Ginzburg has shown, in the optical region of the spectrum this condition is satisfied close to the center of an absorption line. Hence, for a non-gyrotropic medium the new Cerenkov radiation could be observed at the center of the absorption line (at wavelengths such that $\Delta\lambda < 5$ Å, when $\epsilon_0^2|\beta| \sim 1$). In this case the intensity of the new Cerenkov radiation becomes comparable with the intensity of the usual Cerenkov radiation. However, close to the absorption line one must take account of absorption of the radiation in the medium. Estimates carried out in reference 2 indicate that in actual materials the observation of Cerenkov radiation in the optical region of the spectrum would be possible only in sheets which are approximately 10^{-4} cm thick. Thus the experimental observation of the new Cerenkov radiation in an isotropic medium would be difficult because of absorption in the medium.

In terms of the model proposed in reference 3, the real dielectric constant (at one of the natural frequencies of the medium) assumes the following form when spatial dispersion in an isotropic non-gyrotropic medium is considered ($\mathbf{q} = n\boldsymbol{\omega}\mathbf{s}/c$):

$$\varepsilon_{ik}\left(\omega, \frac{\omega^2}{c^2} n^2\right) = \left(1 - \frac{\omega_0^2}{\omega^2 + \omega_0^2 - \beta_0 - \alpha(\omega/c)^2 n^2}\right) \delta_{ik} - \frac{\alpha_1 q_i q_k}{\omega^2 + \omega_0^2 - \beta_0 - \alpha(\omega/c)^2 n^2}. \quad (2.10)$$

The dispersion relation (1.6) now has two solutions, $n_{1,2}^2$, and the Cerenkov radiation is distributed over two cones. The total intensity of the Cerenkov radiation is again given as the sum of two terms:

$$dF = \frac{e^2}{c^2}\sum_{i=1,2}\left(1-\frac{c^2}{v^2 n_i^2}\right)\left|1+\frac{\alpha}{c^2}\frac{\omega^2}{\omega_0^2}(n_i^2-1)^2\right|^{-1}\omega d\omega. \tag{2.11}$$

We now consider Cerenkov radiation in an isotropic gyrotropic medium characterized by spatial dispersion. Since spatial dispersion is important in frequency regions close to one of the resonance frequencies of the medium we use the "inverse" dispersion expansion:

$$E_i = [(1/\varepsilon_0 + \beta n^2)\delta_{ik} + i\gamma\omega\varepsilon_{ikl}n s_l]D_k. \tag{2.12}$$

Eq. (1.1), which characterizes the total energy loss of an electron moving in such a medium, assumes the form*

$$F = \frac{ie^2}{\pi}\int_{-\infty}^{+\infty}\int_0^{k_0}\omega\, d\omega\, k\, dk \times \frac{a+\gamma^2 b}{\left[\frac{v^2\omega^2}{c^2(\omega^2+k^2v^2)}-\frac{1}{\varepsilon_0}-\beta\frac{c^2}{\omega^2}\left(\frac{\omega^2}{v^2}+k^2\right)\right]^2-\gamma^2\frac{c^2}{v^2}(\omega^2+k^2v^2)}, \tag{2.13}$$

where we have introduced the notation

$$\begin{aligned} a &= \left[\frac{1}{\varepsilon_0}+\beta\frac{c^2}{\omega^2}\left(\frac{\omega^2}{v^2}+k^2\right)\right] \times\left[\frac{v^2\omega^2}{c^2(\omega^2+k^2v^2)}-\frac{1}{\varepsilon_0}-\beta\frac{c^2}{\omega^2}\left(\frac{\omega^2}{v^2}+k^2\right)\right] \\ &\times\frac{1}{\omega^2+k^2v^2}\left[\frac{v^2}{c^2}-\frac{1}{\varepsilon_0}-\beta\frac{c^2}{\omega^2}\left(\frac{\omega^2}{v^2}+k^2\right)\right], \\ b &= \frac{c^2}{\omega^2+k^2v^2}\left\{k^2\left[\frac{v^2}{c^2}-\frac{1}{\varepsilon_0}-\beta\frac{c^2}{\omega^2}\left(\frac{\omega^2}{v^2}+k^2\right)\right]\right. \\ &\left.-\frac{\omega^2}{v^2}\left[\frac{1}{\varepsilon_0}+\beta\frac{c^2}{\omega^2}\left(\frac{\omega^2}{v^2}+k^2\right)\right]\right\}. \end{aligned} \tag{2.14}$$

Examination of Eq. (2.13) indicates that Cerenkov radiation at frequency ω is excited in an isotropic gyrotropic medium with spatial dispersion if Eq. (1.5) is satisfied; the $n_i(\omega)$ in this equation are determined from the dispersion equation

$$\left(\frac{1}{n^2}-\frac{1}{\varepsilon_0}-\beta n^2\right)^2-\gamma^2\omega^2 n^2=0,\quad n^2\frac{\omega^2}{c^2}\equiv\frac{\omega^2}{v^2}+k^2. \tag{2.15}$$

In general, Eq. (2.15) yields three different values of $n_i^2(\omega)$ so that in the case being considered the Cerenkov radiation is distributed over the surfaces of three cones with opening angles ϑ_i, which are determined from Eq. (1.7). In this case the total intensity of Cerenkov radiation at frequency ω is given by the expression:

$$dF = -e^2\sum_{i=1,2,3}\omega\, d\omega\,\frac{a_i+\gamma^2 b_i}{\left|2\left(\beta+n_i^{-4}\right)\left(n_i^{-2}-1/\varepsilon_0-\beta n_i^2\right)c^2/\omega^2+\gamma^2 c^2\right|}. \tag{2.16}$$

*It should be kept in mind that Eq. (2.13) gives the correct value of the loss due to Cerenkov radiation only for those frequency regions in which the inverse dispersion relation (2.12) is valid (cf. reference 3).

In frequency regions in which $\gamma\omega\varepsilon_0 n \ll 1$ and $\beta n^2\varepsilon_0 \ll 1$, Eq. (2.15) has two roots which are approximately equal

$$n_{1,2}^2 = n_0^2(1\pm\gamma\omega n_0^3) \tag{2.17}$$

and a third root which is larger

$$n_3^2 = 1/n_0^4(\gamma^2\omega^2 - 2\beta/n_0^2), \tag{2.18}$$

where $n_0^2 = \varepsilon_0$. Consequently, if the radiation intensities for the cones are to be of the same order of magnitude the following condition must be satisfied:

$$n_0^6(\gamma^2\omega^2 - 2\beta/n_0^2) \approx 1. \tag{2.19}$$

In the optical region of the spectrum $\gamma^2\omega^2 \approx 10^{-5}$ and $\beta \approx 10^{-6}$; thus, $n_0^2 = 45$. According to reference 2, this condition is satisfied at wave lengths such that $\Delta\lambda \lesssim 100$ A as measured from the center of the absorption line. It is apparent that absorption does not play an important role in a gyrotropic medium and that the experimental observation of the new Cerenkov waves may be possible.

3. EMERGENCE OF CERENKOV RADIATION THROUGH THE BOUNDARY OF THE MEDIUM

To determine the intensity of the Cerenkov radiation which emerges from a medium it is necessary to consider effects at the boundary. The question of boundary condition then arises. It is apparent that the usual continuity conditions $D_{2n} = D_{1n}$, $H_{2n} = H_{1n}$, $E_{2t} = E_{1t}$ and $H_{2t} = H_{1t}$ still hold. However, new wave solutions are possible when spatial dispersion is taken into account and the usual boundary conditions are found to be inadequate for determining the amplitudes of these waves. As an additional boundary condition Pekar[1] has introduced the condition that the dipole moment per unit volume, due to the excitation of exciton waves in the medium, must vanish

$$4\pi\mathbf{P} = \mathbf{D} - \varepsilon'\mathbf{E} = \sum_{i=1,2}(n_i^2-\varepsilon')\mathbf{E} = 0, \tag{3.1}$$

where the quantity ϵ' takes account of the contribution due to the other resonance frequencies of the medium. The boundary conditions in (3.1) can be used to estimate the intensity of the radiation which emerges from the medium.

Suppose that at the interface between an isotropic non-gyrotropic medium and a vacuum, a plane wave is incident on the medium at an angle $\vartheta_0 < \pi/2$. Two reflected waves arise, corresponding to the two refractive indices $n_1(\omega)$ and $n_2(\omega)$. Suppose that the index associated with the incident wave is $n_1(\omega)$. From the condition that the phases must be equal it is easy to show that the following

relations obtain between the refracted and reflected waves:

$$\vartheta_0 = \vartheta_1, \quad \sin\vartheta_2 / \sin\vartheta_0 = n_1(\omega)\sin\vartheta / n_2(\omega)\sin\vartheta_0 = n_1(\omega), \tag{3.2}$$

where ϑ is the angle of refraction and ϑ_1 and ϑ_2 are the angles of reflection. The boundary conditions (3.1) can be used to determine the amplitudes of the refracted and reflected waves. If the electric vector of the incident wave is perpendicular to the plane of incidence the amplitude of the refracted wave E is related to the amplitude of the incident wave E_0 by the expression

$$\frac{E}{E_0} = \frac{2n_1\cos\vartheta_0(n_1^2 - n_2^2)}{\cos\vartheta(n_1^2 - n_2^2) + n_1\cos\vartheta_0(\varepsilon' - n_2^2) - n_2\cos\vartheta_2(\varepsilon' - n_1^2)}. \tag{3.3}$$

If the incident wave is associated with the index $n_2(\omega)$, we interchange n_1 and n_2 in Eqs. (3.2) and (3.3).

The results obtained above can be used to choose the most convenient experimental geometry for studying these features of Cerenkov radiation in media characterized by spatial dispersion.

In conclusion the authors wish to express their gratitude to V. L. Ginzburg for his interest and for a number of valuable discussions.

[1] S. I. Pekar, J. Exptl. Theoret. Phys. (U.S.S.R.) **33**, 1022 (1957), Soviet Phys. JETP **6**, 785 (1958).

[2] V. L. Ginzburg, J. Exptl. Theoret. Phys. (U.S.S.R.) **35**, 1573 (1958), Soviet Phys. JETP **8**, 1100 (1959).

[3] V. N. Agranovich and A. A. Rukhadze, J. Exptl. Theoret. Phys. (U.S.S.R.) **35**, 982 (1958), Soviet Phys. JETP **8**, 685 (1959).

[4] V. N. Agranovich and A. A. Rukhadze, J. Exptl. Theoret. Phys. (U.S.S.R.) **35**, 1171 (1958), Soviet Phys. JETP **8**, 819 (1959).

[5] L. D. Landau and E. M. Lifshitz, **Электродинамика сплошных сред** (Electrodynamics of Continuous Media) M. 1957.

Translated by H. Lashinsky
32

GENERALIZED FORM OF THE DEPENDENCE OF THE PION CROSS SECTION IN COMPLEX NUCLEI ON THE NUMBER OF NUCLEONS

A. S. BELOUSOV, B. B. GOVORKOV, and V. I. GOL'DANSKIĬ

P. N. Lebedev Physics Institute, Academy of Sciences, U.S.S.R.

Submitted to JETP editor July 10, 1958

J. Exptl. Theoret. Phys. (U.S.S.R.) **36**, 244-248 (January, 1959)

A generalized expression is derived for the dependence of the cross section of photoproduction of π mesons in complex nuclei on the number of nucleons. In addition to the ordinary reabsorption the reabsorption by nucleon pairs at the instant of meson creation has been taken into account. The following two calculations are presented: (1) a calculation for uniform density of the nucleons in the nucleus assuming a particular wave function for the nucleon pair, and (2) a phenomenological calculation without a wave function but for a Fermi distribution of the nucleon density in the nucleus.

1. INTRODUCTION

IT is well known that the dependence of the photoproduction cross section of π mesons in nuclei as a function of the atomic number is determined to a considerable extent by the secondary process of meson reabsorption.

The effect of these processes was analyzed by Brueckner, Serber, and Watson.[1] They gave the following expression for the dependence of the π^0 production cross section as a function of A (or, respectively for π^+ on Z and π^- on N):

$$(\sigma_{\pi^0})_A = (\sigma_{\pi^0})^0_{p,n} A\eta\chi. \qquad (1)$$

The factor χ for the reabsorption has the form

$$\chi = 3[{}^1\!/_2 x^{-1} - x^{-3} + x^{-3}(1+x)e^{-x}],\ x = 2R/\lambda_a,$$

where R — nuclear radius and λ_a — the mean distance for meson absorption in nuclei; $\eta \leq 1$ is a coefficient due to the replacement of free nucleons by nucleons bound in the nucleus.

The secondary meson reabsorption processes can be divided in a rough fashion into single-nucleon and two-nucleon interactions of the meson. At small meson energies the two-nucleon absorption predominates and plays the essential role.

However, as has been pointed out by Wilson[2] and Butler,[3] in the case of meson photoproduction there exists an important specific circumstance which is not accounted for by (1). To be absorbed by a two-nucleon process on its way through the nucleus there have to be present in a certain volume three particles — the meson and two nucleons. Now, at the instant of the production of the meson two particles — the meson and a nucleon — are already contained in this volume and for the two-nucleon absorption process the presence of only a second particle in the same volume is necessary. The circumstance that a quantitative treatment of this effect was not undertaken is the reason for the confrontation "volume production" as described by (1) vs. the so called "surface production." The latter leads to the dependence $\sigma_{\pi^0} \sim A^{2/3}$ independently of the value of λ_a. The necessity of combining these pictures follows from the experimental data on neutral-pion photoproduction in nuclei. In a series of experiments on neutral-pion photoproduction in complex nuclei including our measurements[4-6] it was shown that the dependence of σ_{π^0} on A for nuclei between carbon and lead is close to $A^{2/3}$. Furthermore, the measurements in reference 6 were performed with two counter telescopes in coincidence located 180° apart. They thus counted only π^0 mesons of a limited energy interval (1 to 15 Mev). The mean free path of such mesons in nuclear matter is on the average $\lambda_a \approx 17 r_0 = 17 \times 1.4 \times 10^{-13}$ cm. Nevertheless the dependence of σ_{π^0} on A turned out to be close to $A^{2/3}$. This is clearly in contradiction with the usual optical model formula (1) which for these conditions leads to a dependence close to $\sim A$. On the other hand, the results of reference 6 differ perceptibly from the dependence $\sim A^{2/3}$ of "pure surface production."

In the present paper the influence of the two-nucleon absorption of mesons at the instant of their creation on the dependence of σ_{π^0} on A is estimated in the simplest possible manner.

2. DEPENDENCE OF σ_{π^0} ON A FOR A PARTICULAR WAVE FUNCTION AND DENSITY DISTRIBUTION IN THE NUCLEUS

We follow the method of Wilson,[7] which he applied to the analysis of the photodisintegration of the deuteron. We thus assume that it is necessary and sufficient for a meson to be reabsorbed by a two-nucleon group at the instant of its creation that the nucleons at this time be at a separation $r \leq l = \hbar/\mu c$. We assume for the nucleon pairs the Chew-Goldberger wave function

$$\psi(p) = \sqrt{\alpha\hbar}/\pi(\alpha^2\hbar^2 + p^2), \qquad (2)$$

where $\hbar^2\alpha^2/2m = 18$ Mev (m = nucleon mass). In the coordinate representation this wave function has the form

$$\psi(r) = \sqrt{\alpha/2\pi}\, e^{-\alpha r}/r. \qquad (3)$$

Obviously the probability for the meson not to be absorbed by the quasi-deuteron at the time of its creation equals

$$f_0 = 1 - \int_0^l |\psi(r)|^2 4\pi r^2 dr = e^{-2\alpha l}. \qquad (4)$$

The quantity f_0 characterizes the probability for a meson to be produced in the central parts of the nucleus which are further removed from the surface than the distance l. For the given $\psi(r)$ it has a value 0.075. In the vicinity of the surface this probability increases and equals

$$f_s(y) = \frac{1}{2}\{e^{-2\alpha(R-y)} + e^{-2\alpha l}\} - \frac{\alpha(R^2-y^2)}{2y}\{-\mathrm{Ei}[-2\alpha(R-y)] + \mathrm{Ei}[-2\alpha l]\} + \frac{1}{8\alpha y}\{[1+2\alpha(R-y)]e^{-2\alpha(R-y)} - [1+2\alpha l]e^{-2\alpha l}\}, \qquad (5)$$

where y is distance from the center of the nucleus $[(R-l) \leq y \leq R]$. The overall (i.e., averaged over the nucleus) probability for the meson not to be reabsorbed in a two-nucleon process at the instant of its creation is given by

$$f_q = f_0(1 - A^{-1/3})^3 + \frac{3}{A}\int_{A^{1/3}-1}^{A^{1/3}} z^2 f_s(z)\, dz, \qquad (6)$$

where $z = y/l$.

Curve 1 of Fig. 1 shows the function $f_q A$. The values are plotted with respect to carbon (A = 12). Obviously the curve falls in between the straight line $\sim A$ and the curve $\sim A^{2/3}$. It thus denotes a mixture of "volume" and "surface" production which are characterized respectively by the first and second term of (6).

The dependence of the contribution of "surface production" of π mesons on A (i.e., the production in a surface layer of thickness l) is plotted as curve 1 in Fig. 2.

In addition to the reabsorption of mesons at the instant of their creation one obviously has to take into account the usual reabsorption in the nucleus. The fraction of the "volume-produced" mesons that leave the nucleus will be given approximately by Eq. (1) multiplied by $\exp(-l/\lambda_a)$ for $x = 2(R-l)/\lambda_a$. The fraction of the "surface-produced" mesons that leave the nucleus will be given approximately by

$$\chi_s = \frac{1}{2}\left\{1 + \frac{1-e^{-u}}{u}\right\}, \qquad (7)$$

where

$$u = 2(R - {}^1\!/_2 l)/\lambda_a.$$

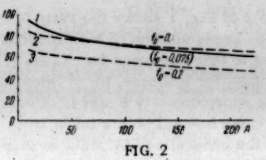

FIG. 2

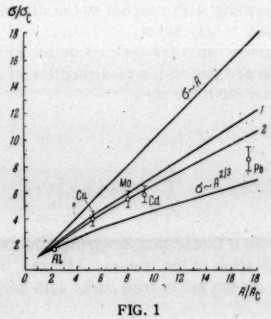

FIG. 1

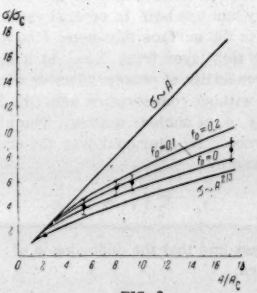

FIG. 3

Curve 2 of Fig. 1 shows the ratio of the photoproduction cross section of slow mesons in different nuclei to that in carbon for $\lambda_a/r_0 = 17$ (this corresponds, for example, to π^0 mesons with an energy of approximately 8 Mev). A comparison with the experimental points taken from reference 6 favors the generalized formula as compared with the usual expression (1) or with the simple dependence $\sim A^{2/3}$.

3. PHENOMENOLOGICAL CALCULATION OF THE DEPENDENCE OF σ_{π^0} ON A FOR A FERMI DENSITY DISTRIBUTION OF THE NUCLEONS IN THE NUCLEUS

The above calculation of the two-nucleon reabsorption of π mesons at the instant of their creation was performed for the case of uniform nucleon density in the nucleus. A consideration of different nucleon density distributions results in considerable complication of all computations. We therefore tried to account for the density distribution purely phenomenologically without assuming any particular form for the two-nucleon wave function. By giving the approximate character of the density distribution of the nucleons in the nucleus and the approximate dependence of the reabsorption probability at the instant of production on the density, we can obtain the dependence of σ_{π^0} on A in terms of the parameter f_0 which describes the probability of a meson to be created in the center of the nucleus without being reabsorbed in a two-nucleon process. Comparing the obtained curves with the experimental results we can establish which value of f_0 gives the closest agreement with the observed A-dependence. The calculation was done for a density distribution which is in agreement with the electron scattering data,[8] i.e., for the Fermi distribution

$$\rho(r) = \rho_0/[e^{(r-c)/t} + 1], \tag{8}$$

where ρ_0 approximately equals the density at $r = 0$ (since $e^{-c/d} \ll 1$), c is the radius at which the density has one half its central value, $d = t/4.4$ where t is the surface thickness (the density changes in this layer from $0.9\rho_0$ to $0.1\rho_0$).

The probability of photoproduction of mesons in a nucleus without reabsorption actually depends on the density ρ of nuclear matter. The photoproduction probability averaged over the nuclear volume is given by

$$f_q^* = \frac{4\pi}{A}\int_0^\infty r^2\rho(r)\,f(\rho)\,dr. \tag{9}$$

We shall assume that the dependence of f on ρ has the form

$$f(\rho) = 1 - (1 - f_0)\,\rho/\rho_0. \tag{10}$$

Then

$$f_q^* = {}^4/_3(\pi c^3/A)\,\rho_0\{f_0[1 + \pi^2(d/c)^2] + (1 - f_0)[3d/c + \pi^2(d/c)^3]\}. \tag{11}$$

The first term in (11) gives the contribution of "volume production" and yields the proportionality $f_q^*A \sim c^3$. The second term, the contribution of "surface production," contains a factor $1/c$ and thus yields $f_q^*A \sim c^2$. The magnitude of the second term is proportional to the volume of the surface layer of the nucleus.

The obtained expression still has to be corrected for the usual reabsorption of the mesons, similarly as in the case treated in Sec. 2.

In Fig. 3 the results of the computation are plotted for $\lambda_a = 17\,r_0$ and for the three values $f_0 = 0$, 0.1, and 0.2.

As one sees from a comparison with the experimental points from reference 6, which are also plotted in Fig. 3, the value of f_0 and the dependence $\sigma_{\pi^0} = f(A)$ agrees with the above obtained results. The relative magnitude of the contribution of "surface production" to the meson production as given by (11) is plotted in Fig. 2 as the dotted curves 2 and 3.

We shall not discuss here different possible reasons for changes in the obtained dependence $\sigma_{\pi^0}(A)$ (e.g., the influence of the binding energy and the momentum distribution of the nucleons, the charge exchange scattering of π^+ mesons etc.). We only wish to point out the as yet unfeasible direct establishment of the facts of the two-nucleon absorption of slow mesons not at the instant of creation but on the subsequent passage through the nucleus. When a fast (~ 70 Mev) π^+ meson is absorbed by a quasideuteron or a fast π^0 meson is absorbed by a pair of protons two protons are emitted with approximately equal energy into roughly opposite directions while the emission is roughly isotropic with respect to the direction of the incoming γ-ray beam.

The cross section for the production of such pairs which are due to the reabsorption of π^+ mesons must have the form

$$\sigma = (\sigma_{\pi^+})_p^*\,\eta_i Z\left\{f_0(1-\chi)\,(1 - A^{-1/3})^3 + \frac{3}{A}(1-\chi_a)\int_{A^{1/3}-1}^{A^{1/3}} z^2 f_a(z)\,dz\right\}\frac{\lambda_a}{\lambda_2}\,\Gamma f_{pp}, \tag{12}$$

where Γ is a factor that describes the two-nucleon correlation in the nucleus ($\Gamma \approx 6$), λ_a and λ_2 are the meson mean free paths with respect to

the total and the two-nucleon absorption respectively, and f_{pp} is the probability that both protons leave the nucleus (equal, for example 0.6 for carbon, 0.4 for iron and 0.25 for lead).

The possibility of actually observing such processes is indicated by the work of Rosengren and Dudley[9] who report the existence of an isotropic component in the angular distribution of photoprotons with an energy close to 70 Mev which is due to the absorption of π mesons by pairs of nucleons.

The authors thank E. M. Leĭkin for his participation in an evaluation of this work.

[1] Brueckner, Serber, and Watson, Phys. Rev. **84**, 258 (1951).

[2] R. Wilson, Phys. Rev. **86**, 125 (1952).

[3] S. T. Butler, Phys. Rev. **87**, 1117 (1952).

[4] Belousov, Tamm, and Shitov, Dokl. Akad. Nauk SSSR **112**, 1017 (1957), Soviet Phys. "Doklady" **2**, 90 (1957).

[5] Govorkov, Gol'danskiĭ, Karpukhin, Kutsenko, and Pavlovskaya, Dokl. Akad. Nauk SSSR **112**, 37 (1957), Soviet Phys. "Doklady" **2**, 4 (1957).

[6] Belousov, Rusakov, and Tamm, J. Exptl. Theoret. Phys. (U.S.S.R.) **35**, 355 (1958), Soviet Phys. JETP **8**, 247 (1959).

[7] R. Wilson, Phys. Rev. **104**, 218 (1956).

[8] R. Hofstadter, Revs. Modern Phys. **28**, 214 (1956).

[9] J. Rosengren and J. Dudley, Phys. Rev. **89**, 603 (1953).

Translated by M. Danos
33

BREAKUP OF A CHARGED LIQUID DROP AND NUCLEAR FISSION

B. T. GEĬLIKMAN

Moscow State Pedagogical Institute

Submitted to JETP editor July 9, 1958

J. Exptl. Theoret. Phys. (U.S.S.R.) **36**, 249-252 (January, 1959)

The disruption of a charged liquid drop is examined. The vibration energies of the parts of the drop are computed, as is the energy of their relative motion. The general results thus obtained are applied to nuclear fission.

IN solving the problem of the breakup of a liquid drop into two parts, and in particular the problem of nuclear fission, the question arises of determining the generalized coordinates and velocities of the fragments of the drop after breakup from the equation of motion of the drop prior to breakup. We shall show below that knowledge of the internal coordinates and velocities of the fragments makes it possible to estimate the excitation energy of the fragments during nuclear fission.

Assume that the liquid is incompressible, that the motion of the liquid prior to and after breakup is potential, and that the radius vectors of the surface of the drop and of its fragments are of the following form (we confine ourselves to an axially-symmetrical case):

$$r(\vartheta)/R = 1 + \Sigma\alpha_n P_n(\cos\vartheta);$$
$$r_i(\vartheta_i)/R_i = 1 + \Sigma\alpha_n^{(i)} P_n(\cos\vartheta_i), \quad i = 1, 2.$$

In each case the origin is located at the center of gravity of the drop. From this condition and from the conservation of volume we obtain the coefficients α_0, α_1, $\alpha_0^{(i)}$, and $\alpha_1^{(i)}$ in terms of the remaining parameters α_n and $\alpha_n^{(i)}$.

Let us consider the change in speed of any mass element of the drop, Δm_d, during the time of breakup of the drop τ_b:

$$\Delta v_d = \int_0^{\tau_b} f_d\,dt/\Delta m_d \approx f_d\tau_b/\Delta m_d.$$

We assume that τ_b is so small, that $\Delta v_d \ll v_d$ (this condition is satisfied in the case of nuclear fission). Then the velocities prior to and after breakup can be considered equal — this corresponds to the so-called shake-up method. Consequently,

$$\operatorname{grad}\varphi(x, y, z(z_i)) = v_c^{(i)} + \operatorname{grad}\varphi_i(x, y, z_i), \quad i = 1, 2. \quad (1)$$

Here $\varphi(x, y, z(z_i))$ is the velocity potential prior to breakup of the drop, referred to the origin of the coordinates of the i-th part of the drop [i.e., z is assumed to be $\mp(z_i - d_c^{(i)})$; $d_c^{(i)}$ are the distances from the center of gravity of the drop to the centers of gravity of its parts]; $\varphi_i(x, y, z_i)$ is the velocity potential of the i-th part after breakup; $v_c^{(i)}$ is the velocity of the center of gravity of the i-th part after breakup:

$$\varphi = \sum_{n=2}^{\infty} \dot{\alpha}_n r^n P_n(\cos\vartheta)/nR^{n-2}; \quad \varphi_i = \sum_{n=2}^{\infty} \dot{\alpha}_n^{(i)} r_i^n P_n(\cos\vartheta_i)/nR_i^{n-2}.$$

Changing to rectangular coordinates in the expressions for φ and φ_i, we obtain from (1):

$$\dot{\alpha}_2^{(i)} = \dot{\alpha}_2 \pm 2\dot{\alpha}_3 b_{ci} + 3\dot{\alpha}_4 b_{ci}^2 \pm \ldots,$$
$$\dot{\alpha}_3^{(i)} = -(\pm\dot{\alpha}_3 + 3b_{ci}\dot{\alpha}_4 \pm \ldots)(A_i/A)^{1/3}; \quad (2)$$
$$\dot{\alpha}_4^{(i)} = (\dot{\alpha}_4 \pm \ldots)(A_i/A)^{1/3}$$

(the minus corresponds to i = 1, the plus to i = 2); the relative velocities of the parts of the drop are

$$v_c = v_c^{(1)} + v_c^{(2)} = \dot{z}_c = [\dot{\alpha}_2(b_{c1} + b_{c2}) - \dot{\alpha}_3(b_{c1}^2 - b_{c2}^2) + \dot{\alpha}_4(b_{c1}^3 + b_{c2}^3) - \ldots]R; \quad b_{ci} = d_c^{(i)}/R.$$

These values of $\dot{\alpha}_n^{(i)}$ and $\dot{z}_c$ can be used as the initial conditions for the equations of motion of the parts of the drop. The initial values of the coordinates $\alpha_n^{(i)}$ and z_c can be readily calculated if the shape of the drop before breakup is known.[1]

In the case of nuclear fission, the potential energy U and the shape of the nucleus prior to fission were calculated for the states corresponding to minimum energy, within the framework of the Frankel and Metropolis[2] drop model (see also reference 3):

$$U(y) = {}^3/_{10}\varepsilon\xi(x, y)A^{2/3}e^2/r_0;$$
$$\xi(x, y) = 2.178\,y^2(1 - x) - 4.09\,y^3(1 - 0.645\,x) + 18.64\,y^4(1 - 0.894\,x) - 13.33\,y^5;$$
$$x = Z^2/A\varepsilon; \quad \varepsilon \equiv (Z^2/A)_{cr} = 48 \div 50;$$
$$r_0 = (1.2 \div 1.5)\cdot 10^{-13}\ \text{cm}.$$
$$\alpha_0 = -y^2(1.06 + 9.76\cdot 10^{-4} f(y)); \quad (3)$$
$$\alpha_2 = y(2.3 + 5.42\cdot 10^{-4} f(y));$$
$$\alpha_4 = y^2[1.6 + y(3 + 2.84\cdot 10^{-3} f(y))];$$
$$\alpha_6 = -2.36\cdot 10^{-5} f(y); \quad \alpha_8 = 2\alpha_6; \quad f(y) = (0.49 - y)^{-1}.$$

The remaining $\alpha_n = 0$. In view of the smallness of α_6 and α_8, we first neglect them; y is a general deformation parameter. The fission barrier corresponds to $y = 1 - x$. The thickness of the neck d_n is close to zero ($d_n/R \sim 0.1$) when $y = y_k \approx 0.35$. If shell effects are taken into account $\alpha_3 \neq 0$. At the experimentally observed value ($A_1/A_2 \gtrsim 0.7$) of the fragment-mass ratio. $\alpha_3 \approx 0.06$.[4] The ratio $\dot{\alpha}_3/\dot{\alpha}_2$ at the break of the neck can be estimated in the following manner:

$$\dot{\alpha}_{3y}/\dot{\alpha}_{2p} \approx \alpha_{3p}/\Delta t_{\alpha_3}[(\alpha_{2p} - \alpha_{2c})/\Delta t_{\alpha_2}]^{-1}$$
$$\approx (1 \div 2)\,\alpha_{3p}\,(\alpha_{2p} - \alpha_{2c})^{-1} \approx 0.07 \div 0.12.$$

(Δt_{α_2} is the time of descent from the saddle point to the break in the neck; Δt_{α_3} is the time of descent from the point at which α_3 stops being equal to zero to the break in the neck; $\Delta t_{\alpha_2}/\Delta t_{\alpha_3} \sim 1$ or 2; α_{2b} is the value of α_2 at the point of the break of the neck, α_{2s} is the value at the saddle point); α_{2b} and α_{2s} were calculated from formula (3) for $x = 0.7$ to 0.8. The value of α_{3b} can thus be neglected (this introduces an error of 4 to 7% for $\dot{\alpha}_n^{(i)}$ and $\dot{z}_c$ when $\dot{\alpha}_3 = 0.1\,\dot{\alpha}_2$).

Since the deformation of the nucleus past the saddle point is slow,[5] one can assume that the nucleus passes through the values α_n corresponding to the minimum of the potential energy and which are consequently determined by formula (3). Then $\dot{\alpha}_n = y d\dot{\alpha}_n/dy$. In particular,

$$\dot{\alpha}_4 = \dot{\alpha}_2\,(d\alpha_4/dy)/(d\alpha_2/dy) = \beta\,(y)\,\dot{\alpha}_2.$$

At the point of breakup, i.e., at $y = y_k \approx 0.35$, we have $\beta \approx 0.8$. The kinetic energy of the drops after the breakup is of the form $T^{(i)} = \sum_{n,m} T_{nm}^{(i)}$. Since $T_{nm} \gg T_{nm}$ ($n \neq m$), we have $T^{(i)} \approx \sum_{n=2}^{n_{max}} T_{nn}^{(i)}$.

In units of e^2/r_0 we have

$$T_{nn}^{(i)} = 3A_i^{5/3} I_n^{(i)}\,[\dot{\alpha}_n^{(i)}]^2/2n\,(2n+1);$$

$$I_n^{(i)} = \frac{n}{2}\int_{-1}^{1} [(P_n^{(1)}(\mu))^2/n^2 + (P_n(\mu))^2]\,[r_i(\mu)/R_i]^{2n+1}\,d\mu.$$

Let us estimate the ratio $T_{44}^{(i)}/T_{22}^{(i)}$ (for $A_1 \approx A_2$). If $I_4^{(i)} \approx I_2^{(i)}$ (see below), we have $T_{44}^{(i)}/T_{22}^{(i)} = 0.02$ to 0.04. One can therefore assume that $\alpha_4^{(i)} \approx 0$. It follows from (3) that $\alpha_4^{(i)} = 0$ when $y \approx 0.35$.[4] We can then confine ourselves to $n_{max} = 3$ in the expression for $r_i(\vartheta_i)$; $\alpha_2^{(i)}$ and $\alpha_3^{(i)}$ were found in reference 4 for various ratios A_1/A_2. When $A_1 = A_2$ we have $\alpha_2^{(i)} \approx 0.26$, $\alpha_3^{(i)} \approx 0.08$, and $2b_{c1} \approx 2.5$. For these values of $\alpha_n^{(i)}$ we have $I_2^{(i)} \approx 1.4$ and $I_3^{(i)} \approx 1.9$. (The values of $\alpha_n^{(i)}$, b_{ci}, and $I_n^{(i)}$ of reference 4a have been revised). Let us estimate the ratio of the kinetic energy $T^{(1)} + T^{(2)}$ of the internal motion of the fragments to the kinetic energy $T_c = \mu v_c^2/2$ of the centers of gravity of the fragments (μ is the reduced mass of the fragments): when $A_1 = A_2$, we find from Eq. (2) ($\dot{\alpha}_4 \approx 0.8\,\alpha_2$) that $(T^{(1)} + T^{(2)})/(T_c + T^{(1)} + T^{(2)}) \sim 0.45$. This estimate is unfortunately not very accurate, for if we include the terms with $\dot{\alpha}_6$ and $\dot{\alpha}_8$ in the expressions for $\dot{\alpha}_n^{(i)}$ and $\dot{z}_c$ [see Eq. (3)], $T^{(1)} + T^{(2)}$ turns out to be on the order of not 45%, but of 90 to 100% of the total energy. In view of the fact that the terms with α_6 and α_8 in (3) have been determined very approximately, we disregard them for the time being. But for further calculations it is essential that formulas (2) be revised.

We note that to determine the absolute value of T_c and $T^{(i)}$ it is essential to replace $\dot{\alpha}_2$ by a certain effective value. As is known, the law of conservation of energy is not obeyed rigorously in the "shake-up" method. Therefore, to satisfy the law of conservation of energy it is necessary to equate the energy $T_c + T^{(1)} + T^{(2)}$, expressed with the aid of formulas (2) in terms of $\dot{\alpha}_2 = (\dot{\alpha}_2)_{eff}$, to the energy of the nucleus prior to the breakup of the neck. If the force of friction for the degrees of freedom α_n in the descent from the saddle point is small, (this corresponds to spontaneous and threshold fission, see reference 1), the nuclear energy prior to the breakup is equal to the difference in the potential energy $U(y)$ at the saddle point and at the point of breakup (for threshold fission), or to the difference in $U(y)$ at the ground state ($y = 0$) and the point of breakup (for spontaneous fission).

To determine the excitation energy of the fragments it is necessary to solve the equations of motion (quantum or classical) for the degrees of freedom $\alpha_n^{(i)}$ and z_c.[1] However, an approximate estimate of the excitation energy can be obtained by considering the sum of the internal kinetic energies $T^{(1)} + T^{(2)}$ and the energy of deformation of both fragments at the point of breakup of the neck: $E_0 = U_d^{(1)} + U_d^{(2)} + T^{(1)} + T^{(2)} = E_0^{(1)} + E_0^{(2)}$. As shown above,

$$T^{(1)} + T^{(2)} \approx \gamma\,[U(y_0) - U(y_d)];$$
$$y_0 = 1 - x \quad \text{or} \quad y_0 = 0; \quad \gamma > 0.45.$$

Bohr and Wheeler[6] calculated $U_d^{(i)}$ in an approxi-

Element	U^{234}		Pu^{240}		Cm^{242}		Cf^{250}	
	Threshold fission	Spontaneous fission	Threshold fission	Spontaneous fission	Threshold fission	Spontaneous fission	Threshold fission	Spontaneous fission
$U_d^{(1)} + U_d^{(2)}$, Mev	18.0		17.9		17.7		18.1	
$T^{(1)} + T^{(2)}$, Mev, $\gamma=0.45$	2.0	0	3.2	0	5.2	1.9	5.4	2.0
$\gamma=0.75$	3.4	0	5.4	0	8.8	3.2	9.2	3.4
E_0, Mev, $\gamma=0.45$	20.0	18.0	21.1	17.9	22.9	19.6	23.5	20.1
$\gamma=0.75$	21.4	18.0	23.3	17.9	26.5	20.9	27.3	21.5

mation that is quadratic in $\alpha_2^{(i)}$ and $\alpha_3^{(i)}$. Correction terms of higher order in $\alpha_n^{(i)}$ were obtained by Present and Knipp.[7] The table lists the values of E_0 calculated for four nuclei with $A_1 = A_2$ for spontaneous and threshold fission, using new values of r_0 and ϵ:[8] $r_0 = 1.22 \times 10^{-13}$ cm and $\epsilon = 50.1$ (and in the quadratic approximation with respect to $\alpha_n^{(i)}$ for $U_d^{(i)}$). These data are also more accurate than those of reference 4a.

As can be seen from the table, $U_d^{(1)} + U_d^{(2)}$ change very little with increasing Z^2/A (they decrease slowly). The increase in E_0 is thus due only to the increase in $T^{(1)} + T^{(2)}$, i.e., $U(y_0) - U(y_d)$. The rapid increase in $|U(y_d)|$ is clearly seen in Fig. 3 of reference 3. From the experimental data on the number of secondary neutrons, ν, it follows that the increase in the fragment excitation energy with increasing Z^2/A corresponds to $\gamma \sim 1$ than to $\gamma = 0.45$ (see reference 9), but $\gamma = 0.45$ is only the lower estimate for γ (see above). Furthermore, E_0 is only approximately equal to the excitation energy of the fragments. At any rate it is clear that the increase in the excitation energy with increasing Z^2/A is due entirely to $T^{(1)} + T^{(2)}$, i.e., to $U(y_0) - U(y_d)$, and not to U_d (if a larger value is assumed for y_d $|U(y_d)|$ will be greater).

Let us now attempt to estimate, for a specified Z^2A, the ratio of the excitation energies of two fragments, or the ratio $E_0^{(1)}/E_0^{(2)}$, in the same approximation, as functions of A_1/A_2. Numerical calculations show that $U_d^{(1)}/U_d^{(2)}$ depends little on A_1/A_2 (it diminishes slowly with diminishing A_1/A_2 when $A_1/A_2 \gtrsim 1$). But since $b_{c1}/b_{c2} = A_2/A_1$ (the distance between the center of gravity of the fragment and the common center of gravity is greater for a lighter fragment than for a heavy one), we have $\dot{\alpha}_n^{(1)} > \dot{\alpha}_n^{(2)}$ for $A_1 < A_2$. According to numerical calculations given in reference 4, $\alpha_n^{(1)}$ is also somewhat greater than $\alpha_n^{(2)}$. Consequently, in spite of the fact that $A_1^{5/3} < A_2^{5/3}$, we nevertheless find that $T^{(1)} > T^{(2)}$. Thanks to this, $E_0^{(1)}$ may turn out to greater than $E_0^{(2)}$ when $A_1 \gtrsim A_2$ (this agrees with the experimental data of reference 10). $E_0^{(1)}/E_0^{(2)}$ diminishes with further increase in A_1/A_2, owing to faster decrease in $U_d^{(1)}/U_d^{(2)}$.

Consequently in this case, too, the main reason for the principal effect ($E_0^{(1)} > E_0^{(2)}$ when $A_1 < A_2$) is $T^{(i)}$ and not $U_d^{(i)}$. We remark that allowance for $\dot{\alpha}_4$ and $\dot{\alpha}_6$ would increase the ratio $E_0^{(1)}/E_0^{(2)}$ substantially, since $\dot{\alpha}_4$ and $\dot{\alpha}_6$ contain high powers of b_{c1} and b_{c2}.

In conclusion, I express my gratitude to I. G. Kruitikova for doing the numerical calculations.

[1] B. T. Geĭlikman, Paper "Fragment Excitation Energy in Nuclear Fission" delivered at the 1958 Geneva Conference.

[2] S. Frankel and N. Metropolis, Phys. Rev. **72**, 914 (1947).

[3] D. Hill and J. Wheeler, Phys. Rev. **89**, 1102 (1953).

[4] B. T. Geĭlikman, (a) Paper delivered at 1958 Geneva Conference; (b) Атомная энергия (Atomic Energy), in press.

[5] B. T. Geĭlikman, Paper delivered at 1955 Geneva Conference.

[6] N. Bohr and J. Wheeler, Phys. Rev. **56**, 426 (1939).

[7] R. Present and J. Knipp, Phys. Rev. **57**, 751 (1940).

[8] T. Maris, Phys. Rev. **101**, 147 (1956).

[9] R. Leachman, Phys. Rev. **101**, 1005 (1956).

[10] J. Fraser and J. Milton, Phys. Rev. **93**, 818 (1954).

Translated by J. G. Adashko
34

CONTRIBUTION TO THE THEORY OF MULTIPLE SCATTERING

M. L. TER-MIKAELYAN

Physics Institute, Academy of Sciences, Armenian S.S.R.

Submitted to JETP editor July 14, 1958

J. Exptl. Theoret. Phys. (U.S.S.R.) **36**, 253-257 (January, 1959)

The article treats a method of calculating multiple-scattering curves with allowance for the finite dimensions of the nucleus. In the calculation use is made of the experimental results on the scattering of fast electrons by nuclei.

LET us denote by $f(\theta_x, \theta_y, t)$ the angular distribution function of charged particles at a depth t (g/cm^2). The scattering angles of the particle are assumed small and be presented in the form of a vector $\boldsymbol{\theta}$ in the plane perpendicular to the direction of motion; θ_x and θ_y are the projections of the scattering angle on two mutually perpendicular planes through the initial direction of motion. The distribution function, for the case of small scattering angles, obeys the following kinetic equation

$$\frac{df(\theta_x\theta_y t)}{dt} = -f(\theta_x\theta_y t)\int_{-\infty}^{\infty}\frac{N}{A}\sigma(\theta_x'\theta_y')\,d\theta_x'd\theta_y' + \int_{-\infty}^{\infty}\frac{N}{A}\sigma(\theta_x'\theta_y')f(\theta_x-\theta_x';\ \theta_y-\theta_y')\,d\theta_x'd\theta_y'. \quad (1)$$

Here N is Avogadro's number, A the atomic weight, $\sigma(\theta_x, \theta_y)$ is the transverse scattering cross section. The boundary condition is chosen in the following form

$$f(\theta_x; \theta_y; 0) = 2\delta(\theta_x)\delta(\theta_y). \quad (2)$$

We shall be interested henceforth in the distribution function for one angle only, either θ_x, or θ_y. This is caused by the fact that it is much easier to measure in a cloud chamber the projection of the scattering angle, than the three-dimensional scattering angle. We must therefore integrate the solution of Eq. (1) over one of the projection angles. The final result can be represented in the following form

$$f(\theta_x, t)\,d\theta_x = \frac{d\theta_x}{\pi}\int_{-\infty}^{\infty}e^{ik_x\theta_x} \times\exp\left\{\frac{Nt}{A}\int_{-\infty}^{\infty}e^{ik_x\theta_x'}\sigma(\theta_x', \theta_y')\,d\theta_x'd\theta_y' - \frac{Nt}{A}\sigma(0,0)\right\}dk_x, \quad (3)$$

where

$$f(\theta_x, t) = \int_{-\infty}^{\infty}f(\theta_x\theta_y, t)\,d\theta_y \quad (4)$$

with the normalization condition $\int_0^{\infty}f(\theta_x, t)\,d\theta_x = 1$. The solution (3) is valid for any scattering law, provided the scattering angles are small.

We are interested so far only in pure Coulomb scattering from a stationary nucleus. This means that $\sigma(\theta_x, \theta_y)$ is the Rutherford scattering cross section with account for both the atomic and nuclear form factors:

$$(Nt/A)\sigma(\theta_x, \theta_y) = 2\chi_c^2q^2F^2/(\theta_x^2+\theta_y^2)^2; \quad (5)$$

we employ the quantity universally used in the theory of multiple scattering

$$\chi_c^2 = (4\pi Nt/A)Z(Z+1)z^2e^4/p^2v^2, \quad (6)$$

where Z is the charge of the scattering nucleus, z the charge of the scattered quantity (henceforth taken as unity); p and v are the momentum and velocity of the scattered particles, q the atomic form factor, and F the nuclear form factor.

Moliere[1,2] has shown how to obtain an exact formula that takes into account the screening of the Coulomb center. This reduces to replacing $q^2/(\theta_x^2+\theta_y^2)^2$ with $(\theta_x^2+\theta_y^2+\varphi_m^2)^{-2}$ where

$$\varphi_m = (\lambda\!\!\!^{-}/0.885R_0Z^{-1/3})\sqrt{1.13+3.76\alpha^2}; \quad (7)$$

Here $\lambda\!\!\!^{-}$ is the wavelength of the incident particle, R_0 is the radius of the hydrogen atom, while $\alpha = zZe^2/\hbar v$.

The nuclear form factor was measured by Hofstadter[3] for a number of elements. For electrons with energies on the order of several hundred Mev, the quantity F^2 in (5) can be approximated by the following expression:[4]

$$F^2 = \{1+k^2a^2(\theta_x^2+\theta_y^2)\}^{-4} \quad (8)$$

The values of a characterize the scattering nucleus. For example, $a = 2.36\times10^{-13}$ cm for lead. It must be noted that the choice of the analytic form (8) for the form factor is dictated exclusively by its suitability for further calculations. From the phys-

ical point of view, this analytical form is not acceptable since it leads to an exponential distribution of the nuclear density. We should consider expression (8) only as an interpolation of the experimental results in the region of electron momenta on the order of 100 Mev/c. It is natural to assume that expression (8) remains valid also for scattering of particles of a different kind in the same range of momentum variation.

Using (5), (7), and (8) we can integrate the exponential function (3) with respect to θ'_y. We obtain

$$f(\theta_x)\,d\theta_x = \frac{2}{\pi}\,d\theta_x \int_0^\infty \cos k_x\theta_x \times \exp\left\{-\frac{2}{3}\chi_c^2 \int_0^\infty (1-\cos k_x\theta'_x)\,B(\theta'_x)\,d\theta'_x\right\}, \quad (9)$$

where

$$B(\theta_x) = 3/2(\varphi_m^2+\theta_x^2)^{-1/2} - 12/\varphi_{nuc}^2(\theta_x^2+\varphi_m^2)^{1/2} + 15\varphi_{nuc}^2/16\,(\theta_x^2+\varphi_{nuc}^2)^{-1/2} + 9\varphi_{nuc}^2/4\,(\theta_x^2+\varphi_{nuc}^2)^{-1/2} + 9/2(\theta_x^2+\varphi_{nuc}^2)^{-1/2} + 12/\varphi_{nuc}^2(\theta_x^2+\varphi_{nuc}^2)^{1/2}. \quad (10)$$

We denote here $\varphi_{nuc} = 1/ka$. It is easy to see that the probability of a single scattering in the interval of the planar angle $\theta_x - \theta_x + \Delta\theta_x$ while traversing the thickness t is $\frac{1}{3}\chi_c^2 B(\theta_x)\,d\theta_x$.

The integral in the exponential of expression (9) is also found analytically; we obtain finally

$$f(\theta_x)\,d\theta_x = \frac{2}{\pi}\,d\theta_x \int_0^\infty d\xi \cos\theta_x\xi \times \exp\left\{-\frac{\chi_c^2\xi^2}{2}\left(\frac{1}{2}-0.577-\ln\frac{\xi\varphi_m}{2}\right) - \frac{8\chi_c^2}{\varphi_{nuc}^2}\left[-0.577+\ln\frac{2}{\xi\varphi_{nuc}} - K_0(\xi\varphi_{nuc})\right] - \frac{13}{3}\frac{\chi_c^2}{\varphi_{nuc}^2}\left[1-\xi\varphi_{nuc}K_1(\xi\varphi_{nuc})\right] + \frac{2}{3}\chi_c^2\xi^2 K_0(\xi\varphi_{nuc}) + \frac{\xi^3\varphi_{nuc}\chi_c^2}{24}K_1(\xi\varphi_{nuc})\right\}. \quad (11)$$

We have incidentally expanded $K_1(\xi\varphi_m)$ and $K_0(\xi\varphi_m)$ in a series, since the important region $\xi\varphi_m \ll 1$. When $\varphi_{nuc} \gg \chi_c$ we arrive at the expression obtained by Moliere[1] for the distribution function on a screened point Coulomb center.

Expression (11) can be reduced to a form amenable to numerical computations. We introduce the variables.

$$\theta_x/\varphi = \theta'_x, \quad \xi\varphi_{nuc} = y, \quad (12)$$

i.e., we measure the scattering angles in units of the nuclear angle.

$$f(\theta_x)\,d\theta_x = \frac{2d\theta'_x}{\pi}\int_0^\infty \cos\theta'_x y \times \exp\left\{-\frac{\chi_c^2}{\varphi_{nuc}^2}\left[\frac{y^2}{2}\left(\frac{1}{2}-0.577-\ln\frac{y\varphi_m}{2\varphi_{nuc}}\right) + 8\left(-0.577+\ln\frac{2}{y}-K_0(y)\right) + \frac{13}{3}(1-yK_1(y)) - \frac{2}{3}y^2K_0(y) - \frac{y^2}{24}K_1(y)\right]\right\}dy. \quad (13)$$

The results of the integration will depend on the two parameters

$$\varphi_{nuc}/\chi_c = (vh/aZe^2)(4\pi Nt/A)^{-1/2}, \quad (14)$$

$$\varphi_m/\varphi_{nuc} = (1.14m_ecZ^{1/3}a/137h)[1.13+3.76(Ze^2/hv)^2]^{1/2}. \quad (15)$$

It is seen from these expressions that both parameters depend only on the velocity of the particle v. This makes it possible to use identical curves for different particles of the same velocity for specified values of t, A, and Z.

Formula (13) was used to calculate the curves for scattering in lead plates 4.5 and 8.5 g/cm^2 thick for velocities of 0.61 c (muon momentum 80 Mev/c), 0.73 c (p = 110 Mev/c), 0.78 c (p = 130 Mev/c), and 0.85 c (p = 170 Mev/c), used in references 5 and 6 to process the experimental results on the scattering of pions and muons, and also protons. It must be noted that it is customary to express the angles in units of the characteristic multiple-scattering angle,[1] $\varphi = \theta_x/\chi_c\sqrt{B}$. We, however, have obtained curves [Eq. (13)] in which the angles are expressed in units of the "nuclear" angle, $\theta'_x = \theta_x/\varphi_{nuc}$. If we rewrite (13) in the following form

$$f(\theta_x)\,d\theta_x = f_1(\theta'_x)\,d\theta'_x = f_2(\varphi)\,d\varphi,$$

it becomes clear that it is easy to change to the variables φ. It is important to know that the use of the scale $(f_1 \cdot \chi_c\sqrt{B}/\varphi_{nuc})$, which must be performed, depends only on the velocity of the particle (but not on its mass), since D is a function of the velocity only. This is why even the recalculated curves can be applied to different particles of the same velocity. The graphs thus obtained were numerically integrated to find the mean values of the scattering angles and their mean squares. For the sake of illustration we list in the table several numbers (lead plate 8.5 g/cm^2 thick). Some boxes contain two values. The upper values are computed for a distribution curve that is cut off at $\varphi = 2.4$, and the lower ones for $\varphi = 2$. The values of $\overline{\varphi}$ and $\overline{\varphi^2}$ for a point nucleus have been calculated from the Moliere distribution curve

while $\bar{\varphi}$ was calculated from the following Moliere formula

$$\bar{\varphi} = \frac{2}{\pi}\bar{\vartheta} = \frac{1}{\pi}\left\{1 + \frac{0.982}{B} - \frac{0.117}{B^2}\right\}$$

(here ϑ is the mean value of the absolute magnitude of the three-dimensional scattering angle). In the calculation of $\overline{\varphi^2}$ for a point nucleus, the same procedure was used as in our case, but the cut-off was at $\varphi = 4$. The fourth line yields $\chi_c\sqrt{B}$ for muons. This quantity must be used to multiply the numbers in the table to obtain the results in degrees.

v/c	0.61	0.78	0.85	Point nucleus
$\bar{\varphi}$	0.53 0.52	0.54 0.537	0.56 0.54	0.60
$(\overline{\varphi^2})^{1/2}$	0.66 0.65	0.69 0.67	0.71 0.66	0.77
$\chi_c\sqrt{B}$	34°.6	20°.2	15°.5	
A	532	550	561	611
B	672	694	711	776

The theory developed above can be used to determine the mass from the scattering angle and range, measured in the cloud chamber. We introduce, after Olbert,[7] the quantity

$$\gamma_i = \theta R^{\alpha}, \tag{16}$$

where R is the range and θ is the scattering angle in radians, while α is determined from the following empirical relation between the range and the quantity $\Pi = pv$:

$$R/mc^2 = A_z(\Pi/mc^2)^{1/\alpha}; \tag{17}$$

m is the mass of the particle, and A_Z is a constant which equals in our case 0.32 g/cm^2 Mev. This relation is valid for the interval $0.05 \leq \Pi/mc^2 \leq 2$. It is easy to see that the distribution function for the quantity η differs from the distribution function for the scattering angles φ only in scale. The values of $\bar{\eta}$ and $\overline{\eta^2}$ are connected with those of $\bar{\varphi}$ and $\overline{\varphi^2}$ as follows

$$\bar{\gamma}_i = \bar{\varphi}\left(\chi_c\sqrt{B}\,\frac{pv}{m_ec^2}\right)(A_zm_ec^2)^{\alpha}\left(\frac{m_e}{m}\right)^{1-\alpha} = A\left(\frac{m_e}{m}\right)^{1-\alpha}, \tag{18}$$

$$(\overline{\gamma_i^2})^{1/2} = (\overline{\varphi^2})^{1/2}\left(\chi_c\sqrt{B}\,\frac{pv}{m_ec^2}\right)(A_zm_ec^2)^{\alpha}\left(\frac{m_e}{m}\right)^{1-\alpha} = B\left(\frac{m_e}{m}\right)^{1-\alpha}; \tag{19}$$

Here m_e is the electron mass. These formulas can be used to determine the mass of the unknown particle m, since the dependence on pv drops out.

The table lists the values of the coefficients [factor in front of $(m_e/m)^{1-\alpha}$], calculated for our case. The coefficients are given for a cut-off at $\varphi = 2.4$. The values of A and B for a different cut-off parameter can be found if the corresponding values of $\bar{\varphi}$ and $\overline{\varphi^2}$ are known for a suitable cut-off (the values given in the table correspond to a cut-off at $\varphi_{max} = 2.4$ and $\varphi_{max} = 2$). It is seen from the above that the results do not depend greatly on the cut-off parameter. Details on the determination of the mass can be found in reference 7. As to the theory of multiple scattering with allowance for the finite dimensions of the nucleus, developed in the same reference, it is a poor approximation to the actual state of affairs.

In conclusion we make several remarks regarding the limits of applicability of the formulas obtained.

We consider first the scattering of particles with nuclear interaction in addition to Coulomb interaction (pions, protons, etc.). In this case one must replace $\sigma(\theta'_X, \theta'_Y)$ and $\sigma(0, 0)$ of Eq. (3) by a particle-scattering cross section that accounts for the nuclear interaction, too. It should be noted that the nuclear scattering has a diffraction character and the cross section for nuclear scattering may amount to a considerable fraction of the total differential cross section (we note that at small angles the cross sections for diffraction scattering may be considerably greater than the geometric cross section).

The plotting of the multiple-scattering curve for the exact differential scattering cross section is made difficult by the lack of sufficient experimental and theoretical data on the single differential cross section. However, certain conclusions with respect to the multiple scattering of nuclear-active charged particles can be made.[5]

Many estimates have been on the scattering of muons. Consideration was given to inelastic interactions that lead to the excitation of the nucleus and that imitate elastic scattering; the possibility of the muon having an anomalous magnetic moment was investigated; estimates were also made of the approximations made in the kinetic equation (for example, the small-angle approximation, of the momentum losses in the plate, and of other corrections. We shall not cite these estimates, in view of the many recent special papers devoted to these problems (for example, references 8 and 9).

I wish to thank F. I. Strizhevskaya who calculated many of the multiple-scattering curves. I am grateful to A. I. Alikhanyan, F. I. Arutyunyan,

and also V. G. Kirillov-Ugryumov and M. I. Daĭon for discussions that have stimulated the performance of this work.

[1] G. Moliere, Z. Naturforsch. **3a**, 78 (1948).
[2] H. Bethe, Phys. Rev. **89**, 1256 (1953).
[3] R. Hofstadter, Revs. Modern Phys. **28**, 214 (1956).
[4] L. Schiff, Phys. Rev. **98**, 756 (1955).
[5] A. I. Alikhaniyan and F. R. Arutyunyan, J. Exptl. Theoret. Phys. (U.S.S.R.) **36**, 32 (1959), this issue.
[6] F. R. Arutyunyan, J. Exptl. Theoret. Phys. (U.S.S.R.) **34**, 800 (1958), Soviet Phys. JETP **7**, 552 (1958).
[7] Annis, Bridge, and Olbert, Phys. Rev. **89**, 1216 (1953).
[8] L. Cooper and J. Rainwater, Phys. Rev. **97**, 492 (1955).
[9] G. Fowler, Nucl. Phys. **1**, 119, 125 (1956).

Translated by J. G. Adashko
35

ABSORPTION OF POLARIZED NEGATIVE MUONS BY NUCLEI AND NEUTRON POLARIZATION

L. D. BLOKHINTSEV

Institute of Nuclear Physics, Moscow State University

Submitted to JETP editor July 15, 1958

J. Exptl. Theoret. Phys. (U.S.S.R.) **36**, 258-263 (January, 1959)

Formulae are obtained for the polarization of neutrons emitted in the absorption of polarized μ^- mesons by nuclei. Estimates are given for O^{16} and Ca^{40}.

IN references 1 and 2, the angular distribution of neutrons produced in the capture of polarized μ^- mesons by nuclei through the reaction

$$\mu^- + P \to N + \nu \qquad (1)$$

was calculated. From measurement of the coefficient of anisotropy, it would be possible to obtain definite information about the type of interaction between μ mesons and nucleons. Measurement of the polarization of the emitted neutrons provides another means of establishing the type of interaction. In this article, the polarization of neutrons produced through reaction (1) in the absorption of polarized μ^- mesons in complex nuclei is calculated. Formulae for the polarization of neutrons produced in the capture of μ^- mesons by free protons are also presented.

1. NEUTRON POLARIZATION

The neutron polarization vector $\mathbf{P}_N$ is defined as the mean value of the neutron spin operator σ:

$$\mathbf{P}_N = \mathrm{Sp}\,(\rho\sigma)\,/\,\mathrm{Sp}\,\rho, \qquad (2)$$

where ρ is the density matrix, the diagonal elements of which determine the probability of neutron emission.

From general considerations, $\mathbf{P}_N$ can be represented as

$$\mathbf{P}_N = a\mathbf{P}_\mu + b\mathbf{k}_N + c\,\mathbf{k}_N \times \mathbf{P}_\mu, \qquad (3)$$

where $\mathbf{P}_\mu$ is the polarization vector of the μ^- meson and $\mathbf{k}_N$ is the neutron momentum. It is clear that the coefficients b and c are different from zero only if spatial parity is not conserved in the process (1). For unpolarized μ^- mesons ($P_\mu = |\mathbf{P}_\mu| = 0$), the neutron polarization is directed along its momentum.

It should be noted that at low energies (~ 1 Mev) it is experimentally difficult to separate neutrons emitted in the direct process from those arising in the decay of the compound nucleus. Therefore, the conclusion reached in reference 1 about the necessity of selecting in the measurements neutrons of energy $E_N \gtrsim 3$ Mev applies here.

The Hamiltonian for the interaction of μ mesons with nucleons, taking into account nonconservation of parity, was taken as

$$H = \sum_k (\bar{\Psi}_N O_k \Psi_P)(\bar{\Psi}_\nu [g_k - g'_k \gamma_5] O_k \Psi_\mu) + \text{Herm. conj.} \qquad (4)$$

in the calculations, where k = s, v, p, t, a denotes the scalar, vector, pseudoscalar, tensor and pseudovector variants of the interaction, respectively. The explicit forms of the operators O_k are given in reference 1.

Calculation of the neutron polarization was carried out under the same assumptions as the calculation of the angular distribution in reference 1. The final formulae are, strictly speaking, only applicable to nuclei having completely filled proton subshells. Two cases were considered. In the first case, the spin-orbit interaction of the neutrons with the nucleus was neglected; in the second case, this interaction was taken into account. The wave functions for the proton in the nucleus Ψ_P, neutron Ψ_N μ^- meson Ψ_μ and neutrino Ψ_ν were given in references 1 and 2.

We choose the coordinate axes in the following way:

$$\mathbf{n}_x = \frac{\mathbf{P}_\mu \times \mathbf{k}_N]}{|\mathbf{P}_\mu \times \mathbf{k}_N|}, \quad \mathbf{n}_y = \frac{\mathbf{k}_N \times [\mathbf{P}_\mu \times \mathbf{k}_N]}{|\mathbf{k}_N \times [\mathbf{P}_\mu \times \mathbf{k}_N]|}, \quad \mathbf{n}_z = \frac{\mathbf{k}_N}{|\mathbf{k}_N|}. \qquad (5)$$

Then the polarization of neutrons of energy E_N, emitted at angle θ to the direction of μ^--meson polarization, with neglect of the spin-orbit interaction of the neutron with the nucleus, is given by the following formulae:*

*The notation used in the following formulae is explained in the appendix.

$$P_N^x(E_N, \theta) = P_\mu \{2B_0(E_N) \operatorname{Im}(h_{st} + h_{sa} + h_{vt} + h_{va})$$
$$- 2B_1(E_N) \operatorname{Im}(h_{pt} + h_{pa}) + G_0(E_N)[(1/2)(h_{ss} + 2\operatorname{Re} h_{sv} + h_{vv})$$
$$- (3/2)(h_{tt} + 2\operatorname{Re} h_{ta} + h_{aa}) + \operatorname{Re}(h_{st} + h_{sa} + h_{vt} + h_{va})]$$
$$+ 2G_1(E_N) \operatorname{Re}(h_{pt} + h_{pa})$$
$$- (1/2) G_2(E_N) h_{pp}\} \sin\theta / W(E_N, \theta); \quad (6a)$$

$$P_N^y(E_N, \theta) = P_\mu \{2[(f_{tt} + 2\operatorname{Re} f_{ta} + f_{aa})$$
$$+ \operatorname{Re}(f_{st} + f_{sa} + f_{vt} + f_{va})] A_0(E_N)$$
$$- (2/3) \operatorname{Re}(f_{ps} + f_{pv})[A_1(E_N) - H(E_N)]$$
$$- (2/3) \operatorname{Re}(f_{pt} + f_{pa})[2A_1(E_N) + H(E_N)]$$
$$+ \operatorname{Im}(f_{ps} + f_{pv} - f_{pt} - f_{pa}) I(E_N)\} \sin\theta / W(E_N, \theta); \quad (6b)$$

$$P_N^z(E_N, \theta) = (\{2[(h_{tt} + 2\operatorname{Re} h_{ta} + h_{aa})$$
$$- \operatorname{Re}(h_{st} + h_{sa} + h_{vt} + h_{va})] B_0(E_N)$$
$$+ 2\operatorname{Re}(h_{ps} + h_{pv}) B_1(E_N)$$
$$+ 2\operatorname{Im}(h_{st} + h_{sa} + h_{vt} + h_{va}) G_0(E_N)$$
$$+ 2\operatorname{Im}(h_{ps} + h_{pv}) G_1(E_N)\} + P_\mu \{[(f_{tt} + 2\operatorname{Re} f_{ta} + f_{aa})$$
$$+ \operatorname{Re}(f_{st} + f_{sa} + f_{vt} + f_{va})] A_0(E_N) - (2/3) \operatorname{Re}(f_{ps} + f_{pv})$$
$$\times [A_1(E_N) + 2H(E_N)]$$
$$- (1/3) \operatorname{Re}(f_{pt} + f_{pa})[A_1(E_N) - H(E_N)]$$
$$- 2\operatorname{Im}(f_{ps} + f_{pv} - f_{pt} - f_{pa}) I(E_N)\} \cos\theta) / W(E_N, \theta) \quad (6c)$$

$$W(E_N, \theta) = \{[(f_{ss} + 2\operatorname{Re} f_{sv} + f_{vv})$$
$$+ 3(f_{tt} + 2\operatorname{Re} f_{ta} + f_{aa})] A_0(E_N) - 2\operatorname{Re}(f_{pt} + f_{pa}) A_1(E_N)$$
$$+ f_{pp} A_2(E_N)\} + P_\mu \{[-(h_{ss} + 2\operatorname{Re} h_{sv} + h_{vv})$$
$$+ (h_{tt} + 2\operatorname{Re} h_{ta} + h_{aa})] B_0(E_N) + 2\operatorname{Re}(h_{pt} + h_{pa}) B_1(E_N)$$
$$- h_{pp} B_2(E_N) + 2\operatorname{Im}(h_{st} + h_{sa} + h_{vt} + h_{va}) G_0(E_N)$$
$$+ 2\operatorname{Im}(h_{pt} + h_{pa}) G_1(E_N)\} \cos\theta. \quad (6d)$$

Formulae for the neutron polarization, taking into account the spin-orbit interaction, are much more lengthy and will not be given here.

In the case of capture of a μ^- meson by a free proton, without taking account of the hyperfine structure of the μ-mesic hydrogen,* calculation with relativistic wave functions leads to the following result†

$$\mathbf{P}_N^{hf} = \frac{P_\mu (c_{hf}\mathbf{n}_x + d_{hf}\mathbf{n}_y) \sin\theta + (k_{hf} + P_\mu l_{hf} \cos\theta)\mathbf{n}_z}{a_{hf} + P_\mu b_{hf} \cos\theta} \quad (7)$$

It should be noted that the influence of the spin-orbit coupling on the polarization of the emitted particle is, in our case, apparently not as important as in scattering. The spin-orbit interaction here does not produce the polarization, although it can change it. Estimates carried out for several special cases show that taking into account the spin-orbit coupling changes the results obtained from Eqs. (6) only little (~ 10 to 15%). Although this result cannot be considered conclusive for the general case, none the less, in view of the complexity of the formulae which take into account the spin-orbit coupling for the neutron, the following considerations and numerical calculations will be based on Eqs. (6), i.e., with neglect of the spin-orbit interaction between neutron and nucleus. Here it might be expected that the spin-orbit coupling would affect the transverse components of polarization P_N^x and P_N^y more strongly than the longitudinal component P_N^z.

Equations (6) make it possible to draw the following conclusions:

(1) As can be seen from Eq. (7), in the case of μ^- capture in mesic hydrogen, P_N^x is not zero only when the Hamiltonian (4) is not invariant not only with respect to reflection of the spatial axes, but also with respect to time reflection. In the case of μ^- capture in nuclei, the interaction of the neutron with the nucleus leads to additional terms in the expression for P_N^x, which do not go to zero even in the case in which temporal parity is conserved.

(2) The presence of a second transverse component P_N^y of polarization is not connected with the degree of nonconservation of spatial parity in the Hamiltonian (4).

(3) In contradistinction to P_N^x and P_N^y, which are proportional to the degree of the μ^--meson polarization P_μ, the longitudinal polarization of the neutron P_N^z does not go to zero for unpolarized μ^- mesons. This fact is valuable, in that — as demonstrated by experiments[5] — the longitudinally-polarized μ^- mesons produced in the decay of π^- mesons are strongly depolarized in slowing down in matter and with formation of mesic atoms; the degree of their polarization in the K orbit is of order[5] ~0.15 to 0.20. Therefore, P_N^z can attain larger values than P_N^x and P_N^y.

We consider several simplifications which can be made in Eqs. (6). Firstly, one can neglect the pseudoscalar interaction, if the pseudoscalar coupling constant g_p is not too large in comparison with other constants. Further, it should be noted

*Gershtein has shown[3] that the hyperfine structure and the effect of the μ^- meson jumping from one hydrogen atom to another lead, under the assumption of a longitudinal neutrino, to neutrons, emitted in the decay of μ-mesic hydrogen, which are completely polarized longitudinally.

†This formula was given for the special case of a longitudinal neutrino by Wolfenstein.[4]

that, as estimates show, $G_0(E_N)$ is much smaller than $A_0(E_N)$. and $B_0(E_N)$. For nuclei with filled proton shells $G_k(E_N) \equiv 0$, if the dependence of the binding energy of the proton in the nucleus on the total angular momentum j is neglected. Finally, it is interesting to look at the special case, important in practice, of a longitudinal neutrino,[6] which corresponds to $g_k = -g'_k$ in Eq. (4).

In the first approximation, leaving out the pseudoscalar interaction and neglecting terms proportional to $G_0(E_N)$, we obtain for the longitudinal neutrino:*

$$P_N^x(E_N, \theta) = \frac{P_\mu 2\,\mathrm{Im}(g_1^* g_2)\,\beta_0(E_N)\sin\theta}{(|g_1|^2+3|g_2|^2) - P_\mu(|g_1|^2-|g_2|^2)\beta_0(E_N)\cos\theta}; \quad (8a)$$

$$P_N^y(E_N, \theta) = \frac{P_\mu 2\,[|g_2|^2 + \mathrm{Re}(g_1^* g_2)]\sin\theta}{(|g_1|^2+3|g_2|^2) - P_\mu(|g_1|^2-|g_2|^2)\beta_0(E_N)\cos\theta}; \quad (8b)$$

$$P_N^z(E_N, \theta) = \frac{2\{[|g_2|^2 - \mathrm{Re}(g_1^* g_2)]\beta_0(E_N) + P_\mu[|g_2|^2 + \mathrm{Re}(g_1^* g_2)]\cos\theta}{(|g_1|^2+3|g_2|^2) - P_\mu(|g_1|^2-|g_2|^2)\beta_0(E_N)\cos\theta}. \quad (8c)$$

Here the quantities $g_1 \equiv g_s + g_v$ and $g_2 \equiv g_t + g_a$, corresponding to the constants of Fermi and Gamow-Teller couplings, have been introduced.

From Eq. (8) it can be seen that measurement of only the longitudinal component P_N^z of polarization makes it possible to determine the ratios of the moduli of the Fermi and Gamow-Teller constants and their relative phase (to within a sign). Analogous information can be obtained from measurement of P_N^y. The sign of the phase can be determined from P_N^x. If the interaction of μ mesons with nucleons is described by the theory of Gell-Mann and Feynman[7] ($g_v = \pm g_a$, $g_s = g_p = g_t = 0$) then, as noted in reference 1, the asymmetry in the angular distribution of the neutrons vanishes. As to the neutron polarization, it follows from Eq. (8) that at least its longitudinal component is not zero.

Equations (6) and (8) relate to a neutron with a definite energy E_N. If integration over the neutron energy E_N is carried out, then we obtain formulae which differ from Eqs. (6) and (8) only in that functions of the energy $A_k(E_N)$, $B_k(E_N)$, ..., $Z(E_N)$, $\beta_0(E_N)$ are replaced by constants $\widetilde{A}_k$, $\widetilde{B}_k$, ..., $\widetilde{Z}$, $\widetilde{\beta}_0$.

2. NUMERICAL EVALUATION FOR $_8O^{16}$ AND $_{20}Ca^{40}$

Since, with neglect of the pseudoscalar interaction, the same coefficients A_0, B_0 and G_0 enter into the expressions for the polarization of the neutron as for the angular distribution, we can use the quantities in reference 1, obtained in the calculation of the angular distribution of neutrons from $_8O^{16}$ and $_{20}Ca^{40}$ nuclei. The assumptions under which the calculation was carried out are described in detail in reference 1.

The neutron polarization, averaged over the spectrum, under the assumption of a longitudinal neutrino, is determined by Eqs. (8) with $\widetilde{\beta}_0$ in place of $\beta_0(E_N)$. For $_8O^{16}$ and $_{20}Ca^{40}$ and two different values of the imaginary part of the potential, describing the interaction of the neutron with the potential, $\widetilde{\beta}_0$ takes on the following values

$$_8O^{16}: \widetilde{\beta}_0 = 0.034 \text{ for } \zeta = 0; \quad \widetilde{\beta}_0 = 0.476 \text{ for } \zeta = -0.15;$$
$$_{20}C^{40}: \widetilde{\beta}_0 = 0.145 \text{ for } \zeta = 0; \quad \widetilde{\beta}_0 = 0.528 \text{ for } \zeta = -0.15.$$

It is easy to show that $|P_N^x(\theta)|$ and $|P_N^y(\theta)|$ are maximal for values of near to $\pm\pi/2$. Then

$$P_N^y\left(\pm\frac{\pi}{2}\right) = \pm P_\mu \frac{2[|g_2|^2 + \mathrm{Re}(g_1^* g_2)]}{|g_1|^2 + 3|g_2|^2}.$$

Thus, the dependence $P(\pm\pi/2)$ on the ratio of Fermi and Gamow-Teller coupling constants turns out to be the same for all nuclei. $P_N^y(\pm\pi/2)$ varies from zero for $g_1 = -g_2$ to P_μ for $g_1 = g_2$. For pure Gamow-Teller coupling $P_N^y(\pm\pi/2) = \pm\frac{2}{3}P_\mu \approx \pm 0.12$. The longitudinal component $|P_N^z(\theta)|$ attains a maximum for $\theta = 0$, if $|g_2|^2 > \mathrm{Re}(g_1^* g_2)$ and for $\theta = \pi$ if $|g_2|^2 < \mathrm{Re}(g_1^* g_2)$. For pure Gamow-Teller coupling and $P_\mu \sim 0.20$ and $\zeta = -0.15$, for $_8O^{16}$ and $_{20}Ca^{40}$ nuclei, $P_N^z(0) = 0.45$ and $P_N^z(\pm\pi/2)$ $\frac{2}{3}\beta_0 \approx 0.33$ (for a free proton, without account of hyperfine structure, $P_N^3(\pm\pi/2) \approx \frac{2}{3}$).

Consequently, the degree of polarization of the neutron, especially the longitudinal component, can become quite large.

In conclusion, I would like to sincerely thank I. S. Shapiro for his interest in the work and discussion of the results.

APPENDIX

Here we explain the notation employed in the article:

$$f_{ik} = g_i^* g_k + g_i'^* g_k', \quad h_{ik} = g_i^* g_k' + g_i'^* g_k; \quad (A.1)$$

$$H(E_N) = C\sum_{nlj}\frac{1}{2}\frac{2j+1}{2l+1}(-1)^l (E_\nu^{nlj}/2Mc^2)^2$$
$$\times \sum_{LL'\Lambda\Lambda'} i^{L+\Lambda-L'-\Lambda'}(2L+1)(2L'+1)(2\Lambda+1)(2\Lambda'+1)$$
$$\times C^{2o}_{Lo\,L'o}C^{2o}_{\Lambda o\,\Lambda' o}C^{1o}_{Lo\,\Lambda o}C^{1o}_{L'o\,\Lambda' o}W(LL'\Lambda\Lambda';\,2l)$$
$$\times \mathrm{Re}\,(b^*_{L\Lambda nlj}(E_N)\,b_{L'\Lambda' nlj}(E_N))\,\varphi_{nlj}(E_N); \quad (A.2)$$

*For $g_k = -g'_k$ we obtain from Eq. (4) that the neutrino is polarized along its direction of motion. If the neutrino produced in μ^- capture is polarized antiparallel to its direction of motion, one should change in Eq. (8) the sign in front of terms containing $\beta_0(E_N)$.

$$I(E_N) = C\sum_{nlj}(2/\sqrt{5})(2j+1)$$
$$\times(-1)^l W(lj1^1/_2;\ ^1/_2\, l)\,(E_\nu^{nlj}/2Mc^2)$$
$$\times\sum_{L\Lambda L'\Lambda'} i^{L+\Lambda-L'-\Lambda'}(2L+1)(2L'+1)$$
$$\times(2\Lambda+1)(2\Lambda'+1)C^{20}_{L0L'0}C^{20}_{\Lambda0\Lambda'0}C^{l0}_{L0\Lambda0}C^{l0}_{L'0\Lambda'0}$$
$$\times X(\Lambda 2\Lambda';\ L2L';\ l1l)\,\mathrm{Im}\,(b^*_{L\Lambda nlt}(E_N)\,b_{L'\Lambda' nlt}(E_N))\,\varrho_{nlt}(E_N); \quad (A.3)$$

$$a_{\mathrm{hf}} = (E_N^{\mathrm{hf}}+M)f_{ss} + (E_N^{\mathrm{hf}}-M)f_{pp}$$
$$+2(2E_N^{\mathrm{hf}}-M-E_\nu^{\mathrm{hf}})f_{vv} + 2(2E_N^{\mathrm{hf}}+M+E_\nu^{\mathrm{hf}})f_{aa}$$
$$+2(3E_N^{\mathrm{hf}}+2E_\nu^{\mathrm{hf}})f_{tt} + 2(E_N^{\mathrm{hf}}+M+E_\nu^{\mathrm{hf}})\,\mathrm{Re}\,f_{sv}$$
$$-2E_\nu^{\mathrm{hf}}\mathrm{Re}\,f_{st} - 2(E_N^{\mathrm{hf}}-M+E_\nu^{\mathrm{hf}})\,\mathrm{Re}\,f_{ap}$$
$$-2E_\nu^{\mathrm{hf}}\mathrm{Re}\,f_{tp} - 4E_\nu^{\mathrm{hf}}\mathrm{Re}\,f_{ta}$$
$$-6(E_N^{\mathrm{hf}}-M+E_\nu^{\mathrm{hf}})\,\mathrm{Re}\,f_{vt} + 6(E_N^{\mathrm{hf}}+M+E_\nu^{\mathrm{hf}})\,\mathrm{Re}\,f_{at}; \quad (A.4)$$

$$b_{\mathrm{hf}} = (E_N^{\mathrm{hf}}+M)h_{ss} + (E_N^{\mathrm{hf}}-M)h_{pp} + 2(M+E_\nu^{\mathrm{hf}})h_{vv}$$
$$-2(M-E_\nu^{\mathrm{hf}})h_{aa} - 2(E_N^{\mathrm{hf}}+2E_\nu^{\mathrm{hf}})h_{tt}$$
$$+2(E_N^{\mathrm{hf}}+M+E_\nu^{\mathrm{hf}})\,\mathrm{Re}\,h_{sv}$$
$$-2E_\nu^{\mathrm{hf}}\mathrm{Re}\,h_{st} - 2(E_N^{\mathrm{hf}}-M+E_\nu^{\mathrm{hf}})\,\mathrm{Re}\,h_{ap} - 2E_\nu^{\mathrm{hf}}\mathrm{Re}\,h_{tp}$$
$$+4E_\nu^{\mathrm{hf}}\mathrm{Re}\,h_{va} + 2(E_N^{\mathrm{hf}}-M+E_\nu^{\mathrm{hf}})\,\mathrm{Re}\,h_{vt}$$
$$-2(E_N^{\mathrm{hf}}+M+E_\nu^{\mathrm{hf}})\,\mathrm{Re}\,h_{at}; \quad (A.5)$$

$$c_{\mathrm{hf}} = 2(E_\nu^{\mathrm{hf}}\,\mathrm{Im}\,h_{sv} - (E_N^{\mathrm{hf}}+M)\,\mathrm{Im}\,h_{sa}$$
$$-(E_N^{\mathrm{hf}}+M+E_\nu^{\mathrm{hf}})\,\mathrm{Im}\,h_{st}$$
$$-(E_N^{\mathrm{hf}}-M)\,\mathrm{Im}\,h_{pv} + E_\nu^{\mathrm{hf}}\,\mathrm{Im}\,h_{pa} + (E_N^{\mathrm{hf}}-M+E_\nu^{\mathrm{hf}})\,\mathrm{Im}\,h_{pt}$$
$$-2(E_N^{\mathrm{hf}}+E_\nu^{\mathrm{hf}})\,\mathrm{Im}\,h_{va} - (E_N^{\mathrm{hf}}+M+3E_\nu^{\mathrm{hf}})\,\mathrm{Im}\,h_{vt}$$
$$-(E_N^{\mathrm{hf}}-M+3E_\nu^{\mathrm{hf}})\,\mathrm{Im}\,h_{at}); \quad (A.6)$$

$$d_{\mathrm{hf}} = 2\{-(E_N^{\mathrm{hf}}-M+E_\nu^{\mathrm{hf}})f_{vv} + (E_N^{\mathrm{hf}}+M+E_\nu^{\mathrm{hf}})f_{aa}$$
$$+2Mf_{tt} - E_\nu^{\mathrm{hf}}\mathrm{Re}\,f_{sv} + (E_N^{\mathrm{hf}}+M)\,\mathrm{Re}\,f_{sa}$$
$$+(E_N^{\mathrm{hf}}+M+E_\nu^{\mathrm{hf}})\,\mathrm{Re}\,f_{st} + (E_N^{\mathrm{hf}}-M)\,\mathrm{Re}\,f_{pv} - E_\nu^{\mathrm{hf}}\mathrm{Re}\,f_{pa}$$
$$-(E_N^{\mathrm{hf}}-M+E_\nu^{\mathrm{hf}})\,\mathrm{Re}\,f_{pt} + 2M\,\mathrm{Re}\,f_{va}$$
$$+(3E_N^{\mathrm{hf}}-M+E_\nu^{\mathrm{hf}})\,\mathrm{Re}\,f_{vt}$$
$$+(3E_N^{\mathrm{hf}}+M+E_\nu^{\mathrm{hf}})\,\mathrm{Re}\,f_{at}\}; \quad (A.7)$$

$$k_{\mathrm{hf}} = 2\{-(E_N^{\mathrm{hf}}-M)h_{vv} - (E_N^{\mathrm{hf}}+M)h_{aa}$$
$$-(2E_N^{\mathrm{hf}}+3E_\nu^{\mathrm{hf}})h_{tt} - E_\nu^{\mathrm{hf}}\mathrm{Re}\,h_{sp} + (E_N^{\mathrm{hf}}+M+E_\nu^{\mathrm{hf}})\,\mathrm{Re}\,h_{sa}$$
$$+(E_N^{\mathrm{hf}}+M)\,\mathrm{Re}\,h_{st} - (E_N^{\mathrm{hf}}-M+E_\nu^{\mathrm{hf}})\,\mathrm{Re}\,h_{pv}$$
$$+(E_N^{\mathrm{hf}}-M)\,\mathrm{Re}\,h_{pt} + 2(E_N^{\mathrm{hf}}+2E_\nu^{\mathrm{hf}})\,\mathrm{Re}\,h_{va}$$
$$+(3E_N^{\mathrm{hf}}-M+3E_\nu^{\mathrm{hf}})\,\mathrm{Re}\,h_{vt}$$
$$-(3E_N^{\mathrm{hf}}+M+3E_\nu^{\mathrm{hf}})\,\mathrm{Re}\,h_{at}\}; \quad (A.8)$$

$$l_{\mathrm{hf}} = 2\{(E_N^{\mathrm{hf}}-M)f_{vv} + (E_N^{\mathrm{hf}}+M)f_{aa}$$
$$+(2E_N^{\mathrm{hf}}+E_\nu^{\mathrm{hf}})f_{tt} - E_\nu^{\mathrm{hf}}\mathrm{Re}\,f_{sp} + (E_N^{\mathrm{hf}}+M+E_\nu^{\mathrm{hf}})\,\mathrm{Re}\,f_{sa}$$
$$+(E_N^{\mathrm{hf}}+M)\,\mathrm{Re}\,f_{st} - (E_N^{\mathrm{hf}}-M+E_\nu^{\mathrm{hf}})\,\mathrm{Re}\,f_{pv}$$
$$+(E_N^{\mathrm{hf}}-M)\,\mathrm{Re}\,f_{pt} + 2E_N^{\mathrm{hf}}\mathrm{Re}\,f_{va} - (E_N^{\mathrm{hf}}-3M+E_\nu^{\mathrm{hf}})\,\mathrm{Re}\,f_{vt}$$
$$+(E_N^{\mathrm{hf}}+3M+E_\nu^{\mathrm{hf}})\,\mathrm{Re}\,f_{at}\}. \quad (A.9)$$

$E_N^{\mathrm{f}} = 4.47$ Mev and $E_\nu^{\mathrm{f}} = 99.1$ Mev, are the energies of the neutron and neutrino, respectively, produced in the decay of μ-mesic hydrogen. The remaining notation encountered in the text of the article and in the appendix is given in references 1 and 2.

[1] É. I. Dolinskiĭ and L. D. Blokhintsev, J. Exptl. Theoret. Phys. (U.S.S.R.) **35**, 1488 (1958), Soviet Phys. JETP **8**, 1040 (1959).

[2] É. I. Dolinskiĭ and L. D. Blokhintsev, J. Exptl. Theoret. Phys. (U.S.S.R.) **34**, 759 (1958), Soviet Phys. JETP **7**, 521 (1958).

[3] S. S. Gershteĭn, J. Exptl. Theoret. Phys. (U.S.S.R.) **34**, 463, 993 (1958), Soviet Phys. JETP **7**, 318, 685 (1958).

[4] L. Wolfenstein, Nuovo cimento **7**, 706 (1958).

[5] Egorov, Ignatenko, Khalupa and Chultém, IV Session of the Scientific Council of the Joint Institute for Nuclear Research, Dubna (1958).

[6] L. D. Landau, J. Exptl. Theoret. Phys. (U.S.S.R.) **32**, 407 (1957), Soviet Phys. JETP **5**, 337 (1958); T. D. Lee and C. N. Yang, Phys. Rev. **105**, 1671 (1957); A. Salam, Nuovo cimento **5**, 299 (1957).

[7] R. P. Feynman and M. Gell-Mann, Phys. Rev. **109**, 193 (1958).

Translated by G. E. Brown
36

CHARGE SYMMETRY PROPERTIES AND REPRESENTATIONS OF THE EXTENDED LORENTZ GROUP IN THE THEORY OF ELEMENTARY PARTICLES

V. I. OGIEVETSKII and CHOU KUANG-CHAO

Joint Institute for Nuclear Research

Submitted to JETP editor July 15, 1958

J. Exptl. Theoret. Phys. (U.S.S.R.) **36**, 264-270 (January, 1959)

The extended Lorentz group, including the complete Lorentz group and charge conjugation, is considered. It is shown that the use of irreducible projective representations of this extended group requires the existence of charge multiplets. Charge symmetry and associated production of strange particles follow from the invariance under reflections and charge conjugation and from the conservation laws for the electric and baryonic charges. The Pauli-Gürsey transformation holds for free nucleons. The extension of the condition of invariance under this transformation to the case of interactions leads to isobaric invariance for strong interactions of all particles.

1. INTRODUCTION

IT is known that the strongly interacting particles form charge multiplets (p, n, π^+, π^0, π^-, K^+, K^0, etc.). Particles belonging to the same multiplet have almost identical masses and identical spins, but differ in their electric charges. In agreement with experiment one adopts the hypothesis of charge symmetry and the stronger hypothesis of charge independence. In the conventional theory this is expressed by the invariance under rotations in a certain formal isobaric space. The particles of a given multiplet are considered as states of the same particle with different projections of the isobaric spin. For example, the proton and the neutron form the nucleon. The description of the nucleon makes use of a reducible eight-component representation of the full Lorentz group. We have a similar situation (reducibility of the representation of the full Lorentz group) for the other strongly interacting particles.

Now the question arises: if it is required that the elementary particles be described only by irreducible representations, would it then be possible to extend the Lorentz group and to find irreducible representations of this extended group which automatically lead to the existence of charge multiplets and charge symmetries? The solution of this question is the subject of the present paper.

We extend the Lorentz group in the following fashion.

The wave functions of quantum theory are complex functions. The operation of charge conjugation C, which takes a particle into its antiparticle, is always represented by the product of a linear operator (matrix) and the antilinear operator of complex conjugation:

$$C: \qquad \psi_c = C_0 \psi^*, \tag{1}$$

where C_0 is determined such that ψ_c transforms according to the same irreducible representation of the proper Lorentz group as ψ.

Besides the proper Lorentz group L, the spatial reflections I, and the time reversal T, we also include the charge conjugation C in the extended group. Together with the conventional irreducible representations of the extended group, we also consider its irreducible projective representations.*

The importance of using the projective representations of the full Lorentz group was pointed out by Gel'fand and Tsetlin[1] in connection with the theory of parity doublets of Lee and Yang. The possibility of using projective representations is connected with the indeterminacy of the phase factor of the quantum theoretical wave function. Subsequent to Gel'fand and Tsetlin, the projective representations of the full Lorentz group were discussed

*We are given a projective representation of the group G, if an operator R(g) is given for each element g of the group G such that the operator $R(g_1g_2) = \alpha(g_1, g_2)R(g_1)R(g_2)$ corresponds to the product of group elements g_1g_2. If $\alpha(g_1, g_2) \equiv 1$, the projective representation reduces to the conventional one. In general, $\alpha(g_1, g_2)$ can also be equal to -1. Anticommuting operators of the projective representation may thus correspond to commuting elements of the group. In particular, the conventional spinor representation is a projective representation (the operations $I = \gamma_4$ and $T = \gamma_4\gamma_5$ anticommute, whereas the spatial and time reflections commute).

by Taylor and McLennan.[2] Taylor notes the connection between these representations and the isobaric invariance. As only the full Lorentz group is considered, protons and neutrons, and $\pi^{\pm}$ and π^0 mesons, differ with respect to their spatial parities. Salam and Pais, at the Seventh Rochester Conference, also discussed the need for a new definition of the operations of space-time reflections from which the charge symmetries would follow.

In this paper we do not consider all irreducible projective representations of the extended group. We restrict ourselves to those necessary for the description of the strongly interacting particles. We shall show that multiplets, charge symmetries, and associated production of strange particles are immediate consequences of the standard conservation laws for the number of baryons and electric charge, and of the invariance with respect to the full Lorentz group and charge conjugation, if the nucleons, Ξ particles, and K mesons are described by the new projective representations of the extended group, while the remaining particles are described in the usual fashion.

In our theory the Pauli-Gürsey transformation holds for free nucleons. This transformation is connected with the isobaric invariance in a natural way. If the requirement of invariance under this transformation is extended to the interaction Lagrangian for the nucleons, the isobaric invariance for strong interactions follows for all particles.

In this theory the Lagrangian for the interaction with electromagnetic fields can be easily written down with the help of the charge operator. It appears that the electromagnetic interactions are invariant only under Wigner time reversal, but not under Schwinger time reversal.

The case of weak interactions, which do not conserve spatial parity, is more complicated and will not be discussed in the present paper.

To be definite, we shall assume that the relative parities of all baryons are identical and that the reflection of the conventional spinors is performed with the help of the operator γ_4. All bosons are considered as pseudoscalars. We start with the discussion of the nucleons.

2. THE FREE NUCLEON FIELD

It is easily shown that the requirement

$$I^2 = T^2 = C^2 = 1, \tag{2}$$

leads, for the case of four-component spinors, to the following expressions for the operators I, T, and C:

$$\begin{aligned} &\text{a) } I: && \psi' = \gamma_4\psi, \\ &\text{b) } T: && \psi' = i\gamma_4\gamma_5\psi^*, \\ &\text{c) } C: && \psi_c = i\gamma_2\psi^*, \end{aligned} \tag{3}$$

where T is the Schwinger time reversal for spinors,[3] and the matrices γ_i are expressed in the Pauli representation.

The following commutation relations hold between the operators I, T, and C:

$$\text{a) } IT = -TI, \quad \text{b) } IC = -CI, \quad \text{c) } TC = -CT. \tag{4}$$

We retain relations (2), but we require that, in contrast to the conventional theory, the sign in relation (4a) is changed for nucleons, i.e., we demand that

$$\text{a) } IT = TI, \quad \text{b) } IC = -CI, \quad \text{c) } TC = -CT. \tag{4'}$$

The commutation relations (2) and (4′) can only be satisfied by 8×8 matrices:

$$\begin{aligned} &\text{a) } I: && \psi' = \tau_3 \times \gamma_4\psi, \\ &\text{b) } T: && \psi' = 1 \times \gamma_4\psi, \\ &\text{c) } C: && \psi_c = i\tau_3 \times \gamma_2\psi^*, \end{aligned} \tag{5}$$

where τ are the Pauli matrices. These operators, together with the operators of the proper Lorentz group (in which γ_μ should everywhere be replaced by $1 \times \gamma_\mu$), form the irreducible projective representation of the extended Lorentz group. The spinors $\psi = \begin{pmatrix} \psi_1 \\ \psi_2 \end{pmatrix}$ have eight components.

In this representation the Lagrangian for the free field is uniquely determined:*

$$L = \bar{\psi}(1 \times \gamma_\mu\partial_\mu + i\tau_2 \times \gamma_5 m)\psi, \tag{6}$$

where $\bar{\psi} = \psi^{*T}(1 \times \gamma_4)$. The field equations have the form

$$1 \times \gamma_\mu\partial_\mu\psi = -i\tau_2 \times \gamma_5 m\psi. \tag{7}$$

The Lagrangian (6) as well as Eq. (7) are invariant with respect to the two one-parameter groups of transformations

$$\psi' = \exp(i\lambda)\psi, \tag{8}$$

$$\psi' = \exp[i\tau_1 \times \gamma_5\lambda]\psi, \tag{9}$$

and with respect to the three-parameter group

$$\psi' = a\psi + b\tau_3 \times \gamma_5\psi_c, \tag{10}$$

where $|a|^2 + |b|^2 = 1$.

The transformations (9) and (10) are the analogs of the Pauli transformations[4] for the neutrino. They are different only in that γ_5 is replaced by $\tau_1 \times \gamma_5$ and $\tau_3 \times \gamma_5$, respectively.

*According to Schwinger $L \to L^T$, where the superscript T signifies transposition of the operators of the Hilbert space.[3]

We introduce the new four-component spinors

$$\psi_p = (\psi_1 + \gamma_5\psi_2)/\sqrt{2}, \quad \psi_{pc} = (\psi_{c1} + \gamma_5\psi_{c2})/\sqrt{2},$$
$$\psi_{nc} = (-\gamma_5\psi_1 + \psi_2)/\sqrt{2}, \quad \psi_n = (\gamma_5\psi_{c1} - \psi_{c2})/\sqrt{2}, \tag{11}$$

they satisfy the ordinary Dirac equation

$$\gamma_\mu\partial_\mu\psi = -m\psi, \tag{12}$$

Under the transformation (9) we obtain

$$\psi'_p = \exp(i\lambda)\,\psi_p, \quad \psi'_n = \exp(i\lambda)\,\psi_n,$$
$$\psi'_{pc} = \exp(-i\lambda)\,\psi_{pc}, \quad \psi'_{nc} = \exp(-i\lambda)\,\psi_{nc}. \tag{13}$$

Transformation (9) may thus be viewed as a gauge transformation connected with the conservation law for the number of baryons. ψp, ψn, ψpc, and ψnc refer to the proton, neutron, antiproton, and antineutron fields respectively.

The following transformation should be related to the conservation law for the electric charge:

$$E:\ \psi' = \exp[(i/2)(1\times 1 + \tau_1\times\gamma_5)\lambda]\,\psi. \tag{14}$$

Indeed, under this transformation:

$$E:\ \psi'_p = \exp(i\lambda)\,\psi_p, \quad \psi'_{pc} = \exp(-i\lambda)\,\psi_{pc},$$
$$\psi'_n = \psi_n, \qquad \psi'_{nc} = \psi_{nc}. \tag{15}$$

The three-parameter trnnsformation (10) is isomorphic to a rotation in the isobaric space. Indeed, if we form the conventional eight-component nucleon field $\psi_N = \begin{pmatrix}\psi_p\\ \psi_n\end{pmatrix}$, we have, under the transformation (10),

$$\psi'_N = \exp[i(\boldsymbol{\tau}\cdot\boldsymbol{\lambda})]\,\psi_N, \tag{16}$$

where λ is a vector with real components λ_1, λ_2, λ_3; τ are the usual 2×2 Pauli matrices, and

$$a = \cos|\lambda| + \frac{i\lambda_3}{|\lambda|}\sin|\lambda|; \quad b = \frac{\sin|\lambda|}{|\lambda|}(\lambda_2 - i\lambda_1). \tag{17}$$

An analogous isomorphism arising from a purely formal doubling of the number of components was pointed out by Gürsey.[5]

3. INTERACTION OF NUCLEONS WITH ORDINARY BOSONS

We first consider the interaction of nucleons with a neutral pseudoscalar field φ_0 with positive "time-parity:"

$$I:\ \tau'_0 = -\tau_0,$$
$$T:\ \tau_0 = \tau_0, \tag{18}$$
$$C:\ \tau_{0c} = \tau_0.$$

The requirement of invariance with respect to I, T, C, transformation (9), and E lead to a unique interaction Lagrangian (in the following we only consider interaction Lagrangians without derivatives):

$$L_0 = ig_0\bar{\psi}\tau_3\times\gamma_5\psi\tau_0 = ig_0(\bar{p}\gamma_5 p - \bar{n}\gamma_5 n)\,\varphi_0 = ig_0\bar{\psi}_N\tau_3\gamma_5\psi_N\varphi_0, \tag{19}$$

the meson field φ_0 couples to the protons and neutrons with a different sign, and φ_0 may be identified with the neutral π^0 meson.

If the neutral meson φ'_0 were a spatial pseudoscalar, but had negative time-parity, we would uniquely obtain the interaction Lagrangian

$$L'_0 = g'_0\bar{\psi}\tau_2\times 1\psi\varphi'_0 = ig'_0(\bar{p}\gamma_5 p + \bar{n}\gamma_5 n)\,\varphi'_0, \tag{20}$$

φ'_0 may be related to the hypothetical ρ_0 meson.

For the Lagrangian describing the interaction of nucleons with a charged pseudoscalar boson field φ:

$$I:\ \varphi' = -\varphi,$$
$$T:\ \varphi' = \varphi, \tag{21}$$
$$C:\ \varphi_c = \varphi^*$$

we similarly obtain the unique expression

$$L = ig(\bar{\psi}_p\psi_c\varphi^* - \bar{\psi}_c\psi_p\varphi) = 2ig(\bar{p}\gamma_5 n\varphi^* + \bar{n}\gamma_5 p\varphi). \tag{21}$$

We may thus assume that φ (φ^*) describes π^- (π^+) mesons.

The charge symmetry (i.e., the possibility of the simultaneous interchange $p \rightleftarrows n$, $\pi^+ \rightleftarrows \pi^-$, $\pi^0 \rightleftarrows -\pi^0$) of the interactions (19) and (20) is obvious. The general form of the Lagrangian for interactions with π mesons is

$$L_\pi = ig_0(\bar{p}\gamma_5 p - \bar{n}\gamma_5 n)\,\pi^0 + 2ig(\bar{p}\gamma_5 n\pi^+ + \bar{n}\gamma_5 p\pi^-). \tag{22}$$

If we now require that not only the free nucleon Lagrangian, but also the interaction Lagrangian be invariant under transformations of the three-parameter group, then $g = g_0/\sqrt{2} = g_\pi/\sqrt{2}$, and

$$L_\pi = ig_\pi\bar{\psi}_N(\boldsymbol{\tau}\cdot\boldsymbol{\pi})\,\psi_N. \tag{23}$$

Under the transformation (10) the meson fields transform according to

$$(\boldsymbol{\tau}\cdot\boldsymbol{\pi})' = \exp[i(\boldsymbol{\tau}\cdot\boldsymbol{\lambda})]\,(\boldsymbol{\tau}\cdot\boldsymbol{\pi})\exp[-i(\boldsymbol{\tau}\cdot\boldsymbol{\lambda})], \tag{24}$$

where the masses of the π^+, π^-, and π^0 mesons must be identical.

We have thus arrived at the conventional isobaric-invariant theory of the interaction between π mesons and nucleons.

4. FREE K MESONS

The conventional representation of the extended Lorentz group for bosons is exhausted by the π mesons. We shall describe the K mesons by the projective representation in which

$$I^2 = 1, \quad C^2 = 1, \quad T^2 = -1, \tag{25}$$
$$IT = TI, \quad IC = CI, \quad TC = CT.$$

The simplest irreducible representation consistent with these commutation relations is two-dimensional, $\varphi = \begin{pmatrix} \varphi_1 \\ \varphi_2 \end{pmatrix}$. The operators I, T, and C have the form

$$\begin{aligned} I&: \quad \varphi' = -\varphi, \\ T&: \quad \varphi' = i\tau_2\varphi, \\ C&: \quad \varphi_c = \varphi^*. \end{aligned} \tag{26}$$

We identify the K^+ meson with φ_1, the K^0 meson with φ_2, the K^- meson with φ_1^*, and the $\overline{K}^0$ meson with φ_2^*. The conservation law for the electric charge is then connected with the transformation

$$E: \quad \varphi' = \exp\left[\frac{1}{2}(1+\tau_3)\lambda\right]\varphi. \tag{27}$$

Indeed, with this transformation,

$$K^{+\prime} = \exp(i\lambda)K^+, \quad K^{-\prime} = \exp(-i\lambda)K^-, \tag{28}$$
$$K^{0\prime} = K^0, \quad \overline{K}^{0\prime} = \overline{K}^0.$$

The conservation law for the hypercharge corresponds to the transformation $\varphi' = \exp(i\tau_3\lambda)\varphi$, so that

$$\begin{aligned} K^{+\prime} &= \exp(i\lambda)K^+, \quad & K^{0\prime} &= \exp(i\lambda)K^0, \\ K^{-\prime} &= \exp(-i\lambda)K^-, \quad & \overline{K}^{0\prime} &= \exp(-i\lambda)\overline{K}^0. \end{aligned} \tag{29}$$

5. INTERACTION OF K MESONS WITH NUCLEONS. Λ AND Σ PARTICLES

We now turn to the investigation of the interaction of K mesons with nucleons. Since both the K mesons and the nucleons transform according to the projective representation of the extended Lorentz group, and since the baryonic charge is conserved, an additional baryon must necessarily participate in the interaction. This requirement inevitably leads to the law of associated production of strange particles. We first consider the case of a neutral baryon. We already said earlier that the relative spatial parities of all baryons are, for definiteness, assumed to be identical:

$$I: \quad Y'_0 = \gamma_4 Y_0. \tag{30}$$

For the nucleon transformation T there are two possibilities for the unknown baryon:

$$T: \quad Y'_0 = -\gamma_4\gamma_5 Y_{0c}, \tag{31}$$
$$Y'_0 = \gamma_4\gamma_5 Y_{0c}. \tag{32}$$

We have to introduce the antibaryon Y_{0C} into equations (31) and (32), since the transformation T for the nucleons anticommutes with the transformation[9] related to the conservation of the baryonic charge.

If we choose (31) for T, then the only form of the Lagrangian invariant under the transformations of the extended Lorentz group and the transformations (9) and E is

$$\begin{aligned} L = ig[&\overline{\psi}(1\times\gamma_5 - \tau_1\times 1)(1\times 1 + \tau_3\times 1)\varphi\times Y_0 \\ &- \overline{\psi}_c(1\times\gamma_5 + \tau_1\times 1)(1\times 1 - \tau_3\times 1)\varphi^*\times Y_0] + \text{Herm. conj.} \end{aligned} \tag{33}$$

In going from ψ and φ to the operators of the nucleon and K meson fields, we obtain the usual form for the Lagrangian for the interaction of nucleons with Λ_0 particles:

$$L = ig_\Lambda(\overline{p}\gamma_5\Lambda_0 K^+ + \overline{n}\gamma_5\Lambda_0 K^0) + \text{Herm. conj.} \tag{34}$$

The transformation law (32) for T leads to a Lagrangian that differs from expression (33) only by a plus sign between the two terms of expression (33). It corresponds to the Σ_0 particle:

$$L = ig_{\Sigma_0}(\overline{p}\gamma_5\Sigma_0 K^+ - \overline{n}\gamma_5\Sigma_0 K^0) + \text{Herm. conj.} \tag{35}$$

We thus arrive at the conclusion that the transformation laws for Λ_0 and Σ_0 corresponding to the transformation T for the nucleons, differ by their signs. We now consider the interaction of nucleons with charged baryons. We can find a Lagrangian which is invariant under charge conjugation, space inversion, and time reversal, and which is consistent with the conservation laws for the electric and baryonic charges, only if we require that, under T,

$$T: \quad \Sigma^+ \to -\gamma_4\gamma_5\Sigma_c^-, \quad \Sigma^- \to -\gamma_4\gamma_5\Sigma_c^+. \tag{36}$$

This implies that the masses of the Σ^+ and Σ^- particles are equal. The Lagrangian has the form

$$\begin{aligned} L = -ig[&\overline{\psi}(1\times 1 - \tau_1\times\gamma_5)(1\times 1 - \tau_3\times 1)\varphi^*\times\Sigma^+ \\ &+ \overline{\psi}_c(1\times 1 + \tau_1\times\gamma_5)(1\times 1 + \tau_3\times 1)\varphi\times\Sigma^-] + \text{Herm. conj.} \end{aligned} \tag{37}$$

In conventional notation this can be written in the form

$$L = ig_{\Sigma^\pm}(\overline{p}\gamma_5\Sigma^+ K^0 + \overline{n}\gamma_5\Sigma^- K^+) + \text{Herm. conj.} \tag{38}$$

The charge symmetry is obvious.

If we now require that the interaction Lagrangian also be invariant under the Pauli-Gürsey type transformation (10), we obtain

$$g_{\Sigma^\pm} = \sqrt{2}\, g_{\Sigma_0} = \sqrt{2}\, g_\Sigma; \tag{39}$$

The masses of Σ^+, Σ^-, and Σ^0 must be equal.

We arrive at the usual isobaric-invariant Lagrangian

$$L = ig_\Sigma[(\bar{p}\gamma_5\Sigma_0 K^+ - \bar{n}\gamma_5\Sigma_0 K^0) + \sqrt{2}\,\bar{p}\gamma_5\Sigma^+ K^0 + \sqrt{2}\,\bar{n}\gamma_5\Sigma^- K^+] + \text{Herm. conj.} \quad (40)$$

6. Ξ PARTICLES

Still another possibility remains within the framework of these representations. In the projective representation (5), we can change the sign between the terms 1×1 and $\tau_1 \times \gamma_5$ in the transformation (14) connected with the conservation law for the electric charge:

$$E:\ \psi' = \exp\left[-\frac{i}{2}(1\times 1 - \tau_1 \times \gamma_5)\lambda\right]\psi. \quad (41)$$

At the same time we retain the transformation (9) connected with the conservation law for the baryonic charge. In all formulas we then simply have to replace p by Ξ^0, n by Ξ^-, K^+ by $\bar{K}^0$, and K^0 by K^-. We again have charge symmetry. If we require invariance under the Pauli transformation even in the case of interaction, we obtain the usual isobaric-invariant Lagrangians.

7. CONCLUSION

We carried out the program which we set ourselves in the beginning of this paper. We introduced the new irreducible projective representation of the extended Lorentz group. We showed that the existence of charge multiplets, charge symmetry, and associated production of strange particles are consequences of the standard conservation laws. The isobaric invariance follows from the invariance under the Pauli-Gürsey type transformation for free nucleons. This transformation is applicable, since the number of components of wave functions transforming according to projective representations necessarily had to be increased.

We did not discuss the weak interactions from this point of view. This task is much more difficult and less unambiguous due to the violation of the parity conservation laws.

The authors express their sincere gratitude to Prof. Gel'fand for valuable comments.

[1] I. M. Gel'fand and M. L. Tsetlin, J. Exptl. Theoret. Phys. (U.S.S.R.) **31**, 1107 (1956), Soviet Phys. JETP **4**, 947 (1957).

[2] J. C. Taylor, Nucl. Phys. **3**, 606 (1957). J. A. McLennan, Jr., Phys. Rev. **109**, 986 (1958).

[3] J. Schwinger, Phys. Rev. **91**, 713 (1953).

[4] W. Pauli, Nuovo cimento **6**, 204 (1957).

[5] F. Gürsey, Nuovo cimento **7**, 411 (1958).

Translated by R. Lipperheide
37

CYCLIC MOTION OF CHARGED PARTICLES IN AN ELECTRIC FIELD

A. A. KOLOMENSKII and FONG SOY-CEN

P. N. Lebedev Physics Institute, Academy of Sciences, U.S.S.R.

Submitted to JETP editor July 24, 1958

J. Exptl. Theoret. Phys. (U.S.S.R.) **36**, 271-276 (January, 1959)

Expressions are obtained for the cyclic motion of charged particles in an electric guide field. This field can be produced by a system of appropriate lenses (weak-focusing or strong-focusing). Resonance acceleration is considered; in particular, we consider phase stability (phase focusing). This is analogous to the usual phase focusing in magnetic fields. An investigation is made of the effect of electromagnetic radiation (including quantum fluctuations) on the motion of electrons in the electric field. The case in which part of the particle trajectory is in an electric field and part in a magnetic field is also treated.

THE cyclic motion of charged particles in various magnetic-field configurations has been considered at great length in the literature. This work pertains chiefly to accelerators, microwave generators, isotope separation, and so on. However, up to now no investigations have been made of the cyclic motion of charged particles in electric fields, although this motion is characterized by a number of interesting features. We may note that various systems of electric lenses can be used and, indeed, have been used (cf. reference 1) in analog models of large magnetic accelerators.* Problems associated with the radiation of relativistic electrons moving in magnetic fields have been considered in a number of papers. From the theoretical point of view it is of interest to compare these results with those obtained when radiation effects are taken into account in analyzing the motion of electrons in an electric guide field. It is also of interest to extend the analysis of phase focusing to the case of cyclic motion in electric fields; phase focusing has, so far, been considered only in connection with the motion of particles in magnetic fields.

1. MOTION OF PARTICLES IN AN AXIALLY SYMMETRIC ELECTRIC FIELD, NEGLECTING RADIATION EFFECTS

We consider a circle of radius r_s in an axially symmetric electric field characterized by the plane of symmetry, $z = 0$. In the first approximation the components of this field, which satisfy the conditions for vanishing divergence, can be written in the form

$$\mathscr{E}_r(r) \approx \mathscr{E}_0(r_s)(1 - n_e x/r_s),$$
$$\mathscr{E}_z(z) \approx -\mathscr{E}_0(r_s)(1 - n_e) z/r_s, \quad x = r - r_s. \tag{1.1}$$

The parameter $n_e = -(r_s/\mathscr{E}_0)\partial\mathscr{E}/\partial r$, which is introduced in analogy with the customary magnetic field index, n, can be called the electric field index. In a cylindrical coordinate system, the equations of motion of a charged particle in a field described by (1.1) and an auxiliary accelerating field $\mathscr{E}_0$, are of the form

$$\frac{d}{dt}(m\dot{r}) = mr\dot{\theta}^2 - e\mathscr{E}_0\left(1 - n_e\frac{x}{r_s}\right), \tag{1.2}$$

$$\frac{d}{dt}(mr^2\dot{\theta}) = eV_0, \tag{1.3}$$

$$\frac{d}{dt}(m\dot{z}) = e\mathscr{E}_0(1 - n_e)\frac{z}{r_s}. \tag{1.4}$$

For resonance acceleration

$$V_0 \approx \frac{V_0}{2\pi}\cos\left[\int_0^t \omega_0 dt - q\theta\right], \tag{1.5}$$

where $q = \omega_0/\omega$ is the frequency multiplication factor and ω_0 and V_0 are the frequency and amplitude of the voltage. In an induction accelerator

$$V_0 \approx (1/2\pi c)\,\partial\Phi/\partial t, \tag{1.6}$$

where Φ is the magnetic flux through the orbit.

The following relations hold in the equilibrium orbit

$$\omega = \frac{e\mathscr{E}_0 c}{E_0}\left[\sqrt{\frac{1}{4} + \left(\frac{E_0}{e\mathscr{E}_0 r_s}\right)^2} - \frac{1}{2}\right]^{1/2}, \quad \frac{\omega}{\dot{\omega}} = \frac{1 - \beta_s^2}{\beta_s^2}\frac{E_s}{\dot{E}_s}, \tag{1.7}$$

where E is the total energy of the particle and

*The practical application of electric guide fields in accelerators is hindered by the fact that the force exerted on a particle by an electric field (expressed in v/cm) is 300 β times smaller than the force exerted by a magnetic field (measured in oersteds). Yet electric fields are used widely in the auxiliary ion and electron optical systems for injection and extraction of particles in large accelerators. Electric fields can be in electron models of proton accelerators.

the subscript s denotes equilibrium quantities.

The motion is analyzed in the manner usually employed in an axially symmetric magnetic accelerator. In particular, it is possible to introduce the notion of betatron (fast) oscillations (radial and vertical) and synchrotron (slow) oscillations. There is, however, an important qualitative difference between the two cases; this distinction can be understood if one assumes that both guide fields remain constant in time. In the magnetic case the force that acts on the particle is perpendicular to the velocity and the particle energy is not changed. In the case of motion in an electric field the force which acts on a particle which executes oscillations is not always perpendicular to the direction of motion. Hence, although the time average of the particle energy remains constant, the energy itself varies with time. We can expand all quantities about the equilibrium orbit. Considering first-order terms [we first consider the case of resonance acceleration, Eq. (1.5)] and introducing the relations

$$\frac{\Delta E}{E_s} = \frac{\beta_s^2}{1-\beta_s^2}\left[\frac{x}{r_s} - \frac{\dot{\varphi}}{q\omega}\right], \tag{1.8}$$

(where φ is the particle phase with respect to the accelerating field), we have from Eqs. (1.2) to (1.4), in the linear approximation,

$$\ddot{x} + \frac{\dot{E}_s}{E_s}\dot{x} + \omega^2(1-n_e)x = \frac{\Delta E}{E_s}\frac{c^2}{r_s}(2-\beta_s^2), \tag{1.9}$$

$$\left(\frac{\Delta \dot{E}}{E_s}\right) = \left(\frac{\dot{\omega}}{\omega} - \frac{\dot{E}_s}{E_s}\right)\frac{\Delta E}{E_s}$$
$$-\beta_s^2\left(\frac{\dot{E}_s}{E_s} + \frac{\dot{\omega}}{\omega}\right)\frac{x}{r_s} - \beta_s^2\frac{\dot{x}}{r_s} - \frac{eV_0\omega}{2\pi E_s}\sin\varphi_s\Delta\varphi, \tag{1.10}$$

$$\ddot{z} + \frac{\dot{E}_s}{E_s}\dot{z} + \omega^2(n_e-1)z = 0. \tag{1.11}$$

The change of energy in the electric guide field is given by the term $-\beta_s^2\dot{x}/r_s$ in Eq. (1.10). The radial betatron and synchrotron oscillations are given by the equations

$$\ddot{x} + \frac{\dot{E}_s}{E_s}\dot{x} + \omega^2(3-n_e-\beta_s^2)x = 0, \tag{1.12}$$

$$\frac{d}{dt}\left(\frac{E_s}{q\omega^2 K_1}\dot{\varphi}\right) - \frac{eV_0}{2\pi}\cos\varphi = -\frac{eV_0}{2\pi}\cos\varphi_s, \tag{1.13}$$

where

$$eV_0\cos\varphi_s = \frac{2\pi r_s \dot{\mathcal{E}}_0}{\omega(1+E_0^2/E_s^2)}, \quad K_1 = \frac{1+n_e(1-\beta_s^2)}{(3-n_e-\beta_s^2)\beta_s^2}. \tag{1.14}$$

The betatron oscillations in the vertical and radial directions are characterized by the following frequencies respectively:

$$\omega_z = \omega\sqrt{n_e-1}, \quad \omega_r = \omega\sqrt{3-n_e-\beta_s^2}. \tag{1.15}$$

For stability the following condition must be satisfied:

$$3-\beta_s^2 > n_e > 1. \tag{1.16}$$

The width of the n_e stability region depends on the particle velocity: when $\beta = 0$ this region is a maximum, when $\beta = 1$ it is a minimum. In this respect the conditions in (1.16) differ essentially from the well-known stability requirement on motion in a magnetic field, $0 < n < 1$; the particle velocity does not enter in the magnetic case.

We may note that the relativistic effect in the dependence of $\omega_{r,z}/\omega$ on β can cause a significant change in the focusing properties of electrostatic lenses. For example, in electron optics it is generally assumed that in a cylindrical condenser ($n_e = 1$) the image is at an azimuthal angle of 127° with respect to the source (cf. for example reference 2). However, examination of Eq. (1.15) indicates that this relation is valid only in the nonrelativistic case, i.e. when $\beta = 0$. The angle indicated above changes at relatively small electron energies, becoming 180° when $\beta = 1$.

We now consider the synchrotron oscillations in an electric field; in some respects these also differ from the synchrotron oscillations in an axially symmetric magnetic field. In the expression for the frequency of synchroton oscillations,

$$\Omega^2 = q\omega^2 eV_0\sin\varphi_s K_1/2\pi E_s \tag{1.17}$$

the quantity K_1 for the magnetic accelerator corresponds to the parameter K defined by the relations

$$\Delta\omega/\omega = -K\Delta E/E_s,$$
$$\Delta r/r_s = \alpha\Delta p/p_s, \quad K = 1-(1-\alpha)/\beta_s^2, \tag{1.18}$$

where p is the particle momentum.

In the present case we have in place of the relation $K_1 = K$

$$K_1 = K/(1+\alpha), \quad \alpha = (2-\beta_s^2)/(1-n_e). \tag{1.19}$$

We may note that in contrast with the magnetic case, where $\alpha = 1/(1-n_m)$, the quantity α depends on the particle velocity. It is apparent at "critical" energies (i.e., energies such that $E = E_{cr} = \sqrt{-n_e E_0}$) $K = 0$ and phase focusing no longer obtains [cf. Eq. (1.19)]. When $n_e > 0$ (i.e., when the electric field falls off radially) there is no critical energy.

2. MOTION OF PARTICLES IN AN AXIALLY SYMMETRIC FIELD WITH RADIATION EFFECTS TAKEN INTO ACCOUNT

In analyzing the motion of a relativistic electron in an electric field it is necessary to take account

of radiation effects. We start with the procedure used in reference 3, analyzing the radiation effects within the framework of classical electrodynamics and assuming that in the equilibrium orbit the radiation losses are compensated by the electric accelerating field. In the right side of Eqs. (12) to (14) we add terms to take account of the radiation (the small parameter is $1/\gamma$ where $\gamma = 1/\sqrt{1-\beta_s^2}$. After some simple transformations we obtain the radial equation

$$\ddot{x} + [2\dot{E}_s/E_s + 3W_s/E_s - 2\dot{\Omega}/\Omega]\dot{x} + \omega^2(2-n_e)\dot{x} + \omega^2[(2-n_e)(\dot{E}_s/E_s - 2\dot{\Omega}/\Omega) + (3-4n_e)W_s/E_s]\dot{x} + \omega^3\Omega^2(2-n_e)x = 0, \quad (2.1)$$

and the equation charcterizing the vertical oscillations

$$\ddot{z} + (\dot{E}_s/E_s + W_s/E_s)\dot{z} + \omega^2(n_e - 1)z = 0, \quad (2.2)$$

where W_s is the radiated power

$$W_s = (2e^4c/3E_0^4)\dot{E}_s^2\mathcal{E}_0^2, \quad (2.3)$$

and Ω is given by Eq. (1.18).

In the first approximation we find that the radiation leads to damping of the oscillations (assuming compensation of the radiation losses); this damping is described by the expressions

$$a_{fr}(t) \sim E_s^{-1/4}\exp\left[-\frac{1}{2}\frac{3+n_e}{2-n_e}\int_0^t\frac{W_s}{E_s}d\xi\right], \quad (2.4)$$

$$a_{sr}(t) \sim E_s^{-1/4}\Omega^{1/4}\exp\left[-\frac{1}{2}\frac{3-4n_e}{2-n_e}\int_0^t\frac{W_s}{E_s}d\xi\right], \quad (2.5)$$

$$a_z(t) \sim E_s^{-1/4}\exp\left[-\frac{1}{2}\int_0^t\frac{W_s}{E_s}d\xi\right], \quad (2.6)$$

where a_{fr} and a_{sr} are respectively the amplitudes of the fast (betatron) and slow (synchrotron) oscillations.

These expressions are analogous to those obtained for motion in a magnetic field by Kolomenskii and Lebedev.[3] As in the magnetic case, the damping term, $a_z(t)$, is independent of n; this follows from the assumption of the existence of a plane of symmetry, $z = 0$. In order for the motion along r and z to be stable in the absence of radiation effects, the quantity n_e (for $\beta = 1$) must satisfy the condition

$$2 > n_e > 1. \quad (2.7)$$

On the other hand, it is apparent from Eqs. (2.4) and (2.5) that to have damping of the radial fast and slow oscillations the following condition must be satisfied when radiation is taken into account:

$$n_e < 3/4. \quad (2.8)$$

Obviously (2.7) and (2.8) cannot be satisfied simultaneously. Thus, the motion of an electron in an axially symmetric electric field is found to be unstable (if the radiation losses are compensated). Under certain conditions, however, stable motion can be achieved, for example, by means of an auxiliary axially symmetric magnetic field. If a magnetic field $H_z = H_{z0}(r_s/r)^{n_m}$ acts on the electron in addition to the electric field $\mathcal{E}_r = \mathcal{E}_{r0}(r_s/r)^{n_e}$, relativistic equilibrium is given by the relation:

$$eH_{z0}r_s = kE_s, \quad c\mathcal{E}_{r0}r_s = (1-k)E_s, \quad 0 \leqslant k \leqslant 1, \quad (2.9)$$

where k characterizes the relative effect of the magnetic field on the circular motion of the particle. When $k = 0$, the field is entirely electric; when $k = 1$, the field is entirely magnetic.

We introduce the effective index

$$n_{eff} = n_m k + n_e(1-k), \quad (2.10)$$

where by n_m and n_e we denote respectively the magnetic and electric field indices. It can be shown that if (2.9) is satisfied the equations of motion become

$$\ddot{x} + \left(2\frac{\dot{E}_s}{E_s} - 2\frac{\dot{\Omega}}{\Omega} + 3\frac{W_s}{E_s}\right)\dot{x} + \omega^2(2-k-n_{eff})\dot{x} + \omega^2\left[(2-k-n_{eff})\left(\frac{\dot{E}_s}{E_s} - 2\frac{\dot{\Omega}}{\Omega}\right) + (3-4n_{eff})\frac{W_s}{E_s}\right]\dot{x} + \omega^2\Omega^2(2-k-n_{eff})x = 0 \quad (2.11a)$$

$$\ddot{z} + \left(\frac{\dot{E}_s}{E_s} + \frac{W_s}{E_s}\right)\dot{z} + \omega^2(n_{eff} - 1 + k)z = 0, \quad (2.12)$$

where

$$\Omega^2 = q\omega^2 eV_0\sin\varphi_s/2\pi E_s(2-k-n_{eff}).$$

The damping associated with compensated radiation is characterized by

$$\zeta_{fr}(t) \sim \exp\left[-\frac{1}{2}\frac{3-3k+n_{eff}}{2-k-n_{eff}}\int_0^t\frac{W_s}{E_s}d\xi\right], \quad (2.11b)$$

$$\zeta_{sr}(t) \sim \exp\left[-\frac{1}{2}\frac{3-4n_{eff}}{2-k-n_{eff}}\int_0^t\frac{W_s}{E_s}d\xi\right], \quad (2.13)$$

$$\zeta_z(t) \sim \exp\left[-\frac{1}{2}\int_0^t\frac{W_s}{E_s}d\xi\right]. \quad (2.14)$$

Since the frequency of the radial betatron oscillations is given by $\omega\sqrt{2-k-n_{eff}}$, the stability conditions (2.7) and (2.8) become

$$1-k < n_{eff} < 2-k, \quad (2.15)$$

$$n_{eff} < 3/4. \quad (2.16)$$

The inequalities in (2.15) and (2.16) yield

$$1-k<n_{\text{eff}}<{}^{3}/_{4},\ {}^{1}/_{4}\leqslant k\leqslant 1. \qquad (2.17)$$

In the n_m-n_e plane the region of stability lies between two parallel lines, one of which passes through the point (0, 1) and the other through the point ($\frac{3}{4}$, $\frac{3}{4}$). The width of the stability region is

$$d=\frac{3}{4}\cos\varphi\left(1-\frac{1}{3}\tan\varphi\right),$$

where

$$\varphi=\tan^{-1}\frac{1-k}{k}$$

is the slope of the lines with respect to the z axis. The maximum and minimum values of d are: $d_{max}=\frac{3}{4}$ ($k=1$) and $d_{min}=0$ ($k=\frac{1}{4}$).

It is also possible to compute the effect of quantum radiation fluctuations on the motion of an electron in axially symmetric electric and magnetic fields. If the condition $E\ll E_{1/2}=m_0c^2\,[rm_0c/h]^{1/2}$ is satisfied this calculation can be carried out by the classical method used in reference 3. Carrying out these computations, we find the mean-square amplitude of the oscillations:

$$\langle a_{\text{fr}}^2\rangle=\frac{55}{24\sqrt{3}}\frac{b\Lambda\omega E_0}{(2-k-n_{\text{eff}})^2E_s}\times\int_0^t\exp\left[-\frac{n_{\text{eff}}+3-3k}{2-k-n_{\text{eff}}}\int_x^t\frac{W_s}{E_s}d\eta_i\right]\frac{E_s^3}{E_0^6}dx, \qquad (2.18)$$

$$\langle a_{\text{sr}}^2\rangle=\frac{55}{24\sqrt{3}}\frac{b\Lambda\omega E_0^{x/z}V^{-1/2}}{(2-k-n_{\text{eff}})^2E_s^{1/2}}\times\int_0^t\exp\left[-\frac{3-4n_{\text{eff}}}{2-k-n_{\text{eff}}}\int_x^t\frac{W_s}{E_s}d\eta_i\right]\frac{E_s^{6.5}}{E_0^{5.5}}V^{-1/2}dx, \qquad (2.19)$$

$$\langle a_z^2\rangle=\frac{13}{24\sqrt{3}}\frac{b\Lambda\omega E_z}{nE_0}\int_0^t\exp\left[-\int_x^t\frac{W_s}{E_s}d\eta_i\right]\frac{E_s^4}{E_0^4}dx, \qquad (2.20)$$

where Λ is the Compton wave length and $b=e^2/m_0c^2$ is the classical radius of the electron. We may note that the mean-square vertical oscillations are given by an expression which formally is the same as that for motion in a magnetic field (without an electric field). This complete similarity does not exist for the radial oscillations, although the corresponding formulas are similar in many respects.

As in systems with magnetic guide fields, it is possible to use strong-focusing in electric guide fields; in this case n_e is a periodic (generally speaking, of alternating sign) function of azimuth $n_e(\vartheta+\vartheta_0)=n_e(\vartheta)$. Generally there is a difference from the motion in a magnetic field characterized by $n_m=n_m(\vartheta)$; this difference lies in the fact that the parameter $\mu_{x,z}$, which describes the frequency of the betatron oscillations (cf. reference 4), depends on the particle velocity. If, however, $|n_e|\gg 2$, these oscillations will be described in the same way as the betatron oscillations in magnetic strong-focusing systems. In particular, all results obtained for such systems when radiation effects are taken into account (cf. references 3, 5 and 6) can be carried over to the electric strong-focusing system.

[1] Cottingam, Plotkin, and Raca, Trans. P.G.N.S., I.R.E., **1**, 12-17 (1954).

[2] O. Klemperer, Electron Optics, Cambridge, 1953, p. 340.

[3] A. A. Kolomenskii and A. N. Lebedev, J. Exptl. Theoret. Phys. (U.S.S.R.) **30**, 205, 1161 (1956), Soviet Phys. JETP **3**, 130 (1956); Nuovo cimento Supp. **12** Ser. X, 43 (1958).

[4] Courant, Livingston, and Snyder, Phys. Rev. **88**, 1190 (1952).

[5] A. A. Kolomenskii and A. N. Lebedev, Атомная энергия (Atomic Energy), **5**, 554 (1958).

[6] Yu. F. Orlov and E. K. Tarasov, J. Exptl. Theoret. Phys. (U.S.S.R.) **34**, 651 (1958), Soviet Phys. JETP **7**, 449 (1958).

Translated by H. Lashinsky
38

DEPOLARIZATION OF THE NEGATIVE MUON IN MESIC-ATOM TRANSITIONS

V. A. DZHRBASHYAN

Physics Institute, Academy of Sciences, Armenian S.S.R.

Submitted to JETP editor July 20, 1958

J. Exptl. Theoret. Phys. (U.S.S.R.) **36**, 277-282 (January, 1958)

A method is developed for calculating the depolarization of μ^--mesons in mesic-atom cascade transitions. An estimate of the expected μ^--meson depolarization is given, which is in good agreement with available experimental data.

As noted by Gol'dman,[1] a μ^--meson is not substantially depolarized in Coulomb collisions. The spin-orbit interaction in mesic atom transitions[2] is mainly responsible for the depolarization.* This results from the fact that for a mesic atom level with fine-structure splitting ν and level width 2γ, the ratio always satisfies the inequality

$$(\nu/2\gamma)^2 \gg 1, \qquad (1)$$

i.e., the period of precession is much less than the lifetime of the level.

Because of its large mass, in comparison with that of the electron, a slow μ^- meson is captured into a highly-excited quantum state of the atom. The principal quantum number n of such a state can be determined[3] from the approximate equality of Bohr radii of the meson and electron, giving $n \sim \sqrt{\mu} \sim 15$.

As noted by Bohr,[4] for a given quantum number n, the meson will be captured in a circular orbit ($l = n-1$) with greatest probability, because of the large statistical weight of this orbit. The comparison with experimental data carried out by Stearns[5] and the subsequent remarks of Day and Morrison[6] indicate that both π^- and μ^- mesons are mainly captured in orbits with high l.

Following this, as a result of subsequent Auger transitions and radiative transitions, the μ^- meson loses energy and drops to the 1s level, from which it either is captured by the atom or decays, depending on Z.

Burbidge and De Borde[3,7] calculated the probability of mesic-atom transitions. According to their calculations, the picture is the following. For large n, dipole Auger transitions with $\Delta n = \Delta l = -1$ take place. Following this, for smaller n (if Z is not very small), the electric-dipole radiative transitions are essential, in which the circular orbits become even more probable because of the maximum probability of a radiative transition to a level with smallest possible n. Thus, in both Auger and radiative transitions, electric-dipole transitions are essential, in which the orbital quantum number decreases by unity ($\Delta l = -1$).

Starting from the above, we consider the depolarization of a μ^- meson in electric dipole transitions. Let the μ^- meson go from a level l_N to a level l_1 by successive dipole emission of either γ-rays or Auger electrons; that is, a cascade down $l_N(1)\, l_{N-1}(1)\, l_{N-2}(1) \ldots l_1(1)$ takes place. To obtain the corresponding density matrix, it is necessary to solve the equations by means of the perturbation theory given by Wigner and Weisskopf,[8] which takes into account the finite width of the level. However, as Abragam and Pound[9] have shown for the case of a single level, one can obtain the final result from the following simple considerations.

The interaction can be included in the expression for the transition probability by means of the operator $u = \exp(-iKt/\hbar)$ which operates on the wave functions of the meson in the given level (K here is the spin-orbit interaction energy operator). It is then necessary to consider the possibility of radiation in the interval t, t+dt, with probability $\exp(-2\gamma t)\, 2\gamma dt$. Integrating such a "supplemented" transition probability over t from 0 to ∞, we obtain the factor $[1 + (\nu_{jj'}/2\gamma)^2]^{-1}$ for each level, leading to the following density matrix

*I. M. Shmushekvich called my attention to this.

$$\rho = \sum a_{\sigma_N} \frac{(j_{N+1} l_{N+1} \mu_{N+1} \sigma_N \mid H_{N+1} \mid j_N l_N \mu_N \sigma_N)\,(j_{N+1} l_{N+1} \mu_{N+1} \sigma_N \mid H_{N+1} \mid j'_N l_N \mu'_N \sigma_N)^*}{1 + (\nu_{l_N l'_N}/2\gamma_N)^2}$$

$$\times \frac{(j_N l_N \mu_N \sigma_{N-1} \mid H_N \mid j_{N-1} l_{N-1} \mu_{N-1} \sigma_{N-1})(j'_N l_N \mu'_N \sigma'_{N-1} \mid H_N \mid j'_{N-1} l_{N-1} \mu'_{N-1} \sigma'_{N-1})^*}{1 + (\nu_{l_{N-1} l'_{N-1}}/2\gamma_{N-1})^2} \cdot \tag{2}$$

$$\ldots \times \frac{(j_3 l_3 \mu_3 \sigma_3 \mid H_3 \mid j_1 l_1 \mu_1 \sigma_1)\,(j'_2 l_2 \mu'_2 \sigma'_1 \mid H_2 \mid j'_1 l_1 \mu'_1 \sigma'_1)^*}{1 + (\nu_{l_1 l'_1}/2\gamma_1)^2}$$

$$\times (j_1 l_1 \mu_1 \sigma \mid H_1 \mid j l \mu \sigma)\,(j'_1 l_1 \mu'_1 \sigma \mid H_1 \mid j l \mu \sigma)^* .$$

The summation here is over all unobserved properties of the radiation and mesic atom, and also over the two values of total angular momentum j_i, j'_i, over the projections of the total angular momentum μ_i, μ'_i and spin projections σ_i, σ'_i of the μ^- meson for each of the i levels ($i = 1, \ldots, N$); a_σ is the probability of the value σ_N for the spin projection on the symmetry axis before the cascade. The levels l_{N+1} and l are introduced formally in order to describe the formation and annihilation of the mesic atom (the decay of the μ^- meson or its capture by the atom).

Because of the inequality (1), all interference terms drop out of the Eq. (2) for the density matrix, and for each transition $l_{i+1}(1)\, l_i$, one can write[9]

$$(j_{i+1} l_{i+1} \mu_{i+1} \sigma_i \mid H_{i+1} \mid j_i l_i \mu_i \sigma_i)\,(j_{i+1} l_{i+1} \mu'_{i+1} \sigma'_i \mid H_{i+1} \mid j_i l_i \mu'_i \sigma'_i)^*$$

$$= (l_{i+1} \mid x \mid l_i)^2 \sum_{m_{i+1}, m_i, m'_{i+1}, m'_i} (-1)^{2\mu_{i+1} + 2\mu_i + m_{i+1} + m'_{i+1}}$$

$$\times (2l_{i+1}+1)\,(2j_{i+1}+1)\,(2j_i+1) \tag{3}$$

$$\times \begin{pmatrix} l_{i+1} & 1/2 & j_{i+1} \\ m_{i+1} & \sigma_i & -\mu_{i+1} \end{pmatrix} \begin{pmatrix} l_i & 1 & l_{i+1} \\ m_i & M_{i+1} & -m_{i+1} \end{pmatrix}$$

$$\times \begin{pmatrix} l_i & 1/2 & j_i \\ m_i & \sigma_i & -\mu_i \end{pmatrix} \begin{pmatrix} l_{i+1} & 1/2 & j_{i+1} \\ m'_{i+1} & \sigma'_i & -\mu_{i+1} \end{pmatrix}$$

$$\times \begin{pmatrix} l_i & 1 & l_{i+1} \\ m'_i & M_{i+1} & -m_{i+1} \end{pmatrix} \begin{pmatrix} l_i & 1/2 & j_i \\ m'_i & \sigma'_i & -\mu_i \end{pmatrix} \delta_{\mu_{i+1}, \mu'_{i+1}}\, \delta_{\mu_i, \mu'_i}.$$

The round brackets denote Wigner 3j symbols. The $(l_{i+1} \mid x \mid l_i)$ denote factors which depend on the properties of the radiation and of the levels $l_{i+1} l_i$, but not on the magnetic quantum numbers. In the transition $l_{N+1} \to l_N$, carrying out summation in Eq. (3) over μ_{N+1}, M_{N+1} and j_{N+1}, we obtain an expression proportional to $(2j_N + 1) \times \begin{pmatrix} l_N & \frac{1}{2} & j_N \\ m_N & \sigma_N & -\mu_N \end{pmatrix}$; analogously, the transition $l_1 \to l$ gives the factor $(2j_1 + 1) \begin{pmatrix} l_1 & \frac{1}{2} & j_1 \\ m_1 & \sigma & -\mu_1 \end{pmatrix}^2$.

In the remaining cases, using the Racah relationship

$$\sum_{m_i, m_{i+1}, \sigma_i} (-1)^{m_{i+1}} \begin{pmatrix} l_i & 1/2 & j_i \\ m_i & \sigma_i & -\mu_i \end{pmatrix} \times \begin{pmatrix} l_{i+1} & 1/2 & j_{i+1} \\ m_{i+1} & \sigma_i & -\mu_{i+1} \end{pmatrix} \begin{pmatrix} l_i & 1 & l_{i+1} \\ m_i & M_{i+1} & -m_{i+1} \end{pmatrix} \tag{4}$$

$$= (-1)^{j_i + l_{i+1} - \mu_i} \begin{Bmatrix} j_i & 1/2 & l_i \\ l_{i+1} & 1 & j_{i+1} \end{Bmatrix} \begin{pmatrix} j_i & 1 & j_{i+1} \\ \mu_i & M_{i+1} & -\mu_{i+1} \end{pmatrix},$$

where the curly brackets denote the Wigner 6j symbol, we obtain

$$\sum_{\sigma_i, \sigma'_i} (j_{i+1} l_{i+1} \mu_{i+1} \sigma_i \mid H_{i+1} \mid j_i l_i \mu_i \sigma_i)\,(j_{i+1} l_{i+1} \mu_{i+1} \sigma'_i \mid H_{i+1} \mid j_i l_i \mu_i \sigma'_i)$$

$$= (l_{i+1} \mid x \mid l_i)^2 (2l_{i+1}+1)\,(2j_{i+1}+1)\,(2j_i+1) \tag{5}$$

$$\times \begin{Bmatrix} j_i & 1/2 & l_i \\ l_{i+1} & 1 & j_{i+1} \end{Bmatrix}^2 \begin{pmatrix} j_i & 1 & j_{i+1} \\ \mu_i & M_{i+1} & -\mu_{i+1} \end{pmatrix}^2.$$

The mean value of the projection of the μ^- spin after the cascade of mesic-atom transitions, is determined by

$$\langle \sigma \rangle = \sum_\sigma \rho\sigma \Big/ \sum_\sigma \rho \tag{6}$$

We note that in Eq. (6) the factors corresponding to formation and annihilation of the mesic atom cancel, making it possible for us to formally introduce the levels l_{N+1}, l (see above).

Expressing σ in terms of the Wigner 3j symbol

$$\sigma = (-1)^{-1/2+\sigma} \sqrt{\frac{3}{2}} \begin{pmatrix} 1/2 & 1 & 1/2 \\ \sigma & 0 & -\sigma \end{pmatrix} \tag{7}$$

and then applying the Racah relationship, we have

$$\sum_{m_1, \sigma} (2j_1 + 1) \begin{pmatrix} l_1 & 1/2 & j_1 \\ m_1 & \sigma & -\mu_1 \end{pmatrix}^2 (-1)^{-1/2+\sigma} \sqrt{\frac{3}{2}} \begin{pmatrix} 1/2 & 1 & 1/2 \\ \sigma & 0 & -\sigma \end{pmatrix} \tag{8}$$

$$= (-1)^{-1/2 + l_1 + 1 - \mu_1} \sqrt{\frac{3}{2}} (2j_1 + 1) \begin{Bmatrix} j_1 & l_1 & 1/2 \\ 1/2 & 1 & j_1 \end{Bmatrix} \begin{pmatrix} j_1 & 1 & j_1 \\ \mu_1 & 0 & -\mu_1 \end{pmatrix}.$$

Employing Eq. (8) for each of the i levels ($i = 1, \ldots, N-1$), we obtain

l_N	$(P/P_0)_{l_N, l_{N-1}, \ldots, 0}$	l_N	$(P/P_0)_{l_N, l_{N-1}, \ldots, \ldots, 0}$
0	1	9	0.192
1	0.407	10	0.188
2	0.301	11	0.185
3	0.257	12	0.183
4	0.234	13	0.181
5	0.219	14	0.179
6	0.209	...	...
7	0.202	∞	0.156
8	0.197		

$$(2l_{i+1}+1)(2j_{i+1}+1)(2j_i+1)\begin{Bmatrix} j_i & 1/2 & l_i \\ l_{i+1} & 1 & j_{i+1}\end{Bmatrix}^2 \sum_{\mu_i, M_{i+1}} (-1)^{\mu_i}$$

$$\times \begin{pmatrix} j_i & 1 & j_{i+1} \\ \mu_i & M_{i+1} & -\mu_{i+1}\end{pmatrix}^2 \begin{pmatrix} j_i & 1 & j_i \\ \mu_i & 0 & -\mu_i\end{pmatrix} \tag{9}$$

$$= (-1)^{j+1-\mu_{i+1}}(2l_{i+1}+1)(2j_{i+1}+1)(2j_i+1)\begin{Bmatrix} j_i & 1/2 & l_i \\ l_{i+1} & 1 & j_{i+1}\end{Bmatrix}^2$$

$$\times \begin{Bmatrix} j_{i+1} & 1 & j_i \\ j_i & 1 & j_{i+1}\end{Bmatrix} \begin{pmatrix} j_{i+1} & 1 & j_{i+1} \\ \mu_{i+1} & 0 & -\mu_{i+1}\end{pmatrix}.$$

Finally

$$(2j_N+1)\sum_{m_N, \mu_N}(-1)^{\mu_N}\begin{pmatrix} j_N & 1/2 & j_N \\ m_N & \sigma_N & -\mu_N\end{pmatrix}^2 \begin{pmatrix} j_N & 1 & j_N \\ \mu_N & 0 & -\mu_N\end{pmatrix} \tag{10}$$

$$= (-1)^{j_N+1-\sigma_N}(2j_N+1)\begin{Bmatrix} 1/2 & l_N & j_N \\ j_N & 1 & 1/2\end{Bmatrix}\begin{pmatrix} 1/2 & 1 & 1/2 \\ \sigma_N & 0 & -\sigma_N\end{pmatrix}.$$

From the unitarity of the matrices of the Wigner 3j symbols, it is easy to show

$$\sum_{\sigma} \rho = \prod_i (l_{i+1} | x | l_i)^2 (2l_N + 1). \tag{11}$$

Thus, substituting Eqs. (2), (5), and (8) to (11) into Eq. (6) and using Eq. (7) for σ_N, we obtain

$$\frac{\langle\sigma\rangle}{\langle\sigma_N\rangle} \equiv \left(\frac{P}{P_0}\right)_{l_N, l_{N-1}, \ldots, l_1} = \sum_{l_N, l_{N-1}, \ldots, l_1} (-1)^{l_1+l_N+N-1}(2j_1+1)$$

$$\times \begin{Bmatrix} j_1 & l_1 & 1/2 \\ 1/2 & 1 & j_1\end{Bmatrix}(2l_2+1)(2j_2+1)(2j_1+1)\begin{Bmatrix} j_1 & 1/2 & l_1 \\ l_2 & 1 & j_2\end{Bmatrix}^2 \begin{Bmatrix} j_2 & 1 & j_1 \\ j_1 & 1 & j_2\end{Bmatrix}$$

$$\times (2l_3+1)(2j_3+1)(2j_2+1) \tag{12}$$

$$\times \begin{Bmatrix} j_2 & 1/2 & l_2 \\ l_3 & 1 & j_3\end{Bmatrix}^2 \begin{Bmatrix} j_3 & 1 & j_2 \\ j_2 & 1 & j_3\end{Bmatrix} \ldots (2j_N+1)(2j_{N-1}+1)$$

$$\times \begin{Bmatrix} j_{N-1} & 1/2 & l_{N-1} \\ l_N & 1 & j_N\end{Bmatrix}^2 \begin{Bmatrix} j_N & 1 & j_{N-1} \\ j_{N-1} & 1 & j_N\end{Bmatrix}(2j_N+1)\begin{Bmatrix} 1/2 & l_N & j_N \\ j_N & 1 & 1/2\end{Bmatrix}.$$

We denote by P_0 and P the degree of polarization of the μ^- meson immediately before and after the cascade considered. Equation (12) gives the final polarization from which it is possible to find the depolarization, equal to $(1 - P/P_0) \times 100\%$. In the future, we will, for simplicity, call P/P_0 the depolarization instead of $(1 - P/P_0)$. We calculate P/P_0 for the cascade down $l_1 = l_1 + i - 1$ $(i = 1, \ldots, N)$.

Rewriting the sum in Eq. (12) in the form

$$\left(\frac{P}{P_0}\right)_{l_N, l_{N-1}, \ldots, l_1} = \sum_{\pm}\left(\frac{P}{P_0}\right)_{l_N \pm \frac{1}{2}, l_{N-1}, \ldots, l_1}, \tag{13}$$

where the $\pm$ under l_i correspond to terms with $j_i = l_i \pm \frac{1}{2}$, it is easy to see that the only terms remaining in Eq. (13) are those in which all pluses stand to the right of the minuses. (Dipole transitions are possible only in this case.)

On the other hand, substituting in values for the Wigner 6j-symbols, we see that addition of pluses to the right of minuses to the left does not change the form of the corresponding term, so that there are terms of three types, which are easy to find:

$$\left(\frac{P}{P_0}\right)_{+, +, +, \ldots, +} = \frac{(2l_N+3)(l_N+1)}{3(2l_N+1)^2};$$

$$\left(\frac{P}{P_0}\right)_{-, -, +, \ldots, +} = -\frac{4l_i^2-5}{3(4l_i^2-1)^2}; \tag{14}$$

$$\left(\frac{P}{P_0}\right)_{\ldots, -, +, \ldots, -} = \frac{(2l_1-1)l_1}{3(2l_1+1)^2}.$$

Thus

$$\left(\frac{P}{P_0}\right)_{l_N, l_{N-1}, \ldots, l_1} \tag{15}$$

$$= \frac{1}{3}\left[\frac{(2l_N+3)(l_N+1)}{(2l_N+1)^2} - \sum_{l=l_1+1}^{l_N}\frac{4l^2-5}{(4l^2-1)^2} + \frac{(2l_1-1)l_1}{(2l_1+1)^2}\right].$$

Setting $l_1 = 0$, we obtain the depolarization for various l_N from Eq. (15) (see table). As one would expect, the main contribution comes from low l. For example $(P/P_0)_{14,13,\ldots,2} = 0.237$.

Analogously, we can introduce the depolarization for other cascades:

$$\left(\frac{P}{P_0}\right)_{l_{N-1}-1,\, l_{N-1},\, l_{N-1}-1,\, l_{N-1}-2, \ldots, l_1} = \frac{1}{3}\left\{\frac{(2l_{N-1}+3)(l_{N-1}+1)}{(2l_{N-1}+1)^2}\right.$$

$$+ \frac{(2l_{N-1}+1)^2(2l_{N-1}-3)(l_{N-1}-1)-4l_{N-1}^2+5}{(2l_{N-1}-1)^2 l_{N-1}} \tag{16}$$

$$\left.\times\left[-\sum_{l=l_1+1}^{l_{N-1}}\frac{4l^2-5}{(4l^2-1)^2} + \frac{(2l_1-1)l_1}{(2l_1+1)^2}\right]\right\}.$$

From Eq. (16) it can be seen that the transition with $\Delta l = +1$ leaves the depolarization practically unchanged.

Thus for $l_{N-1} \gtrsim 5$, with an accuracy to the third decimal place,

$$(P/P_0)_{l_{N-1}-1,\, l_{N-1},\, l_{N-1}-1,\, l_{N-1}-2, \ldots, 0} = (P/P_0)_{l_{N-1},\, l_{N-1}-1, \ldots, 0},$$

If the transition with $\Delta l = +1$ takes place at the end of the cascade ($l_3 = l_1$, $l_2 = l_1 + 1$), then

$$\left(\frac{P}{P_0}\right)_{l_N, l_{N-1}, \ldots, l_1, l_1+1, l_1} = \frac{1}{3}\left\{\frac{1}{(2l_2+1)\,l_2}\left[\frac{(2l_2-1)^2(2l_2+3)(l_2+1)}{(2l_2+1)^2} + \frac{(4l_2^2-5)^2}{(4l_2^2-1)^2(2l_2-1)\,l_2} - \frac{(4l_2^2-5)(2l_2-3)(l_2-1)}{(2l_2-1)^2 l_2}\right] \times \left[\frac{(2l_N+3)(l_N+1)}{(2l_N+1)^2} - \sum_{l=l_1+1}^{l_N}\frac{4l^2-5}{(4l^2-1)^2}\right] + \frac{(2l_2+1)^2(2l_2-3)(l_2-1)}{(2l_2-1)^2 l_2}\left[\frac{(2l_1-1)\,l_1}{(2l_1+1)^2} - \frac{4l_2^2-5}{(4l_2^2-1)^2}\right]\right\}. \quad (17)$$

In particular

$$(P/P_0)_{l_N, l_{N-1}, \ldots, 1, 0, 1, 0} = 0.407\,(P/P_0)_{l_N, l_{N-1}, \ldots, 0}; \quad (18)$$

$$(P/P_0)_{l_N, l_{N-1}, \ldots, 1, 2, 1, 0} = 0.745\,(P/P_0)_{l_N, l_{N-1}, \ldots, 0} - 0.0178.$$

Substituting $l_N = 12$, we obtain

$$(P/P_0)_{12, 11, 10, \ldots, 0, 1, 0} = 0.074,$$

$$(P/P_0)_{12, 11, 10, \ldots, 1, 2, 1, 0} = 0.118,$$

respectively.

Calculation shows that if a quadrupole transition takes place for large l, the result does not differ from that given by Eq. (15).

Thus, the depolarization depends only weakly on the orbital moment of the initial level of the cascade and on the type of transition taking place for large l. This is understandable, in so far as in this case the deflection of $\mathbf{l}$ (and correspondingly of $\mathbf{s}$) which, roughly speaking, is proportional to the moment of force trying to turn $\mathbf{l}$ to l, is less for large l.

From the above, we can estimate the expected depolarization:

$$P/P_0 = \sum_i a_i (P/P_0)_i, \quad \sum_i a_i = 1, \quad (19)$$

where $(P/P_0)_i$ is the depolarization in the i-th cascade and a_i is the probability of this cascade. In Eq. (19) the sum is taken over all possible cascades. As already noted, the value of (19) is determined by the contribution of cascades beginning with large values of l_N.

In capture into a level $n = 15$, $l_N = 14$, a cascade with $\Delta n = \Delta l = -1$ proceeds, and the corresponding depolarization is, according to Eq. (15), equal to 0.179.

For $n = 15$, $l_N = 13$, Auger transitions with $\Delta n = \Delta l = -1$ will take place down to $n \sim 6$; following this, in the first radiative transitions, a transition into a circular orbit with $\Delta n = -2$, $\Delta l = -1$, will be most probable.[3]

Thus, in this case the depolarization will also be described by Eq. (15) in practice, and will be equal to 0.181. Ten times less probable is the cascade with $\Delta n = \Delta l = -1$ down to the 2s state, then[10] an Auger transition to the 2p state, followed by a radiative transition to the 1s state. In this cascade $(P/P_0)_i = 0.074$, i.e., in capture from the level $n = 15$, $l = 13$, $\langle P/P_0 \rangle = 18\%$.

For $n = 15$, $l_N = 12$, and also for smaller values of l, the cascade with $\Delta l = -1$ is again most important because of the probable transition to a circular orbit in the first radiative transitions.

As follows from Eq. (16), the possible transitions with $\Delta l = +1$ do not change matters at all, except for very small l. For small l, according to the Table, the value $(P/P_0)_{l_N, l_{N-1}, \ldots, 0}$ increases somewhat. However, the probability of transitions with $\Delta l = +1$ grows for small l, so that this increase will be compensated for. Thus, the expected value of the expression (18) should be $P/P_0 \sim 18\%$. This value agrees well with available experimental data[11] for carbon.

As seen from Eqs. (15) to (17), the sign of the polarization does not change in mesic atom transitions; these can thus be used to determine the decay scheme of the π^- meson.[2]

The influence of the electron shells in mesic atom transitions can be neglected, since within the lifetime of the levels of the mesic atom, the μ^- meson is not depolarized in this field. This is not true of the final 1s level, the lifetime of which is determined by the decay or capture of the μ^- meson. Taking into account this additional depolarization in the field of the electron shell of total angular momentum j_e, gives a factor $F = (4j_e^2 + 4j_e + 3)/3(2j_e + 1)^2$ in the right-hand sides of Eqs. (15) to (17). For example, in the case of carbon, the electron shells will be the configuration $1s^2 2s^2 2p$ with $j_e = \frac{1}{2}$, $F = \frac{1}{2}$, which gives $P/P_0 \sim 9\%$. However, in condensed material the influence of the neighboring atoms and electrons probably leads to a compensation of the magnetic field of the electron shells, i.e., to $j_e = 0$ and, consequently, to $F = 1$.

Equation (12) is applicable to a nucleus with zero spin. Taking into account the hyperfine structure leads to larger depolarization of the μ^- meson.

The author would like to express his deep gratitude to K. A. Ter-Martirosian for his continued interest in the work, and to A. I. Alikhanyan, M. L. Ter-Mikaelian and I. I. Gol'dman for discussion of the results.

[1] I. I. Gol'dman, J. Exptl. Theoret. Phys. (U.S.S.R.) **34**, 1017 (1958), Soviet Phys. JETP **7**, 702 (1958).

[2] V. A. Dzhrbashyan, J. Exptl. Theoret. Phys.

(U.S.S.R.) **35**, 307 (1958), Soviet Phys. JETP **8**, 212 (1959).

[3] A. de Borde, Proc. Phys. Soc. **A67**, 57 (1954).

[4] N. Bohr, quoted by B. Bruno, Arkiv. Mat. Astron. Fys. **A36**, Paper No. 8, 1948.

[5] M. B. Stearns and M. Stearns, Phys. Rev. **105**, 1573 (1957).

[6] T. Day and P. Morrison, Phys. Rev. **107**, 912 (1957).

[7] G. Burbridge and A. de Borde, Phys. Rev. **89**, 189 (1953).

[8] A. Abragam and R. V. Pound, Phys. Rev. **92**, 943 (1953).

[9] M. Rose, Multipole Fields (Russ. Transl.) IIL, Moscow 1957.

[10] B. L. Ioffe and I. Ya. Pomeranchuk, J. Exptl. Theoret. Phys. **23**, 123 (1952).

[11] Garwin, Lederman, and Weinrich, Phys. Rev. **105**, 1415 (1957).

Translated by G. E. Brown
39

ESTIMATE OF THE CONTRIBUTION OF NUCLEON-ANTINUCLEON INTERACTION IN THE DISPERSION RELATION FOR NUCLEON-NUCLEON SCATTERING

L. I. LAPIDUS

Joint Institute for Nuclear Research

Submitted to JETP editor July 31, 1958

J. Exptl. Theoret. Phys. (U.S.S.R.) **36**, 283-289 (January, 1959)

The relation between the scattering lengths and effective radii in the s and p states, as predicted by the dispersion relations for N-N scattering, are discussed. Estimates are derived for the contribution of the N-N interaction to the dispersion relation for N-N scattering from the experimental data on n-p and p-p scattering at low energies. The N-N interaction contribution has been found to be small. Its magnitude depends pronouncedly on the sign of the scattering path in the s states.

1. INTRODUCTION

An analysis of dispersion relations for N-N scattering and their use for the processing of experimental data is made quite difficult by the presence of contribution of the antinucleon-nucleon interaction. This pertains both to the energy dependence of the total cross sections of the N-N interaction and, in particular, to the observable region that remains even in the case of forward scattering.

There is reason for believing that the influence of the nucleon-antinucleon interaction is slight in the region of low energies. Using this assumption, an attempt can be made[1,2] to obtain dispersion relations for N-N scattering containing no unobservable region.

A clarification of the role of the nucleon-antinucleon interaction in nucleon-nucleon scattering is of interest both from the point of view of obtaining approximate relations and from the general point of view.

In this paper we attempt an estimate of the contribution of the N-N interaction to the scattering of nucleons by nucleons at low energies. For this purpose we use the approach used previously[3] in the analysis of the dispersion relations for π-N scattering, based on the "theory of the effective radius."[4]

For π-N scattering we obtain[3] relations between the scattering paths and the effective radii in different states, and these admitted of direct verification, since the final relations contained quantities that could be determined directly by experiment. It has been shown that the result of the analysis depends strongly on the small scattering phases in the p state.

The analogous relations for N-N scattering contain unknown quantities that characterize the nucleon-antinucleon interactions. The use of data on N-N scattering at low energies (and of the energy dependences of the total cross sections) makes it possible to estimate the contribution of the nucleon-antinucleon interaction to the dispersion relation for the N-N scattering.

Let us consider the dispersion relation for forward N-N scattering. We write the N-N scattering amplitude in the form

$$M = \frac{m}{\omega_b}\{\alpha + \beta(\sigma_1\cdot\mathbf{n})(\sigma_2\cdot\mathbf{n}) + i\gamma(\sigma_1+\sigma_2)\cdot\mathbf{n} + \delta(\sigma_1\cdot\mathbf{m})(\sigma_2\cdot\mathbf{m}) + \varepsilon(\sigma_1\cdot\mathbf{l})(\sigma_2\cdot\mathbf{l})\}, \quad (1)$$

where $\mathbf{l}$, $\mathbf{m}$, and $\mathbf{n}$ are unit vectors in the directions $\mathbf{k}_b \pm \mathbf{k}'_b$ and $\mathbf{k}_b \times \mathbf{k}'_b$, while $\omega_b = \sqrt{m^2 + k_b^2}$ is the energy of one particle in the c.m. system. We confine ourselves to the dispersion relations for the quantity

$$a(\omega) = (\omega_b/4m)\,\mathrm{Sp}\,M(0^\circ).$$

The dispersion relations for N-N scattering were considered by various authors.[5-8] They were treated most fully and in greatest detail by Goldberger, Nambu, and Oehme.[8] Many interesting ideas are due to Ioffe.[6]

2. SCATTERING OF NEUTRONS BY PROTONS

The forward dispersion relation for the a_{np} is represented in the form

$$\mathrm{Re}\left[\alpha_{np}(\omega)-\frac{1}{2}(1+\omega/m)\alpha_{np}(m)-\frac{1}{2}(1-\omega/m)\alpha_{n\bar{p}}(m)\right]$$

$$=(\omega^2-m^2)\left\{\frac{f^2}{4\pi}\frac{1}{2(\omega_\mu+\omega)(\omega_\mu^2-m^2)}\right.$$

$$+\Gamma_a(0)\left(\frac{\omega_d+m}{2m}\right)^{1/2}\frac{1}{(\omega_d-\omega)(\omega_d^2-m^2)}$$

$$+\frac{1}{8\pi^2}\mathrm{P}\int_m^\infty d\omega'\left[\frac{\sigma_{np}(\omega')}{\omega'-\omega}+\frac{\sigma_{n\bar{p}}(\omega')}{\omega'+\omega}\right]$$

$$\left.+\frac{1}{\pi}\int_{\omega(2\mu)}^{\infty}d\omega'\frac{\mathrm{Im}\,\alpha_{np}(\omega')}{(\omega+\omega')(\omega'^2-m^2)}\right\}, \qquad (2)$$

where ω is the total energy of the nucleon in the laboratory system, m and μ are the masses of the nucleon and of the pion, $B=\kappa^2/m$ is the binding energy of the deuteron, and

$$\omega_d=m-2B+B^2/2m,$$

$$\omega_\mu=\mu^2/2m-m,\ \Gamma_a(0)=3(\varkappa/m)/(1-\varkappa r_{0t}).$$

The effective radius r_{0t} is given by Eq. (4.40) of reference 8, the notation of which is used in this article.

The contribution of the nucleon-antinucleon interaction to (2) will be taken to mean the term proportional to the integral from $\omega(2\mu)$ to m (unobservable region) as well as the terms containing $\alpha_{n\bar{p}}(m)$ and $\sigma_{n\bar{p}}(\omega')$.

Since we are interested in the values of $\mathrm{Re}\,\alpha_{np}(\omega)$ for small $\eta_b^2=(k_b/m)^2$, we write the dependence of the scattering phases on the energy in the following form[4]

$$\eta_b^{2L+1}\cot({}^{2S+1}L_J)=\frac{1}{a_L}+\frac{1}{2}r_0^{(L)}\eta_b^2+Q_L\eta_b^4\equiv A({}^{2S+1}L_J), \qquad (3)$$

where $a_L\equiv a({}^{2S+1}L_J)$ is the scattering length (for $\eta\to 0$) in a state with momentum J, parity $(-1)^L$, and spin s; $k_b=\eta_b m$ is the momentum of the nucleon in the center-of-mass system, with

$$k/k_b=\eta/\eta_b=(2+2\omega/m)^{1/2}\approx 2. \qquad (4)$$

The scattering lengths in the ${}^3S_1$ and ${}^1S_0$ states are sometimes denoted $a_t\equiv a({}^3S_1)$ and $a_s\equiv a({}^1S_0)$. In accordance with definition (3) we have $a_t<0$ and $a_s>0$. The symbol b denotes quantities in the center-of-mass system.

Using the expression for α_{np} in terms of the scattering phases, we readily obtain

$$\alpha_{np}^{(b)}(\omega)=\frac{\omega_b}{m}\frac{1}{4k_b}\sum_{J=0}^{\infty}(2J+1)e^{i\delta_J}\sin\delta_J$$

$$=\frac{\hbar}{mc}\frac{\omega_b}{m}\frac{1}{4\tau_{\omega_b}}\sum_{J,\,l,\,S}(2J+1)e^{i\delta_J}\sin\delta_J, \qquad (5)$$

where δ_J denotes the scattering phases in states with total momentum J [the mixing coefficients drop out from (5)]. Since

$$\alpha_{np}=\frac{4\pi}{k_b}\frac{m}{\omega_b}\mathrm{Im}\,\alpha_{np}^{(b)}(\omega_b)=\frac{8\pi}{V\omega^2-m^2}\mathrm{Im}\,\alpha_{np}(\omega), \qquad (6)$$

$\alpha_{np}(\omega)$ is expressed in the laboratory system in terms of $\alpha_{np}^{b}(\omega_b)$ by the following relation ($\lambda_c=\hbar/mc=2.1\times10^{-14}$ cm):

$$\alpha_{np}(\omega)=\frac{k}{2k_b}\frac{m}{\omega_b}\alpha_{np}^{(b)}(\omega_b)$$

$$=\left(\frac{1}{2}+\frac{1}{2}\frac{\omega}{m}\right)^{1/2}\frac{\lambda_c}{4\tau_{\omega_b}}\sum_{JLS}(2J+1)e^{i\delta_J}\sin\delta_J. \qquad (7)$$

From (3) and (7) we have

$$\mathrm{Re}\,\alpha_{np}(m)\equiv D_{np}(m)=\frac{\lambda_c}{4}(3a_t+a_s), \qquad (8)$$

and the expression

$$D_{n\bar{p}}(m)=\frac{\lambda_c}{4}\{3a_{n\bar{p}}({}^3S_1)\exp[-2\beta_{n\bar{p}}({}^3S_1)]$$

$$+a_{n\bar{p}}({}^1S_0)\exp[-2\beta_{n\bar{p}}({}^1S_0)]\} \qquad (9)$$

takes into account the inelastic process — annihilation — with the aid of $\beta_{n\bar{p}}({}^3S_1)$ and $\beta_{n\bar{p}}({}^1S_0)$, the imaginary parts of the phases in the corresponding states of $n\bar{p}$ system.

Using a procedure analogous to that of reference 3, we consider the relation obtained from Eq. (2) when the latter is differentiated with respect to η^2 and η^2 is then set equal to zero. Taking into account the available experimental data, we confine ourselves to a single differentiation. Denoting the derivative of $D_{np}(\omega)$ with respect to η^2 by $D'_{np}(\omega)$, denoting its value at $\omega=m$ by $D'_{np}(m)$, and considering that all the lengths are expressed in terms of λ_c, we get

$$D'_{np}(m)+\frac{1}{4}[D'_{n\bar{p}}(m)-D_{np}(m)]$$

$$=\lambda_c\left\{-\frac{f^2}{4\pi}\left(\frac{m}{\mu}\right)^4+\frac{3}{8}\left(\frac{m}{B}\right)^{1/2}\frac{1}{1-\varkappa r_{0t}}\right.$$

$$+\frac{1}{8\pi^2}\mathrm{P}\int_1^\infty\frac{d\omega'}{\eta'^2}\left[\frac{\sigma_{np}(\omega')}{\omega'-1}+\frac{\sigma_{n\bar{p}}(\omega')}{\omega'+1}\right]$$

$$\left.+\frac{1}{\pi}\int_{\omega(2\mu)/m}^{\infty}d\omega'\frac{\mathrm{Im}\,\alpha_{n\bar{p}}(\omega')}{(\omega'+1)(\omega'^2-1)}\right\} \qquad (10)$$

The contribution of the deuteron state to (2) is calculated with accuracy to terms on the order of B/m, and therefore the terms of order B/m are discarded in the second term of Eq. (10). Terms of the order $(\mu/2m)^2$ have been omitted from the term proportional to f^2.

From Eqs. (3) and (7) we obtain for $D'_{np}(m)$

$$D'_{np}(m) = {}^1/_8 D_{np}(m) - {}^1/_{16}\{a^2({}^1S_0)[a({}^1S_0) + {}^1/_2 r({}^1S_0)] + 3a^2({}^3S_1)[a({}^3S_1) + {}^1/_2 r({}^3S_1)] - a({}^3P_0) - 3[a({}^1P_1) + a({}^3P_1)] - 5a({}^3P_2)\}. \quad (11)$$

According to the experimental data[9,10]

$$a({}^3S_1) = -(0.537 \pm 0.004)\cdot 10^{-12}\,\text{cm} = -(25.6 \pm 0.19)\lambda_c,$$
$$a({}^1S_0) = (2.373 \pm 0.007)\cdot 10^{-12}\,\text{cm} = (113 \pm 0.33)\lambda_c,$$
$$r({}^1S_0) \equiv r_{0s} = 2.7\cdot 10^{-13}\,\text{cm} = 12.84\lambda_c,$$
$$r({}^3S_1) \equiv r_{0t} = 1.7\cdot 10^{-13}\,\text{cm} = 8.1\lambda_c, \quad (12)$$

hence

$$D_{np}(m) = (0.190 \pm 0.0025)\cdot 10^{-12}\,\text{cm} = 9.05\lambda_c,$$
$$D'_{np}(m) = -9.20\cdot 10^4\lambda_c. \quad (12')$$

In calculating $D'_{np}(m)$, the principal contribution is that of the $^1S_0$ state. The triplet s scattering gives a contribution not exceeding 5% of the singlet contribution, while the inaccuracy in the value of a_s leads to an inaccuracy of approximately 1% in the value of $D'_{np}(m)$. Smaller still is the contribution of scattering in p states. We note that if, for a rough estimate, we use the values yielded by the potential of Gammel, Christian and Thaler,[11] the contribution of the p states do not exceed a value determined by the inaccuracy in the calculation of the deuteron term and comparable with $D_{np}(m)$. An estimate based on the potential of Signell and Marshak,[12] yields

$$a({}^1P_1) = -146.4\lambda_c, \quad a({}^3P_0) = 57.2\lambda_c,$$
$$a({}^3P_1) = -46.5\lambda_c, \quad a({}^3P_2) = 27.8\lambda_c.$$

Estimates of various terms in (10) show that numerically the deuteron state is considerably more important than the single-meson term, which played an important role in π-N scattering. In the low-energy region considered here, the presence of $D_{np}(m)$ in Eq. (10), as can be seen from Eqs. (11)' and (12), is hardly significant in practice. The value of $D_{np}(m)$ does not exceed the error in the calculation of the contribution of the deuteron state. The smallness of this term confirms the suggested unimportance of the role of "subtraction" in the nonrelativistic region. Furthermore, this gives grounds for assuming that the contribution of $D_{n\bar{p}}(m)$, which so far cannot be estimated directly, is small.

The contribution of the deuteron state amounts to $+(5450 \pm 13)$ (when B = 2.2 Mev, we have in the right half $1 - \kappa r_{0t} = 0.608$). The contribution of the single-meson state is 162 when $f^2/4 = 0.08$ and -184 when $f^2/4 = 0.09$.

The essential difference between (11), (12), and the analogous formulas of reference 3 lies naturally in the entirely different role of the s and p states in the np and pN scattering. The presence of a "resonance" pN interaction in the p state causes $D_{\pi N}(\omega)$ to be an increasing function at low energies, while the "resonance" interaction of nucleons in the s state makes $D_{np}(\omega)$ diminish at low energies. The sign of $a({}^1S_0)$ becomes significant here.

The calculation of the dispersion integral

$$J_{np}(m) = \frac{1}{8\pi^2} P\int_1^\infty \frac{d\omega' \sigma_{np}(\omega')}{\sqrt{\omega'^2 - 1}(\omega' - 1)} = \frac{F_{np}(m)}{8\pi^2} \quad (13)$$

leads to a value

$$J_{np}(m) = -\frac{7.70\cdot 10^6}{8\pi^2} = -9.65\cdot 10^4. \quad (14)$$

The integral $F_{np}(m)$ is understood to mean the limit

$$F_{np}(m) = \lim_{\omega_c \to 1} P\int_1^\infty \frac{\sigma_{np}(\omega')\, d\omega'}{(\omega' - \omega_0)(\omega'^2 - 1)^{1/2}} = F_s(\omega_0) + 3F_t(\omega_0). \quad (15)$$

The entire interval of integration is broken up into sections, on each of which the function $\sigma_{np}(\omega')$ is approximated by a simple expression. For the region of kinetic energies up to 20 Mev, the formula of Smorodinskiĭ[13] is used

$$\sigma_{np}(E_0) = 1.3\cdot 10^{-24}\left\{\frac{3}{(1.22 - 0.06E_0)^2 + E_0/2} + \frac{1}{(0.27 + 0.0\,E_0)^3 + E_0/2}\right\}\text{cm}^2 \quad (16)$$

(E_0 is the laboratory-system kinetic energy of the neutron in Mev). In other regions, a rough approximation is used. The roughness of the approximation of $\sigma_{np}(\omega)$ at high energies introduces no noticeable error whatever, since the principal role in the calculation of (15) is played, naturally, by the region $\omega' \sim \omega_0$. The contribution of this principal region, when the energy dependence of σ_{np} is given by Eq. (16), is easy to calculate

$$F_1(m) = \lim_{\omega_c \to 1} F_1(\omega_0) = \lim_{\omega_c \to 1}\{3F_{1t}(\omega_0) + F_{1s}(\omega_0)\},$$

where, for example,

$$F_{1s}(\omega_0) = P\int_1^{1+\varkappa^2/2} \frac{d\omega'}{\eta'} \frac{\sigma(\omega')}{\omega' - \omega_0} = \pi a^2({}^1S_0)\left\{-\frac{1}{k_0}\ln\left|\frac{k_0 + \varkappa}{k_0 - \varkappa}\right| + \left(\frac{k_0^2 + k_{2s}^2}{k_{1s}^2 - k_{2s}^2}\right)\frac{2}{k_{1s}}\tan^{-1}\frac{\varkappa}{k_{1s}} - \left(\frac{k_0^2 + k_{1s}^2}{k_{1s}^2 - k_{2s}^2}\right)\frac{2}{k_{2s}}\tan^{-1}\frac{\varkappa}{k_{2s}}\right\} \quad (17)$$

and an analogous expression for the contribution of the triplet state. In Eq. (17) k_{1s}^2 and k_{2s}^2 are the roots of the equation

$$\left(\frac{0.27}{\sqrt{m}}+0.06\sqrt{m}\frac{k_2^2}{2}\right)^2+\frac{k_2^2}{4}=0 \quad (k_1^2>k_2^2).$$

Using (17) and (15) we obtain directly

$$F_{np}^{(1)}(m)=-\frac{2}{\varkappa}\sigma_{np}(m)-6\pi a_t^2\left\{\frac{k_{1t}^2\tan^{-1}(\varkappa/k_{1t})}{k_{1t}(k_{1t}^2-k_{2t}^2)}-\frac{k_{2t}^2\tan^{-1}(\varkappa/k_{1t})}{k_{1t}(k_{1t}^2-k_{2t}^2)}\right\}$$

$$-2\pi a_s^2\left\{\frac{k_{1s}^2\tan^{-1}(\varkappa/k_{2s})}{k_{2s}(k_{1s}^2-k_{2s}^2)}-\frac{k_{2s}^2\tan^{-1}(\varkappa/k_{1s})}{k_{1s}(k_{1s}^2-k_{2s}^2)}\right\}=-7.70\cdot10^6. \quad (18)$$

In Eq. (18) k_{1t}^2 and k_{2t}^2 are the roots of the equation

$$\left(\frac{1.22}{\sqrt{m}}-0.06\sqrt{m}\frac{k_t^2}{2}\right)^2+\frac{k_t^2}{4}=0.$$

The contribution of the entire energy region above 20 Mev is not more than 0.3% of the value given by Eq. (18). In the subsidiary region itself, the energy section above 100 Mev yields approximately 12% of the contribution of this region.

Gathering the results and transferring all the known factors in Eq. (10) to one side, we obtain for the contribution of the nucleon-antinucleon interaction

$$\frac{1}{8\pi^2}\int_1^\infty\frac{d\omega'}{\eta'}\frac{\sigma_{n\bar p}(\omega')}{\omega'+1}+\frac{1}{\pi}\int_{\omega(2\mu)}^1 d\omega'\frac{\operatorname{Im}\alpha_{n\bar p}(\omega')}{(\omega'+1)(\omega'^2-1)}$$

$$-\frac{1}{4}D_{n\bar p}(m)=(-9.2+9.1)10^4=-1000. \quad (19)$$

A direct comparison of the dispersion relations with the experimental data on the n-p scattering at low energies shows therefore that the contribution of the nucleon-antinucleon interaction to the scattering of the nucleons is small in this energy region. It follows hence, in particular, that for this energy region the exact dispersion relation (2) can be replaced, without excessive error, by the approximation

$$D_{np}(\omega)-D_{np}(m)=(\omega^2-m^2)\left\{\left(\frac{\omega_d+\omega}{2m}\right)^{1/2}\frac{\Gamma_\alpha(0)}{(\omega_d-m)(\omega_d^2-m^2)}\right.$$

$$\left.+\frac{1}{8\pi^2}P\int_1^\infty\frac{d\omega'}{\eta'}\frac{\sigma_{np}(\omega')}{\omega'-m}\right\}. \quad (20)$$

Equation (76) of reference 8 may be useful to obtain information on the contribution of the unobservable region at various energies.

3. SCATTERING OF PROTONS BY PROTONS

The amplitude α_{np} can be expressed in terms of the amplitude of N-N scattering in states with definite values of the isotopic spin α_0 and α_1, using the relation

$$2\alpha_{np}=\alpha_0+\alpha_1=\alpha_0+\alpha_{pp}. \quad (21)$$

As a result we obtain for p-p scattering, in lieu of Eq. (10), a relation with a different numerical factor in front of f^2, containing no contribution of the deuteron state. In the unobservable region, naturally, there enter also states of several mesons with T = 1.

In lieu of (8) and (11) we obtain

$$D_{pp}(m)=\frac{1}{2}a(^1S_0)=56.5\lambda_c,$$

$$D'_{pp}(m)=\frac{1}{8}\left\{a_s-a_s^2\left(a_s+\frac{1}{2}r_{0s}\right)\right.$$

$$\left.+a(^3P_0)+3a(^3P_1)+5a(^3P_2)\right\}=-19.00\cdot10^4\lambda_c. \quad (22)$$

Making use of the isotopic invariance and calculating for the corresponding integral only the contribution up to 20 Mev, we obtain with the Smorodinskiĭ formula

$$J_{pp}(m)\approx-\frac{a_s^2}{2\pi}\left\{\frac{1}{\varkappa}+\frac{\tan^{-1}(\varkappa k_{2s})}{k_{2s}}\right\}=-18.75\cdot10^4. \quad (23)$$

Equation (19) is replaced by

$$\frac{1}{8\pi^2}\int_1^\infty\frac{d\omega'}{\eta'}\frac{\sigma_{p\bar p}(\omega')}{\omega'+1}$$

$$+\frac{1}{\pi}\int_{\omega(2\mu)}^1 d\omega'\frac{\operatorname{Im}\alpha_{p\bar p}(\omega')}{(\omega'+1)(\omega'^2-1)}-\frac{1}{4}D_{p\bar p}(m)=-2500, \quad (24)$$

indicating that the corresponding values in p-p and n-p scattering are of the same scale. Analysis shows that this is caused by the fact that the singlet scattering plays the important role in (19) and (23). We can thus use for p-p scattering also an approximate dispersion relation similar to (20) in which $\Gamma_\alpha(0)=0$.

4. SCATTERING OF NUCLEONS IN STATE WITH T = 0

Using (21), it is possible to obtain a dispersion relation for N-N scattering in states with T = 0. The relation will be similar to (2), except that the right hand will not contain the contribution of the single-meson state, while the deuteron contribution is double. Relation (10) is correspondingly transformed:

$$D_{NN}^{(0)}(m)=\frac{3}{2}a(^3S_1)=-38.4\lambda_c. \quad (25)$$

Instead of (11) we get

$$D_{NN}^{(0)\prime}(m)=\frac{1}{4}D_{NN}^{(0)}(m)$$

$$-\frac{3}{8}\left\{\frac{a_t}{2}+a_t^2\left(a_t+\frac{1}{2}r_{0t}\right)-a(^1P_1)\right\}\approx5160\lambda_c. \quad (26)$$

Here the relative role of the p states is naturally greater than in the cases previously considered, but the role of D(m), as before, is insignificant. If, in calculating the dispersion integral

$$J_{NN}^{(0)} = \frac{1}{8\pi^2} P \int_1^\infty \frac{d\omega'}{\eta'} \frac{\sigma_{NN}^{(0)}(\omega')}{\omega' - 1}$$

we again confine ourselves to the contribution of the kinetic-energy region below 20 Mev, we get

$$J_{NN}^{(0)}(m) = -\frac{3}{2}\frac{a_t^2}{\pi}\left\{\frac{1}{\varkappa} + \frac{k_{1t}^2 \tan^{-1}(\varkappa/k_{2t})}{k_{2t}(k_{1t}^2 - k_{2t}^2)} - \frac{k_{2t}^2 \tan^{-1}(\varkappa/k_{1t})}{k_{1t}(k_{1t}^2 - k_{2t}^2)}\right\} = -8.35\, a_t^2 = -5450.$$

The contribution of the deuteron state now amounts to 10900, so that, in analogy with (19) and (24),

$$\frac{1}{8\pi^2}\int_1^\infty \frac{d\omega'}{\eta'}\frac{\sigma_{NN}^{(0)}(\omega')}{\omega'+1} + \frac{1}{\pi}\int_{\omega(2\mu)}^\infty d\omega' \frac{\operatorname{Im}\alpha_{NN}^{(0)}(\omega')}{(\omega'+1)(\omega'^2-1)} - \frac{1}{4} D_{NN}^{(0)}(m) = +300. \quad (27)$$

The approximate dispersion relation differs from (20) in the numerical factor in front of $\Gamma_\alpha(0)$.

5. DISCUSSIONS

The net result of this article is the derivation of estimates like (19), (24), and (27) and the justification of approximate relations like (20). The estimate (27) is the least reliable; nevertheless, all three relationships show the magnitude of the contribution of the nucleon-antinucleon interaction to the dispersion equation for N-N scattering.

The approximate relations (20) may be useful in the analysis of experimental data on N-N scattering at low energies, particularly after more detailed data are obtained on N-N scattering in the p states. An approximate dispersion relation for nucleon-nucleon scattering was first postulated by Blank and Isaev.[1] In the present paper it is corroborated by direct comparison with experimental data. The principal result of this paper — relations of type (10) — can be used to obtain information on the contribution of the unobservable region in the future, when data on the interaction between antinucleons and nucleons become available for a wide range of energies.

It is interesting to note that the deduction that the nucleon-nucleon interaction contributes little is connected with the signs of a_s and a_p.

The dispersion relations for the pion-nucleon scattering was used in its time by many investigators to establish that $D_{\pi+p}$ and α_{33} are positive below resonance.

In the calculations presented here, the signs of a_s and a_t were assumed to be those that follow from data on the scattering of neutrons in para-hydrogen and ortho-hydrogen (see, for example, reference 10).

Since $D'_{pp}(m)$ is determined essentially by the singlet S scattering, while $D'_{np}(m)$ is essentially determined by this scattering, a change in the sign of a ($^1S_0$) would lead to the conclusion that nucleon-antinucleon interaction plays a large role at low energies. It is interesting to call attention to the fact that, from the point of view of dispersion relations, the positive sign of a ($^3S_1$) is determined both by the presence of a real deuteron state and by the fact that follows, from a somewhat different point of view, from the "effective radius theory" (see, for example, reference 14).

The analysis performed can be of interest in the evaluation of data on interactions between nucleons and low-energy antinucleons. The dispersion relation for N-N scattering is obtained from (2) by formally making the substitution $\omega \to -\omega$ and replacing α_{np} by $\alpha_{n\bar{p}}$ in the proper places. The role of single-meson and deuteron states is greatly reduced, but the role of the unobservable region increases noticeably instead. In the presence of necessary data, a relation of type (10) can be obtained to estimate the contribution of the unobservable region in this case.

The author is grateful to the late V. Z. Blank and also to P. S. Isaev for many useful discussions and to Ya. A. Smorodinskiĭ for useful remarks.

[1] V. Z. Blank and P. S. Isaev, Dokl. Akad. Nauk SSSR **117**, 785 (1957), Soviet Phys. "Doklady" **2**, 532 (1957).

[2] D. Y. Wong, Phys. Rev. **107**, 302 (1957). V. I. Serdobol'skiĭ, J. Exptl. Theoret. Phys. (U.S.S.R.) **33**, 1268 (1957), Soviet Phys. JETP **6**, 975 (1958). N. N. Khuri, Phys. Rev. **107**, 1148 (1957); **109**, 198 (1958).

[3] L. I. Lapidus, J. Exptl. Theoret. Phys. (U.S.S.R.) **34**, 453 (1958), Soviet Phys. JETP **7**, 312 (1958).

[4] L. D. Landau and Ya. A. Smorodinskiĭ, J. Exptl. Theoret. Phys. (U.S.S.R.) **14**, 269 (1944). H. A. Bethe, Phys. Rev. **76**, 38 (1949).

[5] V. Ya. Faĭnberg and E. S. Fradkin, Dokl. Akad. Nauk SSSR **109**, 507 (1956), Soviet Phys. "Doklady" **1**, 455 (1956).

[6] B. L. Ioffe, J. Exptl. Theoret. Phys. (U.S.S.R.) **31**, 583 (1956), Soviet Phys. JETP **4**, 534 (1957).

[7] F. M. Kuni, Dokl. Akad. Nauk SSSR **111**, 571 (1956), Soviet Phys. "Doklady" **1**, 686 (1956). F. M. Kuni, Вестн. ЛГУ (Bulletin, Leningrad State Univ.) No. 11, Phys. and Chem. Ser., **2**, 1957, p. 21.

[8] Goldberger, Nambu, and Oehme, Ann. Phys. **2**, 226 (1957).

[9] Lampi, Freier, and Williams, Phys. Rev. **80**, 853 (1950).

[10] G. L. Squires and A. T. Stewart, Proc. Phys. Soc. **230**, 19 (1955).

[11] Gammel, Christian, and Thaler, Phys. Rev. **105**, 311 (1957).

[12] P. S. Signell and R. E. Marshak, Phys: Rev. **106**, 832 (1957). Preprint, 1958.

[13] Ya. I. Smorodinskiĭ, J. Exptl. Theoret. Phys. (U.S.S.R.) **15**, 89 (1945); **17**, 941 (1947).

[14] A. I. Akhiezer and I. Ya. Pomeranchuk, Некоторые вопросы теории ядра (Certain Problems in Nuclear Theory) GITTL, 1950, 3.

Translated by J. G. Adashko
40

A POSSIBLE METHOD FOR THE DETERMINATION OF THE PARITY OF STRANGE PARTICLES

S. M. BILEN' KIĬ

Joint Institute for Nuclear Research

Submitted to JETP editor August 4, 1958

J. Exptl. Theoret. Phys. (U.S.S.R.) **36**, 291-292 (January, 1959)

It is suggested that the K-meson parity can be determined by investigation of the left-right asymmetry in $\pi(K) + p \to Y + K(\pi)$ reactions with a polarized proton target.

In the weak interactions responsible for K-meson and hyperon decays parity is not conserved. Therefore the intrinsic parity of strange particles can be studied only in their strong interactions.

In this note it is pointed out that the intrinsic parity of K mesons and hyperons can be determined from the reactions

$$\pi + p \to \Lambda(\Sigma) + K, \quad K + p \to \Lambda(\Sigma) + \pi \qquad (1)$$

with a polarized proton target. We assume spin $\frac{1}{2}$ for the hyperons and spin 0 for the K mesons in agreement with experimental data. The density matrix for a reaction of type (1) then has the form

$$M = a + \mathbf{b}\cdot\sigma \qquad (2)$$

and is a scalar if the total intrinsic parity in the reaction does not change, a pseudoscalar otherwise (a and **b** are functions of the relative momenta in the initial and final states). Using (2) it is easy to obtain by standard[1] methods the following expression for the differential scattering cross section:[2]

$$\sigma(\theta, \varphi) = \sigma_0(\theta)(1 \pm \mathbf{P}_0\cdot\mathbf{P}_Y). \qquad (3)$$

Here σ_0 is the cross section for an unpolarized target, $\mathbf{P}_0$ is the initial polarization of the protons, $\mathbf{P}_Y$ is the hyperon polarization in a reaction with unpolarized proton targets (the vector $\mathbf{P}_Y$ is perpendicular to the reaction plane).

The plus sign in formula (3) is to be used if $I_Y I_K = I_p I_\pi$, the minus sign if $I_Y I_K = -I_p I_\pi$ (I stands for intrinsic parity of the particle).

If the y axis is taken in the direction of the initial polarization $\mathbf{P}_0$, we can rewrite (3) as follows

$$\sigma(\theta, \varphi) = \sigma_0(1 \pm P_0 P_Y \cos\varphi). \qquad (4)$$

Therefore the asymmetry is given by

$$e(\theta) = \frac{\sigma(\theta, 0) - \sigma(\theta, \pi)}{\sigma(\theta, 0) + \sigma(\theta, \pi)} = \pm P_0 P_Y. \qquad (5)$$

Since the initial polarization P_0 is known, the asymmetry measures directly the hyperon polarization for reactions with unpolarized targets. Most important, the sign of the asymmetry makes it possible to determine the product of the intrinsic parities $I_Y I_K I_p$. To this end an independent measurement is needed of the sign of the hyperon polarization from reactions with unpolarized targets. A ready-made analyzer is provided by the subsequent decay of the polarized hyperon. As is well known,[3] a measurement of the asymmetry of the decay π mesons permits the determination of the product αP_Y (α stands for the asymmetry coefficient). The coefficient α may be obtained by measuring the polarization of the protons from the decay of the hyperon.[4] At the Geneva Conference (1958) such a measurement of the coefficient α for the Λ hyperon was reported ($\alpha = +0.85^{+0.15}_{-0.21}$).[5]

In this manner, utilizing the data on the sign of the polarization obtained from a study of the decay of polarized hyperons, it is possible to deduce uniquely the value of the product $I_Y I_K I_p$ from experiments with a polarized proton target. We would like to emphasize that the basic formula (3) is a rigorous one; the only assumptions in its derivation are that (1) parity is conserved in strong interactions involving K mesons and hyperons, (2) the hyperon spin is $\frac{1}{2}$ and the K-meson spin is 0.

In conclusion we note that the study of various reactions of type (1) with a polarized proton target would permit the determination of relative parities of hyperons. For example, from the reactions

$$\pi^- + p \to \Lambda^0 + K^0, \quad \pi^+ + p \to \Sigma^+ + K^+$$

one finds $I_\Lambda I_K I_p$ and $I_\Sigma I_K I_p$ respectively. Together they determine $I_\Sigma I_\Lambda$.

Finally let us note that all that was said above applies equally well to reactions with polarized spin $\frac{1}{2}$ nuclei where a hypernucleus of spin $\frac{1}{2}$ is formed in the final state.

[1] L. Wolfenstein and J. Ashkin, Phys. Rev. **85**, 947 (1952).

[2] S. M. Bilen'kiĭ and R. M. Ryndin, J. Exptl. Theoret. Phys. (U.S.S.R.) **35**, 827 (1958), Soviet Phys. JETP **8**, 574 (1959).

[3] Lee, Steinberger, Feinberg, Kabir, and Yang, Phys. Rev. **106**, 1367 (1957). Crawford et al., Phys. Rev. **108**, 1102 (1957).

[4] T. D. Lee and C. N. Yang, Phys. Rev. **108**, 1645 (1957).

[5] D. A. Glazer, Report at the Conference on High Energy Physics, Geneva, 1958.

Translated by A. M. Bincer
41

CONDITIONS FOR SUPERFLUIDITY OF THE ATOMIC NUCLEUS AND THE TEMPERATURE OF THE PHASE TRANSITION

V. G. SOLOV' EV

Joint Institute for Nuclear Research

Submitted to JETP editor July 31, 1958

J. Exptl. Theoret. Phys. (U.S.S.R.) **36**, 293-294 (January, 1959)

The conditions for the appearance of a superfluid state in the atomic nucleus are obtained with the aid of a variational principle proposed by N. N. Bogolyubov. The superfluidity conditions reduce to the requirement that attractive forces predominate in the interactions of protons located on the same shell at the energy of the Fermi surface. If the nucleus is in the superfluid state at zero temperature, a transition from the superfluid into the normal phase will take place as the temperature is increased. The critical temperature for this phase transition is found.

IN a preceding paper[1] the author, starting with a shell model for a heavy nucleus, considered the weak interactions of protons (or neutrons) situated on the same shell, and showed that the interactions of protons having equal and opposite projections of their momenta upon the nuclear axis of symmetry lead to the appearance of a superfluid state of the nucleus. In the present paper, using variational principle proposed by Bogolyubov[2] and representing his extension of the statistical variational principle,[3] we shall derive the conditions for the appearance of the superfluid state of the atomic nucleus, as well as the temperature of the phase transition from the superfluid to the normal state.

On the basis of the variational principle we find that the energy of the normal state will not be minimal (and, consequently, that a superfluid state will appear) in the case for which the equation

$$2|E(s_0, m) - E_F|\psi_m(s_0) + \frac{1}{N}\sum_{m'} J(s_0|m, m')\psi_{m'}(s_0) = E\psi_m(s_0) \quad (1)$$

has solutions with negative eigenvalues $E < 0$ (the symbols used are the same as in reference 1). With the object of determining the limits imposed upon $J(s_0|m, m')$, we investigate the asymptotic solutions of Eq. (1) as J tends toward zero while E also tends to zero and remains negative. As a result of these calculations we find that, as for the Fermi system of a metal[4] or of nuclear matter,[5] the superfluidity conditions reduce to the requirement that attractive forces predominate at the energy of the Fermi surface. We thus obtain the conditions for superfluidity of the nucleus in the following form:

$$J(s_0|m_0, m_0) < 0, \quad (2)$$

i.e., attractive forces must predominate between protons situated on an inner shell. On the basis of the statistical variational principle we find that for a temperature Θ different from zero the superfluid state of the atomic nucleus exists in the case for which the equation

$$2|E(s_0, m) - E_F| \coth\frac{|E(s_0, m) - E_F|}{2\Theta}\cdot\psi_m(s_0) + \frac{1}{N}\sum_{m'}' J(s_0|m, m')\psi_{m'}(s_0) = E\psi_m(s_0) \quad (3)$$

has solutions with negative eigenvalues $E < 0$.

It is readily seen that for $\Theta = 0$ Eq. (3) reduces to (2). Let the superfluid state exist for $\Theta = 0$; as the temperature Θ increases E will also increase. At the transition from the superfluid into the normal phase, at the critical temperature Θ_0, the eigenvalue E must become zero. Taking into account the fact that $|E(s_0, m) - E_F|$ is relatively small, and going from the summation to the integral, we obtain the following approximate expression for determination of the critical temperature:

$$\psi_m(s_0) + \frac{1}{4\Theta_0}\int_{m_1}^{m_2} dm'\rho_0(m')J(s_0|m, m')\psi_{m'}(s_0) = 0. \quad (4)$$

Here $\rho_0(m')$ is the level density. In order for (4) to have a non-zero solution, it is necessary that the determinant D be zero. From the equation $D = 0$, in view of the weakness of the interaction, we obtain the following expression for the temperature of the phase transition:

$$\Theta_0 = -\frac{1}{4}\int_{m_1}^{m_2} dm' \rho_0(m') J(s_0; m', m'), \qquad (5)$$

or

$$\Theta_0 \approx -\bar{\rho}_0 \bar{J}/4. \qquad (5')$$

In conclusion, I express my deep gratitude to Academician N. N. Bogolyubov for his constant interest in this work and his always valuable comments.

[1] V. G. Solov'ev, J. Exptl. Theoret. Phys. (U.S.S.R.) **35**, 823 (1958), Soviet Phys. JETP **8**, 572 (1959).

[2] N. N. Bogolyubov, Dokl. Akad. Nauk SSSR **119**, 244 (1958); Soviet Phys. "Doklady" **3**, 292 (1958).

[3] I. A. Kvasnikov and V. V. Tolmachev, Dokl. Akad. Nauk SSSR **120**, 273 (1958); Soviet Phys. "Doklady" **3**, 553 (1958).

[4] Bogolyubov, Tolmachev, and Shirkov, Новый метод в теории сверхпроводимости (New Method in the Theory of Superconductivity), Academy of Sciences Press, Moscow, 1958.

[5] V. G. Solov'ev, Dokl. Akad. Nauk SSSR **123**, 3 (1958); Soviet Phys. "Doklady" (in press).

Translated by S. D. Elliott
42

ON THE MOMENT OF INERTIA OF A MANY-PARTICLE SYSTEM; I.

Yu. K. KHOKHLOV

P. N. Lebedev Physics Institute, Academy of Sciences, U.S.S.R.

Submitted to JETP editor August 5, 1958

J. Exptl. Theoret. Phys. (U.S.S.R.) **36**, 295-299 (January, 1959)

The problem of the determination of the moment of inertia is considered. The formula obtained has as the simplest consequence that, even in the case of a spherically symmetric system, the moment of inertia is different from zero, and is not even very small as compared to the moment of inertia of a rigid body.

THE problem of the determination of the moment of inertia has been considered in a number of papers[1-3] (a more detailed bibliography is given in a paper by Bohr and Mottelson,[3] which is soon to appear). However, as far as we know, a sufficiently general expression for the operator of the moment of inertia has so far not been given. One of the aims of the present paper is to fill this gap to some extent by investigating the problem of the determination of the moment of inertia of a system rotating about a fixed axis.

We also discuss some estimates for the lower limit of the possible values of the moment of inertia. One of these estimates leads to the result that the moment of inertia of a spherically symmetric system (we mainly have in mind the spherically symmetric nucleus) is not only different from zero, as is frequently assumed, but is not even very small as compared to the momentum of inertia of a rigid body.

1. THE COLLECTIVE ANGLE VARIABLE φ

We shall attempt to develop the theory in a form which is independent of the specific method of separation of the collective angular variable. The separation itself is, however, a necessary feature of the theory. It may be achieved in the following manner.

Suppose we have a system of N particles with, in general, different masses. The Hamiltonian of the system is equal to

$$H = \sum^{N} (\hbar^2/2m)\,(\partial^2/\partial x^2 + \partial^2/\partial y^2 + \partial^2/\partial z^2) + U. \qquad (1)$$

The summation in (1) goes over all particles; the particle indices are omitted.

We assume that the potential U is independent of the velocity and commutes with the operator corresponding to the projection of the total angular momentum on the axis of rotation, which we choose as the z axis. We use the notation $M_z \equiv M$, where

$$M = \sum^{N} -i\hbar\,(x\partial/\partial y - y\partial/\partial x). \qquad (2)$$

Then

$$[H, M] = 0. \qquad (3)$$

We introduce a certain operator φ, which depends only on the coordinates x and y and satisfies the condition

$$[M, \varphi] = -i\hbar. \qquad (4)$$

With the help of the equations

$$(i/\hbar)\,[H, \varphi] = -V + M/\hat{I}_0, \quad -\hbar^{-2}\,[[H, \varphi], \varphi] = 1/\hat{I}_0 \qquad (5)$$

we also introduce the operators V and $\hat{I}_0$. Written more explicitly, these operators have the form

$$\frac{1}{\hat{I}_0} = \sum^{N} \frac{1}{m}\left[\left(\frac{\partial\varphi}{\partial x}\right)^2 + \left(\frac{\partial\varphi}{\partial y}\right)^2\right],$$

$$V = \sum^{N} -i\hbar\left[\frac{1}{\hat{I}_0}\left(x\frac{\partial}{\partial y} - y\frac{\partial}{\partial x}\right)\right. \qquad (6)$$

$$\left. - \frac{1}{m}\left(\frac{\partial\varphi}{\partial x}\frac{\partial}{\partial x} + \frac{\partial\varphi}{\partial y}\frac{\partial}{\partial y}\right) - \frac{1}{2m}\left(\frac{\partial^2\varphi}{\partial x^2} + \frac{\partial^2\varphi}{\partial y^2}\right)\right].$$

It follows from equations (3) and (4) that the operators $\hat{I}_0$ and V commute with φ and M. The same obviously holds for the operator H' defined by

$$H = H' - VM + M^2/2\hat{I}_0. \qquad (7)$$

The quantity φ can always be regarded as a new independent variable, by choosing the remaining $3N-1$ variables ξ such that

$$[M, \xi] = 0 \qquad (8)$$

for all ξ. The operator M then has the form

$$M = -i\hbar\partial/\partial\varphi,$$

and the operators H', $\hat{I}_0$, and V are functions of ξ and $\partial/\partial\xi$ only.

The new variable φ can be interpreted as the angle of rotation of the system as a whole (for more detail, cf. Sec. 3). Correspondingly, the variables ξ have the meaning of internal coordinates. The operator H' represents the energy of internal motion. The operator VM represents the energy of interaction of the internal motion with the rotation.

2. MOMENT OF INERTIA

We introduce the complete system of eigenfunctions of the operators H and M:

$$H\Psi_n = E_n\Psi_n; \qquad M\Psi_n = M_n\Psi_n. \tag{9}$$

The functions belonging to the eigenvalue $M_n = 0$ will be denoted by Φ_n.

We consider an initial state Ψ_0 with eigenvalues E_0 and M_0. We may write

$$\Psi_0 = (2\pi)^{-1/2} \exp\left\{\frac{i}{\hbar} M\varphi\right\} \Psi_0', \tag{10}$$

where Ψ_0' is a function depending only on the internal variables ξ. By operating on Ψ_0 with the Hamiltonian (7) we obtain

$$(H' - VM_0 + M_0^2/2\hat{I}_0)\Psi_0 = E_0\Psi_0, \qquad \text{with } M\Psi_0' = 0. \tag{11}$$

Equation (11) is initially obtained for integral values of $M_0/\hbar$. It remains, however, meaningful for arbitrary values of $M_0/\hbar$. It then determines E_0 as a function of some continuous parameter M_0. We assume that, for not too large M_0, this function can be expanded in powers of M_0:

$$E_0(M_0) = E_0(0) + M_0^2/2I + \ldots. \tag{12}$$

One easily sees that the absence of the odd powers of M_0 in expansion (12) is connected with the equivalence of the right and left handed systems of coordinates.

The expansion (12) can be terminated after the quadratic term in M_0. In this case we talk about a purely rotational spectrum. In the presence of higher terms in the expansion, the rotational spectrum will be more or less modified. Nevertheless, in both cases, the quantity I should obviously be interpreted as a moment of inertia. The reciprocal quantity

$$B = 1/I \tag{13}$$

is naturally called the inverse moment of inertia. It follows from (12) that

$$B = (\partial^2 E_0/\partial M_0^2)_{M_0=0}. \tag{14}$$

We note that the expansion (12) is formally just the usual perturbation series for the case that M_0 is a small parameter. The coefficients of this series are well known. In particular, we obtain the coefficient (14) by applying the operator $1/\hat{I}_0$ once and the operator V twice. As a result, we obtain

$$\frac{1}{I} = \left\langle \Phi_0, \frac{1}{\hat{I}_0}\Phi_0 \right\rangle - 2\sum_{n\neq 0} \frac{1}{E_n - E_0} |\langle \Phi_n, V\Phi_0\rangle|. \tag{15}$$

This is the required expression for the moment of intertia for the case of rotation about a fixed axis z.

In operator form we have

$$\frac{1}{I} = \frac{1}{\hat{I}_0} - 2V\mathrm{P}\frac{1}{H' - E_0}V, \tag{16}$$

where P denotes the principal value. The operator $1/\hat{I}$ may be written in a more convenient form by assuming the existence of an operator Λ satisfying the condition

$$V = (i/\hbar)[H', \Lambda], \tag{17}$$

where

$$V_{0n} = (-i/\hbar)(E_n - E_0)\Lambda_{0n}, \qquad V_{n0} = (i/\hbar)(E_n - E_0)\Lambda_{n0}.$$

In this case we may write

$$2\sum_{n\neq 0} \frac{|V_{n,0}|^2}{E_n - E_0} = \frac{i}{\hbar}\sum_n (V_{0n}\Lambda_{n0} - \Lambda_{0n}V_{n0}) = \frac{i}{\hbar}[V, \Lambda]_{00},$$

and therefore

$$1/\hat{I} = 1/\hat{I}_0 - (i/\hbar)[V, \Lambda]. \tag{18}$$

As an example we consider the problem of two interacting two-dimensional rigid rotators, each of which is characterized by its constant moment of inertia μ_i $(i = 1, 2, \ldots, N)$.

The Hamiltonian of this system is

$$H = \sum_{i=1}^{N} (-\hbar^2/2\mu_i)\partial^2/\partial\varphi_i^2 + U. \tag{19}$$

φ_i is the angular coordinate of the i-th rotator.

It is entirely obvious that, by choosing the collective angular variable φ in the form

$$\varphi = \sum_{i=1}^{N} \mu_i\varphi_i / \sum_{i=1}^{N} \mu_i, \tag{20}$$

we achieve a complete separation of the internal and external motions ($V = 0$!). The moment of inertia is equal to

$$I = \hat{I}_0 = \sum_{i=1}^{N} \mu_i. \tag{21}$$

We are, however, interested in the case when φ is chosen such that the operator V is different from zero. We then have to use the general for-

mulas (15) or (18) for the determination of the moment of inertia. In particular, we assume that $\varphi = \varphi_1$; then

$$\hat{I}_0 = \mu_1; \quad V = \frac{1}{\mu_1}\sum_{i=2}^{N} -ik\frac{\partial}{\partial\varphi_i}; \quad \Lambda = \frac{1}{I}\sum_{i=2}^{N}\mu_i(\varphi_i - \varphi). \quad (22)$$

Substituting the operators (22) in formula (18) we again obtain the correct value (20) for the moment of inertia. In the given special case it is thus possible to verify explicitly the independence of the moment of inertia of the choice of φ. This independence corresponds to the fact that the moment of inertia is determined by observable quantities (the energy and the projection of the angular momentum on the axis of rotation), which are, of course, invariant under arbitrary coordinate transformations.

3. ANGULAR VELOCITY OF THE SYSTEM AS A WHOLE

The inverse moment of inertia can also be determined as the derivative of the angular velocity with respect to the projection of the angular momentum on the axis of rotation z. The meaning of the angular velocity of the system is, however, not completely obvious. In this connection it is of interest to investigate the reverse problem: the determination of the angular velocity as that quantity which, upon differentiation with respect to M_0, gives the correct expression for the inverse moment of inertia. It is easily seen that the following quantity has this property:

$$\Omega = \langle \Psi_0, \dot{\varphi}\Psi_0 \rangle, \quad (23)$$

where the dot above the operator denotes the commutator with the Hamiltonian multiplied by i/ħ.

Indeed, we have, according to formula (11),

$$\left(\frac{\partial\Psi_0'}{\partial M_0}\right)_{M_z=0} = \mathrm{P}\frac{1}{H' - E_0}V\Phi_0. \quad (24)$$

Furthermore,

$$\dot{\varphi}\Psi_0 = \left(-V + \frac{M_0}{\hat{I}_0}\right)\Psi_0, \quad (25)$$

hence

$$\left\{\frac{\partial}{\partial M_0}\left[\left(-V + \frac{M_0}{\hat{I}_0}\right)\Psi_0'\right]\right\}_{M_z=0} = \frac{1}{\hat{I}_0}\Phi_0 - V\left(\frac{\partial\Psi_0'}{\partial M_0}\right)_{M_z=0}, \quad (26)$$

and, finally,

$$\left(\frac{\partial\Omega}{\partial M_0}\right)_{M_z=0} = \left\langle\Phi_0, \frac{1}{\hat{I}_0}\Phi_0\right\rangle - 2\left\langle\Phi_0, V\mathrm{P}\frac{1}{H' - E_0}V\Phi_0\right\rangle.$$

This is exactly formula (15).

We can easily determine the angular acceleration by expanding expression (23) for the angular velocity of the system. It may also be used for the determination of the moment of inertia. We again obtain, of course, the same result (15) as before.

4. ESTIMATE OF THE LOWER LIMIT OF THE MOMENT OF INERTIA

Expression (15) for the inverse moment of inertia consists of two structurally different terms. The first term,

$$\frac{1}{I_0} = \left\langle\Phi_0, \frac{1}{\hat{I}_0}\Phi_0\right\rangle, \quad (27)$$

defines some "bare" moment I_0, which plays the role of a generalized "bare" mass corresponding to the generalized coordinate φ. The second term represents a correction to the "bare" moment due to the coupling between the separate particles of the system during the rotation. It is immediately clear from formula (15) that, at least for the ground state of the system, the "bare" moment of inertia is always smaller than the true moment:

$$I_0 < I. \quad (28)$$

The "bare" moment therefore represents a lower limit for the possible values of the total moment. In this connection it is very desirable to find that φ for which the "bare" moment has the largest value. The case mostly considered in the literature so far is that in which φ represents the angle of rotation of the principal axes of the system (see, e.g., reference 2). In this case the operator $\hat{I}_0$ represents the so-called hydrodynamic moment of inertia

$$\hat{I}_0 = \left\{\left[\sum m(x^2 - y^2)\right]^2 + \left[\sum 2mxy\right]^2\right\} \Big/ \sum m(x^2 + y^2).$$

It is an interesting fact that, after averaging over a spherically symmetrical distribution, this quantity takes on a nonvanishing, if small, value.

By choosing φ in the form

$$\varphi = \sum_{i=1}^{N} m_i\rho_i^2\varphi_i \Big/ \sum_{i=1}^{N} m_i\rho_i^2, \quad (29)$$

where ρ_i and φ_i are the cylindrical coordinates of the i-th particle, and $\rho_i = (x_i^2 + y_i^2)^{1/2}$, we may convince ourselves that even in the completely symmetrical case the moment of inertia is not only different from zero, but is not even very small in comparison to the moment of inertia of a rigid body. Indeed, we then obtain the following expression for $\hat{I}_0$:

$$\hat{I}_0 = \sum_{i=1}^{N} m_i \rho_i^2 \Big/ \left\{ 1 + 4 \sum_{i=1}^{N} m_i \rho_i^2 (\varphi_i - \varphi)^2 \Big/ \sum_{i=1}^{N} m_i \rho_i^2 \right\}. \quad (30)$$

The quantity $(\varphi_i - \varphi)^2$ may be replaced by its average value

$$\overline{(\varphi_i - \varphi)^2} = \pi^2/3$$

and can then be taken outside the summation sign. This yields

$$\hat{I}_0 \approx \sum_{i=1}^{N} m_i \rho_i^2 \Big/ \left(1 + \frac{4\pi^2}{3} \right) \approx \frac{1}{14} \sum_{i=1}^{N} m_i \rho_i^2. \quad (31)$$

The moment of inertia of the ground state can therefore not be smaller than $1/14$ of the moment of inertia of a rigid body.

The author is grateful to Prof. A. S. Davydov for a discussion of the results of the present paper.

[1] D. R. Inglis, Phys. Rev. **96**, 1059 (1954).
[2] S. Hayakawa and T. Marumori, Progr. Theoret. Phys. **18**, 396 (1957).
[3] A. Bohr and B. Mottelson, Preprint (1958).

Translated by R. Lipperheide
43

SOVIET PHYSICS JETP VOLUME 36 (9), NUMBER 1 JULY, 1959

PERIPHERAL INTERACTIONS BETWEEN ELEMENTARY PARTICLES

L. B. OKUN' and I. Ya. POMERANCHUK

Submitted to JETP editor September 20, 1958

J. Exptl. Theoret. Phys. (U.S.S.R.) 36, 300-312 (January, 1959)

Modern meson theory can describe in an adequate phenomenological way the peripheral interactions of strongly interacting particles. We propose to isolate the contribution of peripheral interactions, by deriving from experimental data the amplitudes for various processes which require large orbital angular momentum. Large orbital angular momentum corresponds to a large impact parameter. By comparing these amplitudes, derived from experiment, with theoretical calculations, we may obtain many important quantities characterizing the strong interactions of elementary particles, for example, the renormalized coupling-constant of the pion with nucleons and hyperons, the renormalized coupling-constant of two pions or of a pion with a K particle, etc.

1. INTRODUCTION

THE study of existing meson theories has shown that a "naive" extension of these theories to very small regions of space ($r \ll 10^{-13}$ cm) runs into serious contradictions.[1] The resolution of these contradictions will possibly require a change in the foundations of quantum mechanics and perhaps also of relativity. There is still every reason to believe that the present theoretical description is adequate for physical processes taking place at large distances. This paper is concerned with the analysis of strong interactions occurring at large distances ($r > 10^{-13}$ cm).

Suppose that two particles, for example two nucleons, are separated by a distance $r > 1/\mu$, where μ is the mass of a pion. We use units such that $\hbar = c = 1$. The interaction between the two particles depends on the properties of the meson clouds which surround them, and hardly at all on the properties of the inner regions inside the clouds. The nucleons touch each other with their surface regions. A large number of theoretical physicists[2] have understood that existing meson theory can describe this peripheral interaction phenomenologically. But to make use of this fact, one must know how to isolate the effect of the peripheral interaction. The experimental data obtained up till now on the interactions of elementary particles are very rarely suitable for determining peripheral interactions. The processes which have been studied hitherto depend essentially on the nature of the interaction at small distances, where we do not yet know how to make calculations.

A number of authors (Chew, Moravczik, Taylor, Uretskii, Tsifra and others)[3] have proposed a method for isolating the contribution arising from the exchange of one virtual meson. The method of Chew is essentially based on the fact that the function which describes the angular distribution of a process can be extrapolated into the non-physical region $|\cos\theta| > 1$. It can be proved (and will be seen in the following argument), that for a particular value of $|\cos\theta| > 1$ the extrapolated angular distribution defines a one-meson amplitude proportional to g^2, where g is the renormalized pion-nucleon coupling constant. By comparing the values obtained by extrapolation, from the experimental data on N-P scattering and on photoproduction of pions, with the corresponding theoretical quantities, Chew and others could determine the value of g.

We here propose a second method which also allows us to isolate the contributions of peripheral interactions by an analysis of experimental data. Our method is based on the well-known fact that two particles, with a large relative orbital angular momentum l, effectively interact at a distance $\sim l\lambda$, where λ is the particle wavelength. Penetration to smaller distances is hindered by the centrifugal barrier. It follows that, to study peripheral interactions, we need to separate from the experimental data that part which determines the amplitude of a process occurring with sufficiently large values of l.

The possibility of isolating and describing theoretically a peripheral interaction is based on the fact that two particles or systems of particles separated by a large distance exchange between them the smallest possible number of mesons. Thus pion-nucleon scattering at large distances is described by an exchange of two pions, nucleon-nucleon scattering is described by the exchange

of one pion, etc. This allows us for example to describe nucleon-nucleon scattering for large l within the frame of a one-meson approximation, neglecting the exchange of two, three or more pions, and also the contributions of other mesons and baryon pairs, all such effects being included in the renormalized coupling-constant. We emphasize that in this case we may consider only the one-meson term, even though the coupling-constant is considerably larger than one ($g^2/4\pi \sim 15$). The expansion parameter, as we shall see below, is proportional to $(g^2/4\pi)e^{-\mu\lambda l}$, which for sufficiently large l is much smaller than one. In a certain very academic sense, the one-meson approximation for large l is more accurate than the one-photon approximation in electrodynamics, since $e^2/4\pi = \text{const}$, but $(g^2/4\pi)e^{-\mu\lambda l} \to 0$, as $l \to \infty$.

Our method of analysis by orbital angular momentum allows us not only to determine the value of the constant g and other similar constants, but to find relations between various physical quantities, for example scattering phases, describing various processes.

In Sec. 2 we set up a simple model to justify our method. Sections 3 – 6 contain a study of experiments in which peripheral interactions of elementary particles might be observed. In Sec. 3 we consider pion-nucleon experiments, in Sec. 4 strange-particle experiments. In Sec. 5 we study interactions between photons and strongly interacting particles. In Sec. 6 we consider briefly experiments involving leptons. In Sec. 7 we discuss the correlation of the information which could be obtained from the various experiments.

2. STUDY OF A MODEL

To explain our method we consider the interaction of two scalar particles, exchanging neutral scalar mesons with each other. We ignore the symmetry of the amplitudes arising from the identity of the particles. This very unrealistic model allows us to forget the complications of the dependence of the amplitudes on spin and isotopic spin.

We shall compare the behavior for large l of the one-meson and two-meson approximations. We shall also examine to what extent the dependence of the vertex part and the meson Green's function on q^2 influences the one-meson approximation.

The amplitude arising from the exchange of one meson (Fig. 1) is

$$a^{(1)} = \mu f^{(1)}(k^2)\frac{d(q^2)\,\alpha^2(q^2)}{q^2-\mu^2}.$$

Here $\mathbf{k}$ is the momentum of one of the colliding particles in the center-of-mass system; $q^2 = -|\mathbf{q}|^2 = -2k^2(1-\cos\theta)$, θ is the scattering angle, μ is the mass of the virtual meson. The dimensionless function $f^{(1)}$, proportional to the square of the renormalized coupling-constant, depends on k^2 and not on q.

While we allow only one virtual meson to be exchanged between the two particles, we include all the virtual processes which contribute to the meson Green's function and to both the vertex parts. These effects appear in the expression for $a^{(1)}$ as the factors $d(q^2)$ and $\alpha(q^2)$ respectively. By definition $\alpha(\mu^2) = d(\mu^2) = 1$. In Fig. 1 and the other diagrams, blocks containing all possible virtual processes are represented by circles. Henceforth we shall call these block vertices.

The contribution of the one-meson diagram 1 to the scattering amplitude in a state with orbital angular momentum l can easily be obtained from the Legendre polynomial expansion:

$$a^{(1)} = \frac{1}{2ik}\sum_{l=0}(2l+1)\,\eta_l^{(1)}P_l(\cos\theta),$$

$$\eta_l^{(1)} = \exp(2i\delta_l^{(1)}) - 1,$$

This gives

$$\eta_l^{(1)} = \frac{i\mu f^{(1)}(k^2)}{2k}\int_0^\pi \frac{P_l(\cos\theta)\,d(\cos\theta)}{1+\mu^2/2k^2-\cos\theta} = \frac{i\mu f^{(1)}(k^2)}{k}\,Q_l\left(1+\frac{\mu^2}{2k^2}\right),$$

where Q_l is the Legendre polynomial of the second kind. Analytic expressions[4] and tables[5] for Q_l exist. When $l \gg k/\mu \gg 1$,

$$Q_l(1+\mu^2/2k^2) \sim \sqrt{\pi k/2\mu l}\;e^{-\mu l/k}.$$

When $k/\mu \ll 1$, the exponential behavior changes to a power law:

$$Q_l\left(1+\frac{\mu^2}{2k^2}\right) \sim \frac{l!\,2^{l+1}}{(2l+1)!!}\left(\frac{k}{\mu}\right)^{2l+2}.$$

We now estimate the contributions for large l from the two-meson amplitude corresponding to diagram 2. For large l the important effects come from the singularities in the meson Green's functions, and we therefore neglect the dependence of the remaining factors on p and q, and take these factors outside the integrals. We find then

$$a^{(2)} = \frac{f^{(2)}(k^2)}{\mu}\int\frac{d^4p}{|(p-q/2)^2-\mu^2|\,|(p+q/2)^2-\mu^2|},$$

where $f^{(2)}$ is a dimensionless function of k^2. Combining the denominators and changing the variable of integration, we obtain

$$a^{(2)} = \frac{f^{(2)}(k^2)}{\mu}\int_0^1 dx\int\frac{d^4p}{|p^2+q^2(1-x)x-\mu^2|^2}.$$

We next rotate the integration with respect to p^0 onto the imaginary axis.[6,7] The denominator then

becomes positive, and we find

$$\eta_l^{(2)} = -\frac{f^{(2)}(k^2)}{8\mu^2 k}\int_0^1 \frac{dx}{(1-x)x}\int_m^\infty \frac{\partial}{\partial\zeta_l} Q_l\left(1+\frac{\mu^2+t^2}{2k^2(1-x)x}\right) t^2\,dt^2,$$

with $t^2 = |p|^2 + p_0^2$.

When $l \gg k/\mu \gg 1$, we use the asymptotic form of the function Q_l, and carry out the integration to obtain

$$\eta_l^{(2)} \approx -(\pi k f^{(2)}(k^2)/4\mu l^2)\, e^{-2\mu l/k}.$$

We thus see that for large l the two-meson amplitude is exponentially small compared with the one-meson amplitude. We will publish later a detailed analysis of the two-meson amplitude for large l. Here we wish only to remark that, in calculating the contribution for large l, convergence of the momentum integrals is always guaranteed by the presence of the factor $P_l(\cos\theta)$ in the integrand. Thus in the integrals which we considered above $t^2_{\text{eff}} \sim \mu k/l$.

The contribution of the three-meson amplitude for large l ($l \gg k/\mu \gg 1$) must obviously decrease like $\exp(-3\mu l/k)$. When $k/\mu < 1$ the exponential decrease is replaced by a decrease of the form 2^{-2l-2} for the two-meson amplitude and 3^{-2l-2} for the three-meson amplitude.

We now go back to the one-meson amplitude. In deriving the formula for the one-meson amplitude we assumed $\alpha(q^2) = 1$ and $d(q^2) = 1$, supposing that the important values of q^2 in the integral were around μ^2. We now verify the correctness of this approximation. The spectral representations of the Green's functions[8] and the vertex parts[9] give

$$\frac{\alpha^2(q^2)\,d(q^2)}{q^2-\mu^2} = \frac{1}{q^2-\mu^2}(1+S_1(q^2))(1+S_2(q^2))^2,$$

where

$$S_i = (q^2-\mu^2)\int_m^\infty \frac{\rho_i(x^2)\,dx^2}{q^2-x^2}.$$

Keeping only terms linear in S_i, we obtain

$$\eta_l^{(1)} \approx \frac{i\mu f^{(1)}(k)^2}{k}\left\{Q_l\left(1+\frac{\mu^2}{2k^2}\right) + \int_m^\infty Q_l\left(1+\frac{x^2}{2k^2}\right)(\rho_1(x^2)+2\rho_2(x^2))\,dx^2 + \ldots\right\}$$

The quantity m is the smallest sum of masses of particles into which a meson can be transformed. For example, for the pion $m = 3m_\pi$, and for the K particle $m = 2m_\pi + m_K$. For a scalar meson we would have $m = 2\mu$. When $l \gg k/\mu \gg 1$, the correction terms proportional to $e^{-2\mu l/k}$ are therefore exponentially small compared with $Q_l(1+\mu^2/2k^2)$ $\sim e^{-\mu l/k}$. The contribution which comes from the factors $\alpha^2(q^2)$ and $d(q^2)$ is seen to be of the same order as the contribution from exchange of two or more mesons. In the case of virtual pions, this contribution is of the same order as that arising from three-pion exchange. It is easy to verify that the terms of second and third order in S_i would not change this conclusion.

Effects of spin and isotopic spin, while essential in the discussion of actual processes, modify but do not qualitatively change our results.

3. PION-NUCLEON INTERACTION

Nucleon-nucleon scattering. A detailed study of this problem will be published elsewhere.* We therefore discuss here only the essential points.

It is clear from the preceding argument that the peripheral interaction between nucleons is described by the one-meson amplitude

$$M = 4\pi g^2\left\{(\bar{u}_1\gamma_5\tau_3 u_1)(\bar{u}_2\gamma_5\tau_3 u_2)\frac{\alpha^2(q^2)\,d(q^2)}{q^2-\mu^2} - (\bar{u}_2\gamma_5\tau_3 u_1)(\bar{u}_1\gamma_5\tau_3 u_2)\frac{\alpha^2(p^2)\,d(p^2)}{p^2-\mu^2}\right\},$$

as depicted in Fig. 3. Here g is the renormalized pion-nucleon coupling constant, $q = k - k'$, $p = k + k'$, and k and k' are the momentum four-vectors of one of the particles before and after scattering. The factors α and d represent the departure of the values of the vertex part and the meson Green's function at $q^2 < 0$ and $p^2 < 0$ from their values at $q^2 = p^2 = \mu^2$.

From the above expression for M we can calculate the scattering amplitudes with given values of the total angular momentum, just as we did for scalar particles. Estimates made from various models show that at energies of a few tens of Mev the F-wave nucleon-nucleon phase shifts will be accurately obtained from such a calculation.

In the non-relativistic approximation,[11] the nucleon-nucleon scattering amplitude can be written in the form

$$\alpha + \beta(\sigma_1+\sigma_2)\cdot\mathbf{n} + \gamma(\sigma_1\cdot\mathbf{n})(\sigma_2\cdot\mathbf{n}) + \delta(\sigma_1\cdot\mathbf{m})(\sigma_2\cdot\mathbf{m}) + \varepsilon(\sigma_1\cdot\mathbf{l})(\sigma_2\cdot\mathbf{l}),$$

Here $\alpha, \ldots, \epsilon$ are scalar functions of the scattering angles, and $\mathbf{n}$, $\mathbf{l}$, $\mathbf{m}$ are axes along the directions of $\mathbf{k}\times\mathbf{k}'$, $\mathbf{k}-\mathbf{k}'$, $\mathbf{k}+\mathbf{k}'$. The amplitude M contains all the terms of this expression except the second; in the one-meson approximation $\beta = 0$. This means that spin-orbit interaction is not contained in the one-meson approximation, and must appear in the effective nucleon-nucleon potential[12] with a dis-

*Otsuki et al.[10] have calculated nucleon-nucleon scattering phase shifts with the one-meson potential.

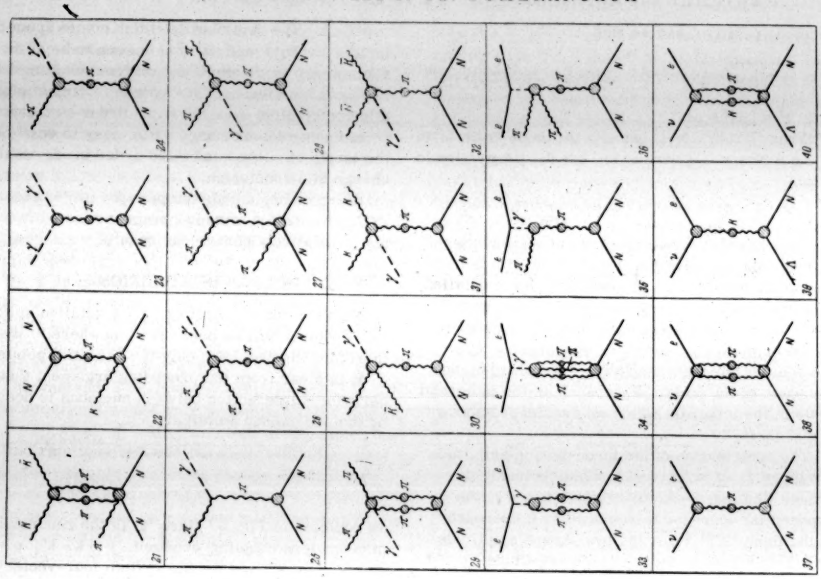

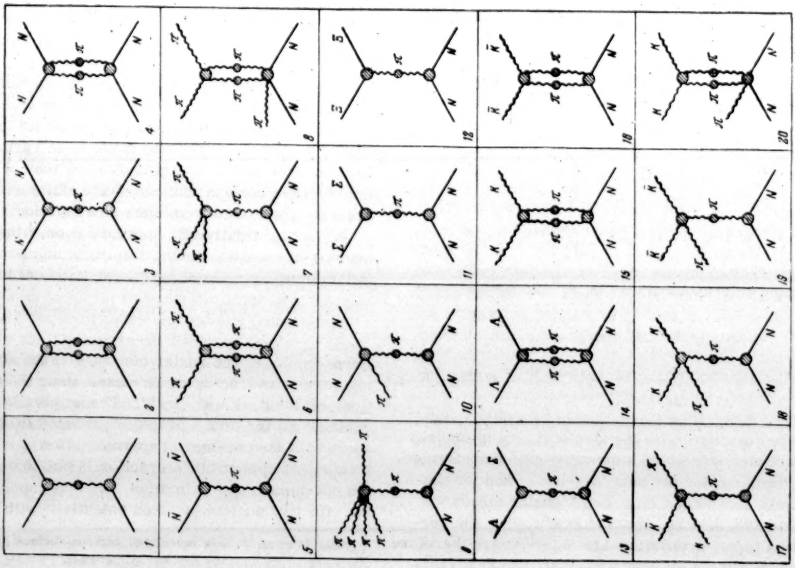

tance-dependence at least as strong as $\exp(-2\mu r)$.

If we can separate from the experimental data a term proportional to β, and measure its contribution to an amplitude with large l, this allows us to determine the magnitude of the two-meson diagram 4. In the one-meson approximation, the spin-dependence of the nucleon-nucleon scattering amplitude is more complicated than nucleon-antinucleon or nucleon-hyperon scattering. In the latter processes there are no exchange forces and the corresponding antisymmetrization of the amplitude is absent.

Nucleon-nucleon scattering allows us to determine the quantity g. Since we may calculate several phases and compare them with different experiments, we can test the consistency of the method. Our procedure thus contains a criterion for estimating the accuracy of the result in each case, without any further theoretical estimates.

Nucleon-antinucleon scattering. Although nucleon-antinucleon scattering differs from nucleon-nucleon scattering in the size of the cross-section and in the character of the interaction, still for large l the nucleon-antinucleon scattering phases are represented by the one-meson diagram 5. Moreover, the phases for $\bar{p} + n \to \bar{p} + n$ and $\bar{n} + p \to \bar{n} + p$ must be equal and opposite to the phases for $p + p \to p + p$, in those states in which the latter process can occur. The phases for $\bar{p} + p$ and $\bar{n} + n$ must be equal and opposite to those for $p + n$ scattering, where however we must remember that the two-nucleon system possesses a symmetry which is absent in the nucleon-antinucleon system. The one-meson amplitude for antinucleon scattering has only one term, and this is of the form $\tau_1\tau_2(\sigma_1 l)(\sigma_2 l)$. Therefore the amplitudes with $T = 0$ and $T = 1$ are for large l related according to

$$a_{T=0} = -3a_{T=1}.$$

The diffraction scattering caused by inelastic nucleon-antinucleon interactions may greatly complicate the isolation of the one-meson contribution.

Pion-nucleon scattering. Pion-nucleon scattering with large l is described by the two-meson diagram 6. The corresponding one-meson diagram is forbidden, since the pion is pseudoscalar and the transition $\pi \to 2\pi$ is impossible.

Lee and Yang[13] proved that a transition in the vacuum from any even number to any odd number of pions is forbidden, by virtue of the invariance of the strong interactions under the combined operation of charge-conjugation and a rotation in isotopic spin space. Therefore in pion-nucleon scattering there are contributions only from diagrams representing the exchange of an even number of pions.

Diagram 6 shows that for large l the pion-nucleon phases are determined by factors arising from two vertices, a pion-pion vertex, and a pion-nucleon vertex in which both pions are virtual.

Pion production in pion-nucleon and nucleon-nucleon collisions. In the production of mesons by mesons ($\pi + N \to N + 2\pi$), the pion-pion vertex which was mentioned above appears in the one-meson diagram 7. In this case the angular-momentum analysis is more complicated, since there are three particles in the final state. For a given angular momentum j_0 of the colliding pion and nucleon, we may choose a variety of angular momenta j_1 and j_2, referring respectively to the relative motion of the pions and to the motion of the nucleon in the final state. Diagram 7 describes a process occurring with a large value of j_2. An experimental determination of these amplitudes would allow us to measure pion-pion scattering. Further, by studying the dependence of the amplitude on j_1, the relative angular momentum of the two pions, one could find out in which orbital states the pions interact most strongly with each other. To carry out this program, a large number of experimental points would be needed. Possibly the simplest case to analyze would be the dependence on j_2 of scattering events in which the two pions emerge with almost equal velocities. Depending on which value of j_1 preponderates, the outgoing pions will be in a state of isotopic spin $T = 1$ if j_1 is odd, or $T = 0, 2$ if j_1 is even. The two-meson diagram 8 gives for large l a contribution small compared with that from diagram 7 but large compared with the other diagrams. For this diagram 8, the large angular momentum by which one should analyze the process is the angular momentum of one pion with respect to the center of mass of the second pion and the nucleon.

Processes of production of larger numbers of pions can be analyzed in the same way. For example, the process $\pi + N \to 4\pi + N$, (diagram 9), may give information about the vertex with six external meson lines.

The production amplitude in a nucleon-nucleon collision $N + N \to N + N + \pi$, when the two nucleons in the final state have large relative angular momentum, is described by the one-meson diagram 10. This contains, besides the pion-nucleon scattering vertex, also the $NN\pi$ vertex.

When any inelastic process is being analyzed into angular momentum states, one must work sufficiently far from the threshold for the process, since near to the threshold the angular momentum

carried away by the nucleon cannot be small.

4. INTERACTION OF STRANGE PARTICLES WITH PIONS AND NUCLEONS

We now turn to processes involving strange particles. We must emphasize that our analysis is much more difficult for processes in which K particles are exchanged. The reason is that the K particle mass is more than three times greater than the pion mass. This makes it hard to separate the contribution of K particles from the contribution of diagrams in which one or two pion lines run parallel to a virtual K-particle line. We therefore consider in what follows only those processes in which the amplitudes for large l are produced by the exchange of pions.

Hyperon-nucleon scattering. Diagrams 11 and 12 represent the scattering of Σ and Ξ hyperons respectively by nucleons. Diagram 13 describes the process $\Sigma + N \to \Lambda + N$, and diagram 14 describes Λ-nucleon scattering. In the last case the one-meson diagram is forbidden, since the $\Lambda\Lambda\pi$ vertex is not isotopically invariant. For all these processes the analysis is similar to that which we gave for nucleon-antinucleon scattering. The antihyperon-nucleon scattering for large l is simply related to the hyperon scattering amplitudes. The form of the $\Sigma + N \to \Lambda + N$ amplitude depends on the relative parity of the Σ and Λ hyperons.

K-particle-nucleon scattering. In K-particle scattering, as in pion scattering, the one-meson diagram is forbidden because the pion is pseudoscalar. At large angular momenta the process is described by the two-meson diagram 15. This diagram is similar to diagram 6 and differs from it only by the replacement of a pion-pion scattering vertex by a K-particle-pion scattering vertex. It is therefore of great interest to compare directly the phases of the processes $\pi + N \to \pi + N$ and $K + N \to K + N$ for large l. For large l the scattering of $\overline{K}$ particles by nucleons (diagram 16) is also determined by a $\pi\pi KK$ vertex.

Production of K particles and pions by K particles. The interaction vertex $\pi\pi KK$, which occurred in the K-particle-nucleon scattering, appears also in many other diagrams. In particular it appears in diagram 17, describing the process $\pi + N \to K + \overline{K} + N$, although the momenta of the incoming particles are now different. This last process must be analyzed in the same way as the process $\pi + N \to \pi + \pi + N$, considering the relative motion of the K particles on the one hand and the motion of their center of mass relative to the nucleon on the other. When the latter angular momentum is large, this process is described by diagram 17. The same vertex $\pi\pi KK$ appears in the one-meson diagrams 18 and 19, describing the production of pions by K particles and by $\overline{K}$ particles: $K + N \to K + \pi + N$ and $\overline{K} + N \to \overline{K} + \pi + N$. The corresponding two-meson diagrams 20 and 21 are similar to diagram 5, and differ from it in having $\pi\pi KK$ instead of $\pi\pi\pi\pi$ at the upper vertex. The creation of K particles in nucleon-nucleon collisions, $N + N \to N + \Lambda(\Sigma) + K$, is described for large l by diagram 22, which is similar to diagram 10 describing the creation of pions.

5. INTERACTION OF PHOTONS WITH MESONS AND BARYONS

Scattering of photons by nucleons. For large l the phases for the Compton scattering $\gamma + N \to \gamma + N$ are represented by diagram 23. The relevance of this diagram was noticed already by Low.[14] The vertex $\pi\gamma\gamma$, which appears in this diagram, describes the decay of a neutrol pion into two photons. Thus a measurement of the Compton scattering of photons by nucleons for large l would be equivalent to a measurement of the lifetime of the neutral pion. The scattering phases defined by diagram 23 are equal and opposite for proton and neutron.

Photoproduction of pions. Peripheral production of charged pions is described by diagram 24. There is a generalized Ward's theorem for the interaction of bosons with real photons.[15] This has the consequence that diagrams 24 and 25 give identical effects, provided that the vertex $\gamma\pi\pi$ and the Green's function of the virtual meson are not renormalized. Thus a measurement of the amplitude for the process $\gamma + N \to \pi + N$ for large l gives a clean determination of the vertex πNN.

The contributions of diagram 25 for the proton and neutron differ only in sign. The process inverse to photoproduction, the radiative capture of a pion by a nucleon, is also described by diagram 25, reading the diagram from right to left.

Diagram 26, containing the vertex $\gamma\pi\pi\pi$, describes the photoproduction of a pair of pions ($\gamma + N \to 2\pi + N$) when the angular momentum of the pair relative to the nucleon is large. Diagram 27 will give a contribution to the same process, when the angular momentum of one meson relative to the center of mass of the other meson and the nucleon is large. The vertex $\gamma\pi\pi\pi$, which appears in diagram 26, appears again in the one-meson diagram 28, which describes the bremsstrahlung of a pion scattered by a nucleon. The bremsstrahlung at large impact parameters (large l) comes

Processes	Vertices a	b	c	d	e	f	g	h	i	j	k	l	m	n	o	p	q	r
$N+N\to N+N$	1,1							2,2										3,3
$\overline{N}+N\to\overline{N}+N$	1,1							2,2										3,3
$\pi+N\to\pi+N$								2	2									
$\pi+N\to 2\pi+N$	1								1,2									2
$N+N\to N+N+\pi$	1							1,2										2
$\Sigma+N\to\Sigma+N$	1	1						2					2					
$\Xi+N\to\Xi+N$	1		1					2						2				
$\Sigma+N\to\Lambda+N$	1			1														
$\Lambda+N\to\Lambda+N$								2				2						
$\overline{\Sigma}+N\to\overline{\Sigma}+N$	1	1						2					2					
$\overline{\Xi}+N\to\overline{\Lambda}+N$	1			1														
$K+N\to K+N$								2		2								
$\overline{K}+N\to\overline{K}+N$								2		2								
$\pi+N\to K+\overline{K}+N$	1									1								
$K+N\to K+\pi+N$	1									1								
$\overline{K}+N\to\overline{K}+\pi+N$	1									1								
$N+N\to N+\Lambda+K$	1											1						
$\gamma+N\to\gamma+N$	1					1												
$\gamma+N\rightleftarrows\pi+N$	1						1											
$\gamma+N\to 2\pi+N$	1						1		1							1		
$\gamma+N\to K+\overline{K}+N$	1															1		
$\pi+N\to\pi+\gamma+N$	1														1			
$K+N\to K+\gamma+N$	1														1			
$e+N\to e+N$						2		2							3			3
$e+N\to\nu+N$	1						1	2									2	

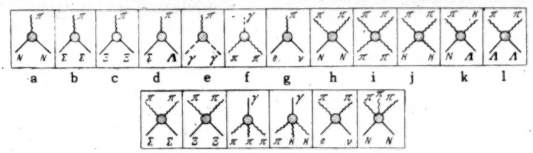

mainly from diagram 28. Because the pion is pseudoscalar, the ordinary classical bremsstrahlung is given by the two-meson diagram 29, and becomes negligible at large l. Bremsstrahlung can also accompany charge-exchange scattering of pions.

Photoproduction of K particles. Diagram 30 describes the photoproduction of a pair $K+\overline{K}$, and contains the vertex $\gamma\pi KK$, which can be determined by the process $\gamma+N\to K+\overline{K}+N$. The same vertex appears in diagrams 31 and 32, which describe the bremsstrahlung emitted by K particles and $\overline{K}$ particles scattered by nucleons. Bremsstrahlung can also accompany charge-exchange scattering of K particles.

Scattering of electrons by nucleons, and production of pions and K particles by electrons. The same vertices which were considered above, with different values of the momenta, appear in the diagrams which describe the interaction of electrons with nucleons. The electron-nucleon scattering amplitude contains two terms, one proportional to τ_3, and the other an isotopic scalar. Goldberger[16] proved that the first of these terms is described by diagram 33, and the second by diagram 34. The vertices $\gamma\pi\pi$ and $\gamma\pi\pi\pi$, which appear in these diagrams with virtual photons having $k^2\neq 0$, also appear in diagrams 35 and 36, which describe the production of pions by electrons, $e+N\to e+\pi+N$ and $e+N\to e+2\pi+N$.

The diagram for the process $e+N\rightleftarrows e+N+K+\overline{K}$ is similar to diagram 36, and differs from it only in the replacement of the vertex $\gamma\pi\pi\pi$ by $\gamma\pi KK$.

Interactions involving neutrinos. The process $e^-+p\to n+\nu$, involving the weak beta-decay interaction, can occur in electron-proton collisions. If the angular distribution of the neutrons from this process could be analyzed into angular momentum states, then for large angular momentum the main contribution comes from diagrams 37 and 38. These diagrams contain the vertices $\pi e\nu$[17] and $\pi\pi e\nu$,[18] the former carrying an axial vector interaction,

the latter a vector interaction. When high-energy electrons collide with protons, hyperon production, for example $e^- + p \to \Lambda + \nu$, is also possible. Diagrams 39 and 40 describe this process and contain the vertices $Ke\nu$ and $K\pi e\nu$. Like the vertices $\pi e\nu$ and $\pi\pi e\nu$, the vertices $Ke\nu$ and $K\pi e\nu$ can be measured independently by studying the decays $\pi \to e + \nu$, $\pi \to \pi + e + \nu$, $K \to e + \nu$, $K \to \pi + e + \nu$. All the remarks in this section apply equally to collisions of μ mesons with nucleons.

6. CORRELATION OF THE VARIOUS PROCESSES

We have enumerated in the table all the processes considered above, and the strongly interacting vertices which can be determined by studying these processes. The numbers 1, 2, 3 denote the number of virtual mesons linking the vertices in the corresponding diagram. Thus for example, in the row corresponding to the process $\pi + N \to 2\pi + N$, the number 1 stands in the column corresponding to the vertices $NN\pi$ and $\pi\pi\pi\pi$. These two vertices appear in diagram 7, and are linked by one virtual pion. In the same row, the numbers 2 correspond to the diagram in which the vertices $\pi\pi\pi\pi$ and $\pi\pi NN$ are linked by two mesons. By examining the one-meson diagrams we shall show how the vertices determined by the various processes can be correlated with one another.

The vertex $NN\pi$, the renormalized coupling constant, can be determined independently from the processes $N + N \to N + N$, $\bar{N} + N \to \bar{N} + N$, $\gamma + N \to \pi + N$. These processes do not contain other unknown vertices. Knowing the vertex $NN\pi$, we can determine the following vertices:

$\pi\pi\pi\pi$	from the process	$\pi + N \to 2\pi + N$,
$NN\pi\pi$	"	$N + N \to N + N + \pi$,
$\Sigma\Sigma\pi$	"	$\Sigma + N \to \Sigma + N$,
$\Sigma\Lambda\pi$	"	$\Sigma + N \to \Lambda + N$,
$\Xi\Xi\pi$	"	$\Xi + N \to \Xi + N$,
$\pi\pi K\bar{K}$	independently from the three different processes	$\pi + N \to K + \bar{K} + N$, $K + N \to K + \pi + N$, $\bar{K} + N \to \bar{K} + \pi + N$.
$\pi NK\Lambda$	from the process	$N + N \to N + \Lambda + K$,
$\pi\gamma\gamma$	"	$\gamma + N \to \gamma + N$,
$\gamma\pi\pi\pi$	"	$\gamma + N \to 2\pi + N$, $\pi + N \to \pi + N + \gamma$,
$\gamma\pi K\bar{K}$	"	$\gamma + N \to \bar{K} + K + N$, $\bar{K} + N \to \gamma + K + N$, $K + N \to \gamma + \bar{K} + N$.

When we determine a vertex from a one-meson diagram, we obtain its value for the special case in which one of the lines incident at the vertex corresponds to a virtual pion.

In a similar way, the two-meson diagrams can determine values of the vertices involving two virtual pions. In many cases the same vertex can be determined from both one-meson and two-meson or three-meson diagrams, for example the vertex $\gamma\pi\pi\pi$. This allows us to find the value of the vertex when the momenta of the incident mesons are in the nonphysical region. It is to be emphasized that the same vertex, when determined from one-meson and two-meson diagrams, appears with different momenta for the incident particles.

We have discussed the amplitudes for various processes with orbital angular momentum $l \gg 1$. Experimental measurement of amplitudes with very large l is of course impossible in practice. However, in case of nucleon-nucleon scattering, we can show that at low energy the experimental amplitude can be described by a peripheral one-meson interaction already when $l = 3$. The shape of the experimental angular distribution of the nucleons in the process $\pi + N \to 2\pi + N$ indicates that the peripheral one-meson interaction can be very large, and can dominate the amplitude for quite small values of l. Thus an experimental study of the processes enumerated above, and a determination of the data necessary for their analysis, may in many cases be possible in the comparatively near future.

Relations, similar to those which exist between the various processes involving nucleons, will also hold for processes in which a deuteron or a more complicated nucleus replaces the nucleon. In particular, by comparing the scattering of nucleons and hyperons by nuclei, we can find the relation between the pion coupling-constants with nucleons and with hyperons.

We emphasize, in conclusion, that all our arguments about peripheral interactions do not depend upon the nature of the strong interactions at short distances. In particular, the arguments are unchanged, whether the pion is an elementary or a compound particle.

The authors are grateful for criticism and helpful comments from V. B. Berestetskiĭ, N. N. Bogolyubov, A. F. Grashin, B. L. Ioffe, L. D. Landau, A. P. Rudik, K. A. Ter-Martirosyan, and I. M. Shmushkevich.

The authors are indebted to Professor Chew for sending a preprint of his paper.

[1] L. D. Landau and I. Ya. Pomeranchuk, Dokl. Akad. Nauk SSSR **102**, 489 (1955). I. Ia. Pomeranchuk, Nuovo cimento **3**, 1186 (1956). Pomeranchuk, Sudakov, and Ter-Martirosyan, Phys. Rev., **103**, 784 (1956). E. S. Fradkin, J. Exptl. Theoret. Phys. (U.S.S.R.) **28**, 750 (1955); Soviet Phys. JETP **1**, 604 (1955). G. Källèn and W. Pauli, Kgl. Dansk. Vid. Selskab. Mat.-Fys. Medd., **30**, No. 7 (1955).

[2] Taketani et al. Supplement to Progr. Theoret. Phys. **3** (1956). G. F. Chew, Proceedings of the seventh Rochester Conference (Interscience, 1957).

V. T. Khoziainov, J. Exptl. Theoret. Phys. (U.S.S.R.) **27**, 445 (1954).

[3] G. F. Chew, to be published. G. F. Chew, Proceedings of the International Conference on High-Energy Physics (Geneva 1958).

[4] M. M. Ryzhik and I. S. Gradshteĭn, Таблицы интегралов, сумм, рядов и произведений (Tables of Integrals, Sums, Series, and Products) Gostekhizdat (Moscow 1951).

[5] Tables of Associated Legendre Functions, Columbia Univ. Press. (New York 1945).

[6] F. J. Dyson, Phys. Rev. **75**, 1736 (1949).

[7] Landau, Abrikosov, and Khalatnikov, Dokl. Akad. Nauk SSSR **95**, 497 (1954).

[8] H. Lehmann, Nuovo cimento **11**, 342 (1954).

[9] Karplus, Sommerfield, and Wichmann, Phys. Rev. **111**, 1187 (1958) (and other references quoted therein).

[10] Otsuki, Tamagaki, and Watari, Proceedings of the Second Geneva Conference on the Peaceful Uses of Atomic Energy, 1958.

[11] R. Oehme, Phys. Rev., **98**, 216 (1955). Wolfenstein, Ann. Rev. Nucl. Sci. **6** (1956); Russian translation in Usp. Fiz. Nauk **62**, 71 (1957). Puzikov, Ryndin, and Smorodinskiĭ, J. Exptl. Theoret. Phys. (U.S.S.R.) **32**, 592 (1957); Soviet Phys. JETP **5**, 489 (1957).

[12] S. Okubo and R. E. Marshak, Ann. of Phys. **4**, 166 (1958).

[13] T. D. Lee and C. N. Yang, Nuovo cimento **3**, 749 (1956).

[14] F. Low, reported by G. F. Chew, Ref. 3.

[15] I. Ya. Pomeranchuk, Dokl. Akad. Nauk SSSR **100**, 41 (1955).

[16] J. Bernstein and M. Goldberger, Revs. Modern Phys. **30**, 465 (1958).

[17] M. Goldberger and S. Treiman, Phys. Rev. **110**, 1178 (1958).

[18] R. P. Feynman and M. Gell-Mann, Phys. Rev. **109**, 193 (1958).

Translated by F. J. Dyson
44

Letters to the Editor

QUANTUM CORRECTIONS TO RADIATION FROM A RIGID ROTATOR

L. B. IOGANSEN

Moscow State Pedagogical Institute

Submitted to JETP editor June 25, 1958

J. Exptl. Theoret. Phys. (U.S.S.R.) **36**, 313-314 (January, 1959)

A series of Soviet and foreign papers, quite complicated mathematically, have been devoted to the calculation of quantum corrections to synchrotron electron radiation (in particular, see reference 1.) The authors begin from the equations of motion for particles in an axially-symmetric magnetic field that assures circular motion and provides weak-focusing forces around the stable orbit.

It is shown in the present note that practically the same results can be obtained by entirely neglecting the excitation due to the betatron oscillations and considering the electron to be an absolutely rigid rotator. The character of the forces that ensures such a rigid focus are not specified. A possible interaction of the electron spin with the focusing fields is not taken into account.

We taken the orbit of radius a to lie in the xy plane, with its center at the origin. Dirac's equation for free azimuthal motion has the form

$$(\hbar c/ia)(\sin\varphi\alpha_x - \cos\varphi\alpha_y)\,\partial\psi/\partial\varphi = (E + \beta mc^2)\psi. \qquad (1)$$

We obtain the positive energy eigenvalues

$$E_l = \hbar\omega_l = \{(\hbar c/a)^2 l(l+1) + (mc^2)^2\}^{1/2} \qquad (l = 1, 2, \ldots). \qquad (2)$$

Two eigenfunctions correspond to each E_l:

$$\Psi_l^{(-)} = \frac{e^{il\varphi}}{\sqrt{2\pi(1+\varkappa_{l-}^2)}}\begin{pmatrix} i \\ 0 \\ 0 \\ \varkappa_{l-}e^{i\varphi} \end{pmatrix};$$

$$\Psi_l^{(+)} = \frac{e^{il\varphi}}{\sqrt{2\pi(1+\varkappa_{l+}^2)}}\begin{pmatrix} 0 \\ -ie^{i\varphi} \\ \varkappa_{l+} \\ 0 \end{pmatrix};$$

$$\varkappa_{l-} = \frac{E_l + mc^2}{(\hbar c/a)(l+1)}, \qquad \varkappa_{l+} = \frac{E_l + mc^2}{(\hbar c/a)\,l}. \qquad (3)$$

They are also eigenfunctions of the z component of the angular momentum, belonging to the eigenvalue $\hbar(l + \frac{1}{2})$. In the nonrelativistic approximation $\Psi_l^{(-)}$ corresponds to the z components of orbital angular momentum $m = l + 1$ and spin $s = -\frac{1}{2}$, while $\Psi_l^{(+)}$ corresponds to $m = l$ and $s = +\frac{1}{2}$.

We are interested in motion at relativistic velocities in a circle of macroscopic radius a. Such motion is quasi-classical, that is, $l \gg 1$, so $l(l+1) \approx l^2$, therefore, $\varkappa_l = \varkappa_{l+} = \varkappa_{l-}$. We consider the transition of an electron from the state $\Psi_l^{(-)}$ to the state Ψ_{l_1}; furthermore, we shall take $l - l_1 = n \ll l$, so that we can restrict ourselves to the first order in an expansion in powers of n/l. The frequency of the photon emitted in this transition is

$$\omega_n = \omega_l - \omega_{l_1} = \sigma n\frac{c}{a}; \quad \sigma = \beta\left[1 - \frac{1-\beta^2}{2}\frac{n}{l}\right]; \quad \beta = \sqrt{1-\gamma^{-2}}; \quad \gamma = \frac{E_l}{mc^2}. \qquad (4)$$

It is easy to see that the probability of a transition $\Psi_l^{(\pm)} \to \Psi_l^{(\mp)}$ with a change in the z component of the spin is proportional to $(n/l)^2$; therefore, only transitions with conservation of the spin component play a role in our approximation.

In first-order perturbation theory, the intensity of radiation of frequency ω_n in a solid angle $d\Omega$, given in terms of the angles θ' and φ', is equal to

$$I_n d\Omega = \frac{e^2c}{2\pi a^2}\sigma^2 n^2\left\{[\cot^2\theta' J_n^2(n\sigma\sin\theta') + \sigma^2 J_n'^2(n\sigma\sin\theta')] + \frac{n}{l}\left[\frac{\beta^2\sqrt{1-\beta^2}}{\sigma}\frac{1+\cos^2\theta'}{\sin\theta'}J_n(n\sigma\sin\theta')\,J_n'(n\sigma\sin\theta')\right]\right\}d\Omega. \qquad (5)$$

In the limit $l \to \infty$ we get precisely the classical formula.[2] Integrating Eq. (5) over the angles, we get the full power for the n-th harmonic:

$$I_n = \frac{e^2cn}{a^2}\left\{\left[2\sigma^3 J_{2n}'(2n\sigma) - \sigma(1-\sigma^2)\int_0^{2n\sigma} J_{2n}(x)\,dx\right] + \frac{n}{l}\beta^2\sqrt{1-\beta^2}\left[J_{2n}(2n\beta) - \frac{1}{2n\beta}\int_0^{2n\beta} J_{2n}(x)\,dx\right]\right\}. \qquad (6)$$

In the most interesting, ultrarelativistic case, when $\gamma \gg 1$, $\beta \approx 1$, it is possible to calculate the total radiated power.

For this we sum Eq. (6) over n and with the help of an asymptotic formula (see reference 3) we find

$$W = \frac{2e^2c}{3a^2}\gamma^4\left[1 - \left(\frac{385}{32\sqrt{3}} - \frac{3}{2}\right)\frac{\hbar}{mac}\gamma^2\right]. \qquad (7)$$

The result obtained has the same appearance as that of motion in a magnetic field,[1] but the numerical coefficients are somewhat different for the quantum correction.

In conclusion, I should like to express my gratitude to Professor M. S. Rabinovich for much valuable advice.

[1] Sokolov, Klepikov, and Ternov, J. Exptl. Theoret. Phys. (U.S.S.R.) **23**, 632 (1952) and **24**, 249 (1953). Also J. Schwinger, Proc. Natl. Acad. Sci. (U.S.A.) **40**, 132 (1954).

[2] G. A. Schott, Electromagnetic Radiation, Cambridge, 1912.

[3] J. Schwinger, Phys. Rev. **75**, 1912 (1949).

Translated by W. Ramsay
45

ENERGY SPECTRUM OF FRAGMENTS FROM THE PHOTOFISSION OF U^{238}

B. S. KOVRIGIN, M. Ya. KONDRAT'KO and K. A. PETRZHAK

Leningrad Technological Institute

Submitted to JETP editor June 24, 1958

J. Exptl. Theoret. Phys. (U.S.S.R.) **36**, 315-317 (January, 1959)

A systematic study of the variation of the nature of fission with excitation is possible by comparison of the energy spectra of any one isotope for different excitation energies. This should show a preference for excitation of the nucleus by gamma quanta, since the number of nucleons in the nucleus is not changed by this method. Some data for such a comparison can be gained at present from the behavior of U^{238}, for which the spectrum of spontaneous fission fragments[1,2] and the spectrum of fragments from photofission for a maximum gamma-ray energy of 16.7 Mev[3] have been investigated. The purpose of the present work was to obtain the energy spectrum of fragments from the photofission of U^{238} at a maximum betatron gamma-ray energy of 12.5 Mev.

The measurement of the kinetic energy of the photofission fragments was made in an apparatus consisting of a differential pulse ionization chamber, an amplifying channel, and a photo-recording pulsed oscillograph. The chamber had two parts — working and compensating — with a common collecting electrode and high voltage electrodes of opposite sign. The working part of the chamber was an ordinary pulse chamber with a grid. The compensating part of the chamber gave better compensation in the absence of a grid electrode within it. A layer of U_3O_8, which had been a target for a beam of gamma-rays and had a surface density of 0.4 mg/cm^2, was placed on the negative electrode. No collimation of the direction of the fragments was made.

The angular distribution of fragments in photofission is anisotropic with a maximum in the direction perpendicular to the gamma-ray beam. When the orientation of the chamber axis was parallel to the beam axis an additional distortion of the fragment spectrum could have arisen at the expense of absorption, since a significant part of the fragments could have flown out at very small angles to the plane of the preparation. Therefore in practice the chamber axis was set up at an angle of 15° to the beam axis.

The energy spectrum of fragments from the photofission of U^{238} for a maximum betatron bremsstrahlung energy of 12.5 Mev is shown in Fig. 1. The energy distribution of fragments from the slow neutron fission of U^{235} was obtained with the same apparatus and with the same preparation. This distribution is also shown in Fig. 1.

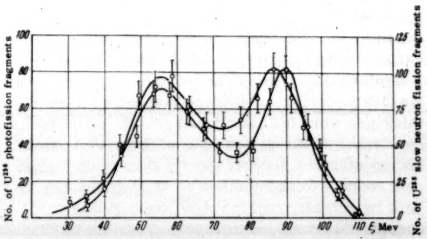

FIG. 1. Fragment energy spectra: ● – photofission of U^{238} at a maximum gamma-ray energy of 12.5 Mev, □ – slow neutron fission of U^{235}.

The spectrum of the photofission fragments has the most probable energies of (55.1 ± 1) and (86.9 ± 1) Mev for the groups of heavy and light fragments, respectively. To take the absorption in the preparation layer into account, these values must each be increased by approximately 5 Mev.

In Fig. 2 the U^{238} photofission spectrum is compared with the spontaneous fission spectrum obtained in reference 2. The comparison was made by means of the energy spectra of fragments from

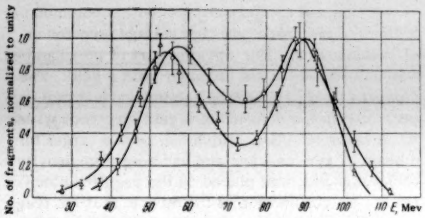

FIG. 2. Comparison of energy spectra of fragments from: ○ – photofission and Λ – spontaneous fission of U^{238}.

the slow neutron fission of U^{235}, determined, by the way, both in the present work and in reference 2.

Owing to the different thicknesses of the preparations (the surface density of the preparation in reference 2 amounted to 0.15 mg/cm^2), the neutron fission spectra differ somewhat among themselves. The main difference consists in the most probable energies of the spectrum in the present work being 2 Mev less, on the average, than those of the spectrum found in reference 2. Moreover, the increase of the thickness of the preparation is connected with an additional distortion of the spectrum, which consists in each peak obtaining some spread and becoming more asymmetrical at the expense of the appearance of a "tail" in the low-energy region. It is evident that if the neutron fission spectrum undergoes a distortion, then the photofission spectrum will undergo a similar distortion. However, the two neutron fission spectra do not differ from each other in form within the limits of error. Therefore the corrections to the distortions of the spectrum form caused by the large preparation thickness were not introduced into the photofission spectrum. In the comparison of the photofission and spontaneous fission spectra they were shifted with respect to one another so as to guarantee the best superposition of the U^{235} neutron fission spectra obtained in both cases. Thus the influence of the difference in the surface densities of the preparations was eliminated.

Comparison of the spectra shows that they differ mainly in the ratio of the notch height to the height of the light fragment peak. For the photofission spectrum this quantity is 0.60, and for the spontaneous fission spectrum it is 0.33.

This difference may depend both on the large excitation of the nucleus in photofission and on the superposition of fluctuations of the compensated gamma background. These fluctuations are due to a differential effect between the gamma pulses in the two parts of the chamber. The average magnitude of the pulse fluctuations on a pulse amplitude scale graduated in fragment energy units is about 4 Mev. The fluctuation pulses were superposed on the fragment pulses, producing a small broadening of the energy spectrum peaks. However, an estimate showed that the increase of the half-widths of the photofission spectrum peaks from this cause consisted of not more than 1 Mev, which can lead to an increase of the ratio of the notch height to the peak height of approximately 0.05. Hence, the main increase in the ratio of the notch height to the peak height by 0.22 should be carried at the expense of an increase in the number of symmetric fissions due to the high excitation of the fissioning nucleus in photofission.

Notwithstanding the considerable excitation energy, there is no essential increase observed of the most probable fragment energies and of the total kinetic energy in photofission compared with spontaneous fission. One can note also a certain pulling together of the photofission spectrum peaks compared with those of the spontaneous fission spectrum.

[1] W. J. Whittehouse and W. Galbraith, Phil. Mag. **41**, 429 (1950).

[2] B. S. Kovrigin and K. A. Petrzhak, Атомная энергия (Atomic Energy) **4**, 547 (1958).

[3] Korotkova, Cerenkov, and Chuvilo, Dokl. Akad. Nauk SSSR **106**, 811 (1956), Soviet Phys. "Doklady" **1**, 104 (1956).

Translated by Malcolm A. McLeod
46

THE BETA SPECTRA OF F^{20} *AND* F^{17}

S. S. VASIL' EV and L. Ya. SHAVTVALOV

Submitted to JETP editor July 5, 1958

J. Exptl. Theoret. Phys. (U.S.S.R.) **36**, 317-318 (January, 1959)

THE beta spectrum of F^{20} has been investigated with the aid of a beta-ray spectrometer with a magnetic lens. A beam of 4-Mev deuterons, accelerated in the cyclotron of the Research Institute for Nuclear Physics, Moscow State University, was led into the chamber of the beta-ray spectrometer. The arrangement of the experiment was described by us earlier.[1] LiF of about 0.4 mg/cm^2 served as a target. The beta spectrum obtained by us is a superposition of the beta spectrum of F^{20} (pro-

duced by the reaction $F^{19}(d, p)F^{20}$) on the beta spectrum of Li^8 (produced by the reaction $Li^7(d, p)Li^8$). Since the upper limit of the Li^8 beta spectrum exceeds that of F^{20} by more than a factor of two, approximately half of the area under the Li^8 beta spectrum curve lies beyond the upper limit of the F^{20} beta spectrum.

The beta spectrum of F^{20} was obtained as a result of subtracting the beta spectrum of Li^8 from the beta spectrum of Li^8 and F^{20}, the corresponding section of which was obtained by us separately (see Fig. 1. $H\rho$ in kilogauss-cm).

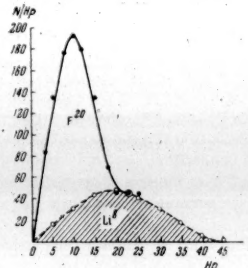

FIG. 1

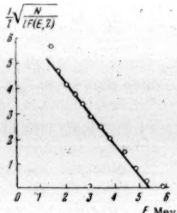

FIG. 2

A Kurie plot for F^{20} is presented in Fig. 2. As is obvious from the figure, the Kurie plot obtained is a straight line. The upper limit of the F^{20} beta spectrum is (5.45 ± 0.05) Mev. An estimate of the half-life made for the region of the spectrum around 1840 kev by separation in the beta-ray spectrometer gave the value (12.5 ± 2) sec. The results obtained were found in agreement with the data of Wong,[2] Alburger,[3] and Littauer[4] who investigated the F^{20} beta spectrum with the aid of magnetic spectrometers.

When a thin target of LiF is irradiated with deuterons, the relative number of radioactive Li^8 and F^{20} nuclei in the target and, hence, the relative intensity of their beta radiation in radioactive equilibrium is proportional to the ratio of the total cross-sections of the reactions $Li^7(d, p)Li^8$ and $F^{19}(d, p)F^{20}$. Since the half-lives of Li^8 and F^{20} are sufficiently short and the target current during the experiment varied only slightly and slowly, one can assume that the measurements have been made under equilibrium conditions. Consequently, taking the isotopic composition of the target into account, one can determine $\sigma(F^{19})/\sigma(Li^7)$ from the ratio of the areas (normalized to $H\rho = 20$ kilogauss-cm, i.e., beyond the upper limit of the F^{20} beta spectrum) under the beta spectra curves of Li^8 and F^{20}. This ratio turns out to be about 1.5 for deuteron energies around 4 Mev.

We also plotted the beta spectrum of F^{17} (produced according to the reaction $O^{16}(d, n)F^{17}$). The target used was celluloid film $(C_6H_{10}O_5)_x$ about 0.5 mg/cm^2 thick rather than the lead oxide usually used in such cases. The advantage of the celluloid film over a film of lead oxide is that the former contains no heavy elements, hence the positron scattering effect appears much weaker. The deviation from a straight line Kurie plot for F^{17} begins at approximately 800 kev, i.e., at approximately the same energy at which a deviation is observed in those cases when lead oxide is used as a target. Therefore the deviation from a straight line Kurie plot for F^{17} is apparently not connected with the scattering of positrons in the target. On the other hand, in the beta decay of F^{17} to the ground level of O^{17} the total spin of the nucleus does not change, $\ln \tau f = 3.38$, i.e., the transition must be allowed, and, consequently, the Kurie plot must be a straight line. One may suppose that the beta spectrum of F^{17} is a superposition of two partial spectra and that the decay also proceeds to an excited level which the nucleus has at 880 kev. However, this supposition requires further experimental verification. Besides, the change of the total nuclear moment in the decay to the excited level is $2(\frac{5}{2} - \frac{1}{2})$, which strongly decreases the probability of such a beta transition. The half-life and the upper limit have the previous values.[1]

We shall make use of this opportunity to express our gratitude to Yu. M. Shirokov for valuable discussions, to B. M. Makun' and Z. I. Tikhomirovaya for help in the work, and to the cyclotron crew, particularly G. V. Koshelyaev, A. A. Danilov, V. P. Khlapov, and A. P. Ozyabkin.

[1] S. S. Vasil'ev and L. Ya. Shavtvalov, Izv. Akad. Nauk SSSR, Ser. Fiz. **22**, 788 (1958) [Columbia Tech. Transl., in press].

[2] C. Wong, Phys. Rev. **95**, 761 (1954).

[3] D. F. Alburger, Phys. Rev. **88**, 1257 (1952).

[4] R. M. Littauer, Phil. Mag. **41**, 1214 (1950).

[5] Hornyak, Dougherty, and Lauritsen, Phys. Rev. **74**, 1727 (1948).

[6] C. Wong, Phys. Rev. **92**, 529 (1953); **95**, 765 (1954).

[7] L. Koester, Z. Naturforsch. **9a**, 104 (1954).

[8] V. Perez-Mendez and P. Lindenfeld, Phys. Rev. **80**, 1097 (1950).

[9] Warren, Laurie, James, and Erdman, Can. J. Phys. **32**, 563 (1954).

Translated by Malcolm A. McLeod
47

SUPERCONDUCTING ALLOYS AT FINITE TEMPERATURES

A. A. ABRIKOSOV and L. P. GOR'KOV

Institute for Physical Problems, Academy of Sciences, U.S.S.R.

Submitted to JETP editor July 16, 1958

J. Exptl. Theoret. Phys. (U.S.S.R.) **36**, 319-320 (January, 1959)

WE have recently[1] formulated the electrodynamics of superconductors that contain small atomic concentrations of impurities at $T = 0$. The method of reference 1 is not applicable at finite temperatures.

The authors of the present paper obtained, together with I. E. Dzyaloshinskii, a generalization of the method applied at $T = 0$. It was basically founded upon the formulation of the thermodynamic theory proposed by Matsubara.[2] An exposition of this method will be given in a separate paper. We note here only that the evaluation of the basic functions at $T \neq 0$ is formally very similar to the calculations at $T = 0$. In the case of equilibrium practically the only change involved is the replacement of the integrals over the frequency by sums over the discrete variable

$$\frac{1}{2\pi}\int_{-\infty}^{\infty} d\omega f(\omega) \to \frac{iT}{\hbar}\sum_{n=-\infty}^{\infty} f(i\omega_n), \qquad (1)$$

where $\omega_n = (\pi T/\hbar)(2n + 1)$, and T is the temperature in energy units.

This method was applied by us to study the equilibrium properties of superconducting alloys at finite temperatures. All calculations are exactly the same as the evaluations performed[1] for $T = 0$ apart from the transformation (1).

The evaluation of the functions $G(x, x')$ and $F(x, x')$ leads to the conclusion that in alloys, as at $T = 0$, these functions are simply multiplied by an exponential factor

$$G(x, x') = G_0(x, x')\exp\{-|\mathbf{x} - \mathbf{x}'|/2l\},$$
$$F(x, x') = F_0(x, x')\exp\{-|\mathbf{x} - \mathbf{x}'|/2l\}, \qquad (2)$$

where l is the mean free path in the normal state.

To find the thermodynamic functions it is sufficient to determine the particle density $N(\mu, T)$ as a function of the chemical potential and temperature:

$$N = \langle\psi^+(x)\psi(x)\rangle = -i[G(x, x')]_{x=x', t=t'-0}. \qquad (3)$$

One sees easily that the function $N(\mu, T)$ is the same as in the case of a pure superconductor. In the model under consideration, where one assumes that the impurities do not influence the interaction between the electrons, but only scatter them, the occurrence of impurities will therefore not change the thermodynamic functions. In particular, the critical temperature T_c is not shifted. We emphasize once again that this result is, of course, valid only if the impurity concentration is supposed to be small.

We have considered the behavior of alloys in a constant magnetic field. The connection between the current and the vector potential is local in the London case. At finite temperatures it is of the form

$$\mathbf{j} = -Q\mathbf{A}, \qquad (4)$$

$$Q = \frac{Nc^2}{mc}\,2\pi T\Delta^2\sum_n^{\infty}\frac{1}{[(\hbar\omega_n)^2 + \Delta^2]\left(\sqrt{(\hbar\omega_n)^2 + \Delta^2} + \hbar/2\tau_{tr}\right)} \qquad (5)$$

where $\omega_n = (\pi T/\hbar)(2n + 1)$; $\Delta(T)$ the temperature dependent "gap" occurring in the paper by Bardeen, Cooper, and Schrieffer;[3] $\tau_{tr} = [\int w(\theta)(1 - \cos\theta)\,d\Omega]^{-1}$ is the transport collision time for the metal in its normal state, and N is the electron density.

From Eq. (4) together with the Maxwell equation one obtains the connection between Q and the penetration depth:

$$\delta = \sqrt{c/4\pi Q}. \qquad (6)$$

In the limiting case of large free paths, $\Delta\tau_{tr}/\hbar \gg 1$, this formula goes over into the usual result for a pure London superconductor, i.e., a superconductor with $\delta \gg \hbar v/\Delta$:

$$\delta = \sqrt{mc^2/4\pi N_s e^2}, \qquad (7)$$

where N_s is the number of superconducting electrons (see Ref. 3),

$$N_s/N_0 = 2\pi T\Delta^2\sum_n[(\hbar\omega_n)^2 + \Delta^2]^{-3/2} = \frac{1}{4T}\int_{\Delta}^{\infty}\frac{z\,dz}{\cosh^2\frac{\varepsilon}{2T}\sqrt{\varepsilon^2 - \Delta^2}}. \qquad (8)$$

In the opposite limiting case, $\Delta\tau_{tr}/\hbar \ll 1$,

$$\delta = (c/2\pi)[\hbar/\Delta\sigma\tanh(\Delta/2T)]^{1/2}, \qquad (9)$$

where $\sigma = Ne^2\tau_{tr}/m$ is the conductivity of the alloy in the normal state.

It is well known that superconductors fall into two classes. For London superconductors $\delta > \hbar v/\Delta$. In that case the connection between Δ and $\hbar/\tau_{tr}$ can be arbitrary. In the case of the Pippard superconductors, for which $\delta < \hbar v/\Delta$, the condition $\delta \gg l$ leads to $\Delta\tau_{tr}/\hbar \ll 1$. Hence, only Eq. (9) refers to Pippard superconductors.

As was noted in reference 1, all formulae obtained for δ can by analogy with this be applied for the characteristics of films of thickness $d \ll \delta$.

In that case the quantity δ no longer plays the role of the penetration depth, but this quantity goes over into the effective dielectric constant for low frequencies and determines the magnetic susceptibility. Since the connection between $\mathbf{j}$ and $\mathbf{A}$ is local, ϵ and χ, expressed in terms of δ, have the usual, London form:

$$\varepsilon = -c^2/\omega^2\delta^2, \tag{10}$$

$$\chi = \frac{1}{4\pi}\left(1 - \frac{2\delta}{d}\tanh\frac{d}{2\delta}\right) \approx -\frac{1}{12\pi}\left(\frac{d}{2\delta}\right)^2. \tag{11}$$

In conclusion the authors express their gratitude to Academician L. D. Landau for discussions of this paper.

[1] A. A. Abrikosov and L. P. Gor'kov, J. Exptl. Theoret. Phys. (U.S.S.R.) **35**, 1558 (1958), Soviet Phys. JETP **8**, 1090 (1959).

[2] T. Matsubara, Progr. Theoret. Phys. **14**, 351 (1955).

[3] Bardeen, Cooper, and Schrieffer, Phys. Rev. **108**, 1175 (1957).

Translated by D. ter Haar
48

PARTICLE ENERGY LOSSES DUE TO THE EXCITATION OF LONGITUDINAL WAVES

B. A. LYSOV

Moscow State University

Submitted to JETP editor September 3, 1958

J. Exptl. Theoret. Phys. (U.S.S.R.) **36**, 321-322 (January, 1959)

IT has been pointed out[1-3] that longitudinal plane waves are excited if a medium exhibits spatial dispersion; Ginzburg has noted[1] that a very convenient means for the excitation of these new waves may be the Cerenkov effect.

In this connection it is of interest to develop the theory of the Cerenkov effect as applied to the case in which longitudinal electromagnetic waves are excited by an electron. We consider an isotropic medium. We start by noting that one cannot use the usual Lagrangian $L = (\epsilon\mathbf{E}^2 - \mathbf{H}^2)/8\pi$ because the energy density of the field, given by the expression $(\epsilon\mathbf{E}^2 + \mathbf{H}^2)/8\pi$, vanishes for longitudinal waves (both $\mathbf{H}$ and ϵ vanish).

In order to avoid this difficulty we start with the Fock-Podolsky Lagrangian,[4] making the necessary extension to the case of an isotropic madium. We have

$$L = \left\{(n\mathbf{E})^2 - \mathbf{H}^2 - \left(\operatorname{div}\mathbf{A} + \frac{n^2}{c}\frac{\partial\varphi}{\partial t}\right)^2\right\}, \tag{1}$$

where $\mathbf{E}$ and $\mathbf{H}$ are the intensities of the electric and magnetic fields respectively, $\mathbf{A}$ is the vector potential, φ is the scalar potential and n is the index of refraction (n is considered an operator, cf. reference 5).

Introducing the existence condition for a longitudinal field, curl $\mathbf{A} = 0$, and the fact that there are no free charges, $(\varphi = 0)$, using the analysis in reference 1 we find the following expressions for $\mathbf{A}$ and the energy density respectively:

$$\{\Delta - (n^2\partial^2/c^2\partial t^2)\}\,\mathbf{A} = 0,$$
$$T_{44} = \{(\operatorname{div}\mathbf{A})^2 + (\partial n\mathbf{A}/c\partial t)^2\}/8\pi. \tag{2}$$

In order for Eq. (2) (vector potential) to be consistent with the field equation in the medium, the condition $\epsilon\mathbf{E} = n^2\{\mathbf{E} - \boldsymbol{\kappa}_0(\mathbf{E}\cdot\boldsymbol{\kappa}_0)\}$ must be satisfied; this follows from the analysis in reference 1.

Now, writing the solution of Eq. (2) in the form

$$A = L^{-3}\sum_{\mathbf{x}}\sqrt{2\pi c\hbar/\varkappa n}\left\{\mathbf{a}\exp\left(-ic\frac{\varkappa}{n}t + i\boldsymbol{\varkappa}\cdot\mathbf{r}\right)\right.$$
$$\left. + \mathbf{a}^+\exp\left(ic\frac{\varkappa}{n}t - i\boldsymbol{\varkappa}\cdot\mathbf{r}\right)\right\},$$

we find the energy of the longitudinal field:

$$H = \sum_{\mathbf{x}}(c\hbar\varkappa/n)(\mathbf{a}^+\mathbf{a}), \tag{3}$$

where $\hbar\boldsymbol{\kappa}$ and $c\hbar\kappa/n$ are the momentum and energy of the longitudinal photon. To satisfy the existence condition for longitudinal waves explicitly we write

$$\mathbf{a} = g\boldsymbol{\varkappa}_0, \quad \mathbf{a}^+ = g^+\boldsymbol{\varkappa}_0, \quad \boldsymbol{\varkappa}_0 = \boldsymbol{\varkappa}/\varkappa, \tag{4}$$

then, using Eq. (3) in the usual way (cf. reference 6), we find that the operators g and g^+ satisfy the Bose commutation relations. The phenomenological quantum electrodynamics developed above for the longitudinal field agrees in form with that given in reference 6 — the only differences lie in the meanings of the operators $\mathbf{a}$ and $\mathbf{a}^+$. Hence, in applying the analysis to the Cerenkov effect we can use the results obtained by Sokolov.[7,8] Substituting Eq. (4) in Eq. (8) of the paper by Sokolov and Loskutov[8] and assuming that there are no longitudinal photons at $t = 0$, after some elementary transformations we find the following expression for the energy radiated per unit length of path in the form of longitudinal waves:

$$W^{(1/2)} = \frac{e^2}{2c^2}\int_{\omega_1}^{\omega_2}\omega\left[2\cos^2\eta - \frac{\hbar\omega}{cp}(n\cos\eta + 1/\beta)\right]d\omega \qquad (5)$$

for a particle with half-integral spin and

$$W^{(0)} = \frac{e^2}{c^2}\int_{\omega_1}^{\omega_2}\omega\left(\cos^2\eta - \frac{\hbar\omega n}{cp}\cos\eta\right)d\omega \qquad (6)$$

for a particle of zero spin. Here

$$\cos\eta = 1/\beta n + (n\omega\hbar/2pc)(1 - n^{-2}) \qquad (7)$$

($\mathbf{p}$ is the initial momentum of the electron, θ is the angle between $\mathbf{p}$ and the direction of photon emission). The integrations in Eqs. (5) and (6) are taken over the frequency regions for which the inequality $\cos\theta \leq 1$ is satisfied.

The following remarks may be made concerning the derivation of Eqs. (5) and (6): first, the quantum correction is proportional to $\hbar$ as in the case of the transverse field of longitudinally polarized electrons;[9] second, in the case of the longitudinal field there is no specific quantum correction proportional to $\hbar^2$ due to the electron spin in the transverse field. The latter situation leads one to believe that the indicated correction is due to the transverse field rather than the spin of the electron. There is at least one important difference from the case of the transverse field; in the classical analysis of Cerenkov radiation of transverse waves there is no radiation threshold; in the case of longitudinal waves, however, the radiation remains finite at the threshold, even in the classical approximation. Thus, neglecting terms of order $\hbar$ and higher in Eq. (5) we have

$$W^{(1/2)} = W^{(0)} = (e^2/2c^2)(\omega_2^2 - \omega_1^2). \qquad (8)$$

I wish to thank A. A. Sokolov for his interest in the present work and a number of stimulating remarks and Yu. M. Loskutov for valuable discussions.

[1] V. L. Ginzburg, J. Exptl. Theoret. Phys. (U.S.S.R.) **34**, 1593 (1958), Soviet Phys. JETP **7**, 1096 (1958).

[2] S. I. Pekar, J. Exptl. Theoret. Phys. (U.S.S.R.) **33**, 1022 (1957), Soviet Phys. JETP **6**, 785 (1958).

[3] S. I. Pekar, J. Exptl. Theoret. Phys. (U.S.S.R.) **34**, 1176 (1958), Soviet Phys. JETP **7**, 813 (1958).

[4] W. Fock and B. Podolsky, Sow. Phys. **1**, 801 (1932).

[5] D. D. Ivanenko and A. A. Sokolov, Классическая теория поля (Classical Theory of Fields) Gostekhizdat, M.-L., 1951.

[6] A. Sokolov and D. Ivanenko, Квантовая теория поля (Quantum Theory of Fields) Gostekhizdat, M.-L., 1952.

[7] A. A. Sokolov, Dokl. Akad. Nauk SSSR **28**, 415 (1940).

[8] A. A. Sokolov and Yu. M. Loskutov, J. Exptl. Theoret. Phys. (U.S.S.R.) **32**, 630 (1957), Soviet Phys. JETP **5**, 523 (1957).

[9] A. A. Sokolov and Yu. M. Loskutov, J. Exptl. Theoret. Phys. (U.S.S.R.) **34**, 1022 (1958), Soviet Phys. JETP **7**, 706 (1958).

Translated by H. Lashinsky
49

COULOMB EXCITATION OF NEON

D. K. ALKHAZOV, A. P. GRINBERG, I. Kh. LEMBERG, and V. V. ROZHDESTVENSKII

Leningrad Physico-Technical Institute, Academy of Sciences, U.S.S.R.

Submitted to JETP editor September 13, 1958

J. Exptl. Theoret. Phys. (U.S.S.R.) **36**, 322-324, (January, 1959)

In studying Coulomb excitation of nuclei one can observe various excitations in the target nucleus. It is also possible to observe excitations in the bombarding particle if the latter exhibits levels for which the Coulomb excitation cross section is large. In most of the work on Coulomb excitation the bombarding particles have been protons or α particles. Inasmuch as H^1 and He^4 do not have suitable levels the effect noted above has not been observed. In certain cases, however, the use of heavy ions as bombarding particles makes it possible to observe the excitation of nuclear excitations in these particles.

The present authors have investigated Coulomb excitation in Ne^{20} and Ne^{22}. The first excited levels are at 1.63 and 1.275 Mev respectively. Coulomb excitation of these levels has still not been studied because the intensity of the γ rays produced when neon is bombarded by protons or α particles is low unless the latter have high energies, i.e., energies comparable with the potential barrier. For this reason the measurements are complicated by background effects. In the usual method, when the element being investigated serves as the target (if a thick gas target is used), it is difficult to measure the beam current. It is probably for this reason that in the work reported in references 1 and 2, concerning an investigation of Coulomb excitation of krypton and xenon, the authors were able to determine only the relative values of the γ yields.

In the present work accelerated neon ions have been used as the bombarding particles. Neutral neon was admitted to the ion source of the cyclotron. The cyclotron was tuned for the different ions (Ne^{20} or Ne^{22}) by varying the magnetic field, keeping the frequency of the accelerating field fixed. The average beam current at the target was 1.5×10^{-8} amp for Ne^{20} and 1.5×10^{-9} amp for Ne^{22} (these figures correspond to the isotropic composition of the neutral neon). The energy of the $Ne^{20.4+}$ ions was approximately 23.5 Mev, the energy of the $Ne^{22.4+}$ ions was 25.8 Mev. The following materials were used as targets: Be, B, C, Mg, Al, Si, $Mg^{24}O$, $Mg^{25}O$, $Mg^{26}O$ and ScO. Calculations indicate that the γ-ray intensity associated with the Coulomb excitation of Ne^{20} or Ne^{22} falls off rapidly with increasing atomic number of the target. For this reason only light targets were used in the present experiments.

The γ rays were detected with a γ spectrometer in which a NaI(Tl) crystal was used.[3,4] The energy losses of the neon ions in these targets were computed by means of the method proposed by Longchamp[5] and by the range-energy curve for neon ions in lead, plotted by A. Papineau using a method suggested in reference 6.* In the latter case the calculation of stopping power in the element of interest was carried out using the ratio of the specific energy loss in lead (obtained experimentally) to that in the given element for protons with the same velocity as the neon ions. The values of dE/dpx obtained by both methods agreed to within 12%.

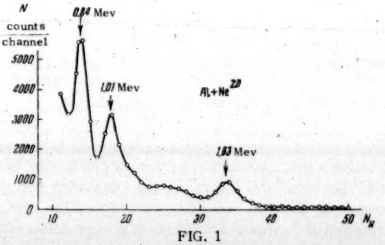

FIG. 1

In Figs. 1 and 2 are shown the spectra of γ rays emitted in the Coulomb excitation of the level characterized by $\Delta E = 1.63$ Mev for Ne^{20} ions and the level characterized by $\Delta E = 1.275$ Mev for Ne^{22} ions. In both cases the target is aluminum. Similar spectra were observed in the bombardment of the other targets. The only exceptions were boron and beryllium. No peak for $E = 1.63$ Mev was observed in bombardment by Ne^{20} ions because of the very strong γ background due to nuclear reactions. In

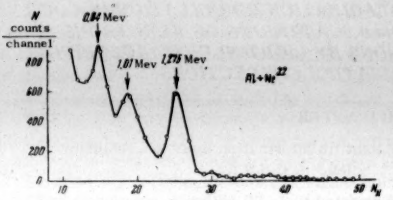

FIG. 2

the bombardment with Ne^{22} there was a well-defined peak for $E = 1.275$ Mev but the calculation of B(E2) gave a value which was considerably higher (in the case of beryllium, a factor of 10) than those obtained with the other targets. This is apparently due to the fact that in the $(Be + Ne^{22})$ and $(B + Ne^{22})$ reactions the collision energy is approximately the same as the value of the Coulomb barrier.

The mean values of B(E2) are $0.041\,e^2 \times 10^{-48}$ cm^4 for the Ne^{20} level characterized by $\Delta E = 1.63$ Mev and $0.025\,e^2 \times 10^{-48}$ cm for the Ne^{22} level characterized by $\Delta E = 1.275$ Mev. The mean life times for these states (τ) are respectively 8.6×10^{-13} sec and 4.8×10^{-12} sec. The indicated value of $\tau(Ne^{20})$ is in good agreement with the value reported in reference 7 in which τ was measured from the Doppler broadening of the γ-line and found to be $(7.6 \pm 3.3) \times 10^{-13}$ sec.

We wish to thank A. B. Girshin, and the cyclotron crew, for providing uninterrupted operation of the cyclotron.

*We are indebted to A. Papineau who kindly furnished us with a number of calculated curves.

[1] Heydenburg, Pieper, and Anderson, Phys. Rev. **108**, 106 (1957).

[2] Pieper, Anderson and Heydenburg, Bull. Am. Phys. Soc. **3**, 38 (1958).

[3] Alkhazov, Andreev, Grinberg, and Lemberg, Izv. Akad. Nauk SSSR, Ser. fiz. **20**, 1365 (1956). [Columbia Tech. Transl. **20**, 1249 (1956)].

[4] Alkhazov, Andreev, Erokhina, and Lemberg, J. Exptl. Theoret. Phys. (U.S.S.R.) **33**, 1347 (1957), Soviet Phys. JETP **6**, 1036 (1958).

[5] J. P. Longchamp, J. Phys. et radium, **14**, 89 (1956).

[6] A. Papineau, Compt. rend. **242**, 2933 (1956).

[7] Devons, Manning, and Towle, Proc. Phys. Soc. **A69**, 173 (1956).

Translated by H. Lashinsky
50

POLARIZATION CORRELATION IN COULOMB SCATTERING OF ELECTRONS AND MUONS BY LIGHT NUCLEI INCLUDING RADIATIVE CORRECTIONS

I. G. IVANTER

Scientific Information Institute, Academy of Sciences, U.S.S.R.

Submitted to JETP editor September 15, 1958

J. Exptl. Theoret. Phys. (U.S.S.R.) **36**, 325-326 (January, 1958)

THE general expression for the Coulomb scattering cross section of electrons with prescribed directions for the spin and momentum before and after scattering, and with neglect of radiative corrections, was given by Tolhoek.[1] However that work contains an error. Some results were also obtained by Passatore.[2]

We make use of the projection operators method developed by Tolhoek, de Groot, Fano, and Michel.[1]

If lowest order radiative corrections are taken into account one must include the second Born approximation in the calculations. The second Born approximation for this problem was first considered by Mott[3] in connection with the question of asymmetry in double scattering. Dalitz[4] has given the matrix element for the second Born approximation in the Feynman form.

The matrix element for the transition, including the second Born approximation and radiative corrections, has the form

$$M = A\gamma_4 - iB\hat{q} + C. \qquad (1)$$

A, B, and C contain no Dirac matrices; $\hat{q} \equiv \hat{p}_2 - \hat{p}_1$, where p_1 and p_2 are the four-momenta of the particle before and after scattering. Further $A = A_0 + A_1$ where $A_0 = 2\pi i Ze^2/|\mathbf{q}|^2$. Terms bilinear in the small quantities A_1, B, and C may be neglected in the matrix element squared.[5]

For the cross section for pure elastic scattering we find

$$d\sigma_s = \frac{1}{2\pi v}\rho_f \frac{d\omega}{4\varepsilon^2}\frac{1}{4}\mathrm{Sp}\{(A\gamma_4 - iB\gamma_4\hat{q} + C)(1 + i\hat{S}_1\gamma_5)(\hat{p}_1 + m) \times (A^*\gamma_4 + iB^*\hat{q}\gamma_4 + C^*)(1 + i\hat{S}_2)(\hat{p}_2 + m)\}. \qquad (2)$$

where v is the velocity and ϵ the energy of the particle, and S_1 and S_2 are Stokes' four-vectors; the indices 1 and 2 refer to before and after scattering respectively. Expression (2) can be written as the sum of four terms

$$d\sigma_s = {}^1/_2 d\overline{\sigma_s} + {}^1/_2 d\sigma_s(1) + d\sigma_s(2) + d\sigma_s(1, 2). \qquad (3)$$

Here $\overline{d\sigma_S}$ is the cross section averaged over the polarizations of the incident particle and summed over the polarizations of the scattered particle. The ratio $d\sigma_S(1)/\overline{d\sigma_S}$ gives the asymmetry in the scattering of polarized particles, the ratio $2d\sigma_S(2)/\overline{d\sigma_S}$ gives the degree of polarization in the scattering of unpolarized particles. The ratio $2d\sigma_S(1, 2)/\overline{d\sigma_S}$ corresponds to the "degree of polarization correlation" of the scattered and incident particles, or in other words it describes the spin rotation. Mott[3] obtained expressions for $d\sigma_S(1)$ and $d\sigma_S(2)$. Lowest order radiative corrections do not contribute to $d\sigma_S(1)$ and $d\sigma_S(2)$ (i.e., they do not affect the asymmetry in the scattering of polarized particles, nor the polarization in the scattering of unpolarized particles).

For pure elastic scattering we find for $d\sigma_S(1, 2)$:*

$$d\sigma_s(1, 2) = \frac{1}{2\pi v}\frac{\rho_f d\omega}{4\varepsilon^2}\{[\,|A_0|^2 + 2\mathrm{Re}(A_0A_1^*) + 4\mathrm{Im}(A_0B^*)m] \times (-1)F_1 + [2\,\mathrm{Re}(A_0C^*) + 4\,\mathrm{Im}(A_0B^*)\varepsilon]F_2\}. \qquad (4)$$

Here

$$F_1 \equiv -[(\mathbf{p}_1\cdot\mathbf{J}_1)(\mathbf{p}_2\cdot\mathbf{J}_2) + [(\varepsilon - m)/(\varepsilon + m)]\,[(\mathbf{p}_2\cdot\mathbf{J}_2)(\mathbf{p}_2\cdot\mathbf{J}_1) + (\mathbf{p}_1\cdot\mathbf{J}_1)(\mathbf{p}_1\cdot\mathbf{J}_2)] + (\mathbf{J}_1\cdot\mathbf{J}_2)(-m^2 - \varepsilon^2) - (\mathbf{J}_1\cdot\mathbf{J}_2)(\mathbf{p}_1\cdot\mathbf{p}_2) + (\mathbf{p}_2\cdot\mathbf{J}_1)(\mathbf{p}_1\cdot\mathbf{J}_2) - [2/(\varepsilon + m)^2](\mathbf{p}_2\cdot\mathbf{J}_2)(\mathbf{p}_1\cdot\mathbf{J}_1)(\mathbf{p}_1\cdot\mathbf{p}_2);$$

$$F_2 \equiv [(\varepsilon - m)/(\varepsilon + m)]\,[(\mathbf{p}_1\cdot\mathbf{J}_1)(\mathbf{p}_1\cdot\mathbf{J}_2) + (\mathbf{p}_2\cdot\mathbf{J}_2)(\mathbf{p}_2\cdot\mathbf{J}_1)] + 2\varepsilon m(\mathbf{J}_1\cdot\mathbf{J}_2) - [2/(\varepsilon + m)^2](\mathbf{p}_2\cdot\mathbf{J}_2)(\mathbf{p}_1\cdot\mathbf{J}_1)(\mathbf{p}_1\cdot\mathbf{p}_2). \qquad (4a)$$

$\mathbf{J}_1$, $\mathbf{J}_2$ are the spin directions of the particles in their rest system before and after scattering. The total differential cross section, which includes the emission of long wave length photons accompanying scattering with an energy change $\Delta\epsilon$, is of the same form as (4) with A_1 replaced by some A_1'. The expressions for A, B, and C are given in reference 5.

The expression for F_1 assumes a simple form if longitudinal polarization is considered:

$$F_{1\,\mathrm{long}} \equiv F_{1a} \sim [(\varepsilon^4 + m^4)\cos\theta + \varepsilon^4 + m^4 - 2\varepsilon^2m^2]/(\varepsilon^2 - m^2).$$

It follows that in scattering through an angle $\theta_0 = \cos^{-1}[(\epsilon^2 - m^2)^2/(\epsilon^4 + m^4)]$, F_{1a} vanishes but F_{2a} does not. Thus it may be expected that the measurement of residual longitudinal polarization after scattering through an angle θ_0 will provide the best experiment for the study of radiative corrections and the second Born approximation. It should be noted that the contribution to F_{2a} from the second Born approximation decreases with increasing energy. Thus, at $\epsilon = 4m$ the ratio of the contributions from the second Born approximation and the radiative corrections is already Z/10.6.

At low energies, on the other hand, the contribu-

tion from the second Born approximation is dominant.

The author expresses his gratitude to K. A. Ter-Martirosyan for many helpful discussions.

*The error in reference 1 consists of having the sum $[(\mathbf{p}_1\cdot\mathbf{J}_1)(\mathbf{p}_2\cdot\mathbf{J}_2)+(\mathbf{p}_1\cdot\mathbf{J}_2)(\mathbf{p}_2\cdot\mathbf{J}_1)]\,\mathbf{p}_2\cdot\mathbf{p}_1$ instead of $2(\mathbf{p}_1\cdot\mathbf{J}_2)\times(\mathbf{p}_1\cdot\mathbf{J}_1)(\mathbf{p}_2\cdot\mathbf{p}_1)$. It is easy to see that if $\hat{S}_1$, $\hat{S}_2$, $\hat{p}_1$ and $\hat{p}_2$ enter the square of the matrix element as factors only once it is impossible to obtain the second term of the sum.

[1] H. A. Tolhoek, Revs. Modern Phys. **28**, 277 (1956).

[2] G. Passatore, Nuovo cimento **6**, 850 (1957).

[3] N. F. Mott, Proc. Roy. Soc. (London) **A124**, 425 (1929).

[4] R. Dalitz, Proc. Roy. Soc. (London) **A206**, 509 (1951).

[5] A. I. Akhiezer and V. B. Berestetskii, Квантовая электродинамика (Quantum Electrodynamics) GITTL, 1953, pp. 358-364. [Engl. Transl. by U. S. Dept. of Commerce].

Translated by A. M. Bincer
51

K-LEVEL X-RAYS FROM FISSION FRAGMENTS AND DISTRIBUTION OF FRAGMENTS BY CHARGES

V. V. SKLYAREVSKII, E. P. STEPANOV, and B. A. MEDVEDEV

Submitted to JETP editor September 13, 1958

J. Exptl. Theoret. Phys. (U.S.S.R.) **36**, 326-328 (January, 1959)

We have observed earlier[1] that the 30-kev line appearing in the gamma-ray spectrum of U^{235} fission is not monochromatic; it has been supposed that this line represents K-level x-rays from heavy fission fragments with different Z, arising apparently in the internal conversion of the harder gamma rays due to fission. We report here the results of new measurements of the spectrum of soft gamma rays from the fission of U^{235}; these data have been used to estimate the widths of the distributions of the light and heavy fragments by charges.

The experimental setup consisted of an ionization chamber with a layer of U^{235} placed in the thermal-neutron beam of the RFT reactor of the U.S.S.R. Academy of Sciences, and a xenon proportional counter for the gamma rays. The spectra of the gamma-ray pulses coincident with the fission-fragment pulses were measured with an ELA-2 amplitude analyzer.[2]

The diagram shows the gamma-ray spectrum of U^{235} fission in the 10 — 50 kev range. Curve A is the spectrum of all the γ-f coincidences, curve C the random-coincidence spectrum, and curve B the spectrum of true coincidences from hard gammas and fission neutrons. This curve was obtained by measuring the spectrum of the γ-f coincidences with an 180-μ lead absorber placed between the chamber and counter. Curve D was obtained by subtracting B and C from A.

Calibration was with the 32.2-kev barium K line, emitted from a Cs^{137} source, and the Np 17.7-kev L_β line emitted from an Am^{241} source. The Cs^{137} and Am^{241} sources were thin layers of the substance, deposited on aluminum disks. During the measurements these disks were placed in the same position relative to the counter as the U^{235} layer. The half-widths of the calibration 17.7 and 32.2 kev lines were 20 and 14% respectively.

As seen from the diagram, the spectrum contains two intense non-monochromatic lines, whose maxima correspond to 16 ± 1 and 31 ± 1.5 kev, and whose half-widths are 35 and 22%, respectively. There is no doubt that these lines represent the K-level x-rays from the fragments of the light and heavy groups.

It is obvious that the energy distribution of the K-level x-rays of the fragments, W(E), is connected with the charge distribution of the fragments, W(Z). It is therefore possible to estimate the width of W(Z) from the results obtained. For such an estimate we can assume that the distributions W(E) and W(Z) are Gaussian with total widths at half height δ_E and δ_Z. Then $\delta_Z = \delta_E dZ/dE$ and, since $Z \approx 10\,E^{1/2}(\text{kev}) + 1$, where E is the energy of the K-level x-rays from an atom with

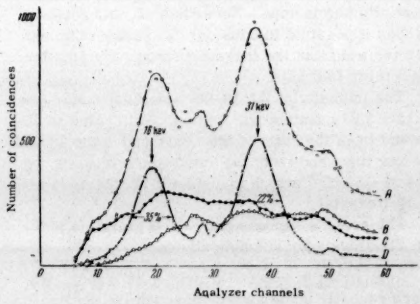

charge Z (Moseley formula), $\delta_Z/Z_0 = \delta_E/2E_0$, where E_0 corresponds to the position of the maximum on the distribution relative to E; the values of E_0 are 16 ± 1 and 31 ± 1.5 kev, and the values of Z_0 are 40 ± 1.5 and 56 ± 1.5.

It is necessary, in the determination of δ_E, to take into account the instrument line width. Since the line shape, for a proportional counter, can be assumed Gaussian with a half-width δ_k, the connection between the value of δ_E and the experimental line width, δ_{exp}, is given by $\delta_E = (\delta^2_{exp} - \delta^2_k)^{1/2}$. From the experimental values of δ_{exp}/E_0, 35 ± 4 and 22 ± 2 percent for the 31 and 16 kev lines respectively, and from the values of δ_k/E_0, which are 20 ± 2 and 14 ± 1 percent for the corresponding calibration lines, we get values of δ_Z/Z_0 of 14.5 ± 1.5 and 17 ± 3 percent respectively for the light and heavy group. These values are approximately the same as the known half-widths of the fragment mass distribution, which are 17% for the light group of fragments and 11.5% for the heavy one.[3]

It has been assumed in the foregoing analysis that the probability ν of emission of a K line is the same for fragments with different Z, which, in general, is not correct. In our paper devoted to the measurement of capture gamma-ray spectra,[4] we determined the yields of x-ray K radiation for several rare-earth elements:

Element	Eu_{63}	Gd_{64}	Dy_{66}	Ho_{67}	Er_{68}	Hf_{72}
Number of x-ray quanta to capture one neutron	0.34	0.15	0.15	0.8	0.45	0.39

The above data show that ν is not a monotonic function of Z, and that its deviations from the mean value reach ±70%. For fission gamma rays, ν should vary in a much narrower range than for capture gamma rays, since the fission gammas are emitted by a wide range of isotopes, while the capture gammas are emitted in most cases by essentially one isotope. Nevertheless, this factor makes it possible to consider the values obtained for the widths of the fragment charge distribution as a mere estimate.

The intensity of the 16-kev line was found to be 0.10 ± 0.03 quantum per fission. This value is obtained from the ratio of the areas under the 16 and 31 kev lines and from the value of the intensity of the 31-kev line, which is 0.42 ± 0.12, obtained with a NaI crystal.[1]

The authors express their deep gratitude to V. M. Strutinskii for valuable advice.

Note added in proof (November 26, 1958). We were recently made aware (through Dr. R. B. Litchman at the Second International Conference on Peaceful Uses of Atomic Energy, Geneva, 1958) of the results of Carter, Wagner, and Wayman, who observed in the gamma-ray spectrum of U^{235} fission (measured with a scintillation spectrometer with a NaI crystal) 18 and 32 kev peaks corresponding K-level x-rays from the fission fragments. In the spectrum measured with an argon-filled proportional counter, they found 2.1 and 3.6 kev peaks, corresponding to L-level x-rays from the fragments. No data are given on the intensities of these rays.

[1] Sklyarevskii, Fomenko, and Stepanov, J. Exptl. Theoret. Phys. **32**, 256 (1957), Soviet Phys. JETP **5**, 220 (1957).

[2] Mel'nikov, Artemenkov, and Golubev, Приборы и техника эксперимента (Instruments and Meas. Engg.) No. 6, p. 57 (1957).

[3] A. N. Murin, in Физика деления атомных ядер (Physics of Nuclear Fission), Atomizdat, M. 1957.

[4] Sklyarevskii, Stepanov, and Obinyakov, Атомная энергия (Atomic Energy) No. 1, p. 22 (1958).

Translated by J. G. Adashko
52

CONCERNING A 100-kev TRANSITION IN THE SPECTRUM OF Ce^{144}

A. V. GNEDICH, L. N. KRYUKOVA, and V. V. MURAV'EVA

Institute of Nuclear Physics, Moscow State University

Submitted to JETP editor September 22, 1958

J. Exptl. Theoret. Phys. (U.S.S.R.) **36**, 329 (January, 1959)

ALTHOUGH the radiation from Ce^{144} has been investigated by many authors, there is still no established $Ce^{144} - Pr^{144}$ decay scheme.

Conversion transitions between certain levels of Pr^{144} on different shells give very close electronic lines. This feature makes it difficult to interpret the conversion spectrum of Ce^{144} and makes the existence of certain transitions doubtful. In particular, there is no unequivocal answer to the question of whether a 100-kev transition is present.[1-4] This is a low-intensity transition between the 134 and 34 kev levels. The electron line ob-

served in the Ce^{144} spectrum near 58 kev has been interpreted as either K-100 or M-59. The L line of the 100-kev transition has not been separated, since it is located near the K-134 line, which is the most intense one in the spectrum; this made the presence of this transition doubtful.

We investigated the conversion spectrum of Ce^{144} with the aid of a spiral beta spectrometer having a resolution of 0.25%.

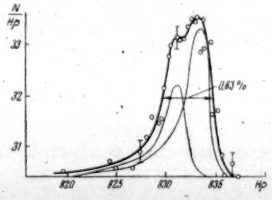

The diagram shows the 57.7-kev conversion line. The shape of this line and the fact that its half-width (0.63%) is greater than the single lines of this spectrum* make it obvious that this is a complex line. A graphical resolution of this line yielded two components with energies 57.76 and 57.45 kev. These energy values are in good agreement with the energy values of K-100 and M-59 and confirm the presence of both transitions. We also resolved the L_1-100 line, with $E_e = 92.83$ kev. According to our data, a more exact value of the energy of the 100-kev transition is 99.7 ± 0.1 kev. From the ratio of the areas under the K and the L_1 lines we obtain a ratio $\alpha_K/\alpha_{L_1} = 3.3 \pm 0.8$ kev for the ratio of the conversion coefficient of this transition. The possible contribution of the M-95 line has been estimated by us and is included in the error. The value obtained for the ratio of the conversion coefficients corresponds to an M3 transition.[5,6]

*The 38-kev K-80 line has a half-width of 0.38%.

[1] Cork, Brice, and Schmid, Phys. Rev. **96**, 1295 (1954).

[2] J. Pullman and P. Axel, Phys. Rev. **102**, 1366 (1956).

[3] Hickok, McKinley, and Fultz, Phys. Rev. **109**, 113 (1958).

[4] Parfenova, Forafrontov, and Shpinel', Izv. Akad. Nauk SSSR, Ser. Fiz. **21**, 1601 (1957), [Columbia Tech. Transl. **21**, 1590 (1957)].

[5] L. A. Sliv and I. M. Band, Таблицы коэффициентов внутренней конверсии (Tables of Internal Conversion Coefficients, part 1, K Shells). Acad. Sci. Press, M-L, 1956.

[6] L. A. Sliv and I. M. Band, Таблицы коэффициентов внутренней конверсии (Tables of Internal Conversion Coefficients, part 2, L Shells). Acad. Sci. Press, M-L, 1958.

Translated by J. G. Adashko
53

CONCERNING THE Ce^{141} *DECAY SCHEME*

N. V. FORAFONTOV and A. A. SOROKIN

Moscow State University

Submitted to JETP editor September 22, 1958

J. Exptl. Theoret. Phys. (U.S.S.R.) **36**, 330-331 (January, 1959)

We have measured the γ-γ and e^--γ coincidences to improve the accuracy of the decay scheme[1-5,7,8] of Ce^{144}.

The γ-γ coincidences were measured with a scintillation coincidence spectrometer.[6] Figure 1 shows the singles spectrum for Ce^{144} and the coincidence spectrum for γ rays in the 80-kev region. Peaks corresponding to x-rays from Pr^{144} and to γ-rays with an energy ~ 53 kev were visible in the coincidence spectrum. The peak at ~ 46 kev in the coincidence spectrum corresponds to Compton electrons from 134-kev γ rays and is due to the scattering of quanta from crystal to crystal. When the analyzer window is set at the 134-kev peak, the coincidence spectrum has no noticeable peaks up to 80 kev. To determine the upper limit for the intensity of the proposed 41 to 134 kev γ-γ cascade, comparative measurements were made for Ce^{144} and Sm^{153}. It was found that

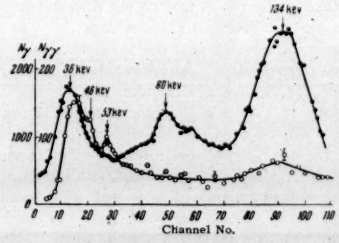

FIG. 1. •) Singles γ-ray spectrum; ○) $\gamma - \gamma$ coincidence spectrum (with random coincidence background included).

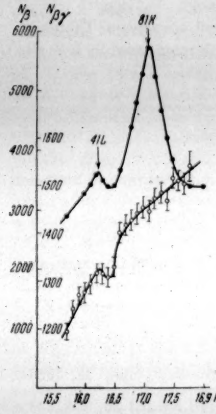

FIG. 2. •) β spectrum; o) $e^- - \gamma$ coincidence spectrum.

the intensity of the γ ray in cascade with the 134-kev line in Ce^{144} is less than 4×10^{-4} of that for the 134-kev transition. This value is defined by the statistical accuracy of the measurements. However, in a previous study,[7] we found an indication of a soft β spectrum with $E_\beta \simeq 130$ kev and we suggested that there may be a 41 to 134 kev cascade.

The absence of coincidences among the γ rays has prompted us to investigate coincidences of the 134-kev γ line with the 35-kev conversion line that had been observed in the primary β spectrum and that was identified as an L conversion transition of the 41-kev level. These coincidences were measured with a device described previously.[6,7] Figure 2 shows a portion of the coincidence spectrum which was obtained from one of a series of measurements. Also shown in Fig. 2 is the corresponding portion of the singles β spectrum. These data indicate that the 41L conversion line is in coincidence with the 134-kev γ line.

All these data are in agreement with a decay scheme which includes a 175-kev level.[2,4,7] In this case one must assume that the 41-kev transition undergoes practically total conversion. The values computed for the conversion coefficient in the L shell[9] show that for a multipolarity which is not less than E2, or even for E2 with an admixture of M1, the conversion coefficient is close to unity, and this is in complete agreement with the data from our measurements of γ-γ and e^--γ coincidences.

We wish to express our gratitude to A. G. Khudoverdyan and L. P. Zherebtsova for their assistance with the measurements.

[1] F. T. Porter and C. S. Cook, Phys. Rev. **87**, 464 (1952).

[2] Emmerich, Auth, and Kurbatov, Phys. Rev. **94**, 110 (1954).

[3] W. E. Kreger and C. S. Cook, Phys. Rev. **96**, 1276 (1954).

[4] Cork, Brice, and Schmid, Phys. Rev. **96**, 1295 (1954).

[5] J. Pullman and P. Axel, Phys. Rev. **102**, 1366 (1956).

[6] Delyagin, Sorokin, Forafontov and Shpinel', Izv. Akad. Nauk SSSR, Ser. Fiz. **20**, 913 (1956) [Columbia Tech. Transl. **20**, 828 (1956)].

[7] Parfenova, Forafontov, and Shpinel', Izv. Akad. Nauk SSSR, Ser. Fiz. **21**, 1601 (1957) [Columbia Tech. Transl. **21**, 1590 (1957)].

[8] Hickok, McKinely, and Fultz, Phys. Rev. **109**, 113 (1958).

[9] G. F. Dranitsina, Коэффициенты внутренней конверсии на L_I, L_{II}, L_{III} подоболочках (The Coefficients of Internal Conversion in the L_I, L_{II}, and L_{III} Subshells) Acad. Sci. Press (1957).

Translated by A. Skumanich
54

THE ELASTIC SCATTERING OF POLARIZED DIRAC PARTICLES BY A SHORT RANGE CENTER OF FORCE IN THE DAMPING THEORY

I. I. GUSEĬNOV

Moscow State University

Submitted to JETP editor September 24, 1958

J. Exptl. Theoret. Phys. (U.S.S.R.) **36**, 331-333 (January, 1959)

THE elastic scattering of Dirac particles by a fixed short range center of force including the effect of damping was investigated in references 1 and 2 (in the following we shall adhere to the notations of these papers). Reference 2 also took into account the polarization effects for the special case of scattering from a δ-function potential.

In the present note we consider the elastic scattering of Dirac particles by an arbitrary center of force with the inclusion of the polarization effects, using the damping theory. The solution of the fundamental integral equation of the damping theory is [cf. formula (28) of reference 2]

$$B'_{m_{s'}} = \frac{8\pi^2\hbar}{kK} \sum_{n,l,m} \frac{c_l^{(n)}}{1+ic_l^{(n)}} \Omega_{lm}^{(n)}(\mathbf{k}', m_{s'}) \Omega_{lm}^{*(n)}(\mathbf{k}, m_s) B_{m_s} \quad (1)$$

$B_{m_s} \equiv B_{m_s}(\mathbf{k})$ and $B'_{m_{s'}} \equiv B_{m_{s'}}(\mathbf{k}')$ are the amplitudes corresponding to the projection of the spin of the particle on the z axis ($m_s = \pm\frac{1}{2}$) in the initial and final states; $\Omega_m^{(n)}(\mathbf{k}, m_s)$ are the components of the spherical spinors; the quantities

$$c_l^{(n)} = -\tan\gamma_l^{(n)}$$

$$= \frac{1}{2}\left[\left(1+\frac{k_0}{K}\right)c_l + \left(1-\frac{k_0}{K}\right)c_{l\pm1}\right] \quad (n=1,2), \quad (2)$$

$$c_l = -\tan\gamma_l = \frac{\pi K}{c\hbar}\int_0^\infty rV(r)J_{l+1/2}^2(kr)dr \quad (3)$$

determine the scattering phase shifts for Dirac and spinless relativistic particles, respectively; n = 1, 2 denotes the value of the quantum number j for given l: $j = l + \frac{1}{2}$ for n = 1, and $j = l - \frac{1}{2}$ for n = 2.

The differential cross section for elastic scattering, taking into account the direction of the spin of the incoming and scattered particles, is given by

$$d\sigma_{m_{s'}m_s} = (K^2/4\pi^2c^2\hbar^2)\left(B'^*_{m_{s'}}B'_{m_{s'}} \Big/ \sum_{m_s} B^*_{m_s}B_{m_s}\right)d\Omega', \quad (4)$$

where $d\Omega' = \sin\theta'\,d\theta'\,d\varphi'$ is the element of solid angle.

With the z axis taken along the momentum of the incoming particle ($\mathbf{k} \parallel z$), we obtain for the amplitudes $B'_{m_{s'}}$:

$$B'_{1/2} = \frac{2\pi c\hbar}{K}[f(\vartheta')B_{1/2} - g(\vartheta')e^{-i\varphi'}B_{-1/2}],$$
$$B_{-1/2} = \frac{2\pi c\hbar}{K}[g(\vartheta')e^{i\varphi'}B_{1/2} + f(\vartheta')B_{-1/2}], \quad (5)$$

where

$$f(\vartheta') = \frac{1}{2ik}\sum_l\left[(l+1)(e^{2i\eta_l^{(1)}}-1) + l(e^{2i\eta_l^{(2)}}-1)\right] \times P_l(\cos\vartheta'), \quad (6)$$

$$g(\vartheta') = \frac{1}{2ik}\sum_l\left[-e^{2i\eta_l^{(1)}} + e^{2i\eta_l^{(2)}}\right]P_l^1(\cos\vartheta'). \quad (7)$$

From (4) we find the following expression for the differential cross section, for an arbitrary initial direction of the spins,

$$d\sigma = \sum_{m_{s'}} d\sigma_{m_{s'}m_s} = |f(\vartheta')|^2 + |g(\vartheta')|^2 + (g^*(\vartheta')f(\vartheta') - g(\vartheta')f^*(\vartheta'))$$
$$\times\{(B^*_{1/2}B_{-1/2}e^{-i\varphi'} - B^*_{-1/2}B_{1/2}e^{i\varphi'}) / (B^*_{1/2}B_{1/2} + B^*_{-1/2}B_{-1/2})\}. \quad (8)$$

It follows from these formulas that the scattering of an initially unpolarized beam ($B^*_{1/2}B_{1/2} + B^*_{-1/2}B_{-1/2} = 1$; $B^*_{1/2}B_{1/2} + B^*_{-1/2}B_{-1/2} = B^*_{1/2}B_{-1/2} = B^*_{-1/2}B_{1/2} = 0$) is accompanied by a partial polarization according to the relations

$$B'^*_{1/2}B'_{1/2} - B'^*_{-1/2}B'_{-1/2} \neq 0,$$
$$B'^*_{1/2}B'_{-1/2} = -e^{2i\varphi'}B'^*_{-1/2}B'_{1/2}$$
$$= 2\pi^2c^2\hbar^2K^{-2}e^{i\varphi'}(f^*(\vartheta')g(\vartheta') - g^*(\vartheta')f(\vartheta')),$$
$$B'^*_{1/2}B'_{1/2} + B'^*_{-1/2}B'_{-1/2} = 4\pi^2c^2\hbar^2K^{-2}(|f(\vartheta')|^2 + |g(\vartheta')|^2). \quad (9)$$

The polarization of the scattered beam can be observed by a second scattering. Indeed, denoting the quantities corresponding to the second scattering by a double prime ($\mathbf{k}' \parallel z$), we find for the differential cross section [formulas (8) and (9)]:

$$d\sigma(\vartheta'', \varphi'') = d\sigma_0(\vartheta'')(1 + \varepsilon(\vartheta', \vartheta'')\cos(\varphi'' - \varphi')), \quad (10)$$

where

$$\varepsilon(\vartheta', \vartheta'') = p(\vartheta')p(\vartheta''), \quad p(\vartheta)$$
$$= i(f(\vartheta)g^*(\vartheta) - g(\vartheta)f^*(\vartheta)) / (|f(\vartheta)|^2 + |g(\vartheta)|^2),$$
$$d\sigma_0(\vartheta'') = (|f(\vartheta'')|^2 + |g(\vartheta'')|^2)d\Omega'';$$

$d\sigma_0$ is the differential cross section for the scattering of an unpolarized beam in the damping theory; the quantities $p(\vartheta')$ and $p(\vartheta'')$ determine the polarization acquired by the initially unpolarized beam in the first and second scattering, respectively.

Formulas (8) and (10) have the same appearance as the formulas of Mott.[3] However, in the case considered by Mott, the quantities $f(\theta)$ and $g(\theta)$ must be determined from differential equations and can only in special cases be obtained in exact form. In the damping theory, on the other hand, these quantities have a completely definite form for an arbitrary short range scattering potential with spherical symmetry.

It is seen from formulas (10) that the asymmetry effect disappears in the general case for $\epsilon(\theta', \theta'') \to 0$, and that the unpolarized incoming beam remains unpolarized after the second scattering. In particular, for small energies ($k \ll k_0$) there will be no polarization at all, since in this case the scattering amplitude $g(\theta)$, and hence $\epsilon(\theta', \theta'')$ go to zero. Reversely, at high energies, the polarization plays an essential role.

It can be easily shown that formula (10) goes over into formula (36) of reference 2 in the case of scattering from a δ-function potential. The latter formula describes the double scattering of Dirac particles by a δ-function potential.

We remark that the polarization effects disappear if the damping effects are neglected [$f^*(\theta) = f(\theta)$ and $g^*(\theta) = g(\theta)$]. This corresponds to the first approximation in perturbation theory.

[1] Sokolov, Guseĭnov, and Kerimov, J. Exptl. Theoret. Phys. (U.S.S.R.) **34**, 110 (1958), Soviet Phys. JETP **7**, 76 (1958).

[2] Sokolov, Kerimov, and Guseĭnov, Nucl. Phys. **5**, 390 (1958).

[3] N. Mott and G. Massey, Theory of Atomic Collisions, Clarendon Press, Oxford, 1933 (Russ. trans. IIL, 1951).

Translated by R. Lipperheide
55

DECAY OF A BERYLLIUM HYPERFRAGMENT

A. O. VAĬSENBERG and V. A. SMIRNITSKIĬ

Submitted to JETP editor October 8, 1958

J. Exptl. Theoret. Phys. (U.S.S.R.) **36**, 333-335 (January, 1959)

A systematic scanning of Ilford G-5 emulsions[1] irradiated at an approximate altitude of 25 km we observed a non-mesonic decay of a beryllium hyperfragments, which permits a relatively accurate measurement of the binding energy of the Λ^0 particle.

A primary star of the 12 + 4p type (see microphotograph) emits a slow particle hf. It is stopped in the same layer and forms a secondary three-prong star. The hf range is 60 microns. An estimate of the charge, made by comparing the thickness of hf track with the thicknesses of the tracks of the Be^8 fragments and the alpha particles from the Be^8 decay yields $Z \approx 4$. An analogous estimate was made for tracks 1, 2, and 3. The measurement details are listed in the table.

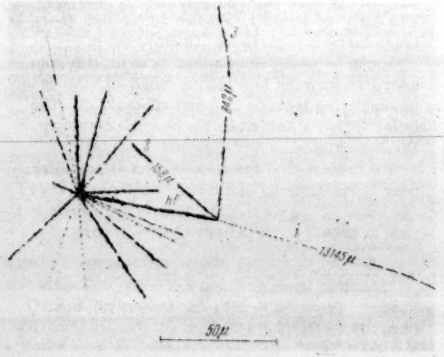

Track of Hyperfragment

Primary star	12 + 4p
Connected phenomena	None observed
Length, μ	60 ± 2
Angle with undeveloped emulsion	28° + 30′
Proof of stopping	Thinning
Charge hf	4
Energy of nucleon, Mev	≈ 3.9, if Be^8

Secondary Star

Track	1	2	3
Nature of particle	p	He^4	d
Range	13145	158	842
Experimental error	± 120	± 2	± 10
Measured mass, $m_e(\alpha, R)$	1820 ± 250	–	3400 ± 1300
Energy, Mev	61.4 ±0.8	19.1± 0.2	17.6± 0.3
Angle of inclination, θ	−1° 10′	41° 50′	−15° 50′
Error $\Delta\theta$	± 10′	± 30′	± 30′
Polar angle φ	182° 40′	17° 4p′	64°
Error $\Delta\varphi$	± 0.50	± 1°	± 1°

The total momentum of particles 1, 2, and 3 is 345.7 ± 2 Mev. Assuming that an equal and opposite momentum has been carried away by the neutron, we arrive at the following decay scheme:

$$^{*}_{\Lambda^0}Be^8 \rightarrow He^4 + d + p + n + Q, \quad Q = (160.0 \pm 1.3) \text{ Mev}.$$

We obtain for the binding energy of Λ^0 in the Be^8 nucleus $B_{\Lambda^0} = 9.2 \pm 1.6$ Mev.

The measured values of B_{Λ^0} for the known decays of $^{*}_{\Lambda^0}Be^8$ are 3.7 ± 3 (reference 2), 0 ± 5 (reference 3), 9.3 or 6.6 (depending on the decay scheme, reference 4), and 5.9 ± 0.5 (mesonic decay, reference 5).

The three decay schemes

$$^{*}_{\Lambda^0}Be^9 \rightarrow He^5 + d + p + n + Q;$$
$$^{*}_{\Lambda^0}Be^8 \rightarrow He^3 + H^3 + p + n + Q;$$
$$^{*}_{\Lambda^0}Be^9 \rightarrow He^4 + H^3 + p + n + Q$$

can be eliminated, for they lead to large negative values of B_{Λ^0}, equal respectively to 13.6 ± 1.8, −18.3 ± 1.8, and −27.5 ± 2.2 Mev.

Decay schemes with several neutral particles cannot be excluded, but are less probable. In the processing of the data we used the values of the constants from Shapiro's review[6] and the range-energy relations from the paper by Fry, Gottstein, and Hain.[7]

[1] A. O. Vaĭsenberg and V. A. Smirnitskiĭ, J. Exptl. Theoret. Phys. (U.S.S.R.) **32**, 736 (1957), Soviet Phys. JETP **5**, 607 (1957).

[2] Fry, Schneps, and Swani, Phys. Rev. **101**, 1526 (1956).

[3] M. Blau, Phys. Rev. **102**, 495 (1956).

[4] Gottstein, Roederer, Roederer, Varshneya, and Waloshek, Z. Naturforsch. **11a**, 152 (1956).

[5] Levi-Setti, Slater, and Telegdi, Preprint, 1958.

[6] A. M. Shapiro, Revs. Modern Phys. **28**, 161 (1956).

[7] Fry, Gottstein, and Hain, Nuovo cimento Suppl. No. 2, 234 (1954).

Translated by J. G. Adashko
56

ON THE PROBABILITY OF DOUBLE BETA DECAY

F. YANOUKH

Institute of Nuclear Physics, Moscow State University

Submitted to JETP editor October 8, 1958

J. Exptl. Theoret. Phys. (U.S.S.R.) **36**, 335-337 (January, 1959)

As is well known, the experimental searches for double β decay undertaken up to now have not met with success, although the accuracy of the experiments has increased so greatly that one of the latest papers[1] gives for the lower limit on the half-life $T_{1/2}$ a value of 0.7×10^{19} years. On the other hand theoretical calculations give for $T_{1/2}$ (in the Majorana scheme, $\nu \equiv \tilde{\nu}$) a quantity of the order of 10^{12} to 10^{19} years.[2-6] Therefore the negative results of searches for double decay can be interpreted as an indication that the neutrino is not a Majorana particle. At present, however, the accuracy of the experiments is still not great enough for the discovery of double β decay with Dirac neutrinos ($\nu \neq \tilde{\nu}$).

In view of the new situation in the theory of β decay it is useful to make a theoretical reexamination of the problem of the probability of double β decay, with due regard to effects of parity nonconservation and nonconservation of the leptonic charge (the latter possibility is evidently not very probable, but cannot as yet be finally rejected). The Hamiltonian of the β interaction with nonconservation of parity and leptonic charge has been discussed by Pauli,[7] Enz,[8] starting from Pauli's results, obtained the expression in general form for the probability of double β decay. We note the fact that the probability of double β decay is proportional to a combination of the squares of the quantities

$$I_{ij} = C_i C_j - C_i' C_j', \quad J_{ij} = C_i C_j - C_i' C_j'. \tag{1}$$

where C and C′ are the coupling constants for the terms conserving parity and not conserving it, and the indices i, j take the values S, V, T, A, P.

It can be seen from Eq. (1) that (for i = j) even in the case of the Majorana neutrino the probability of double β decay can be much smaller than the value previously given if $|C| \approx |C'|$, or can even be exactly zero if $|C| = |C'|$. One can get an idea of the ratio of the constants C and C′ from the data of experiments to measure the longitudinal polarization of β-ray electrons or the circular polarization of γ-ray quanta. At present the precision of these experiments is such that the equality $|C| = |C'|$ is established with an accuracy of 10 to 20 percent. In this scheme the theoretical value of the half-value period of double β decay can be written as follows (i = j = V; the order of magnitude of $T_{1/2}$ is practically independent of the choice of type of interaction):

$$T_{1/2} \leqslant 1 \cdot 10^{19} \frac{(ft)^2}{|I|^2 K(\epsilon)} \frac{A^{4/3}}{Z^2} \text{ sec}, \tag{2}$$

where ft is the well known quantity characteristic of β decay, Z and A are the atomic number and mass number, and $K(\epsilon)$ is a function depending on the energy ϵ of the transition (its values* for several nuclei are given in the table).† Setting $|C| = 0.8|C'|$, we get for Ca^{48} the result $T_{1/2} \leq 2 \cdot 10^{19}$ years.

As can be seen from Eq. (1), in the case of equality of the constants, $|C| = |C'|$, double β decay can occur only for the following choice of the signs of the constants: $C_i = -C_i'$, $C_j = C_j'$, or $C_i = C_i'$, $C_j = -C_j'$. But the very latest data on the polarization of β-ray electrons evidently agree with $C_S/C_S' = C_T/C_T' = 1$ and $C_V/C_V' = C_A/C_A' = -1$.[9] Using also the fact that the Fierz interference terms vanish, we get only the following two possible combinations of interaction types with which double β decay can occur: i = S, j = A, and i = V, j = T. It is well known, however, that double β decay occurs mainly between nuclei in 0^+ states. The probability of double β decay will be proportional to the product of the squares of the Fermi (M_F) and Gamow-Teller (M_{GT}) matrix elements. For allowed transitions M_F gives the selection rules $\Delta J = 0$ (no), whereas the allowed M_{GT} give the rules $\Delta J = 0, \pm 1$ (no), with $0 \rightarrow 0$ forbidden. Therefore double β decay can occur only through the level 1^- (or through levels with higher angular momentum), but then both the first transition ($Z \rightarrow Z + 1$) and the second transition ($Z + 1 \rightarrow Z + 2$) will be singly forbidden. The

Element	$K(\varepsilon)$	$F(\varepsilon)$
Ca^{48}	$2.4 \cdot 10^3$	$2.0 \cdot 10^3$
Zr^{96}	$4.8 \cdot 10^2$	$4.4 \cdot 10^2$
Te^{130}	$2.7 \cdot 10^2$	$2.4 \cdot 10^2$
Cd^{116}	$3.2 \cdot 10$	$2.8 \cdot 10$
Sn^{124}	3.5	2.8

latest data on the β decay of neutrons[9] evidently show that in β decay the V and A interaction types are realized; the precision of the experiment does not, however, exclude the possibility that there may also be present small amounts of the S and T types. Therefore it is of interest to calculate the probability of double β decay also in this scheme (transitions $0^+ \to 1^- \to 0^+$). We have obtained the following expression for the half-value period

$$T_{1/2} \lesssim 2 \cdot 10^{15} (ft)^2 Z^2 / (|I|^2 + |J|^2) F(\varepsilon) \text{ sec}, \qquad (3)$$

where $F(\epsilon)$ is a function that depends on the energy ϵ of the transition (see table). A large uncertainty in the value of $T_{1/2}$ is introduced by the quantity ft, which for the transitions in question can neither be calculated theoretically nor satisfactorily estimated from the experimental data. Making the usual assumption that $ft = 10^7$ for first-forbidden transitions,[10] and supposing that $|C_S/C_A| = 0.1$ (or $|C_T/C_V| = 0.1$), we get for Ca^{48} the value $T_{1/2} = 2 \times 10^{22}$ years.

The results of our calculations show that at the present time the question of the existence of neutrinoless double β decay cannot be regarded as finally settled by the work of Dobrokhov and others[1] and the search for this effect for the purpose of establishing higher values of the lower limit on $T_{1/2}$ is of real interest for the theory.

In conclusion the writer expresses his deep gratitude to I. S. Shapiro for the suggestion of this topic and help in studying it.

*The function $f(\varepsilon)$ used in references 2, 5, and 6 differs from our $K(\varepsilon)$ by the fact that in obtaining it account was taken of the energy dependence of the Coulomb correction factors. In references 5 and 6 the Coulomb factors are regarded as independent of the energy, but the writers use $f(\varepsilon)$ instead of $K(\varepsilon)$.

†In Eqs. (2) and (3) the β-decay constant is included in ft, so that $0 < |C| \leq 1$.

[1] Dobrokhotov, Lazarenko, and Luk'yanov, J. Exptl. Theoret. Phys. (U.S.S.R.), **36**, 76 (1959), Soviet Phys. JETP **9**, 54 (1959) (this issue).

[2] W. H. Furry, Phys. Rev. **56**, 1184 (1939).

[3] B. Touschek, Z. Physik **125**, 108 (1948).

[4] H. Primakoff, Phys. Rev. **85**, 888 (1952).

[5] L. Sliv, J. Exptl. Theoret. Phys. (U.S.S.R.) **20**, 1035 (1950).

[6] Zel'dovich, Luk'yanov, and Smorodinskii, Usp. Fiz. Nauk **54**, 361 (1954).

[7] W. Pauli, Nuovo cimento **6**, 204 (1957).

[8] C. P. Enz, Nuovo cimento **6**, 250 (1957).

[9] P. Nataf, Rapport au Congres Intern. de Phys. Nucl., Paris 1958.

[10] K. Siegbahn, Beta and Gamma Ray Spectroscopy, 1955, p. 435.

Translated by W. H. Furry
57

PAIR PRODUCTION BY A CIRCULARLY POLARIZED PHOTON

I. M. NADZHAFOV

Moscow State University

Submitted to JETP editor October 14, 1958

J. Exptl. Theoret. Phys. (U.S.S.R.) **36**, 337-339 (January, 1959)

THE theoretical prediction and experimental detection of longitudinally polarized electrons and positrons in the β decay of non-oriented nuclei has heightened interest in the problem of bremsstrahlung and electron-positron pair production, taking into account the polarization properties of the particles participating in these processes. Since the bremsstrahlung of a polarized electron has already been examined in references 1 to 4, we confine our investigation here to the pair production process. The bremsstrahlung and pair production process in the ultrarelativistic case was considered in reference 5.

In the present work, we investigate pair production by a circularly polarized photon in the field of a point nucleus. The treatment is general, and is suitable for all values of angles and energies.

In the Born approximation, the effective cross section for pair production is given by the formula

$$d\sigma_p(\eta_+, \eta_-)\, d\Omega_+ d\Omega_- = \frac{Z^2}{\pi^2}\left(\frac{e^2}{c\hbar}\right)^3 \frac{K_+ K_- k_+ k_- dK_+}{\kappa\kappa'^4} (S^+S)_p\, d\Omega_+ d\Omega_-, \qquad (1)$$

where $(S^+S)_p$ is the square of the matrix element for pair production, $E_\pm = c\hbar K_\pm = c\hbar\sqrt{k_0^2 + k_\pm^2}$, $\hbar k_\pm$ are the total energies and momenta of the positron and the electron, $\epsilon_{ph} = c\hbar\kappa = E_+ + E_-$, $\hbar\kappa$ are the energy and momentum of the photon, $\hbar\kappa' = \hbar\kappa - \hbar k_+$

$-\hbar\mathbf{k}_-$ is the momentum transferred to the nucleus, and $d\Omega_\pm$ are the solid angles of the emerging positron and electron.

Taking the spins of the photon, positron, and electron into account we obtain the following expression for $(S^+S)_p$:

$$(S^+S)_p = (4K_+K_-\varkappa^2)^{-1}\{F_{p0}(\theta_+,\theta_-) + s_+s_-F_{p1}(\theta_+,\theta_-) - ls_+F_{p2}(\theta_+,\theta_-) - ls_-F_{p3}(\theta_+,\theta_-)\}, \quad (2)$$

where

$$F_{p0}(\theta_+,\theta_-) = -(K_-^2-\varkappa^2/4)\,k_+^2\sin^2\theta_+/\Delta_+^2 - (K_+^2-\varkappa^2/4)\,k_-^2\sin^2\theta_-/\Delta_-^2 + (\varkappa^2/2-K_+K_--\varkappa^2/4) \times 2\delta/\Delta_+\Delta_- + (k_+^2\sin^2\theta_+ + k_-^2\sin^2\theta_-)\varkappa^2/2\Delta_+\Delta_-,$$

$$F_{p1}(\theta_+,\theta_-) = -(2k_+k_-)^{-1}\{[2(k_0^2-K_+K_-)(K_-^2-\varkappa^2/4) - k_0^2(3K_-^2+K_+^2)]\,k_+^2\sin^2\theta_+/\Delta_+^2 + [2(k_0^2-K_+K_-)(K_+^2-\varkappa^2/4) - k_0^2(3K_+^2+K_-^2)]\,k_-^2\sin^2\theta_-/\Delta_-^2 - 2[2(k_0^2-K_+K_-)(\varkappa^2/2 - K_+K_--\varkappa^2/4) - k_0^2(K_--K_+)^2]\,\delta/\Delta_+\Delta_- + \varkappa k_0^2(K_--K_+)\,\delta(\Delta_+^{-2}-\Delta_-^{-2}) + 4k_0^2\varkappa^2K_+K_-/\Delta_+\Delta_- + \varkappa^2K_+K_-(k_-^2\sin^2\theta_+ + k_+^2\sin^2\theta_-)/\Delta_+\Delta_- + \varkappa k_0^2(K_--K_+)\,(k_+^2\sin^2\theta_+ - k_-^2\sin^2\theta_-)/\Delta_+\Delta_- - \varkappa^2k_0^2(K_-/\Delta_- + K_+/\Delta_+) - \varkappa^2k_0^2(K_-(K_-+\varkappa^0\mathbf{k}_-)/\Delta_+^2 + K_+(K_++\varkappa^0\mathbf{k}_+)/\Delta_-^2)\},$$

$$F_{p2}(\theta_+,\theta_-) = -(2k_+)^{-1} \times \{(K_+\boldsymbol{\varkappa}\cdot\mathbf{k}_- - K_-\boldsymbol{\varkappa}\cdot\mathbf{k}_+ + K_-\varkappa^2 - \varkappa k_0^2)\,k_+^2\sin^2\theta_+/\Delta_+^2 + (K_+\boldsymbol{\varkappa}\cdot\mathbf{k}_- - K_+\boldsymbol{\varkappa}\cdot\mathbf{k}_+ - K_+\varkappa^2 + \varkappa k_0^2)\,k_-^2\sin^2\theta_-/\Delta_-^2 - 2K_-(\boldsymbol{\varkappa}\cdot\mathbf{k}_- - \boldsymbol{\varkappa}\cdot\mathbf{k}_+)\,\delta/\Delta_+\Delta_- + \varkappa(K_+\varkappa - k_0^2)(k_+^2\sin^2\theta_+ - k_-^2\sin^2\theta_-)/\Delta_+\Delta_- - \varkappa k_0^2\delta(\Delta_+^{-2}-\Delta_-^{-2}) + \varkappa^2k_0^2(k_-^2\sin^2\theta_- - k_+^2\sin^2\theta_+)/\Delta_-^2\Delta_+\},$$

$$F_{p3}(\theta_+,\theta_-) = -(2k_-)^{-1}\{(K_-\boldsymbol{\varkappa}\cdot\mathbf{k}_- - K_-\boldsymbol{\varkappa}\cdot\mathbf{k}_+ + K_-\varkappa^2 - \varkappa k_0^2)\,k_+^2\sin^2\theta_+/\Delta_+^2 + (K_-\boldsymbol{\varkappa}\cdot\mathbf{k}_- - K_-\boldsymbol{\varkappa}\cdot\mathbf{k}_+ - K_-\varkappa^2 + \varkappa k_0^2)\,k_-^2\sin^2\theta_-/\Delta_-^2 - 2K_-(\boldsymbol{\varkappa}\cdot\mathbf{k}_- - \boldsymbol{\varkappa}\cdot\mathbf{k}_+)\,\delta/\Delta_+\Delta_- - \varkappa k_0^2\delta(\Delta_+^{-2}-\Delta_-^{-2}) + \varkappa(K_-\varkappa - k_0^2)(k_+^2\sin^2\theta_+ - k_-^2\sin^2\theta_-)/\Delta_+\Delta_- + \varkappa^2k_0^2(k_-^2\sin^2\theta_- - k_+^2\sin^2\theta_+)/\Delta_+\Delta_-\},$$

$$\cos\theta_\pm = \mathbf{x}^0\cdot\mathbf{k}_\pm/k_\pm,\quad \Delta_\pm = K_\pm - k_\pm\cos\theta_\pm,$$

$$\delta = k_+k_-\sin\theta_+\sin\theta_-\cos(\varphi_+-\varphi_-),\quad \mathbf{x}^0 = \boldsymbol{\varkappa}/\varkappa. \quad (3)$$

The quantities l, s_+, $s_- = \pm 1$ in Eq. (2) determine the projections of the spins of the photon (in units of $\hbar$), the positron and the electron (in units of $\hbar/2$), respectively, in the directions of their motion.

Integrating the effective cross section over the angle of emergence θ_- of the electron, we obtain

$$d\sigma_p(\theta_+)\,d\Omega_+ = C_p\{Q_{p0}(\theta_+) + s_+s_-Q_{p1}(\theta_+) - ls_-Q_{p2}(\theta_-) - ls_+Q_{p3}(\theta_+)\}\,d\Omega_+, \quad (4)$$

where

$$Q_{pi}(\theta_+) = \int (F_{pi}(\theta_+,\theta_-)\,d\Omega_-)/\varkappa^4,\ i = 0,1,2,3,$$

can be expressed in terms of elementary functions (which we do not present here), and

$$C_p = Z^2(e^2/ch)^3\,k_+k_-dK_+/4\pi^2\varkappa^3.$$

After integrating Eq. (4) over θ_+, we obtain

$$d\sigma_p = C_p\{G_{p0} + s_+s_-G_{p1} - ls_-G_{p2} - ls_+G_{p3}\},$$

$$G_{pi} = \int Q_{pi}(\theta_+)\,d\Omega_+,\ i = 0,1,2,3. \quad (5)$$

for the effective cross section.

In the general case, the expressions for G_{pi} are quite unwieldy. However, in the ultra-relativistic case, they are substantially simplified:

$$G_{p0} = \eta_{ip}(2K_+K_- + 3K_+^2 + 3K_-^2),\quad G_{p1} = -\eta_{ip}(K_- - K_+)^2,$$
$$G_{p2} = -\eta_{ip}\varkappa(3K_+ - K_-),\quad G_{p3} = -\eta_{ip}\varkappa(3K_- - K_+),$$
$$\eta_{ip} = 2(L_p-1)\pi^2/3K_+K_-k_0^2,\quad L_p = 2\ln(2E_+E_-/\varepsilon_{ph}mc^2). \quad (6)$$

The result obtained by McVoy and Dyson[5] follows from Eqs. (5) and (6) as a special case.

In the case of complete screening, the quantity $L_p - 1$ in Eq. (6) is replaced by $2\ln(183\,Z^{-1/3})$ (to within $^2/_9$).

The degree of polarization of the pair can be determined as follows:

$$P_1(\theta_+) = \frac{d\sigma_p(\theta_+)_{\uparrow\uparrow} - d\sigma_p(\theta_+)_{\downarrow\downarrow}}{d\sigma_p(\theta_+)_{\uparrow\uparrow} + d\sigma_p(\theta_+)_{\downarrow\downarrow}},$$

$$P_2(\theta_+) = \frac{d\sigma_p(\theta_+)_{\uparrow_+} - d\sigma_p(\theta_+)_{\downarrow_+}}{d\sigma_p(\theta_+)_{\uparrow\downarrow} + d\sigma_p(\theta_+)_{\downarrow\uparrow}}, \quad (7)$$

where the first and second of the symbols $\uparrow$ and $\downarrow$ correspond to the values $+1$ and -1 of the spins s_+ and s_-. In the general case, Eqs. (4), (5), and (7) determine the angular and energy dependence of the effective cross section and the degree of polarization of the pair.

Recently, Olsen and Maximon investigated the process of bremsstrahlung and pair production in the ultra-relativistic case, taking Coulomb corrections and screening into account[6] (the effective cross section was averaged over the final spin states of the electron). It turned out that these corrections have no significant influence on the degree of polarization.

In conclusion, I would like to thank Prof. A. A. Sokolov for guidance, and B. K. Kerimov for discussion of the results.

[1] B. K. Kerimov and I. M. Nadzhafov, Izv. Akad. Nauk SSSR, Ser. Fiz. 22, 886 (1958) [Columbia Tech. Transl., in press]; Научн. докл. Высш. школы

(Scientific Reports of the Higher Schools) **1**, 95 (1958).

[2] I. M. Nadzhafov, Вестник МГУ (Bulletin, Moscow State Univ.) Mat. Mech. Astr. Phys. and Chem. Ser., No. 3, 1958.

[3] Vysotskiĭ, Kresnin, and Rozentsveĭg, J. Exptl. Theoret. Phys. (U.S.S.R.) **32**, 1078 (1957), Soviet Phys. JETP **5**, 883 (1957).

[4] Kirk W. McVoy, Phys. Rev. **106**, 828 (1957).

[5] Kirk W. McVoy and F. J. Dyson, Phys. Rev. **106**, 1360 (1957).

[6] H. Olsen and L. C. Maximon, Phys. Rev. **110**, 589 (1958).

Translated by D. Lieberman
58

RADIATION FROM A SPIN-2 PARTICLE MOVING UNIFORMLY IN A MEDIUM

A. I. BEDRITSKIĬ

Vitebsk Pedagogical Institute

Submitted to JETP editor October 13, 1958

J. Exptl. Theoret. Phys. (U.S.S.R.) **36**, 339-341 (January, 1959)

THE energy radiated from a particle with spin 2, moving uniformly in a medium with a velocity higher than the phase velocity of light in that medium (Cerenkov effect), can be determined in analogy to the phenomenological theory of this effect for the electron (see reference 1, §32).

The free field operator for a particle with spin 2 has, according to the general, relativistically-covariant equations of first order,[2] the form

$$D = i\hbar\gamma_4\partial/\partial t - \hbar c(\gamma\nabla) - mc^2, \qquad (1)$$

where the matrices γ, of dimension thirty, are known from references 3 and 4. The interaction of charged particles with the electromagnetic field is obtained by changing the operator $\partial/\partial x_k$ to the operator $\partial/\partial x_k - (ie/\hbar c)A_k$. The field of virtual photons interacting with the particle moving in a dielectric with a refraction coefficient $n = c/c'$ is obtained from the fundamental formula (1) in analogy to the theory for the electron.[1] The result is

$$w^+(\mathbf{r}, t) = -ieL^{-3/2}\sum_{\mathbf{K}}\sqrt{2\pi c'\hbar/K}\,(\boldsymbol{\gamma}\cdot\mathbf{a}^+) \times \exp(ic'K_0 t - i\mathbf{K}\cdot\mathbf{r}), \qquad (2)$$

where e is the charge of the particle, K_1, K_2, K_3, and $K_0 = K = \sqrt{K_1^2 + K_2^2 + K_3^2}$ form the four-dimensional wave vector of the photon, $\mathbf{a}^+(a_1^+, a_2^+, a_3^+)$ are the amplitudes of the photon field acting on a function of the number of photons included in the wave function. The a_n^+ satisfy the commutation relations

$$a_n^+ a_{n'} = 0, \quad a_n a_{n'}^+ = \delta_{nn'} - K_n K_{n'}/K^2 \qquad (3)$$

and the condition of transversality $(\mathbf{K}\cdot\mathbf{a}^+) = 0$.

The probability for the radiation process can be determined by considerations similar to those of the electron case. The energy W radiated from the particle per unit time is

$$W = c^2 c \int_0^{\omega_m} \frac{k_0' K^2}{nk} G\,dK, \quad G = \frac{1}{5Kn}\sum_{s,s'} \frac{b^+(\boldsymbol{\gamma}^+\mathbf{a})\gamma_4^+ b' \cdot b'^+\gamma_4(\boldsymbol{\gamma}\mathbf{a}^+)\,b}{b'^+\gamma_4^+ b' \cdot b'^+\gamma_4 b}, \qquad (4)$$

where b and b′ are thirty-component functions of the wave vectors k_e and k_e'; the primes refer to the state of the particle after radiation; ω_m is the maximal radiation frequency, which depends on the momentum of the particle according to the formula

$$\omega_m = \frac{2pc}{n\hbar}\,\frac{1 - 1/n^2}{1 - n^{-2}}, \qquad (5)$$

the direction of the radiation is determined by

$$\cos\vartheta = 1/n\beta + (K/2k)(1 - n^{-2}), \qquad (6)$$

$\beta = v/c$, where v is the velocity of the particle. The conservation laws are fulfilled: $\mathbf{k}' = \mathbf{k} - \mathbf{K}$, $k_0' = k_0 - K/n$. The frequency of the light radiated from the particle is equal to $\omega = cK/n$.

The classification of the wave functions according to the projection of the spin on the momentum of the particle and the normalization with respect to the charge $\psi^* A\gamma_4 = 1$ in the calculation of the quantity G were carried out with the help of the covariant method proposed by Fedorov.[5]

In the general case, as well as in the nonrelativistic approximation, we were faced with exceedingly complex calculations, which we were unable to master. The comparatively simple calculation in the extreme relativistic case leads, with (4), to

$$W = \frac{e^2E^2}{5120\,cE_0^4}\int_0^{\omega_m}\omega\left\{32\frac{(E - n\hbar\omega\cos\vartheta)^4}{(E - \hbar\omega)^2} + 32(E - n\hbar\omega\cos\vartheta)^2 + \frac{(\hbar\omega)^2\sin^2\vartheta}{E - \hbar\omega}(E - n\hbar\omega\cos\vartheta) + (E - \hbar\omega)(E - n\hbar\omega\cos\vartheta) + 4\cos^2\vartheta\left[\frac{n^6(\hbar\omega)^6\sin^6\vartheta}{(E - \hbar\omega)^4} + 4\frac{n^4(\hbar\omega)^4\sin^4\vartheta}{(E - \hbar\omega)^2} + 3n^2(\hbar\omega)^2\sin^2\vartheta\right] + 8\cos\vartheta\sin\vartheta\left[\frac{n^5(\hbar\omega)^5\sin^5\vartheta}{(E - \hbar\omega)^4}(E - n\hbar\omega\cos\vartheta) + 8\frac{n^3(\hbar\omega)^3\sin^3\vartheta}{E - \hbar\omega} + 3\frac{n^3(\hbar\omega)^3\sin^3\vartheta}{(E - \hbar\omega)^2}(E - n\hbar\omega\cos\vartheta)\right]\right\}d\omega, \qquad (7)$$

where

$$\cos\theta = \frac{1}{n} + \frac{\hbar\omega}{2E}\left(n - \frac{1}{n}\right), \quad \omega_m = \frac{2pc}{(n+1)\hbar},$$

E is the initial energy of the particle, and $E_0 = mc^2$ is the rest energy.

For a medium with a refraction index close to unity ($\cos\theta \approx 1$, $\sin\theta \approx 0$), we obtain from (7):

$$W = \frac{13}{1024}\frac{e^2E^2}{cE_0^4}\int_0^{\omega_m}\omega(E-\hbar\omega)^2\,d\omega, \quad \omega_m = \frac{pc}{\hbar}. \qquad (8)$$

If the energy of the emitted quantum is significantly smaller than the energy of the particle ($\hbar\omega \ll E$), then $\cos\theta = 1/n$, and we have for the radiation energy, from (7),

$$W = \frac{13}{1024}\frac{e^2}{c}\left(\frac{E}{E_0}\right)^4\int_0^{\omega_m}\omega\,d\omega, \qquad (9)$$

where only $\omega_m = 2pc/(n+1)\hbar$ ($n \gg 1$) depends on the index of refraction.

A specific feature of these results is the unlimited increase of the radiation energy with growing initial energy of the particle. This is in agreement with the latest experimental data on the intensity of the Cerenkov radiation caused by the particles of the cosmic radiation. Jelley notes[6] that Bassi and his co-workers have established, in a series of experiments on the changes in the intensity of the Cerenkov radiation of cosmic-ray particles, that the yield of light increases with increasing energy for very high particle energies. Jelley's view[6] is that this increase of radiation for high energies cannot be explained by knock-on electrons, nor by any other cause, and that the results of these experiments confirm the conclusions of Budini, who predicted a logarithmic increase of the radiation of the particles at extremely relativistic energies in dense media, in analogy to the increase of the ionization losses at such energies.

I express my sincere gratitude to Prof. F. I. Fedorov for valuable advice.

[1] A. A. Sokolov and D. D. Ivanenko, Квантовая теория поля (Quantum Theory of Fields), M.-L., 1952.

[2] I. M. Gel'fand and A. M. Yaglom, J. Exptl. Theoret. Phys. (U.S.S.R.) **18**, 703 (1948).

[3] F. I. Fedorov, Уч. зап. Белорус. гос. ун., серия физ.-мат. (Sci. Notes, Belorussian State Univ., Phys.-Math. Series) **12**, 156 (1951).

[4] A. I. Bedritskiĭ, J. Exptl. Theoret. Phys. (U.S.S.R.) **35**, 1278 (1958), Soviet Phys. JETP **8**, 892 (1959).

[5] F. I. Fedorov, J. Exptl. Theoret. Phys. (U.S.S.R.) **35**, 493 (1958). Soviet Phys. JETP **8**, 339 (1959).

[6] J. V. Jelley, Progr. Nucl. Phys. **3**, 84-130 [Russ. Transl., Usp. Fiz. Nauk **58**, 231 (1956)].

Translated by R. Lipperheide
59

DISAPPEARANCE OF THE ISOTHERMAL JUMP AT LARGE RADIATION DENSITY

V. A. BELOKON'

Institute of Chemical Physics, Academy of Sciences, U.S.S.R.

Submitted to JETP editor October 18, 1958

J. Exptl. Theoret. Phys. (U.S.S.R.) **36**, 341-343 (January, 1959)

THE theory of finite disturbances in gas, based on the differential equations of hydrodynamics without supplementary assumptions, leads, in the complete absence of dissipative factors and continuous initial conditions, to absurd triple-valued flow parameters.[1] To eliminate this difficulty, Stokes and Riemann postulated a flow discontinuity that satisfies the boundary conditions.[2] Rankin and Rayleigh,[3] staying within the framework of a continuum, examined a heat-conduction mechanism by which "jumps" can be realized, and considered the results of Stokes, Riemann, and Hugoniot as a trivial neglect of the dissipation mechanism. Rayleigh observed here that the heat-conduction structure of a compression wave with a profile that remains unchanged in time can be continuous only if

$$p_{+\infty}/p_{-\infty} \leqslant (\varkappa+1)/(3-\varkappa) \equiv (i+1)/(i-1). \qquad (1)$$

Waves of greater amplitude experience an "overturn" similar to the Riemannian overturn of adiabatic wave. The "isothermal jump" (see reference 4) resolves the Rayleigh paradox, although the meaning of such a solution again reduces somehow to ignoring, within the scope of the stated problem, dissipative factors other than heat conduction (such as viscosity and diffusion). In this solution one has in mind a radiant heat conduction, but the radiation density is neglected, and the conclusion is that the structure of a wave of amplitude (1), with the inequality sign reversed, includes the isothermal jump.

Considering, as before, the gas to be a continuous heat-conducting medium that retains local ther-

modynamic equilibrium, we shall show that the isothermal jump vanishes in a sufficiently hot gas.

We determine the equation of state

$$p_a + p_\gamma = \rho RT + a_0 T^4/3 = p; \quad \rho = 1/V \qquad (2)$$

and the enthalpy

$$H = c_p T + \frac{4}{3} a_0 T^4 V = \left(\frac{i+2}{2} p_a + 4p_\gamma\right) V \qquad (3)$$

with allowance for the radiation density. By virtue of the fact that in such a gas the isothermal velocity of sound increases relatively slowly,

$$a_T^2 \equiv (\partial p/\partial \rho)_T = (\partial/\partial \rho)_T (\rho RT + {}^1/_3 a_0 T^4) = RT = p_a V, \qquad (4)$$

the following relation is satisfied behind the shock wave at certain amplitudes

$$\begin{aligned} -V_{+\infty}^2 (p_{+\infty} - p_{-\infty})/(V_{+\infty} - V_{-\infty}) \\ = u_{+\infty}^2 > a_T^2 = -V_{+\infty}^2 (\partial p/\partial V)_{T,+\infty} \end{aligned} \qquad (5a)$$

or

$$\begin{aligned} -(\partial p/\partial V)_{T,+\infty} = (p_{+\infty} - p_{\gamma,+\infty})/V_{+\infty} \\ \leqslant -(p_{+\infty} - p_{-\infty})/(V_{+\infty} - V_{-\infty}), \end{aligned}$$

which leads to the condition

$$\begin{aligned} (p_\gamma/p)_{+\infty} (V_{-\infty}/V_{+\infty} - 1) \\ \geqslant (V_{-\infty}/V_{+\infty} - 2) + p_{-\infty}/p_{+\infty}. \end{aligned} \qquad (5b)$$

It is easy to see, for example from the p-V diagram, that condition (5a) is equivalent to stating that the temperature is monotonic along the line of evolution of the heat-conducting gas within the shock wave:

$$-\frac{p_{+\infty} - p_{-\infty}}{V_{+\infty} - V_{-\infty}} = -\frac{dp}{dV} = j^2 \equiv (\rho u)^2 = \text{const}.$$

This is correct also for a non-radiating gas [in the latter case we obtain Eq. (1)]. For strong waves, from the conservation conditions for the flow of energy and momentum

$$\begin{aligned} j^2 (V_{-\infty}^2 - V_{+\infty}^2) = V_{+\infty} [(6-i) p_{\gamma,+\infty} + (i-2) p_{+\infty}], \\ j^2 (V_{-\infty} - V_{+\infty}) = p_{+\infty}, \end{aligned}$$

we get the total compression on the wave in the radiating gas:

$$\begin{aligned} V_{-\infty}/V_{+\infty} = i + 1 + (6-i) p_{\gamma,+\infty}/p_{+\infty} \to 7 \\ \text{for } p_{\gamma,+\infty}/p_{+\infty} \to 1. \end{aligned} \qquad (6)$$

Expressing $(p_\gamma/p)_{+\infty}$ in terms of $V_{-\infty}/V_{+\infty}$ in (5b) we obtain the inequality

$$(V_{-\infty}/V_{+\infty})^2 - 8V_{-\infty}/V_{+\infty} + 13 - i \geqslant 0, \qquad (7)$$

which means that waves on which

$$V_{-\infty}/V_{+\infty} \geqslant 4 + \sqrt{3+i} = 6.45 \text{ (for } i = 3) \qquad (8)$$

(we disregard the second root, for we specified large amplitudes) have a monotonic temperature profile in the heat-conduction approximation. The equality corresponds to the transformation of the isothermal jump into isothermal sound.

In conclusion, I consider it my pleasant duty to express my indebtedness to my associates at the Institute of Chemical Physics, K. E. Gubkin, O. S. Ryzhov, and A. A. Milyutin, for valuable discussions.

[1] R. Sauer, Flow of Compressible Fluid, Russ. Transl. IIL, 1954, pp. 272 ff. [Ecoulement des Fluides Compressibles, Paris, Beranger, 1951.]

[2] B. Riemann, Collected Works, GITTL, 1948, pp. 383-385.

[3] Lord Rayleigh, Scientific Papers, Vol. 5, pp. 247-284.

[4] L. D. Landau and E. M. Lifshitz, Механика сплошных сред (Mechanics of Continuous Bodies) GITTL, 1951, §88.

Translated by J. G. Adashko
60

THE CONDUCTIVITY OF SEMI-CONDUCTORS IN AN ULTRASONIC FIELD

V. A. ZHURAVLEV and M. I. KOZAK

L'vov State Medical Institute

Submitted to JETP editor August 30, 1958

J. Exptl. Theoret. Phys. (U.S.S.R.) **36**, 343-344 (January, 1959)

In the literature there are several references to the effect of ultrasonics on the luminescence[1-4] and photoconductivity of semiconductors.[5]

We have examined the influence of ultrasonics on the conductivity of a number of semiconductors, and have studied specimens of selenium, cadmium sulphide, lead sulphide, cuprous oxide, stannic oxide and germanium, irradiated with 10 w/cm^2 of ultrasound at 600 Kcs. In all cases a change of conductivity was found on irradiation, but analysis of these changes shows that the ultrasound does not have a specific action on the conductivity, but that the effects follow from the heating of the specimen. The conductivity did not change immediately on switching on the ultrasound, but increased or decreased (depending on the sign of the temperature coefficient for the specimen) during the heating of the sample on irradiation. Simultaneous measurement of the temperature and conductivity shows that the latter varies as $\sigma = \sigma_0 \exp\{-E/kT\}$, i.e.,

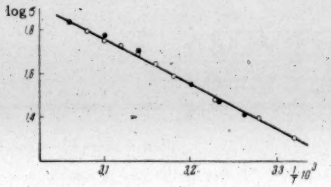

FIG. 1

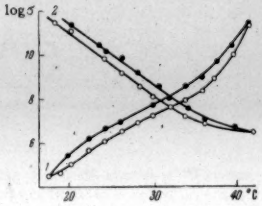

FIG. 2

there is no variation in conductivity over and above the temperature effect. On switching off the ultrasound, the specimen cools down and one finds that any temperature corresponds to the same value of conductivity, whether it is reached during irradiation or during cooling. This shows clearly the purely temperature action of the ultrasound. These results are illustrated in Fig. 1, which shows the dependence of conductivity on temperature for lead sulfide, on a log σ vs. 1/T plot, during irradiation (full circles) and on cooling at the end of the irradiation (open circles).

Similar results were obtained with copper oxide, stannic oxide, cadmium sulfide, and germanium, but there were some differences in the case of selenium. We examined two groups of selenium specimens, one with positive and the other with negative temperature coefficients. On increasing the temperature by irradiation the conductivity of the former increased while for the latter it decreased. The conductivity of selenium showed some hysteresis on heating and cooling (this is shown in Fig. 2, in which curve 1 applies to a specimen with positive temperature coefficient and curve 2 to a negative coefficient). The cause of this instability in conductivity was examined in studies of the temperature dependence of the conductivity of selenium.[6] Investigation of the influence of ultrasound on the photoconductivity of cadmium sulfide and of selenium also shows that this effect corresponds to a thermal action.

In view of the foregoing, it is essential to have some confirmation of a specific action of ultrasound on luminescence,[4] as Leistner did not measure the temperature of the irradiated specimen. Some differences between the variation of the intensity of luminescence with irradiation and with external heating could be explained by the different heating conditions in these two cases.

[1] H. Schreiber and W. Degner, Ann. Physik **7**, 275 (1950).

[2] I. G. Polotskii, J. Phys. Chem. (U.S.S.R.) **22**, 787 (1948).

[3] V. Bredin, Usp. Fiz. Nauk. **42**, 584 (1950).

[4] M. Leistner, Ann. Physik **20**, 129 (1957).

[5] L. Helforth and J. Krumbiegel, Naturwiss. **42**, 39 (1955).

[6] R. Yu. Kadań, J. Exptl. Theoret. Phys. (U.S.S.R.) **24**, 714 (1953).

Translated by R. Berman
61

ANNOUNCEMENT

Beginning with the current issue, this journal will change its transliteration system from that of the Library of Congress to that known as the British Standard. This latter has recently achieved wide adoption in England, and will be used in 1959 by a large number of abstracting journals in the United States.

The changes from the Library of Congress system are few; they are listed below. The primary advantage of the new system is that it permits unambiguous re-transliteration from English to Russian. At the same time, there is strong reason to hope, and grounds for believing, that this system will achieve virtually universal adoption, at least in the Anglo-American scientific community.

The changes are as follows:

Russian	Library of Congress	British Standard
й	i	ĭ
тс	ts	t-s
ы	y	$\bar{y}$
э	e	é
ю	iu	yu
я	ia	ya

The bar will be placed over the letter y only if the Russian ы is followed by a y or a.

SOVIET PHYSICS JOURNALS

Published in English by the American Institute of Physics

Soviet Physics – JETP

A translation, beginning with 1955 issues of "Journal of Experimental and Theoretical Physics" of the USSR Academy of Sciences. Leading physics journal of Soviet Union. Similar to "The Physical Review" in quality and range of topics. Outstanding new work is most likely to appear in this journal.

Twelve issues, approximately 3,500 pages. $75 domestic, $79 foreign. Libraries $35 domestic, $39 foreign. Single copies, $8.*

Soviet Physics – SOLID STATE

A translation, beginning with 1959 issues of "Fizika Tverdogo Tela" of the USSR Academy of Sciences. Offering results of theoretical and experimental investigations in the physics of semiconductors, dielectrics, and on applied physics associated with these problems. Also publishes papers on electronic processes taking place in the interior and on the surface of solids.

Twelve issues, approximately 2,000 pages. $55 domestic, $59 foreign. Libraries $25 domestic, $29 foreign. Single copies, $8.*

Soviet Physics – TECHNICAL PHYSICS

A translation, beginning with the 1956 issues of the "Journal of Technical Physics" of the USSR Academy of Sciences. Contains work on plasma physics and magnetohydrodynamics, aerodynamics, ion and electron optics and radio physics. Also publishes articles in mathematical physics, the physics of accelerators and molecular physics.

Twelve issues, approximately 2,000 pages, $55 domestic, $59 foreign. Libraries $25 domestic, $29 foreign. Single copies, $8.*

Soviet Physics– ACOUSTICS

A translation, beginning with 1955 issues of "Journal of Acoustics" of USSR Academy of Sciences. Devoted principally to physical acoustics but includes electro, bio, and psycho acoustics. Mathematical and experimental work with emphasis on pure research.

Four issues, approximately 400 pages. $12 domestic, $14 foreign. (No library discounts) Single copies, $4.

Soviet Physics – DOKLADY

A translation, beginning with 1956 issues of "Physics Sections" of Proceedings of USSR Academy of Sciences. All-science journal offering four-page reports of recent research in physics and borderline subjects.

Six issues, approximately 1,500 pages. $35 domestic, $38 foreign. Libraries $15 domestic, $18 foreign. Single copies Vols. 1 and 2, $5; Vol. 3 and later issues, $7.*

Soviet Physics – CRYSTALLOGRAPHY

A translation, beginning with 1957 issues of the journal "Crystallography" of USSR Academy of Sciences. Experimental and theoretical papers on crystal structure, lattice theory, diffraction studies, and other topics of interest to crystallographers, mineralogists, and metallurgists.

Six issues, approximately 1,000 pages. $25 domestic, $27 foreign. Libraries $10 domestic, $12 foreign. Single copies, $5.*

SOVIET ASTRONOMY – AJ

A translation, beginning with 1957 issues of "Astronomical Journal" of USSR Academy of Sciences. Covers various problems of interest to astronomers and astrophysicists including solar activity, stellar studies, spectroscopic investigations of radio astronomy.

Six issues, approximately 1,100 pages. $25 domestic, $27 foreign. Libraries $10 domestic, $12 foreign. Single copies, $5.*

Soviet Physics – USPEKHI

A translation, beginning with September, 1958 issue of "Uspekhi Fizicheskikh Nauk" of USSR Academy of Sciences. Offers reviews of recent developments comparable in scope and treatment to those carried in "Reviews of Modern Physics." Also contains reports on scientific meetings within the Soviet Union, book reviews, and personalia.

Six issues, approximately 1,700 pages. (Contents limited to material from Soviet sources.) $45 domestic, $48 foreign. Libraries $20 domestic, $23 foreign. Single copies, $9.*

*For libraries of non-profit degree-granting academic institutions.

Subscription prices subject to annual variation depending on size of Russian originals.

Please send orders and inquiries to

American Institute of Physics

335 East 45 Street, New York 17, N. Y.

CONTENTS--continued

	Page	Russian Reference
Gamma Oscillations of the Surface of an Atomic Nucleus . . . . . A. S. Davydov and D. A. Zaikin	157	36, 233
Cerenkov Radiation of an Electron Moving in a Medium with Spatial Dispersion . . . . . V. N. Agranovich, V. E. Pafomov, and A. A. Rukhadze	160	36, 238
Generalized Form of the Dependence of the Pion Cross Section in Complex Nuclei on the Number of Nucleons . . . . . A. S. Belousov, B. B. Govorkov, and V. I. Gol'danskii	164	36, 244
Breakup of a Charged Liquid Drop and Nuclear Fission . . . . . B. T. Geilikman	168	36, 249
Contribution to the Theory of Multiple Scattering . . . . . M. L. Ter-Mikaelyan	171	36, 253
Adsorption of Polarized Negative Muons by Nuclei and Neutron Polarization . . . . . L. D. Blokhintsev	175	36, 258
Charge Symmetry Properties and Representations of the Extended Lorentz Group in the Theory of Elementary Particles . . . . . V. I. Ogievetskii and Chou Kuang-Chao	179	36, 264
Cyclic Motion of Charged Particles in an Electric Field . . . . . A. A. Kolomenskii and Fong Soy-Cen	184	36, 271
Depolarization of the Negative Muon in Mesic-Atom Transitions . . . . . V. A. Dzhrbashyan	188	36, 277
Estimate of the Contribution of Nucleon-Antinucleon Interaction in the Dispersion Relation for Nucleon-Nucleon Scattering . . . . . L. I. Lapidus	193	36, 283
A Possible Method for the Determination of the Parity of Strange Particles . . . . . S. M. Bilen'kii	199	36, 291
Conditions for Superfluidity of the Atomic Nucleus and the Temperature of the Phase Transition . . . . . V. G. Solov'ev	201	36, 293
On the Moment of Inertia of a Many-Particle System; I. . . . . Yu. K. Khokhlov	203	36, 295
Peripheral Interactions between Elementary Particles . . . . . L. B. Okun' and I. Ya. Pomeranchuk	207	36, 300
LETTERS TO THE EDITOR		
Quantum Corrections to Radiation from a Rigid Rotator . . . . . L. B. Iogansen	216	36, 313
Energy Spectrum of Fragments from the Photofission of U^{238} . . . . . B. S. Kovrigin, M. Ya. Kondrat'ko, and K. A. Petrzhak	217	36, 315
The Beta Spectra of F^{20} and F^{17} . . . . . S. S. Vasil'ev and L. Ya. Shavtvalov	218	36, 317
Superconducting Alloys at Finite Temperatures . . . . . A. A. Abrikosov and L. P. Gor'kov	220	36, 319
Particle Energy Losses Due to the Excitation of Longitudinal Waves . . . . . B. A. Lysov	221	36, 321
Coulomb Excitation of Neon . . . . . D. K. Alkhazov, A. P. Grinberg, I. Kh. Lemberg, and V. V. Rozhdestvenskii	222	36, 322
Polarization Correlation in Coulomb Scattering of Electrons and Muons by Light Nuclei Including Radiation Corrections . . . . . I. G. Ivanter	224	36, 325
K-Level X-Rays from Fission Fragments and Distribution of Fragments by Charges . . . . . V. V. Sklyarevskii, E. P. Stepanov, and B. A. Medvedev	225	36, 326
Concerning a 100-kev Transition in the Spectrum of Ce^{144} . . . . . A. V. Gnedich, L. N. Kryukova, and V. V. Murav'eva	226	36, 329
Concerning the Ce^{141} Decay Scheme . . . . . N. V. Forafontov and A. A. Sorokin	227	36, 330
The Elastic Scattering of Polarized Dirac Particles by a Short Range Center of Force in the Damping Theory . . . . . I. I. Guseinov	228	36, 331
Decay of a Beryllium Hyperfragment . . . . . A. O. Vaisenberg and V. A. Smirnitskii	230	36, 333
On the Probability of Double Beta Decay . . . . . F. Yanouki	231	36, 335
Pair Production by a Circularly Polarized Photon . . . . . I. M. Nadzhafov	232	36, 337
Radiation from a Spin-2 Particle Moving Uniformly in a Medium . . . . . A. I. Bedritskii	234	36, 339
Disappearance of the Isothermal Jump at Large Radiation Density . . . . . V. A. Belokon'	235	36, 341
The Conductivity of Semi-Conductors in an Ultrasonic Field . . . . . V. A. Zhuravlev and M. I. Kozak	236	36, 343

CONTENTS

	Page	Russian Reference
Depth of Penetration and Character of Distribution of Atoms Injected into Si^{30} Isotope Targets . . . M. I. Guseva, E. V. Inopin, and S. P. Tsytko	1	**36,** 3
Showers Produced by Positrons in 100 to 400 Mev Range . . . Yu. D. Prokoshkin and T'ang Hsiao-Wei	6	**36,** 10
Cloud Chamber Investigations in the Cores of Extensive Air Showers . . . O. I. Dovzhenko, S. I. Nikol'skii, and I. V. Rakobol'skaya	11	**36,** 17
Beta-Gamma Angular Correlation in Ba^{139} Decay and the Relative Sign of the Beta-Interaction Coupling Constants . . . N. A. Vlasov and V. P. Rudakov	17	**36,** 24
Gd^{146} and Eu^{146} Conversion-Electron Spectra . . . N. M. Anton'eva, A. A. Bashilov, B. S. Dzhelepov, and B. K. Preobrazhenskii	20	**36,** 28
The Scattering of Muons in Lead . . . A. I. Alikhanyan and F. R. Arutyunyan	23	**36,** 32
Ionization of Air by H^+ and H_2^+ Ions . . . R. N. Il'in, V. V. Afrosimov, and N. V. Fedorenko	29	**36,** 41
Hodoscope Investigation of the Penetrating Component of Extensive Air Showers . . . R. E. Kazarov	35	**36,** 49
(d, p) Stripping Reactions in the Silicon Isotopes . . . V. G. Sukharevskii	37	**36,** 52
The Energy of Formation and Migration of Vacancies in Gold and Platinum . . . B. G. Lazarev and O. N. Ovcharenko	42	**36,** 60
Energy Spectra of Alpha Particles from the Long-Lived Isotopes Th^{232} and U^{238} . . . G. E. Kocharov, A. P. Komar, and G. A. Korolev	48	**36,** 68
A Search for Double Beta Decay in Ca^{48} . . . E. I. Dobrokhotov, V. R. Lazarenko, and S. Yu. Luk'yanov	54	**36,** 76
Symmetry Group of the Isotropic Oscillator . . . Yu. N. Demkov	63	**36,** 88
Angular Momentum and Parity Conservation Laws in the Statistical Theory of Multiple Production . . . V. B. Magalinskii	67	**36,** 93
Dual Scattering of Relativistic Pions by Nucleons . . . V. A. Astaf'ev	70	**36,** 98
Electrical, Optical, and Elastic Properties of Crystals of the Diamond Type. III. Dispersion and Absorption of Light . . . V. S. Mashkevich	76	**36,** 108
Frequency Spectrum of Electron Spin Double Resonance at Color Centers in Alkali Halide Crystals . . . V. Ya. Zevin	81	**36,** 116
The Two-Nucleon **LS** Potential in Nonrelativistic Meson Theory . . . Yu. V. Novozhilov and I. A. Terent'ev	89	**36,** 129
Remarks Regarding Heisenberg's Paper on the Lee Model . . . L. A. Maksimov	97	**36,** 140
Electroacoustic Phenomena in a Degenerate Electron-Ion Plasma . . . P. S. Zyryanov and G. G. Taluts	100	**36,** 145
On the Energy Spectrum of a Mott Exciton in Ionic Crystals . . . S. A. Moskalenko and K. B. Tolpygo	103	**36,** 149
Effects of a Resonant Pion-Pion Interaction in Fermi's Statistical Theory of Multiple Particle Production . . . V. I. Rus'kin	113	**36,** 164
A System of Magnetic Moments in a Weak Variable Magnetic Field . . . G. V. Skrotskii and A. A. Kokin	116	**36,** 169
Paramagnetic Resonance of F Centers in Static Magnetic Fields of Arbitrary Strength . . . M. F. Deĭgen and L. B. Roĭtsin	120	**36,** 176
Parentage Coefficients in the Generalized Nuclear Model . . . V. G. Neudachin and Yu. F. Smirnov	127	**36,** 186
Beta-Gamma Correlation in First-Forbidden Beta Transitions . . . Yu. V. Gaponov	131	**36,** 193
Green's Function for the Resonance Radiation Diffusion Equation . . . V. A. Veklenko	138	**36,** 204
Polarization Effects in Σ^--Hyperon Capture by Deuterons . . . S. G. Matinyan and O. D. Cheishvili	143	**36,** 212
On the Theory of Relaxation Processes in Ferrodielectrics at Low Temperatures . . . A. I. Akhiezer, V. G. Bar'yakhtar, and S. V. Peletminskii	146	**36,** 216
Phenomenological Theory of Kinetic Processes in Ferromagnetic Dielectrics. II. Interaction of Spin Waves with Phonons . . . M. I. Kaganov and V. M. Tsukernik	151	**36,** 224

(Contents continued on inside back cover)